Pacific Northwest
NATIONAL LABORATORY

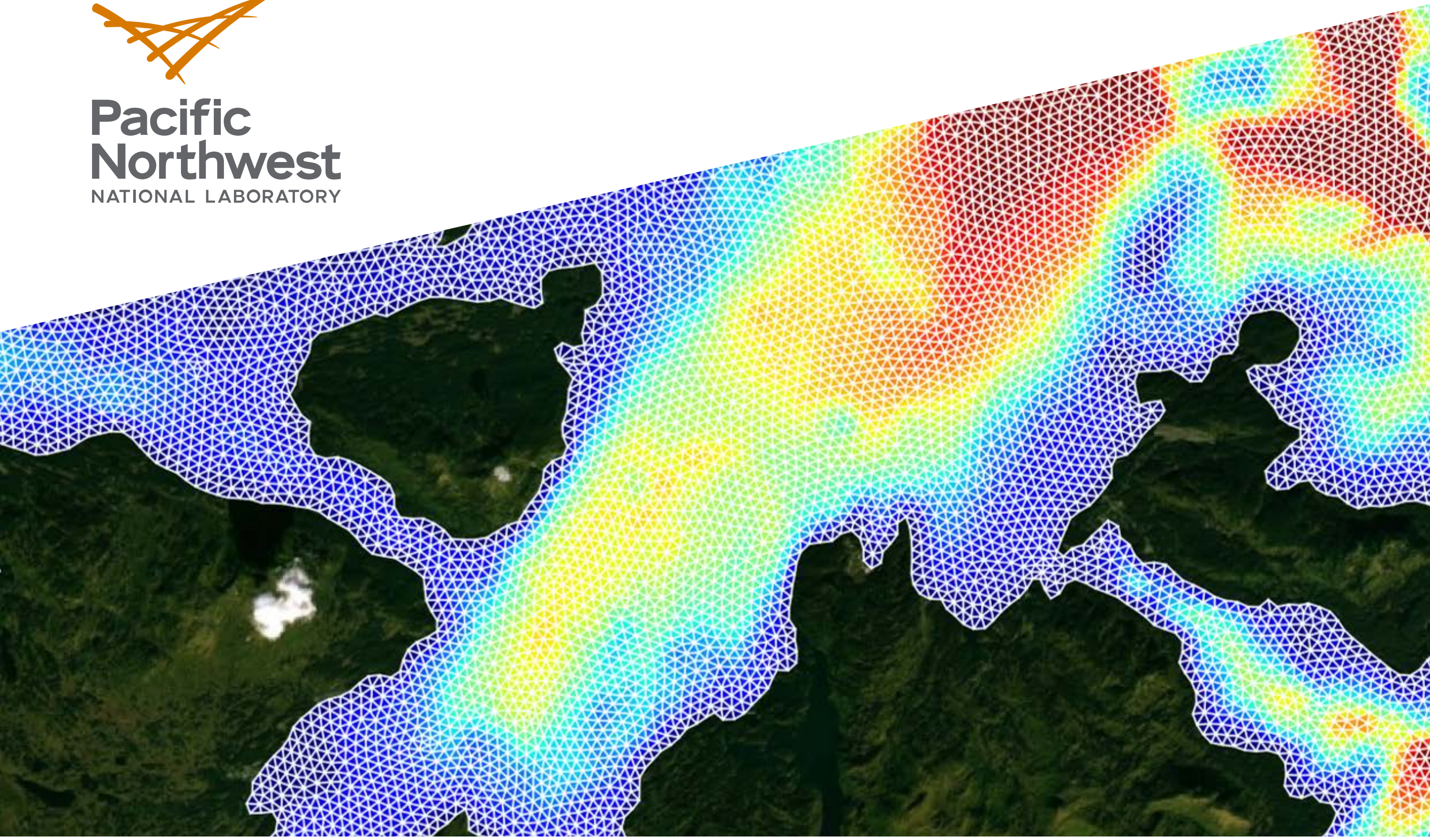

PNNL- 29479

High-Resolution Regional Wave Hindcast for the U.S. Alaska Coast

December 2019

Z Yang
WC Wu
T Wang
G García-Medina
L Castrucci

U.S. DEPARTMENT OF ENERGY

Prepared for the U.S. Department of Energy
under Contract DE-AC05-76RL01830

PACIFIC NORTHWEST NATIONAL LABORATORY
operated by
BATTELLE
for the
UNITED STATES DEPARTMENT OF ENERGY
under Contract DE-AC05-76RL01830

Printed in the United States of America

Available to DOE and DOE contractors from the
Office of Scientific and Technical Information,
P.O. Box 62, Oak Ridge, TN 37831-0062;
ph: (865) 576-8401
fax: (865) 576-5728
email: reports@adonis.osti.gov

Available to the public from the National Technical Information Service
5301 Shawnee Rd., Alexandria, VA 22312
ph: (800) 553-NTIS (6847)
email: orders@ntis.gov <https://www.ntis.gov/about>
Online ordering: http://www.ntis.gov

PNNL- 29479

High-Resolution Regional Wave Hindcast for the U.S. Alaska Coast

December 2019

Z Yang
WC Wu
T Wang
G García-Medina
L Castrucci

Prepared for
the U.S. Department of Energy
under Contract DE-AC05-76RL01830

Pacific Northwest National Laboratory
Richland, Washington 99354

Summary

Regional long-term wave hindcast with state-of-art third-generation models is essential for characterization of regional wave resources. This report summarizes modeling efforts for the simulation of the wave climate along southern Alaska, which used an unstructured, nested-grid modeling approach that incorporates a global-regional nested grid using WAVEWATCH III® and the high-resolution SWAN (Simulating Waves Nearshore) model. Wave resource and wave bulk parameters were simulated for a 32-year period from 1979 to 2010 and were subsequently validated with wave buoy data in the model domain. Error statistics of model skill were calculated at all buoy stations. Overall, model results, both resource and bulk parameters, match observations well. The model hindcast was able to reproduce the seasonal variation of the sea state with large waves that occur in the winter and early spring months when wind forcing is strong and the calm sea state during the summer when wind forcing is weak. The hindcast also considers the effect of sea ice on wave growth, which affects the southern Bering Sea. The hindcast results, including resource and bulk parameters, were archived at every model grid point for the entire model domain at three-hour intervals. In addition, spectral results were saved at National Data Buoy Center buoy stations and selected nearshore locations at hourly intervals. The nested-grid modeling framework employed in this study provides a powerful and efficient modeling approach for accurately simulating wave climate at regional and long-term temporal scales with sufficiently fine resolutions in the nearshore region.

Acknowledgments

This study was funded by the U.S. Department of Energy (DOE), Office of Energy Efficiency and Renewable Energy, Water Power Technologies Office under Contract DE-AC05-76RL01830 to Pacific Northwest National Laboratory (PNNL).

A steering committee, chaired by Dr. Bryson Robertson of Oregon State University, provided external oversight of this modeling study. Steering committee members include Dr. Henrique Alves of the National Oceanic and Atmospheric Administration; Dr. Brian Polagye of Pacific Marine Energy Center at University of Washington; Dr. Julie Thomas of the Coastal Data Information Program at the University of California San Diego; Dr. Pukha Lenee-Bluhm of Columbia Power; Bill Staby of Resolute Marine Energy; and Mr. Sean Anderton of Ocean Renewable Power Company.

The model computations were performed using resources available through Research Computing at PNNL. PNNL is operated by Battelle for DOE under Contract DE-AC05-76RL01830.

Acronyms and Abbreviations

AOOS	Alaska Ocean Observing System
CDIP	Coastal Data Information Program
CFL	Courant–Friedrichs–Lewy
CFSR	Climate Forecast System Reanalysis
DFO	(Canada's) Department of Fisheries and Oceans
EEZ	Exclusive Economic Zone
EPRI	Electric Power Research Institute, Inc.
GSE	Garden Sprinkler Effect
Hz	hertz
IEC	International Electrotechnical Commission
km	kilometer(s)
kW/m	kilowatt(s) per meter
m	meter(s)
NDBC	National Data Buoy Center
NCEP	National Centers for Environmental Prediction
NOAA	National Oceanic and Atmospheric Administration
NREL	National Renewable Energy Laboratory
PE	percentage error
R	correlation coefficient
RMSE	root-mean-square-error
s	second(s)
SI	scatter index
ST	source term
SWAN	Simulating WAves Nearshore
TS	Technical Specification
UnSWAN	unstructured-grid Simulating WAves Nearshore
UTC	Coordinated Universal Time
SWAN	Simulating WAves Nearshore
WEC	wave energy converter
WWIII	WAVEWATCH III
yr	year(s)

Contents

Figures

Tables

1.0 Introduction

Ocean waves are the greatest energy resource of the U.S. marine and hydrokinetic energy resources, which include waves, tidal and ocean currents, ocean thermal gradients, and river streams. The first U.S. nationwide wave resource assessment was conducted by The Electric Power Research Institute (EPRI) based on the 4 arc-minute resolution, 51-month wave hindcasts generated by the National Oceanic and Atmospheric Administration (NOAA) using the nested-grid WAVEWATCHIII® model (WWIII) (EPRI, 2011; H.L. Tolman & WAVEWATCH III Development Group, 2014). EPRI's study showed that Alaska has the largest wave resource of all U.S. major coastal regions. The national assessment provided first-order estimates of wave resource locations and variability. However, a 51-month hindcast does not provide records of adequate length to characterize the decadal trends of wave power. There are concerns that the shallow-water processes in the nearshore regions were not well reproduced because of the coarse-grid resolution, which could result in high uncertainty in resource estimates, especially in the nearshore region (National Research Council, 2013). Most wave energy converters (WECs) are designed for deployment in nearshore areas because of the associated low deployment and maintenance costs, as well as low risk under extreme sea states. Therefore, it is important to conduct a long-term, high-resolution wave hindcast, especially in nearshore shallow-water areas to improve the accuracy of hindcasts and reduce the uncertainties of the previous resource assessment by EPRI (2011).

The U.S. Department of Energy, Office of Energy Efficiency and Renewable Energy, Water Power Technologies Office funded a joint project by National Renewable Energy (NREL), Pacific Northwest National Laboratory (PNNL), and Sandia National Laboratories to conduct field measurements, validate numerical models, and develop classification schemes to improve U.S. wave and tidal resource characterization and assessment. Specifically, PNNL was funded to conduct high-resolution model simulations of wave climates and provide high-quality hindcast results to improve resource characterization in the Alaska region. Simulation of wave climate with fine-grid resolution at a regional scale requires extensive computational resources. The unstructured-grid modeling approach not only provides flexibility in accurately fitting the mesh boundary to the shoreline and refining the grid resolution in the area of interest, but it also maintains great computational efficiency for a large model domain. In recent years, many studies have been conducted using unstructured-grid Simulating WAves Nearshore (UnSWAN) to simulate wave climates in many regions around the world (Cobell, Zhao, Roberts, Clark, & Zou, 2013; Gallagher, Tiron, & Dias, 2014; Mao, van der Westhuysen, Xia, Schwab, & Chawla, 2016; Mediavilla & Sepulveda, 2016; Roland & Ardhuin, 2014; Wu, Yang, & Wang, 2018; Yang, Wu, Wang, & Castrucci, 2018; Yuk, Kim, Jung, & Choi, 2016; Zijlema, 2010).

In this study, a nested-grid, unstructured-grid modeling approach was applied to simulate high-resolution wave climates in Alaska using two widely used third-generation wave models─WWIII and SWAN. International Electrotechnical Commission (IEC) wave resource parameters, as well as long-term wave bulk parameters, were simulated and validated against measurements at wave buoys maintained by NOAA's National Data Buoy Center (NDBC). Wave partition output was collected along selected lines of equal distance (from 1 to 5 km) from the shore to support wave classification. An analysis of the distribution of the wave resource parameters both spatially and temporally was conducted.

Model configurations for both WWIII and SWAN, including model grids, spectral and directional resolutions, model run time steps, and wind forcing are provided in Section 2. Wave buoy data for model validation are also described. Model simulations and validation results are presented in Section 3. Spatial and temporal distributions of wave resource parameters are also discussed in Section 3. The conclusions of the study are given in Section 4. Monthly and yearly distributions of simulated wave bulk parameters are listed in Appendix A. Comparisons of simulated wave bulk parameter time series with buoy data and the model performance metrics are provided in Appendices B and C, respectively. Similar products for IEC resource parameters are provided in Appendices D, E, and F.

2.0 Methods

A nested-grid modeling approach using WWIII and SWAN models was used in this study. Three levels of nested grids using the WWIII model were set up to simulate wave climates from global to regional scales and provide open boundary conditions to the high-resolution unstructured-grid SWAN (SWAN, 2015) for the Alaska Exclusive Economic Zone (EEZ). The SWAN model domain extends from the southern border of Alaska and British Columbia to the north end of Bristol Bay, Alaska. Details about the WWIII and SWAN model configurations are provided in ensuing sections.

2.1 WWIII Model Configuration

To drive the high-resolution SWAN model for Alaska, a nested-grid modeling approach was employed. This method allows for models that have different resolutions and spatial coverages to operate simultaneously and focus the computational resources on shelf scales without neglecting oceanic scale effects, which are important for accurately characterizing swells. Like other wave resource characterization studies (García-Medina, Özkan-Haller, & Ruggiero, 2014; García-Medina, Özkan-Haller, Ruggiero, & Oskamp, 2013; Wu et al., 2018; Yang et al., 2017; Yang et al., 2018), this study used three levels of structured-grid WWIII models. All three levels are based on the NOAA National Centers for Environmental Prediction (NCEP) operational WWIII model.

The Level 1 grid (L1) is the global model that has a resolution of 0.5 arc-degree. Level 2 (L2) and Level 3 (L3) grids have resolutions of 10 arc-minutes and 4 arc-minutes, respectively. The model domain coverage and spatial resolution for all three levels of WWIII models are summarized in Table 2.1. Model output from WWIII provides open boundary conditions for the SWAN model. The source term ST4 physics package (Ardhuin et al., 2010) was used in all WWIII model runs conducted in this study using default parameters for WWIII v5.16.

Table 2.1. Summary of nested WWIII model grids.

Grid Name	Coverage	Resolution (long x lat)
Global (L1)	77.5°S – 77.5°N; 0 – 360°W	0.5° × 0.5°
Alaska 10m (L2)	44° – 75°N; 140°E – 120°W	0.25° × 0.167° (15' × 10')
Alaska 4m (L3)	48° – 74°N; 165°E – 122°W	8' × 4'

Model time steps used in WWIII are summarized in Table 2.2. For WWIII, each model grid requires four time steps: (1) the global time step Δt_g, (2) the spatial propagation time step Δt_{xy}, (3) the intra-spectral propagation time step Δt_k, and (4) the source term time step Δt_s (Tolman et al. 2014). WWIII employs an explicit scheme for spatial propagation, thus the propagation time step Δt_{xy} must satisfy the Courant–Friedrichs–Lewy (CFL) criterion to ensure model stability.

Table 2.2. Model run time steps for the WWIII model (L1–L3 grids).

WWIII Nested Grid	Δt_g (s)	Δt_{xy} (s)	Δt_k (s)	Δt_s (s)
L1 (global)	1,800	600	900	30
L2	1,800	225	900	15
L3	600	150	300	15

The WWIII L2, L3, and SWAN model domains are shown in Figure 2-1.

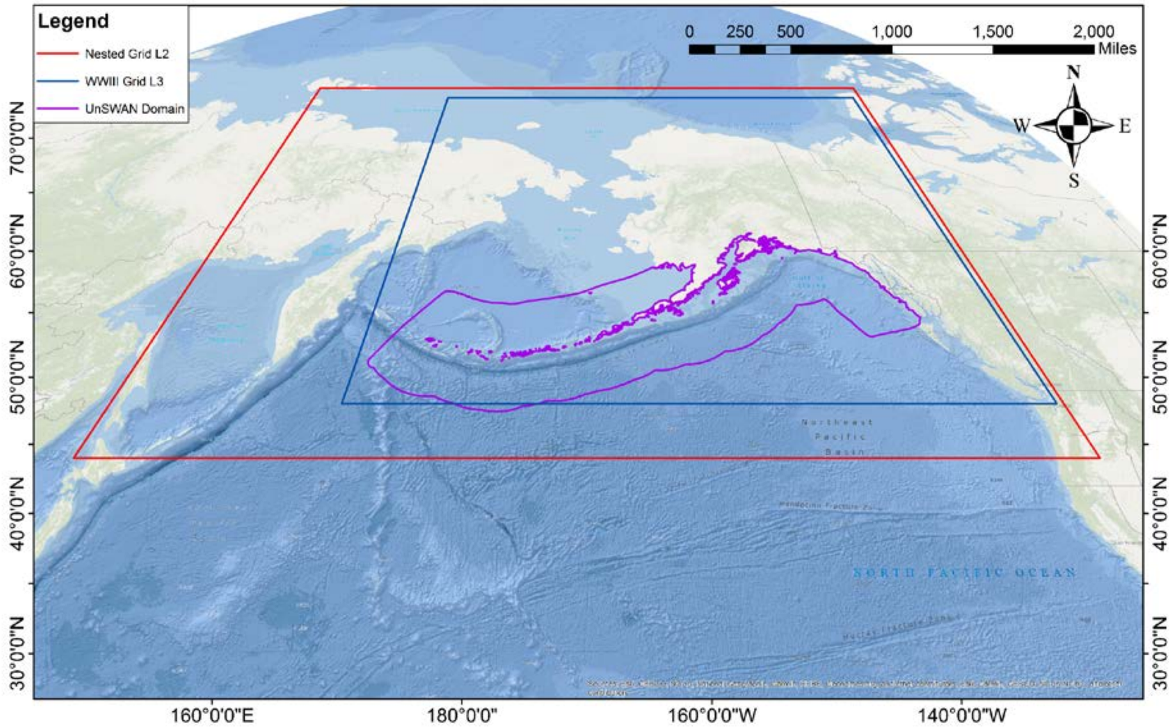

Figure 2-1. Model domains of Alaska. Red and blue lines represent the WWIII L2 and L3 model domains, respectively. The purple line represents the high-resolution SWAN Alaska model domain.

All WWIII simulations used 29 frequency bins, 24 direction bins, a logarithmic increment factor of 1.1, a minimum frequency of 0.035 Hz, and a maximum frequency of 0.505 Hz. This spectral resolution meets the minimum requirements specified by the IEC Technical Specification (IEC, 2015), i.e., a minimum of 25 frequency components and 24 to 48 directional components and a frequency range covering at least 0.04 to 0.5 Hz.

2.2 SWAN Model Configuration

A Level 4 of nested grid is implemented using unstructured-grid SWAN. The SWAN model domain covers the Alaska EEZ from the U.S.-Canada border in southeast Alaska to the north end of Bristol Bay. The bathymetry within the model domain is shown in Figure 2-2. The model grid has a resolution of approximately 300 m in the nearshore region from the shoreline to 30 km offshore. This allows the model to resolve the wave field with high resolution in the shallow areas nearshore. An example of the model mesh near the western Aleutian Islands is shown in Figure 2-2. From 30 to 40 km from shore, the resolution was gradually reduced to 2,500 m. From 40 km from shore to the EEZ (370.4 km from shore), the model resolution was kept constant at 2,500 m. Finally, between the EEZ and the model boundary, the resolution was reduced to 4,000 m to allow for a smooth transition between the WWIII forcing and the SWAN model domains. The resulting unstructured grid consists of 3,894,283 nodes and 7,719,870 elements. The model bathymetry was interpolated from the Southern Alaska Coastal Relief Model (Lim, Eakins, & Wigley, 2011) and the digital elevation models from NOAA Fisheries covering the Aleutian Islands (Zimmermann, Prescott, & Rooper, 2013), Cook Inlet (Zimmermann & Prescott, 2014), and the Central Gulf of Alaska (Zimmermann & Prescott, 2015), where the latter data set had priority because they were of higher resolution and the former was used where no high-resolution data were available.

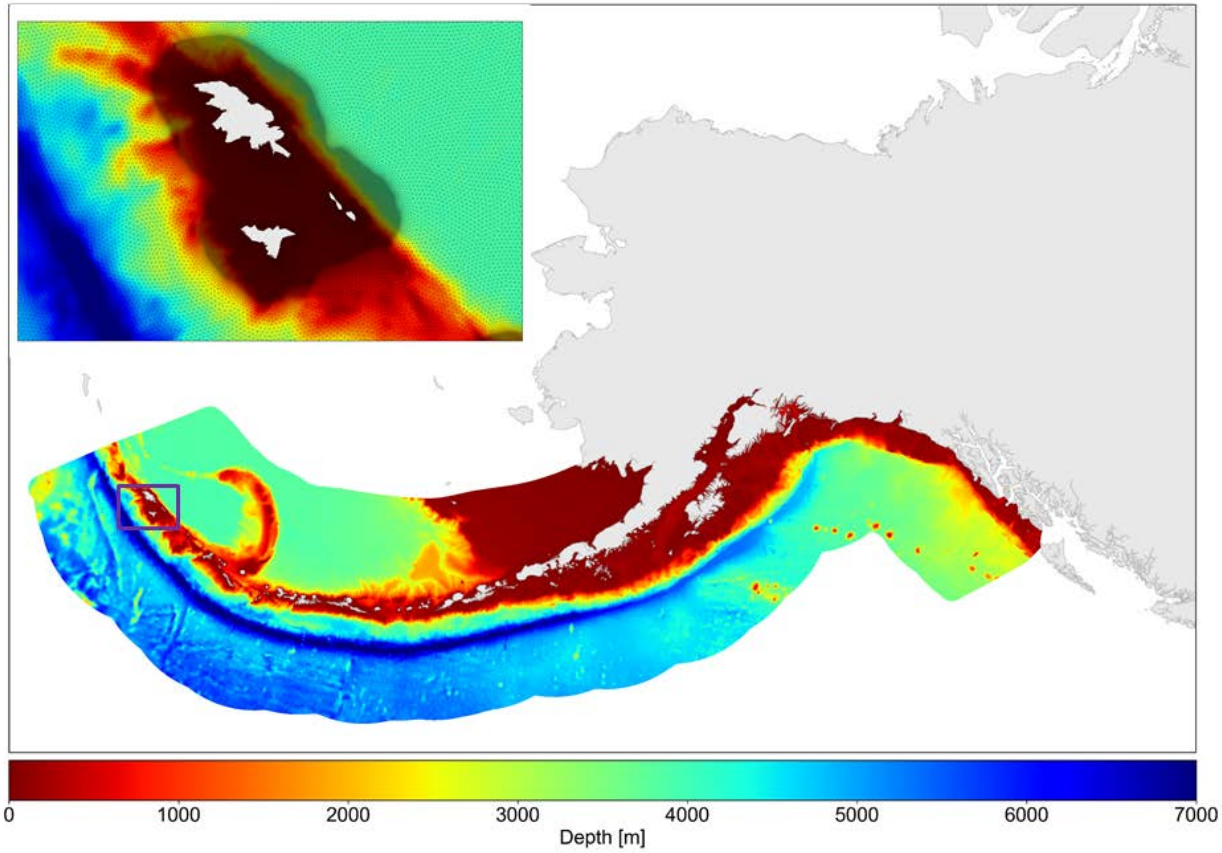

Figure 2-2. Bathymetry distribution of the SWAN model for the Alaska Coast. The two map inserts show the close-up model grid and the overall model bathymetry.

A time step of 10 minutes was used in SWAN simulations. This time step is sufficient to solve the temporal variations of wave climates. SWAN solves the action balance equation with an implicit solver and thus the time step is not constrained by the CFL criterion. Another factor that affects the accuracy of the model results is the number of iterations. The model sensitivity to the iterations was tested by considering 20 (default), 10, 5, and 2 iterations. The model results were not sensitive to the maximum number of iterations, so to save computation time, two iterations where chosen to solve the model equations.

Because of the combination of narrow channels between the islands and deep waters along the Aleutian Arc, significant Garden Sprinkler Effect (GSE) is present, a phenomenon of discrete swell fields as a result of coarse spectral-directional resolution (H. L. Tolman, 2002). To mitigate the GSE, the directional resolution of the spectral domain is increased. Based on a qualitative assessment from model simulations that had a directional resolution of 15°, 10°, and 5°, the latter was chosen (Figure 2-3). Finally, to be consistent to WWIII configuration, the frequency range was specified from 0.035 to 0.505 Hz with a logarithmic spacing that increased by a factor of 1.1, resulting in 29 frequency bins.

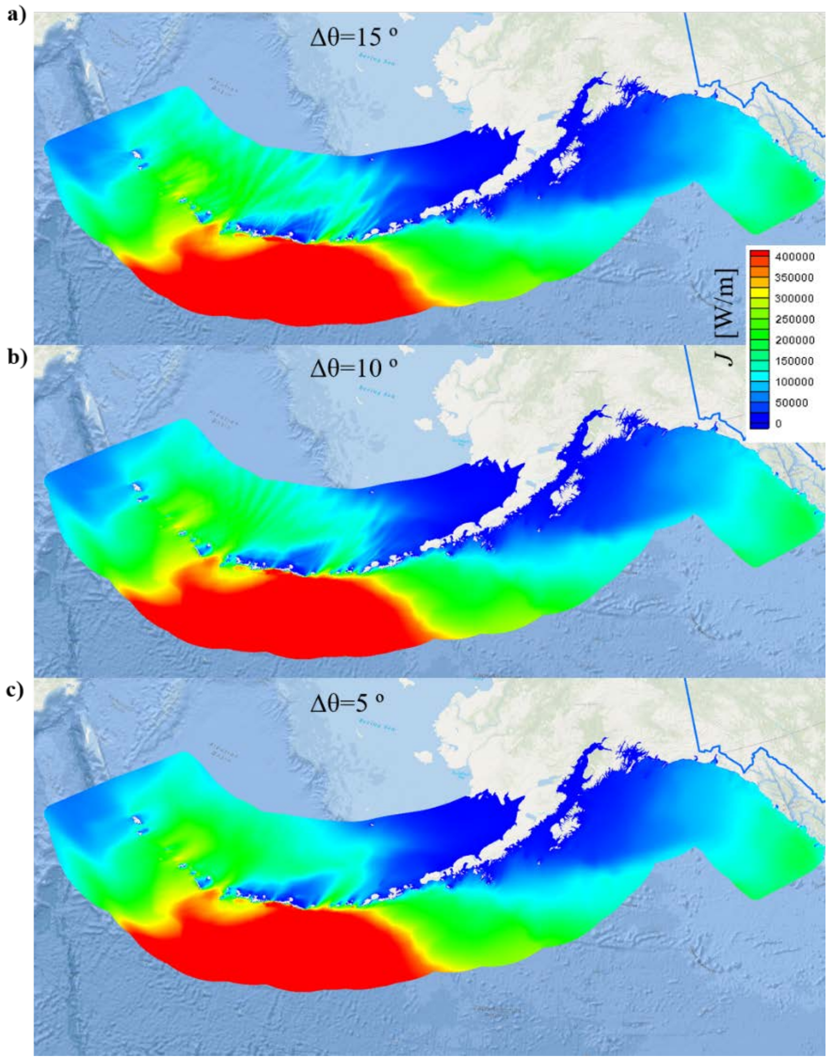

Figure 2-3. Simulated wave power (*J*) in Alaska with direction resolutions of (a) 15°, (b) 10°, and (c) 5°. With a relatively coarse directional resolution of 15°, the GSE is clearly seen, with a ray of discrete swell fields spreading out through the narrow channels between Aleutian Islands. As the directional resolution is increased to 10°, the swell fields are improved and finally with a direction resolution of 5°, the GSE is mitigated.

2.3 Model Forcing

In this study, the model hindcast covered 32 years from 1979 to 2010, which corresponds to the sea surface wind data availability period of the Climate Forecast System Reanalysis (CFSR), produced by NCEP (Saha et al., 2010). The wind forcing data (wind speeds and directions) for the wave hindcast were obtained from CFSR and interpolated onto model grid points. Comparison of CFSR wind speed with observed data at a number of NDBC buoy stations indicated that the CFSR wind speed is generally in good agreement with the observed speed and reasonably captures the diurnal and seasonal variabilities. Figure 2-4 shows an example of global CFSR wind speed distribution on 23 October 2004. On that day, a severe winter storm generated large storm surges on the coast of western Alaska. The wave heights associated with this event are shown in Figure 2-5. The storm generated significant wave heights in excess of 7 m in the southern Bering Sea.

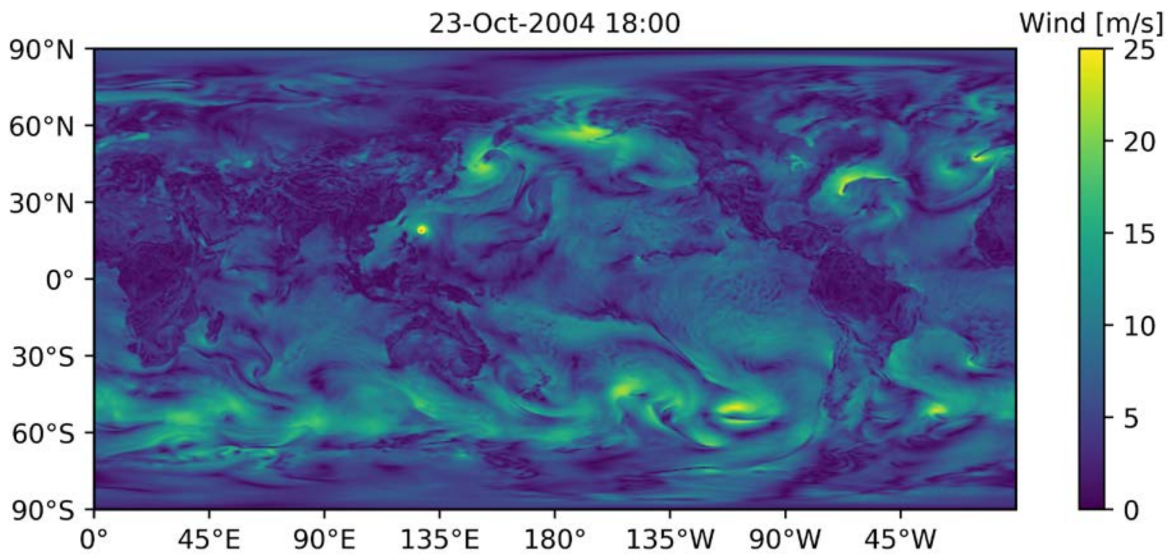

Figure 2-4. Instantaneous global wind speed distribution from CFSR for 23 October 2004 at 18:00 UTC.

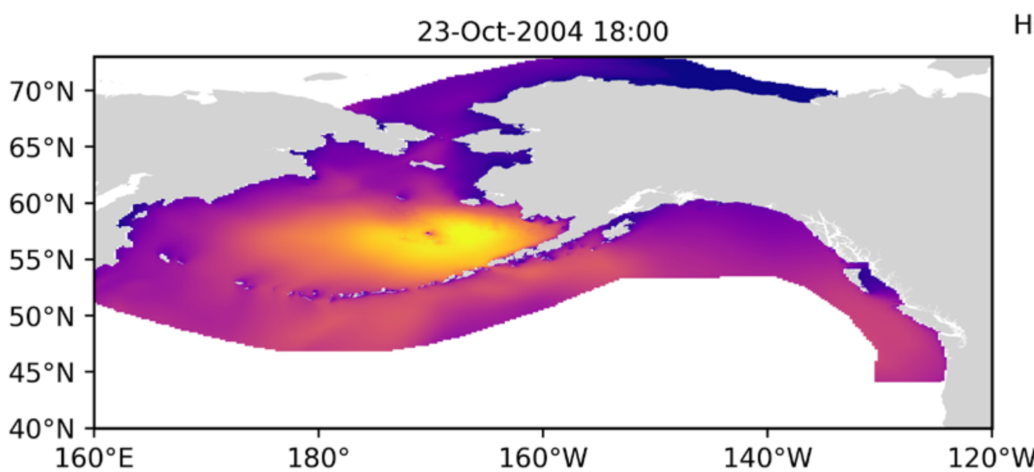

Figure 2-5. Instantaneous significant wave height fields from WW3 L2 and L3 during 23 October 2004 at 18:00 UTC.

The sea ice coverage data were obtained from the same NCEP CFSR data set as the wind data, except that the original sea ice data were defined in the NCEP T382 Gaussian Grid that has a spatial resolution of 38 km. The sea ice data were subsequently re-projected onto the same 0.5 × 0.5 arc-degree regular grid as the wind forcing data and implemented at daily temporal resolution. The currents induced by tides and ocean circulations were not considered in this study.

Because most of the wave buoys in Alaska started to collect directional wave data after 2010, a simulation for 2017 was conducted for model validation with IEC resource parameters, in addition to the 1979–2010 hindcast. NREL conducted a shallow-water measurement campaign near Kodiak, Alaska during which directional wave properties were measured. The model configuration for the 2017 simulation is the same as that used for the 32-year hindcast. Wind forcing was obtained from the second version of CFSR (CFSv2, Saha et al. (2014)), which covers the period from 2011 to the present.

The SWAN model was driven by the WWIII model outputs along the SWAN model open boundary. Full 2-D spectral boundary conditions were used at the open boundary to allow for the propagation of multimodal sea states. There is a strong seasonal variability in the wave forcing as seen in Figure 2-6**,** where the winters are more energetic than the summers at basin scale.

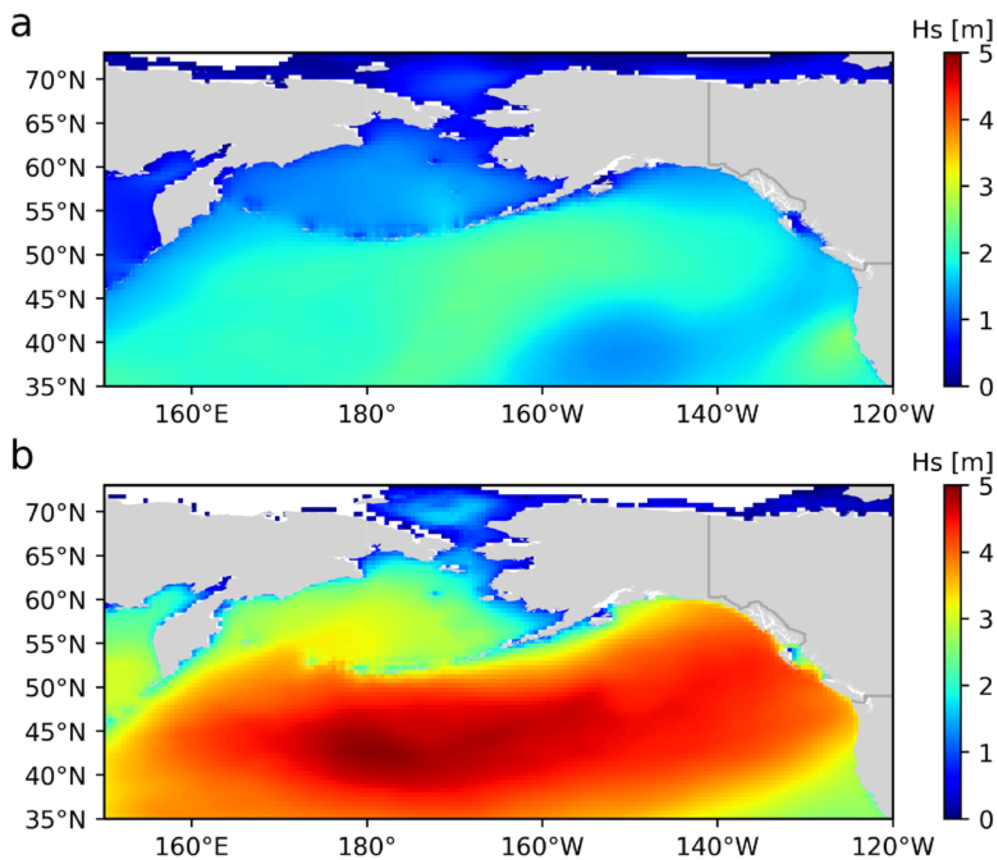

Figure 2-6. Monthly average significant wave height (m) simulated by WWIII for (a) July and (b) November.

2.4 Wave Buoy Data for Model Validation

Model validation was conducted using measured data from wave buoys. A total of 48 buoys measuring either bulk parameters or spectral data are in the Alaska coastal region. Of the 48 buoys, 24 are maintained by NDBC, 5 by the Coastal Data Information Program (CDIP), 14 by Canada's Department of Fisheries and Oceans (DFO), 4 by Shell Arctic, and 1 by the Alaska Ocean Observing System (AOOS) (Table 2.3). Most NDBC buoys measure spectral data after 2010. All CDIP buoys measure bulk wave parameters only, except Buoy 46264, which was deployed by NREL as part of the joint project. All DFO buoys have at least 25 years of spectral data and are active up to present, except Buoys 46138 and 48021.

Because the model simulation period is from 1979 to 2010, buoys with measurement periods outside of the simulation period are not included for model validation. A few buoys are also eliminated from the model validation process because they have a short measurement period, are outside of the model domain, or are close to other buoy locations. A total of 20 final NDBC buoys were selected for model validation because they had data records corresponding to the hindcast period (Table 2.4). These buoys are distributed along the extensive Alaskan coast, from the Aleutian Islands to southeastern Alaska, providing sufficient measured data for a thorough model validation Figure 2-7.

Table 2.3. Inventory of wave buoys with directional-spectral data and bulk parameters in the Alaska region

Agency	Buoy	Longitude	Latitude	Depth (m)	Period		Years	
					Param	Spec	Param	Spec
NDBC	46001	-147.949	56.232	4054	1979-2018	2017	40	1
NDBC	46035	-177.738	57.026	3658	1985-2012 2014-2018	2014-2018	33	5
NDBC	46060	-146.805	60.584	440.1	1995-2018	2007-2018	24	12
NDBC	46061	-146.843	60.230	220	1995-2018	2014-2018	24	5
NDBC	46066	-155.047	52.785	4545	2000-2011 2013-2018	2013-2018	18	6
NDBC	46070	175.153	55.082	3835	2006-2009 2011-2017	2015-2017	11	3
NDBC	46071	179.012	51.125	1681	2004-2009 2012 2016-2017	2016-2017	9	2
NDBC	46072	-172.058	51.656	3048	2002-2016	2016	15	1
NDBC	46073	-172.001	55.031	3051.5	2005-2011 2014-2017	2014-2017	11	4
NDBC	46075	-160.817	53.983	2392.7	2004-2018	2016-2018	15	3
NDBC	46076	-147.990	59.502	195.1	2005-2018	2015-2018	14	4
NDBC	46077	-154.175	57.910	202	2005-2014 2017-2018	2017-2018	12	2
NDBC	46078	-152.582	55.556	5380	2004-2018	2013-2018	15	6
NDBC	46080	-150.042	57.947	254.5	2002-2012 2014-2018	2017-2018	16	2
NDBC	46081	-148.263	60.799	434	2003-2018		16	0
NDBC	46082	-143.372	59.681	300	2002-2018	2015-2018	17	4
NDBC	46083	-137.997	58.300	136	2001-2013 2015-2018	2015-2018	17	4
NDBC	46084	-136.101	56.600	1408	2002-2008 2010-2017	2016-2017	16	3
NDBC	46085	-142.492	55.868	3736.3	2007-2012 2014-2018		11	0
NDBC	48011	-164.185	67.582	17.3	2000-2001	2000-2001	2	2
NDBC	46003	-155.850	51.831		1979-1999		21	0
NDBC	46105	-152.233	59.049	126.5	2008 2011- 2012	2008 2011-2012	3	3
NDBC	46106	-152.090	59.760	45.7	2007-2010	2007-2010	4	4
NDBC	46107	-147.992	59.925	105.5	2008-2010	2008-2010	3	3
CDIP	46108	-151.829	59.597	32.9	2013 2015-2018	2013 2015-2018	5	5
CDIP	46246	-145.200	50.033	4252	2010-2017	2010-2017	8	8

Agency	Buoy	Longitude	Latitude	Depth (m)	Period Param	Period Spec	Years Param	Years Spec
CDIP	46264	-151.695	57.479	86	2017-2018	2017-2018	2	2
CDIP	175	-152.004	59.733	25.6	2011-2013	2011-2013	3	3
CDIP	205	-131.763	55.604	387.1	2014-2018	2014-2018	5	5
Shell Arctic	48211	-146.040	70.370		2013		1	0
Shell Arctic	48213	-164.133	71.502		2012-2015		4	0
Shell Arctic	48214	-165.248	70.872		2012-2015		4	0
Shell Arctic	48216	-167.952	71.758		2015		1	0
AOOS	48114	-169.454	65.011	51	2014-2015		2	0
DFO	46205	-134.320	54.190	2675	1988-2018	1988-2018	31	31
DFO	46004	-136.100	50.930	3600	1988-2018	1988-2018	31	31
DFO	46208	-132.690	52.520	2950	1990-2018	1990-2018	29	29
DFO	46183	-131.100	53.620	65	1991-2018	1991-2018	28	28
DFO	46147	-131.220	51.830	2000	1993-2018	1993-2018	26	26
DFO	46138	-129.795	52.437	230	2010-2011	2010-2011	2	2
DFO	46207	-129.920	50.870	2125	1989-2018	1989-2018	30	30
DFO	46145	-132.440	54.370	255	1991-2018	1991-2018	28	28
DFO	46181	-128.830	53.830	23	1988-2018	1988-2018	31	31
DFO	46185	-129.790	52.420	230	1991-2018	1991-2018	28	28
DFO	46204	-128.770	51.380	222	1989-2018	1989-2018	30	30
DFO	46132	-127.930	49.740	2040	1994-2018	1994-2018	25	25
DFO	46184	-138.850	53.910	3200	1987-2018	1987-2018	32	32
DFO	48021	-133.000	70.350	36	2014-2015	2014-2015	2	2

Table 2.4 Summary of wave buoys distributed in the Alaska region.

					Period		Years	
Agency	Buoy	Longitude	Latitude	Depth (m)	Param	Spec	Param	Spec
NDBC	46001	-147.949	56.232	4054	1979-2010		32	0
NDBC	46060	-146.805	60.584	440.1	1995-2010	2007-2010	16	4
NDBC	46061	-146.843	60.230	220	1995-2010		16	0
NDBC	46066	-155.047	52.785	4545	2000-2010		11	0
NDBC	46070	175.153	55.082	3835	2006-2009		4	0
NDBC	46071	179.012	51.125	1681	2004-2009		6	0
NDBC	46072	-172.058	51.656	3048	2002-2010		9	0
NDBC	46073	-172.001	55.031	3051.5	2005-2010		6	0
NDBC	46075	-160.817	53.983	2392.7	2004-2010		7	0
NDBC	46076	-147.990	59.502	195.1	2005-2010		6	0
NDBC	46077	-154.175	57.910	202	2005-2010		6	0
NDBC	46078	-152.582	55.556	5380	2004-2010		7	0
NDBC	46080	-150.042	57.947	254.5	2002-2010		9	0
NDBC	46082	-143.372	59.681	300	2002-2010		9	0
NDBC	46083	-137.997	58.300	136	2001-2010		10	0
NDBC	46084	-136.101	56.600	1408	2002-2008 2010		8	0
NDBC	46003	-155.850	51.831	4730	1976-1999		24	0
NDBC	46105	-152.233	59.049	126.5	2008	2008	1	1
NDBC	46106	-152.090	59.760	45.7	2007-2010	2007-2010	4	4
NDBC	46107	-147.992	59.925	105.5	2008-2010	2008-2010	3	3

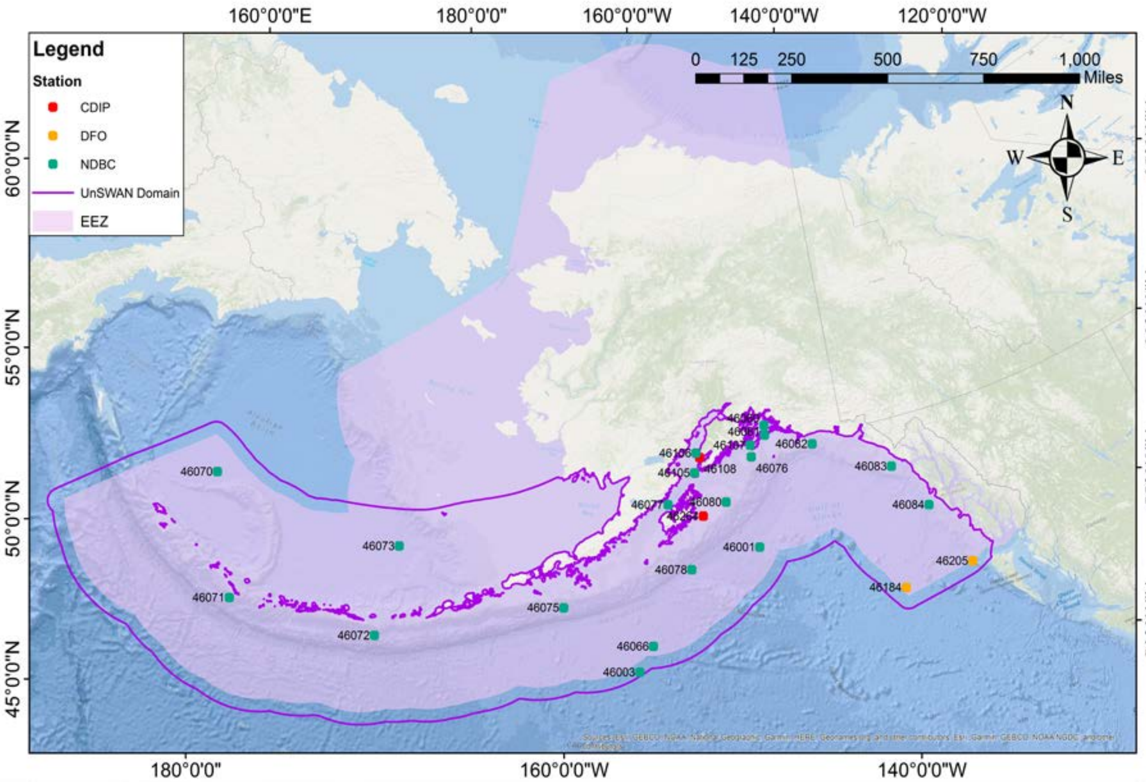

Figure 2-7. Unstructured-grid SWAN model domain and distribution of wave buoys inside the model domain. Only NDBC buoys were selected for model validation in Alaska because they had data records corresponding to the hindcast period.

3.0 Model Hindcast and Validation

The regional wave hindcast for the Alaska Coast was conducted for the period of 1979–2010, and 2017. Model hindcast and validation for both wave bulk parameters and resource parameters are described in this section.

3.1 Simulation of IEC Resource Parameters

The six wave resource parameters recommended by the IEC Technical Specification (2015) were calculated based on model results of directional wave spectra and measured wave spectral data. The six IEC parameters are omnidirectional wave power, significant wave height, energy period, spectral width, direction of maximum directionally resolved wave power, and directionality coefficient, which are defined below.

The omnidirectional wave power, J, is the total wave power in a single point. It is computed as the sum of the contributions to energy flux from each of the components of the wave spectrum,

$$J = \rho g \sum_{i,j} c_{g,i} S_{ij} \Delta f_i \, \Delta\theta_j \tag{1}$$

where
ρ = the density of sea water,
g = the acceleration due to gravity,
$c_{g,i}$ = the group velocity,
Δf_i = the frequency bin width at each discrete frequency index i, and
$\Delta\theta_i$ = the direction bin width at each discrete direction index j.

Directionally integrated parameters are calculated from one-dimensional frequency variance density using the equation

$$S_i = \sum_j S_{ij} \Delta\theta_j. \tag{2}$$

For the purpose of the present study the significant wave height is defined as the zeroth spectral moment:

$$H_s \sim H_{m0} = 4\sqrt{m_0}\,, \tag{3}$$

where the moments of a variance spectrum are defined as

$$m_n = \sum_i f_i^{\,n} S_i \Delta f_i. \tag{4}$$

H_s is typically paired with the energy period, T_e, calculated as

$$T_e = \frac{m_{-1}}{m_0}, \tag{5}$$

to define a wave climate’s sea state. The energy period is the variance-weighted mean period of the directionally unresolved variance density spectrum. It is preferred over the peak period, because it is less sensitive to the spectral shape.

The spectral width, ϵ_0,

$$\epsilon_0 = \sqrt{\frac{m_0 m_{-2}}{(m_{-1})^2} - 1}, \tag{6}$$

is a measure of the spreading of energy along the wave spectrum. The directionally resolved wave power is the sum of the wave power at each direction, θ:

$$J_\theta = \rho g \sum_{i,j} c_{g,i} S_{ij} \Delta f_i \, \Delta\theta_j cos(\theta - \theta_j)\delta \tag{7}$$
$$\begin{cases} \delta = 1, & cos(\theta - \theta_j) \geq 0 \\ \delta = 0, & cos(\theta - \theta_j) < 0 \end{cases}$$

where J_θ is the directionally resolved wave power in direction θ. The maximum time-averaged wave power propagating in a single direction, J_{θ_J}, is the maximum value of J_θ. The corresponding direction, θ_J, is the direction of maximum directionally resolved wave power and describes the characteristic direction of the sea state.

The directionality coefficient, d, is the ratio of maximum directionally resolved wave power to the omnidirectional wave power,

$$d_\theta = \frac{J_{\theta_{jmax}}}{J}, \tag{8}$$

which is a characteristic measure of directional spreading of wave power.

Examples of monthly averaged 2-D distributions of the six IEC parameters were presented in Figure 3-1 and Figure 3-2 for the months of July and December, respectively. In general, there is strong seasonality between summer (July) and winter (December) seasons, especially for omnidirectional wave power, significant wave height, and energy period. In winter, high wave power and wave height occur along the southern coast of the Aleutian Islands, Aleutian Peninsula, and southern Alaska. The energy period in winter generally is greater than in the summer. Wave power drops rapidly north of the Aleutian Islands and Kodiak. Although not as strong as J, H_s, and T_e, weak seasonal variations are observed in ϵ_0 and θ_J, and both are slightly greater in the summer. Spatial distribution of spectral width ϵ_0 is quite uniform over the entire model domain and varies in a small range seasonally, from approximately 0.3 in winter to 0.5 in summer. The mean direction of maximum directionally resolved wave power is typically from northeast and east along the southern coast of the Aleutian Islands and Gulf of Alaska, and from the north and northwest in the southern Bering Sea. The directionality coefficient of the Alaska region is generally above 0.7, with little seasonal variation.

Horizontal 2-D plots of monthly and yearly bulk parameters and six resource parameters are presented in Appendix A and Appendix D, respectively.

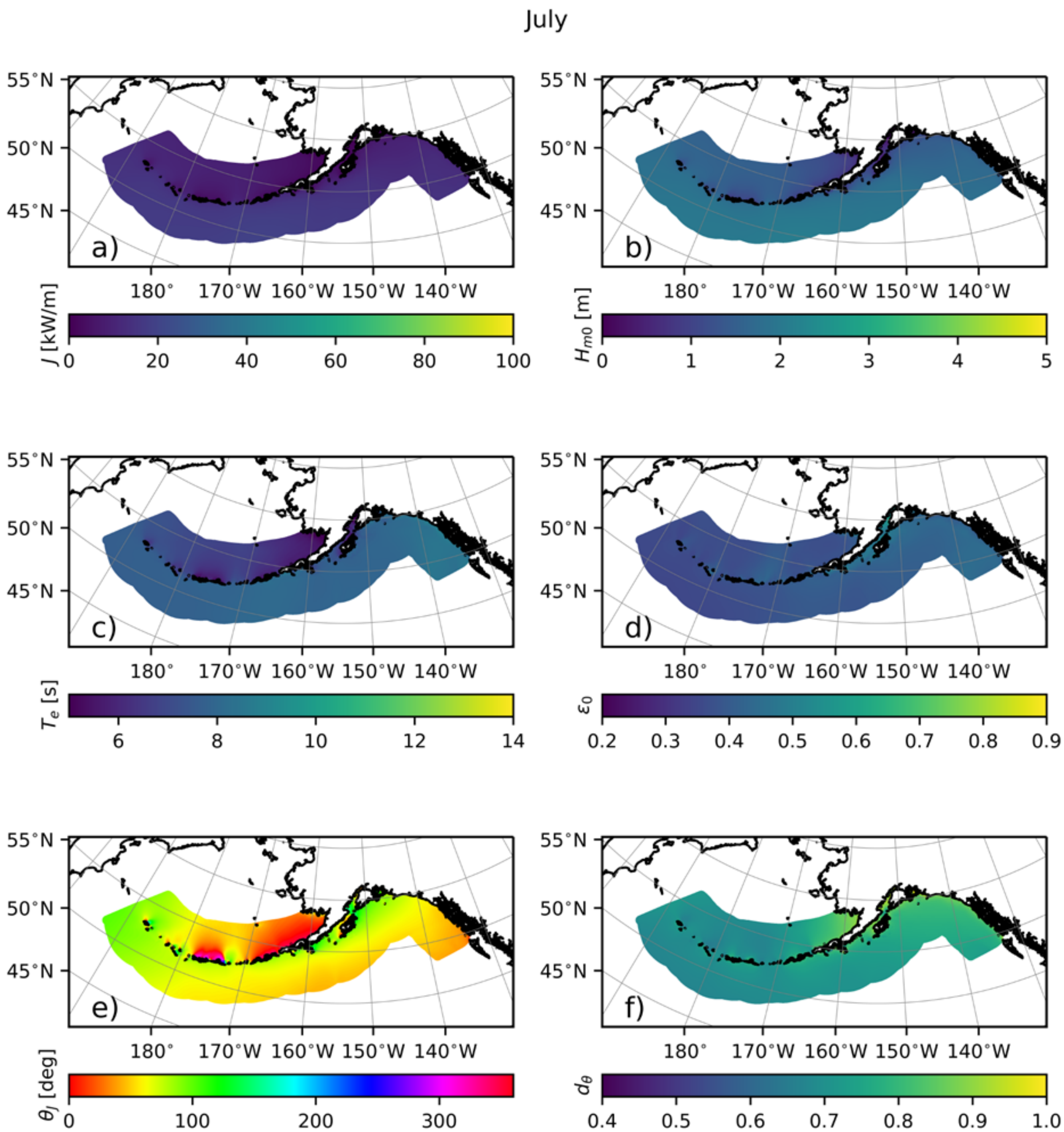

Figure 3-1. Simulated monthly six IEC wave resource parameters in July: (a) omnidirectional wave power, (b) significant wave height, and (c) energy period, (d) spectral width, (e) direction of maximum directionally resolved wave power, and (f) directionality coefficient.

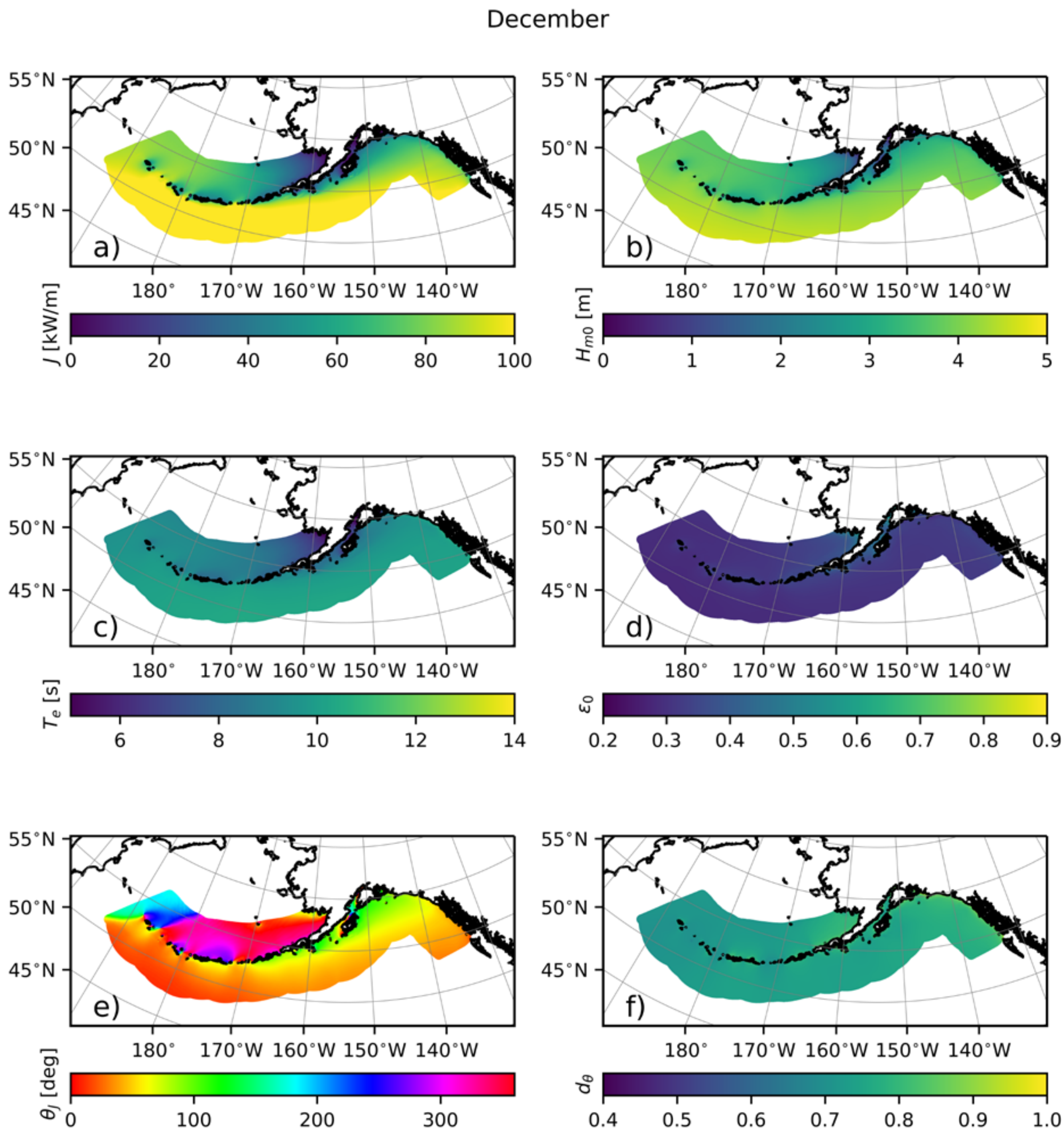

Figure 3-2. Simulated monthly six IEC wave resource parameters in December: (a) omnidirectional wave power, (b) significant wave height, and (c) energy period, (d) spectral width, (e) direction of maximum directionally resolved wave power, and (f) directionality coefficient.

3.2 Model Validation

The following model performance metrics used in previous studies (García-Medina et al., 2014; García-Medina et al., 2013; Wu et al., 2018; Yang et al., 2017; Yang et al., 2018) were adopted in this study for model validation.

The root-mean-square-error (*RMSE*), *aka* root-mean-square-deviation, is defined as

$$RMSE = \sqrt{\frac{\sum_{i=1}^{N}(P_i - M_i)^2}{N}} \tag{9}$$

where N is the number of observations, M_i is the measured value, and P_i is the predicted value. *RMSE* represents the sample standard deviation of the differences between predicted values and measured values.

The percentage error (*PE*) is defined as

$$PE(\%) = \frac{100}{N}\sum_{i=1}^{N}\left(\frac{P_i - M_i}{M_i}\right) \tag{10}$$

and is the average *PE* over the period of comparison.

The scatter index (*SI*) is the *RMSE* normalized by the average of all measured values over the value of comparison, where

$$SI = \frac{RMSE}{\bar{M}}, \tag{11}$$

where the overbar indicates the mean of the measured values.

Model bias, which represents the average difference between the predicted and measured value, is defined as

$$Bias = \frac{1}{N}\sum_{i=1}^{N}(P_i - M_i). \tag{12}$$

Percentage bias, which is defined as

$$Bias(\%) = \frac{\sum_{i=1}^{N}P_i - \sum_{i=1}^{N}M_i}{\sum_{i=1}^{N}M_i} \cdot 100 \tag{13}$$

is also commonly used to normalize bias.

The linear correlation coefficient, R, is defined as

$$R = \frac{\sum_{i=1}^{N}(M_i - \bar{M})(P_i - \bar{P})}{\sqrt{\left(\sum_{i=1}^{N}(M_i - \bar{M})^2\right)\left(\sum_{i=1}^{N}(P_i - \bar{P})^2\right)}} \tag{14}$$

and is a measure of the strength of the linear relationship between the predicted and measured values.

Model validation was first conducted by comparing simulated and measured bulk parameters (1979–2010) because most of the buoys did not start to collect directional-spectral data until after 2010. Even for bulk parameters, observed data for peak wave direction were not available at most of the buoy stations before 2010. Therefore, error statistics were not calculated for peak direction. A total of 191 station-years are compared and the temporal averages of the error statistics for the entire data records at every buoy station are summarized in Table 3.1. Comparisons of time series and scatter plots of simulated and observed significant wave height and mean period are provided in Appendix B. The results of the yearly averages of performance metrics (error statistics) for significant wave height and mean wave period were calculated for all buoys and are summarized in Appendix C. The significant wave height is very well simulated with high linear correlations. Errors in the periods are larger than the wave heights but are still considered to be small. Larger errors in the periods are not uncommon in these models, because they are at the development state (i.e., source terms) and most model validations are done with respect to wave heights.

Table 3.1 Summary of temporal averages of Performance Metrics for Simulated Wave Bulk Parameters.

Buoy #	Parameter	RMSE	PE (%)	SI	Bias	Bias (%)	R
46001	H_s (m)	0.48	8.03	0.17	0.08	3.00	0.94
	T_m (s)	1.29	15.82	0.17	1.03	15.58	0.87
46060	H_s (m)	0.26	12.07	0.37	0.02	2.26	0.83
	T_m (s)	2.10	28.79	0.34	1.20	24.86	0.48
46061	H_s (m)	0.43	16.84	0.25	0.15	9.87	0.92
	T_m (s)	1.37	16.41	0.19	0.95	15.55	0.74
46066	H_s (m)	0.47	7.58	0.16	0.07	2.80	0.95
	T_m (s)	1.28	16.64	0.17	1.07	16.40	0.89
46070	H_s (m)	0.45	0.76	0.17	-0.11	-4.04	0.96
	T_m (s)	1.16	15.80	0.17	0.95	15.78	0.90
46071	H_s (m)	0.54	8.93	0.19	0.06	2.81	0.95
	T_m (s)	1.17	13.32	0.16	0.86	13.02	0.87
46072	H_s (m)	0.59	6.27	0.19	0.03	1.32	0.92
	T_m (s)	1.25	13.18	0.16	0.89	12.87	0.83
46073	H_s (m)	0.43	11.44	0.17	0.11	4.90	0.96
	T_m (s)	0.75	5.61	0.11	0.37	5.90	0.90
46075	H_s (m)	0.49	7.82	0.18	0.04	1.65	0.94
	T_m (s)	1.03	10.99	0.14	0.70	10.76	0.86
46076	H_s (m)	0.41	11.31	0.20	0.06	2.99	0.95
	T_m (s)	1.34	17.75	0.19	1.00	16.81	0.78
46077	H_s (m)	0.56	-20.53	0.63	-0.35	-28.20	0.77
	T_m (s)	1.28	10.09	0.26	0.35	7.67	0.39
46078	H_s (m)	0.47	5.93	0.17	0.04	1.57	0.94
	T_m (s)	1.07	11.98	0.15	0.77	11.81	0.85

Buoy #	Parameter	RMSE	PE (%)	SI	Bias	Bias (%)	R
46080	H_s (m)	0.46	3.75	0.20	-0.07	-2.52	0.94
	T_m (s)	0.91	9.16	0.13	0.57	9.04	0.83
46082	H_s (m)	0.54	0.96	0.24	-0.14	-5.51	0.94
	T_m (s)	1.37	17.80	0.18	1.10	17.08	0.83
46083	H_s (m)	0.46	4.88	0.20	-0.06	-2.45	0.95
	T_m (s)	1.38	17.97	0.18	1.11	17.27	0.84
46084	H_s (m)	0.43	6.01	0.17	0.01	0.63	0.96
	T_m (s)	1.38	17.91	0.18	1.14	17.35	0.87
46003	H_s (m)	0.65	13.07	0.20	0.21	7.08	0.91
	T_m (s)	1.31	16.29	0.17	1.08	15.74	0.86
46105	H_s (m)	0.71	0.42	0.50	-0.22	-13.54	0.81
	T_m (s)	1.24	4.11	0.23	0.10	1.92	0.51
46106	H_s (m)	0.54	-20.24	0.75	-0.32	-29.90	0.69
	T_m (s)	1.23	-6.91	0.32	-0.41	-9.68	0.19
46107	H_s (m)	0.36	33.72	0.30	0.22	22.15	0.88
	T_m (s)	1.42	12.49	0.21	0.69	11.40	0.67

For model validation against directional-spectral data, comparisons of time series and scatter plots of the six IEC parameters were conducted between model results and observed data performed for year 2017. A total of 29 year-station time series and scatter plots that compare model results and observed data are presented in Appendix E. Error statistics for the six IEC resource parameters were calculated and are provided in Appendix F.

Figure 3-3 shows model-data comparisons for 2017 at Buoy 46076 in the Gulf of Alaska. Overall, the model results match the observed data well. The time series show strong seasonal variability with energetic winters and calmer summers. However, it is not uncommon during the spring and autumn for some storms to generate waves more than 5 m high. These events that appear in the data are well captured in the model, showing good overall seasonal performance.

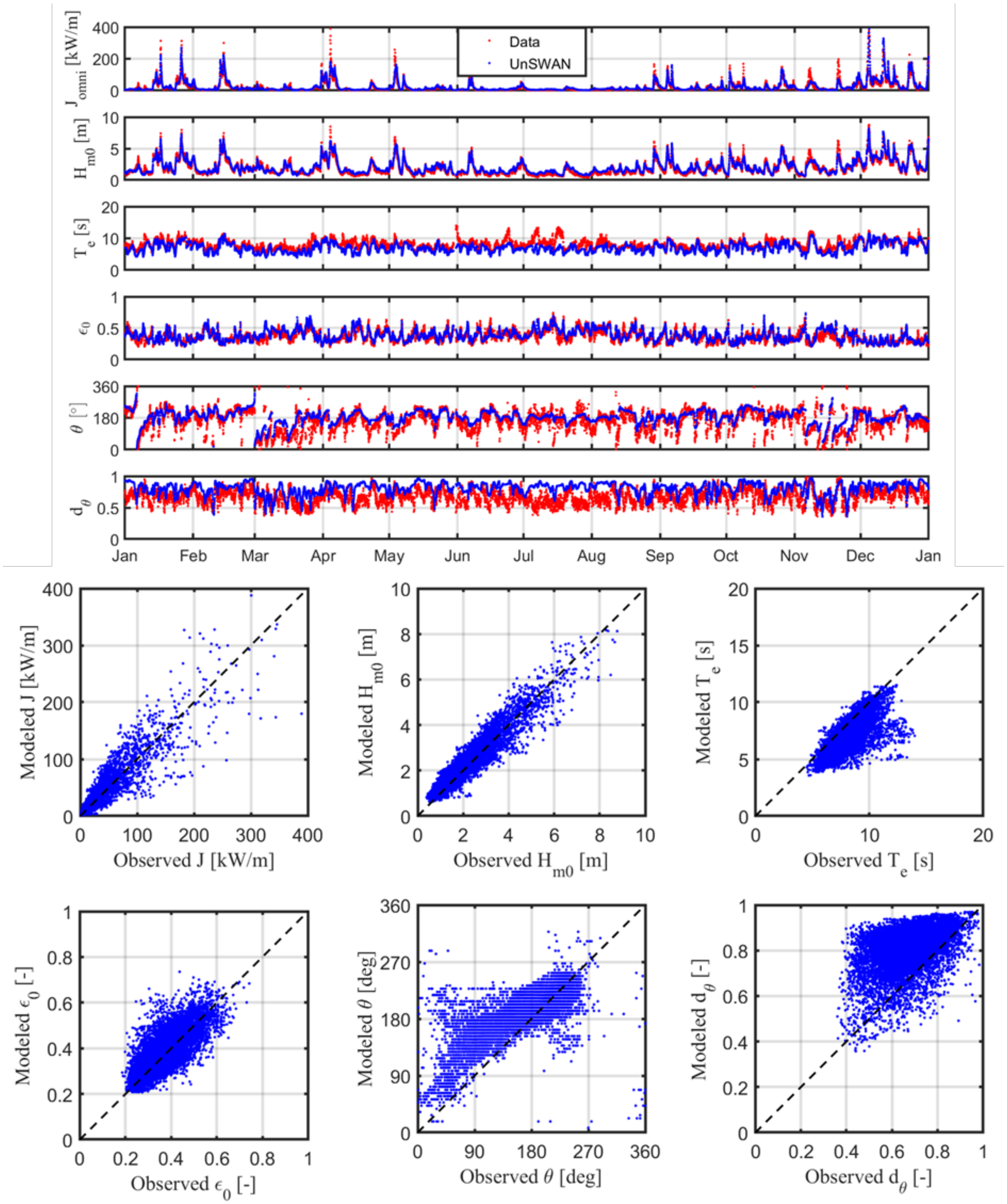

Figure 3-3. Time series (top) and scatter plots (bottom) of the six modeled and observed IEC wave resource parameters for 2017 at Buoy 46076 in the Gulf of Alaska.

As an example, the performance at Buoy 46078, 100 nautical miles (185 km) south of Kodiak Island is shown in Table 3.2. The error statistics are generally good with slight overprediction in the wave power and wave height and underprediction in the energy period, which represents the general trend observed at all buoys. Overall, error statistics between model results and observed data show good model performance in simulating the six IEC parameters.

Table 3.2. Performance metrics of the six simulated IEC resource parameters for 2017 at Buoy 46078.

Parameter	RMSE	PE (%)	SI	Bias	Bias (%)	R
J (kW/m)	26	51	0.72	8.31	22.8	0.92
H_s (m)	0.51	18	0.21	0.28	11.3	0.95
T_e (s)	1.19	-10	0.14	-0.84	-10.1	0.85
ϵ_0 (-)	0.05	3	0.16	0.01	1.9	0.79
θ (degrees)	38.36	27	0.20	21.4	11.0	0.90
d_θ (-)	0.10	5	0.14	0.03	3.6	0.70

4.0 Conclusion

Wave hindcasts are critical to providing accurate wave resource characterization and assessment. This study applies a nested-grid modeling approach to simulate wave climates in the Alaska EEZ for a period of 32 years. High-resolution hindcast in the nearshore region was accomplished using an unstructured-grid SWAN model, driven by nested-grid WWIII models from global to regional scales. The IEC wave resource parameters were simulated and subsequently validated by wave buoy data within the model domain. Overall, the six simulated IEC wave resource parameters match well with the measured data. SWAN was able to reproduce the seasonal variation of the sea states. The hindcast results from this study can be used to inform the deployment of WECs and other nearshore instrumentation/devices in nearshore regions, assist in prioritizing hotspots for near-term market opportunities, and update wave resource assessment data for the U.S. Department of Energy Marine and Hydrokinetic Energy Atlas.[1] Furthermore, these results can also be used to assess decadal cycles in the wave fields because of the long record of the hindcast (1979–2010).

[1] https://maps.nrel.gov/mhk-atlas

5.0 References

Ardhuin, F., Rogers, E., Babanin, A. V., Filipot, J.-F., Magne, R., Roland, A., . . . Collard, F. (2010). Semiempirical Dissipation Source Functions for Ocean Waves. Part I: Definition, Calibration, and Validation. *Journal of Physical Oceanography, 40*(9), 1917-1941. doi:10.1175/2010jpo4324.1

Cobell, Z., Zhao, H. H., Roberts, H. J., Clark, F. R., & Zou, S. (2013). Surge and Wave Modeling for the Louisiana 2012 Coastal Master Plan. *Journal of Coastal Research*, 88-108. doi:10.2112/SI_67_7

EPRI. (2011). *Mapping and Assessment of the United States Ocean Wave Energy Resource*. Retrieved from Palo Alto, California:

Gallagher, S., Tiron, R., & Dias, F. (2014). A long-term nearshore wave hindcast for Ireland: Atlantic and Irish Sea coasts (1979-2012). *Ocean Dynamics*, *64*(8), 1163-1180. doi:10.1007/s10236-014-0728-3

García-Medina, G., Özkan-Haller, H. T., & Ruggiero, P. (2014). Wave resource assessment in Oregon and southwest Washington, USA. *Renewable Energy, 64*, 203-214. doi:10.1016/j.renene.2013.11.014

García-Medina, G., Özkan-Haller, H. T., Ruggiero, P., & Oskamp, J. (2013). An Inner-Shelf Wave Forecasting System for the U.S. Pacific Northwest. *Weather and Forecasting*, *28*(3), 681-703. doi:10.1175/waf-d-12-00055.1

IEC. (2015). *Marine energy – wave, tidal and other water current converters – Part 101: Wave energy resource assessment and characterization* (IEC TS 62600-101). Retrieved from Geneva, Switzerland:

Lim, E., Eakins, B. W., & Wigley, R. (2011). Coastal relief model of southern Alaska: procedures, data sources, and analysis. *NOAA Technical Memorandum NESDIS NGDC-43*.

Mao, M., van der Westhuysen, A. J., Xia, M., Schwab, D. J., & Chawla, A. (2016). Modeling wind waves from deep to shallow waters in Lake Michigan using unstructured SWAN. *Journal of Geophysical Research-Oceans, 121*(6), 3836-3865. doi:10.1002/2015JC011340

Mediavilla, D. G., & Sepulveda, H. H. (2016). Nearshore assessment of wave energy resources in central Chile (2009-2010). *Renewable Energy*, *90*, 136-144. doi:10.1016/j.renene.2015.12.066

National Research Council. (2013). *An Evaluation of the U.S. Department of Energy's Marine and Hydrokinetic Resource Assessments*. Retrieved from Washington, DC:

Roland, A., & Ardhuin, F. (2014). On the developments of spectral wave models: numerics and parameterizations for the coastal ocean. *Ocean Dynamics, 64*(6), 833-846. doi:10.1007/s10236-014-0711-z

Saha, S., Moorthi, S., Pan, H. L., Wu, X. R., Wang, J. D., Nadiga, S., . . . Goldberg, M. (2010). The Ncep Climate Forecast System Reanalysis. *Bulletin of the American Meteorological Society, 91*(8), 1015-1057. doi:10.1175/2010bams3001.1

Saha, S., Moorthi, S., Wu, X. R., Wang, J., Nadiga, S., Tripp, P., . . . Becker, E. (2014). The NCEP Climate Forecast System Version 2. *Journal of Climate, 27*(6), 2185-2208. doi:10.1175/Jcli-D-12-00823.1

SWAN. (2015). *SWAN: User Manual, Cycle III version 41.01A*. Retrieved from Delft, The Netherlands: http://www.swan.tudelft.nl

Tolman, H. L. (2002). Alleviating the Garden Sprinkler Effect in wind wave models. *Ocean Modelling, 4*(3-4), 269-289. doi:10.1016/S1463-5003(02)00004-5

Tolman, H. L., & WAVEWATCH III Development Group. (2014). *User manual and system documentation of WAVEWATCH III® version 4.18* (MMAB Contribution No. 316). Retrieved from College Park, MD 20740:

Wu, W.-C., Yang, Z., & Wang, T. (2018). Wave Resource Characterization Using an Unstructured Grid Modeling Approach. *Energies, 11*(3), 15. doi:10.3390/en11030605

Yang, Z., Neary, V. S., Wang, T., Gunawan, B., Dallman, A. R., & Wu, W. (2017). A wave model test bed study for wave energy resource characterization. *Renewable Energy*. doi:10.1016/j.renene.2016.12.057

Yang, Z., Wu, W. C., Wang, T., & Castrucci, L. (2018). *High-Resolution Regional Wave Hindcast for the U.S. West Coast* (PNNL-28107). Retrieved from Richland, WA:

Yuk, J. H., Kim, K. O., Jung, K. T., & Choi, B. H. (2016). Swell Prediction for the Korean Coast. *Journal of Coastal Research, 32*(1), 131-141. doi:10.2112/Jcoastres-D-14-00208.1

Zijlema, M. (2010). Computation of wind-wave spectra in coastal waters with SWAN on unstructured grids. *Coastal Engineering, 57*(3), 267-277. doi:10.1016/j.coastaleng.2009.10.011

Zimmermann, M., & Prescott, M. (2014). Smooth Sheet Bathymetry of Cook Inlet, Alaska. *NOAA Technical Memorandum NMFS-AFSC-275*.

Zimmermann, M., & Prescott, M. (2015). Smooth sheet bathymetry of the central Gulf of Alaska. *NOAA Technical Memorandum NMFS-AFSC-287*.

Zimmermann, M., Prescott, M., & Rooper, C. N. (2013). Smooth sheet bathymetry of the Aleutian Islands. *NOAA Technical Memorandum NMFS-AFSC-250*.

Appendix A – Monthly and Yearly Distributions of Simulated Wave Bulk Parameters from 1979–2010 on the Alaska Coast

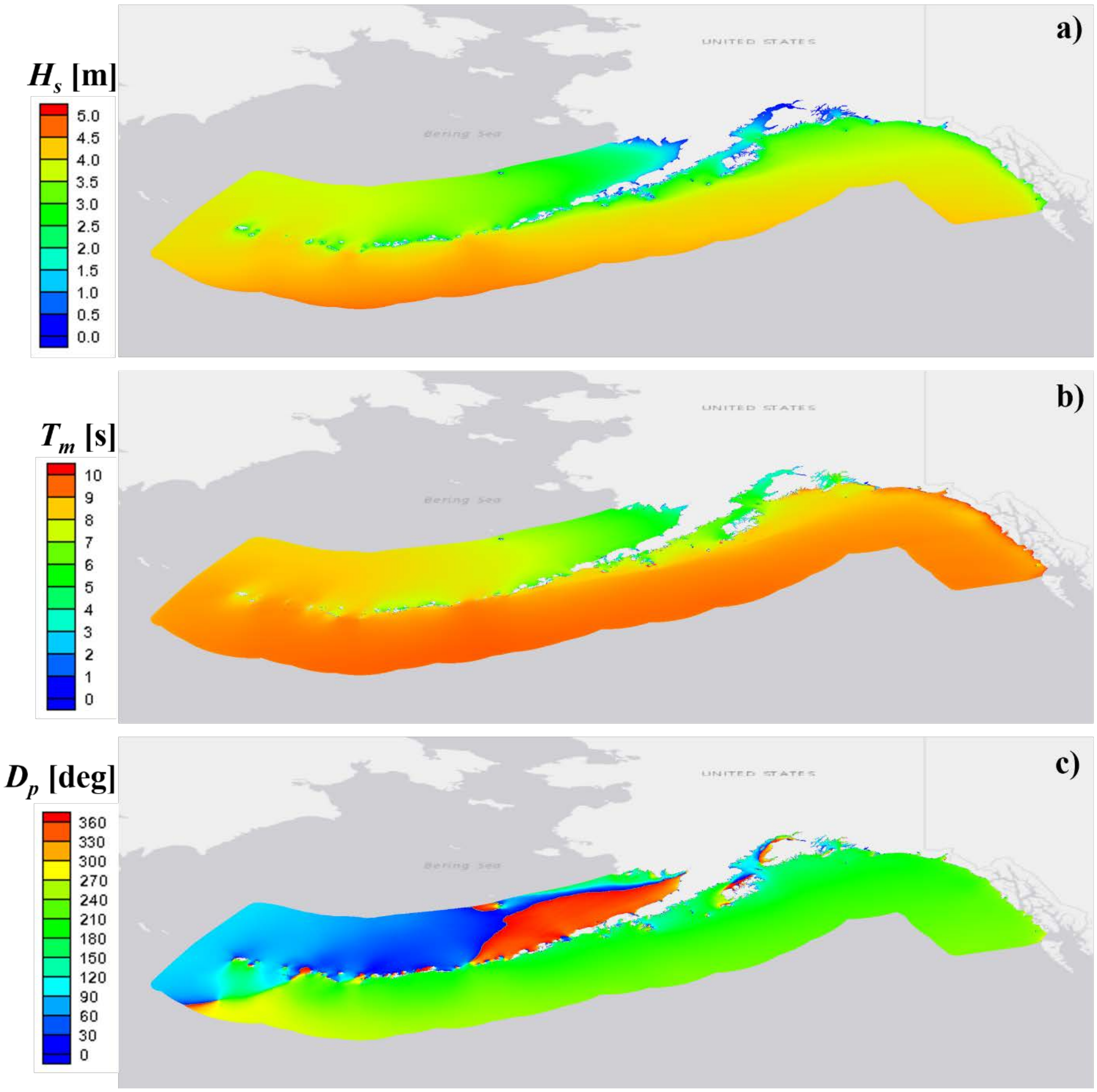

Figure A.1. Monthly distributions of three wave bulk parameters in January: (a) significant wave height, (b) mean wave period, and (c) peak wave direction on the Alaska Coast.

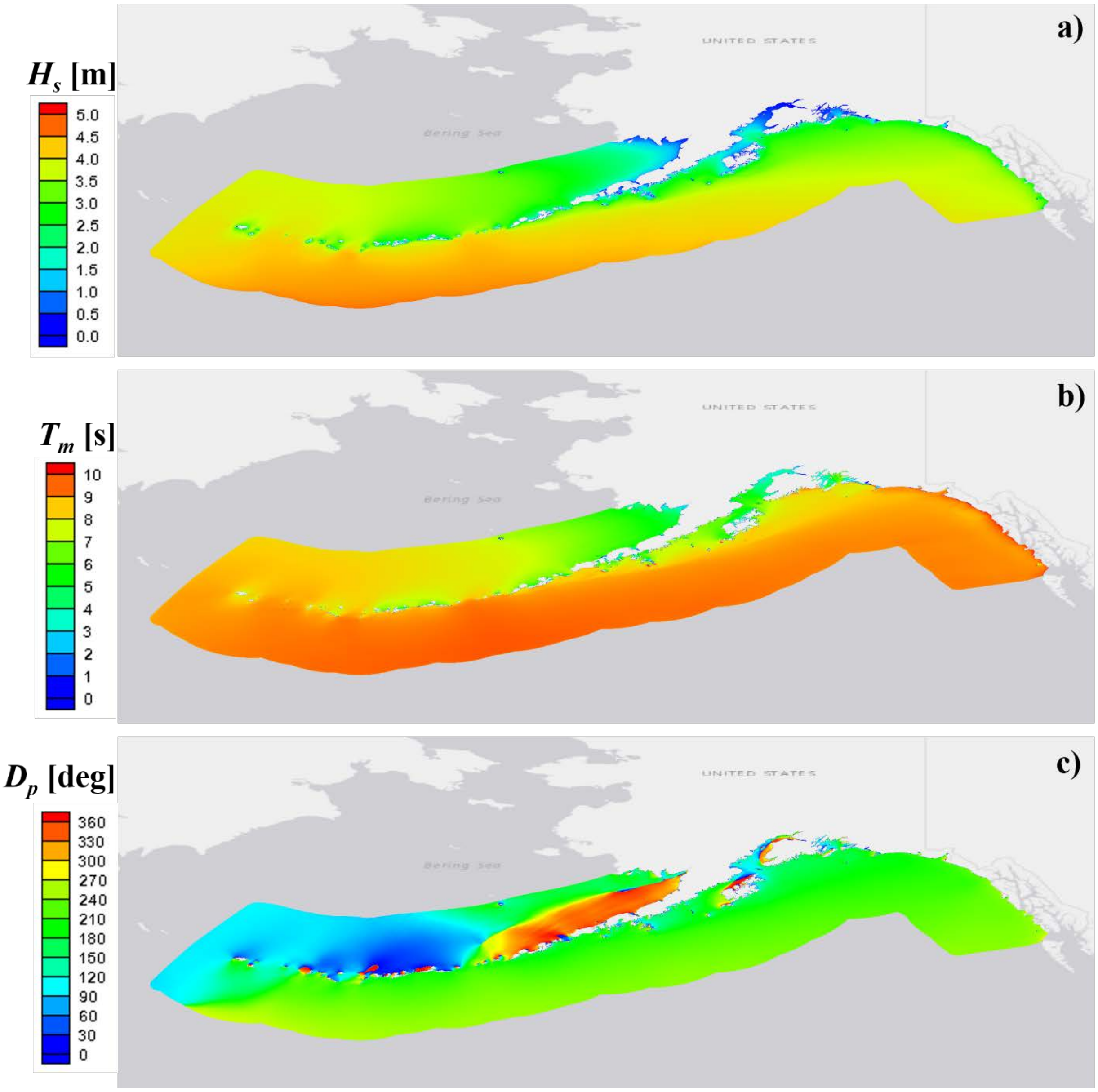

Figure A.2. Monthly distributions of three wave bulk parameters in February: (a) significant wave height, (b) mean wave period, and (c) peak wave direction on the Alaska Coast.

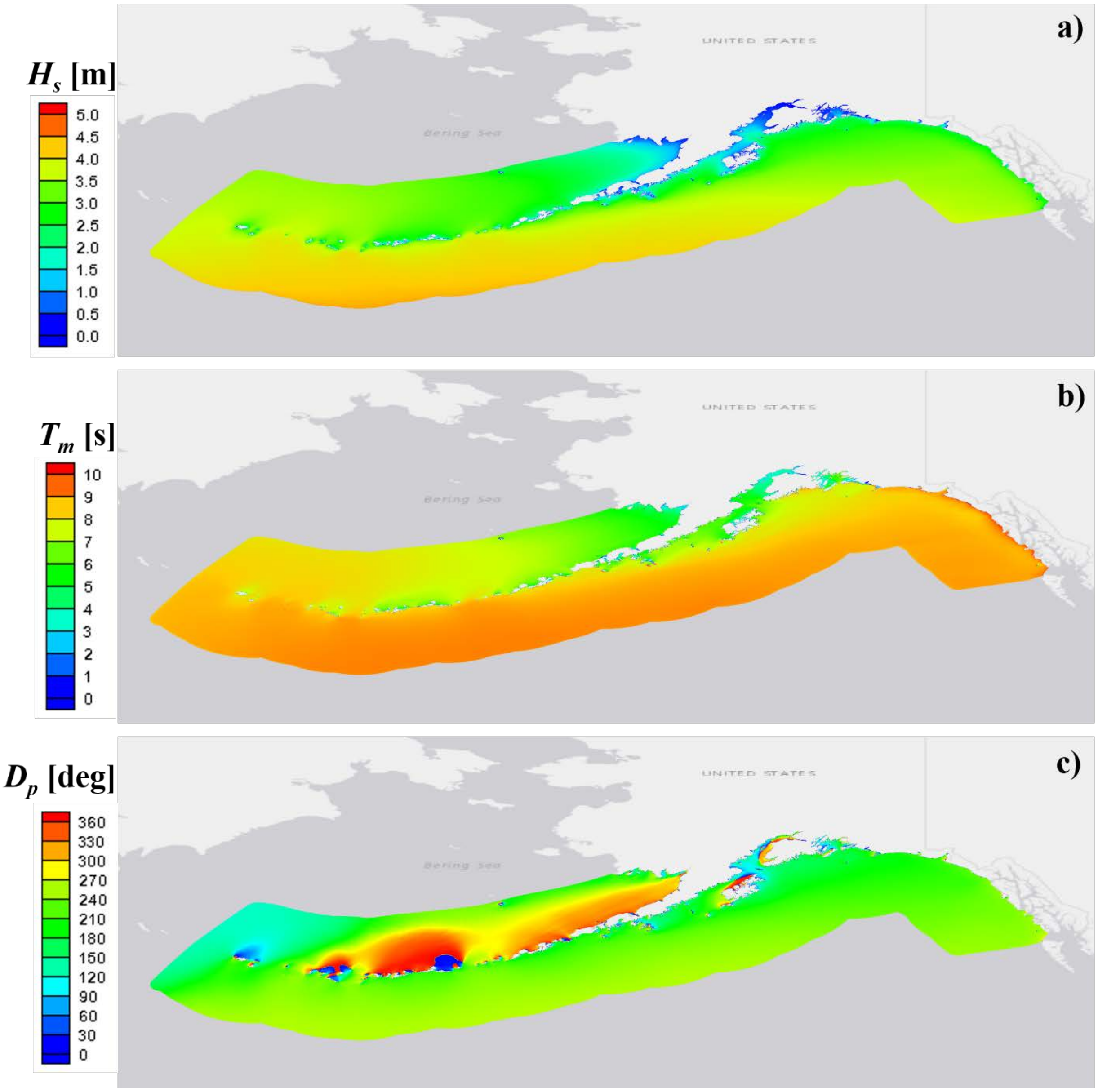

Figure A.3. Monthly distributions of three wave bulk parameters in March: (a) significant wave height, (b) mean wave period, and (c) peak wave direction on the Alaska Coast.

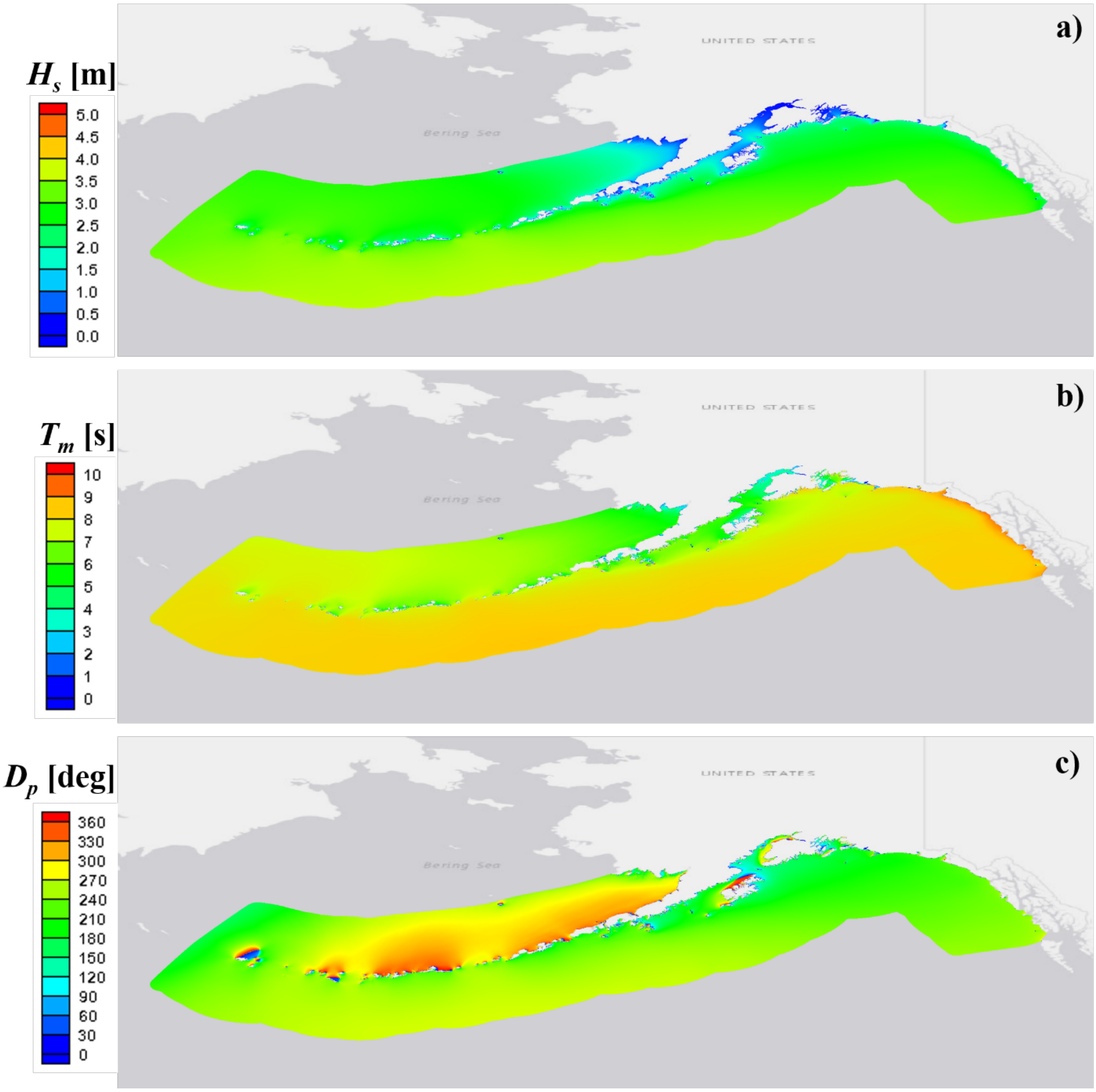

Figure A.4. Monthly distributions of three wave bulk parameters in April: (a) significant wave height, (b) mean wave period, and (c) peak wave direction on the Alaska Coast.

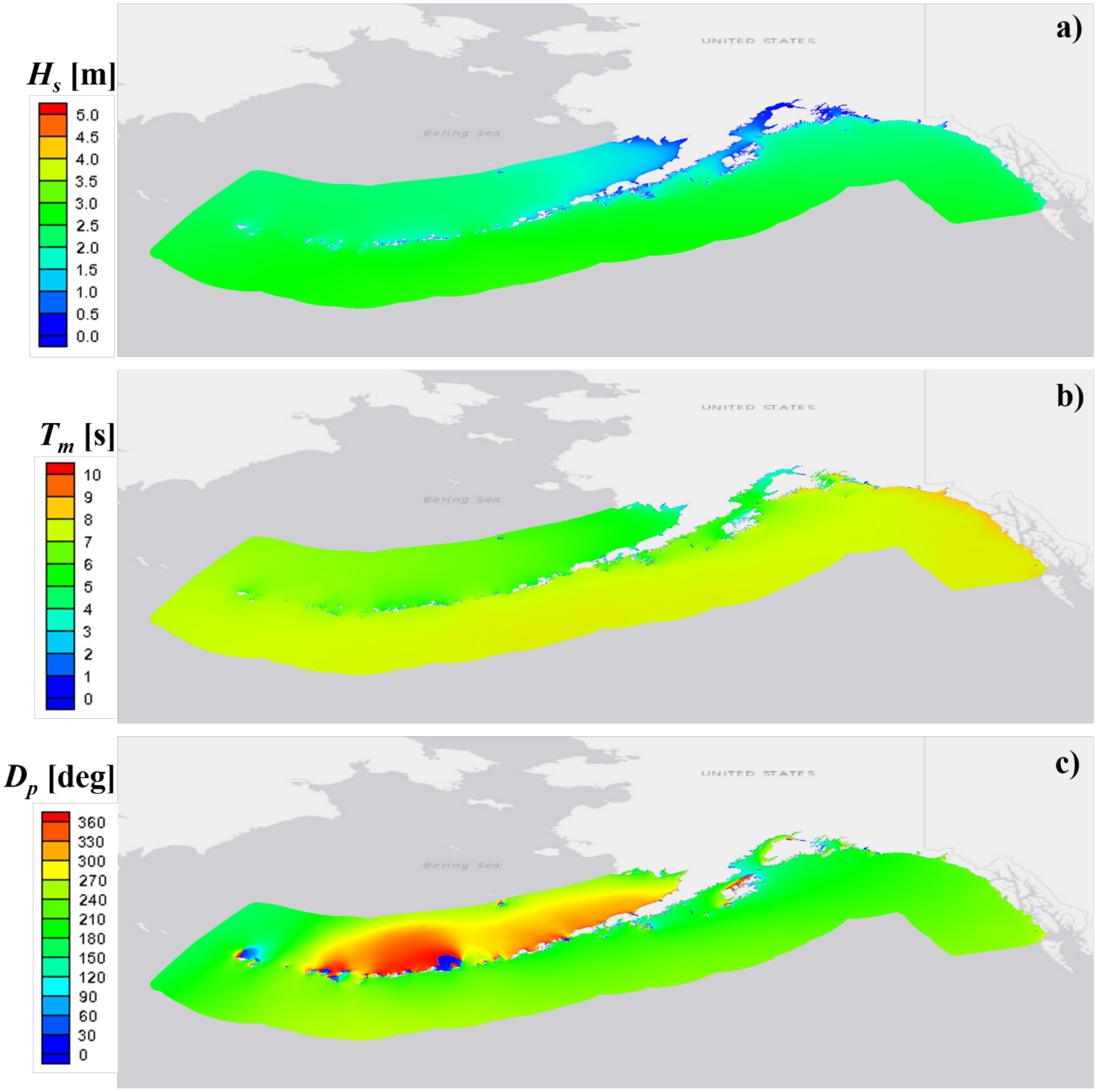

Figure A.5. Monthly distributions of three wave bulk parameters in May: (a) significant wave height, (b) mean wave period, and (c) peak wave direction on the Alaska Coast.

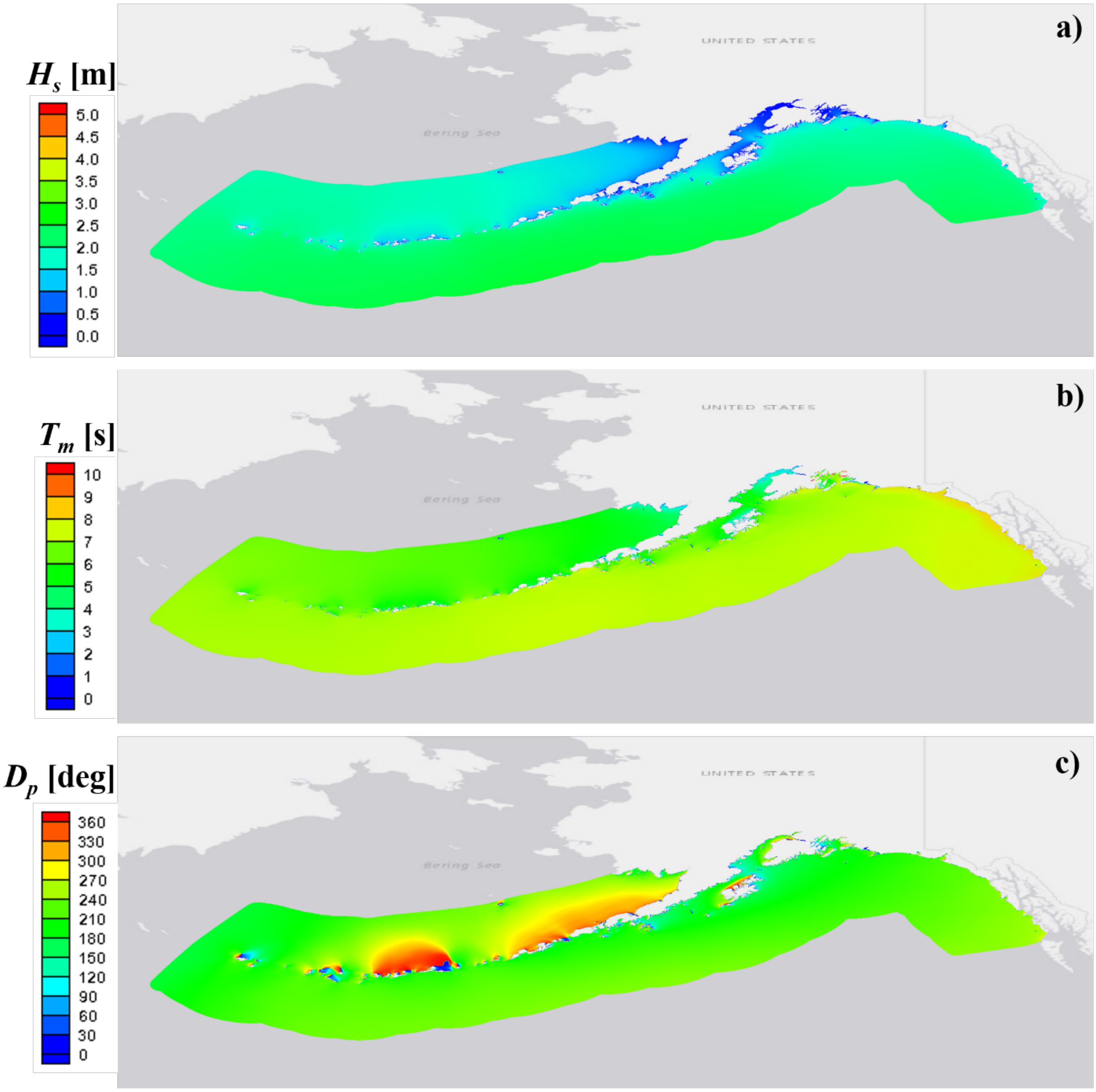

Figure A.6. Monthly distributions of three wave bulk parameters in June: (a) significant wave height, (b) mean wave period, and (c) peak wave direction on the Alaska Coast.

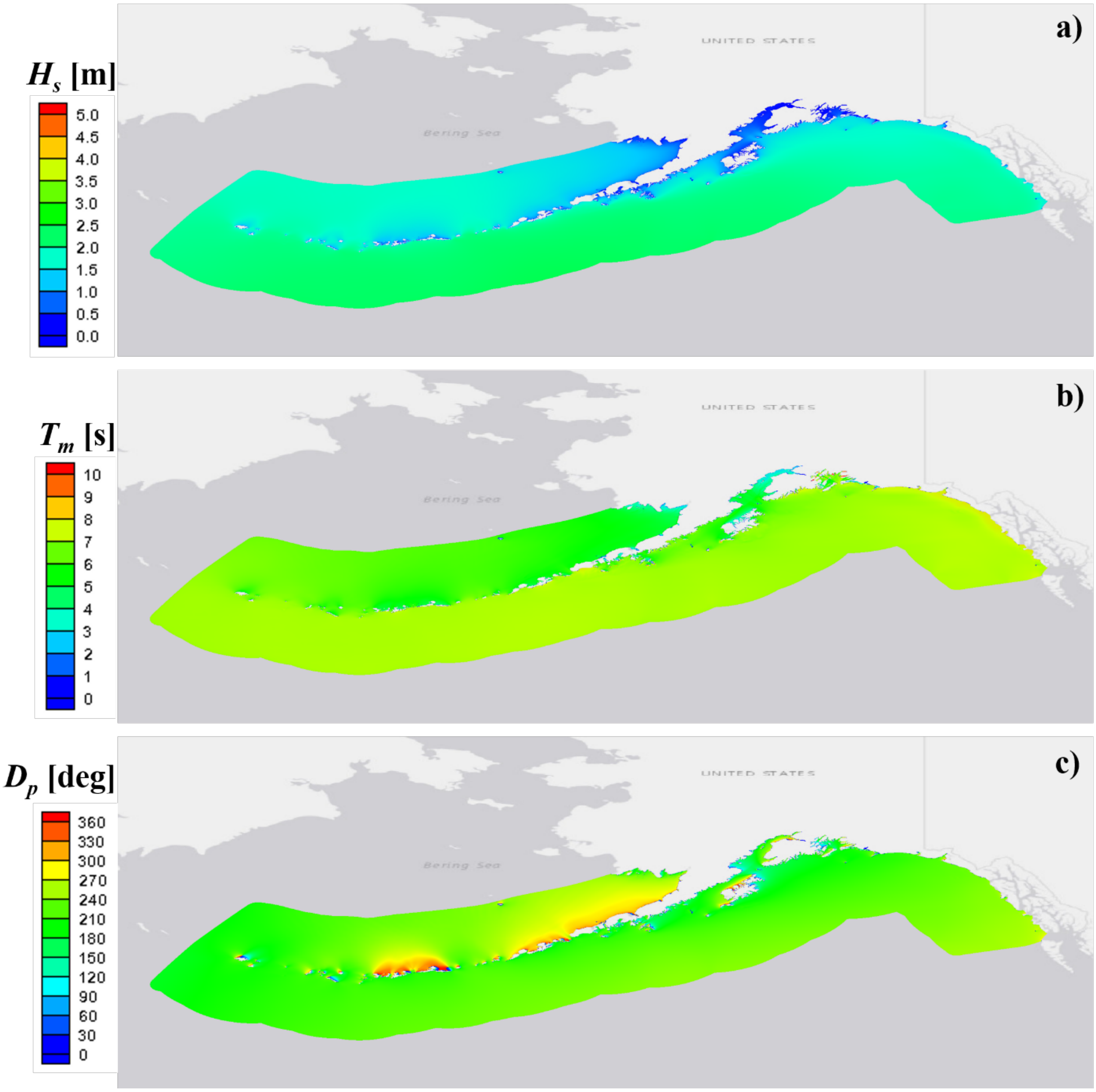

Figure A.7. Monthly distributions of three wave bulk parameters in July: (a) significant wave height, (b) mean wave period, and (c) peak wave direction on the Alaska Coast.

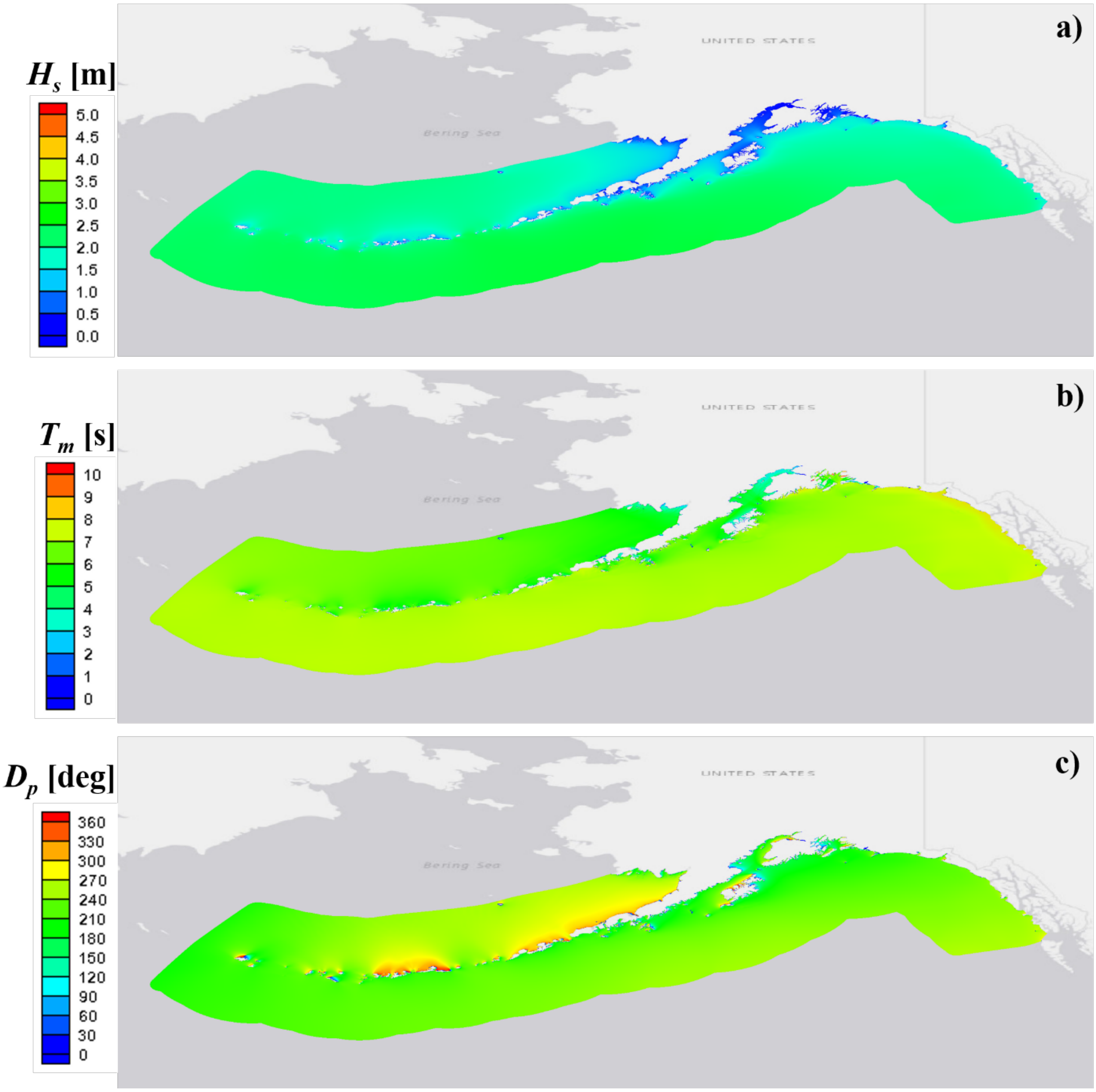

Figure A.8. Monthly distributions of three wave bulk parameters in August: (a) significant wave height, (b) mean wave period, and (c) peak wave direction on the Alaska Coast.

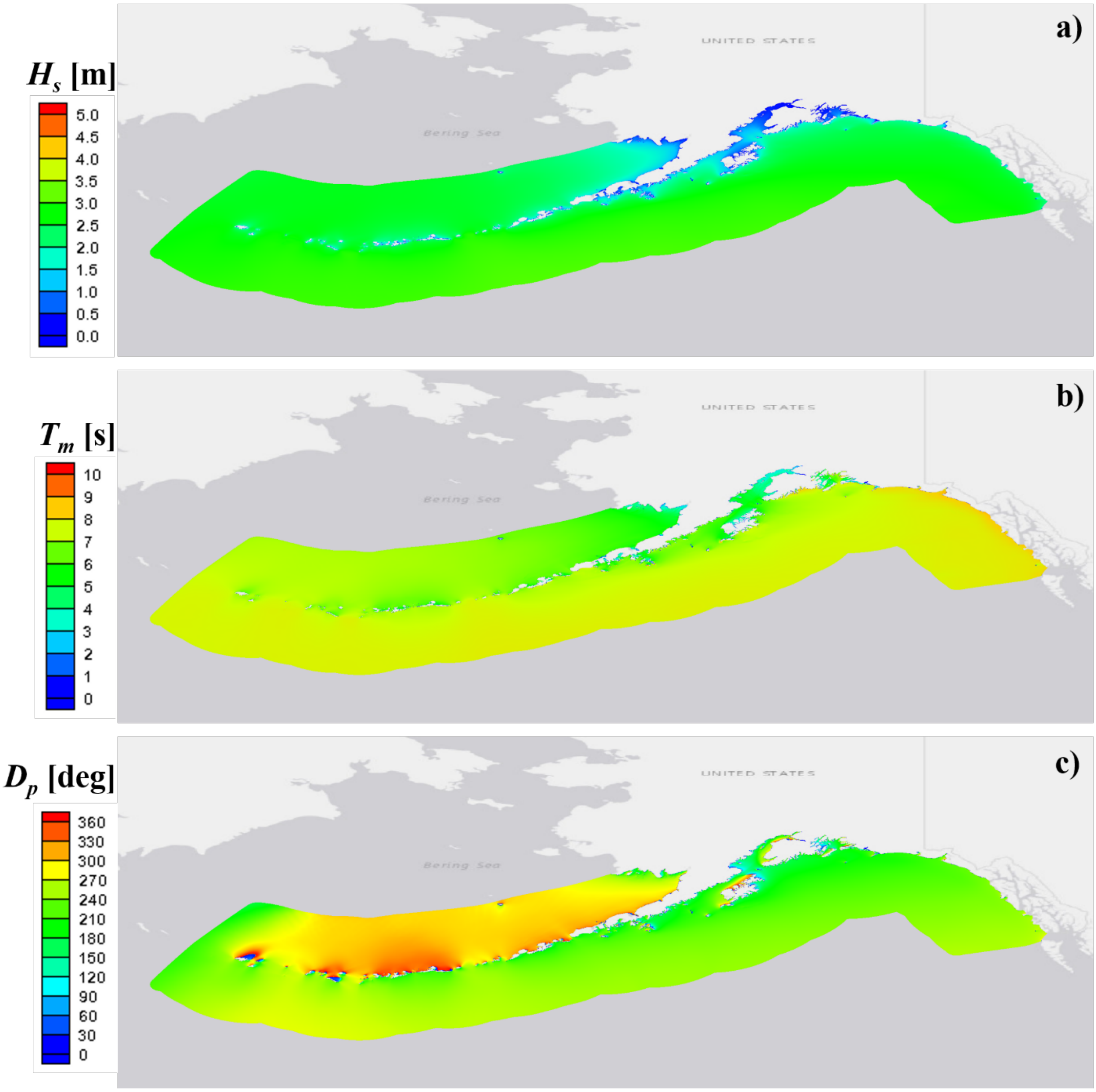

Figure A.9. Monthly distributions of three wave bulk parameters in September: (a) significant wave height, (b) mean wave period, and (c) peak wave direction on the Alaska Coast.

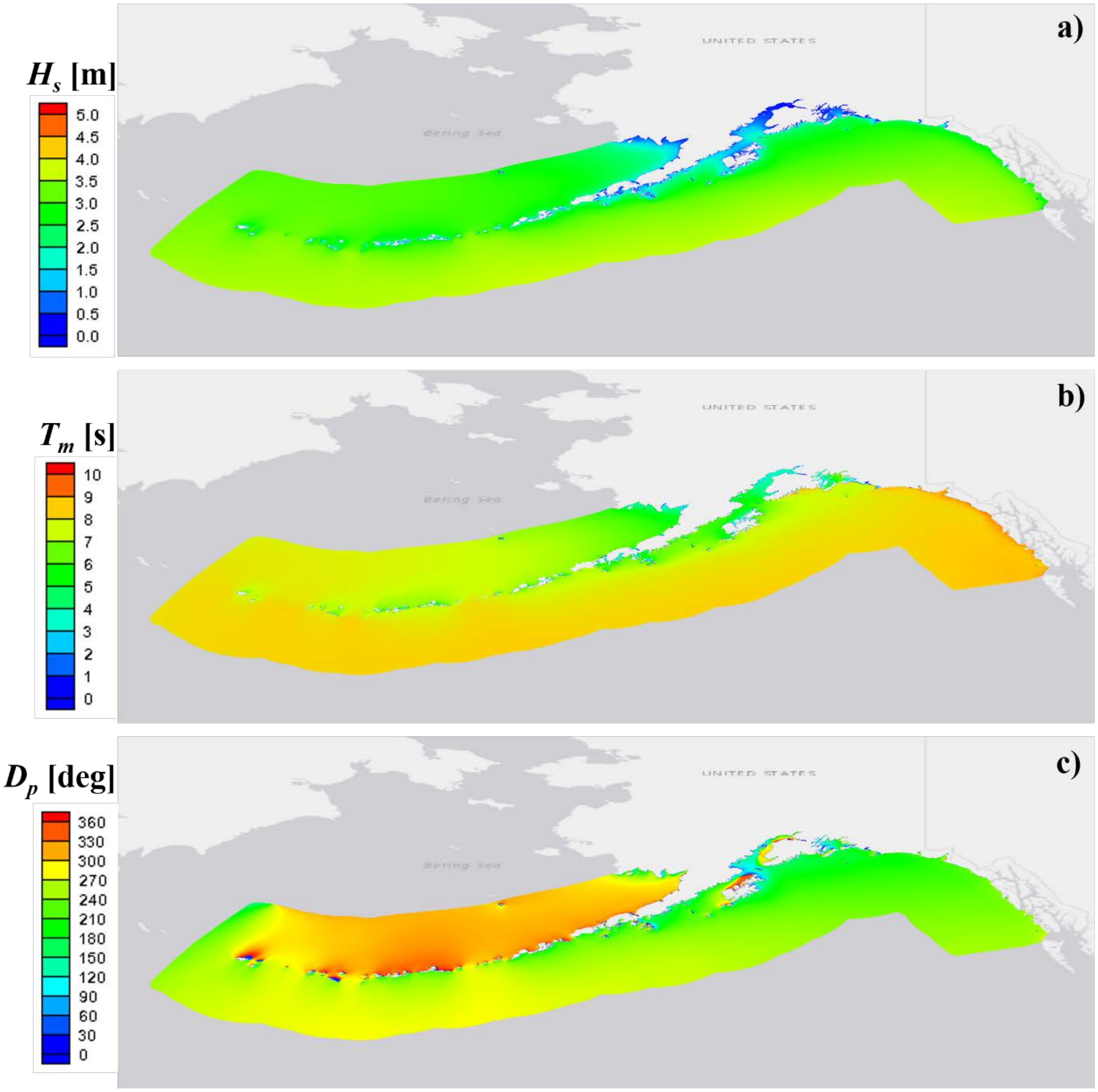

Figure A.10. Monthly distributions of three wave bulk parameters in October: (a) significant wave height, (b) mean wave period, and (c) peak wave direction on the Alaska Coast.

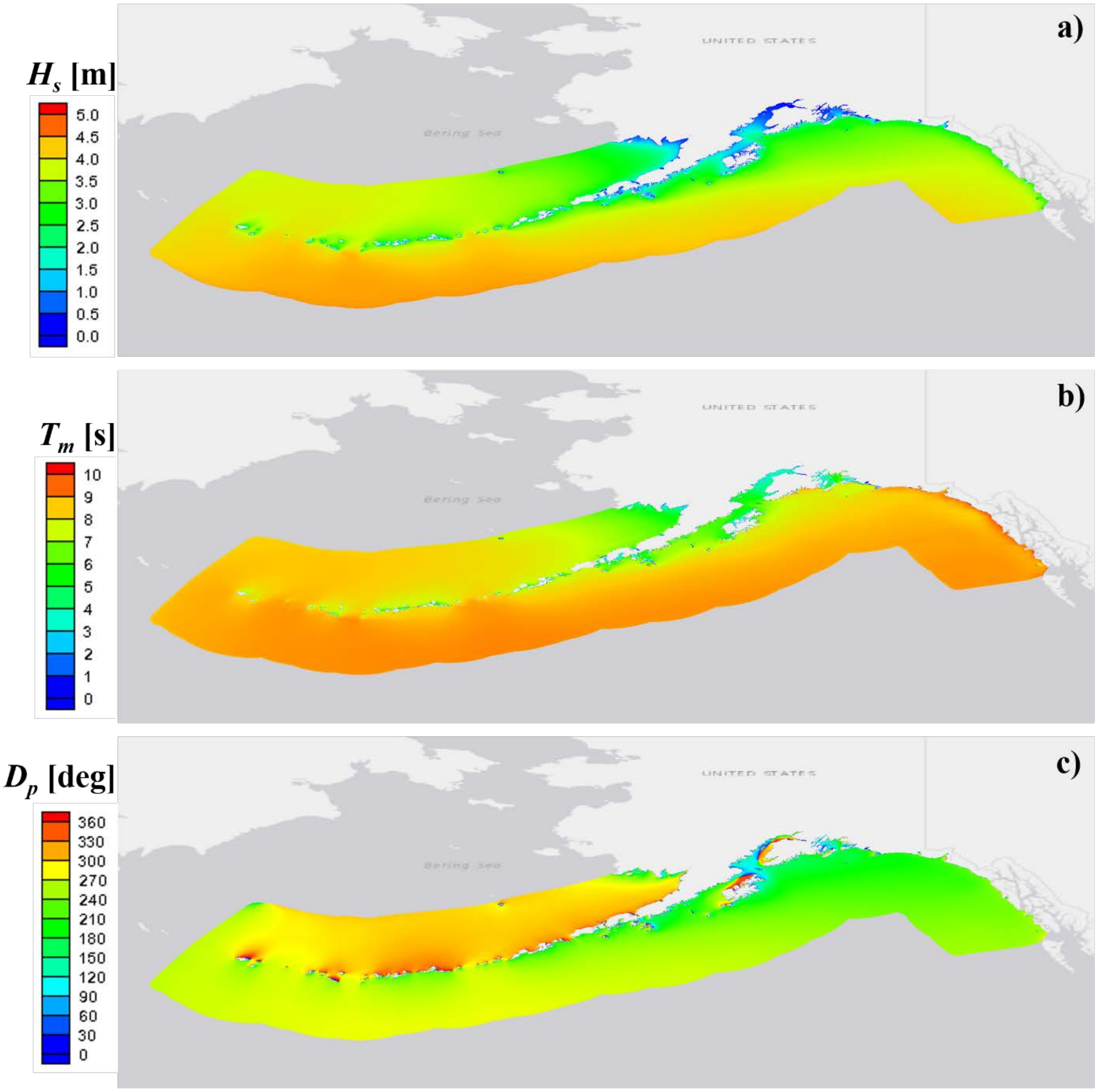

Figure A.11. Monthly distributions of three wave bulk parameters in November: (a) significant wave height, (b) mean wave period, and (c) peak wave direction on the Alaska Coast.

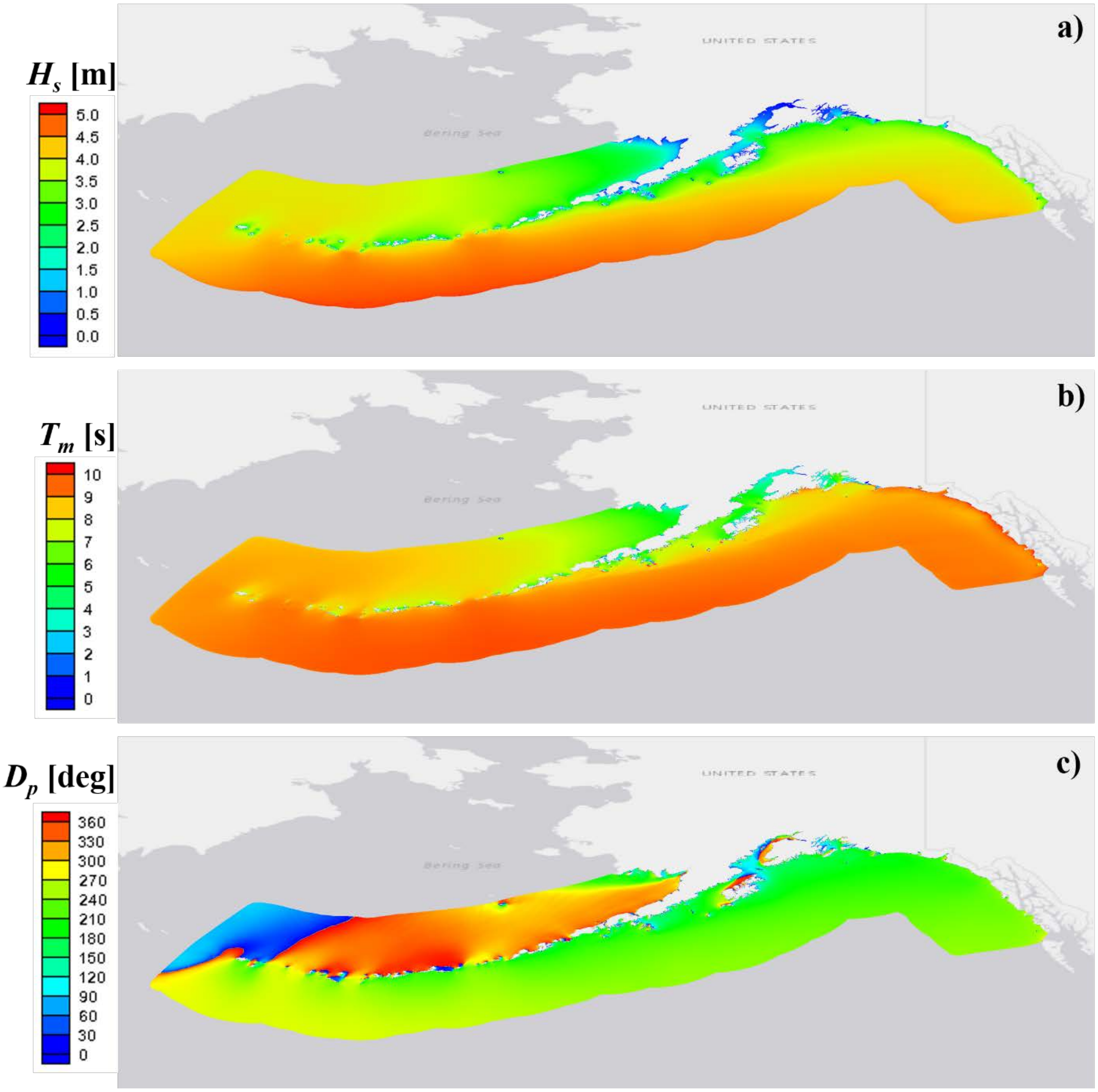

Figure A.12. Monthly distributions of three wave bulk parameters in December: (a) significant wave height, (b) mean wave period, and (c) peak wave direction on the Alaska Coast.

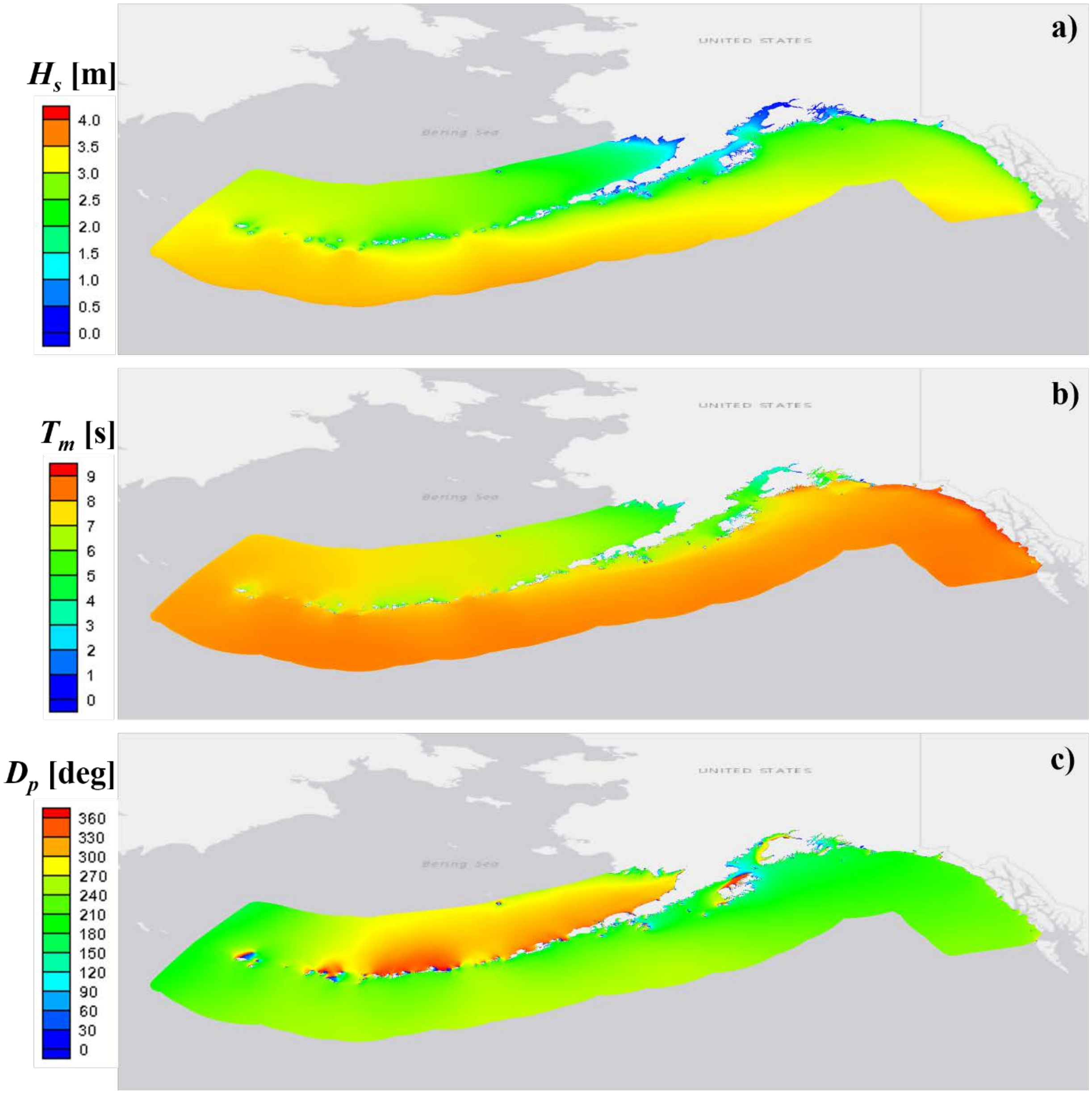

Figure A.13. Yearly distributions of three wave bulk parameters in 2010: (a) significant wave height, (b) mean wave period, and (c) peak wave direction on the Alaska Coast.

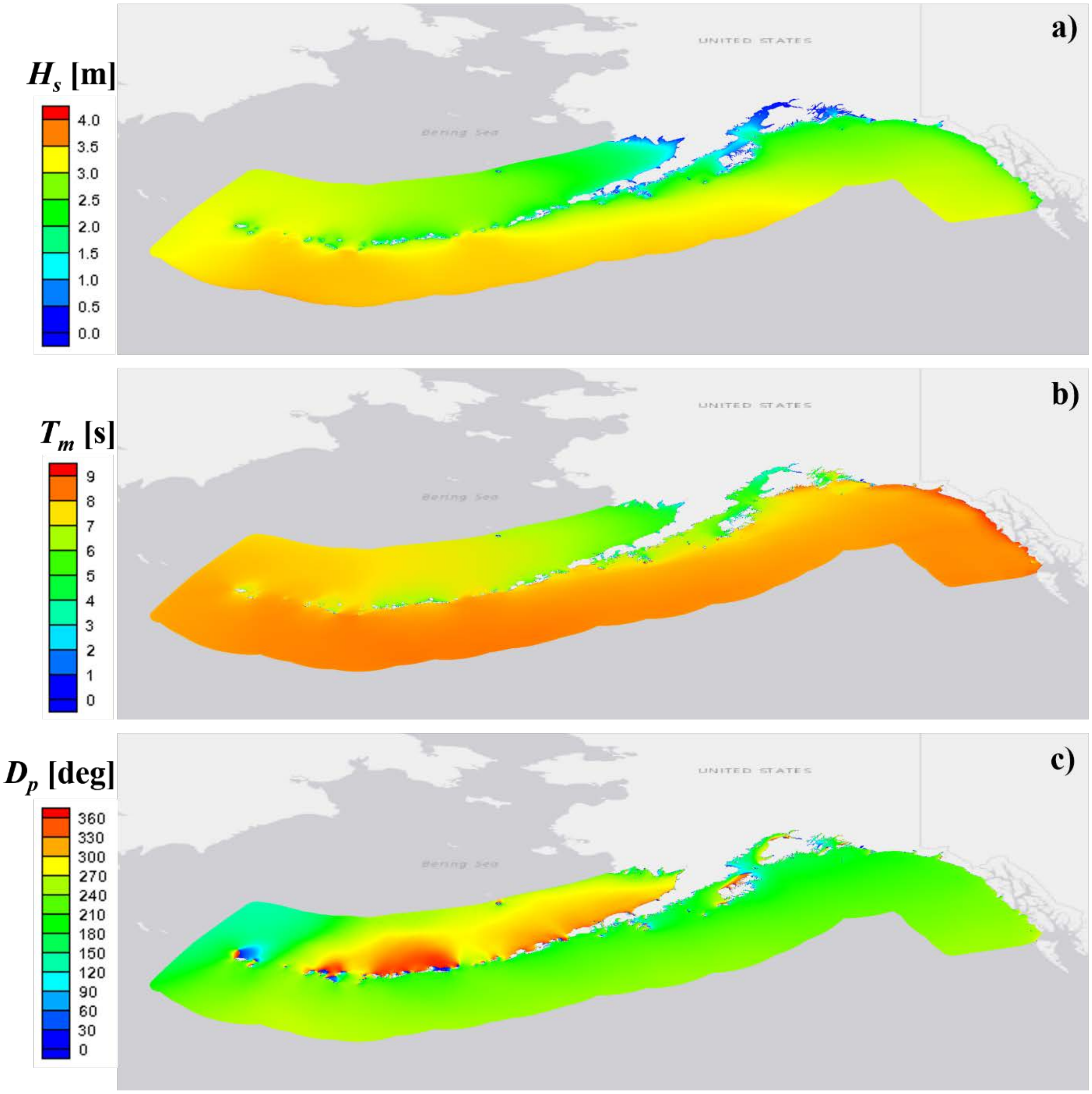

Figure A.14. Yearly distributions of three wave bulk parameters in 2009: (a) significant wave height, (b) mean wave period, and (c) peak wave direction on the Alaska Coast.

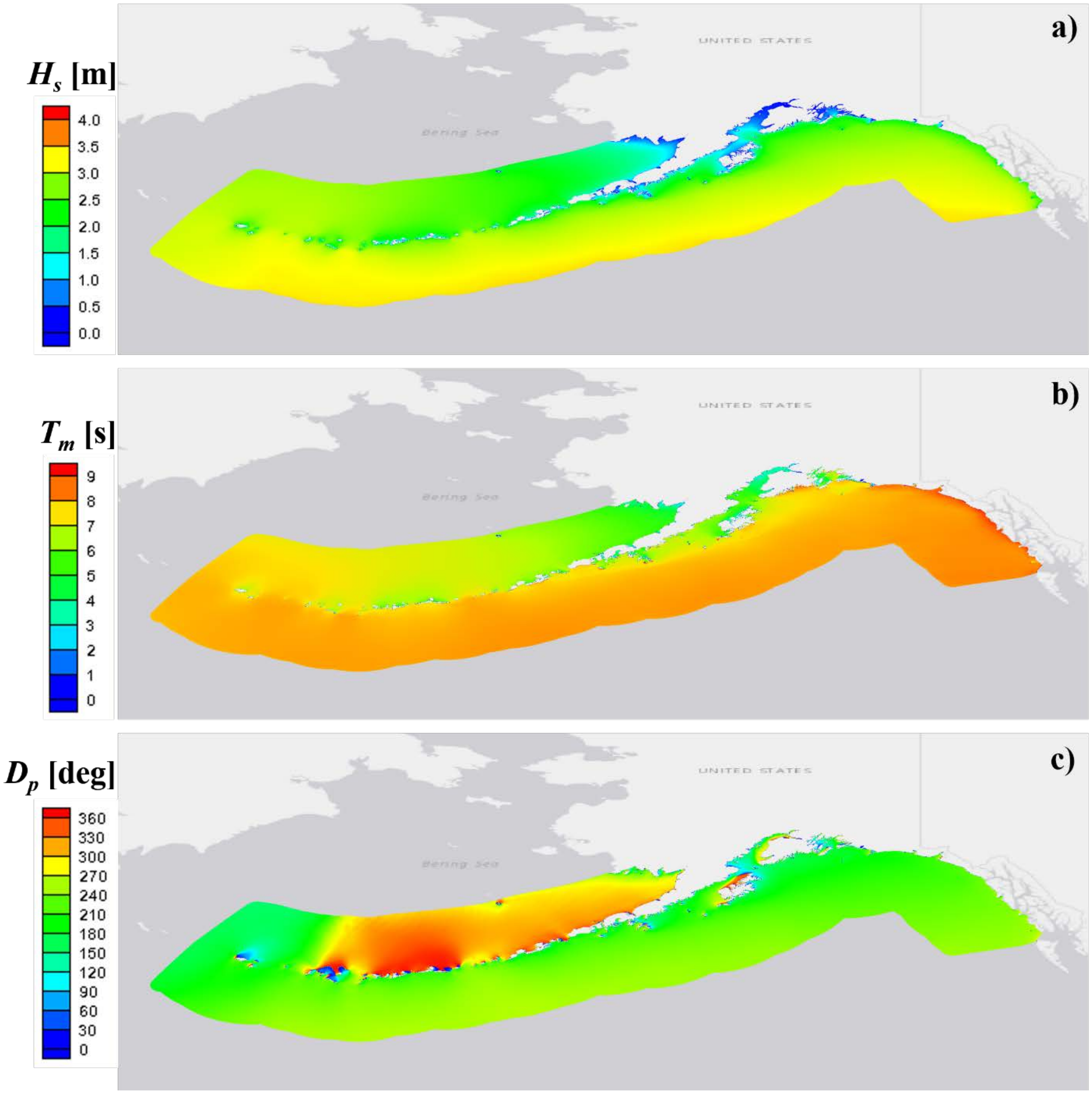

Figure A.15. Yearly distributions of three wave bulk parameters in 2008: (a) significant wave height, (b) mean wave period, and (c) peak wave direction on the Alaska Coast.

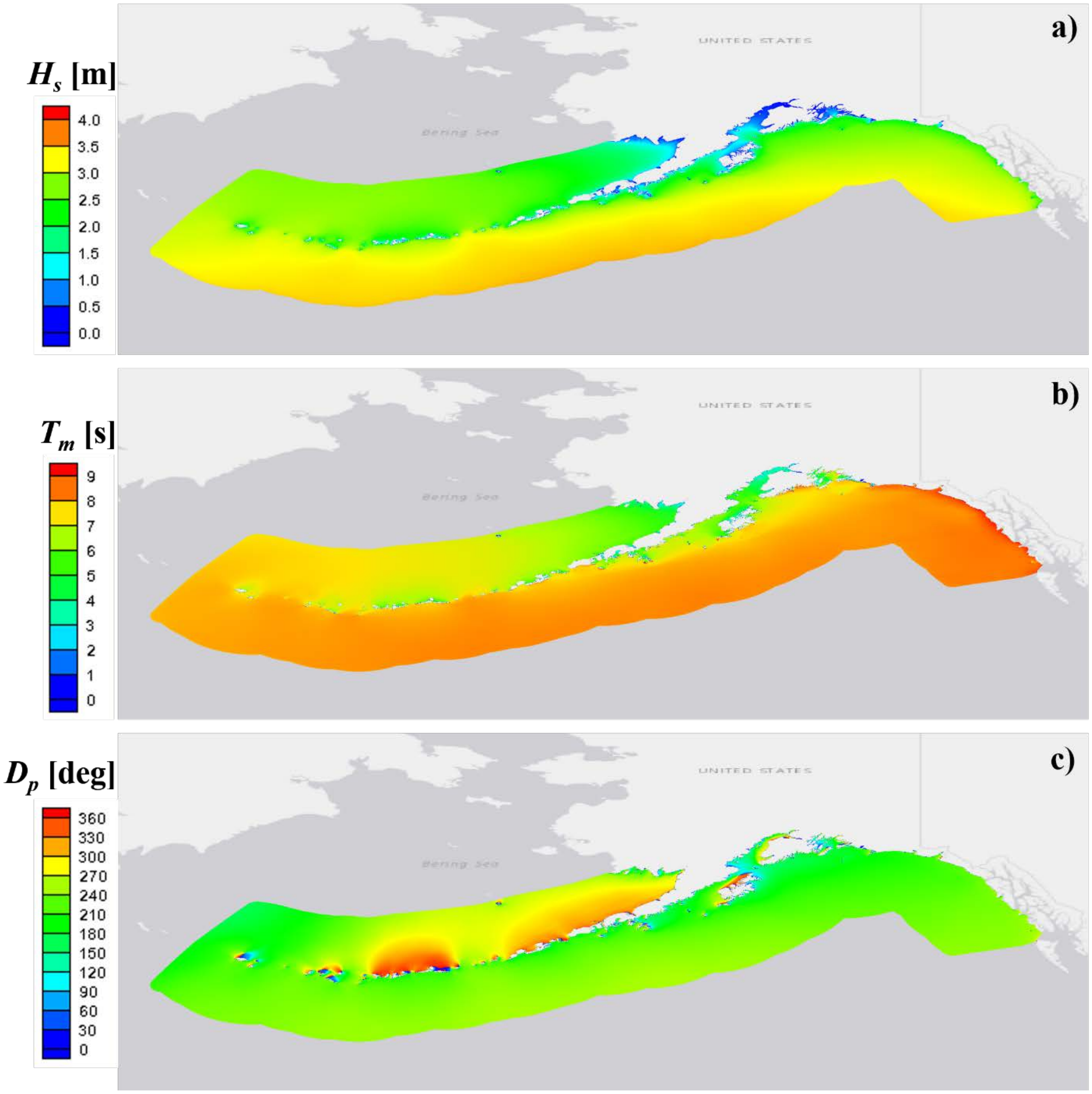

Figure A.16. Yearly distributions of three wave bulk parameters in 2007: (a) significant wave height, (b) mean wave period, and (c) peak wave direction on the Alaska Coast.

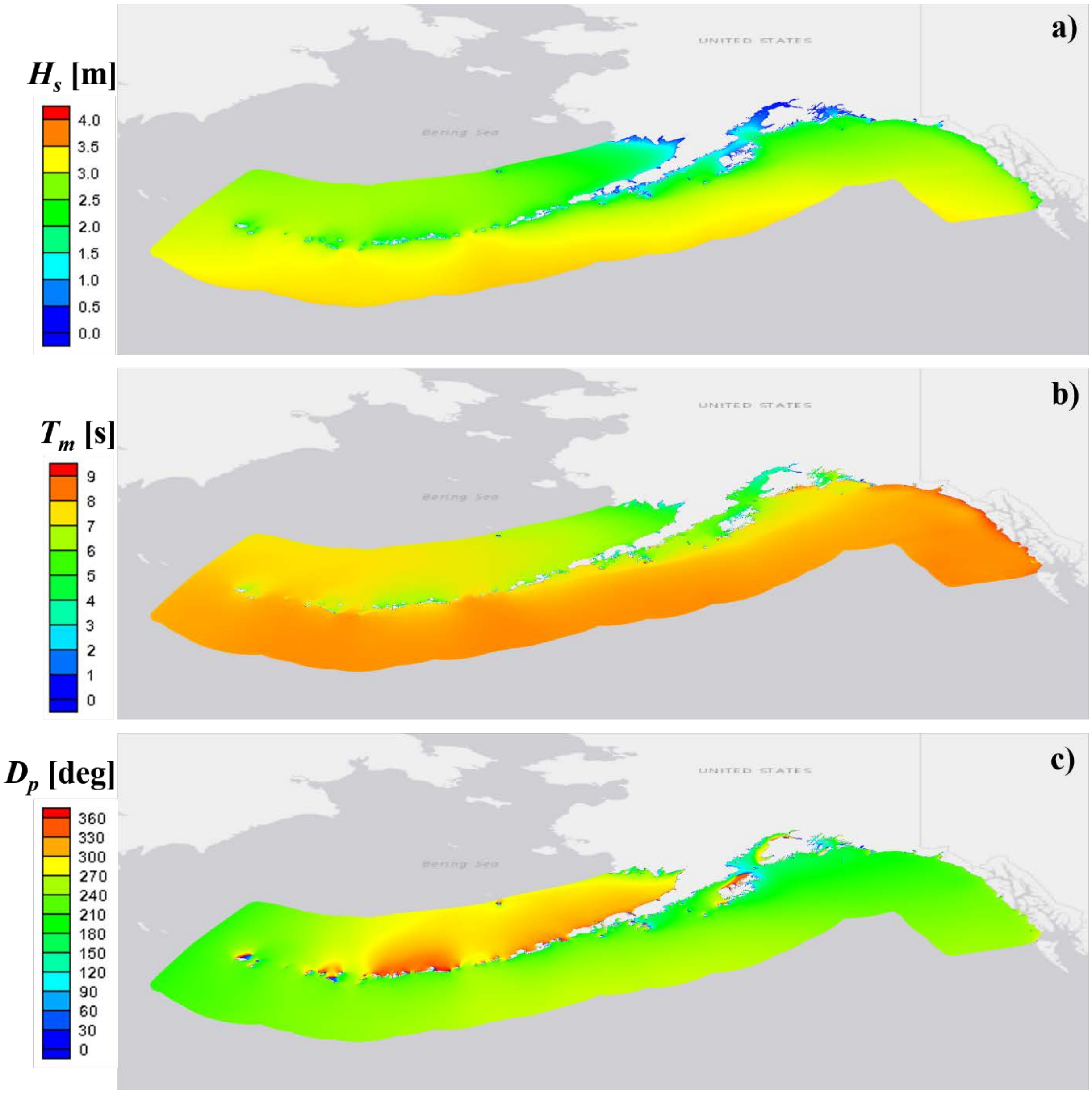

Figure A.17. Yearly distributions of three wave bulk parameters in 2006: (a) significant wave height, (b) mean wave period, and (c) peak wave direction on the Alaska Coast.

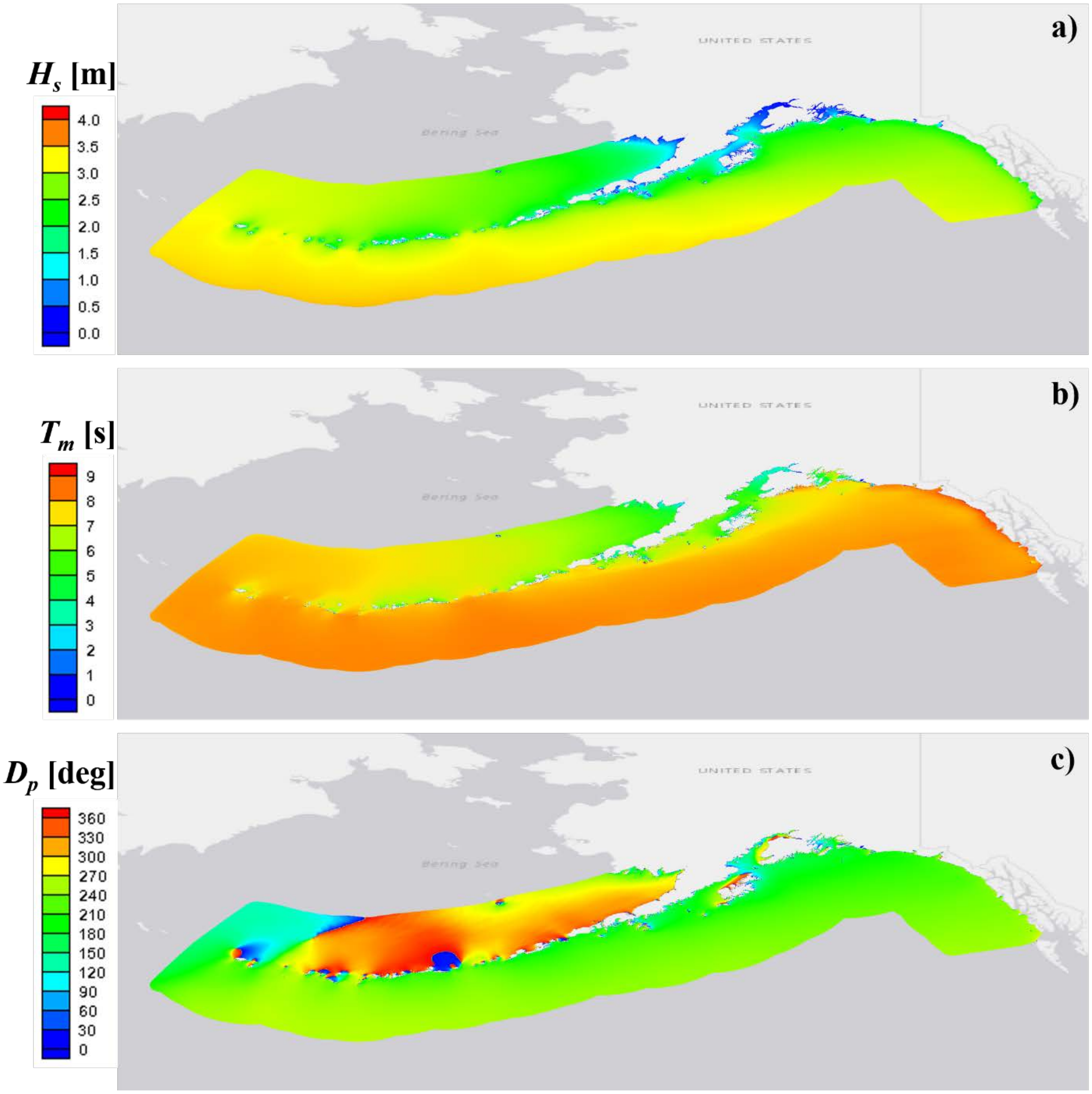

Figure A.18. Yearly distributions of three wave bulk parameters in 2005: (a) significant wave height, (b) mean wave period, and (c) peak wave direction on the Alaska Coast.

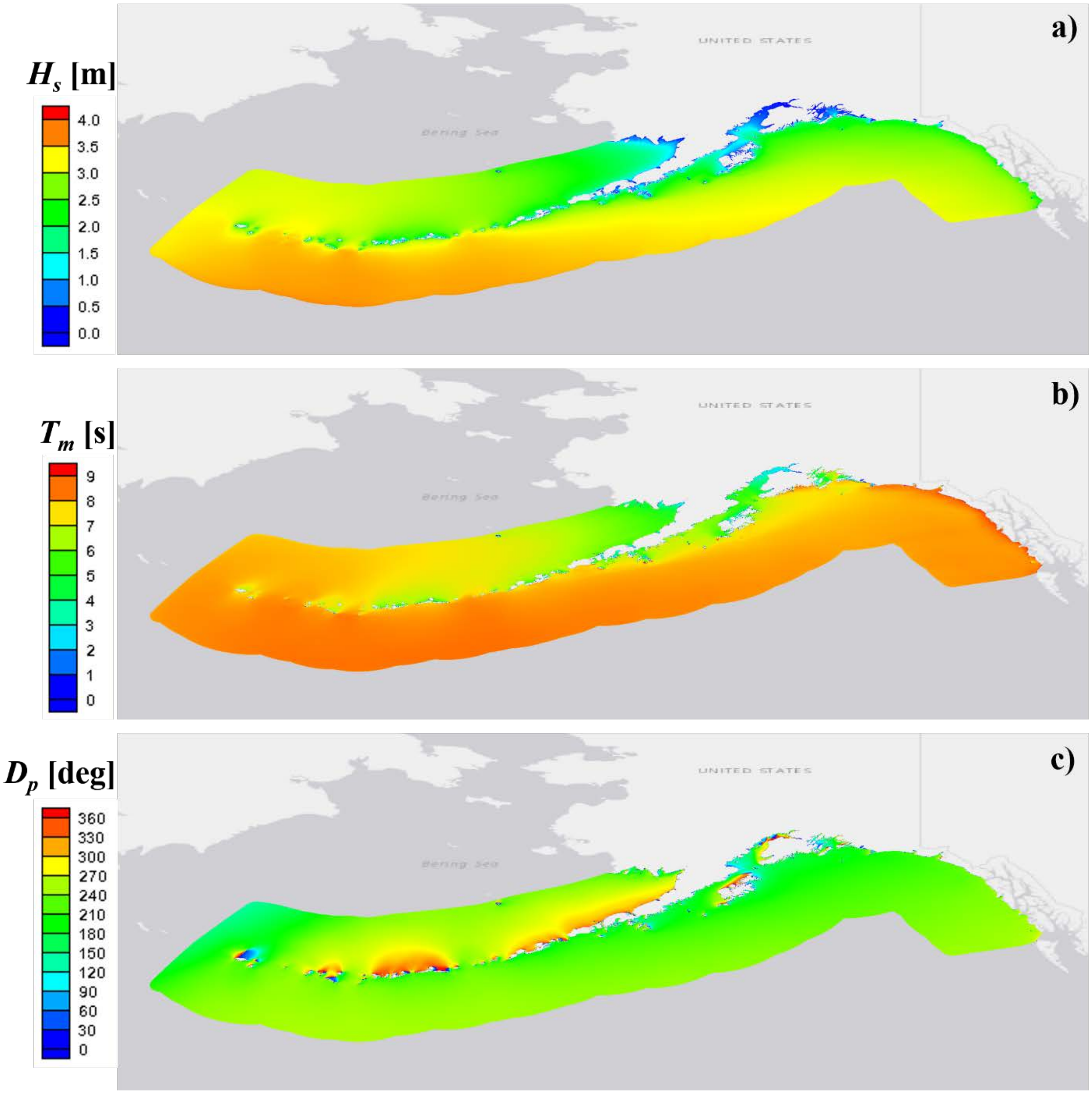

Figure A.19. Yearly distributions of three wave bulk parameters in 2004: (a) significant wave height, (b) mean wave period, and (c) peak wave direction on the Alaska Coast.

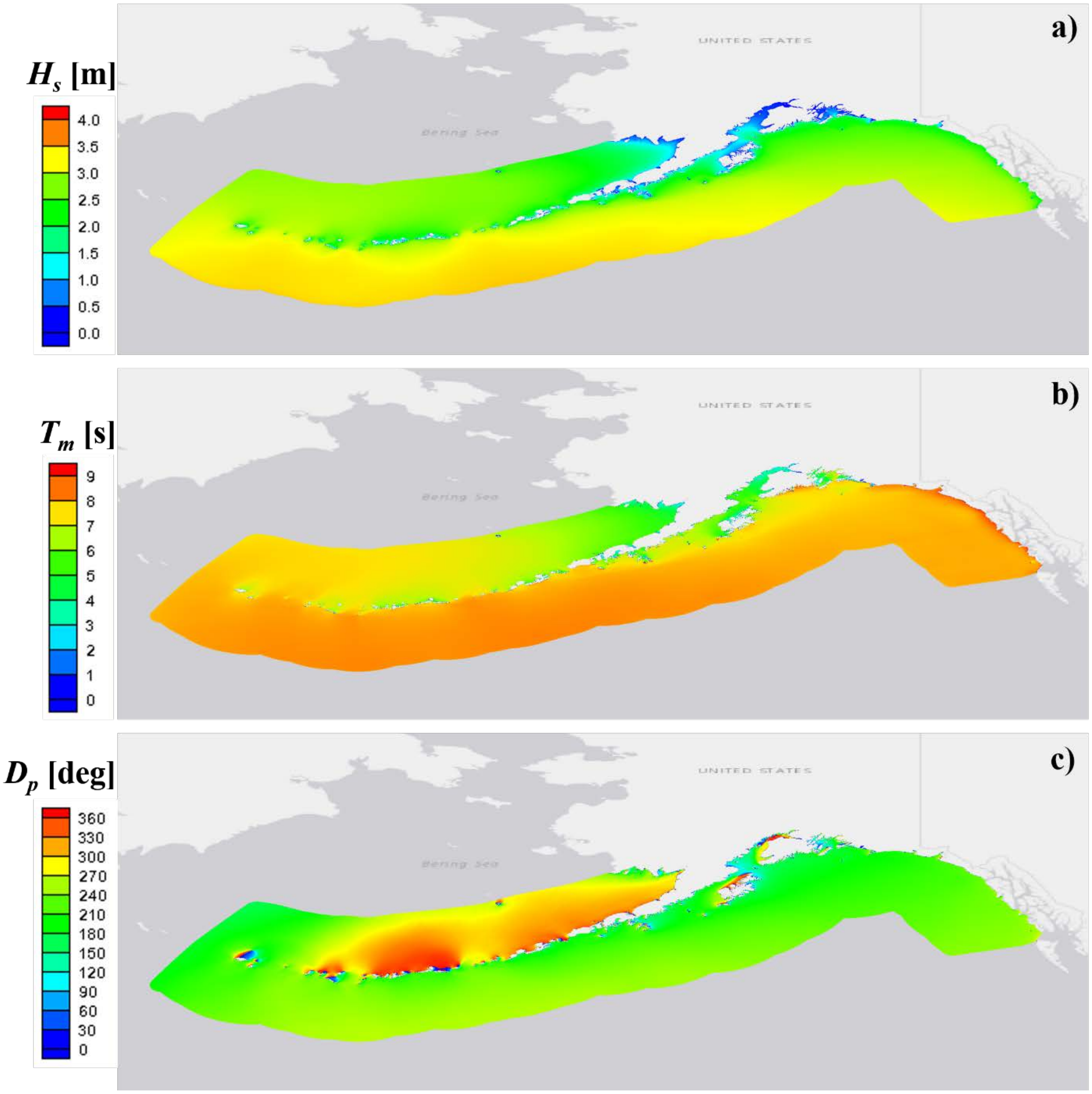

Figure A.20. Yearly distributions of three wave bulk parameters in 2003: (a) significant wave height, (b) mean wave period, and (c) peak wave direction on the Alaska Coast.

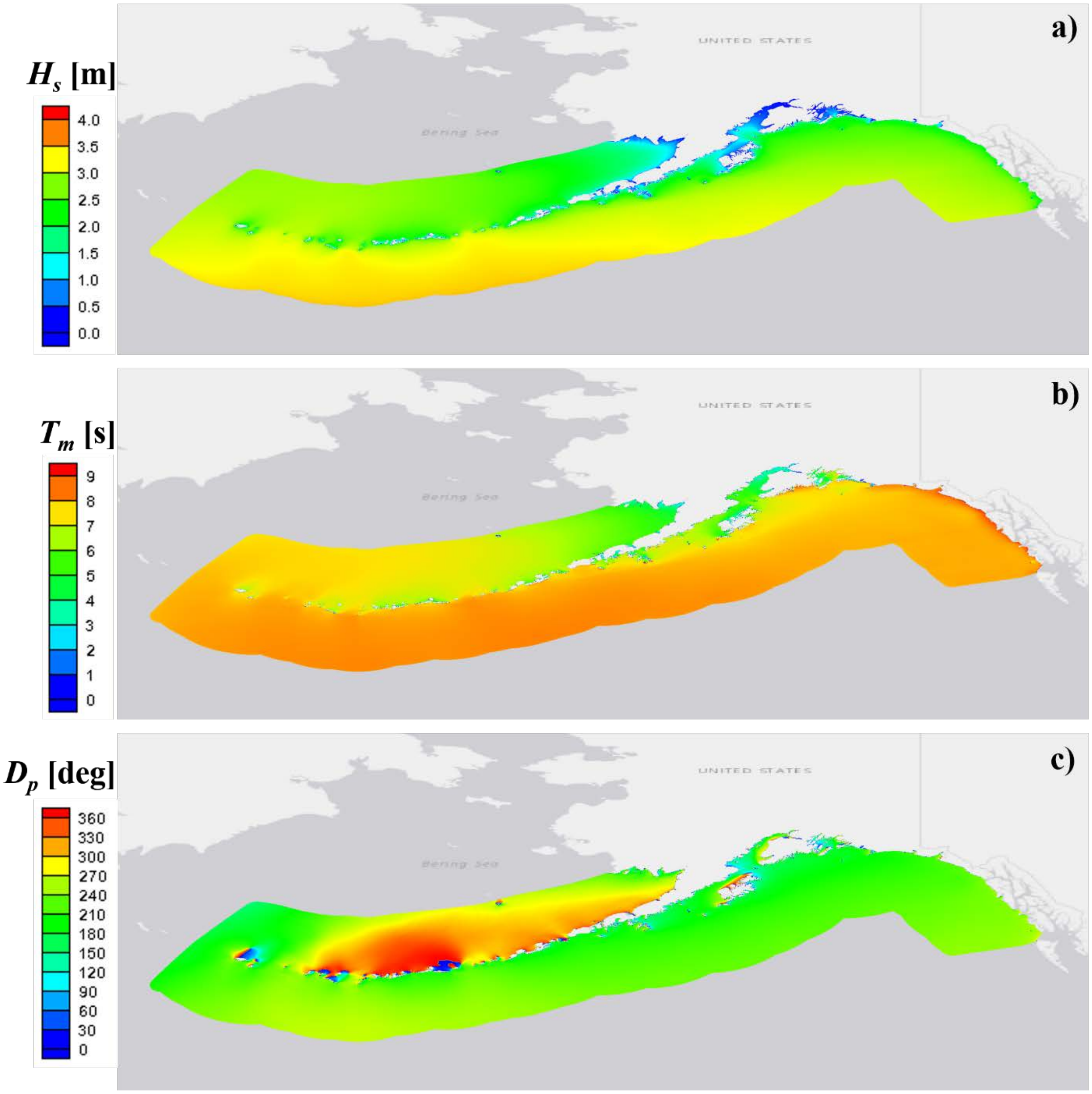

Figure A.21. Yearly distributions of three wave bulk parameters in 2002: (a) significant wave height, (b) mean wave period, and (c) peak wave direction on the Alaska Coast.

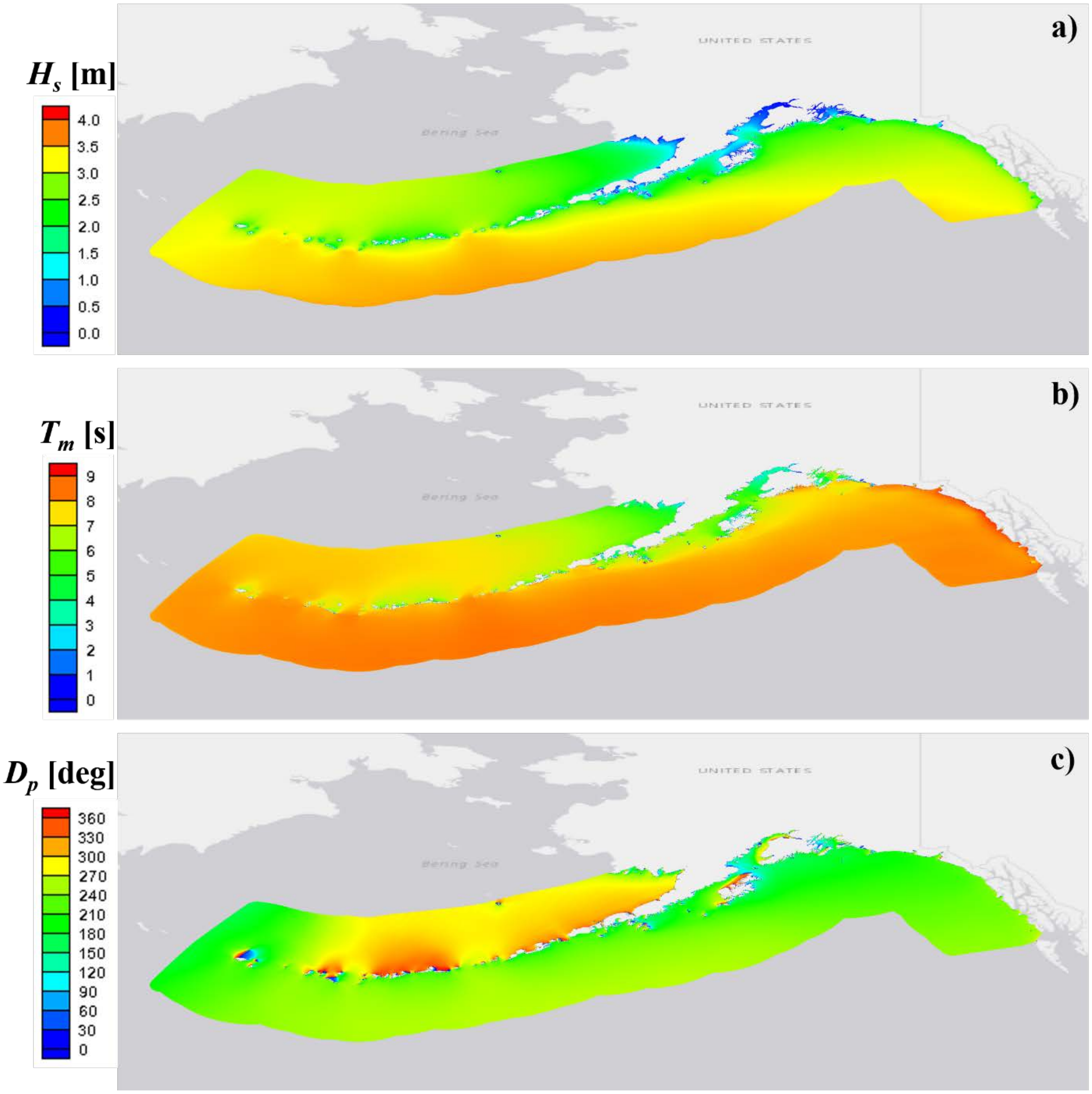

Figure A.22. Yearly distributions of three wave bulk parameters in 2001: (a) significant wave height, (b) mean wave period, and (c) peak wave direction on the Alaska Coast.

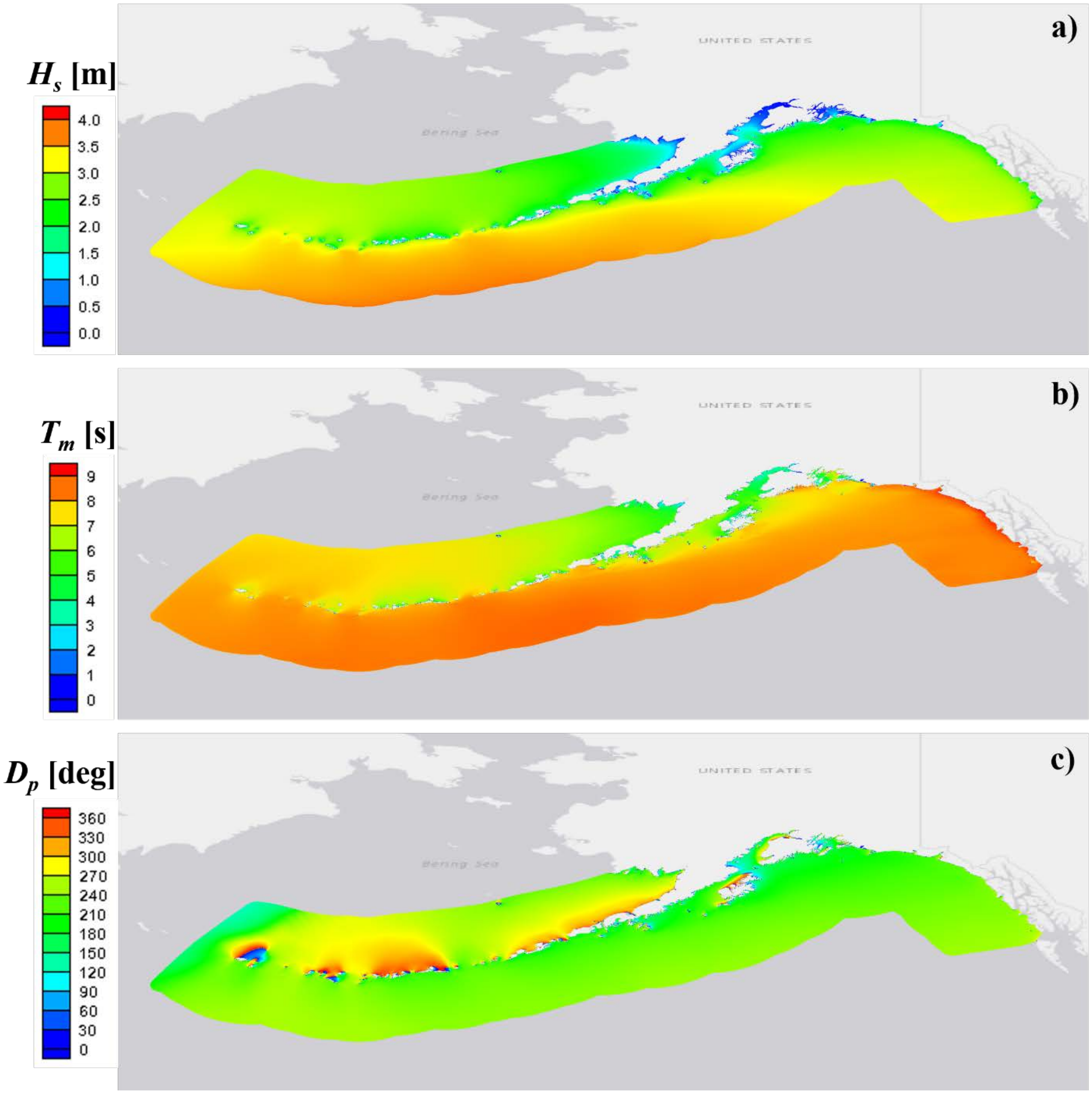

Figure A.23. Yearly distributions of three wave bulk parameters in 2000: (a) significant wave height, (b) mean wave period, and (c) peak wave direction on the Alaska Coast.

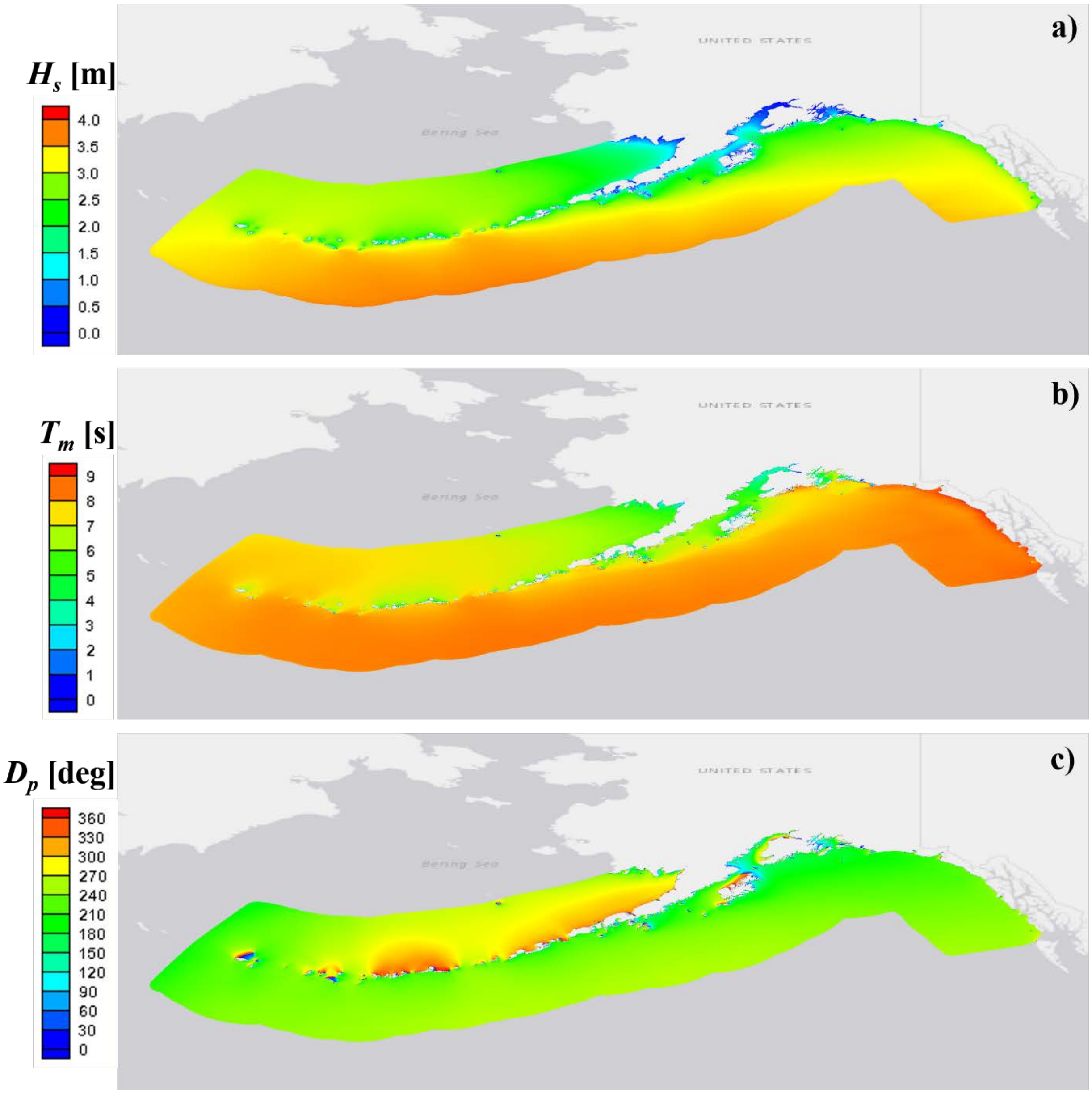

Figure A.24. Yearly distributions of three wave bulk parameters in 1999: (a) significant wave height, (b) mean wave period, and (c) peak wave direction on the Alaska Coast.

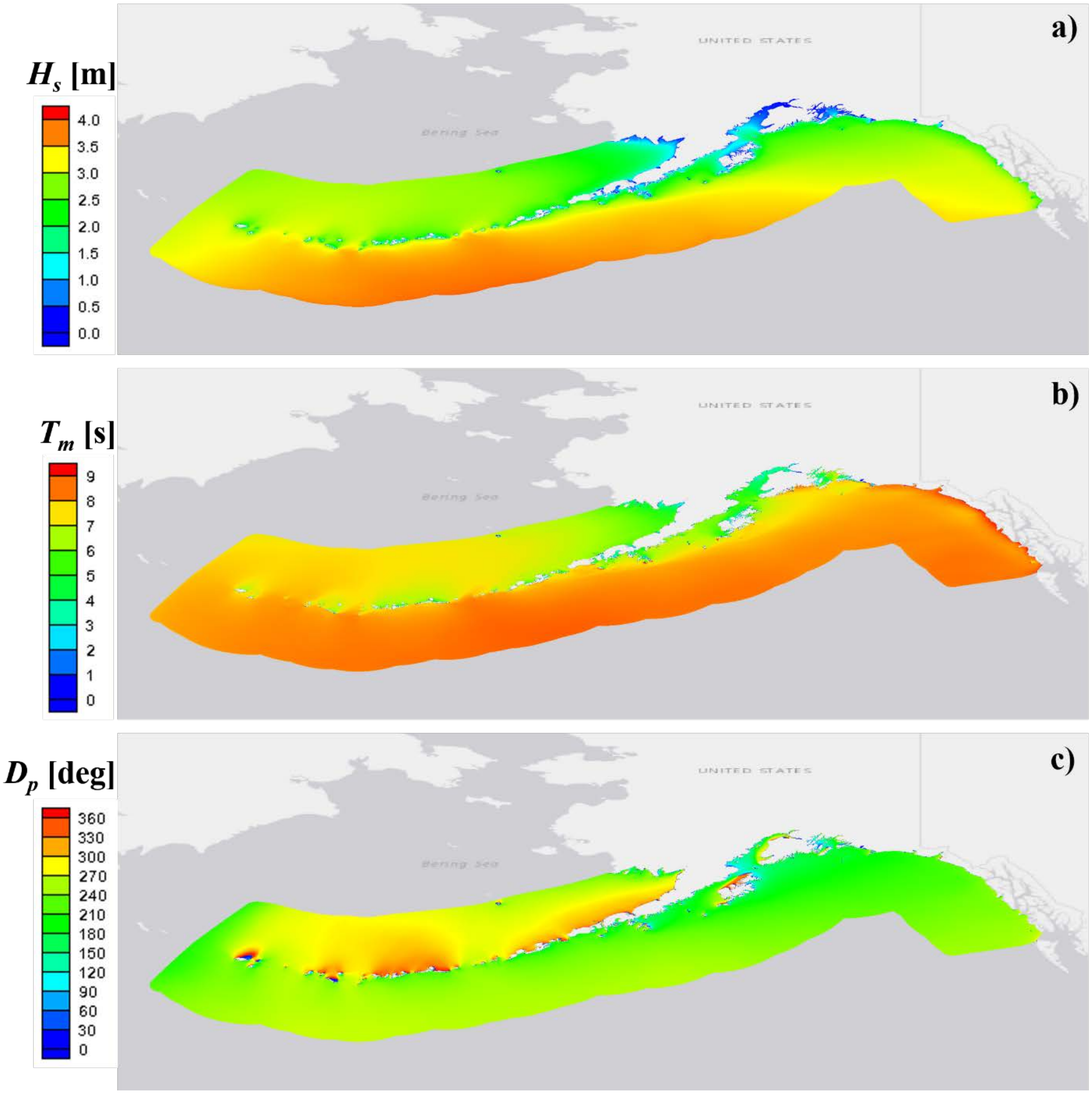

Figure A.25. Yearly distributions of three wave bulk parameters in 1998: (a) significant wave height, (b) mean wave period, and (c) peak wave direction on the Alaska Coast.

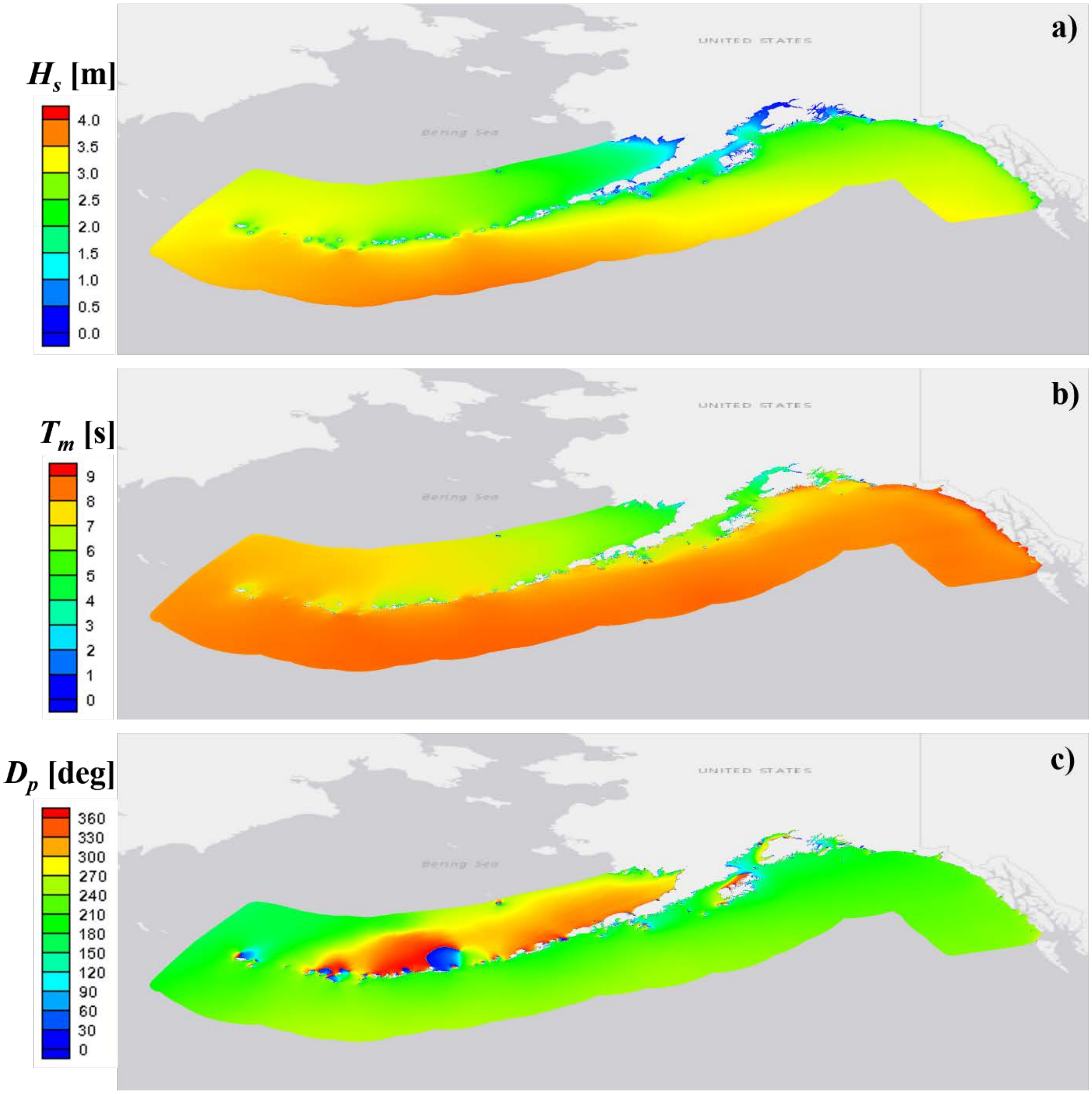

Figure A.26. Yearly distributions of three wave bulk parameters in 1997: (a) significant wave height, (b) mean wave period, and (c) peak wave direction on the Alaska Coast.

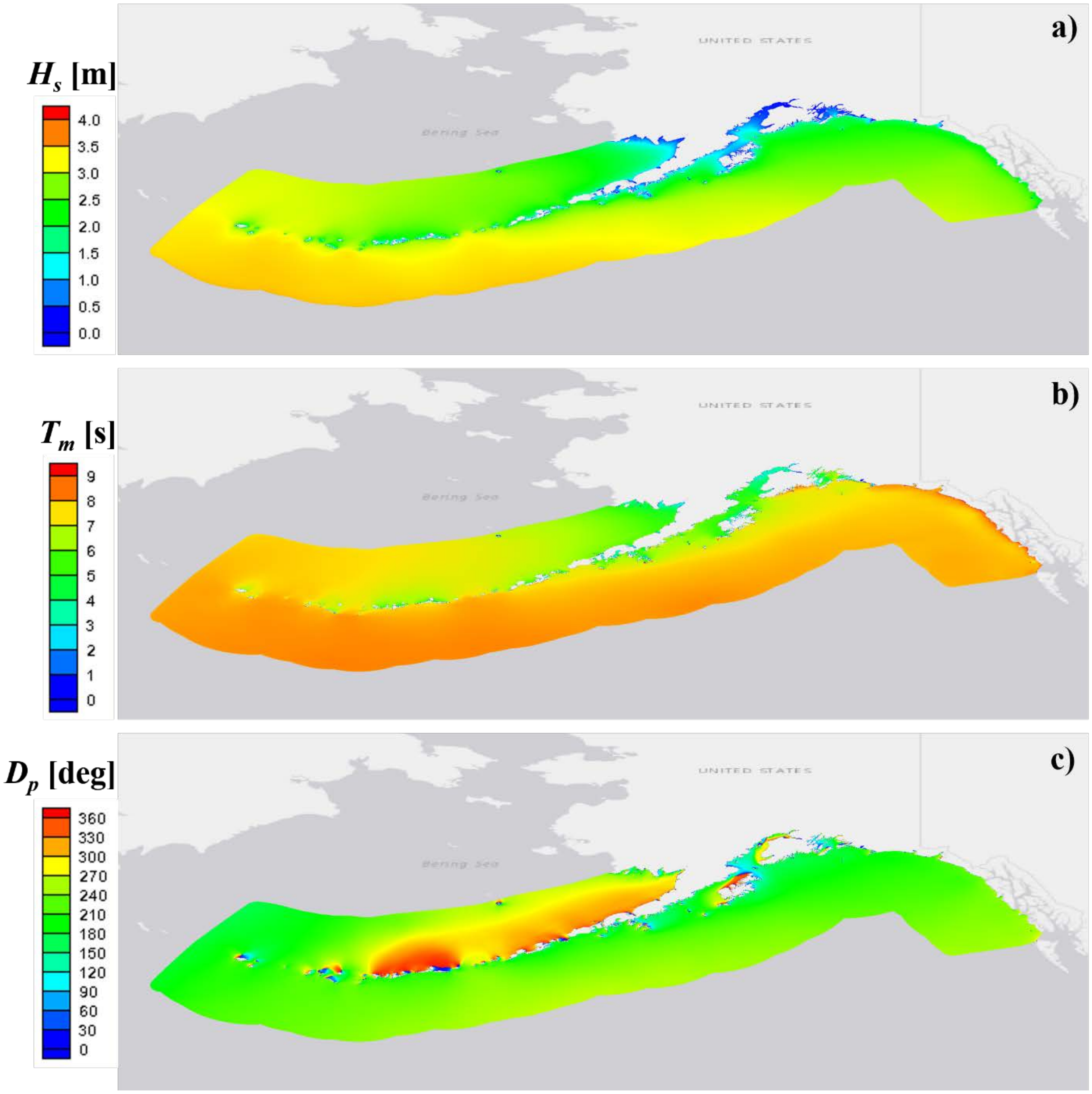

Figure A.27. Yearly distributions of three wave bulk parameters in 1996: (a) significant wave height, (b) mean wave period, and (c) peak wave direction on the Alaska Coast.

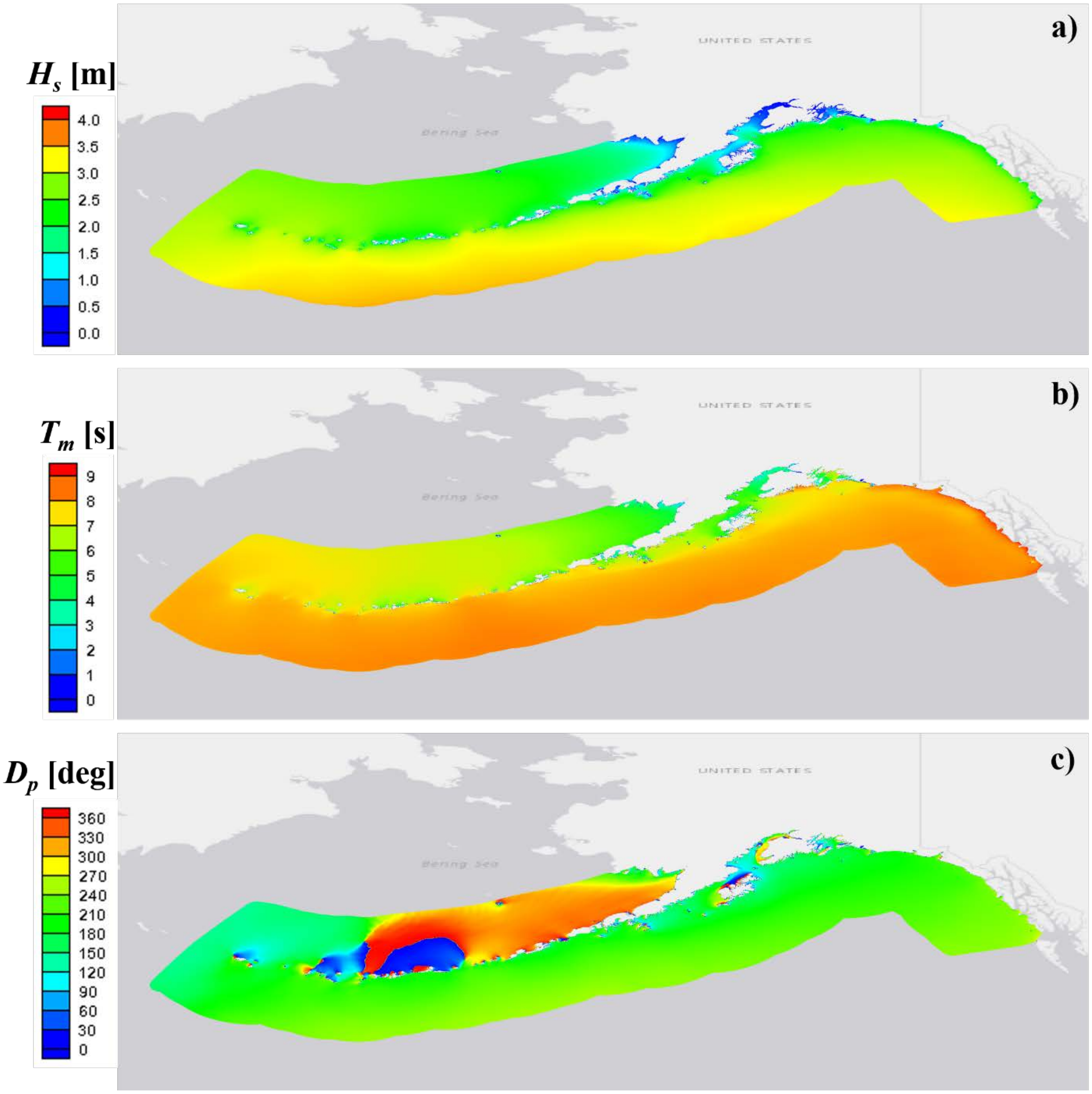

Figure A.28. Yearly distributions of three wave bulk parameters in 1995: (a) significant wave height, (b) mean wave period, and (c) peak wave direction on the Alaska Coast.

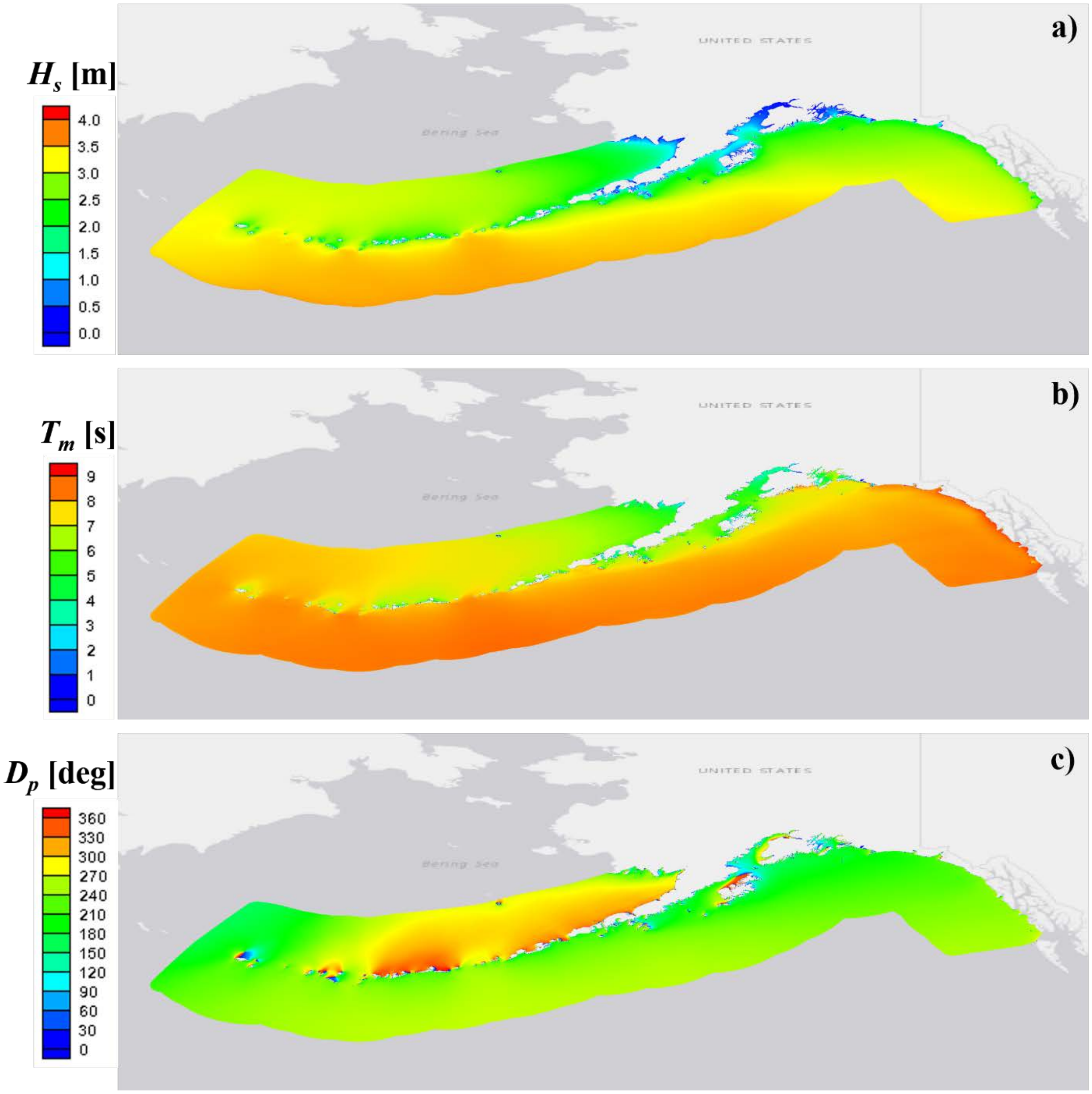

Figure A.29. Yearly distributions of three wave bulk parameters in 1994: (a) significant wave height, (b) mean wave period, and (c) peak wave direction on the Alaska Coast.

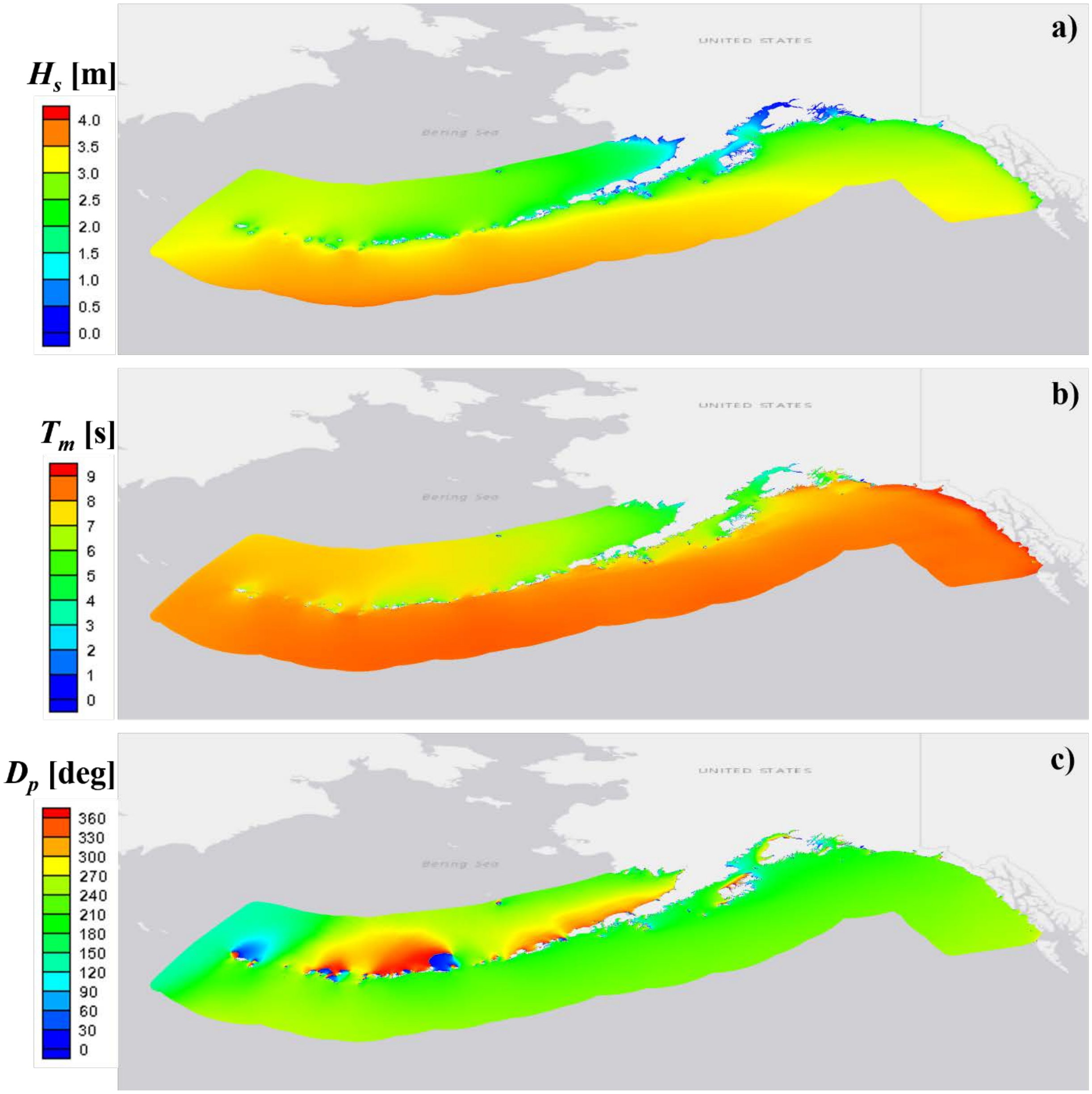

Figure A.30. Yearly distributions of three wave bulk parameters in 1993: (a) significant wave height, (b) mean wave period, and (c) peak wave direction on the Alaska Coast.

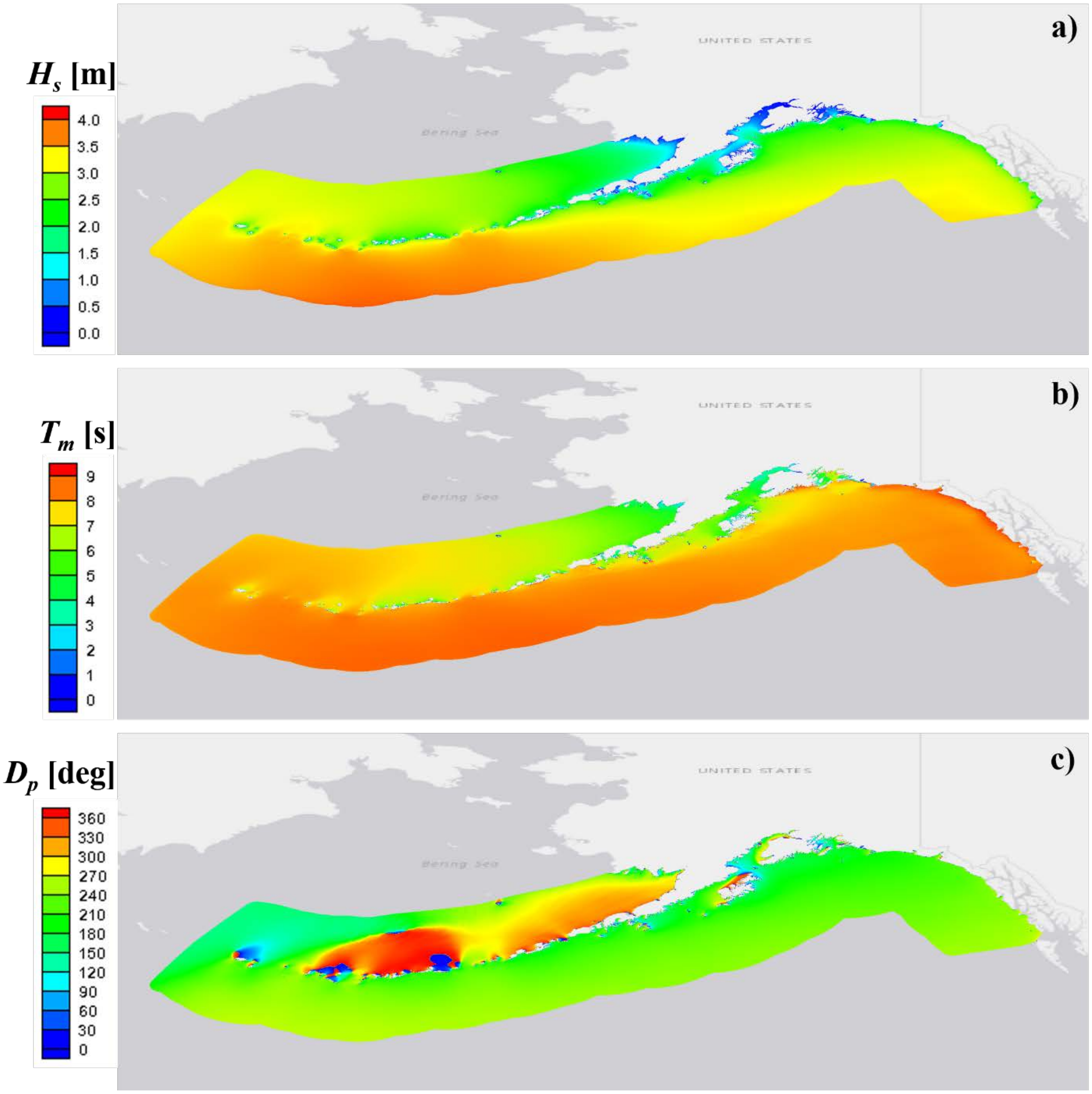

Figure A.31. Yearly distributions of three wave bulk parameters in 1992: (a) significant wave height, (b) mean wave period, and (c) peak wave direction on the Alaska Coast.

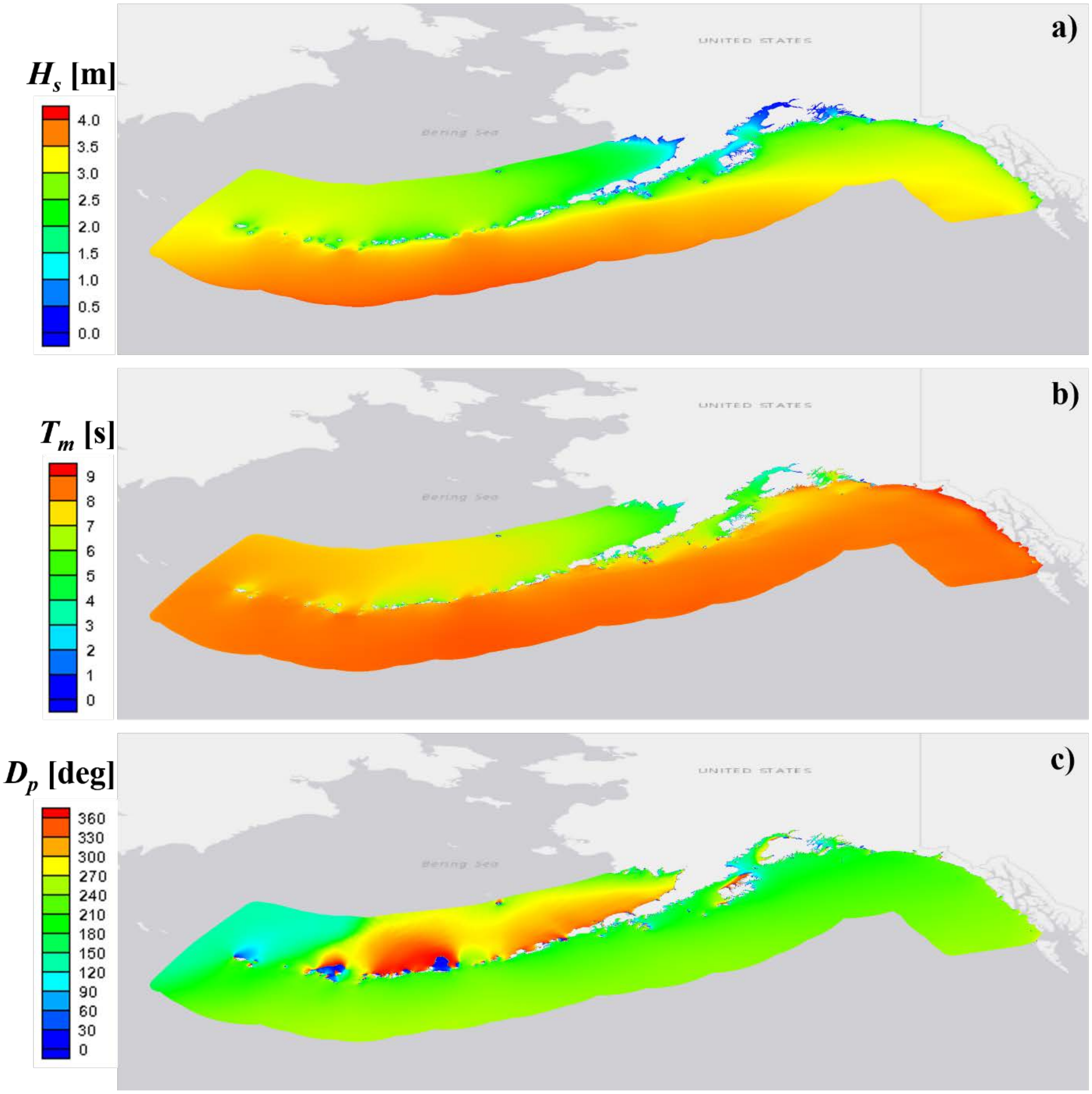

Figure A.32. Yearly distributions of three wave bulk parameters in 1991: (a) significant wave height, (b) mean wave period, and (c) peak wave direction on the Alaska Coast.

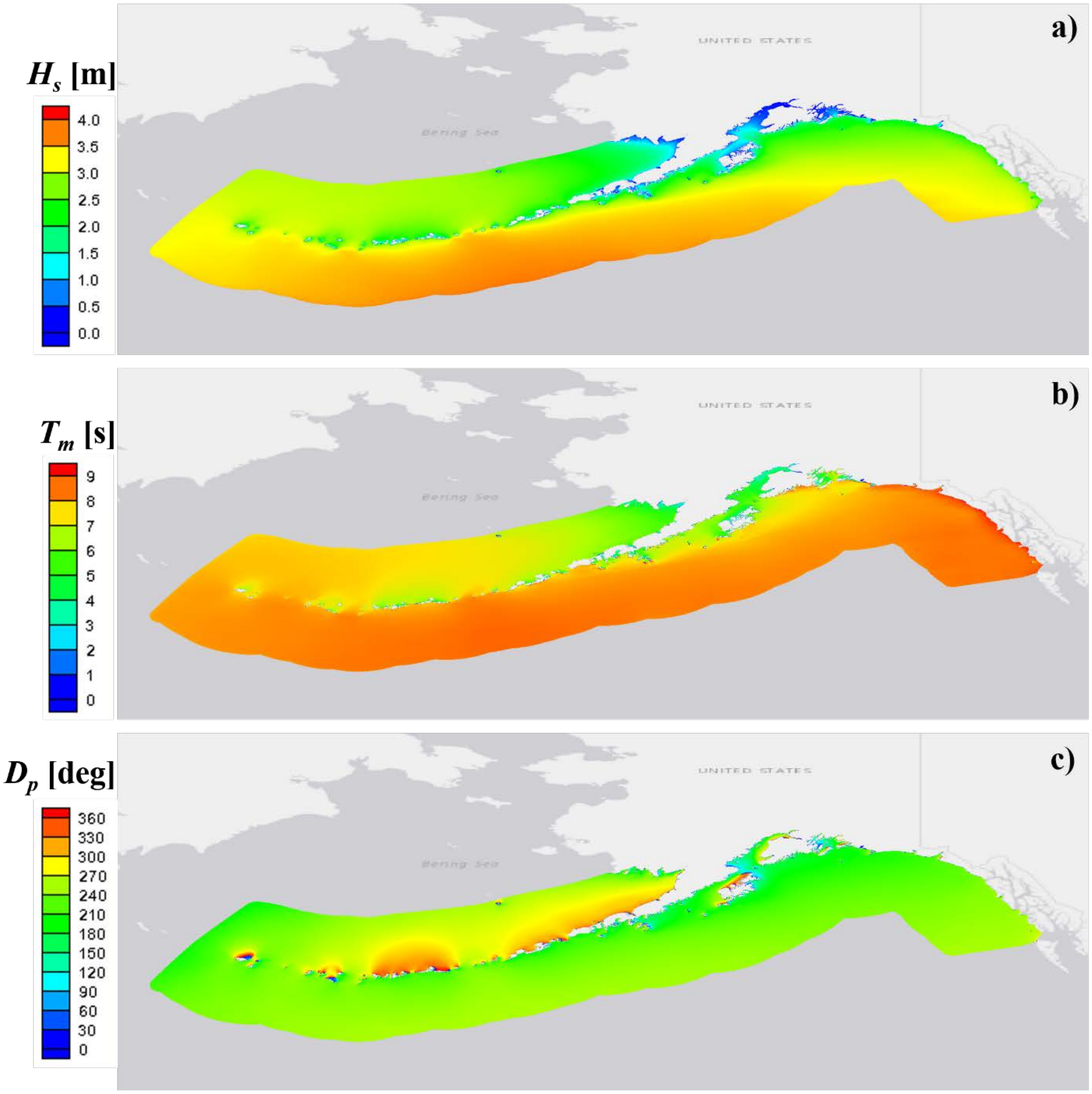

Figure A.33. Yearly distributions of three wave bulk parameters in 1990: (a) significant wave height, (b) mean wave period, and (c) peak wave direction on the Alaska Coast.

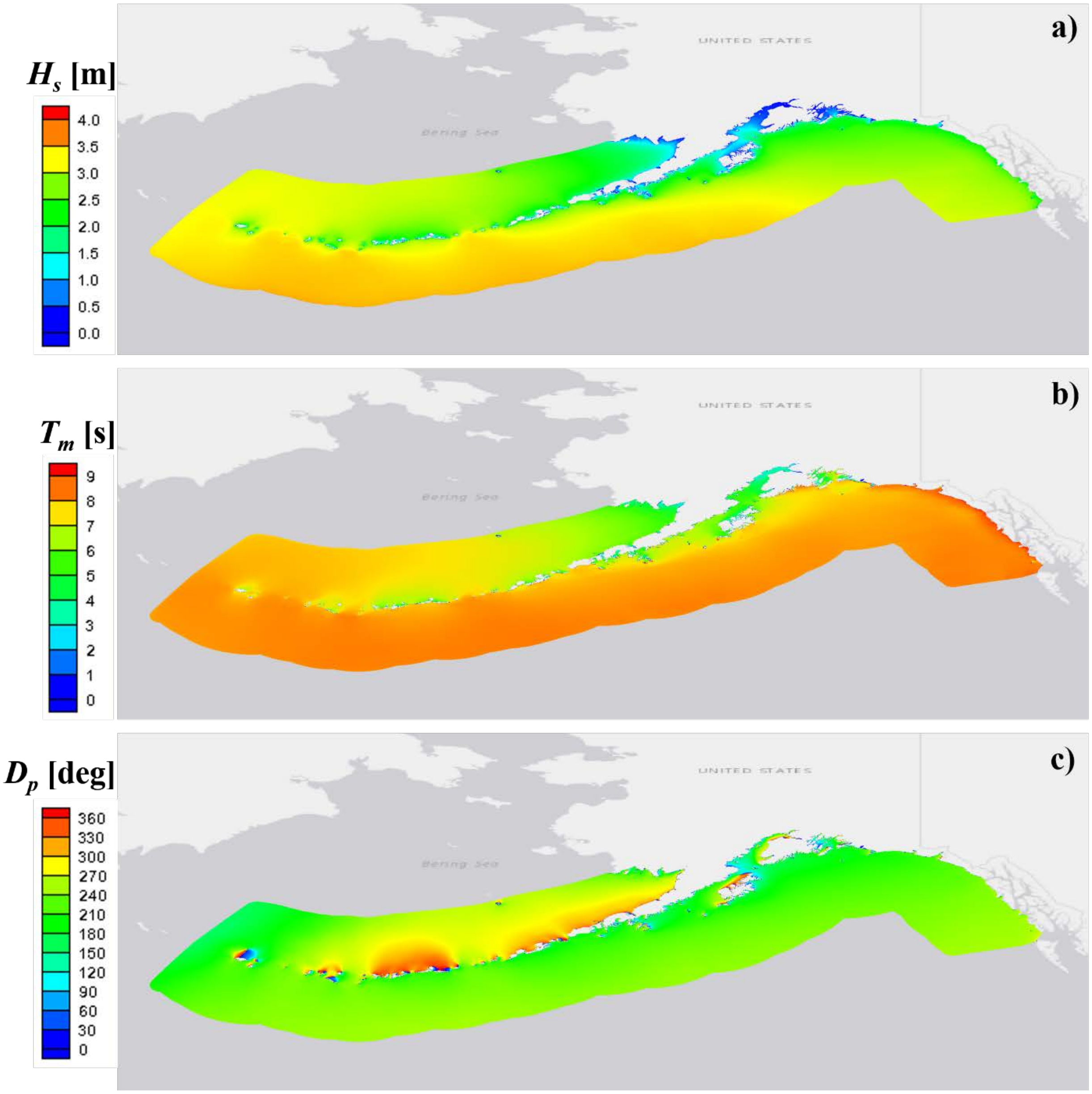

Figure A.34. Yearly distributions of three wave bulk parameters in 1989: (a) significant wave height, (b) mean wave period, and (c) peak wave direction on the Alaska Coast.

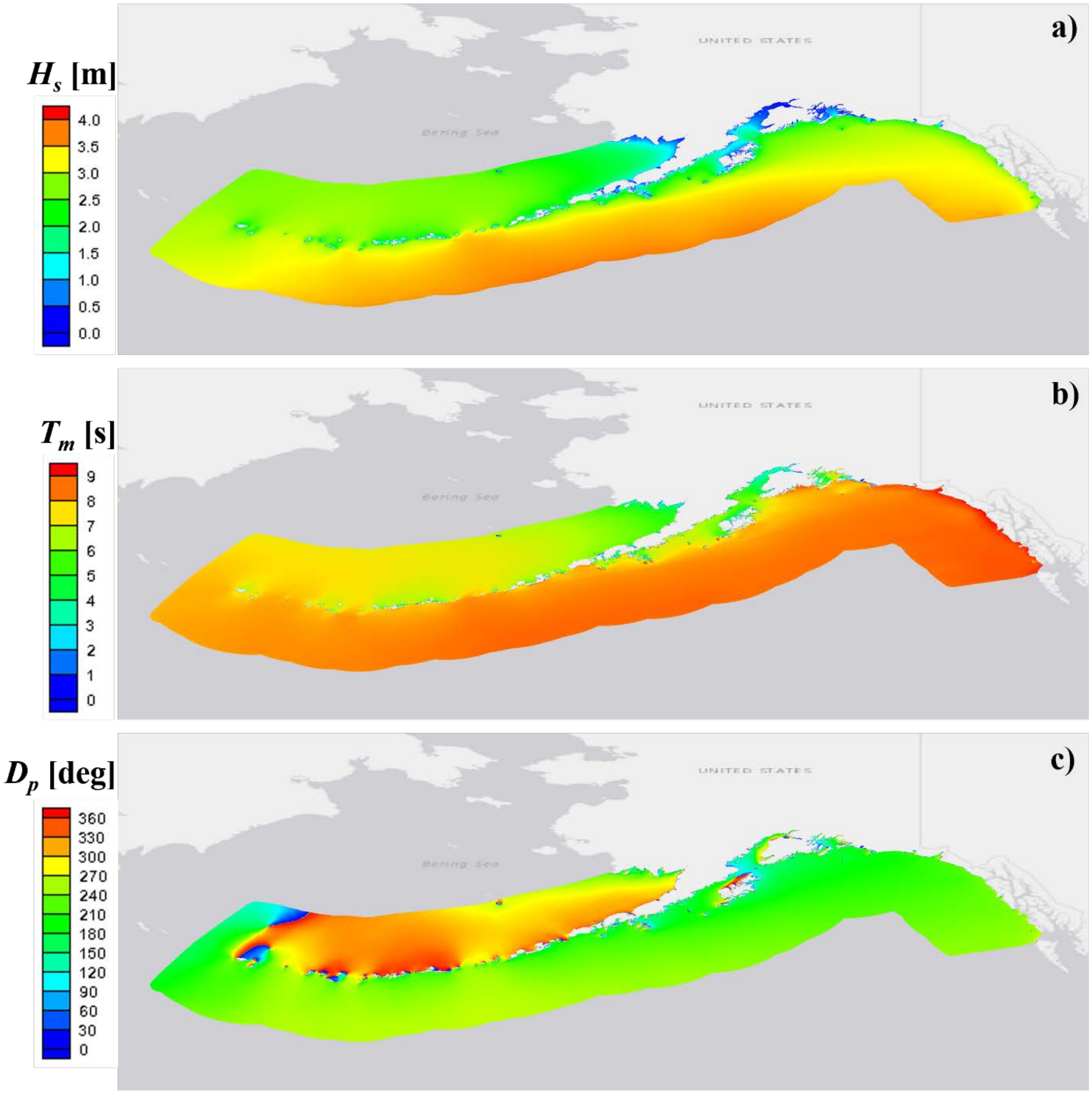

Figure A.35. Yearly distributions of three wave bulk parameters in 1988: (a) significant wave height, (b) mean wave period, and (c) peak wave direction on the Alaska Coast.

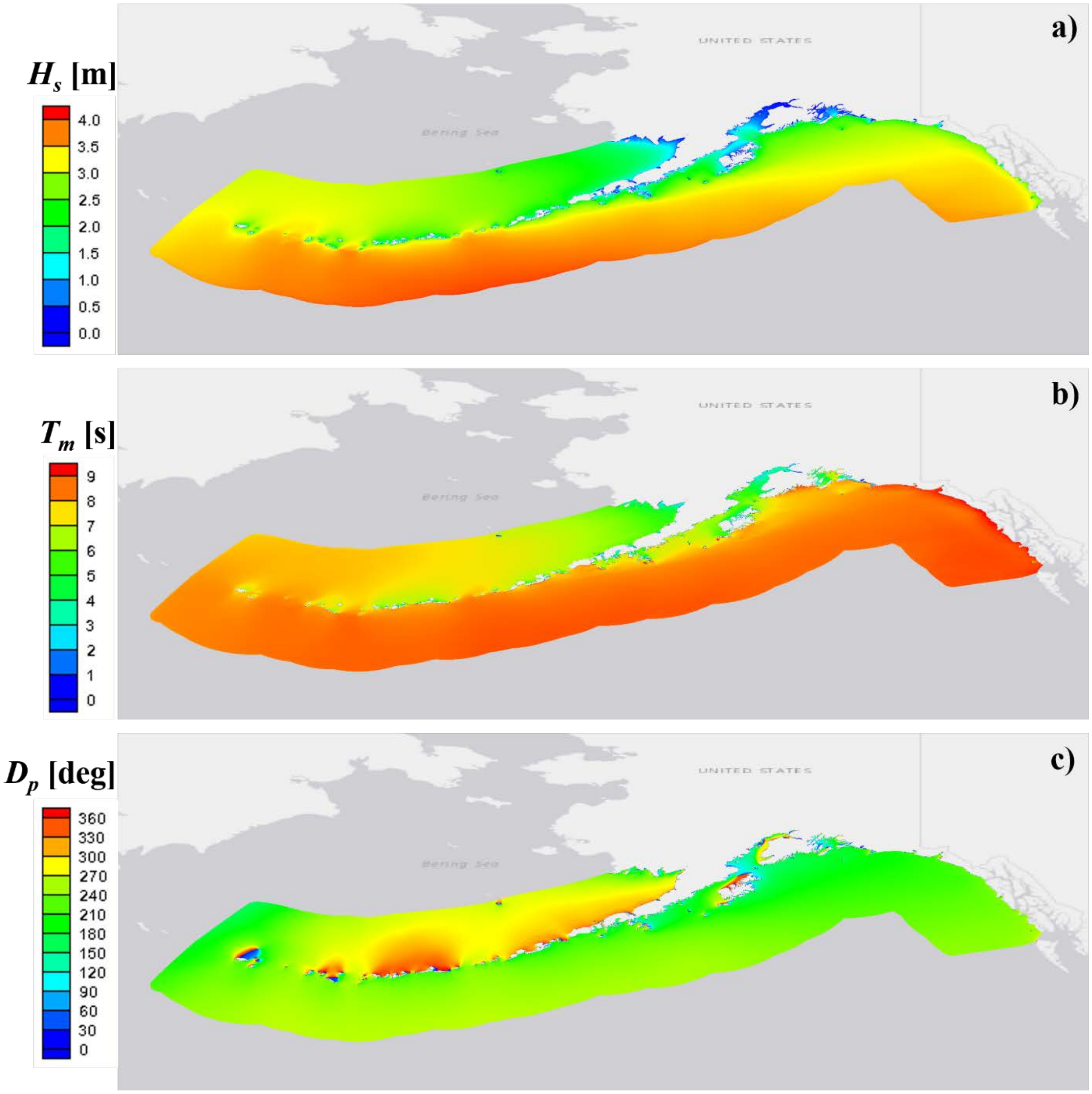

Figure A.36. Yearly distributions of three wave bulk parameters in 1987: (a) significant wave height, (b) mean wave period, and (c) peak wave direction on the Alaska Coast.

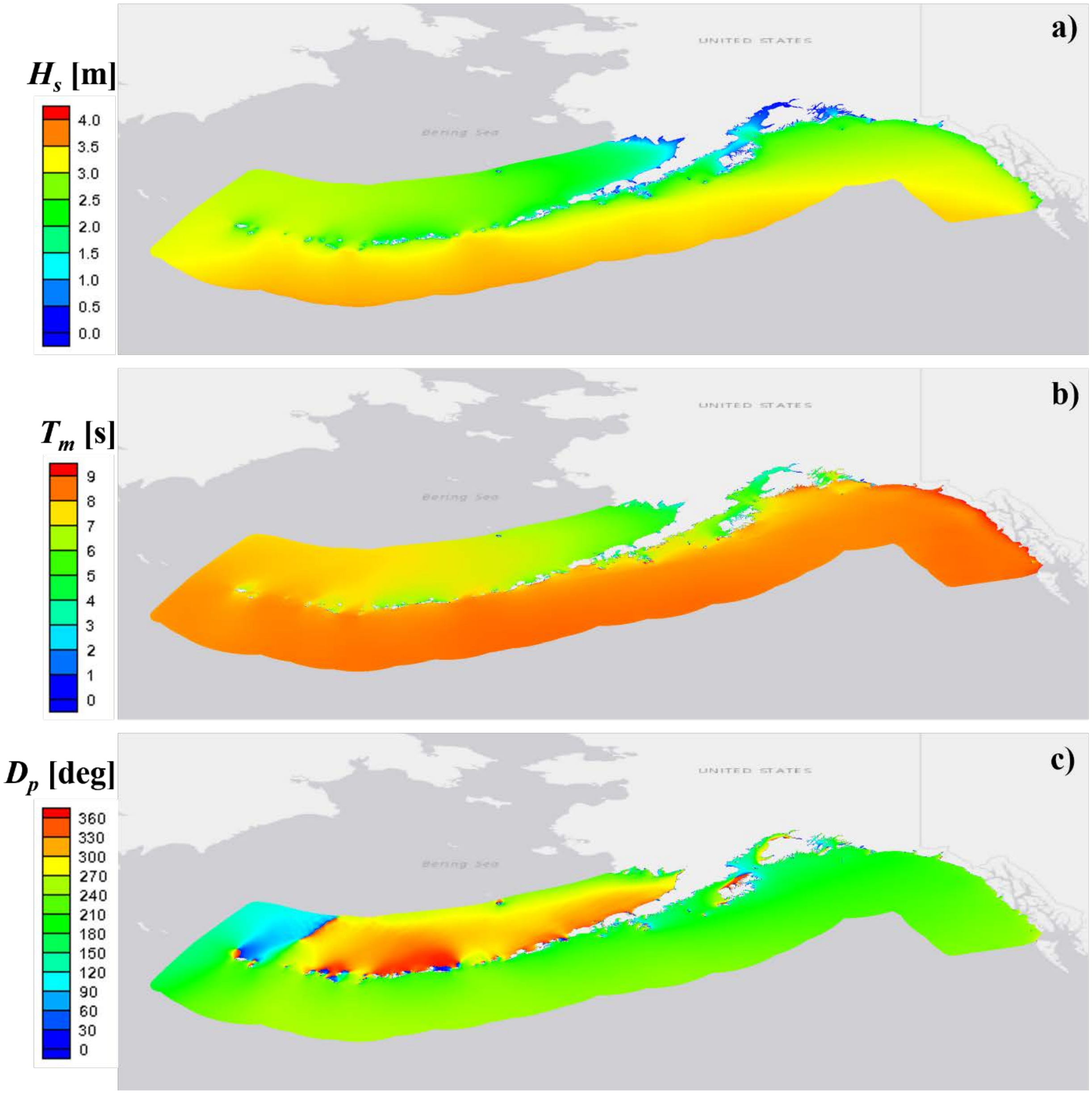

Figure A.37. Yearly distributions of three wave bulk parameters in 1986: (a) significant wave height, (b) mean wave period, and (c) peak wave direction on the Alaska Coast.

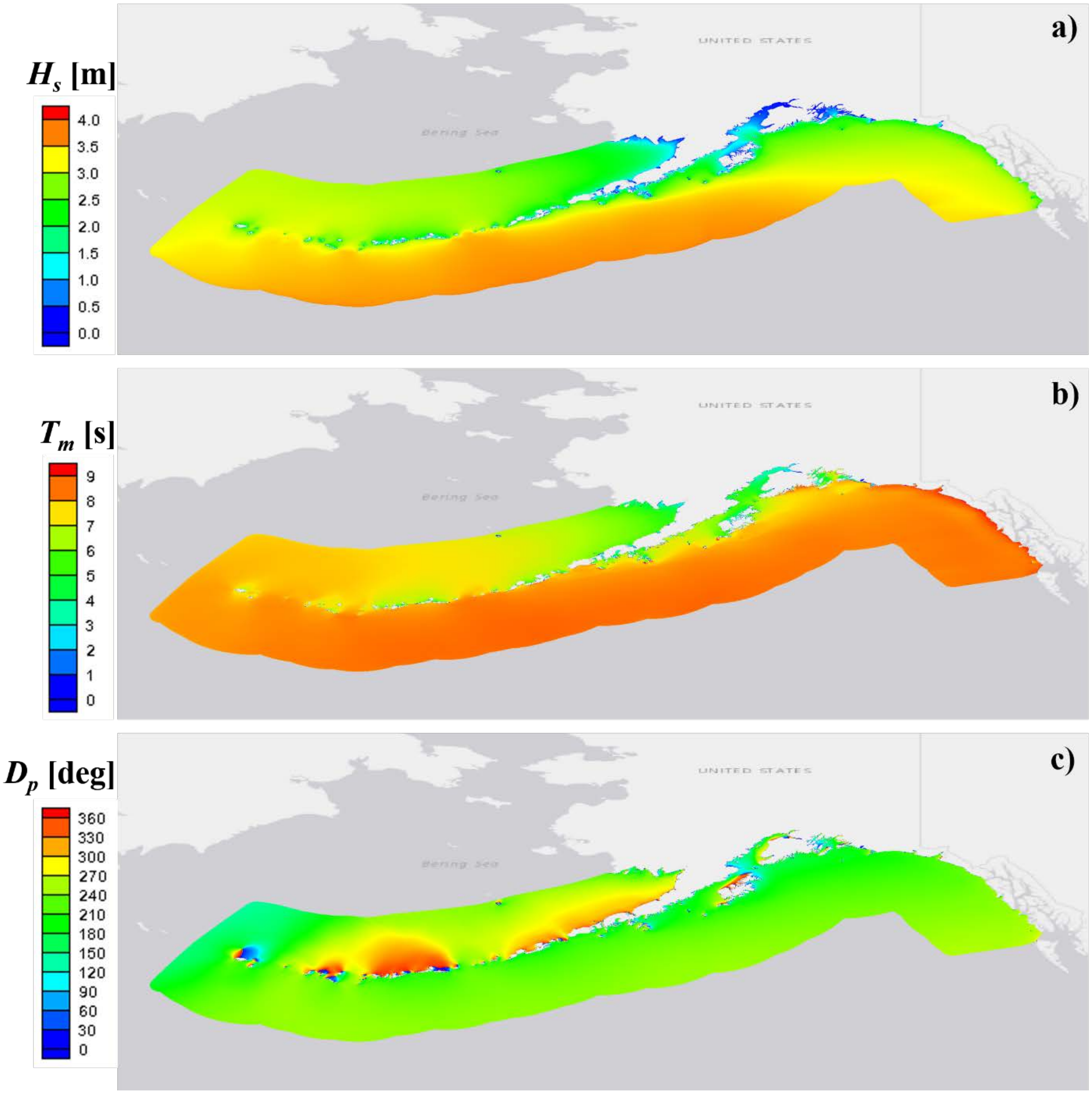

Figure A.38. Yearly distributions of three wave bulk parameters in 1985: (a) significant wave height, (b) mean wave period, and (c) peak wave direction on the Alaska Coast.

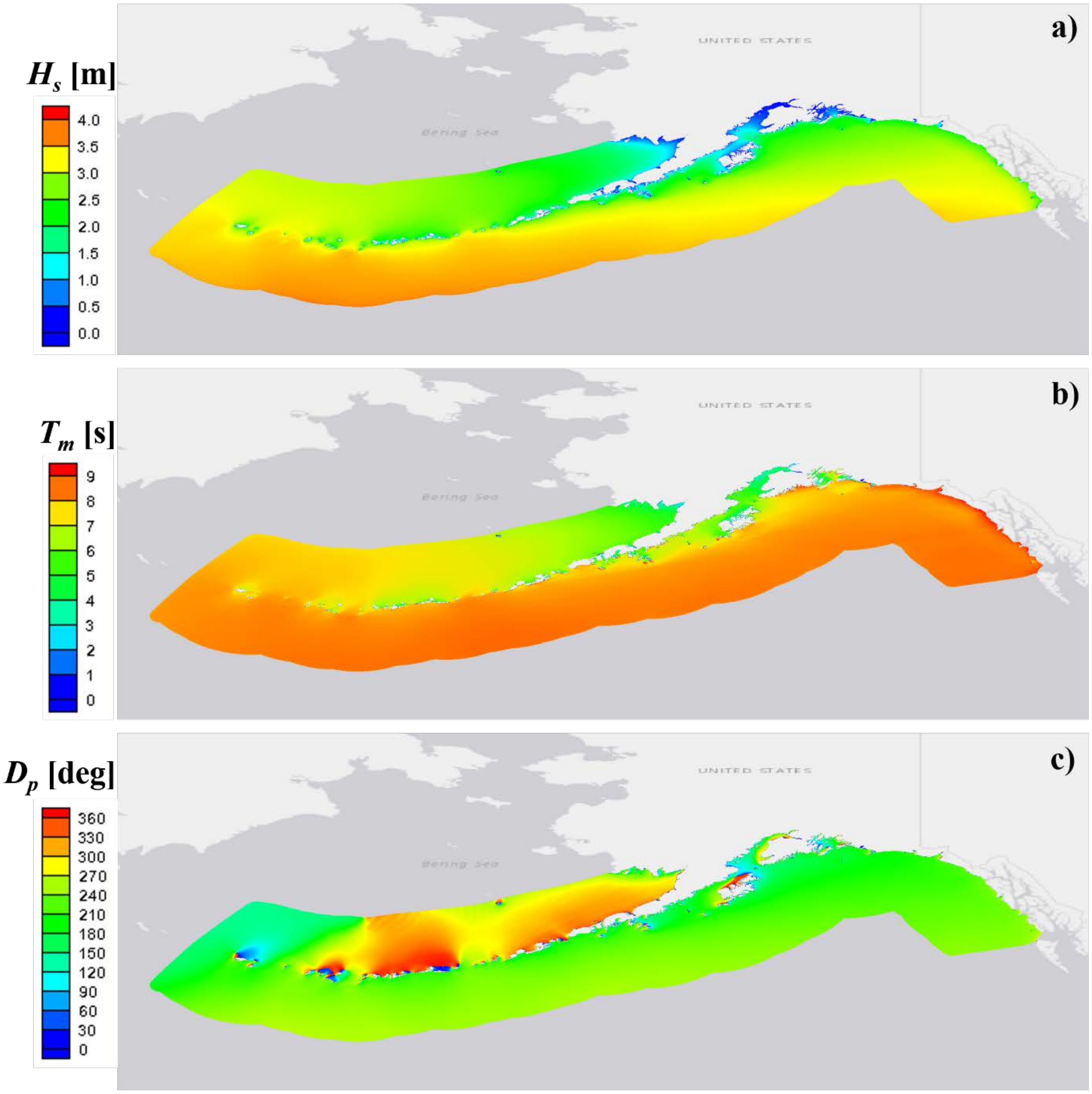

Figure A.39. Yearly distributions of three wave bulk parameters in 1984: (a) significant wave height, (b) mean wave period, and (c) peak wave direction on the Alaska Coast.

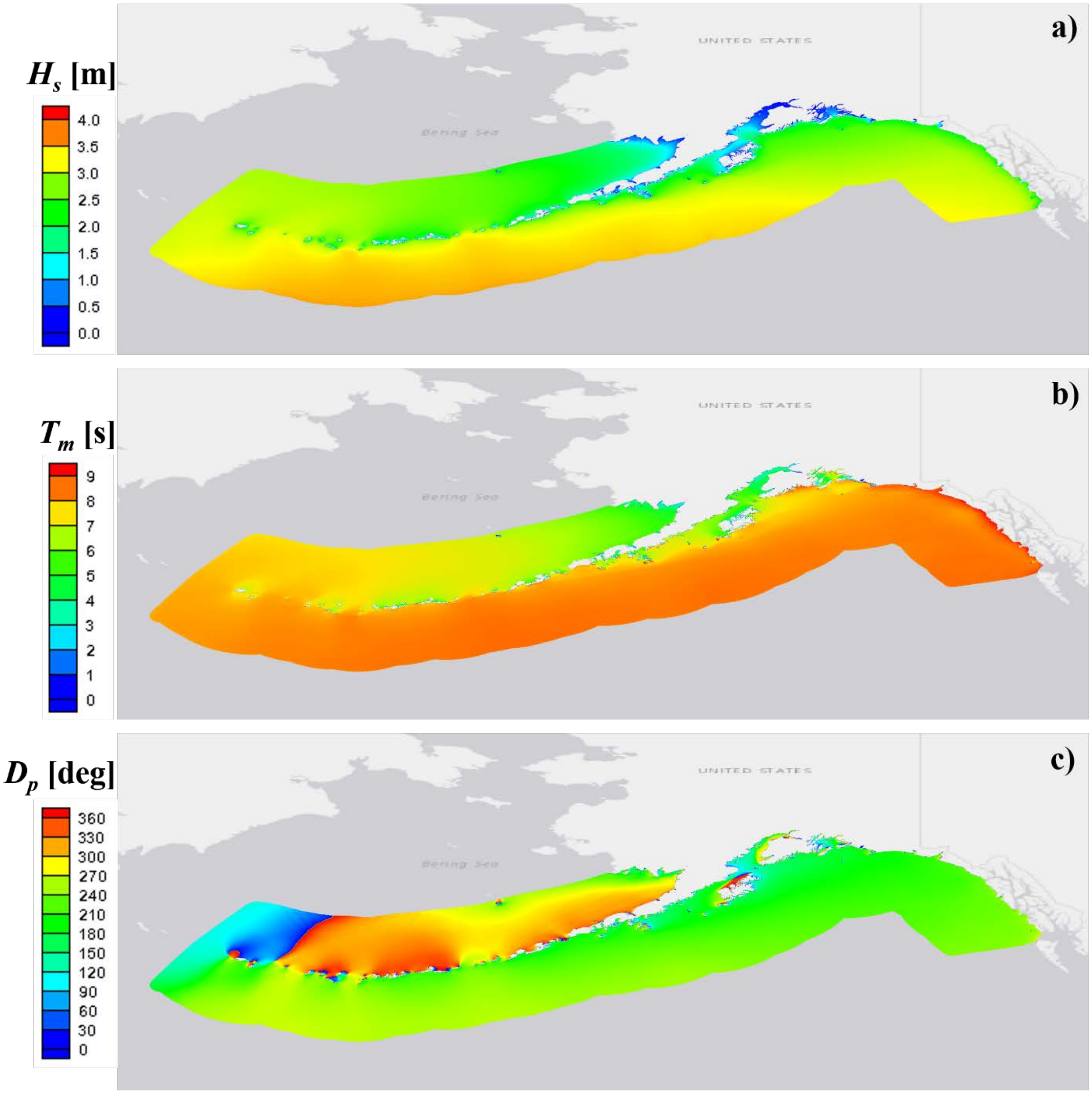

Figure A.40. Yearly distributions of three wave bulk parameters in 1983: (a) significant wave height, (b) mean wave period, and (c) peak wave direction on the Alaska Coast.

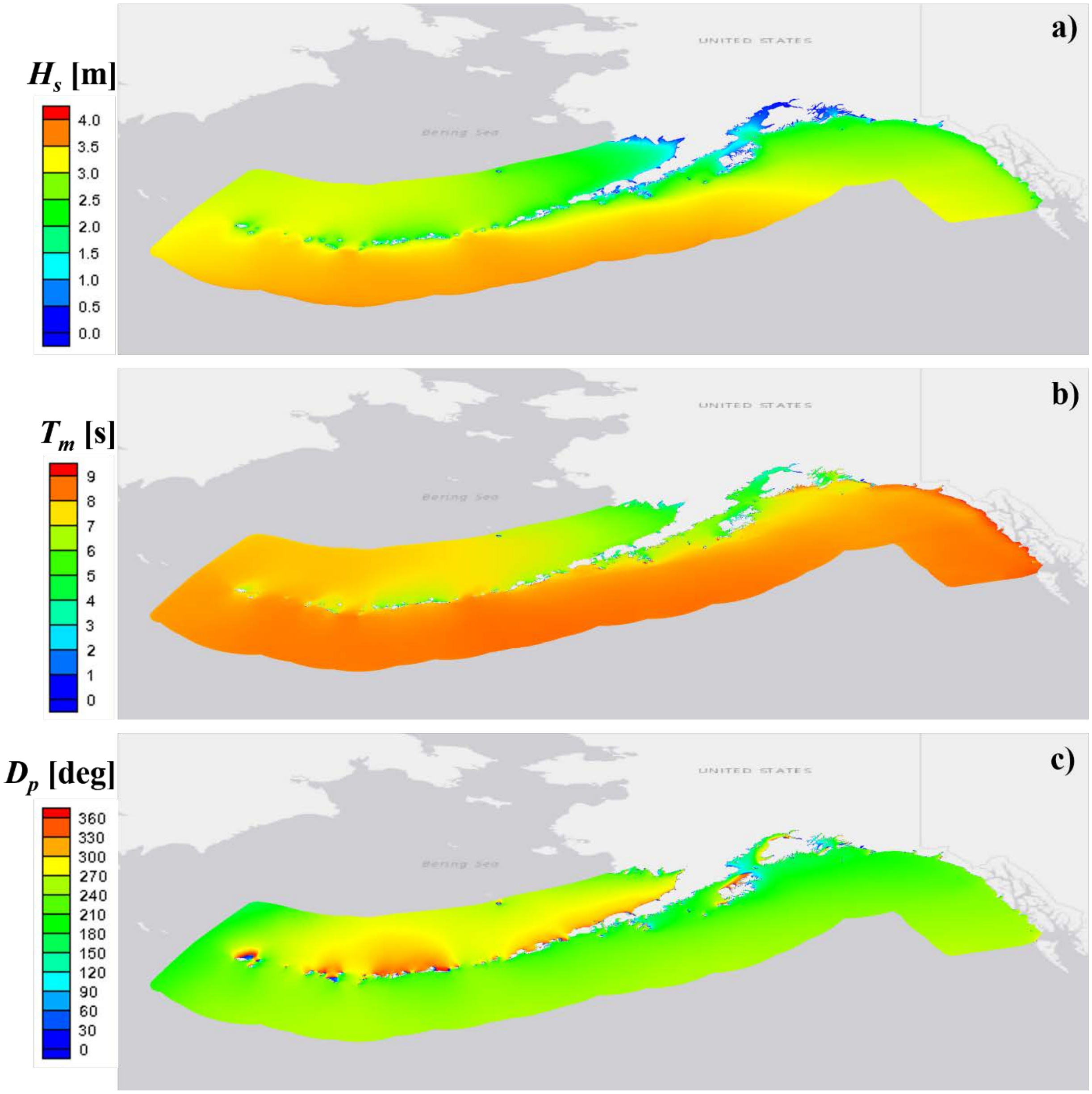

Figure A.41. Yearly distributions of three wave bulk parameters in 1982: (a) significant wave height, (b) mean wave period, and (c) peak wave direction on the Alaska Coast.

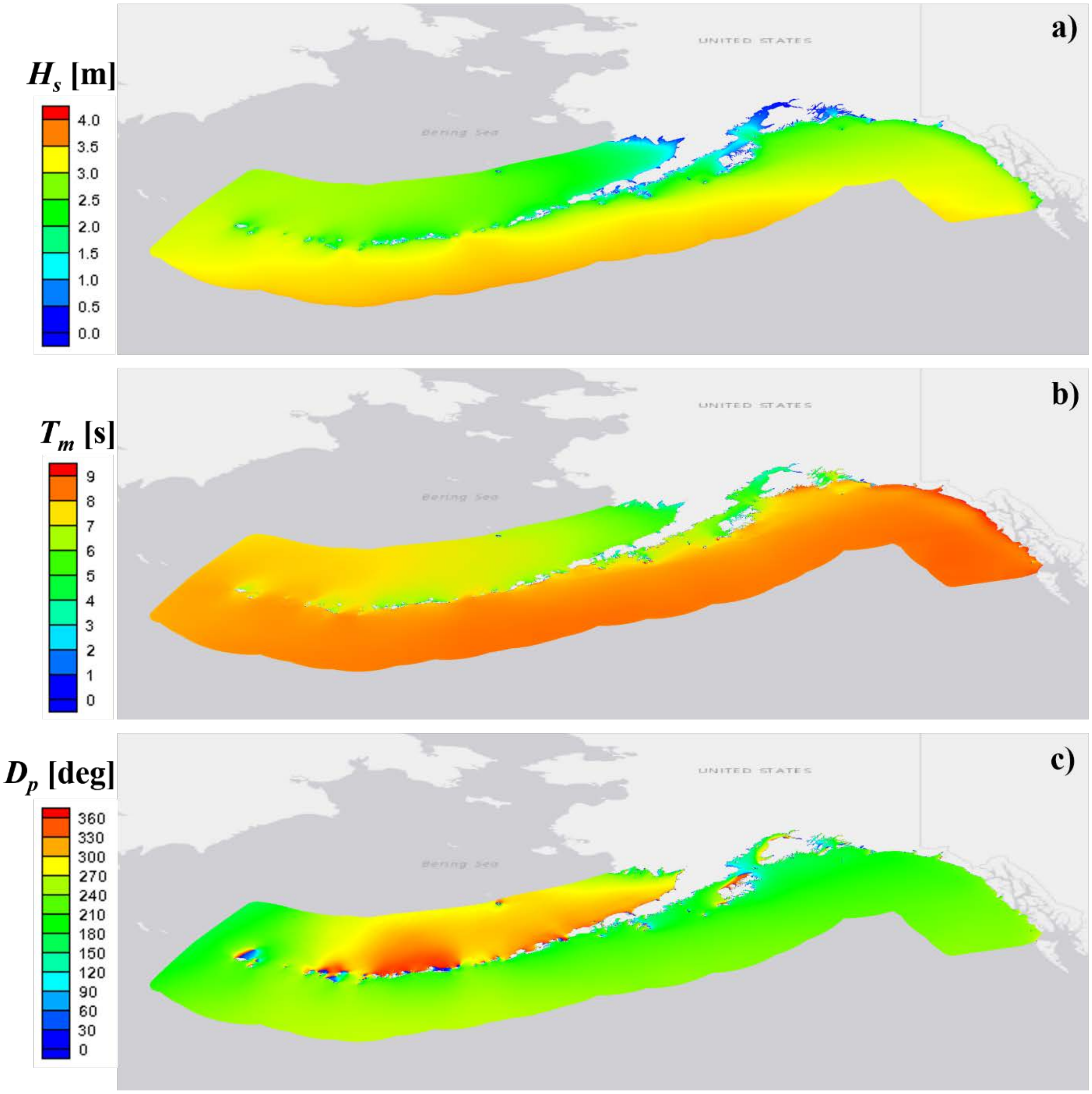

Figure A.42. Yearly distributions of three wave bulk parameters in 1981: (a) significant wave height, (b) mean wave period, and (c) peak wave direction on the Alaska Coast.

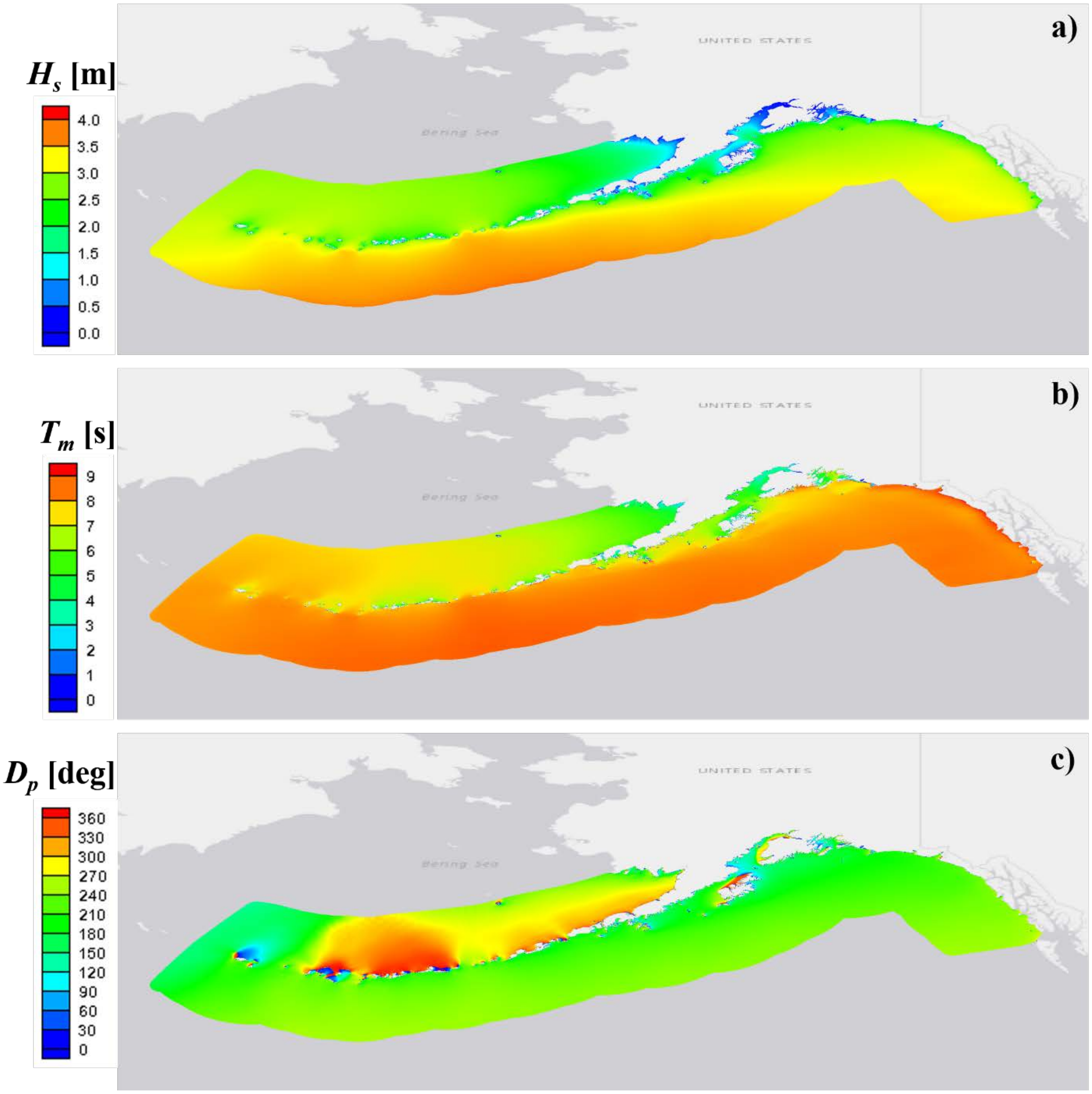

Figure A.43. Yearly distributions of three wave bulk parameters in 1980: (a) significant wave height, (b) mean wave period, and (c) peak wave direction on the Alaska Coast.

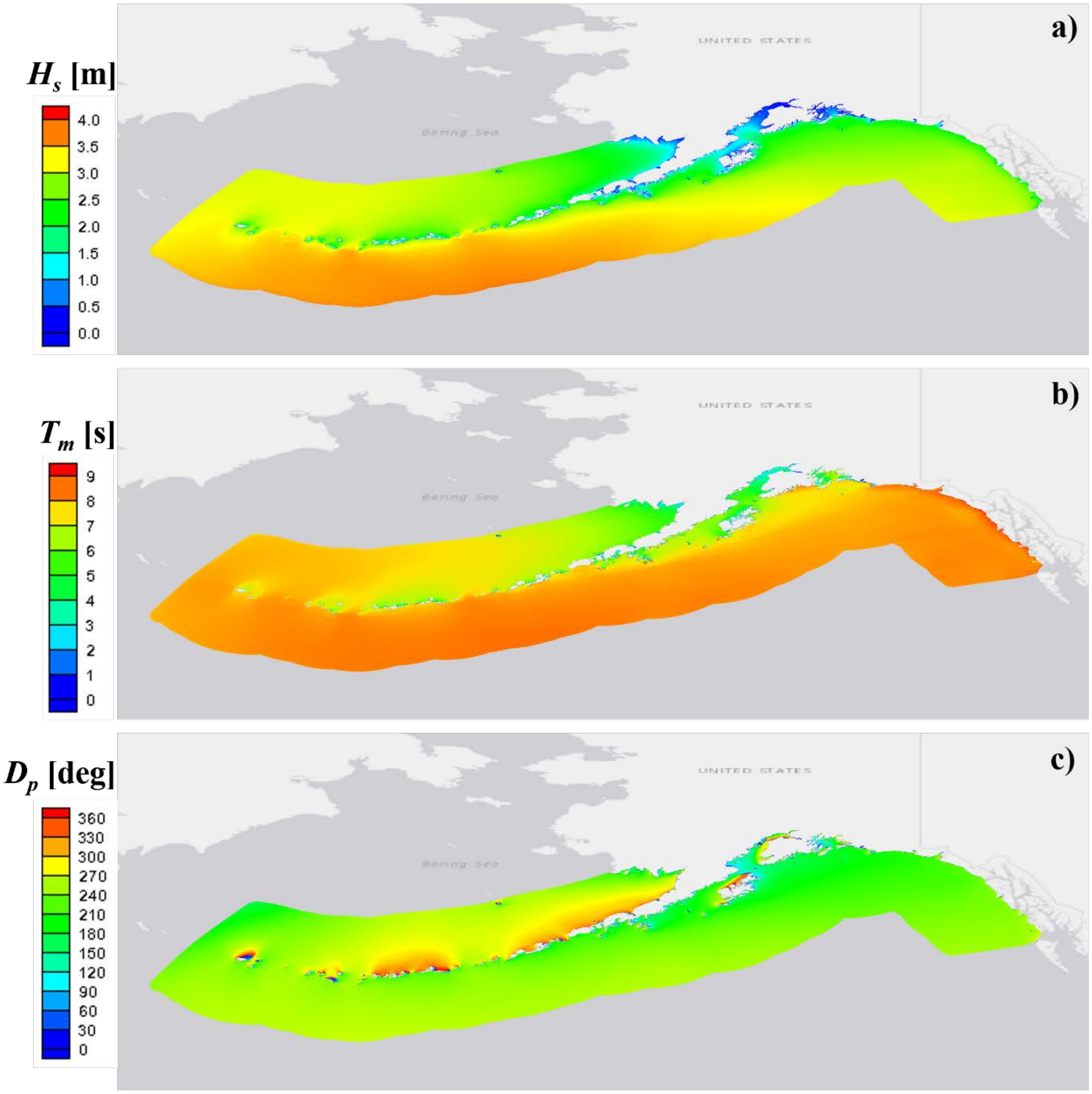

Figure A.44. Yearly distributions of three wave bulk parameters in 1979: (a) significant wave height, (b) mean wave period, and (c) peak wave direction on the Alaska Coast.

Appendix B – Comparisons of Model-Simulated Wave Bulk Parameters with Buoy Data

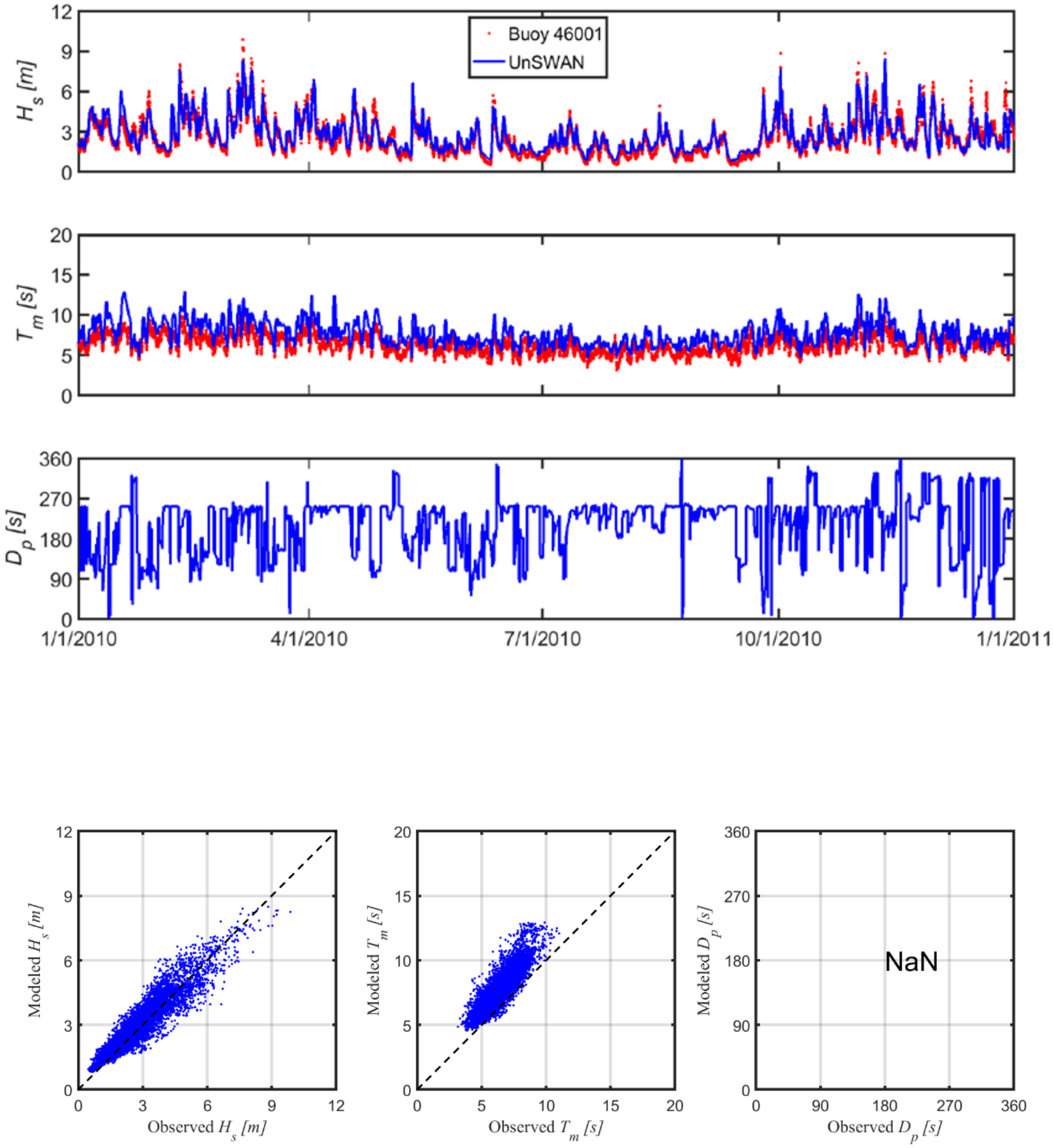

Figure B.1. Comparisons of time series (top) and scatter plots (bottom) of the three UnSWAN model-simulated bulk parameters with observed data at NDBC Buoy 46001 for 2010.

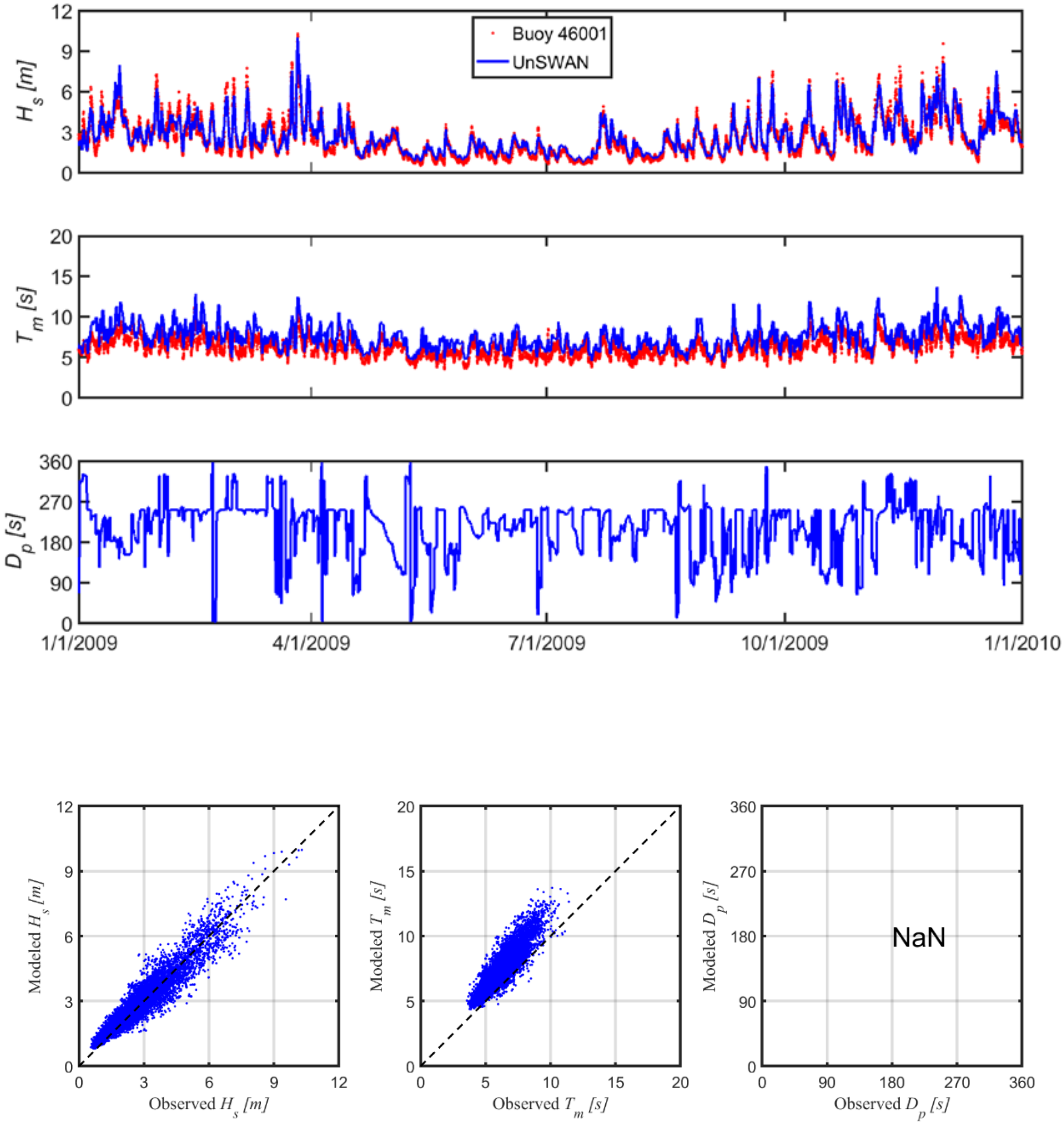

Figure B.2. Comparisons of time series (top) and scatter plots (bottom) of the three UnSWAN model-simulated bulk parameters with observed data at NDBC Buoy 46001 for 2009.

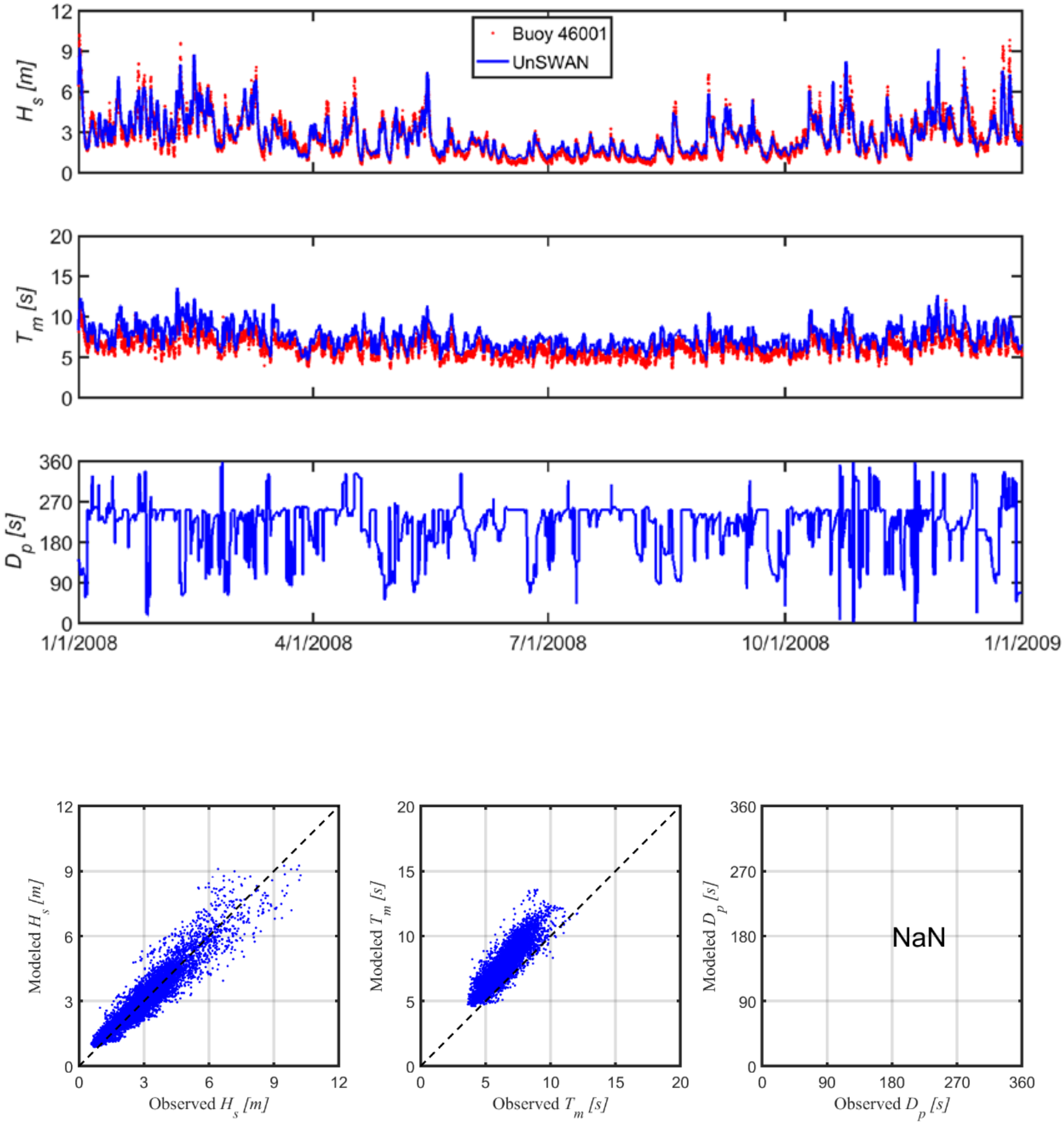

Figure B.3. Comparisons of time series (top) and scatter plots (bottom) of the three UnSWAN model-simulated bulk parameters with observed data at NDBC Buoy 46001 for 2008.

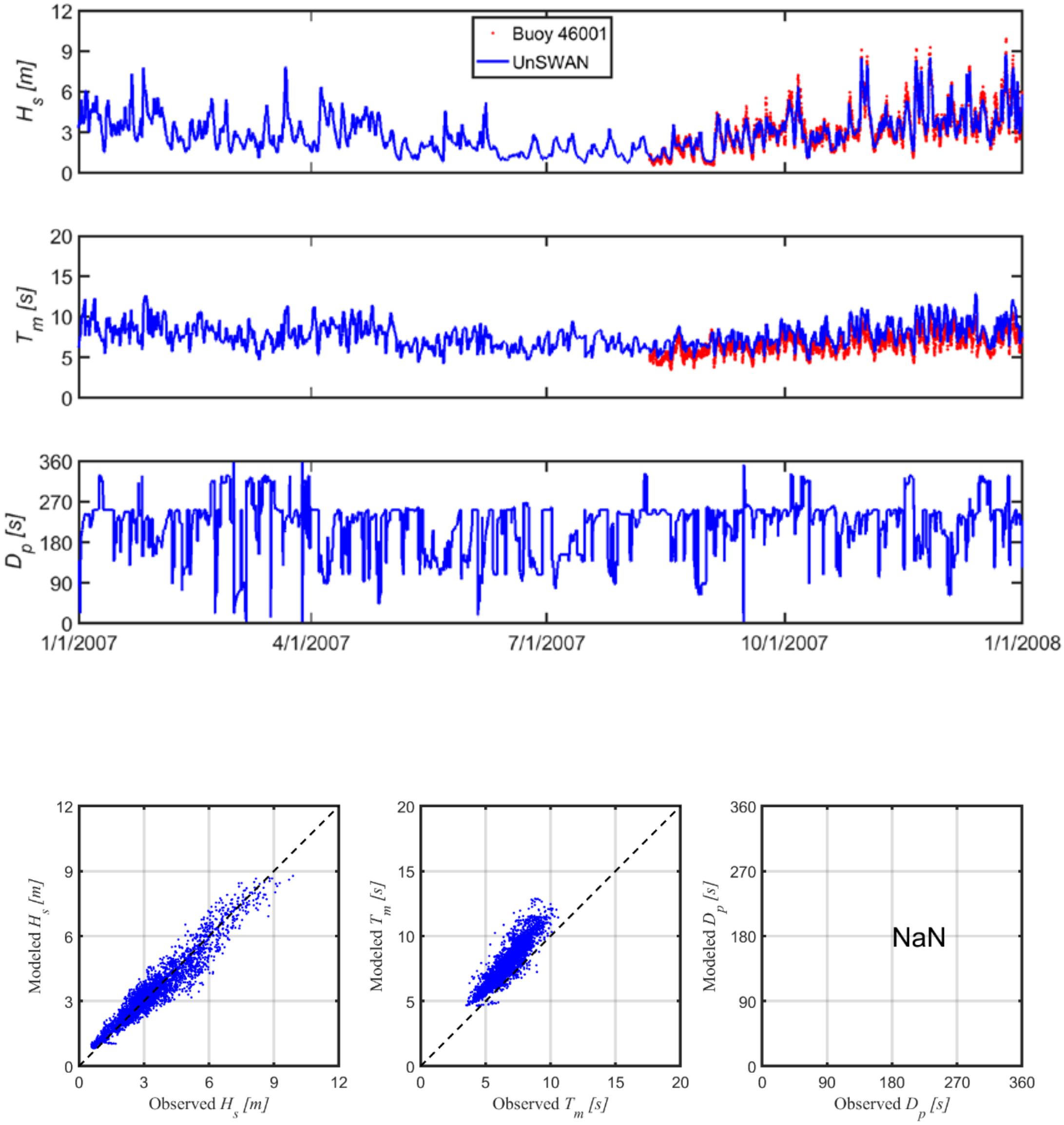

Figure B.4. Comparisons of time series (top) and scatter plots (bottom) of the three UnSWAN model-simulated bulk parameters with observed data at NDBC Buoy 46001 for 2007.

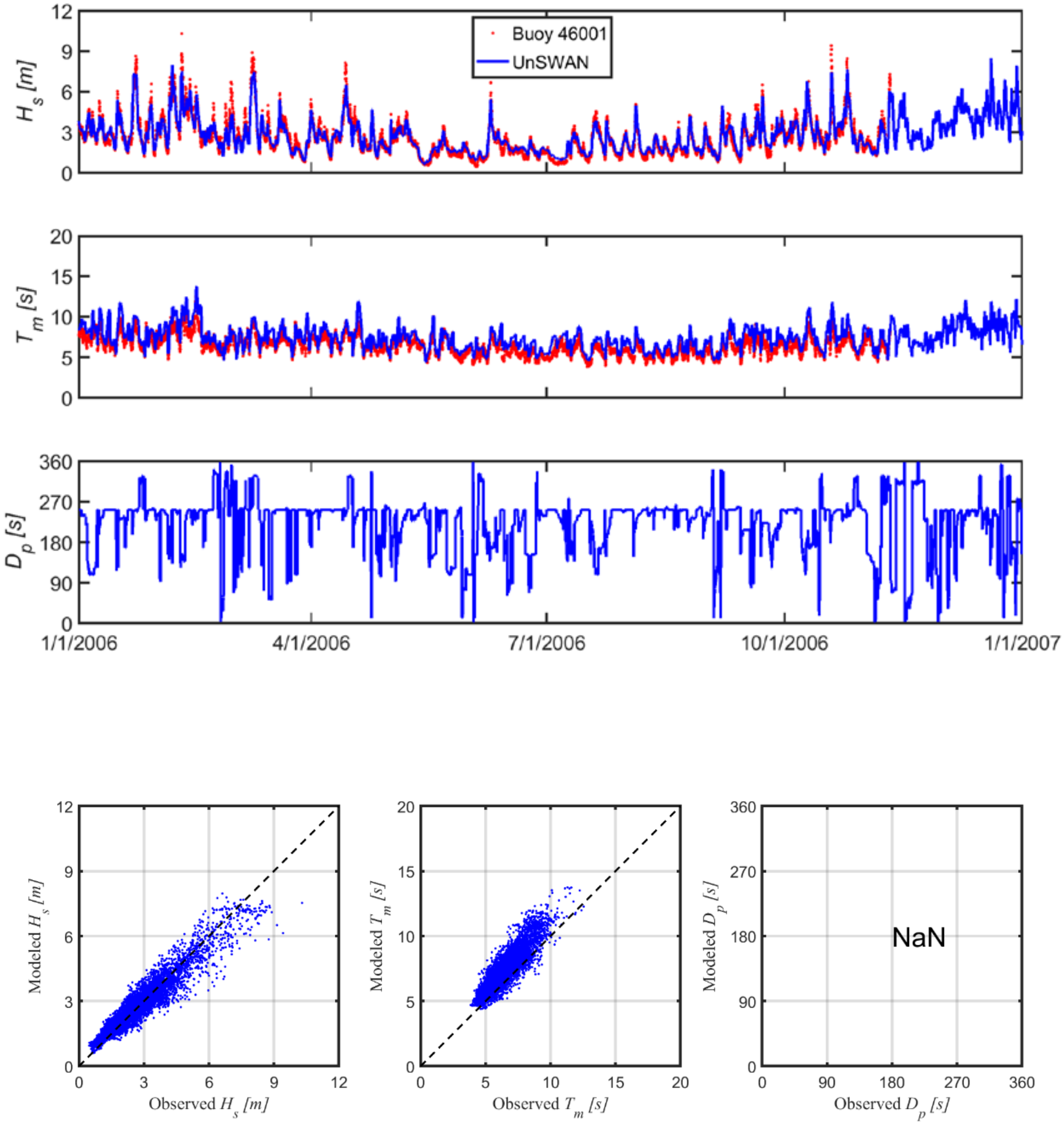

Figure B.5. Comparisons of time series (top) and scatter plots (bottom) of the three UnSWAN model-simulated bulk parameters with observed data at NDBC Buoy 46001 for 2006.

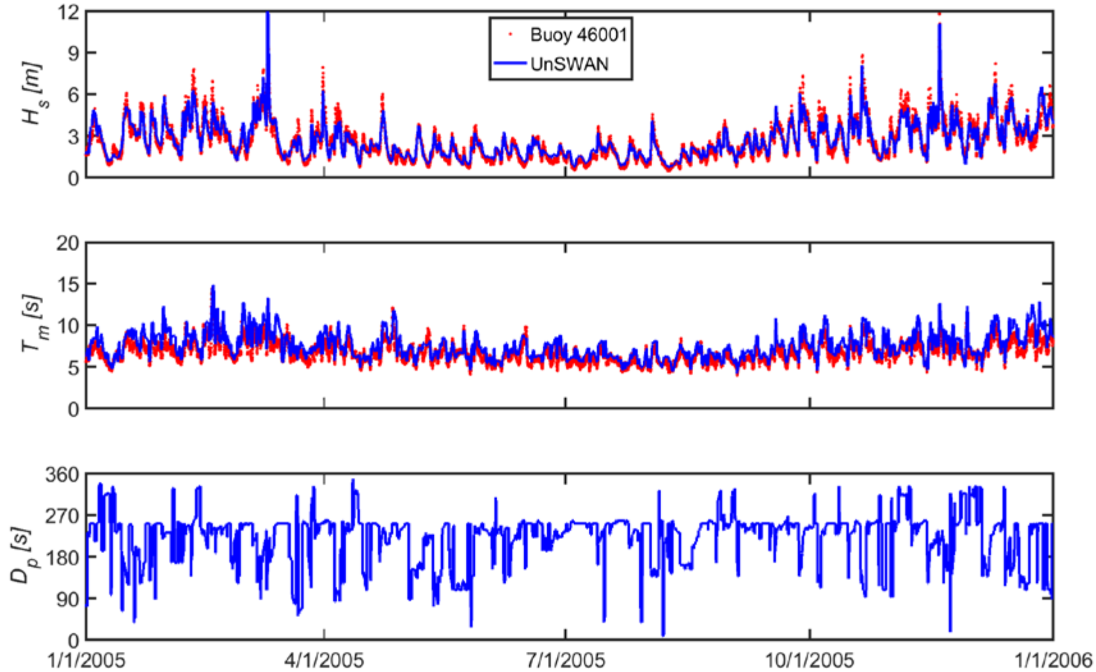

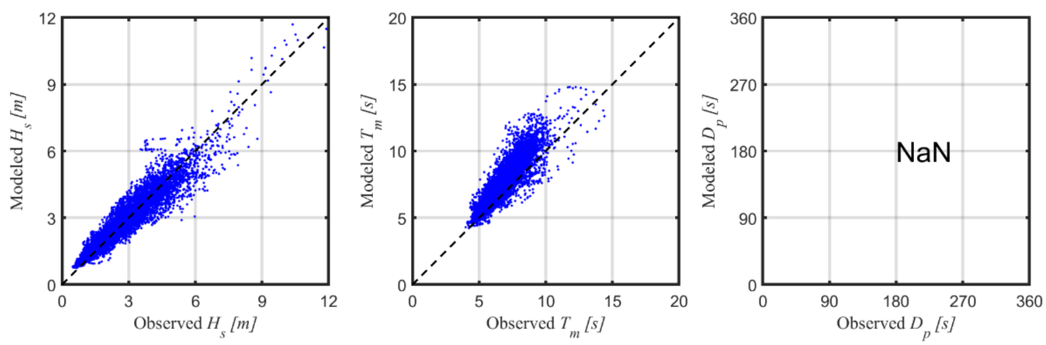

Figure B.6. Comparisons of time series (top) and scatter plots (bottom) of the three UnSWAN model-simulated bulk parameters with observed data at NDBC Buoy 46001 for 2005.

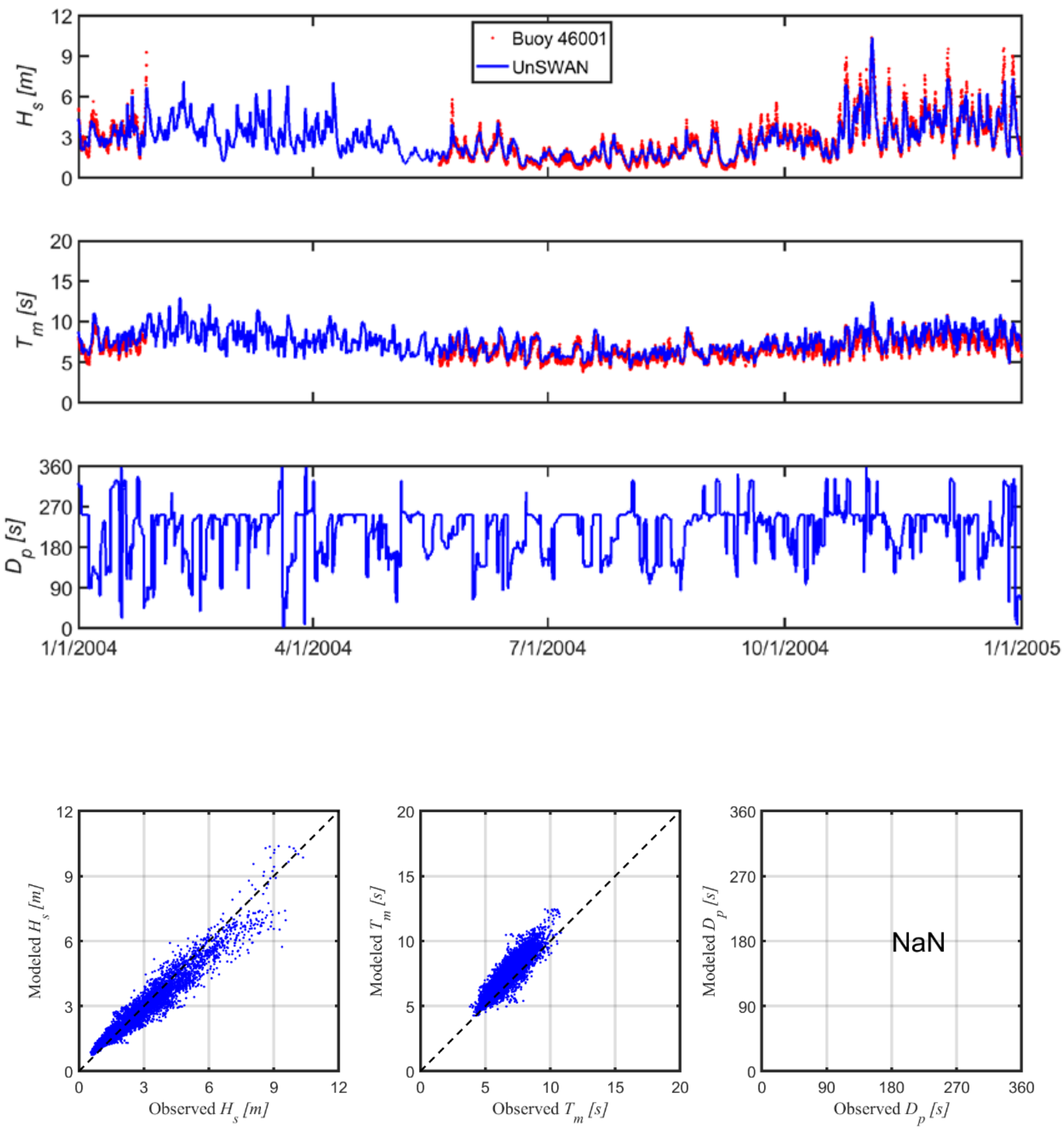

Figure B.7. Comparisons of time series (top) and scatter plots (bottom) of the three UnSWAN model-simulated bulk parameters with observed data at NDBC Buoy 46001 for 2004.

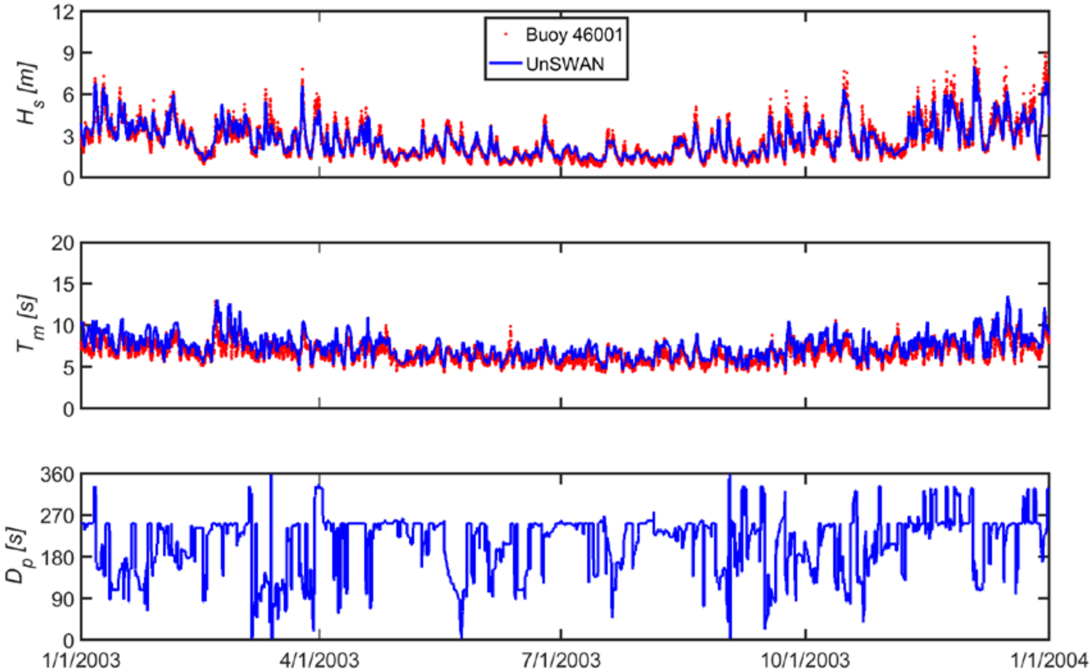

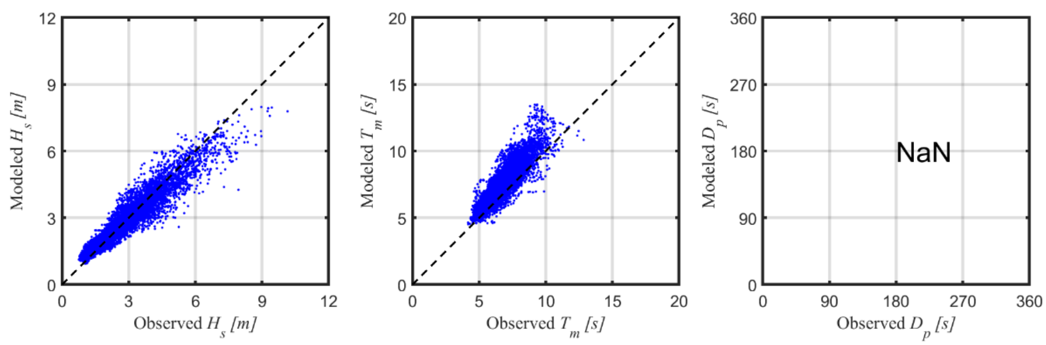

Figure B.8. Comparisons of time series (top) and scatter plots (bottom) of the three UnSWAN model-simulated bulk parameters with observed data at NDBC Buoy 46001 for 2003.

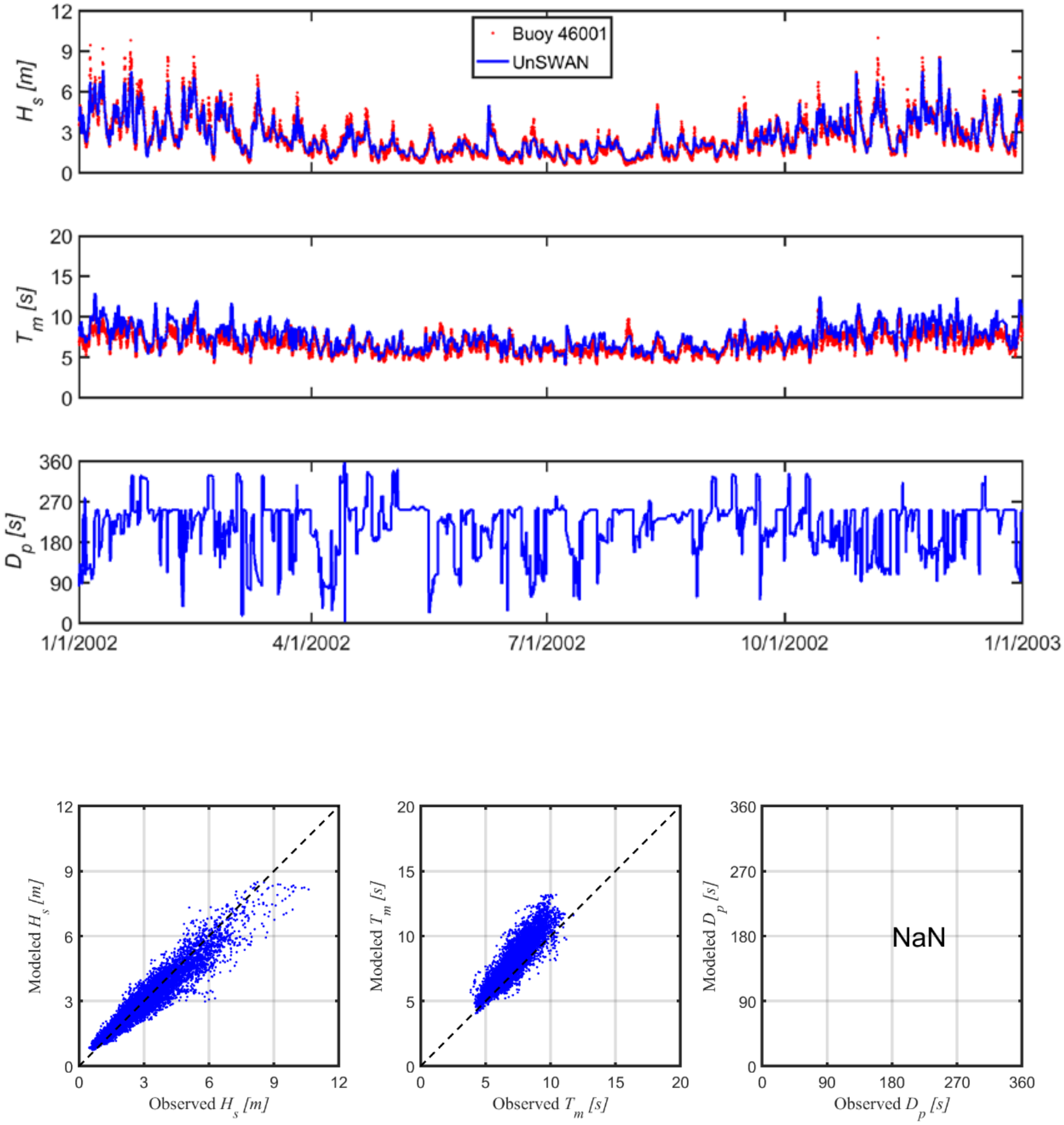

Figure B.9. Comparisons of time series (top) and scatter plots (bottom) of the three UnSWAN model-simulated bulk parameters with observed data at NDBC Buoy 46001 for 2002.

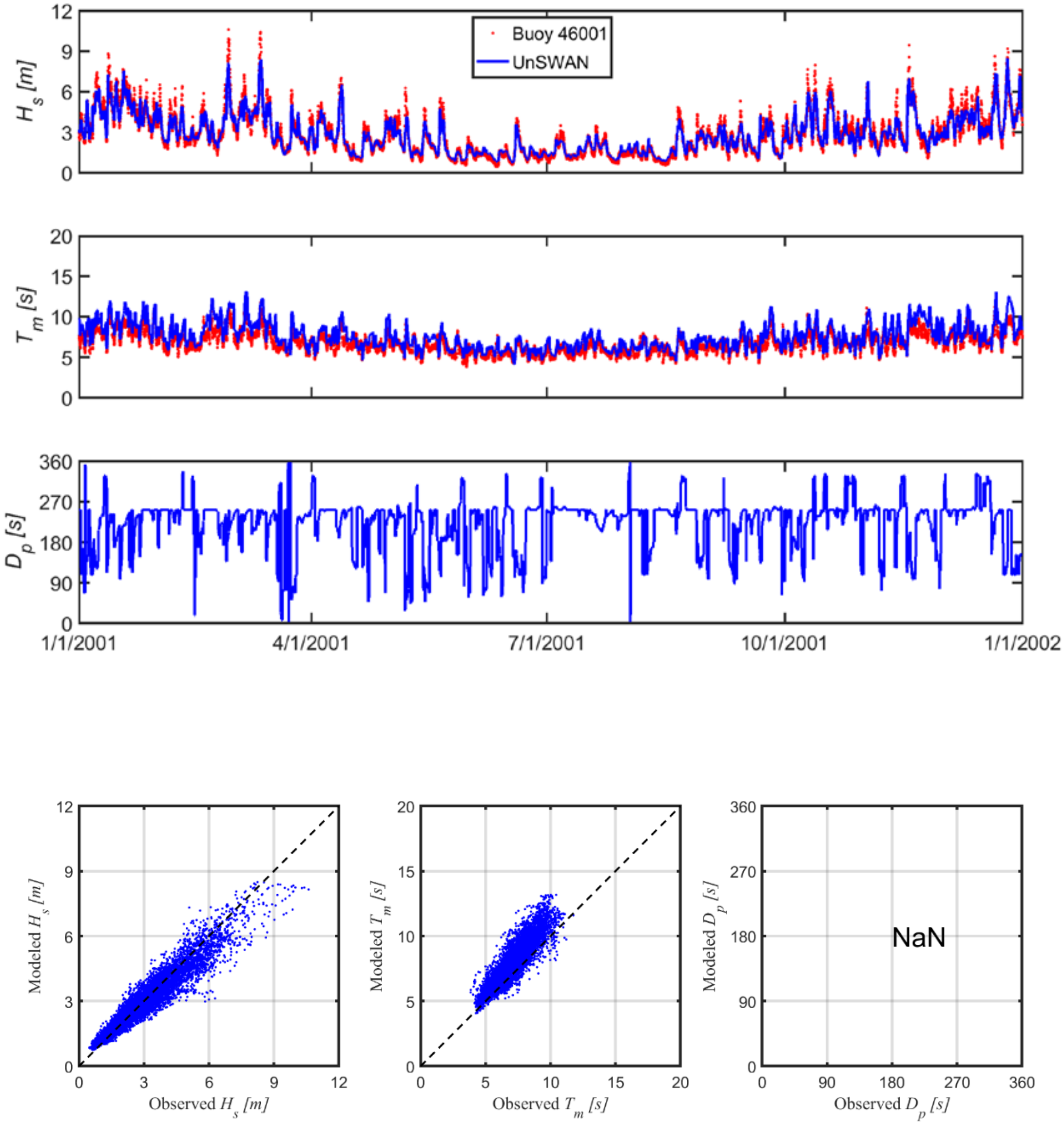

Figure B.10. Comparisons of time series (top) and scatter plots (bottom) of the three UnSWAN model-simulated bulk parameters with observed data at NDBC Buoy 46001 for 2001.

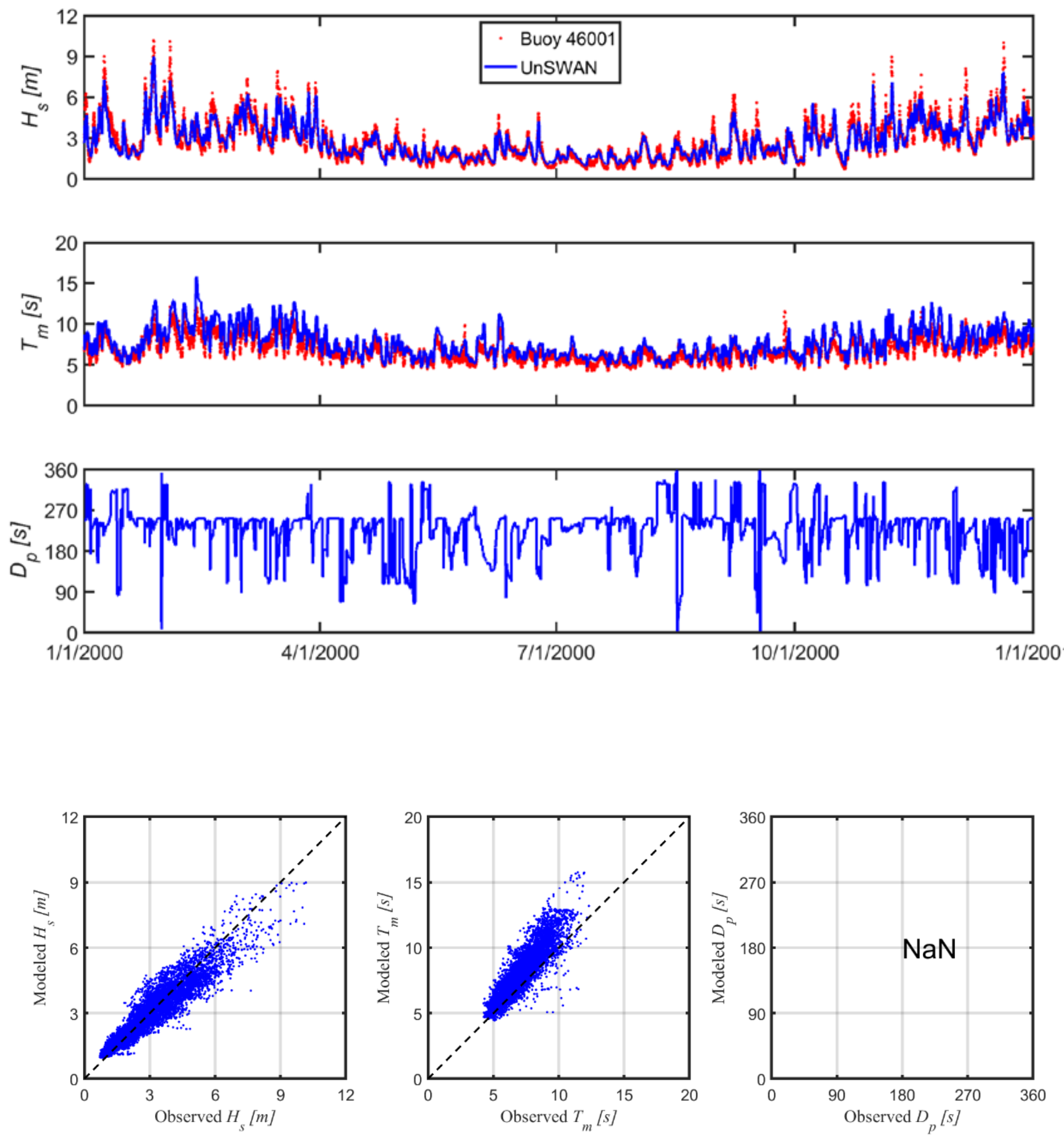

Figure B.11. Comparisons of time series (top) and scatter plots (bottom) of the three UnSWAN model-simulated bulk parameters with observed data at NDBC Buoy 46001 for 2000.

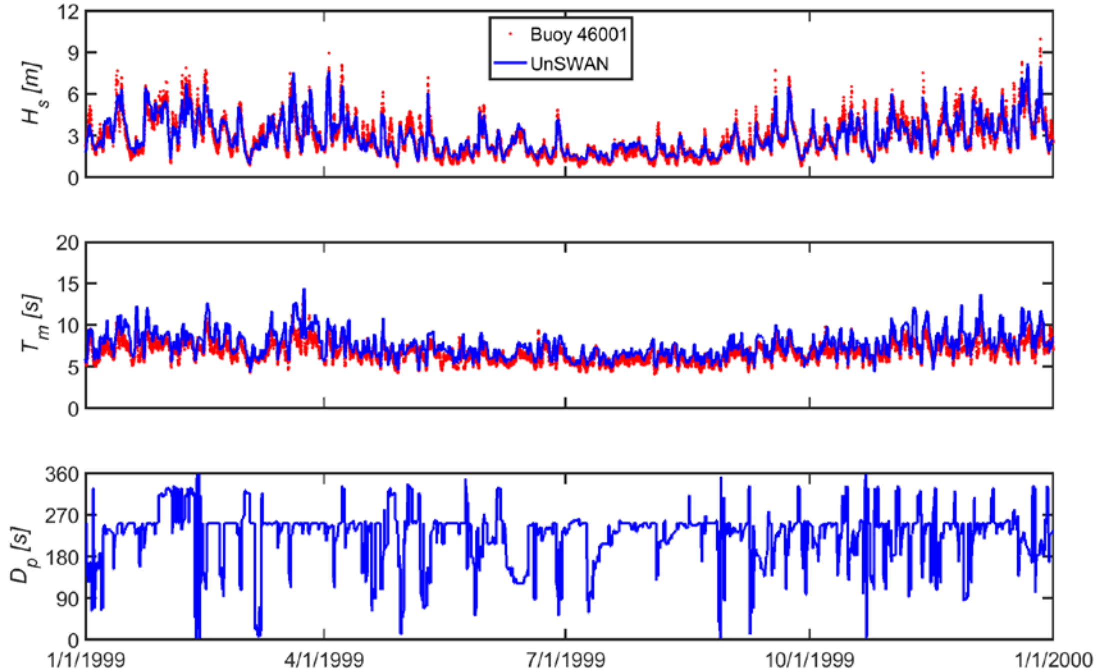

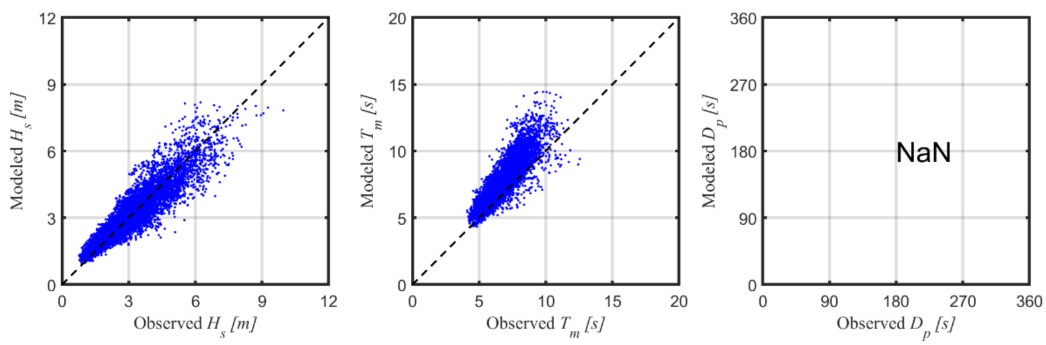

Figure B.12. Comparisons of time series (top) and scatter plots (bottom) of the three UnSWAN model-simulated bulk parameters with observed data at NDBC Buoy 46001 for 1999.

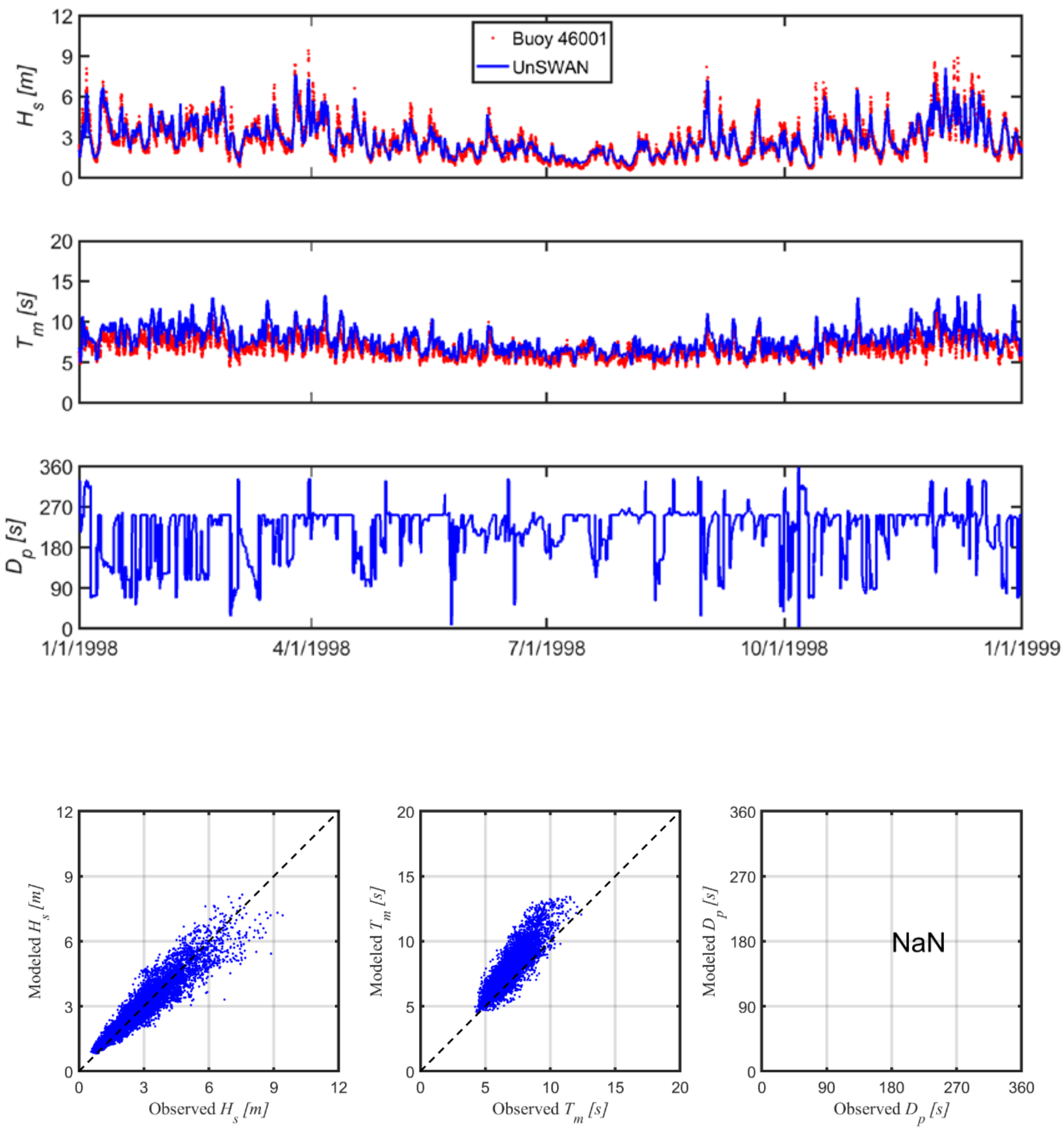

Figure B.13. Comparisons of time series (top) and scatter plots (bottom) of the three UnSWAN model-simulated bulk parameters with observed data at NDBC Buoy 46001 for 1998.

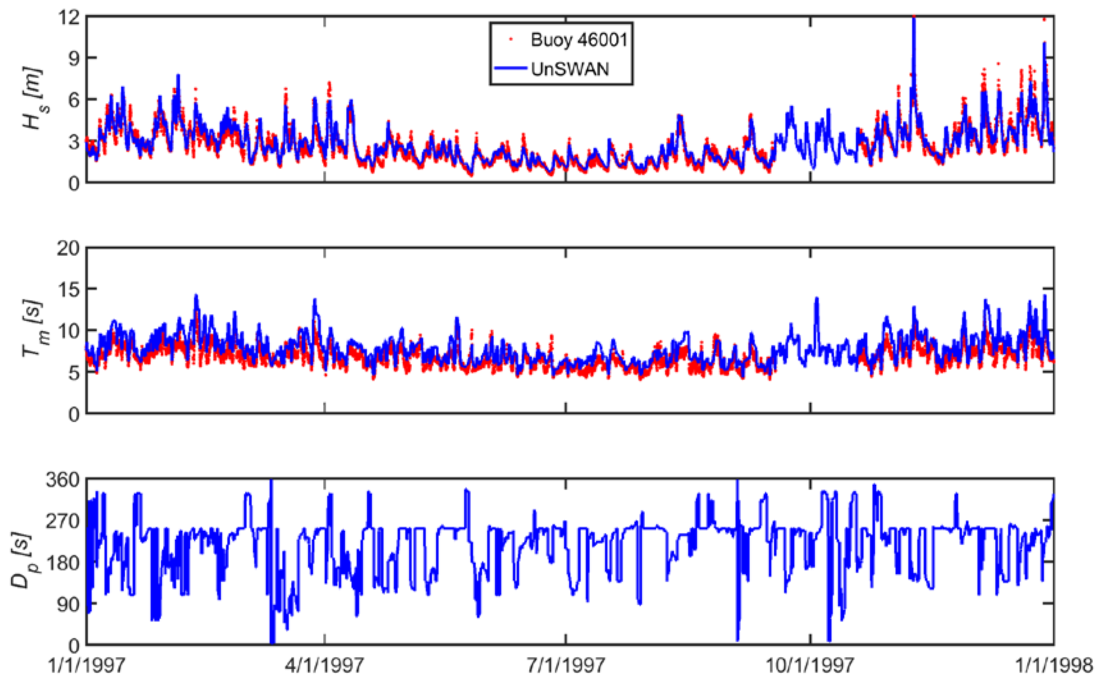

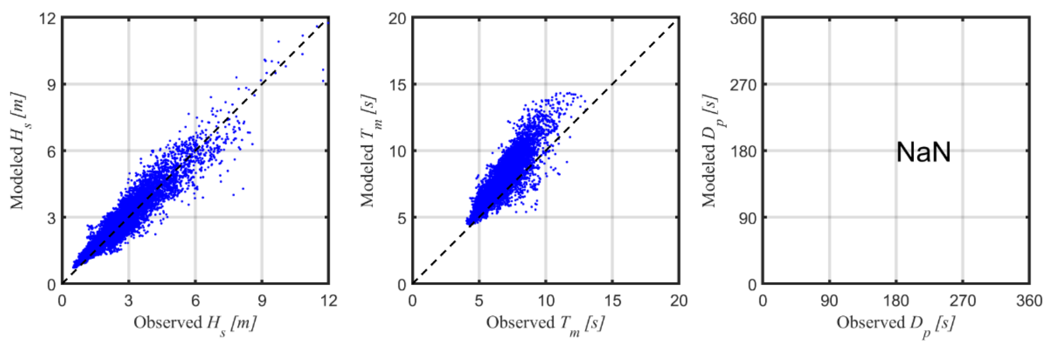

Figure B.14. Comparisons of time series (top) and scatter plots (bottom) of the three UnSWAN model-simulated bulk parameters with observed data at NDBC Buoy 46001 for 1997.

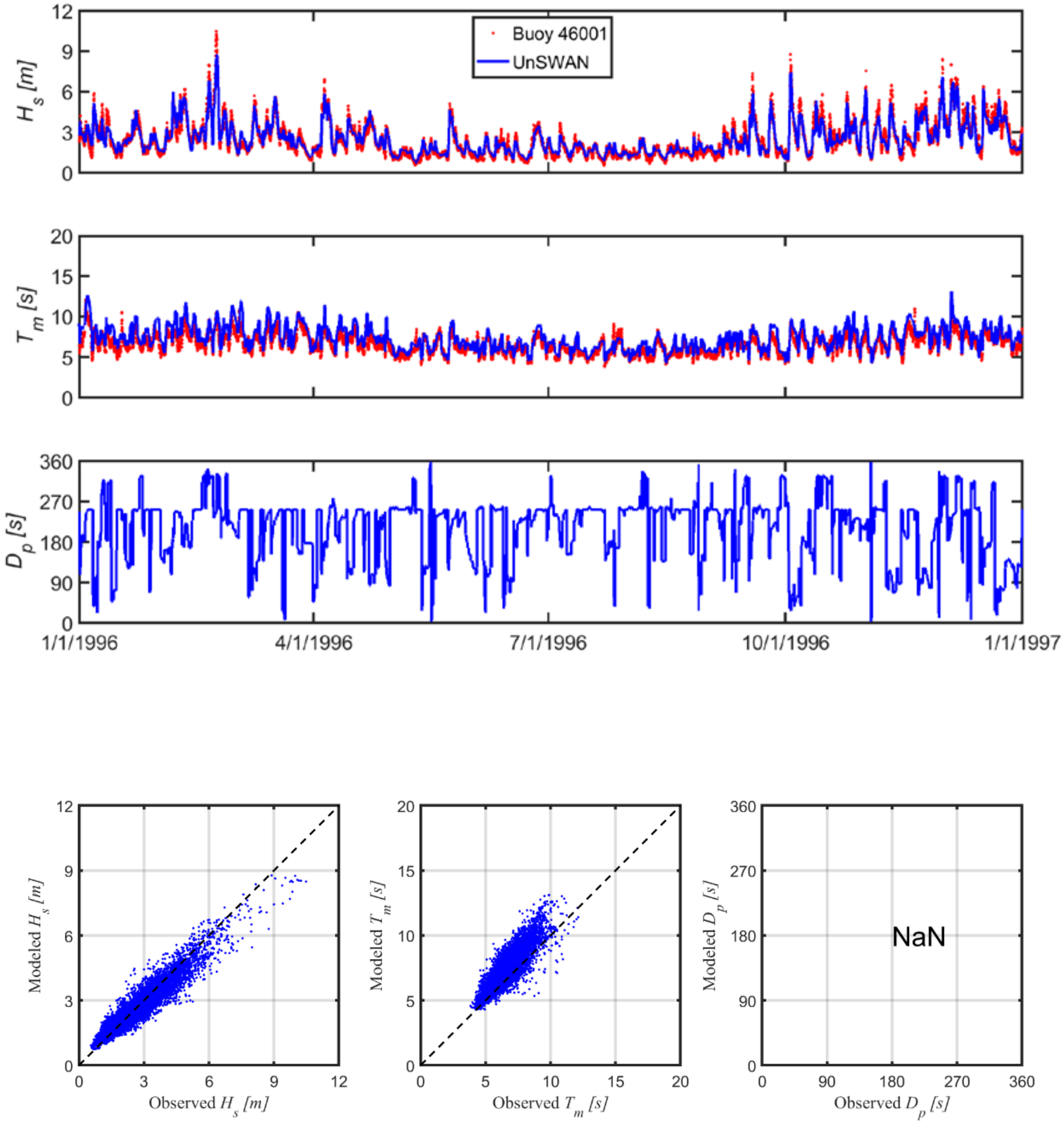

Figure B.15. Comparisons of time series (top) and scatter plots (bottom) of the three UnSWAN model-simulated bulk parameters with observed data at NDBC Buoy 46001 for 1996.

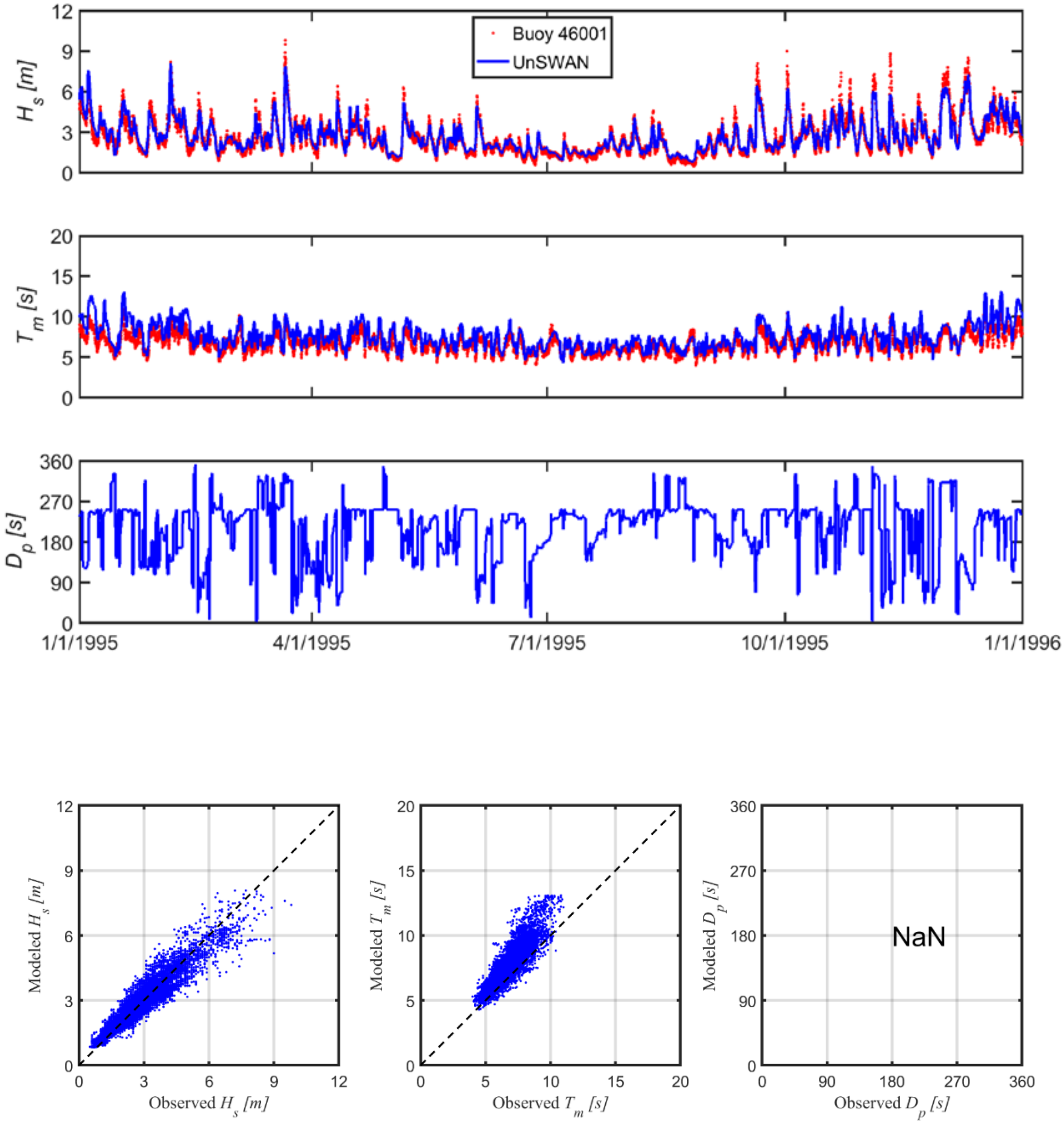

Figure B.16. Comparisons of time series (top) and scatter plots (bottom) of the three UnSWAN model-simulated bulk parameters with observed data at NDBC Buoy 46001 for 1995.

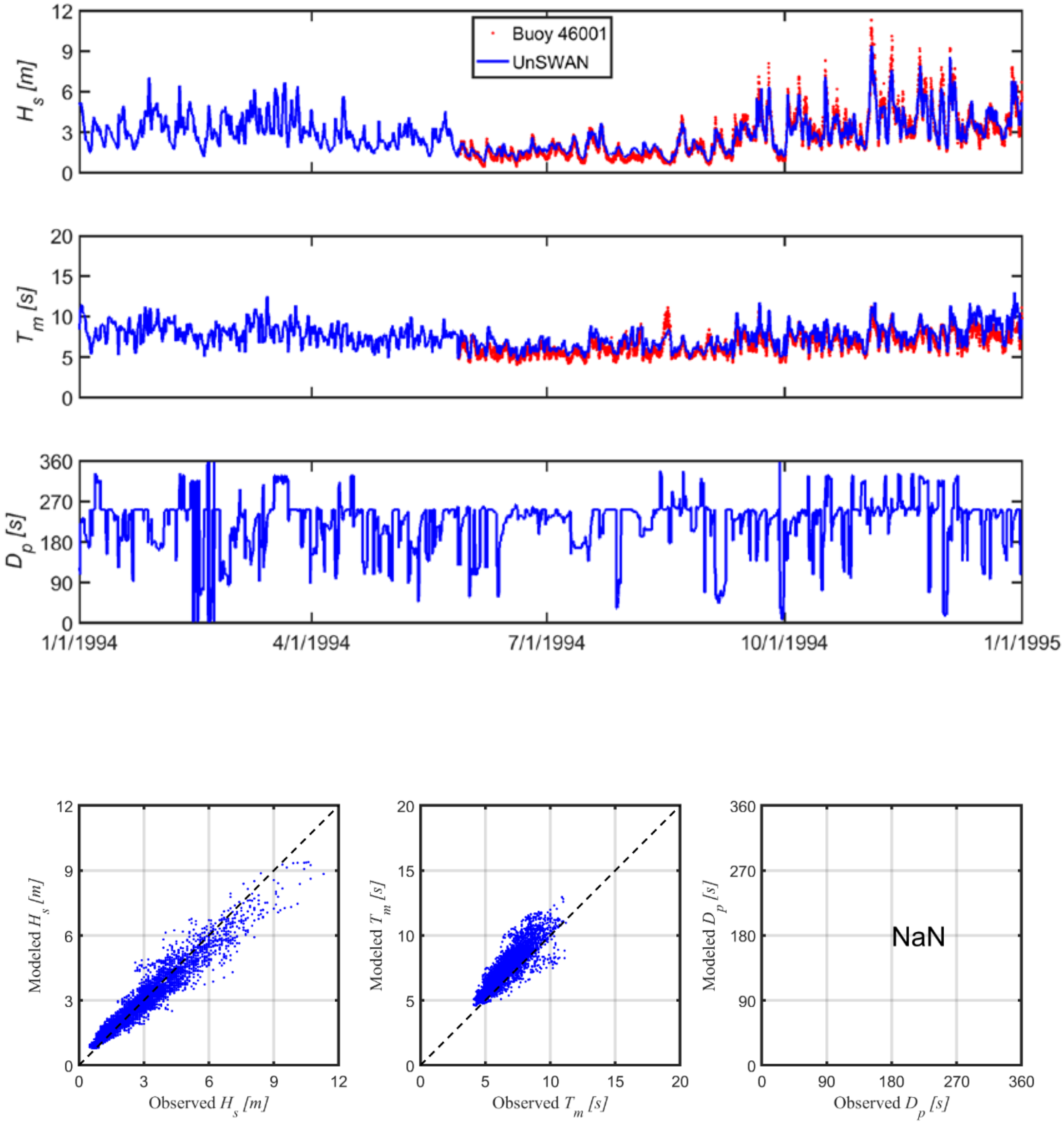

Figure B.17. Comparisons of time series (top) and scatter plots (bottom) of the three UnSWAN model-simulated bulk parameters with observed data at NDBC Buoy 46001 for 1994.

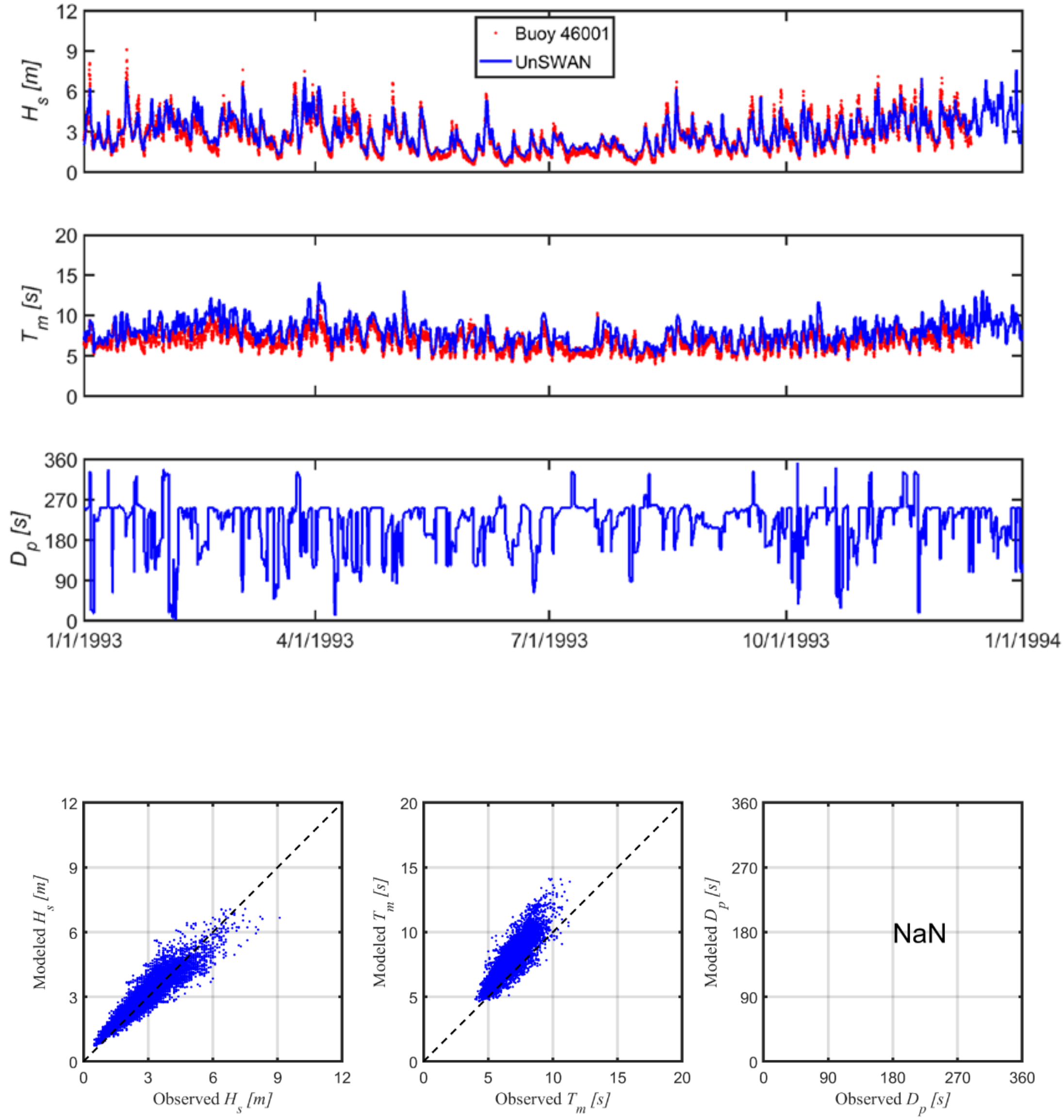

Figure B.18. Comparisons of time series (top) and scatter plots (bottom) of the three UnSWAN model-simulated bulk parameters with observed data at NDBC Buoy 46001 for 1993.

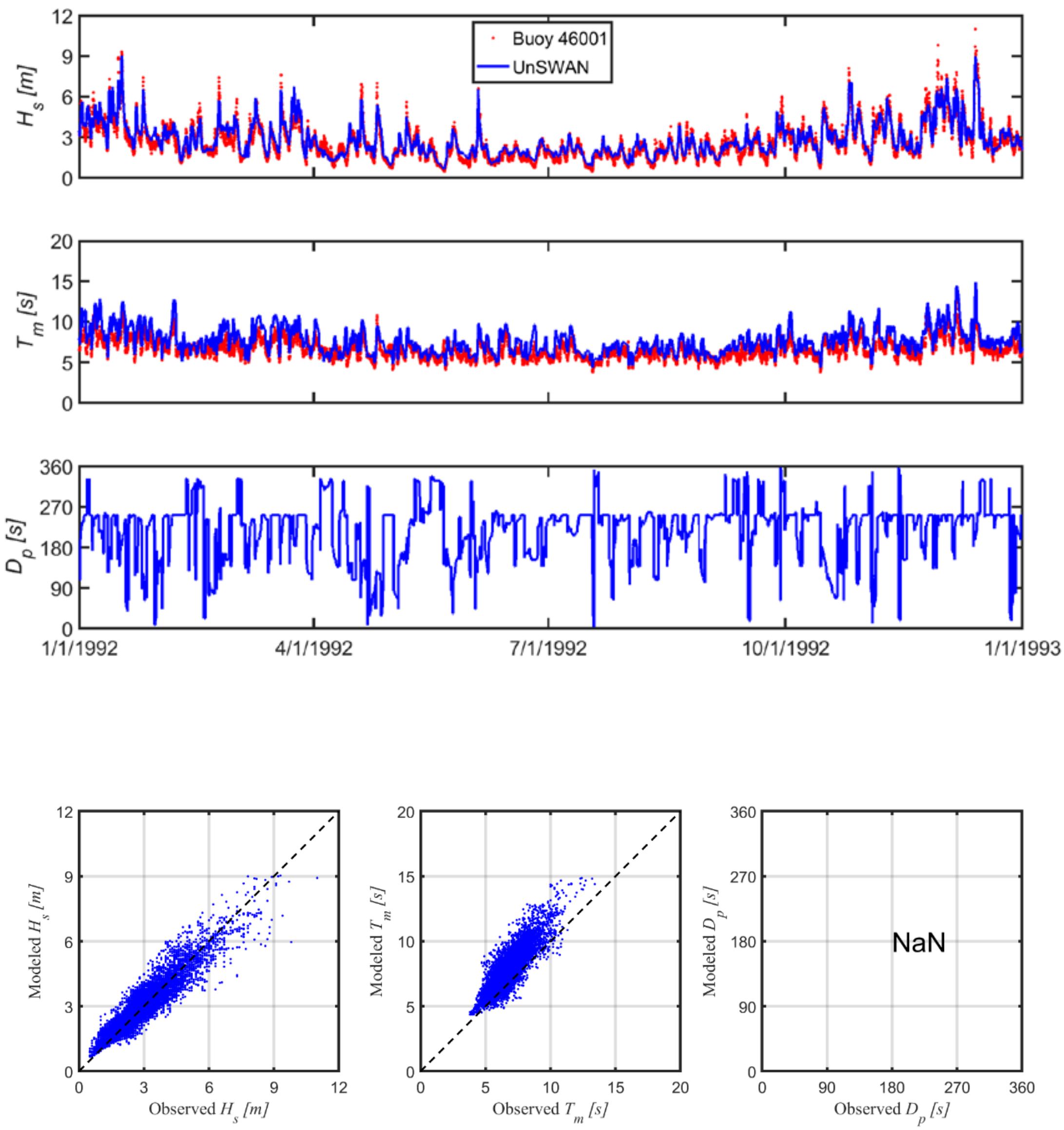

Figure B.19. Comparisons of time series (top) and scatter plots (bottom) of the three UnSWAN model-simulated bulk parameters with observed data at NDBC Buoy 46001 for 1992.

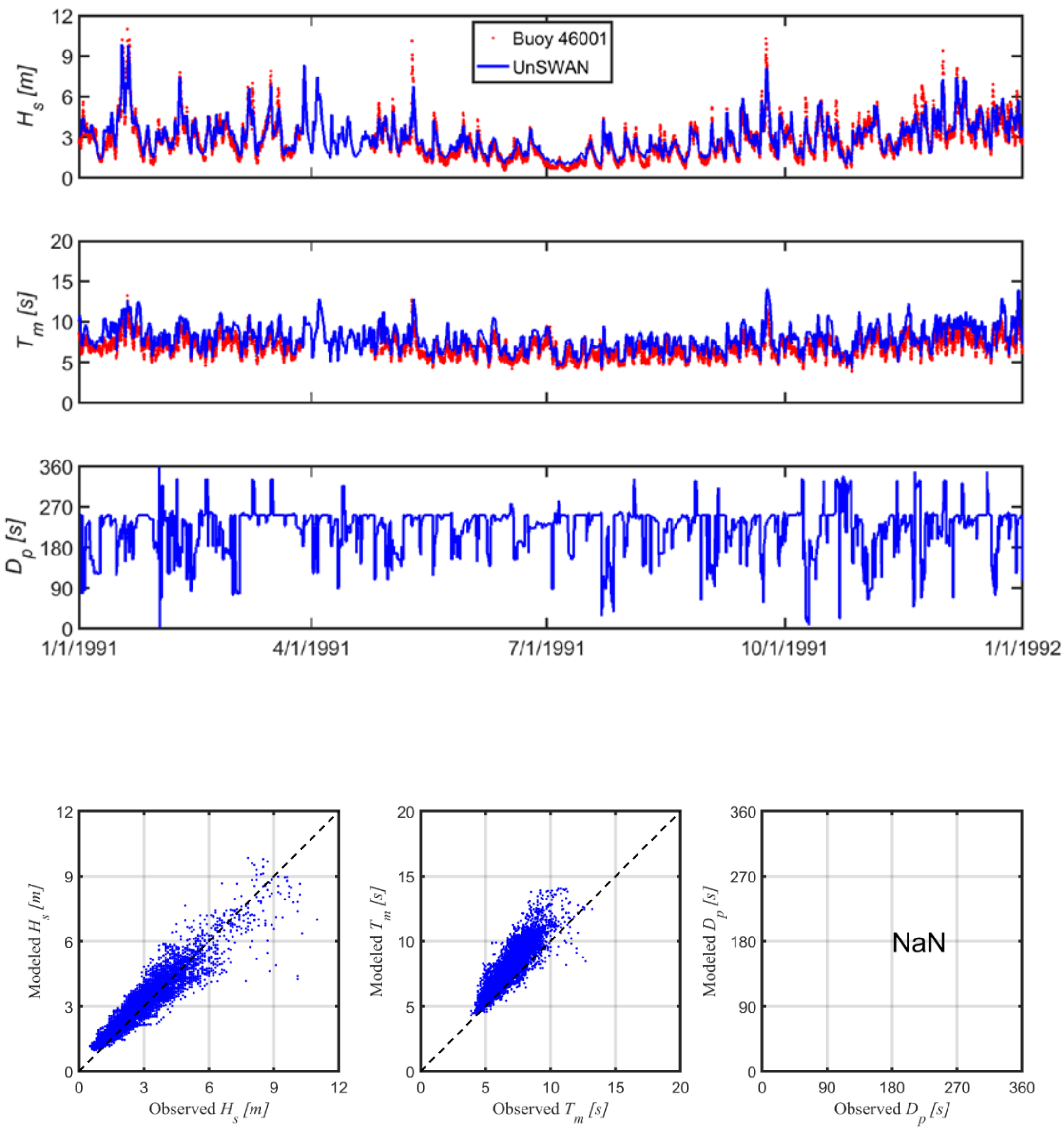

Figure B.20. Comparisons of time series (top) and scatter plots (bottom) of the three UnSWAN model-simulated bulk parameters with observed data at NDBC Buoy 46001 for 1991.

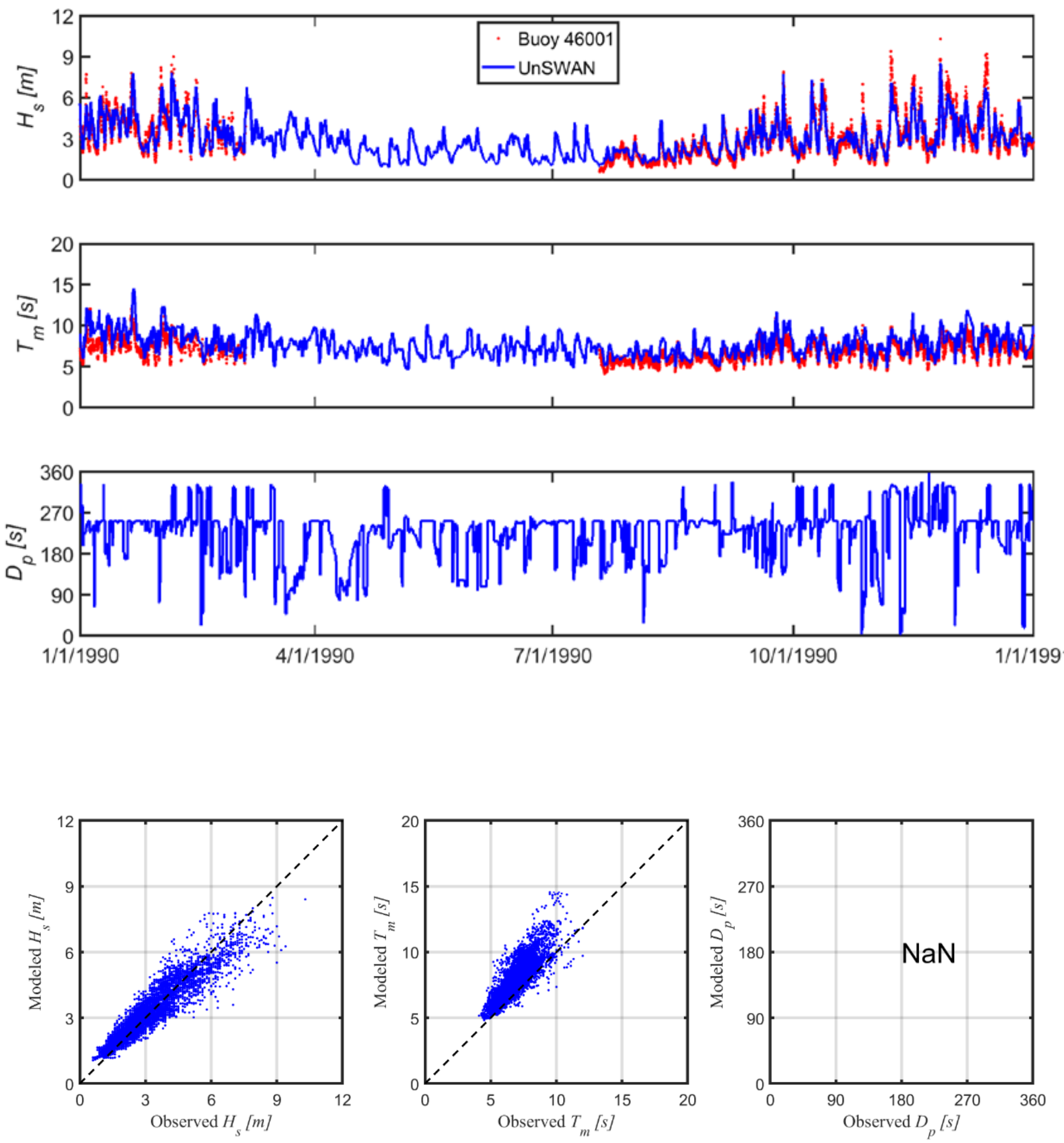

Figure B.21. Comparisons of time series (top) and scatter plots (bottom) of the three UnSWAN model-simulated bulk parameters with observed data at NDBC Buoy 46001 for 1990.

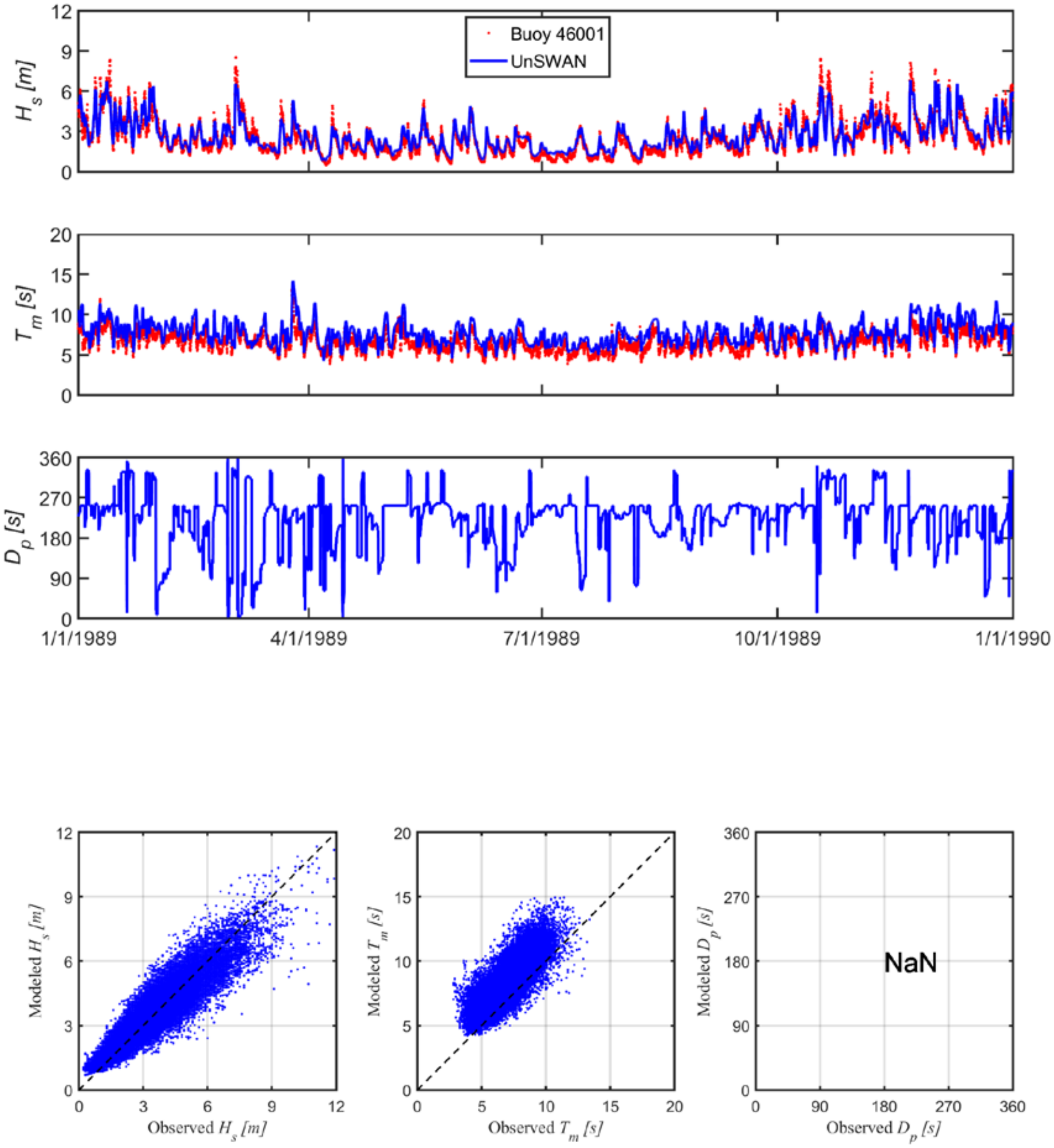

Figure B.22. Comparisons of time series (top) and scatter plots (bottom) of the three UnSWAN model-simulated bulk parameters with observed data at NDBC Buoy 46001 for 1989.

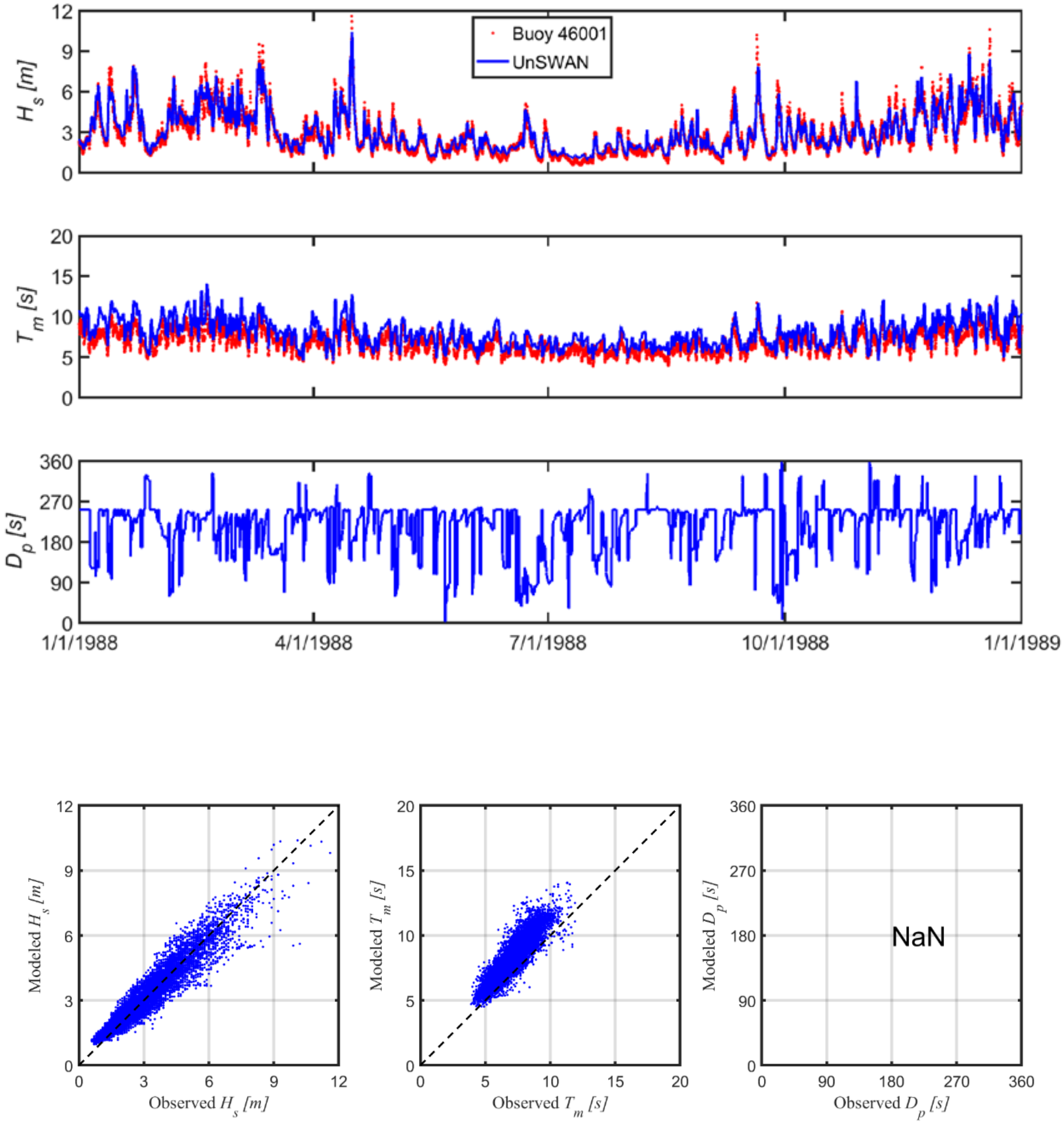

Figure B.23. Comparisons of time series (top) and scatter plots (bottom) of the three UnSWAN model-simulated bulk parameters with observed data at NDBC Buoy 46001 for 1988.

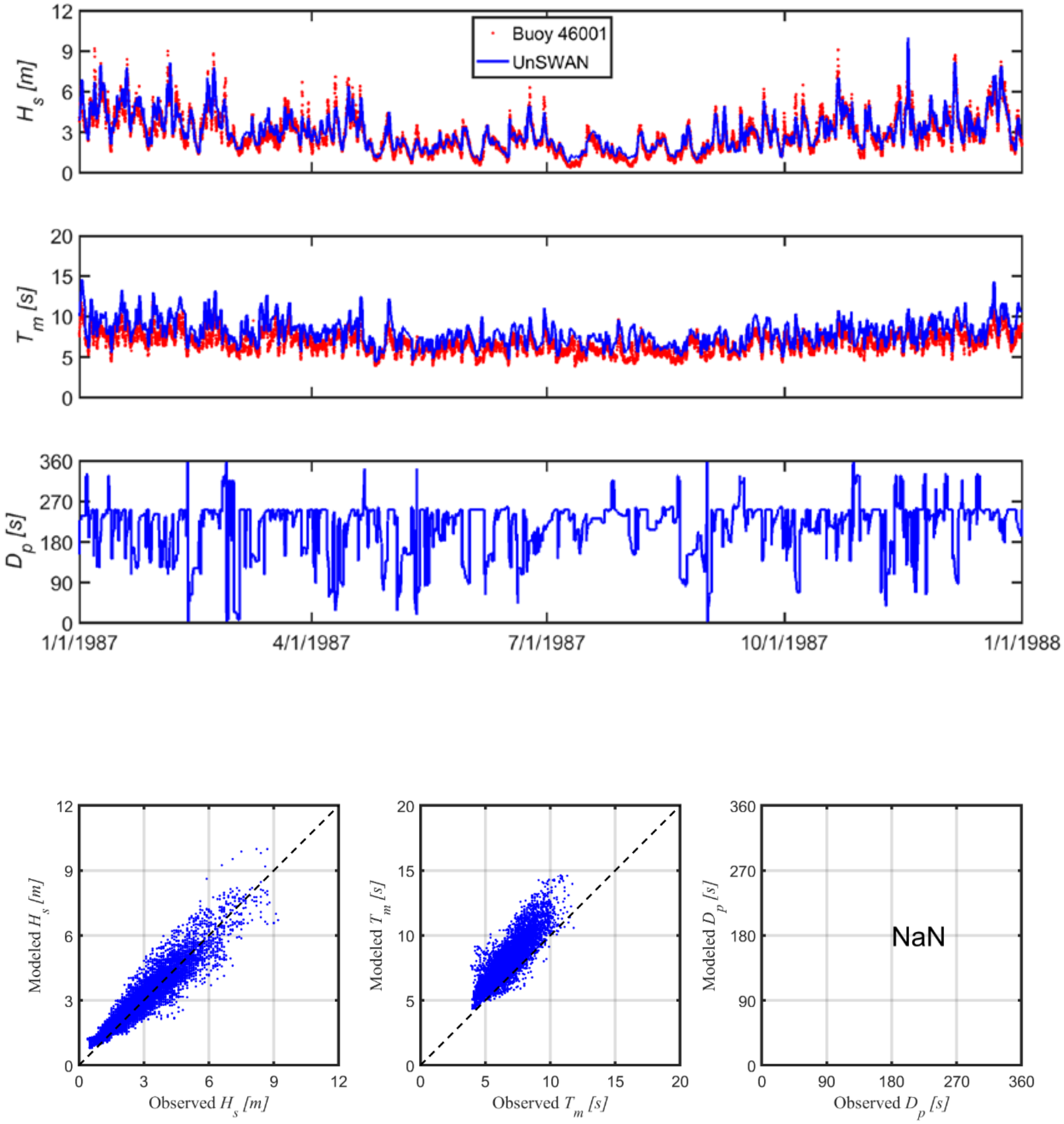

Figure B.24. Comparisons of time series (top) and scatter plots (bottom) of the three UnSWAN model-simulated bulk parameters with observed data at NDBC Buoy 46001 for 1987.

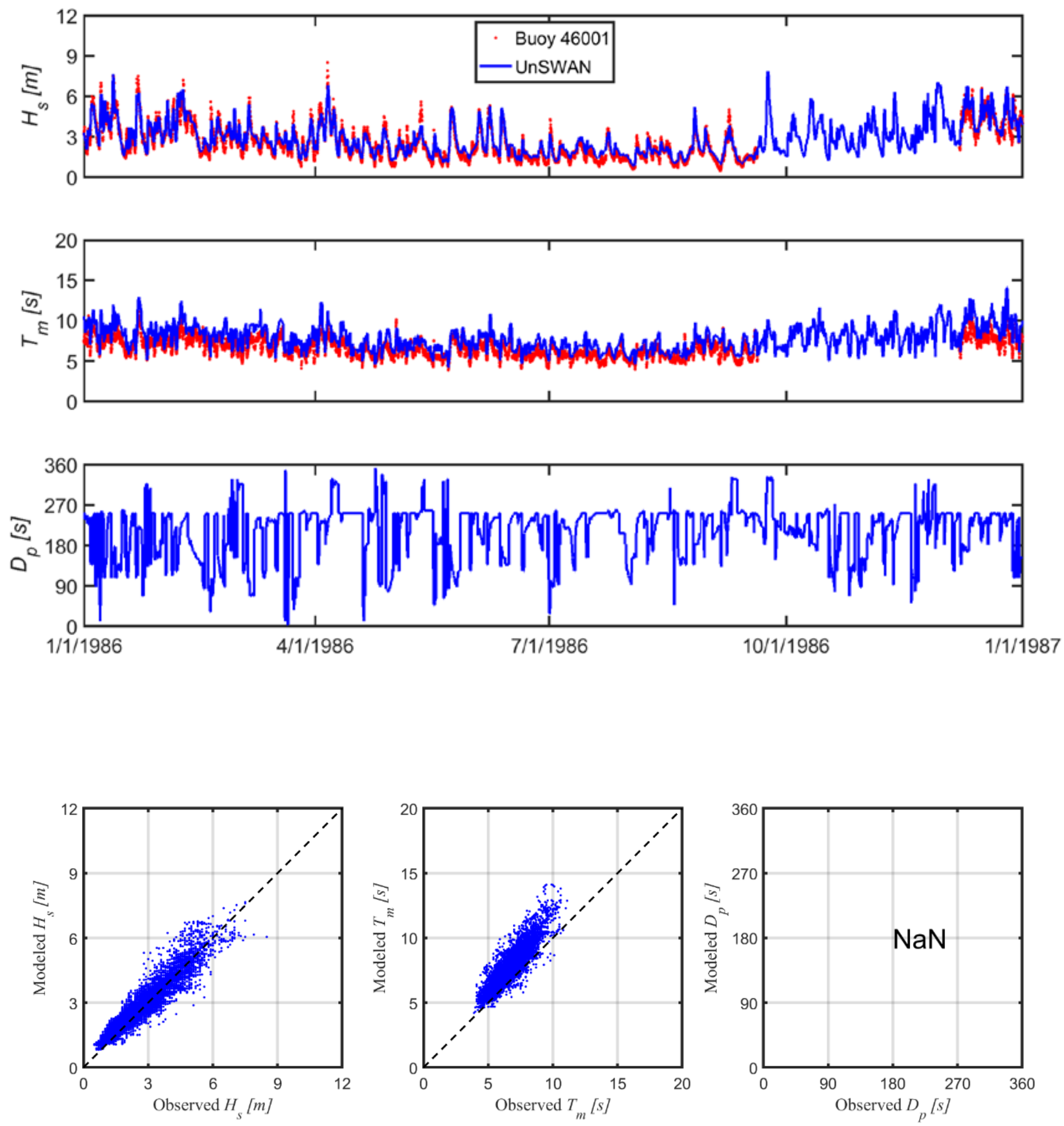

Figure B.25. Comparisons of time series (top) and scatter plots (bottom) of the three UnSWAN model-simulated bulk parameters with observed data at NDBC Buoy 46001 for 1986.

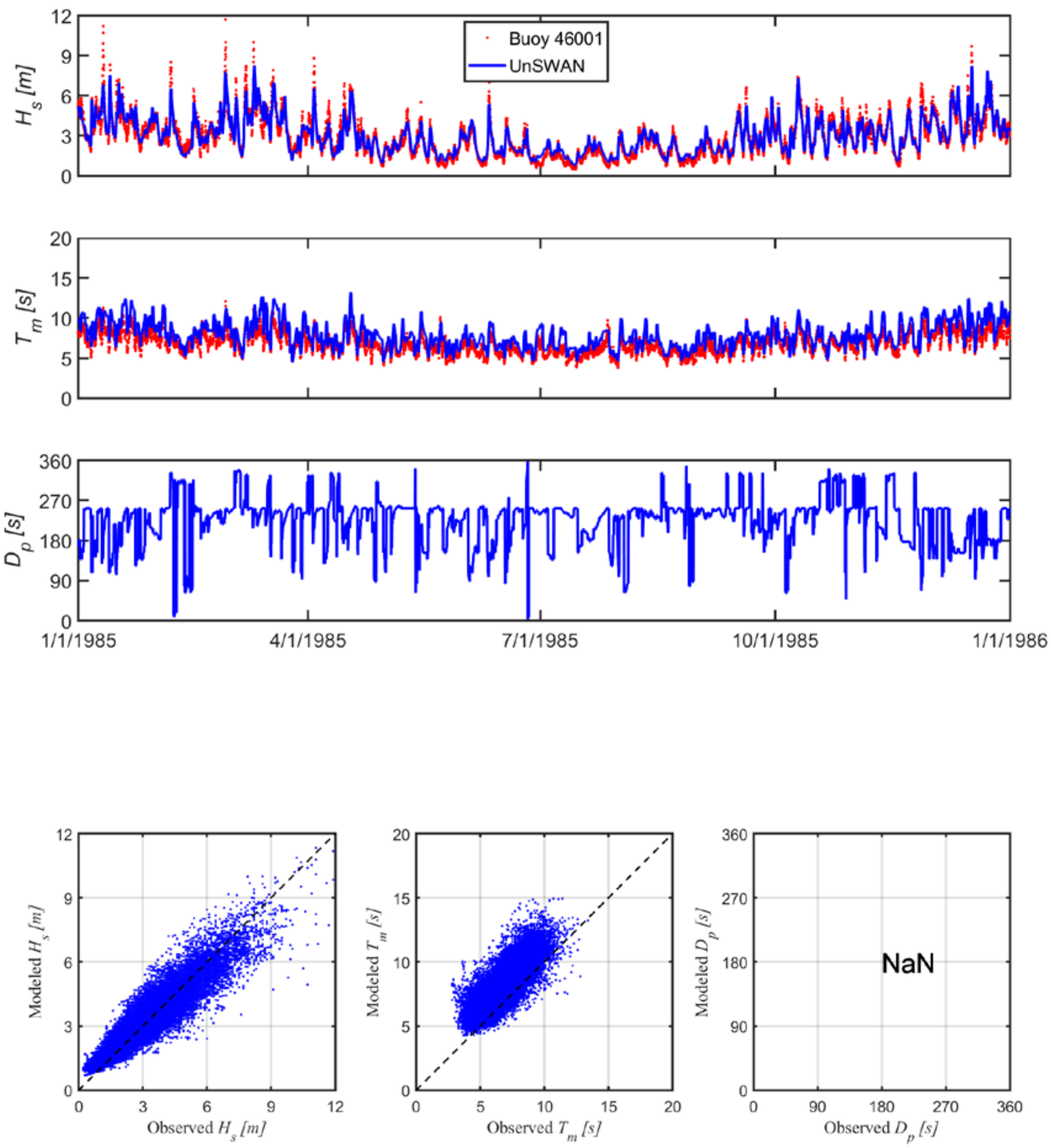

Figure B.26. Comparisons of time series (top) and scatter plots (bottom) of the three UnSWAN model-simulated bulk parameters with observed data at NDBC Buoy 46001 for 1985.

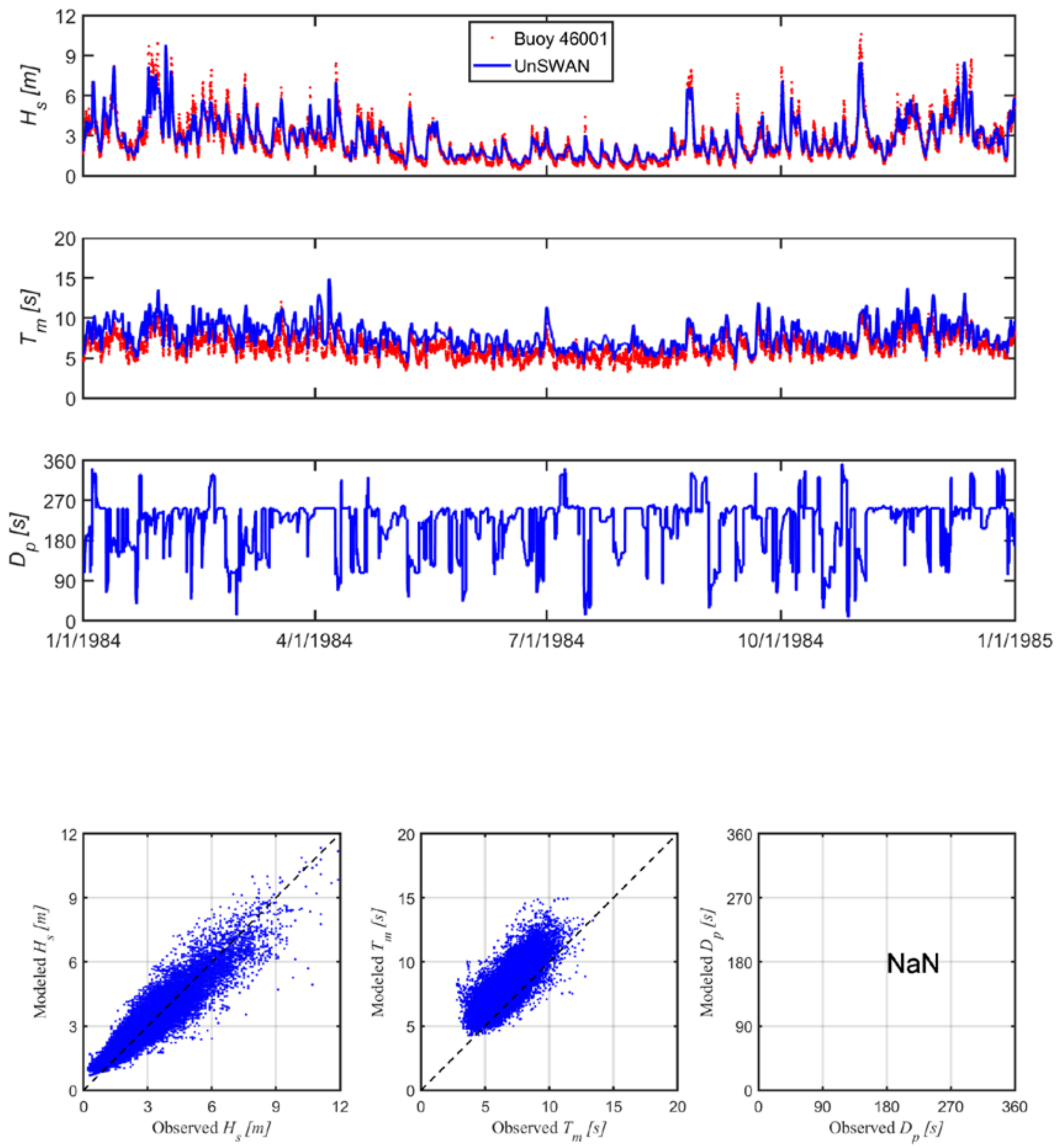

Figure B.27. Comparisons of time series (top) and scatter plots (bottom) of the three UnSWAN model-simulated bulk parameters with observed data at NDBC Buoy 46001 for 1984.

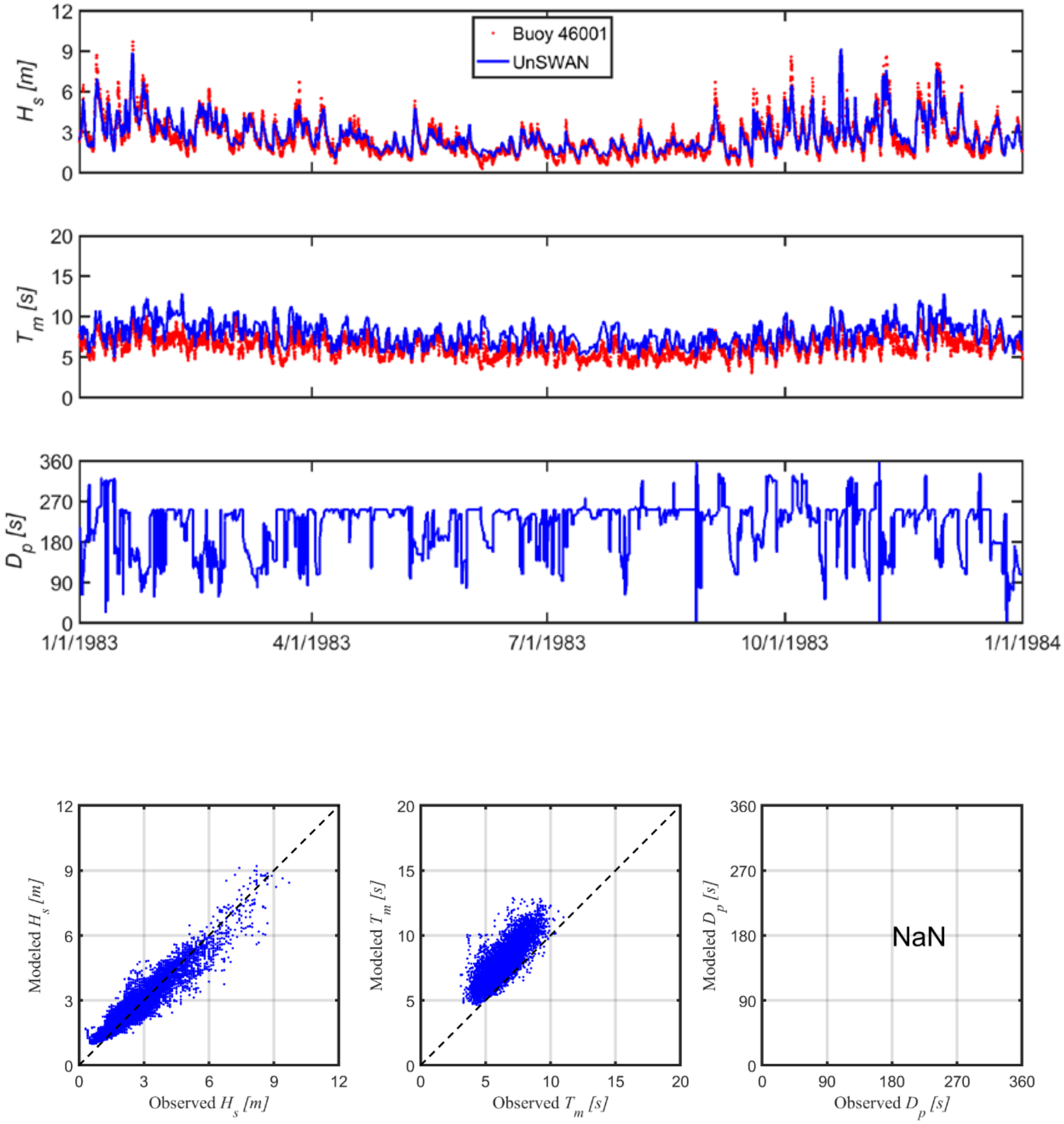

Figure B.28. Comparisons of time series (top) and scatter plots (bottom) of the three UnSWAN model-simulated bulk parameters with observed data at NDBC Buoy 46001 for 1983.

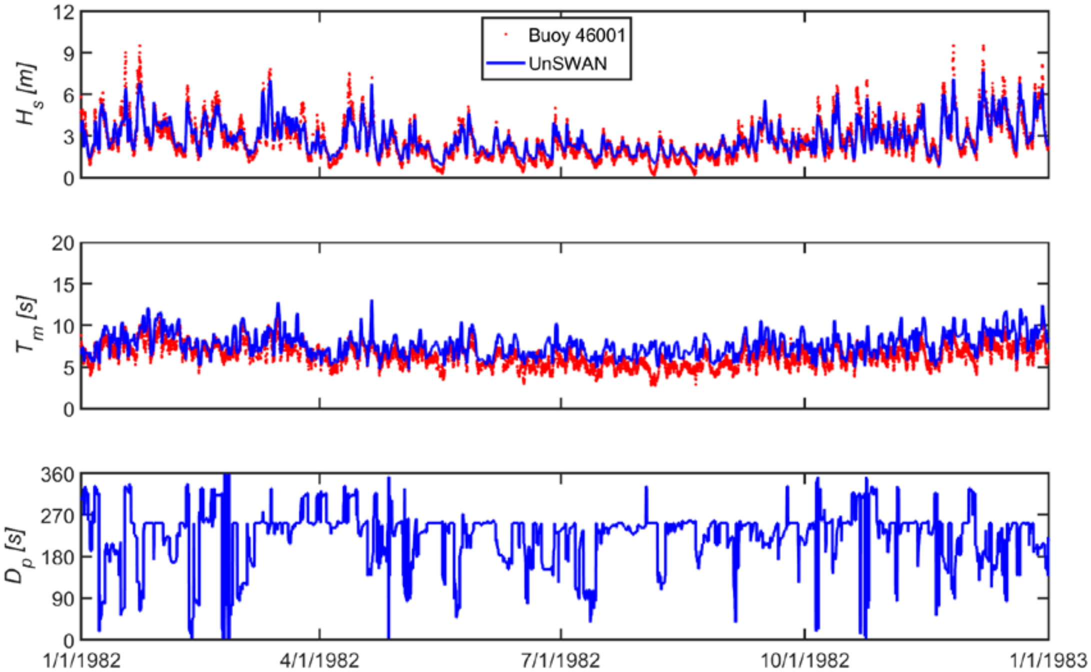

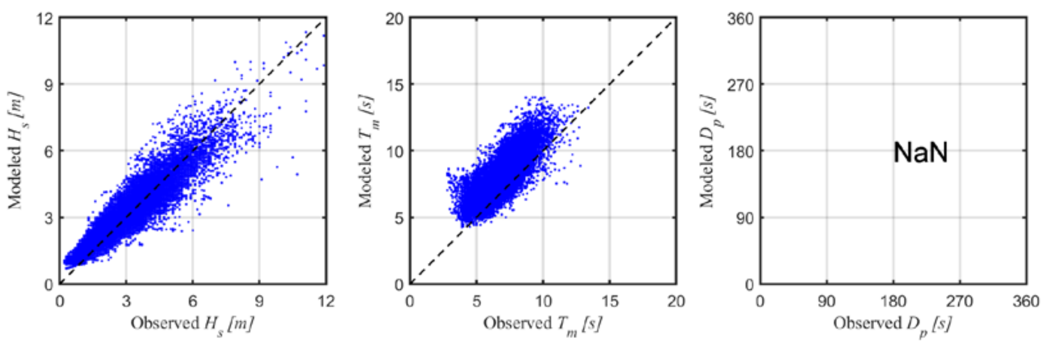

Figure B.29. Comparisons of time series (top) and scatter plots (bottom) of the three UnSWAN model-simulated bulk parameters with observed data at NDBC Buoy 46001 for 1982.

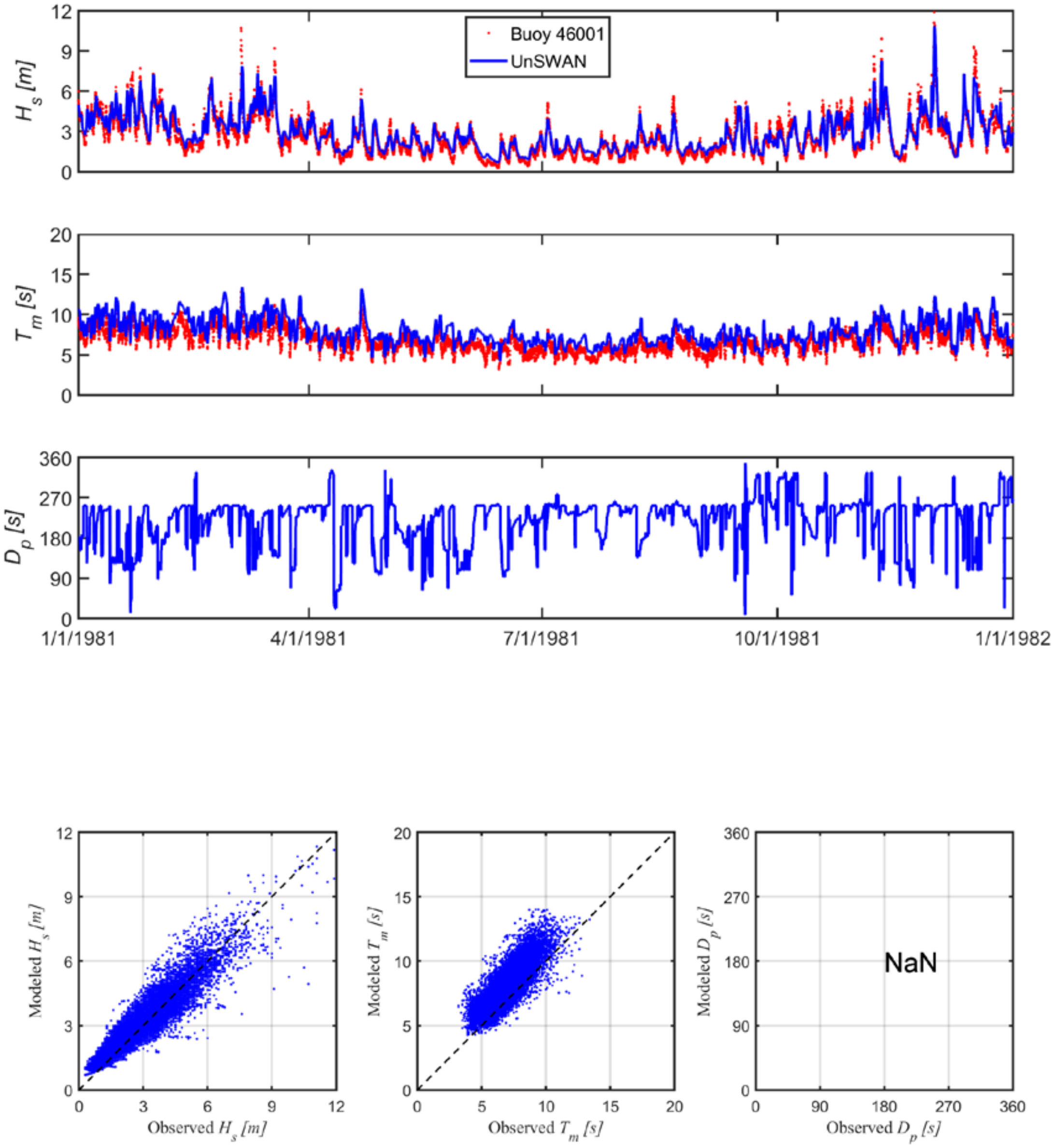

Figure B.30. Comparisons of time series (top) and scatter plots (bottom) of the three UnSWAN model-simulated bulk parameters with observed data at NDBC Buoy 46001 for 1981.

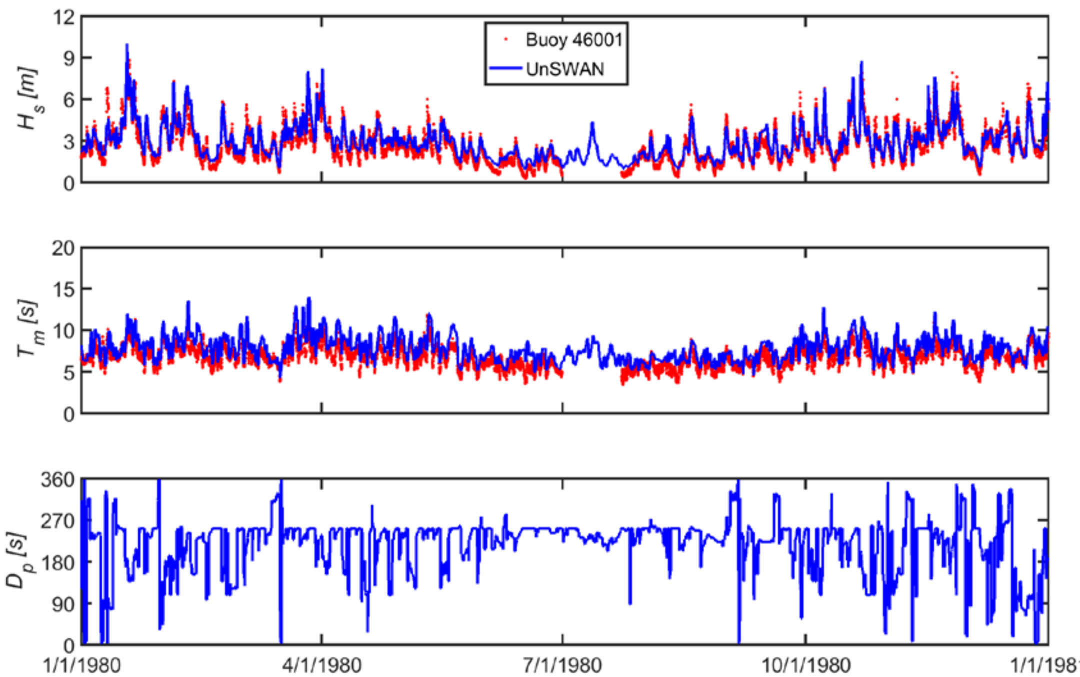

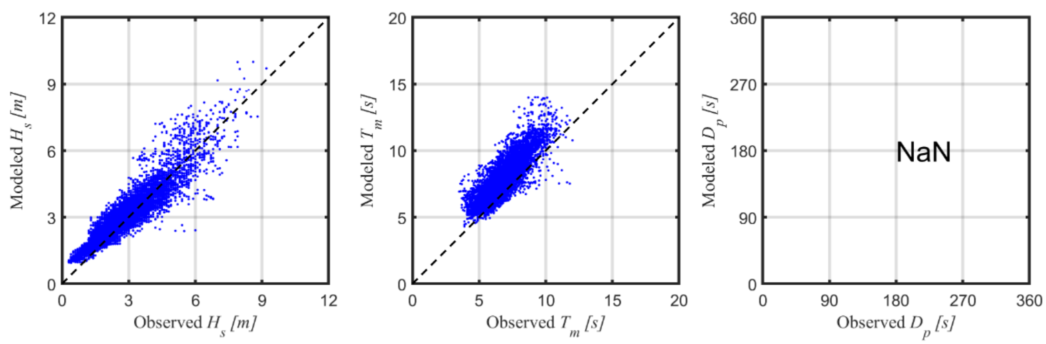

Figure B.31. Comparisons of time series (top) and scatter plots (bottom) of the three UnSWAN model-simulated bulk parameters with observed data at NDBC Buoy 46001 for 1980.

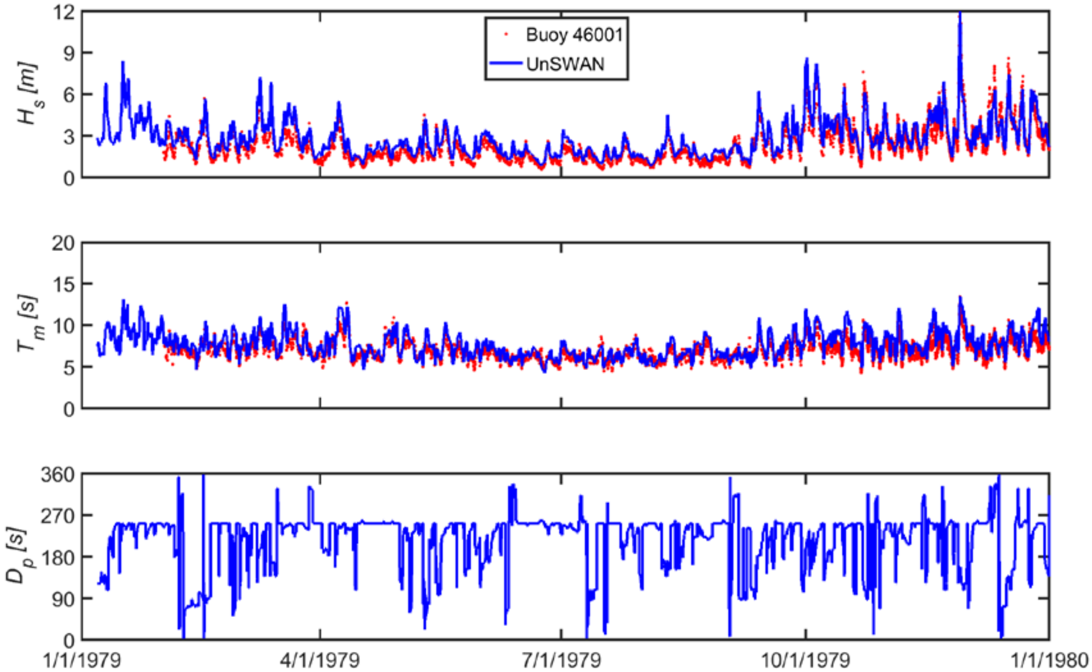

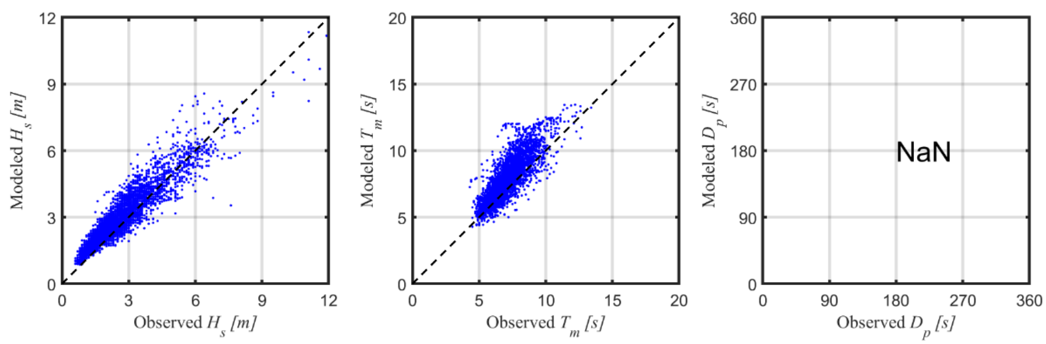

Figure B.32. Comparisons of time series (top) and scatter plots (bottom) of the three UnSWAN model-simulated bulk parameters with observed data at NDBC Buoy 46001 for 1979.

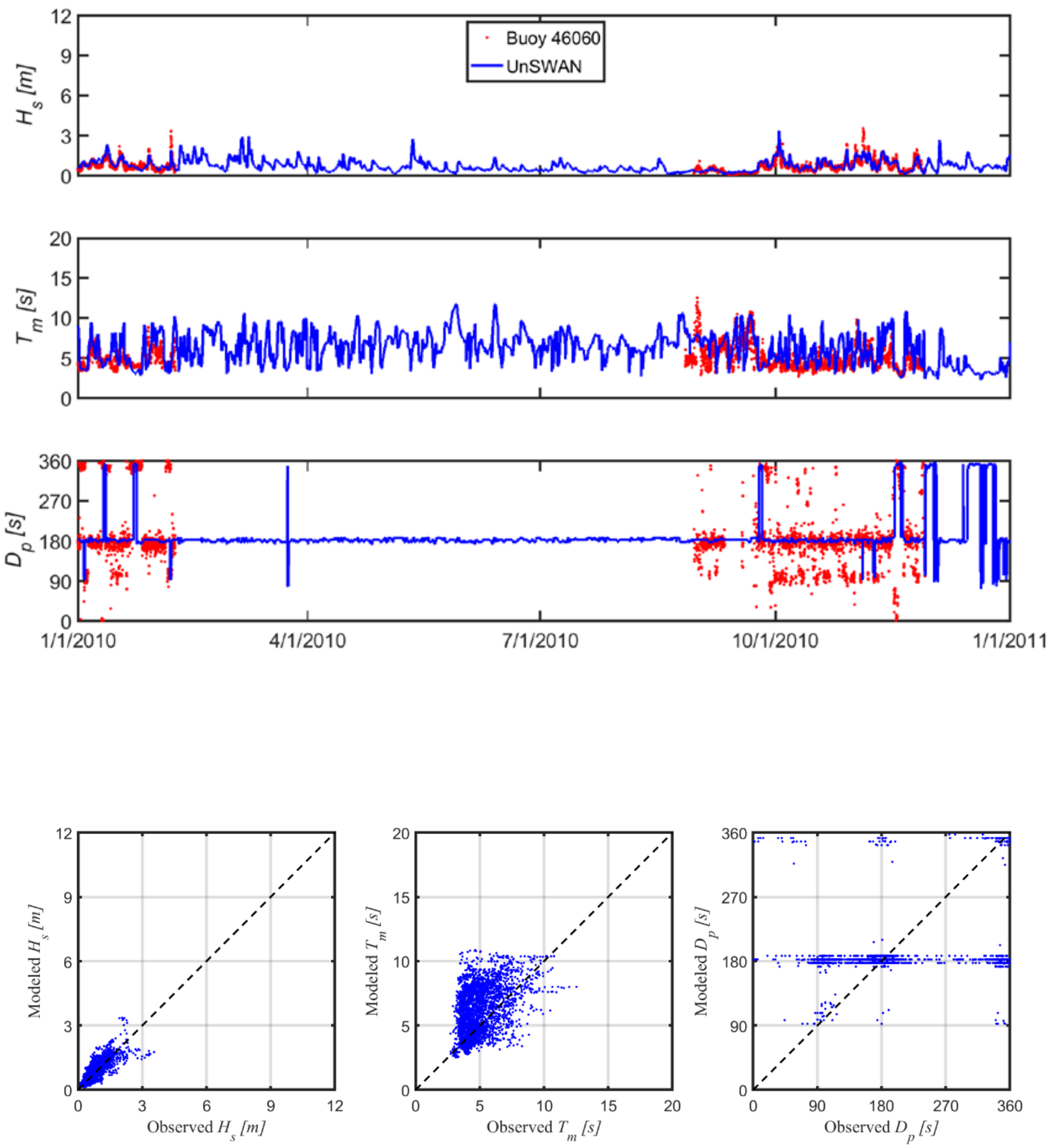

Figure B.33. Comparisons of time series (top) and scatter plots (bottom) of the three UnSWAN model-simulated bulk parameters with observed data at NDBC Buoy 46060 for 2010.

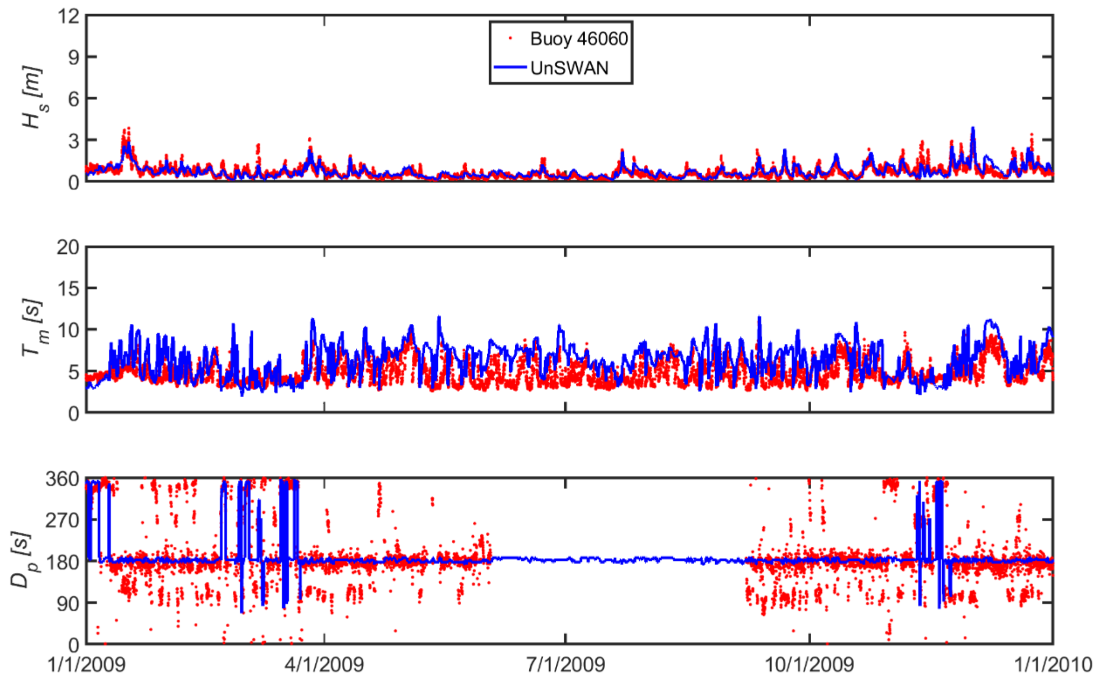

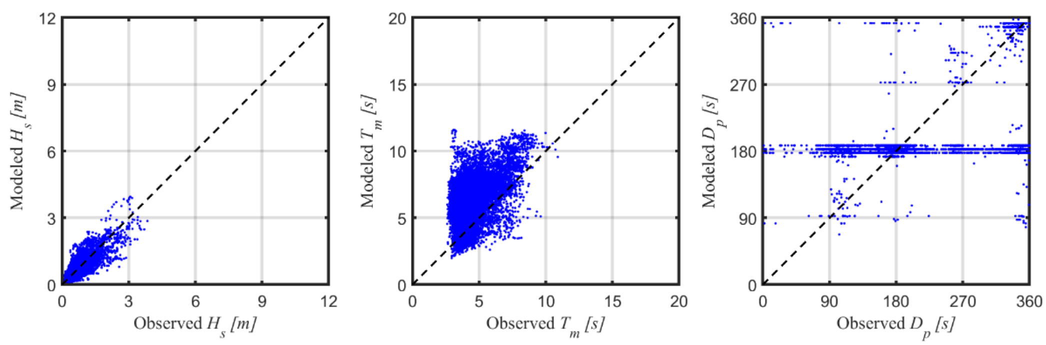

Figure B.34. Comparisons of time series (top) and scatter plots (bottom) of the three UnSWAN model-simulated bulk parameters with observed data at NDBC Buoy 46060 for 2009.

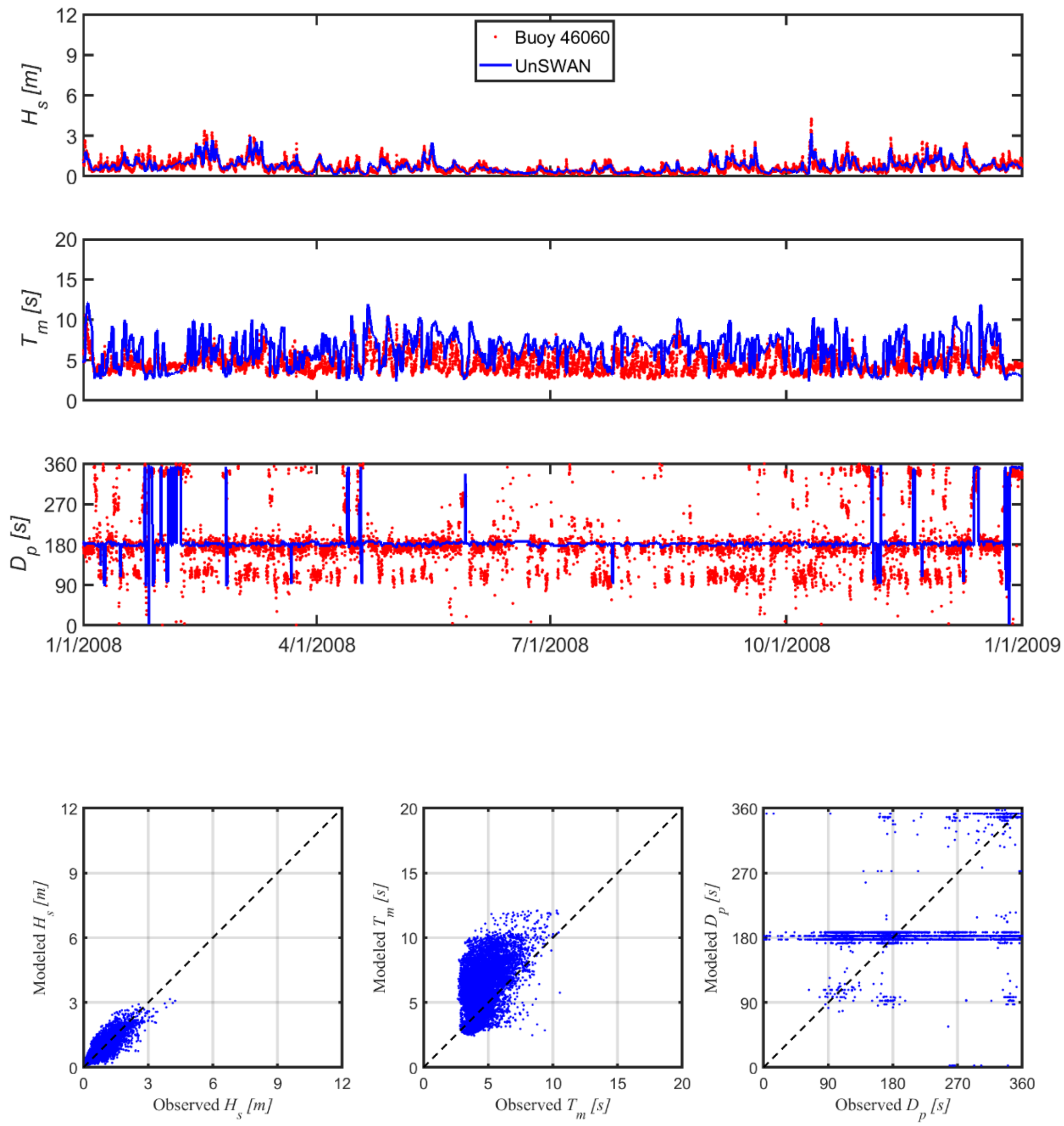

Figure B.35. Comparisons of time series (top) and scatter plots (bottom) of the three UnSWAN model-simulated bulk parameters with observed data at NDBC Buoy 46060 for 2008.

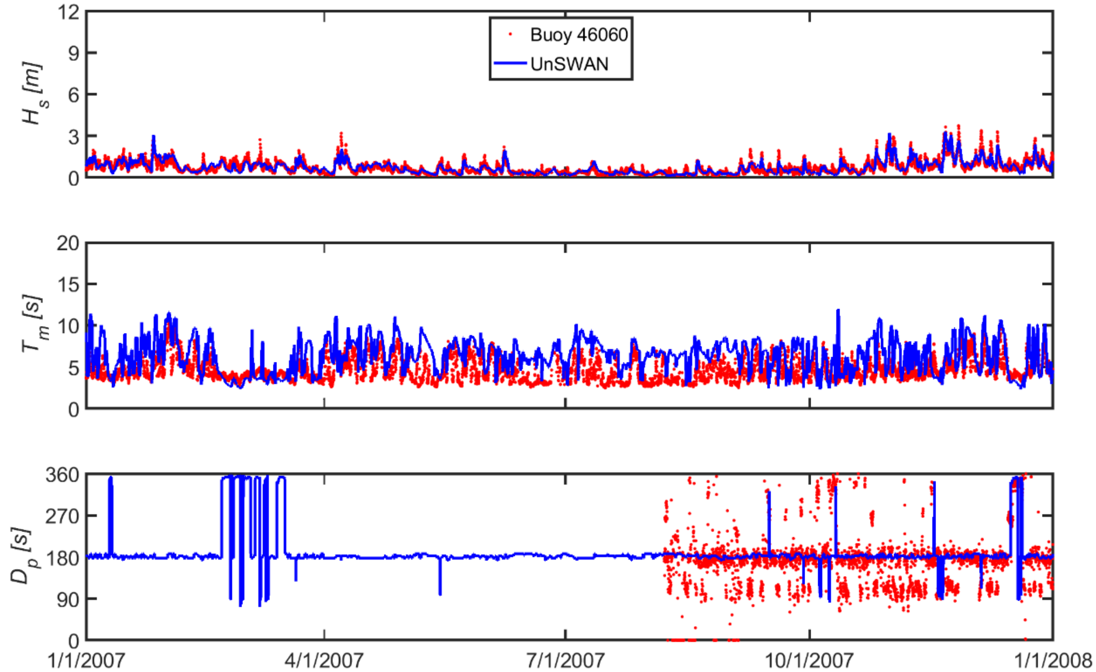

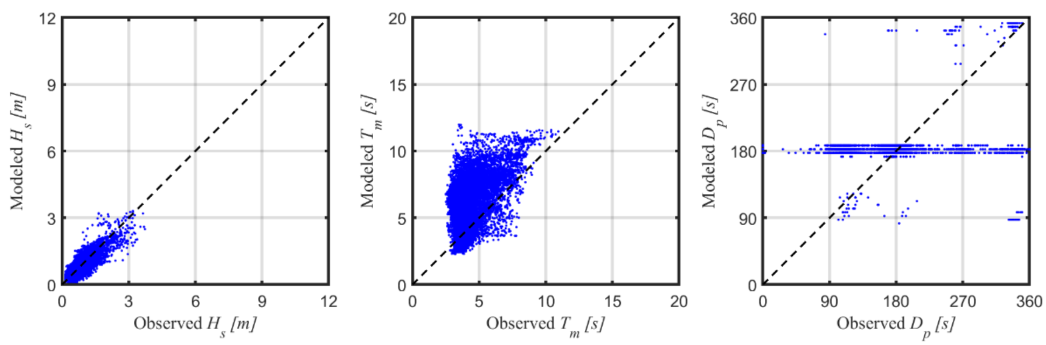

Figure B.36. Comparisons of time series (top) and scatter plots (bottom) of the three UnSWAN model-simulated bulk parameters with observed data at NDBC Buoy 46060 for 2007.

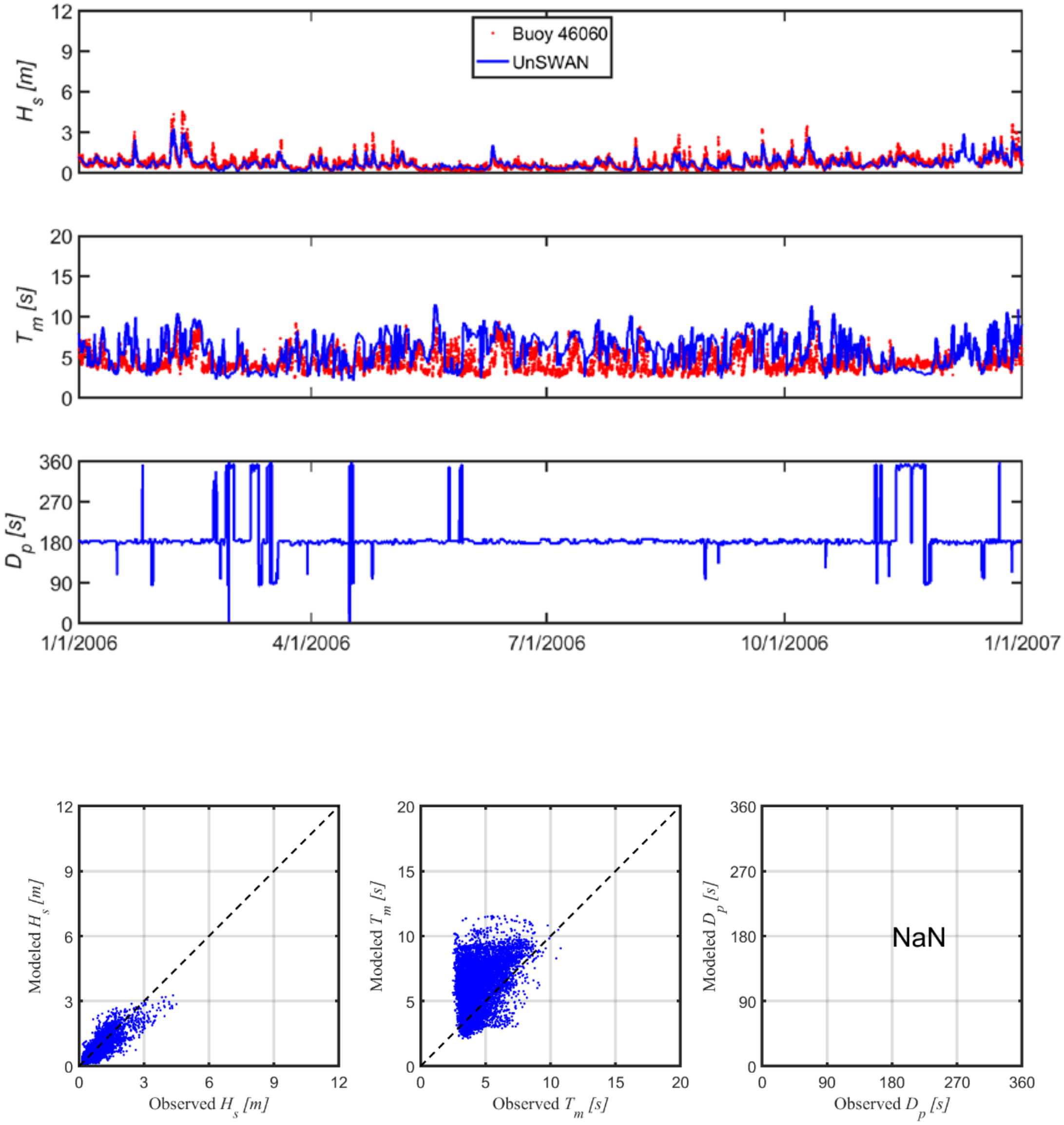

Figure B.37. Comparisons of time series (top) and scatter plots (bottom) of the three UnSWAN model-simulated bulk parameters with observed data at NDBC Buoy 46060 for 2006.

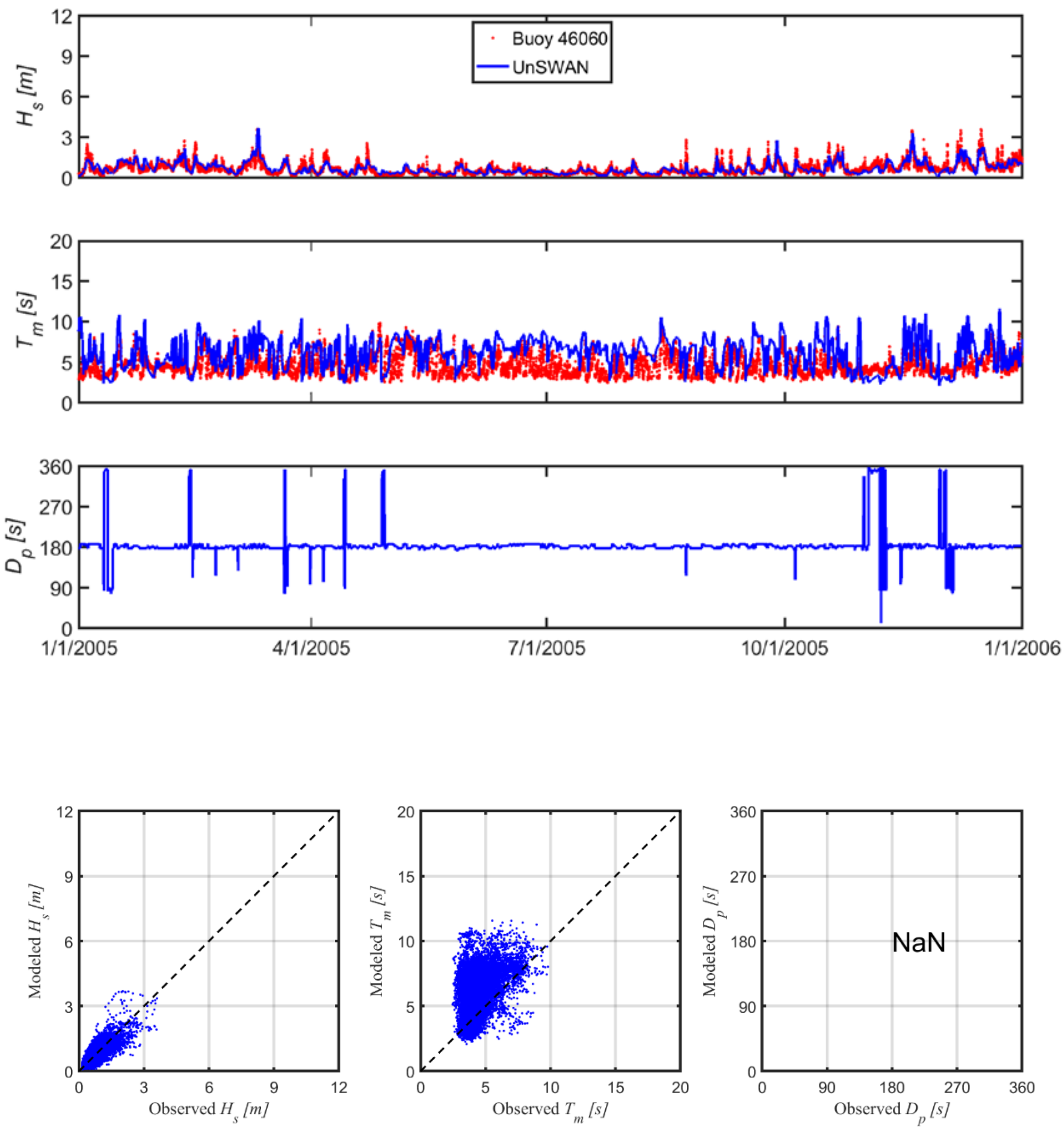

Figure B.38. Comparisons of time series (top) and scatter plots (bottom) of the three UnSWAN model-simulated bulk parameters with observed data at NDBC Buoy 46060 for 2005.

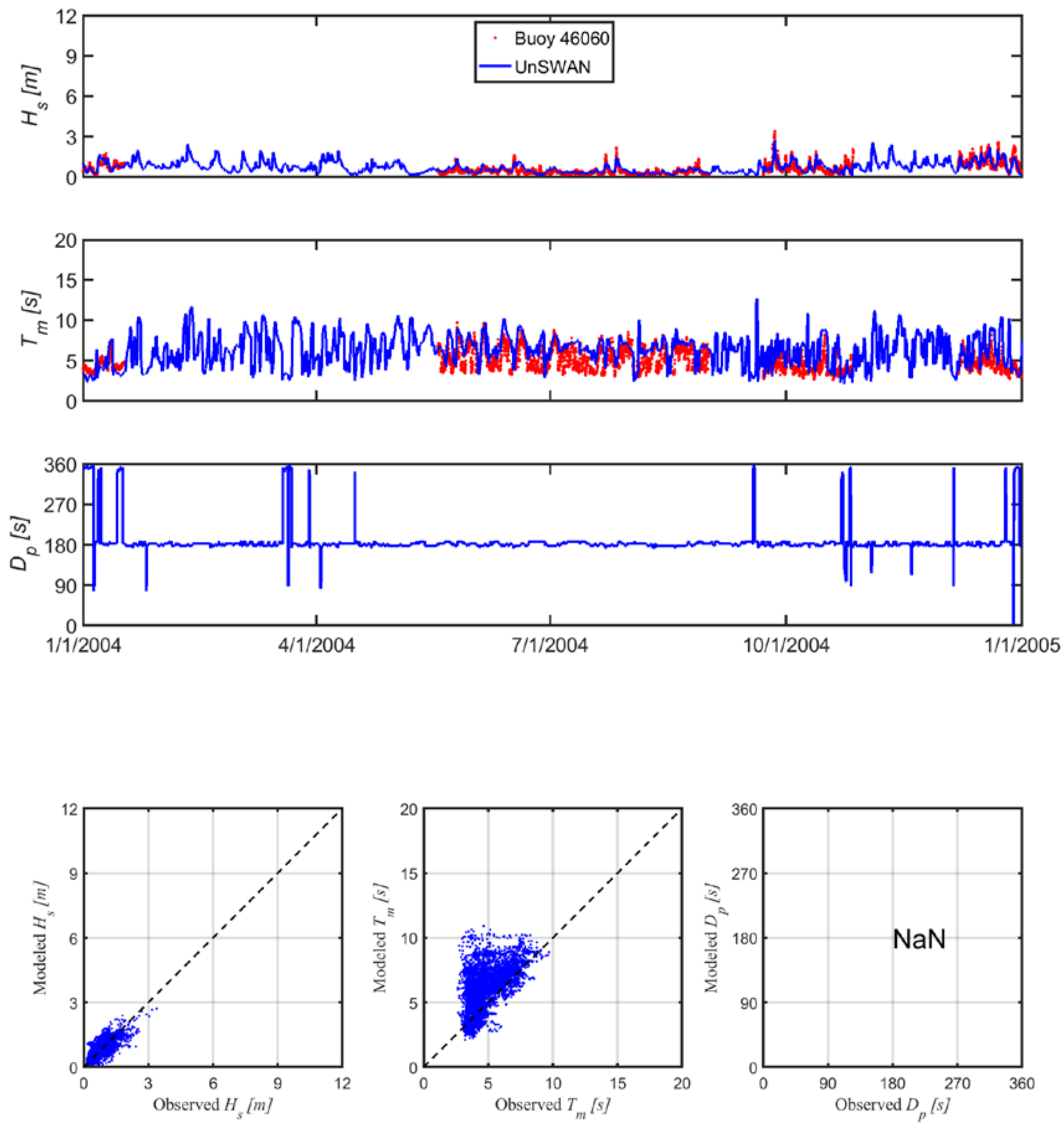

Figure B.39. Comparisons of time series (top) and scatter plots (bottom) of the three UnSWAN model-simulated bulk parameters with observed data at NDBC Buoy 46060 for 2004.

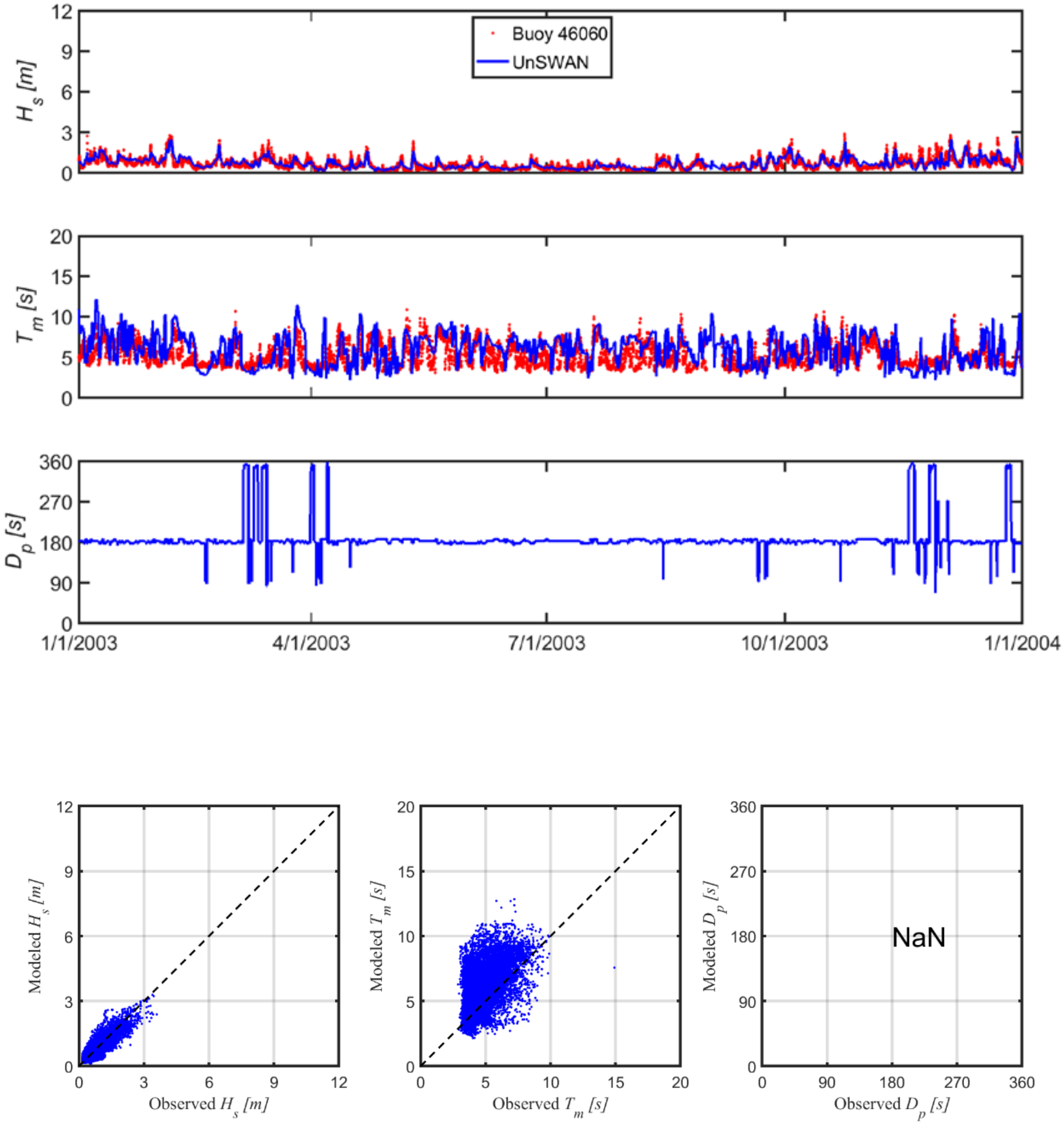

Figure B.40. Comparisons of time series (top) and scatter plots (bottom) of the three UnSWAN model-simulated bulk parameters with observed data at NDBC Buoy 46060 for 2003.

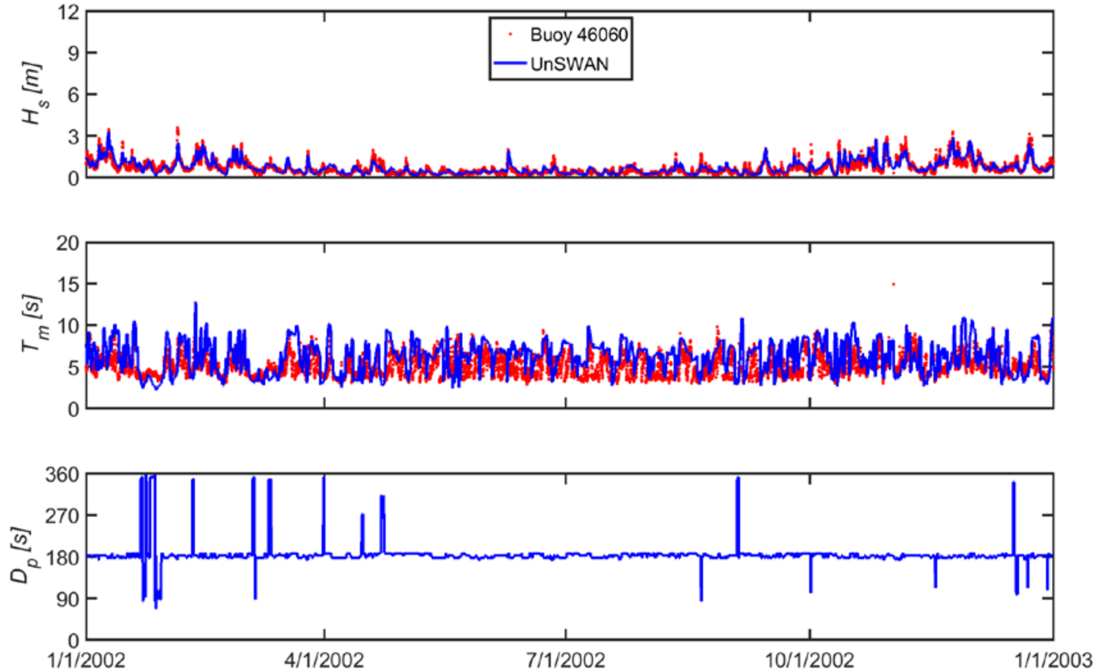

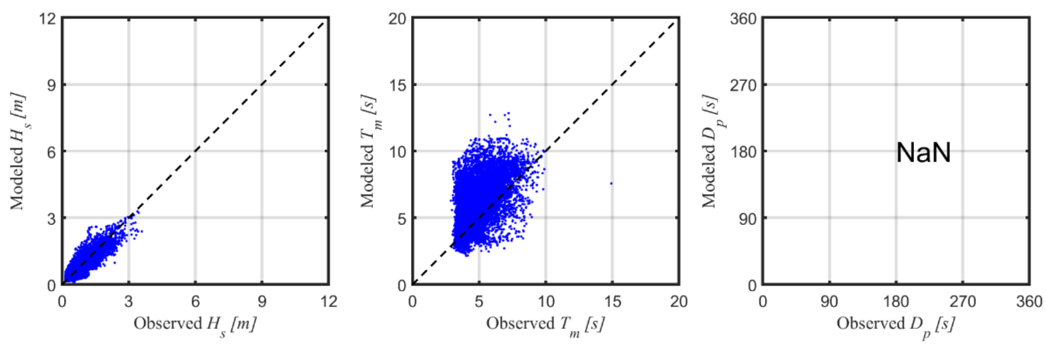

Figure B.41. Comparisons of time series (top) and scatter plots (bottom) of the three UnSWAN model-simulated bulk parameters with observed data at NDBC Buoy 46060 for 2002.

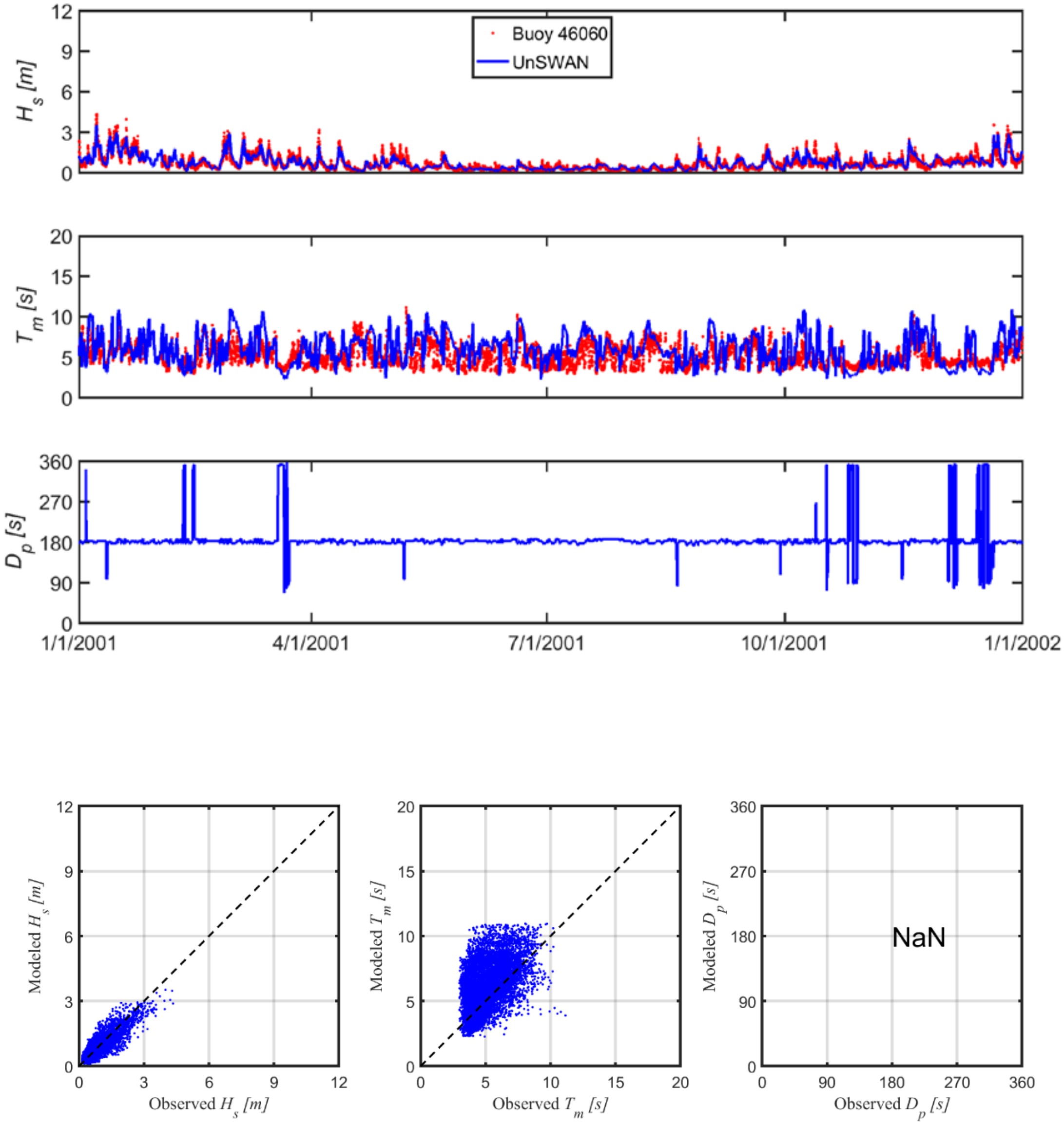

Figure B.42. Comparisons of time series (top) and scatter plots (bottom) of the three UnSWAN model-simulated bulk parameters with observed data at NDBC Buoy 46060 for 2001.

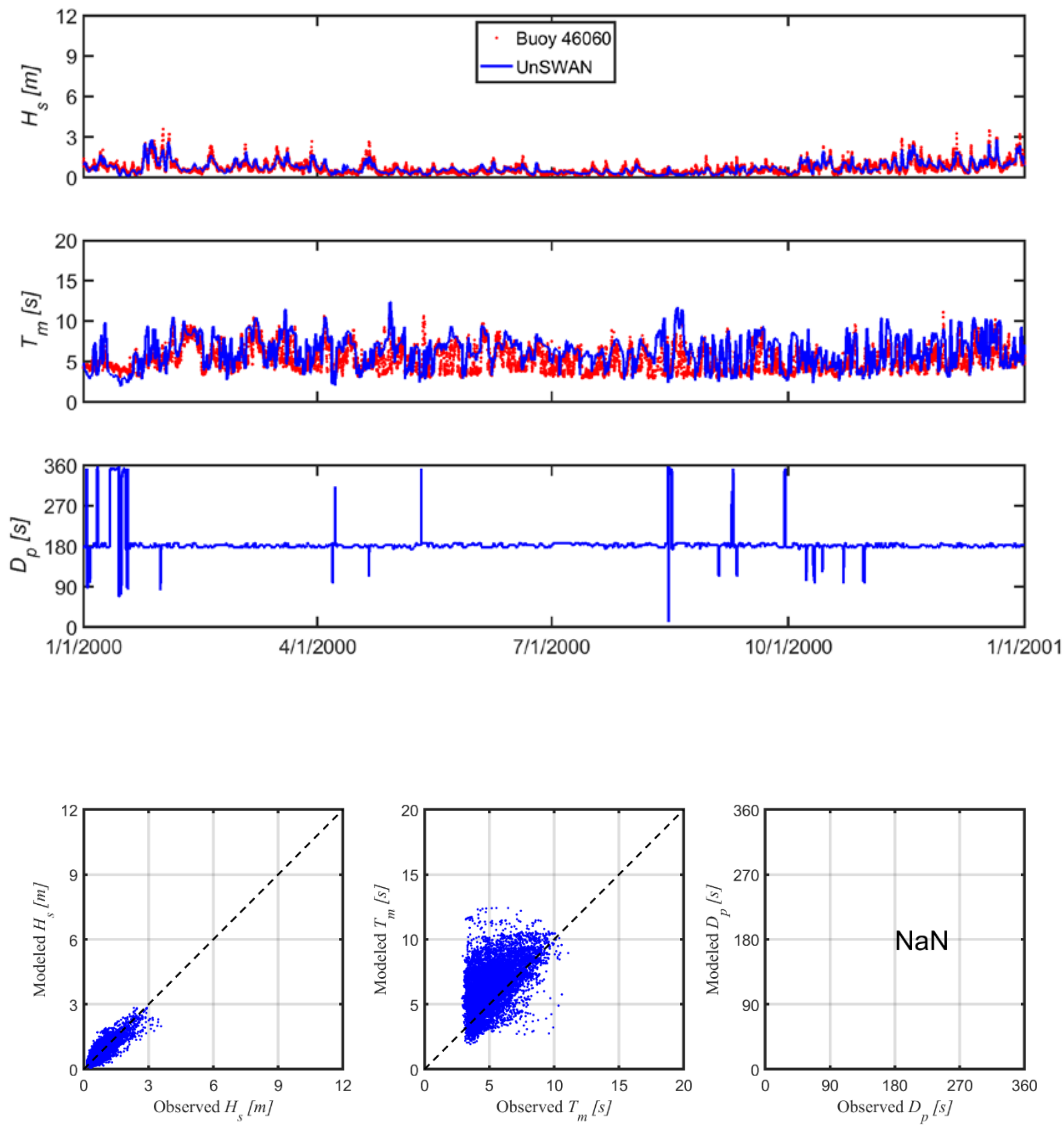

Figure B.43. Comparisons of time series (top) and scatter plots (bottom) of the three UnSWAN model-simulated bulk parameters with observed data at NDBC Buoy 46060 for 2000.

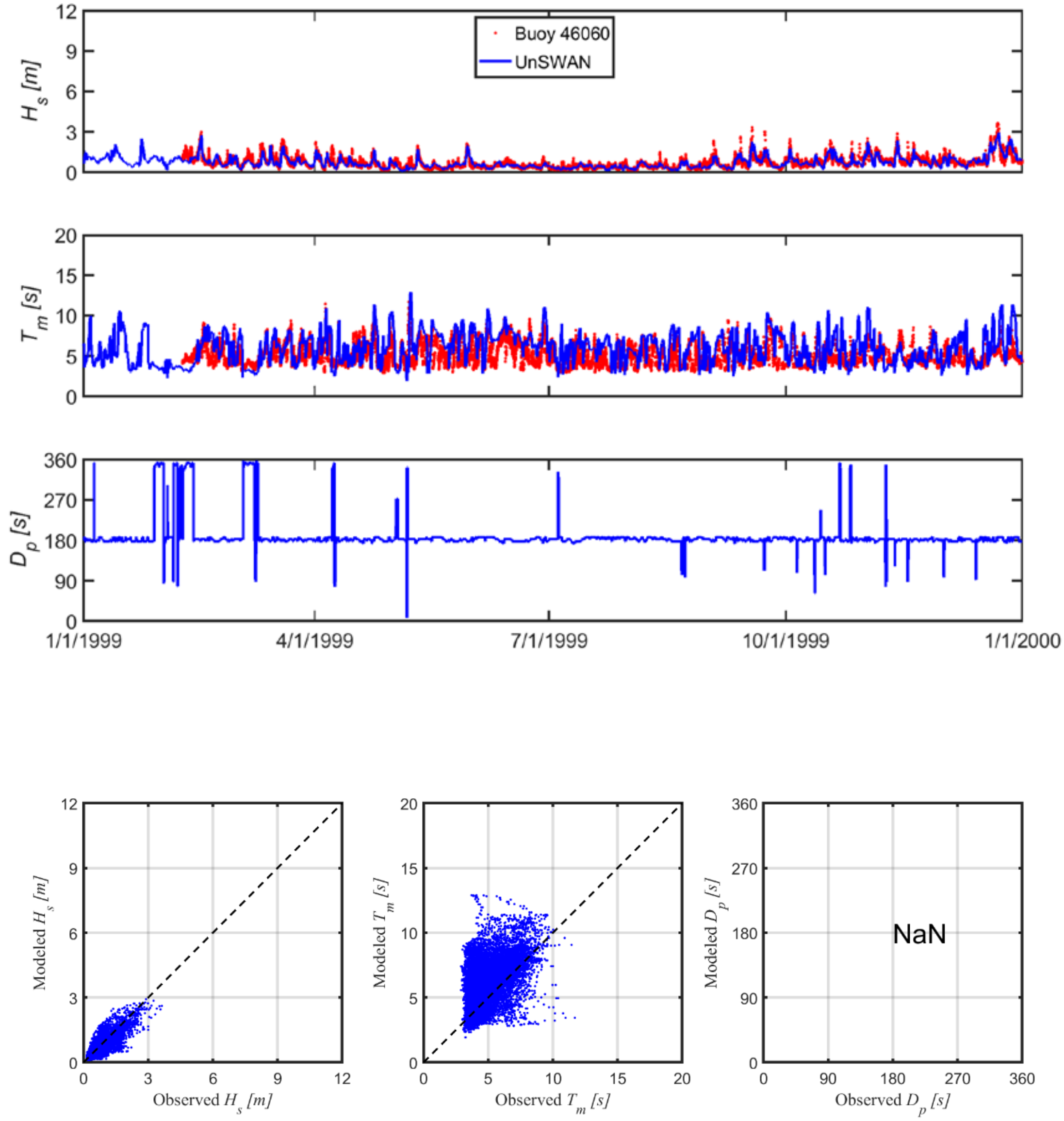

Figure B.44. Comparisons of time series (top) and scatter plots (bottom) of the three UnSWAN model-simulated bulk parameters with observed data at NDBC Buoy 46060 for 1999.

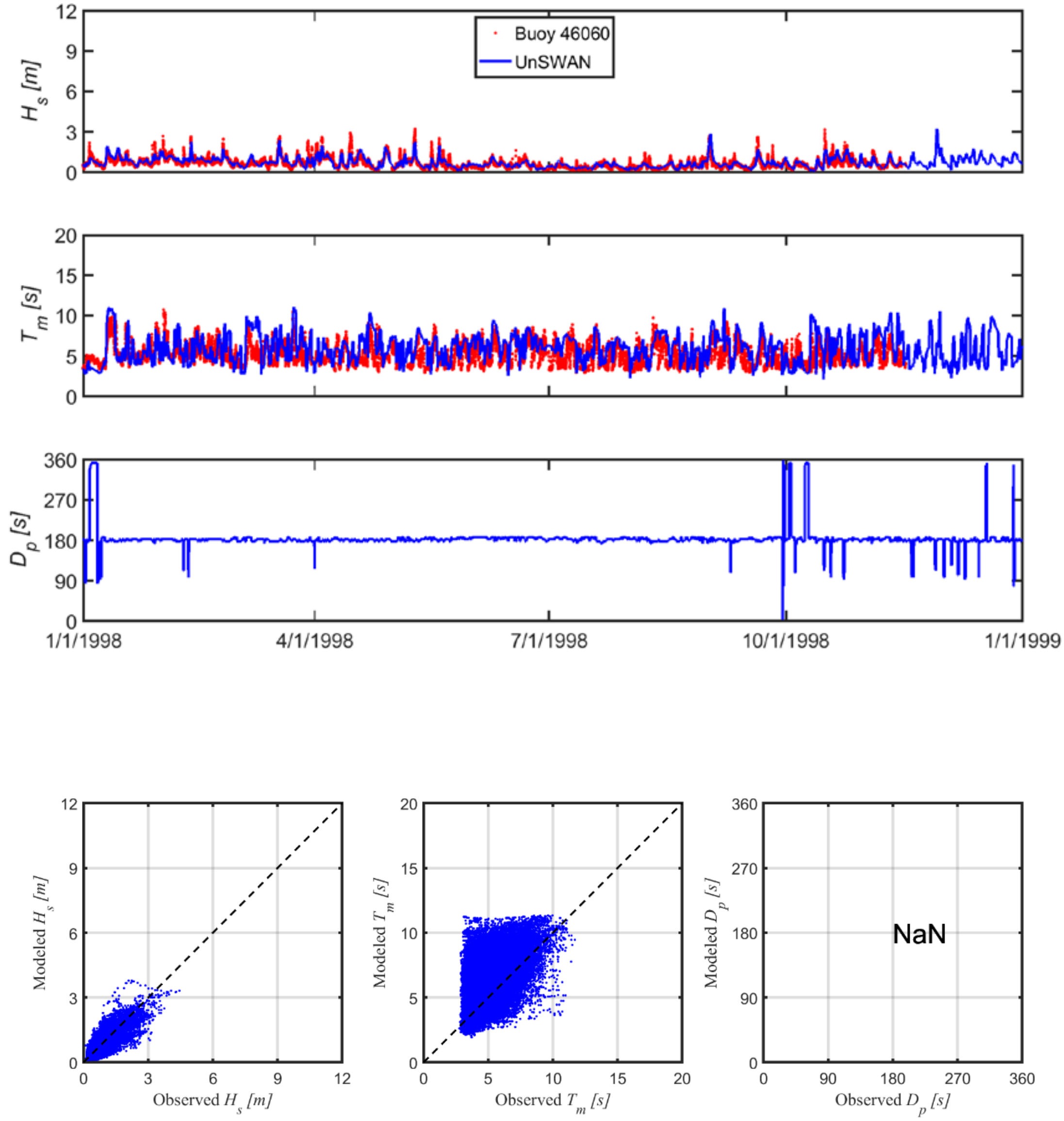

Figure B.45. Comparisons of time series (top) and scatter plots (bottom) of the three UnSWAN model-simulated bulk parameters with observed data at NDBC Buoy 46060 for 1998.

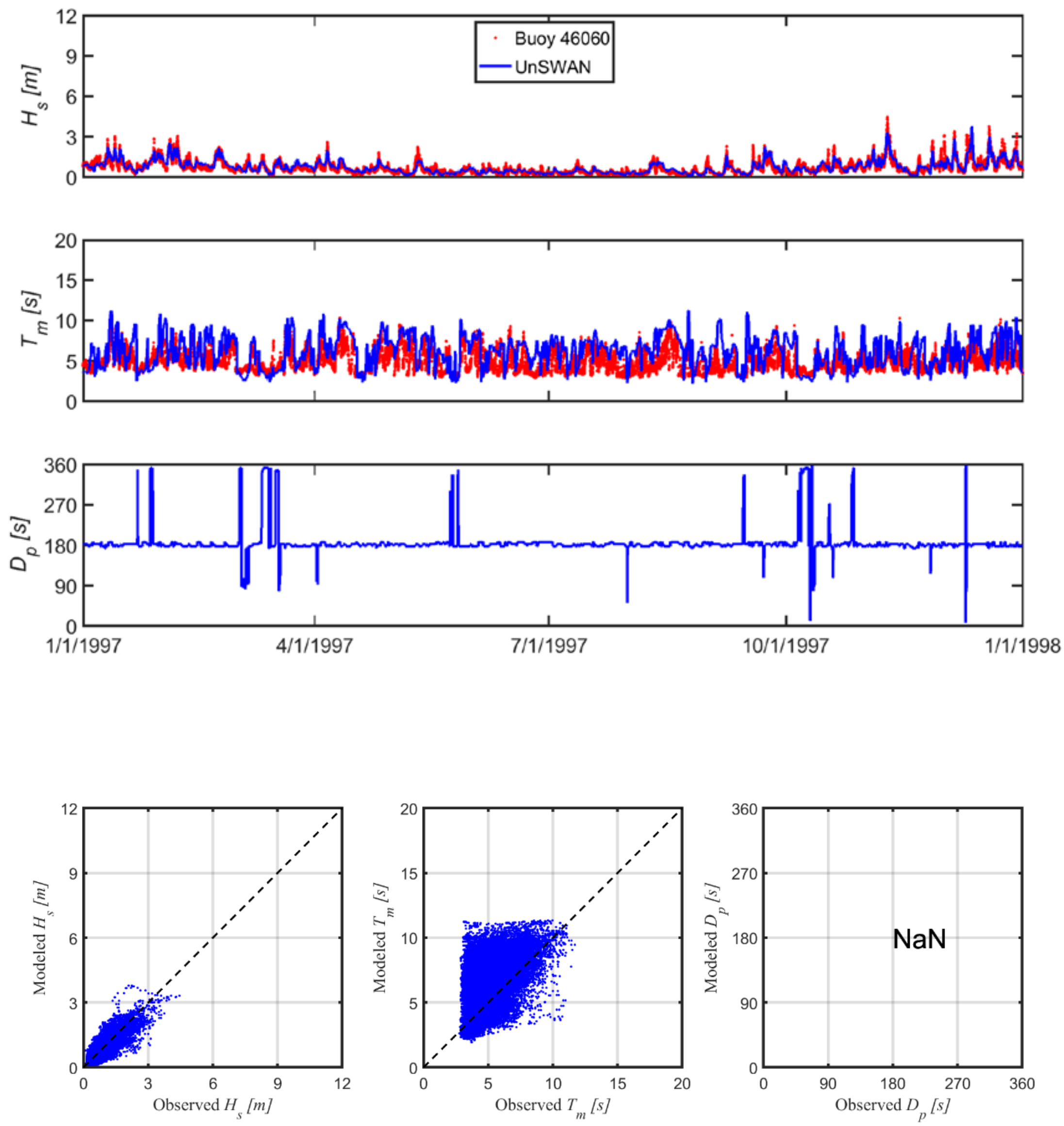

Figure B.46. Comparisons of time series (top) and scatter plots (bottom) of the three UnSWAN model-simulated bulk parameters with observed data at NDBC Buoy 46060 for 1997.

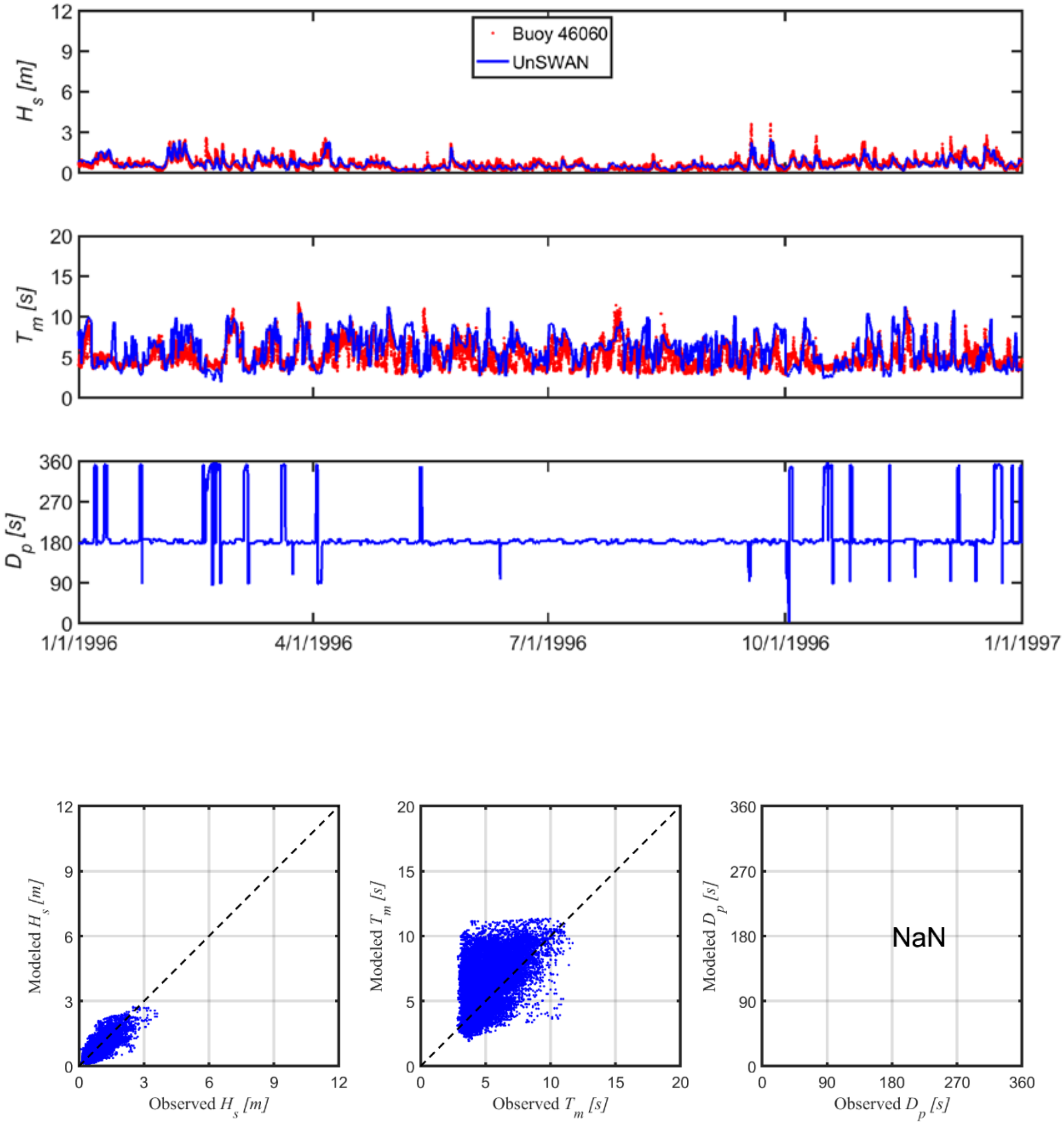

Figure B.47. Comparisons of time series (top) and scatter plots (bottom) of the three UnSWAN model-simulated bulk parameters with observed data at NDBC Buoy 46060 for 1996.

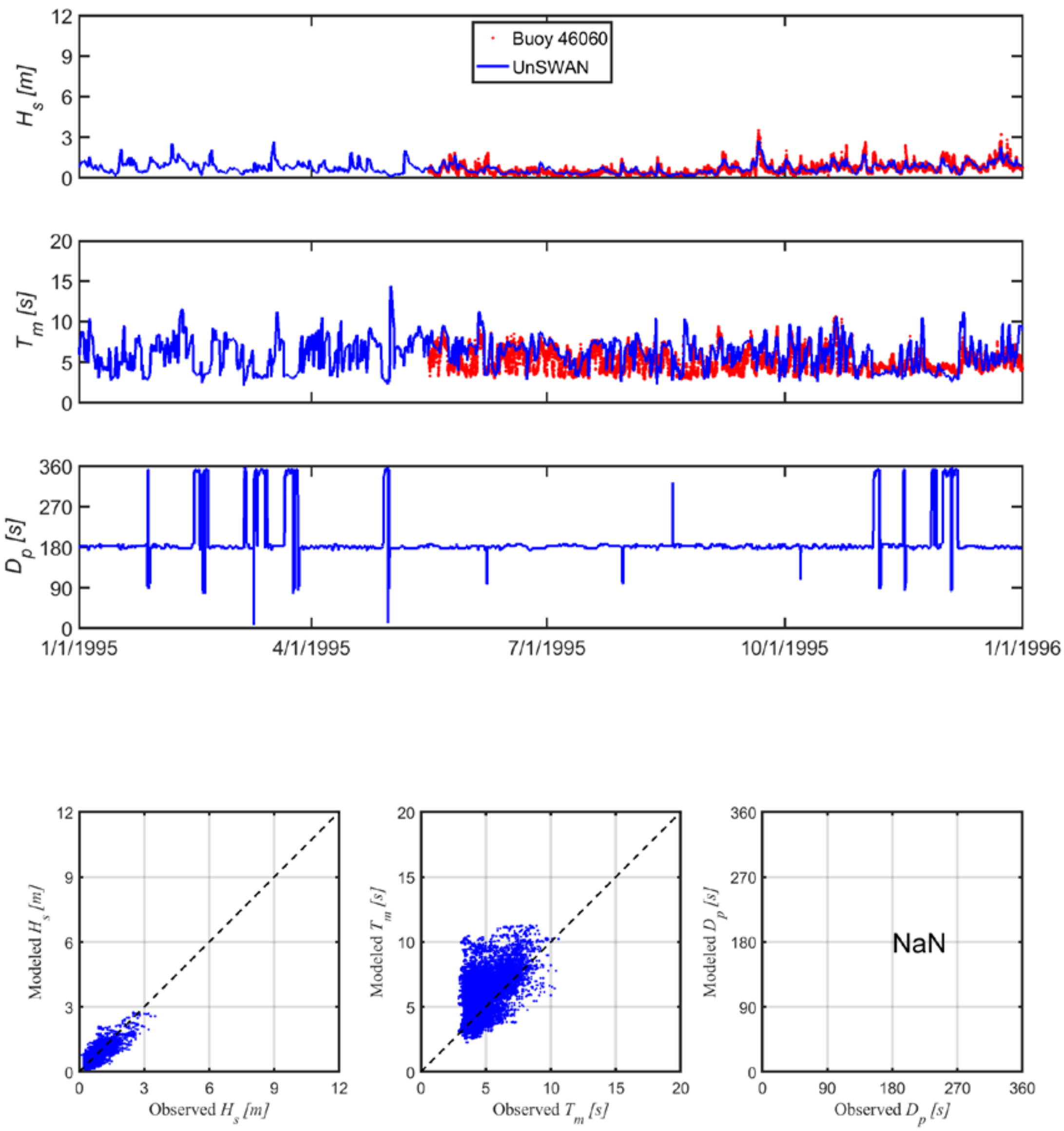

Figure B.48. Comparisons of time series (top) and scatter plots (bottom) of the three UnSWAN model-simulated bulk parameters with observed data at NDBC Buoy 46060 for 1995.

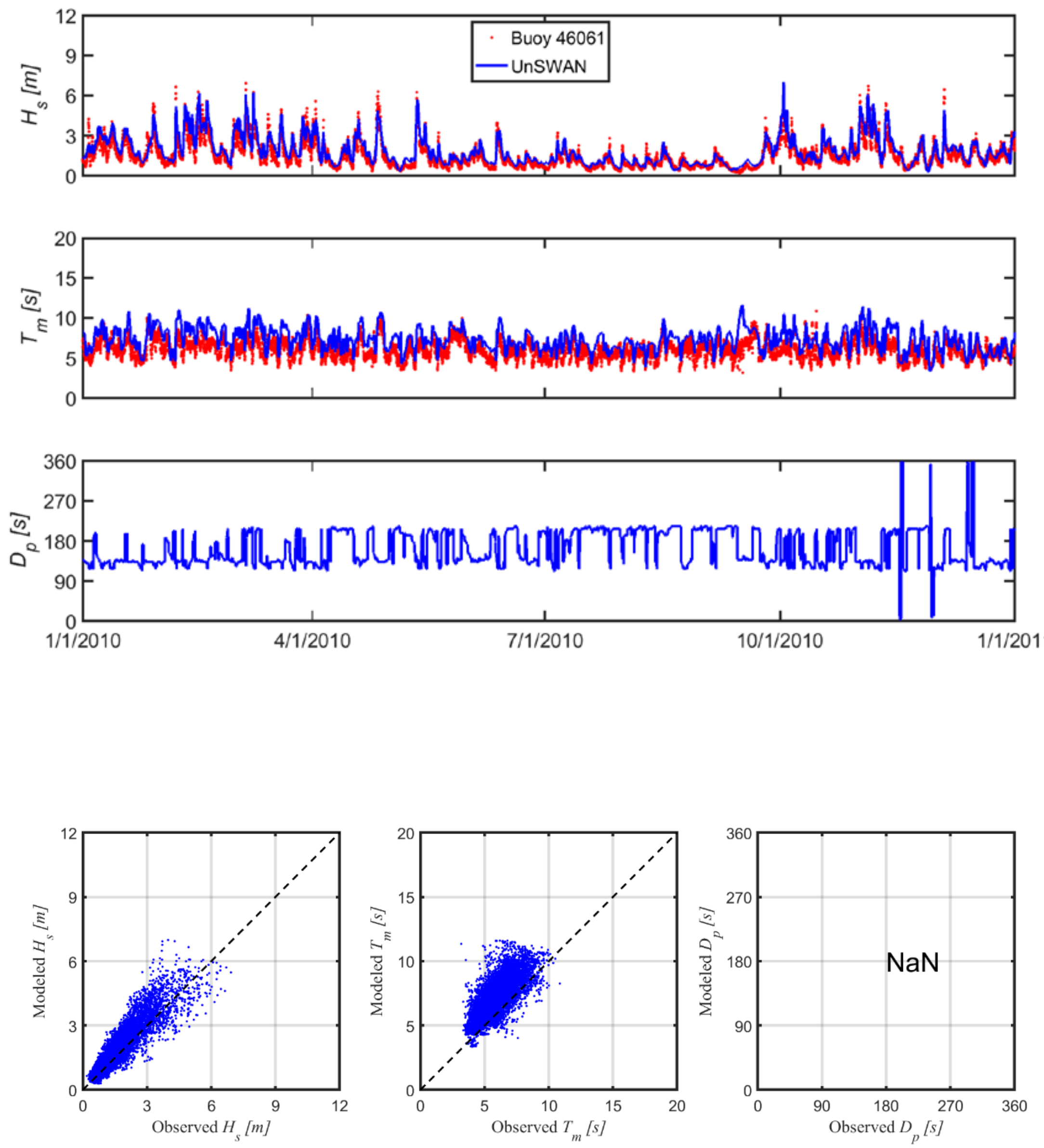

Figure B.49. Comparisons of time series (top) and scatter plots (bottom) of the three UnSWAN model-simulated bulk parameters with observed data at NDBC Buoy 46061 for 2010.

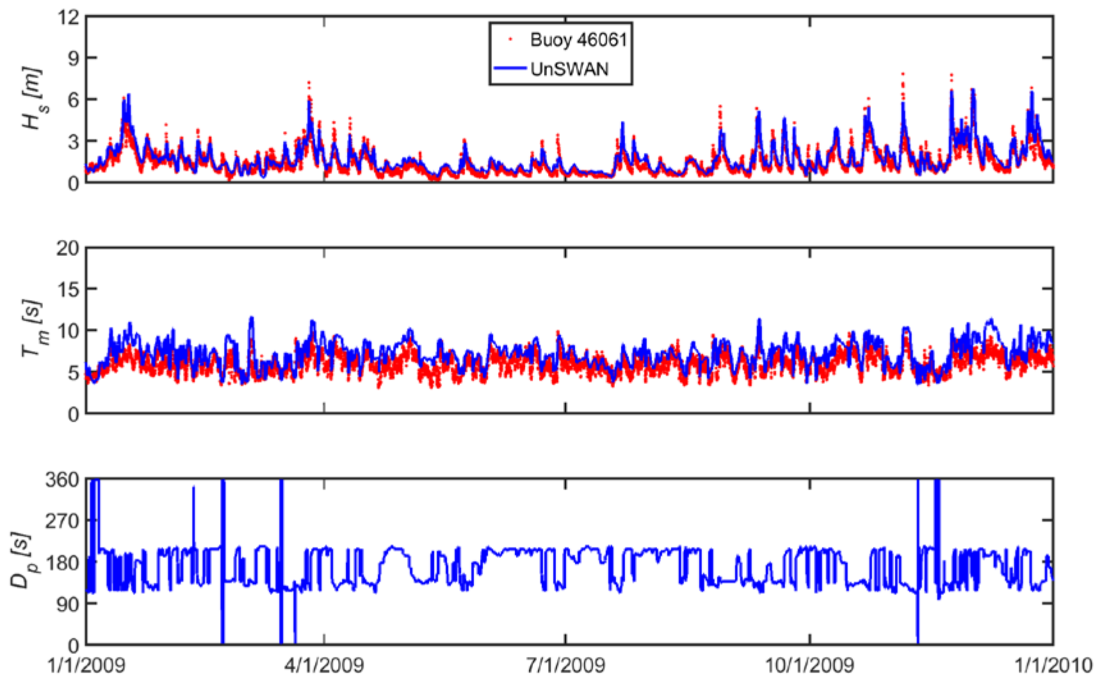

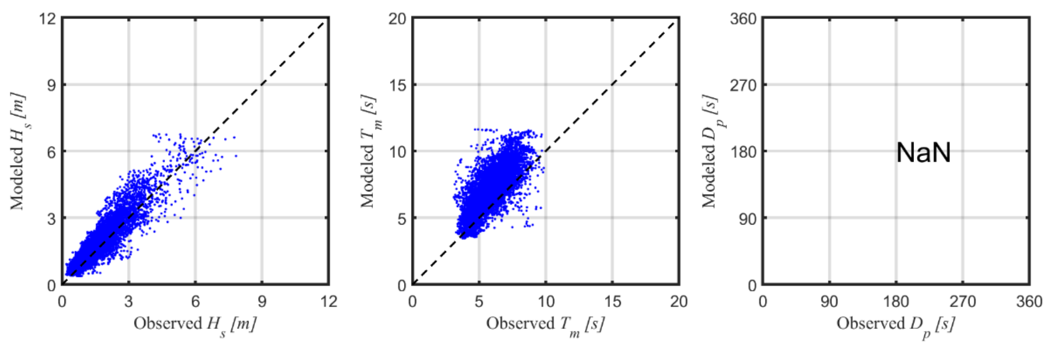

Figure B.50. Comparisons of time series (top) and scatter plots (bottom) of the three UnSWAN model-simulated bulk parameters with observed data at NDBC Buoy 46061 for 2009.

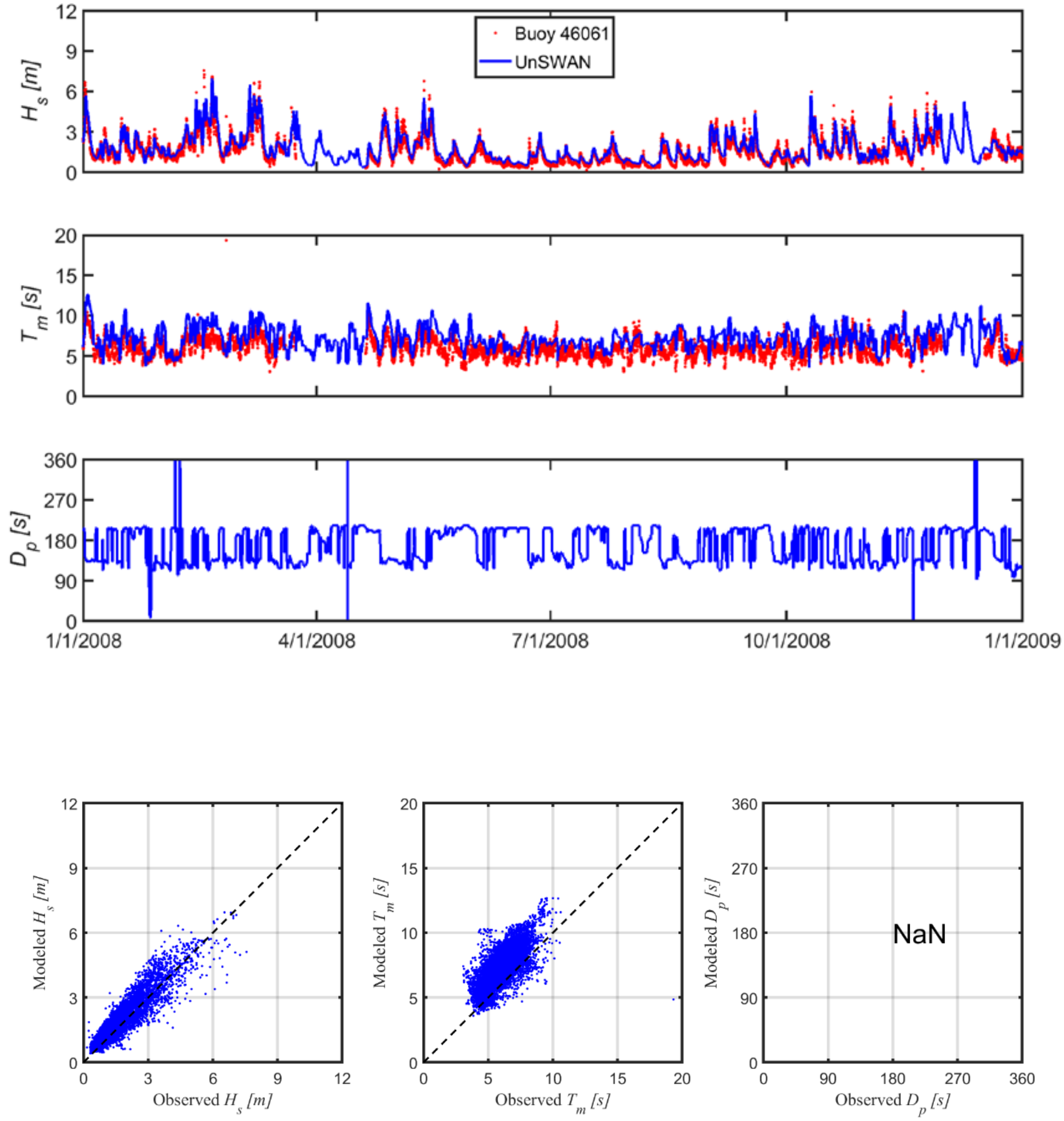

Figure B.51. Comparisons of time series (top) and scatter plots (bottom) of the three UnSWAN model-simulated bulk parameters with observed data at NDBC Buoy 46061 for 2008.

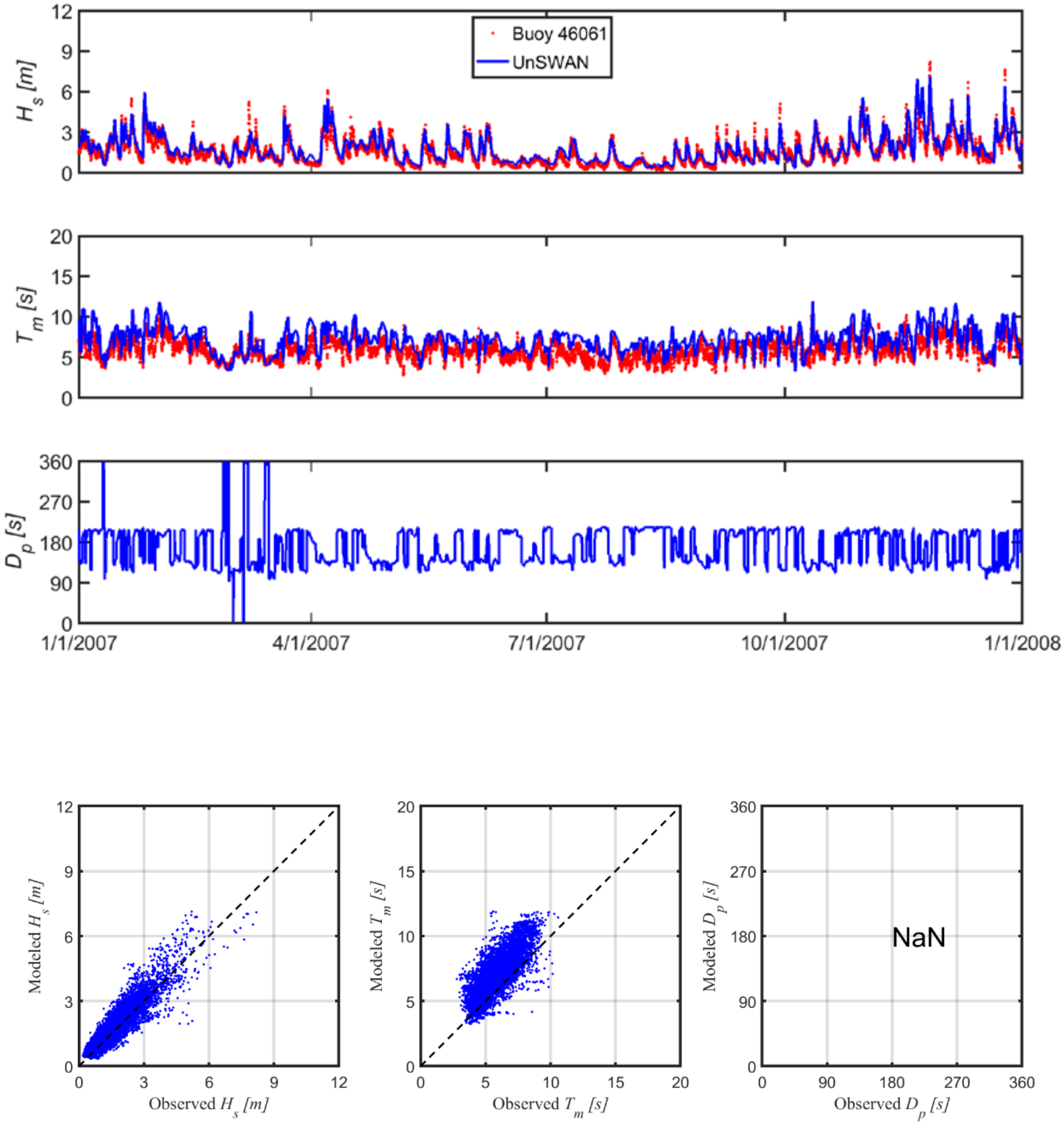

Figure B.52. Comparisons of time series (top) and scatter plots (bottom) of the three UnSWAN model-simulated bulk parameters with observed data at NDBC Buoy 46061 for 2007.

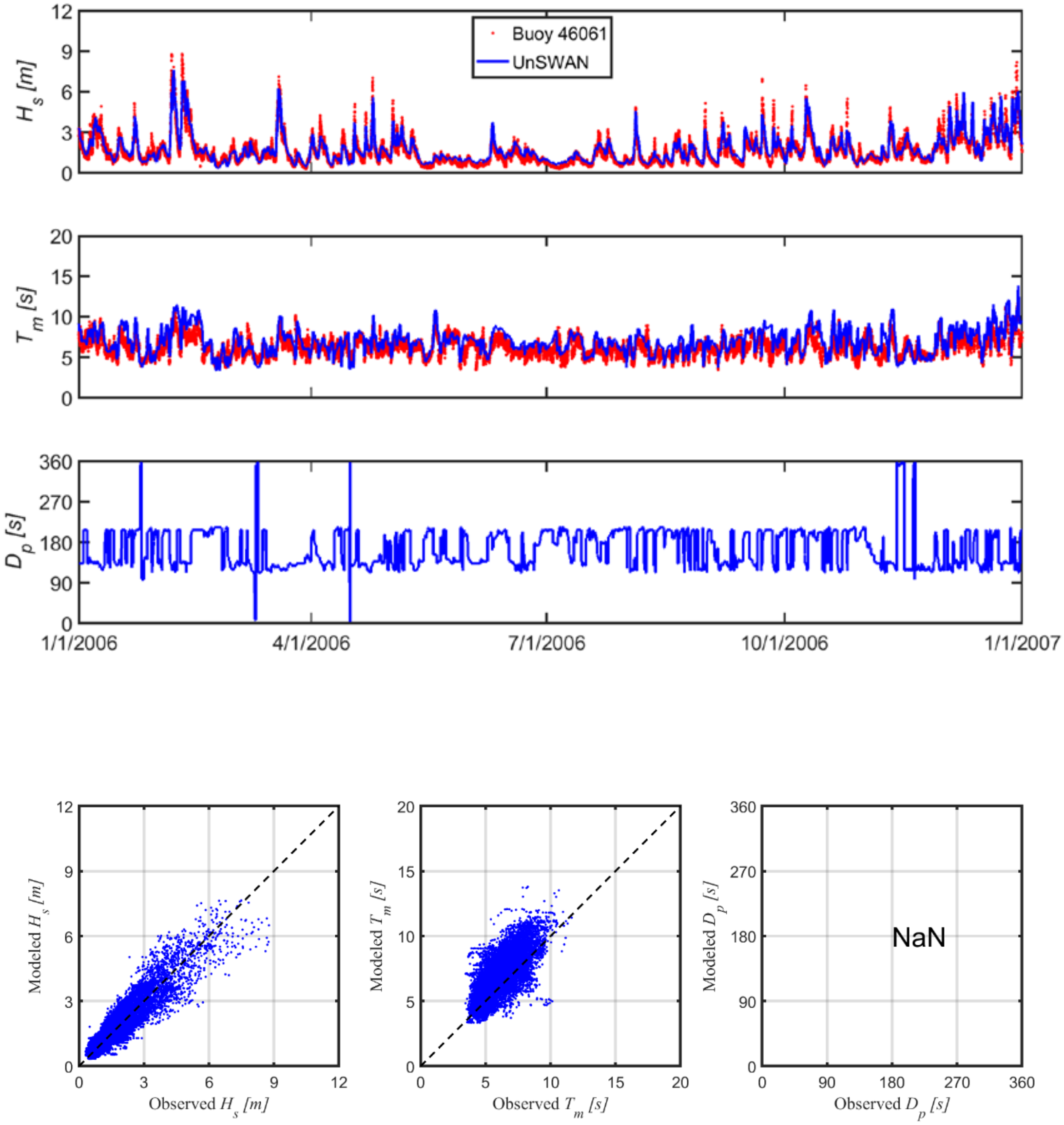

Figure B.53. Comparisons of time series (top) and scatter plots (bottom) of the three UnSWAN model-simulated bulk parameters with observed data at NDBC Buoy 46061 for 2006.

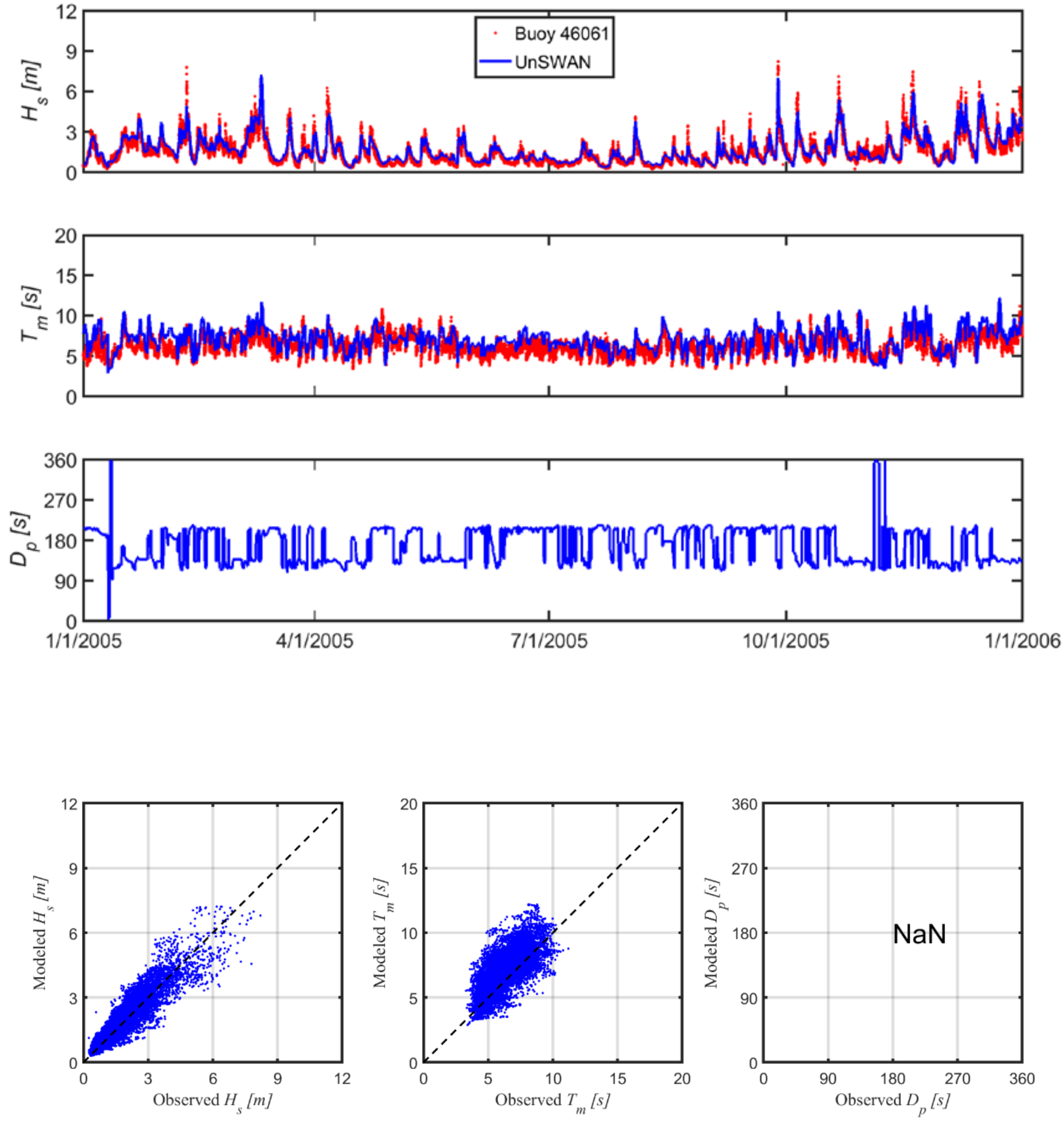

Figure B.54. Comparisons of time series (top) and scatter plots (bottom) of the three UnSWAN model-simulated bulk parameters with observed data at NDBC Buoy 46061 for 2005.

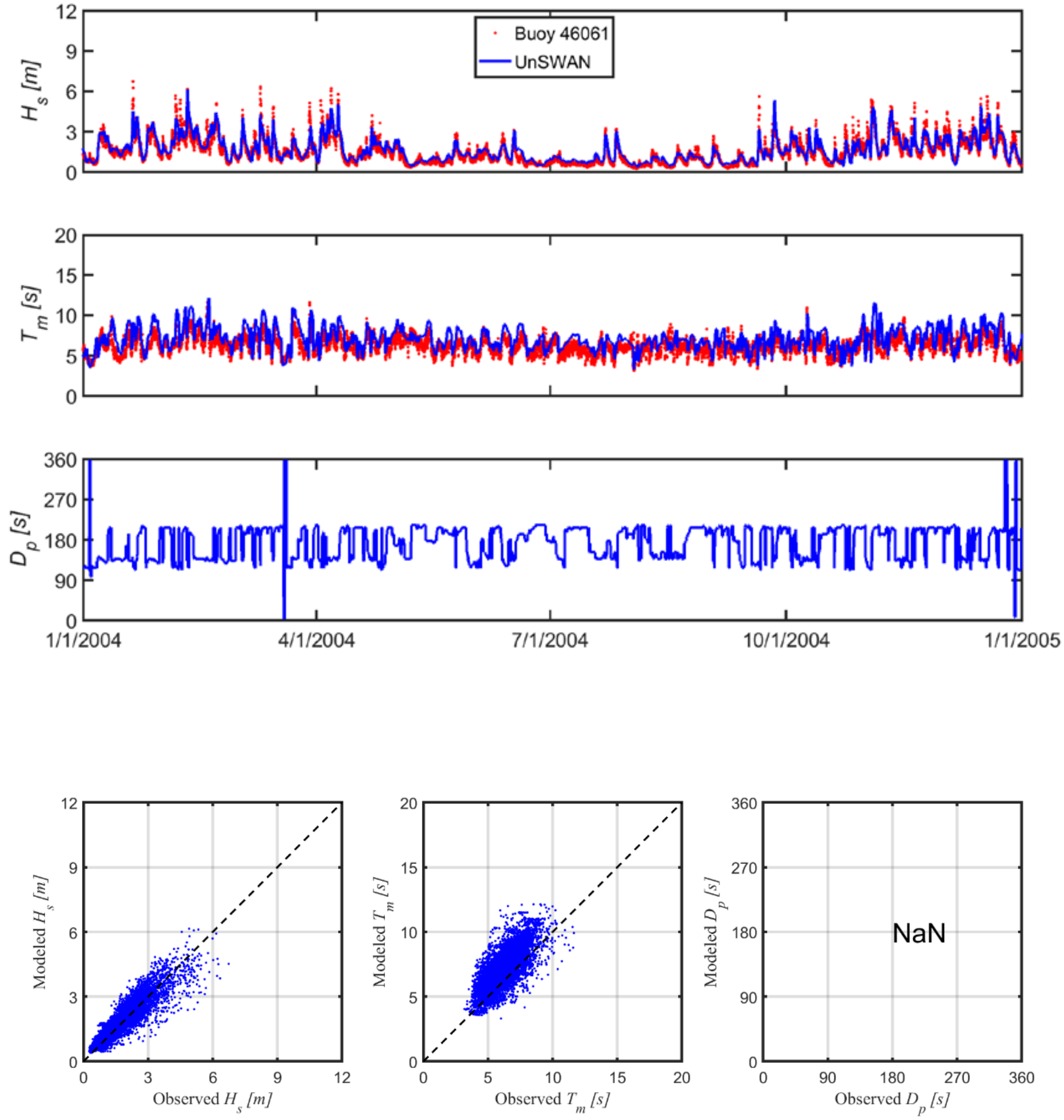

Figure B.55. Comparisons of time series (top) and scatter plots (bottom) of the three UnSWAN model-simulated bulk parameters with observed data at NDBC Buoy 46061 for 2004.

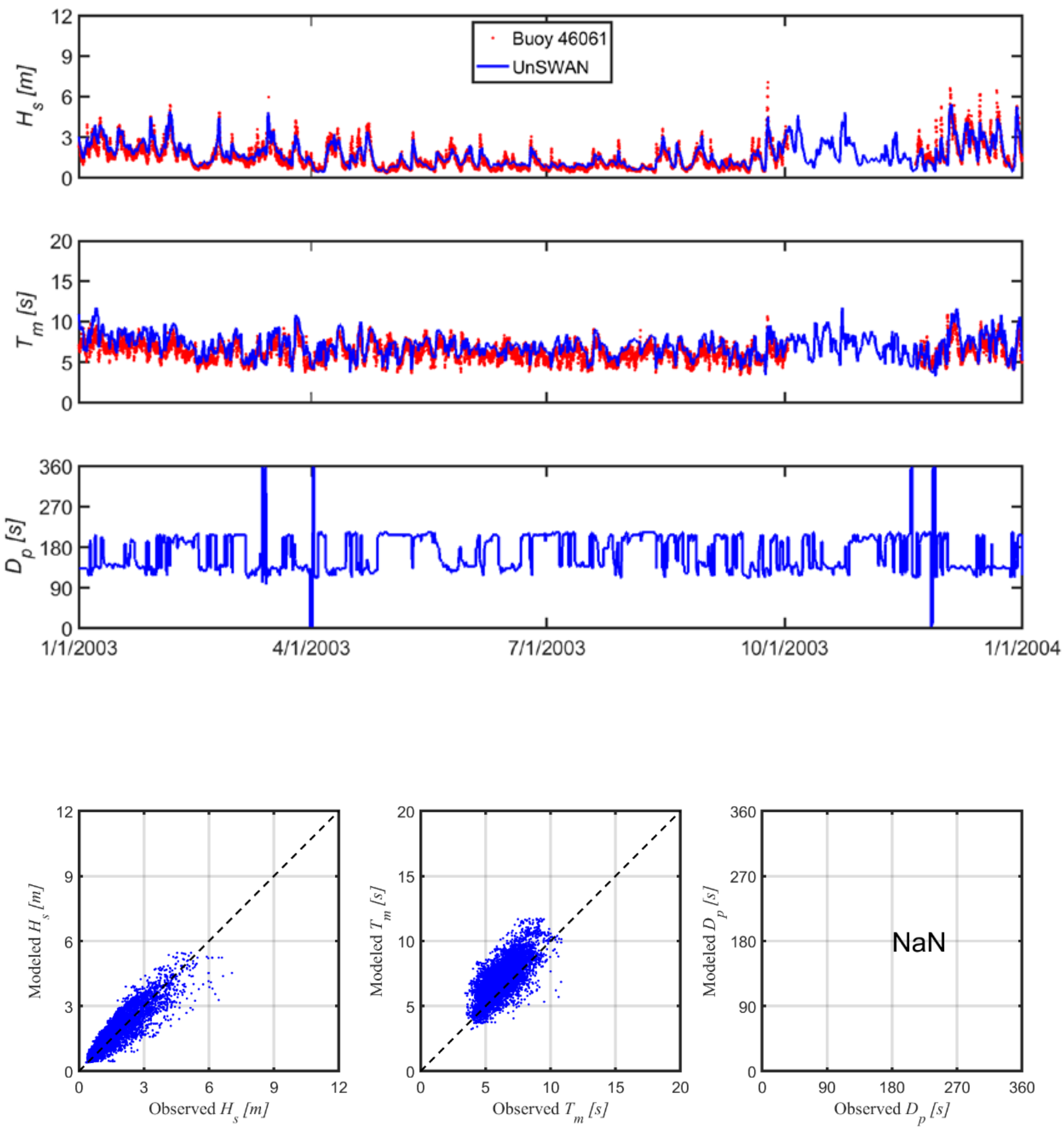

Figure B.56. Comparisons of time series (top) and scatter plots (bottom) of the three UnSWAN model-simulated bulk parameters with observed data at NDBC Buoy 46061 for 2003.

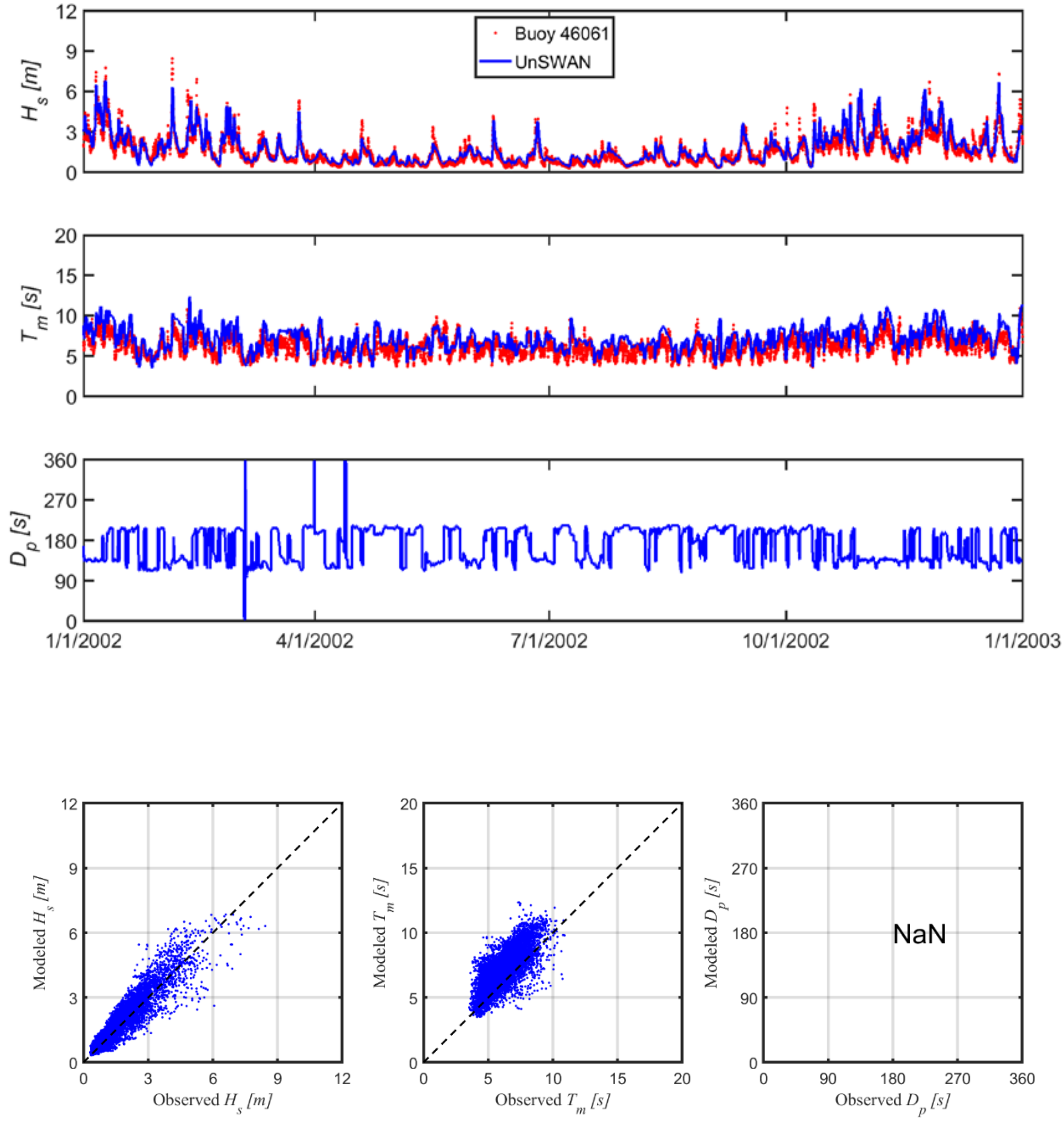

Figure B.57. Comparisons of time series (top) and scatter plots (bottom) of the three UnSWAN model-simulated bulk parameters with observed data at NDBC Buoy 46061 for 2002.

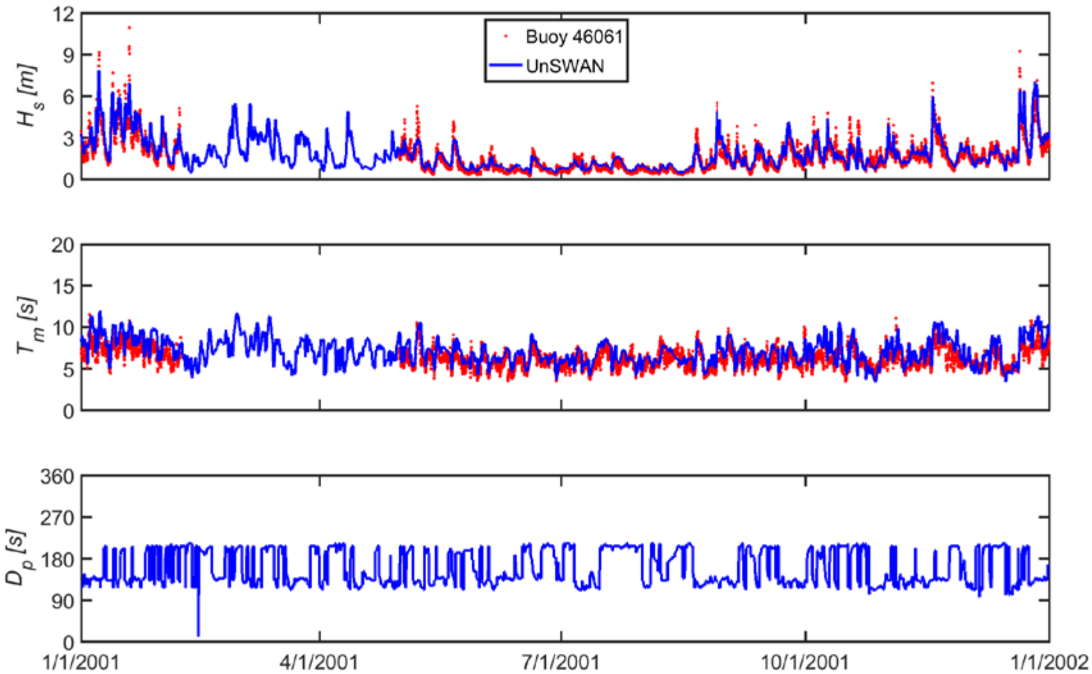

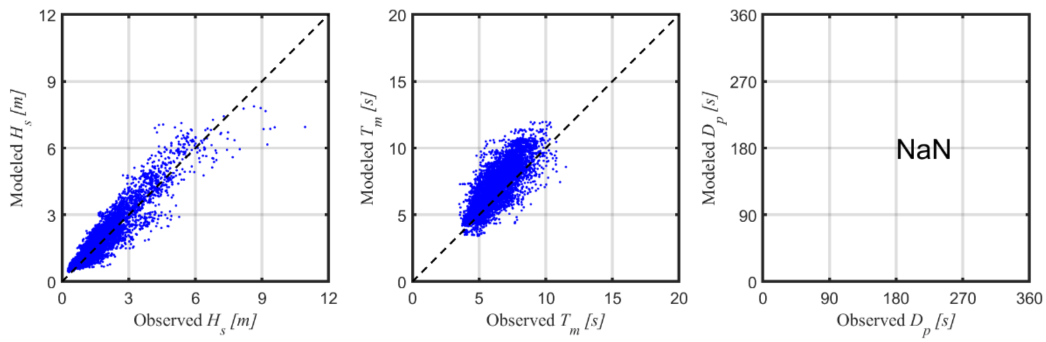

Figure B.58. Comparisons of time series (top) and scatter plots (bottom) of the three UnSWAN model-simulated bulk parameters with observed data at NDBC Buoy 46061 for 2001.

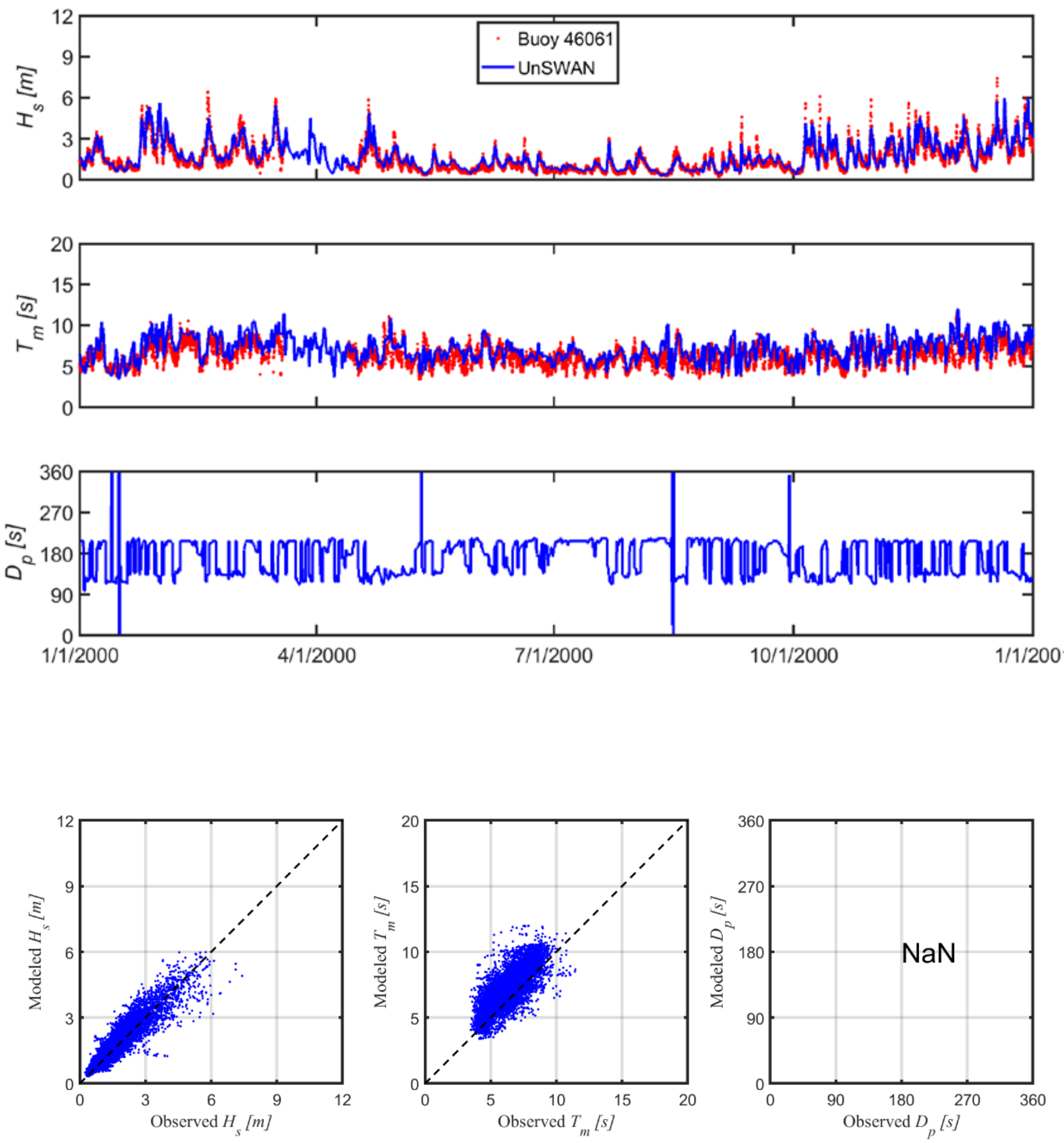

Figure B.59. Comparisons of time series (top) and scatter plots (bottom) of the three UnSWAN model-simulated bulk parameters with observed data at NDBC Buoy 46061 for 2000.

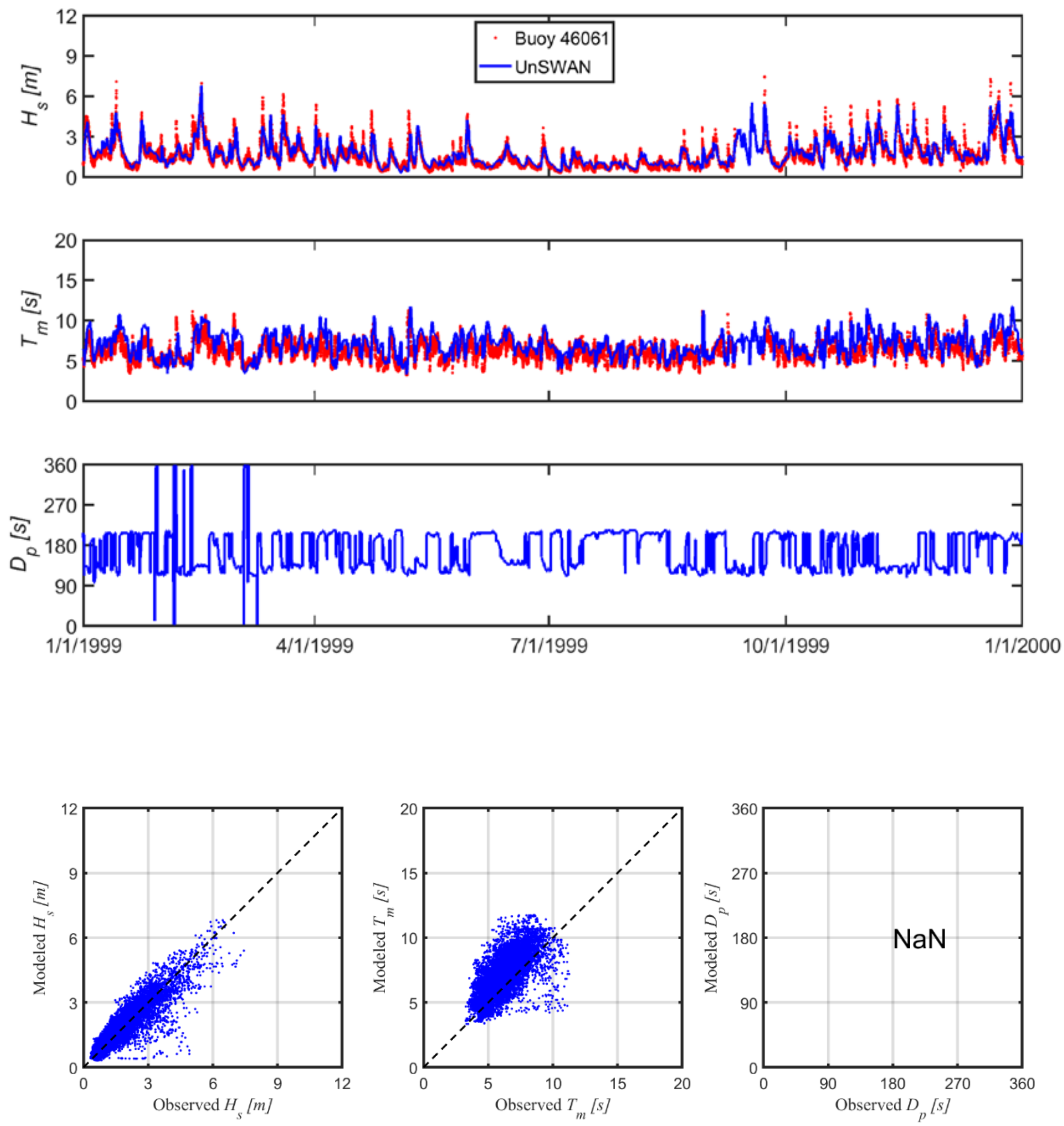

Figure B.60. Comparisons of time series (top) and scatter plots (bottom) of the three UnSWAN model-simulated bulk parameters with observed data at NDBC Buoy 46061 for 1999.

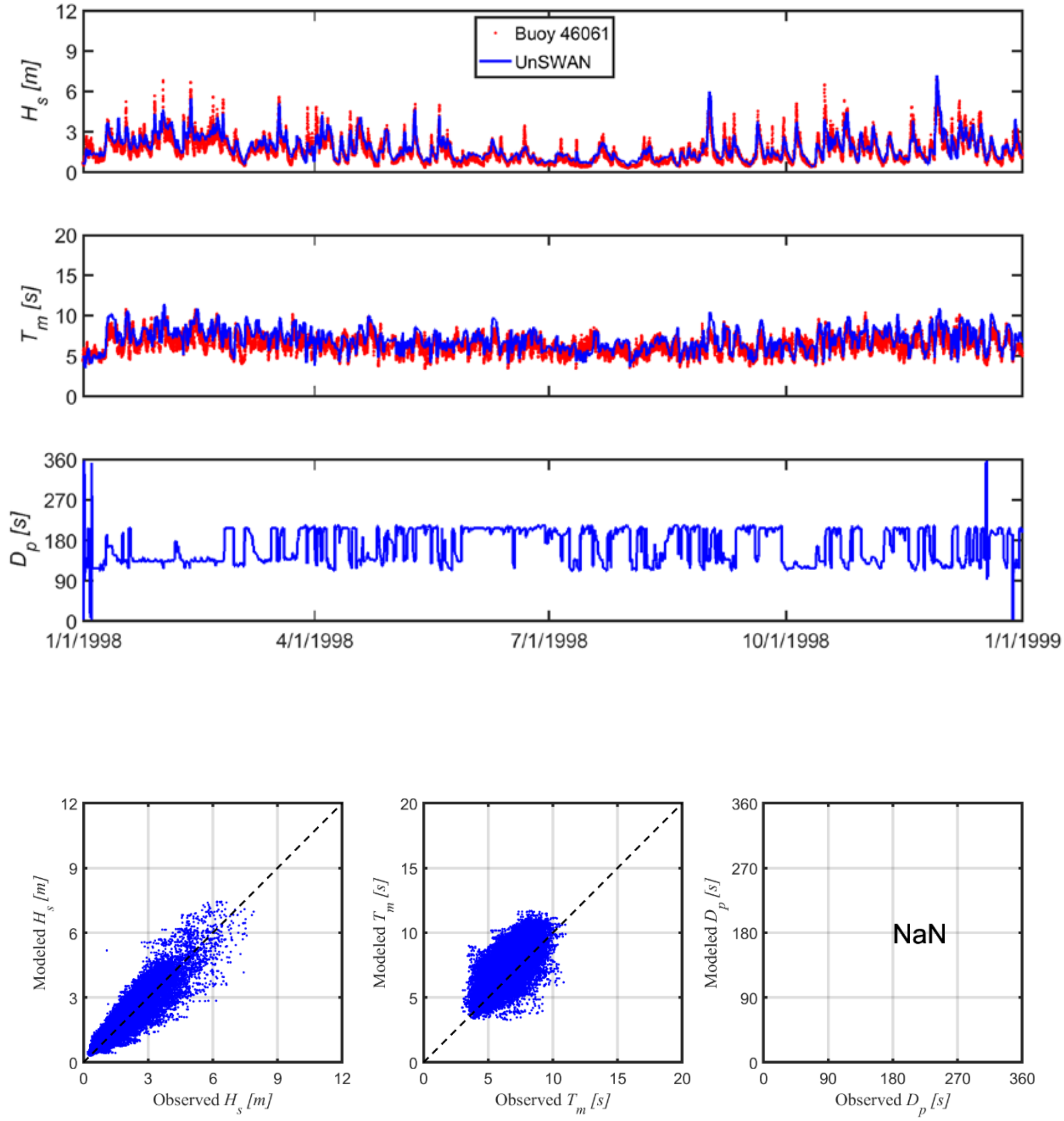

Figure B.61. Comparisons of time series (top) and scatter plots (bottom) of the three UnSWAN model-simulated bulk parameters with observed data at NDBC Buoy 46061 for 1998.

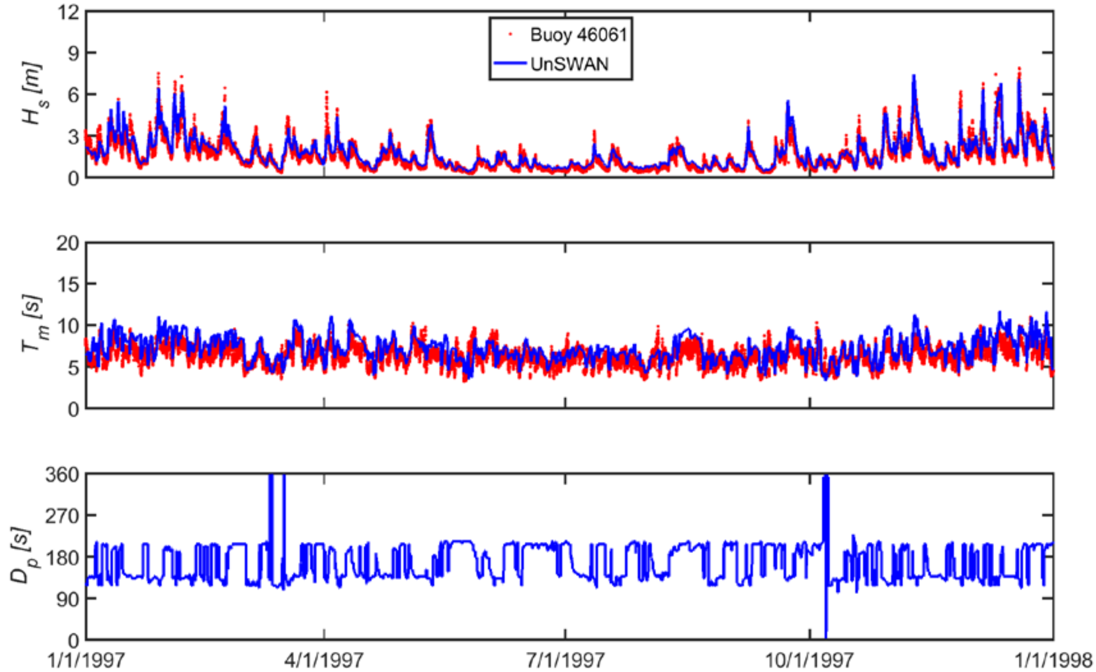

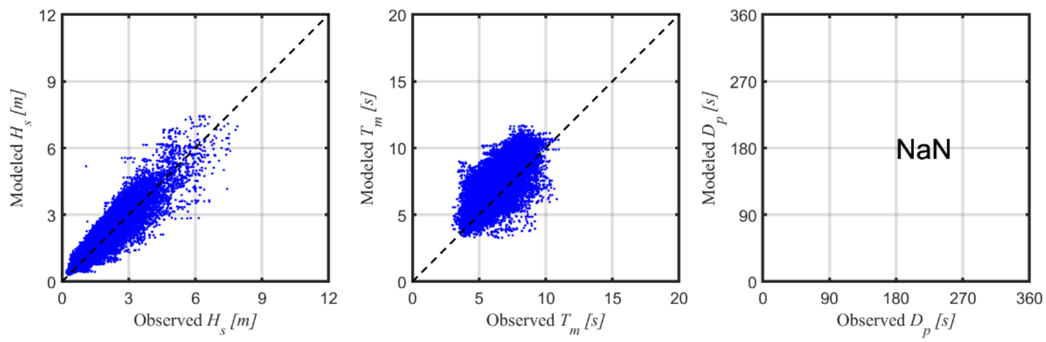

Figure B.62. Comparisons of time series (top) and scatter plots (bottom) of the three UnSWAN model-simulated bulk parameters with observed data at NDBC Buoy 46061 for 1997.

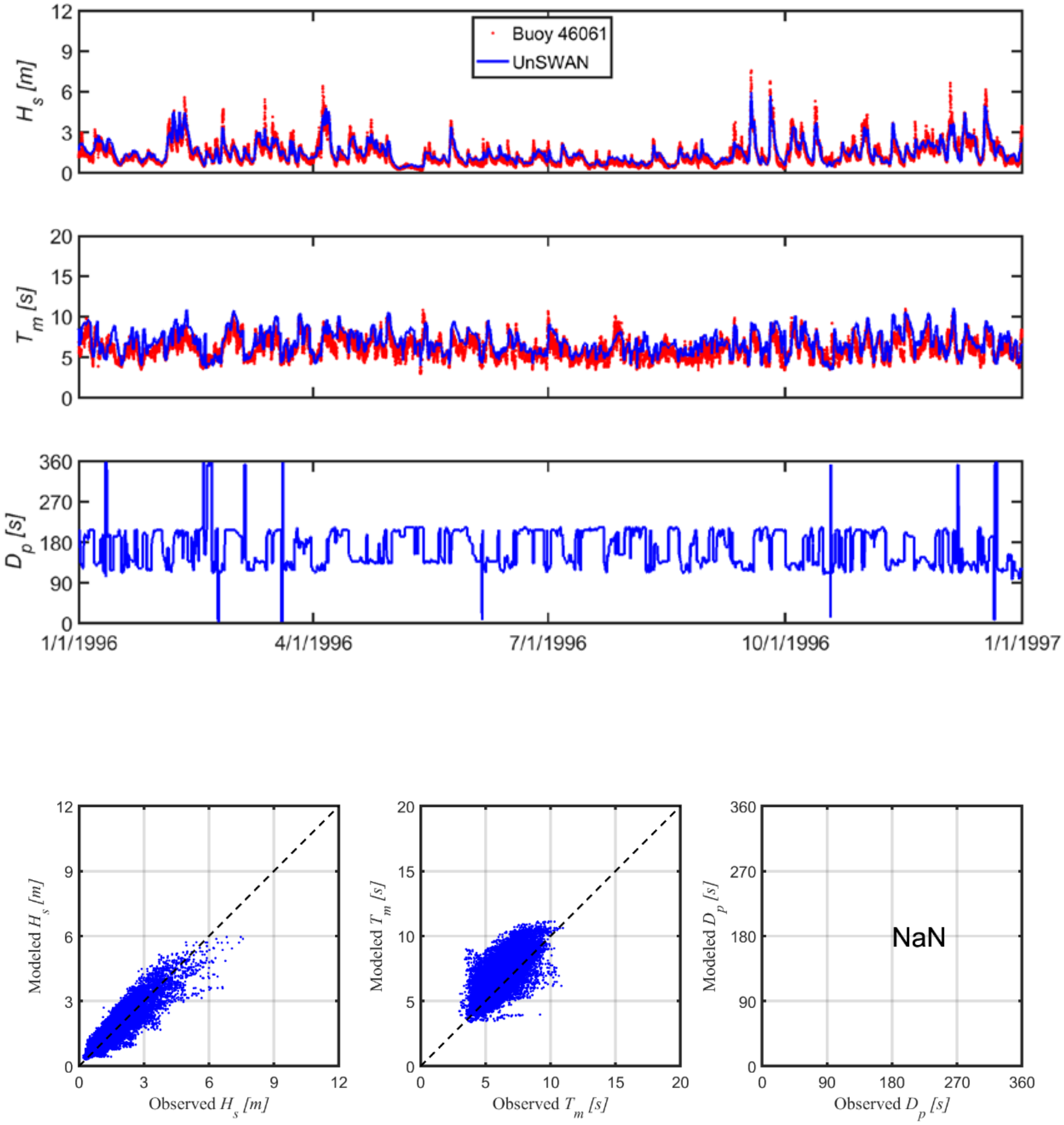

Figure B.63. Comparisons of time series (top) and scatter plots (bottom) of the three UnSWAN model-simulated bulk parameters with observed data at NDBC Buoy 46061 for 1996.

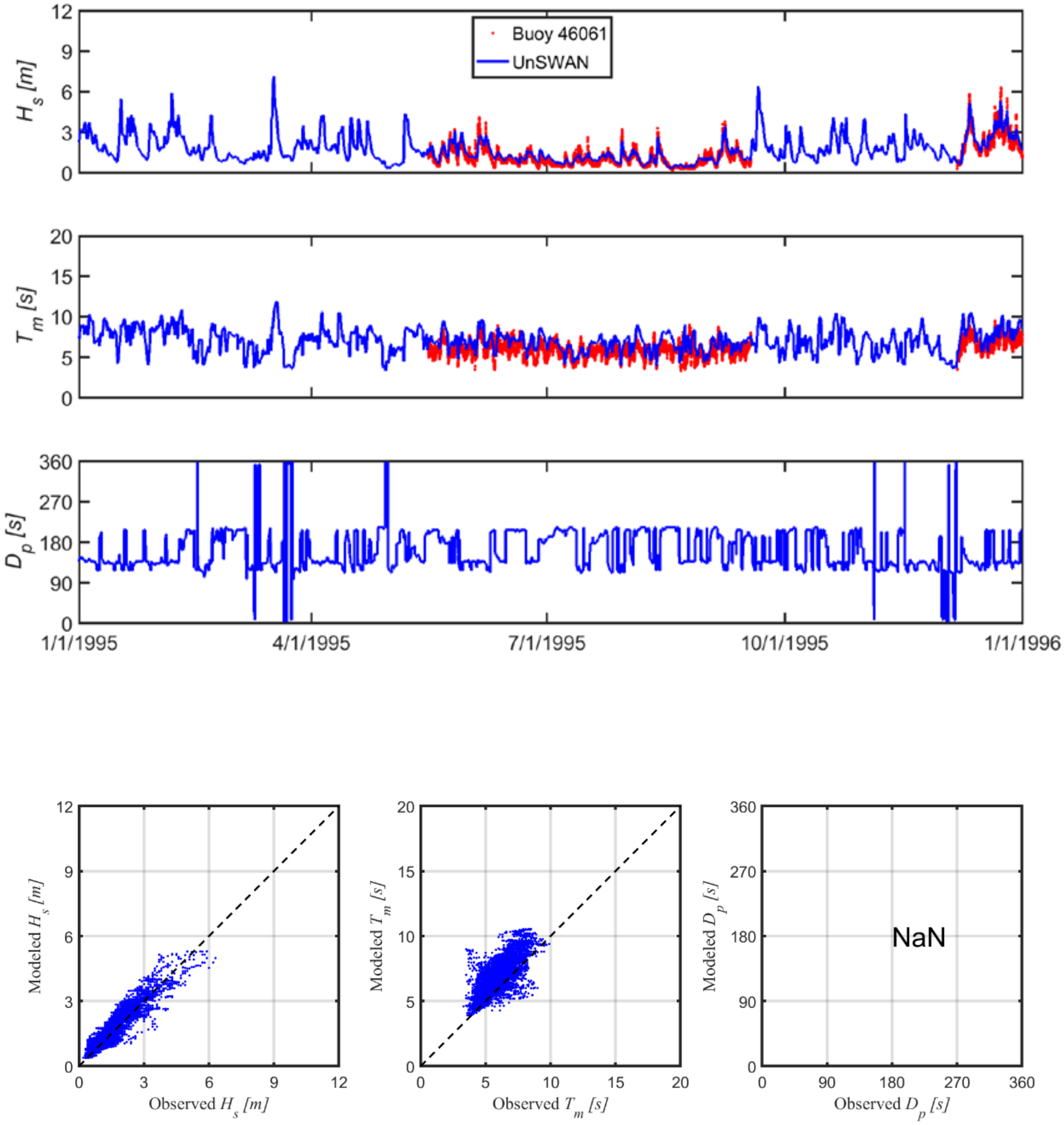

Figure B.64. Comparisons of time series (top) and scatter plots (bottom) of the three UnSWAN model-simulated bulk parameters with observed data at NDBC Buoy 46061 for 1995.

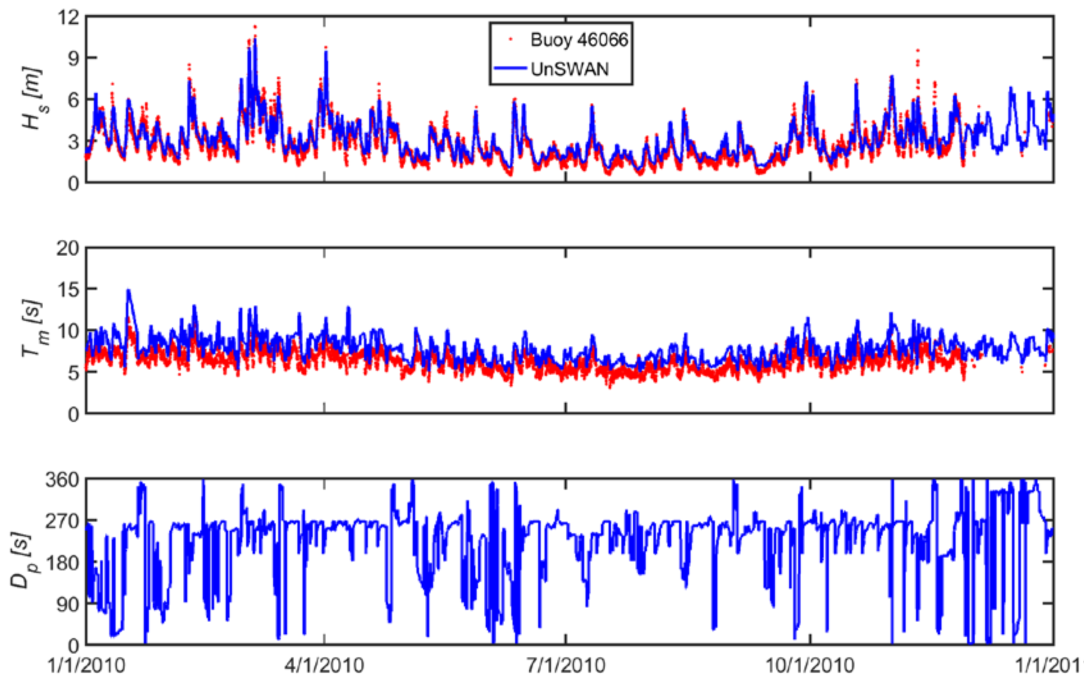

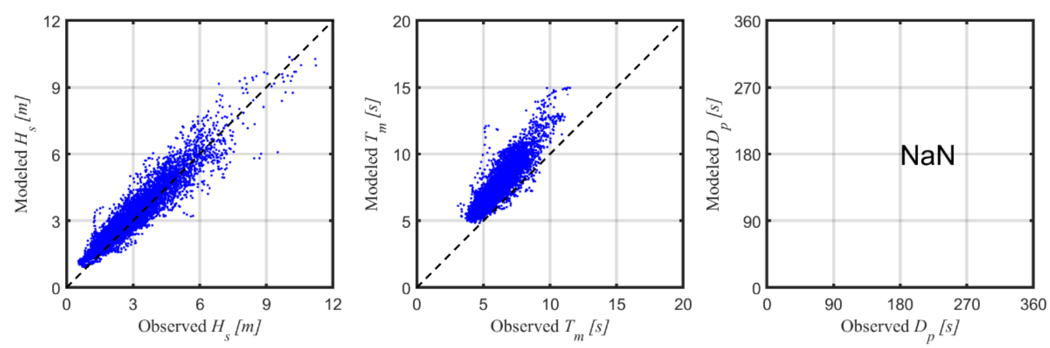

Figure B.65. Comparisons of time series (top) and scatter plots (bottom) of the three UnSWAN model-simulated bulk parameters with observed data at NDBC Buoy 46066 for 2010.

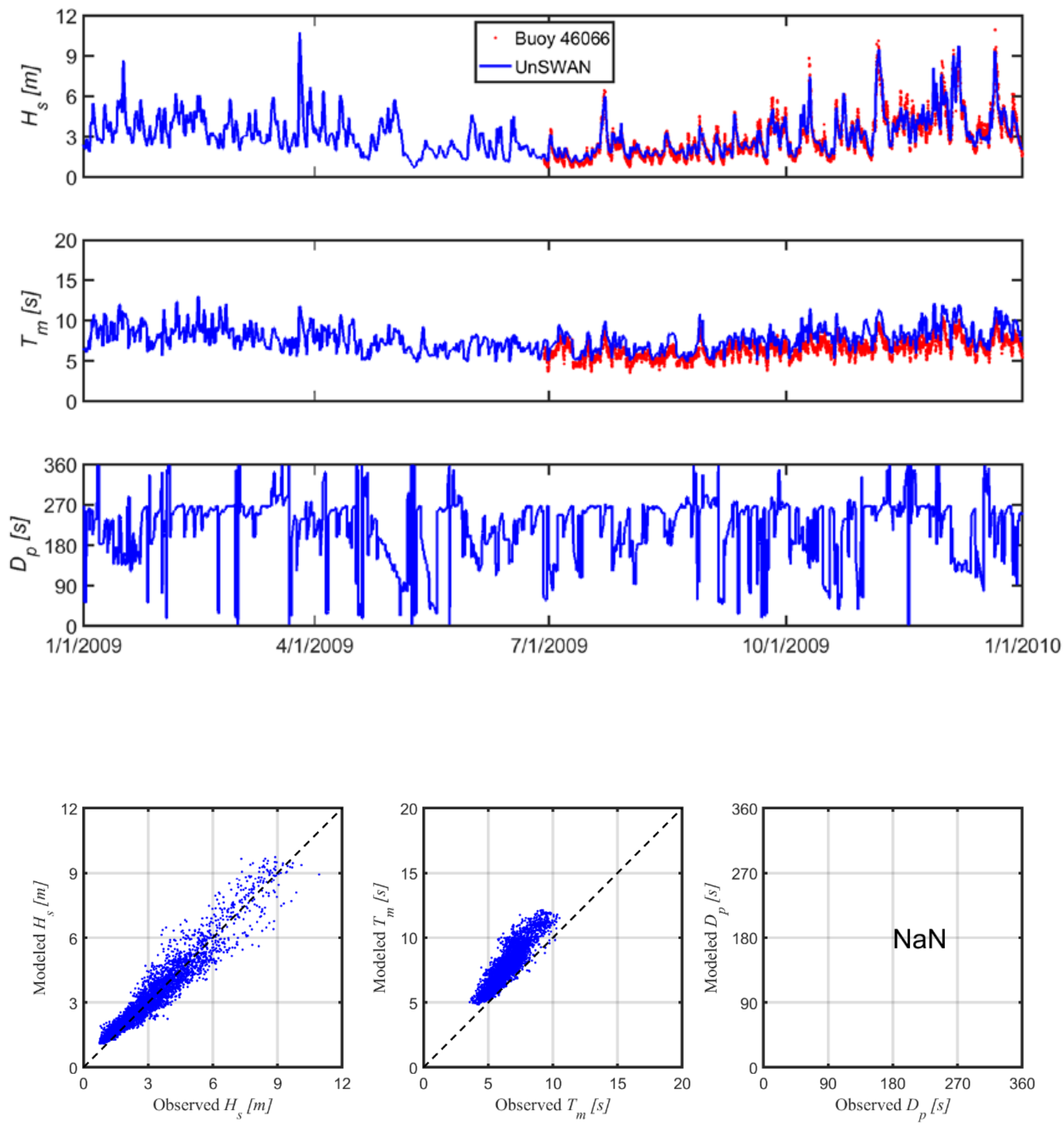

Figure B.66. Comparisons of time series (top) and scatter plots (bottom) of the three UnSWAN model-simulated bulk parameters with observed data at NDBC Buoy 46066 for 2009.

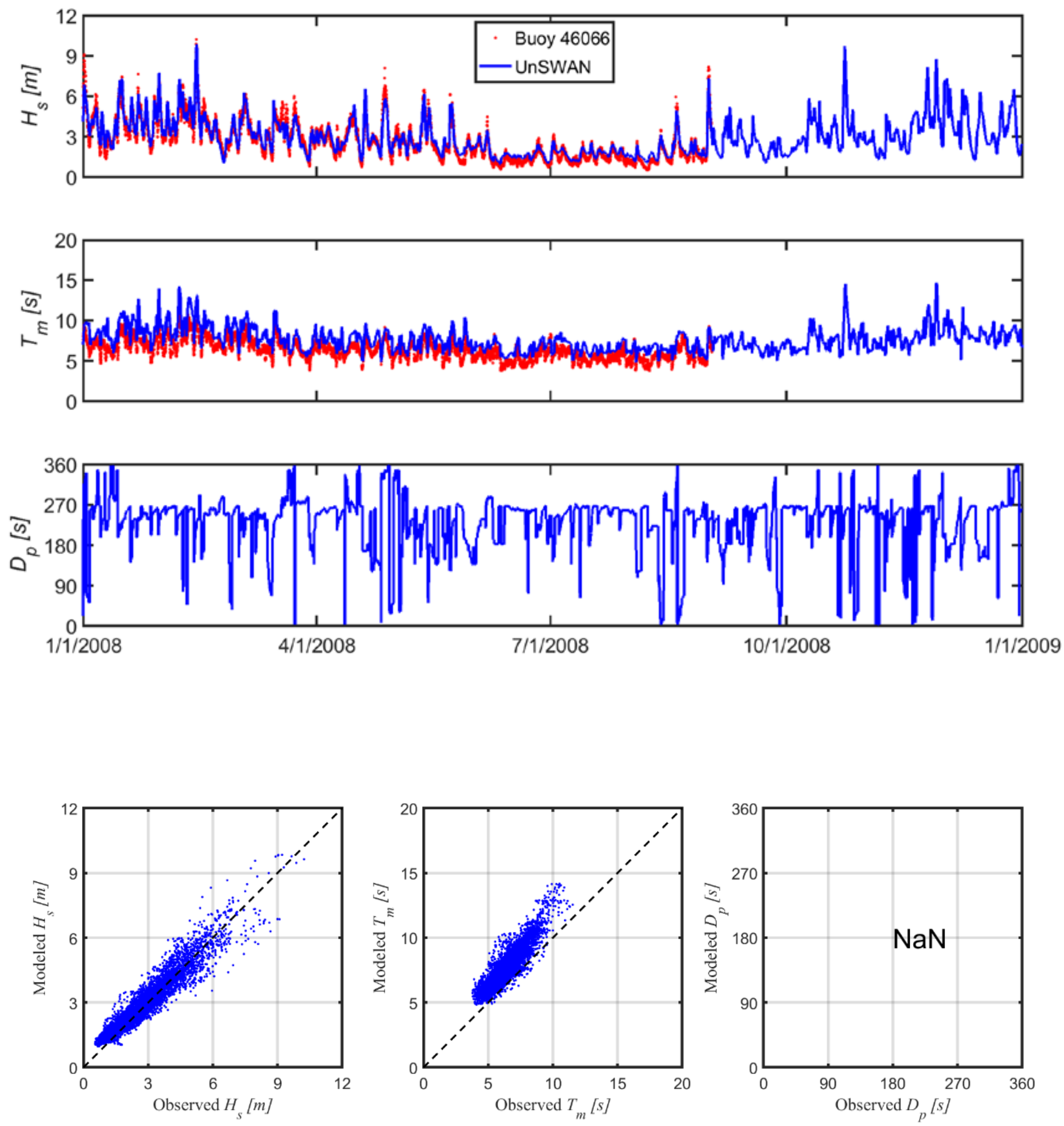

Figure B.67. Comparisons of time series (top) and scatter plots (bottom) of the three UnSWAN model-simulated bulk parameters with observed data at NDBC Buoy 46066 for 2008.

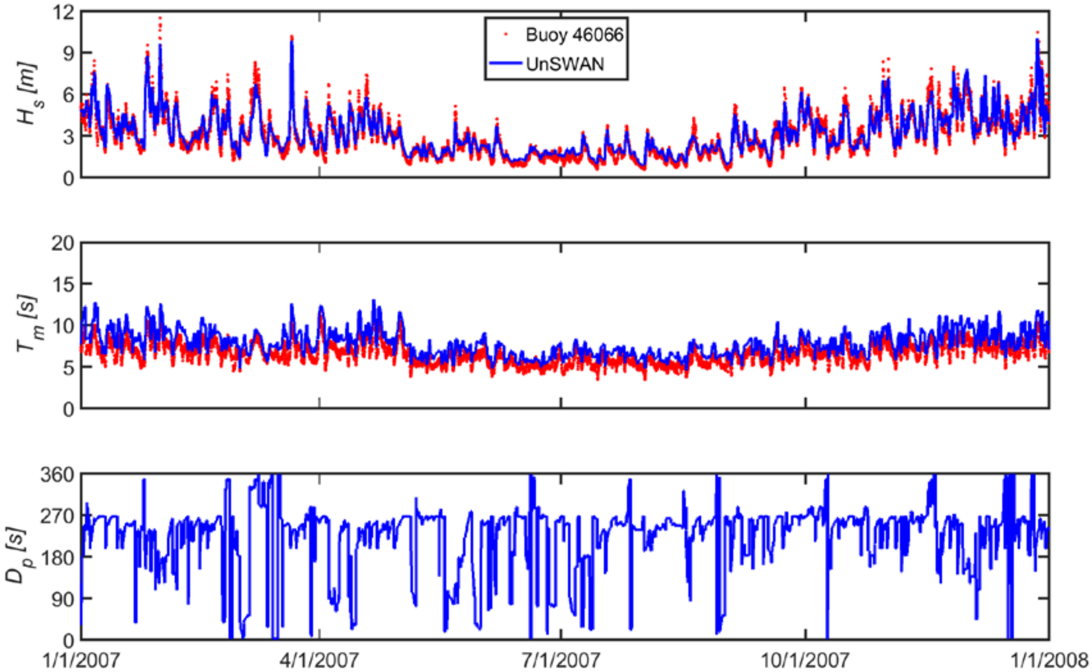

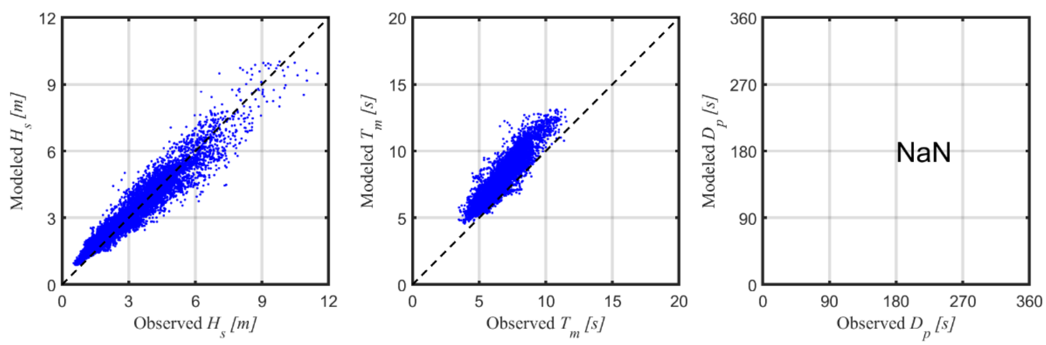

Figure B.68. Comparisons of time series (top) and scatter plots (bottom) of the three UnSWAN model-simulated bulk parameters with observed data at NDBC Buoy 46066 for 2007.

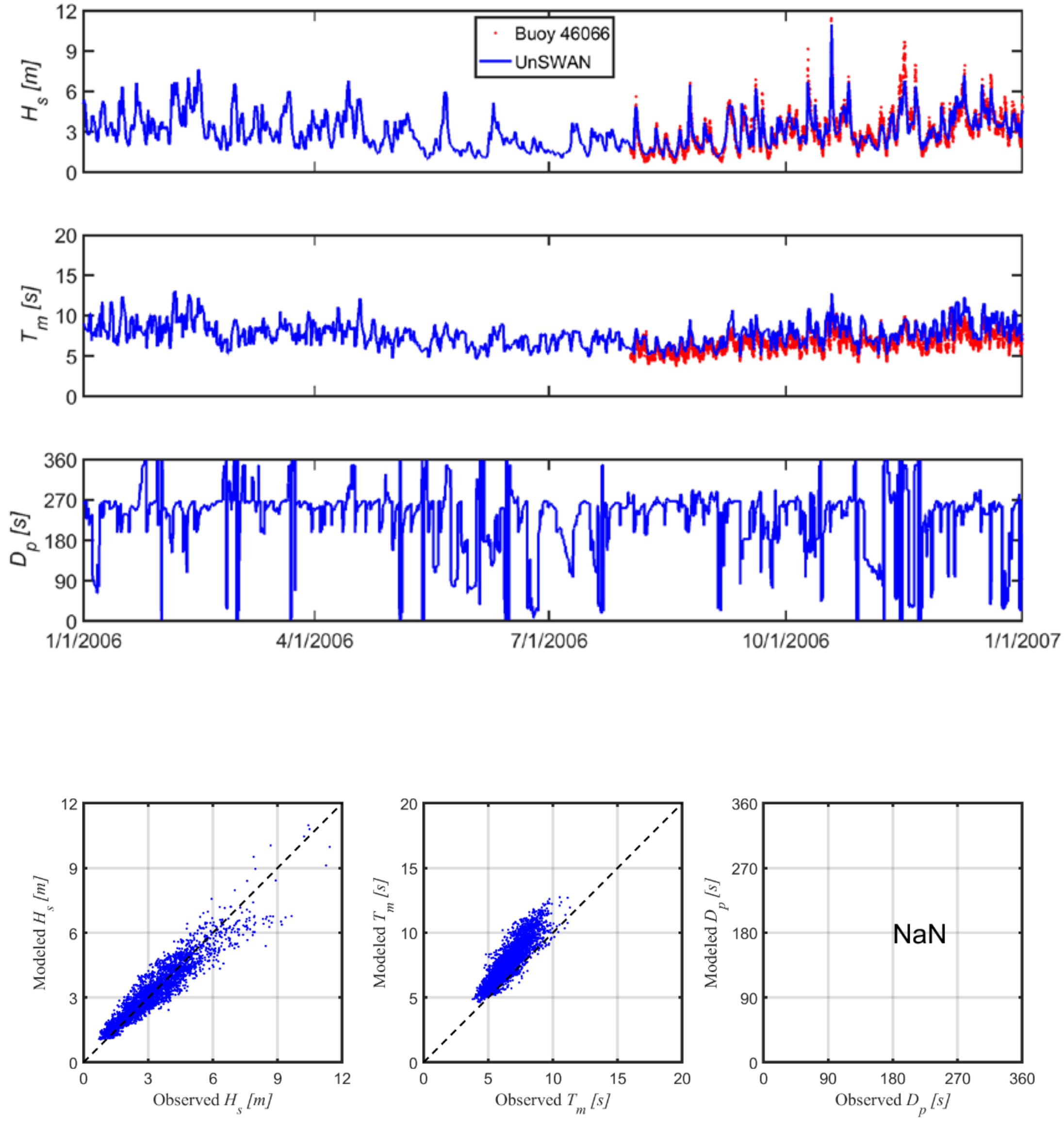

Figure B.69. Comparisons of time series (top) and scatter plots (bottom) of the three UnSWAN model-simulated bulk parameters with observed data at NDBC Buoy 46066 for 2006.

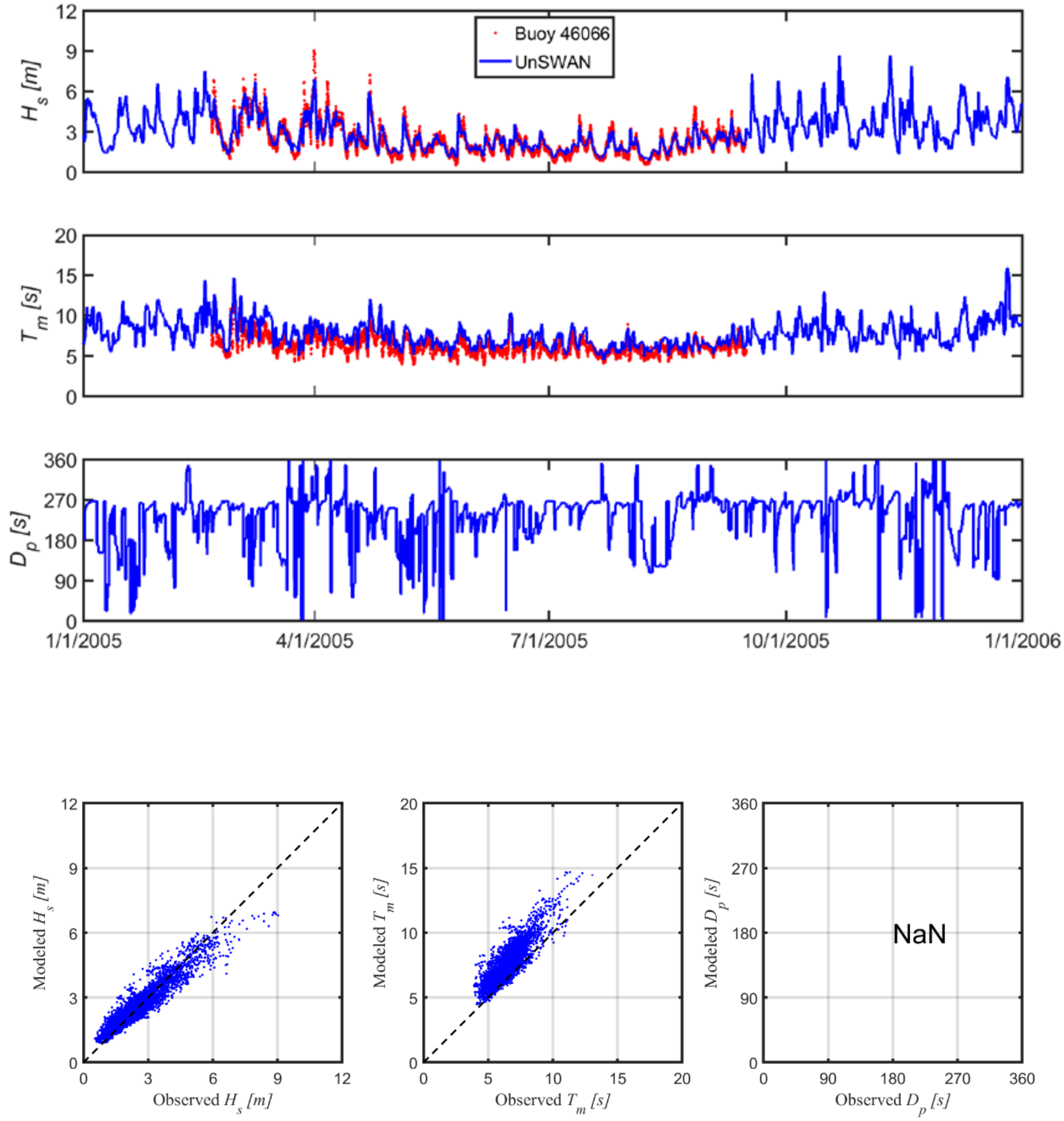

Figure B.70. Comparisons of time series (top) and scatter plots (bottom) of the three UnSWAN model-simulated bulk parameters with observed data at NDBC Buoy 46066 for 2005.

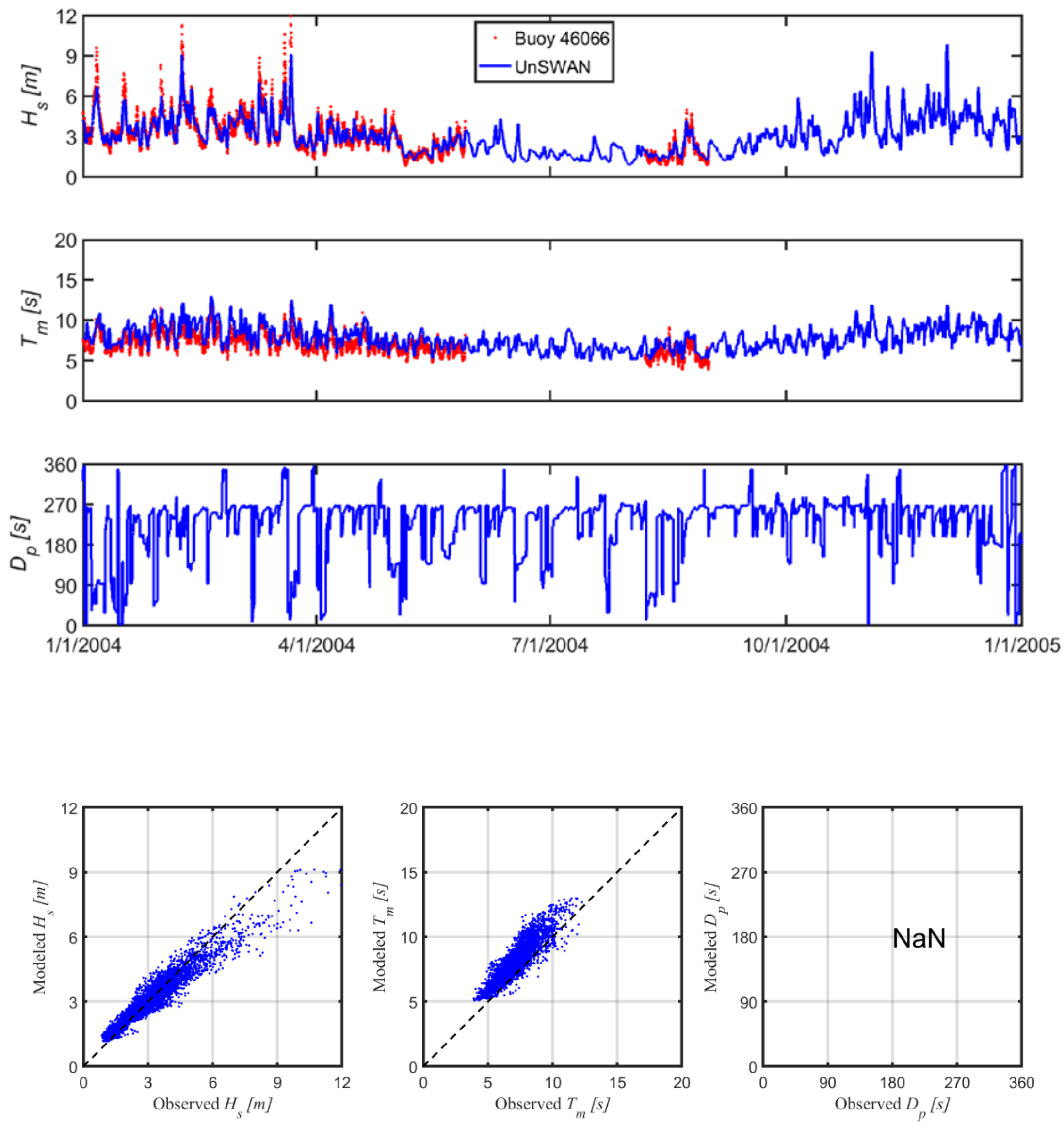

Figure B.71. Comparisons of time series (top) and scatter plots (bottom) of the three UnSWAN model-simulated bulk parameters with observed data at NDBC Buoy 46066 for 2004.

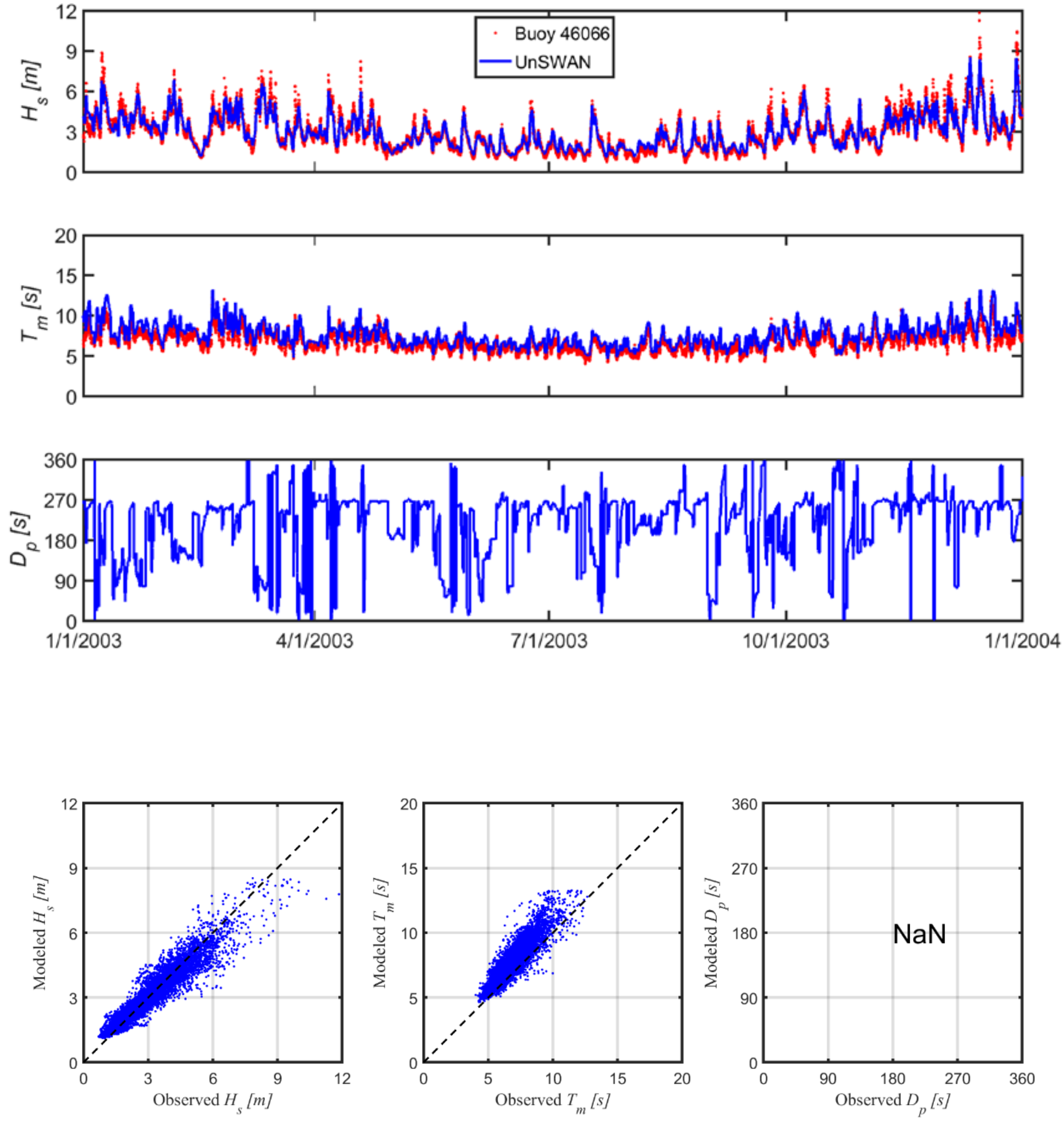

Figure B.72. Comparisons of time series (top) and scatter plots (bottom) of the three UnSWAN model-simulated bulk parameters with observed data at NDBC Buoy 46066 for 2003.

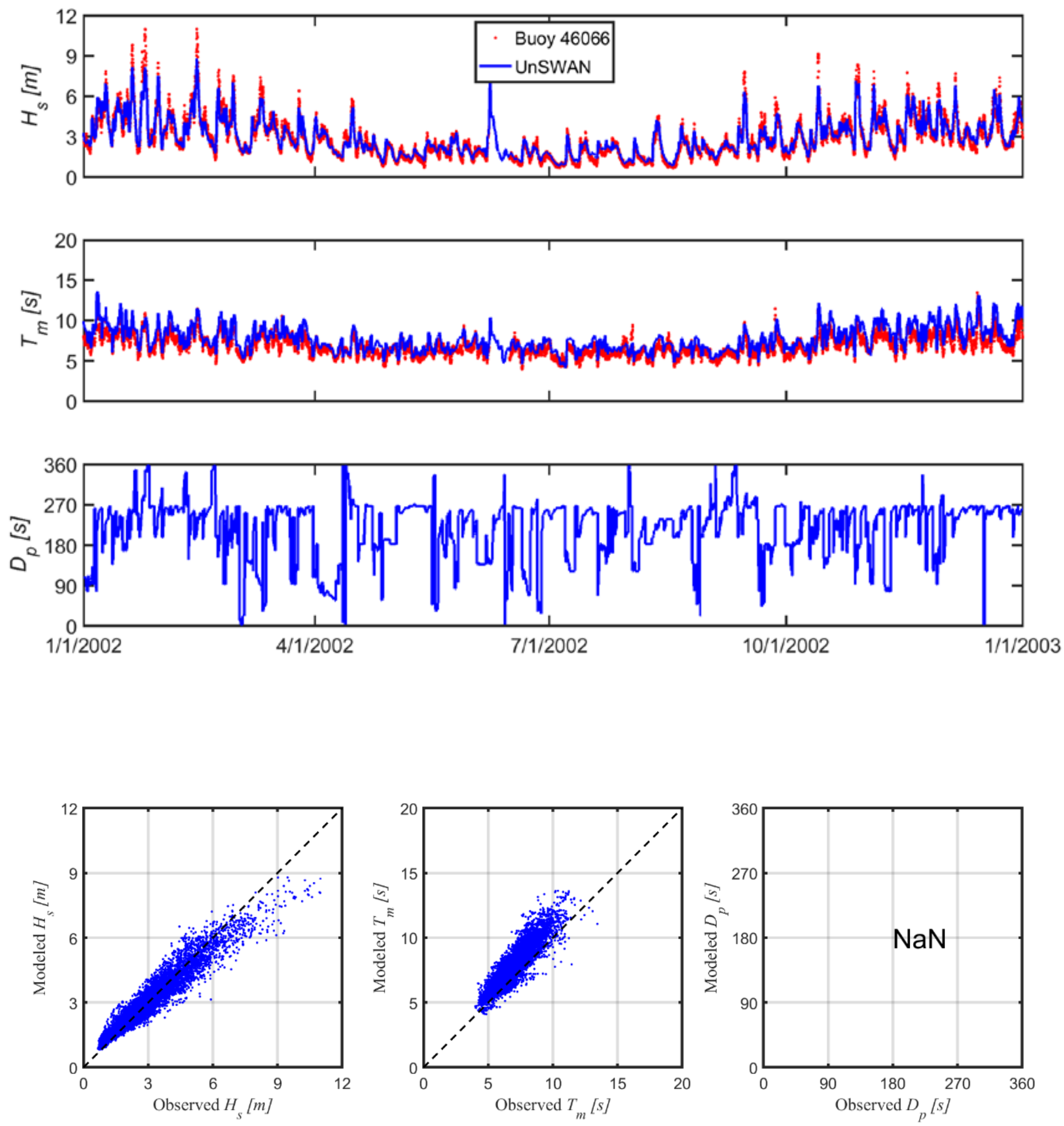

Figure B.73. Comparisons of time series (top) and scatter plots (bottom) of the three UnSWAN model-simulated bulk parameters with observed data at NDBC Buoy 46066 for 2002.

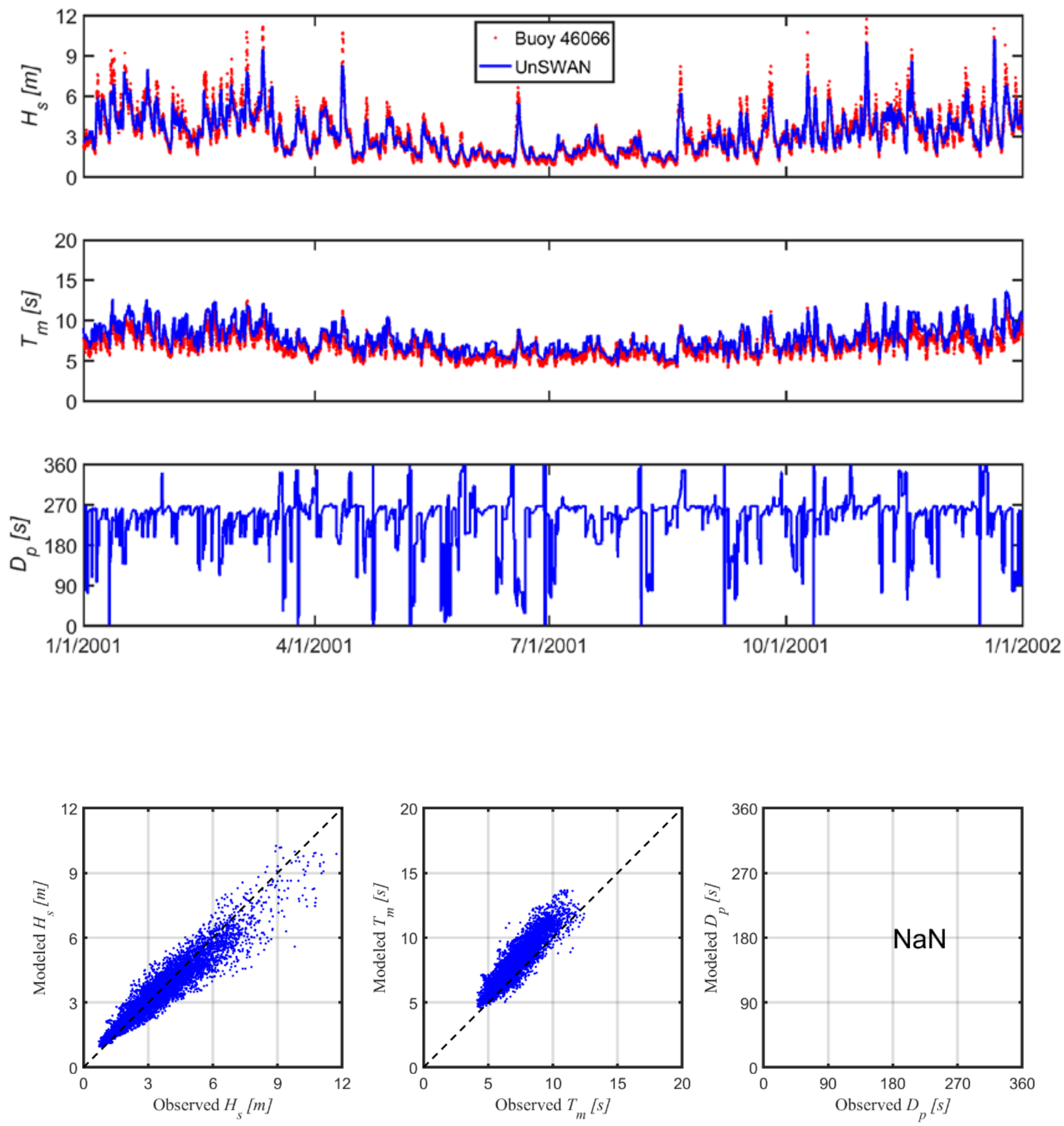

Figure B.74. Comparisons of time series (top) and scatter plots (bottom) of the three UnSWAN model-simulated bulk parameters with observed data at NDBC Buoy 46066 for 2001.

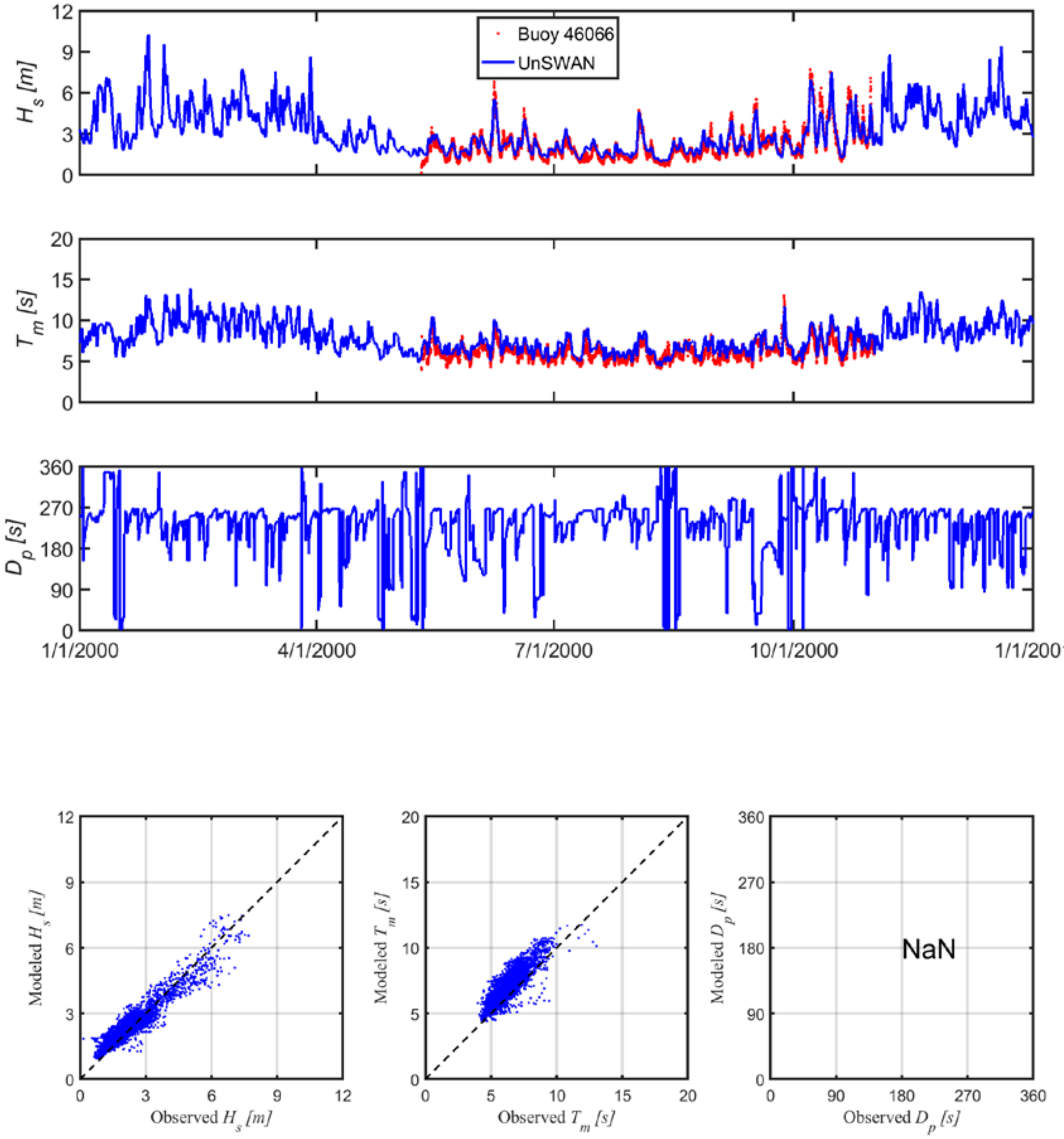

Figure B.75. Comparisons of time series (top) and scatter plots (bottom) of the three UnSWAN model-simulated bulk parameters with observed data at NDBC Buoy 46066 for 2000.

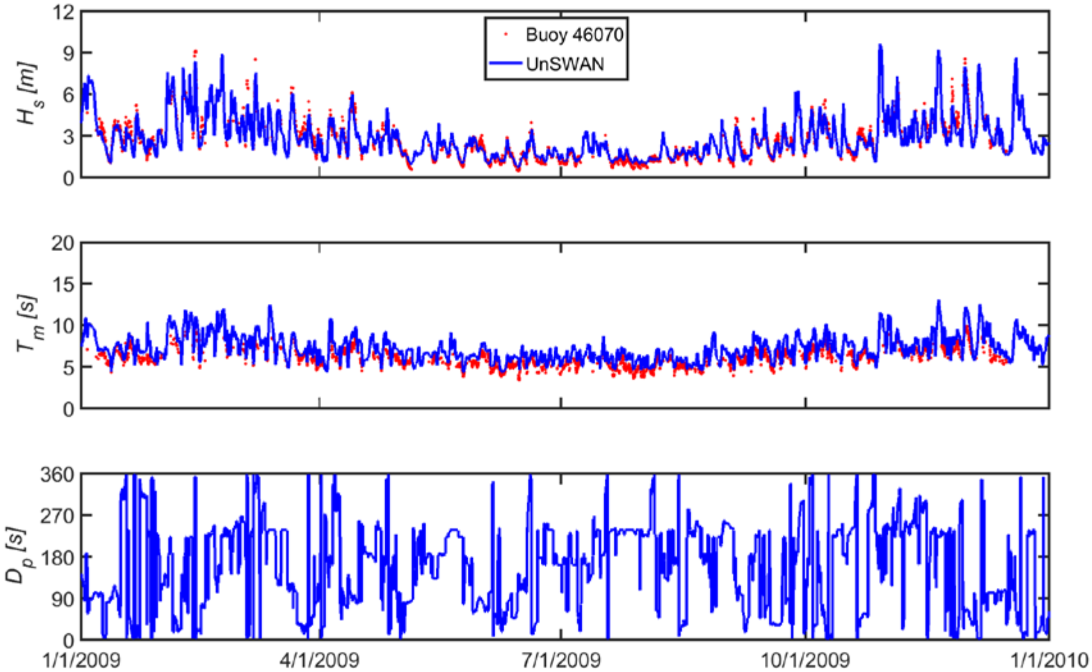

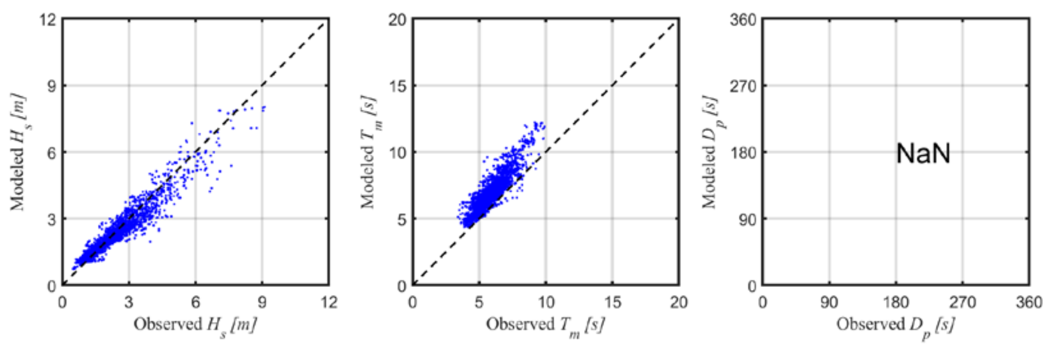

Figure B.76. Comparisons of time series (top) and scatter plots (bottom) of the three UnSWAN model-simulated bulk parameters with observed data at NDBC Buoy 46066 for 2009.

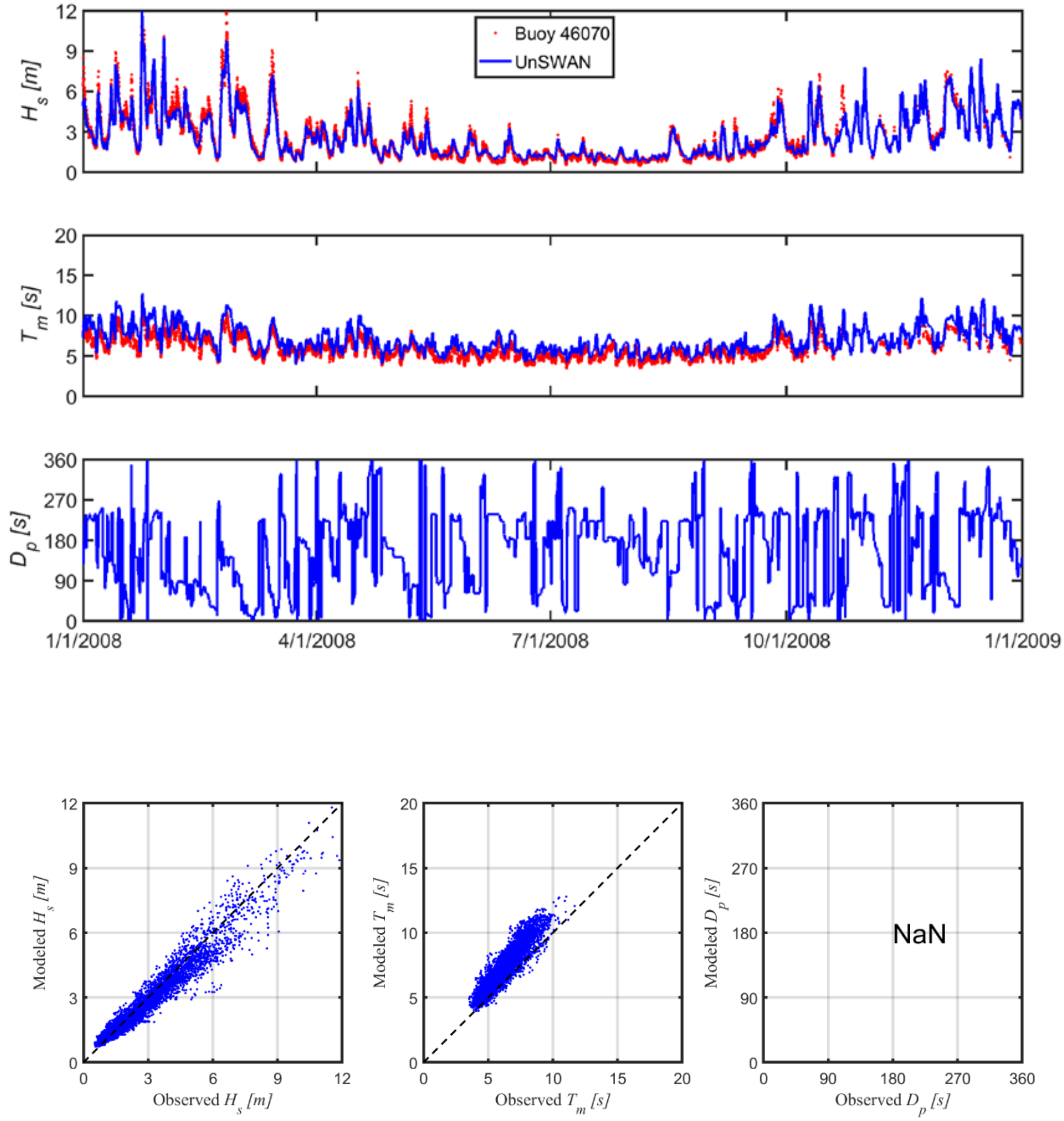

Figure B.77. Comparisons of time series (top) and scatter plots (bottom) of the three UnSWAN model-simulated bulk parameters with observed data at NDBC Buoy 46070 for 2008.

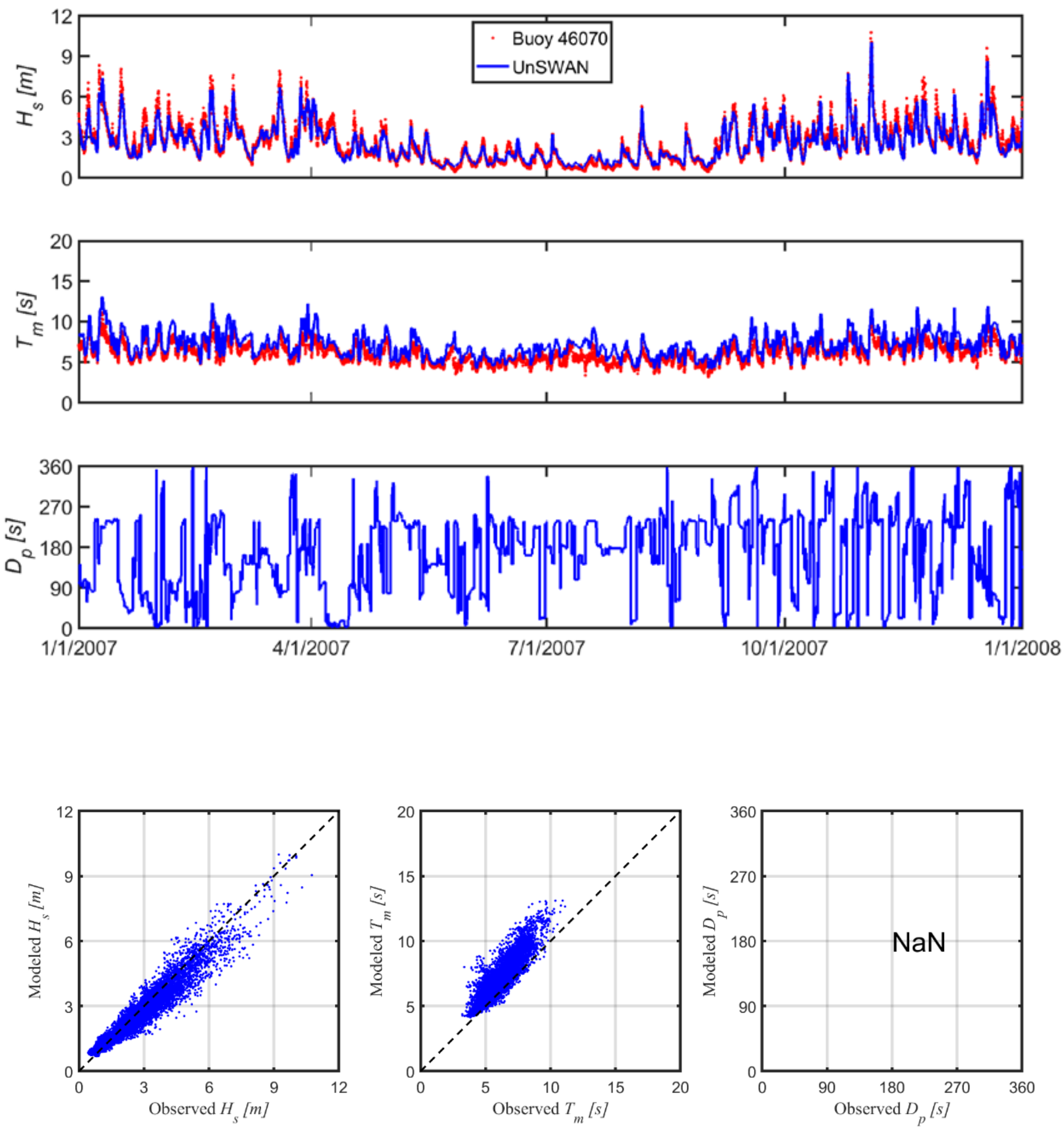

Figure B.78. Comparisons of time series (top) and scatter plots (bottom) of the three UnSWAN model-simulated bulk parameters with observed data at NDBC Buoy 46070 for 2007.

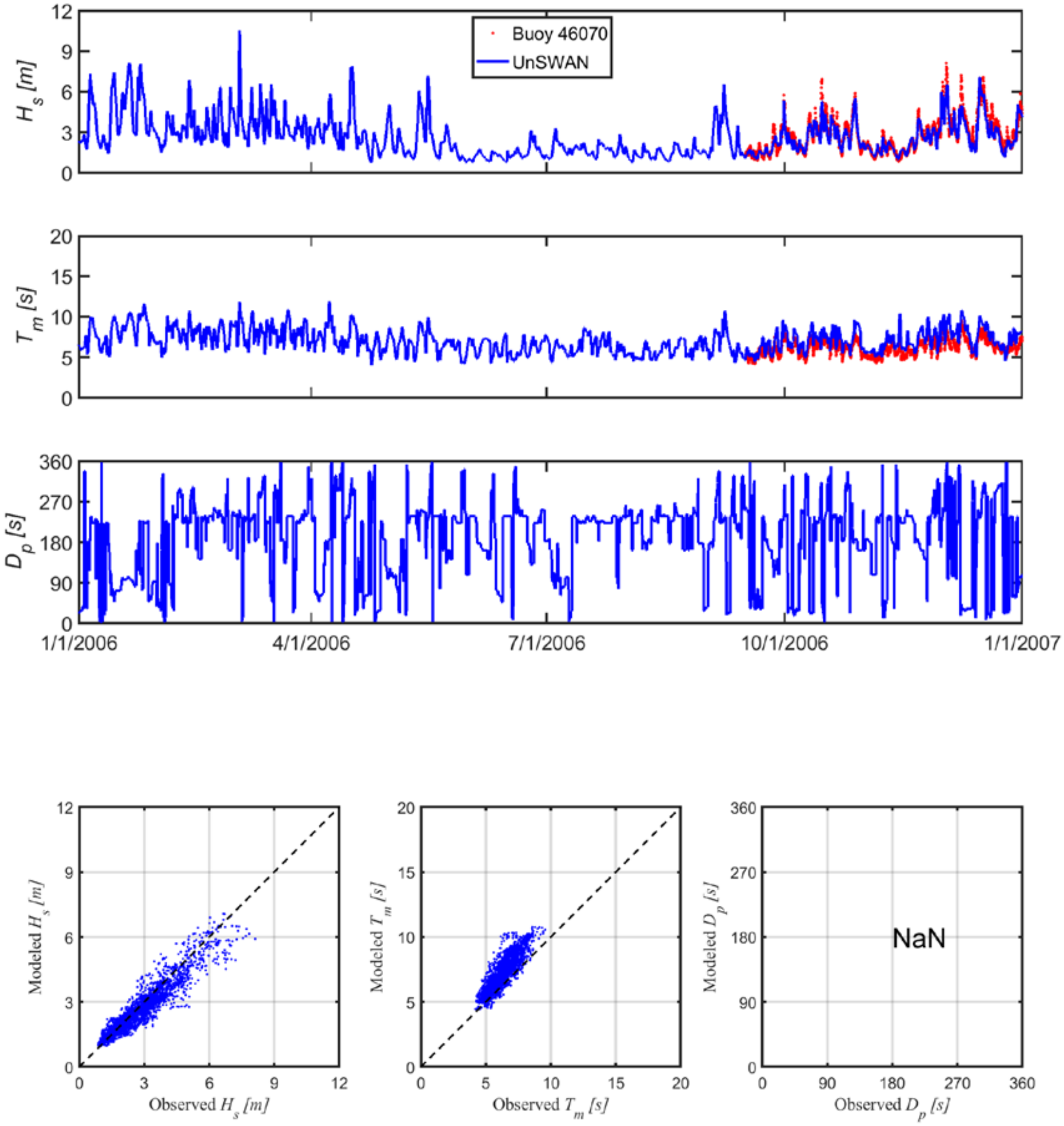

Figure B.79. Comparisons of time series (top) and scatter plots (bottom) of the three UnSWAN model-simulated bulk parameters with observed data at NDBC Buoy 46070 for 2006.

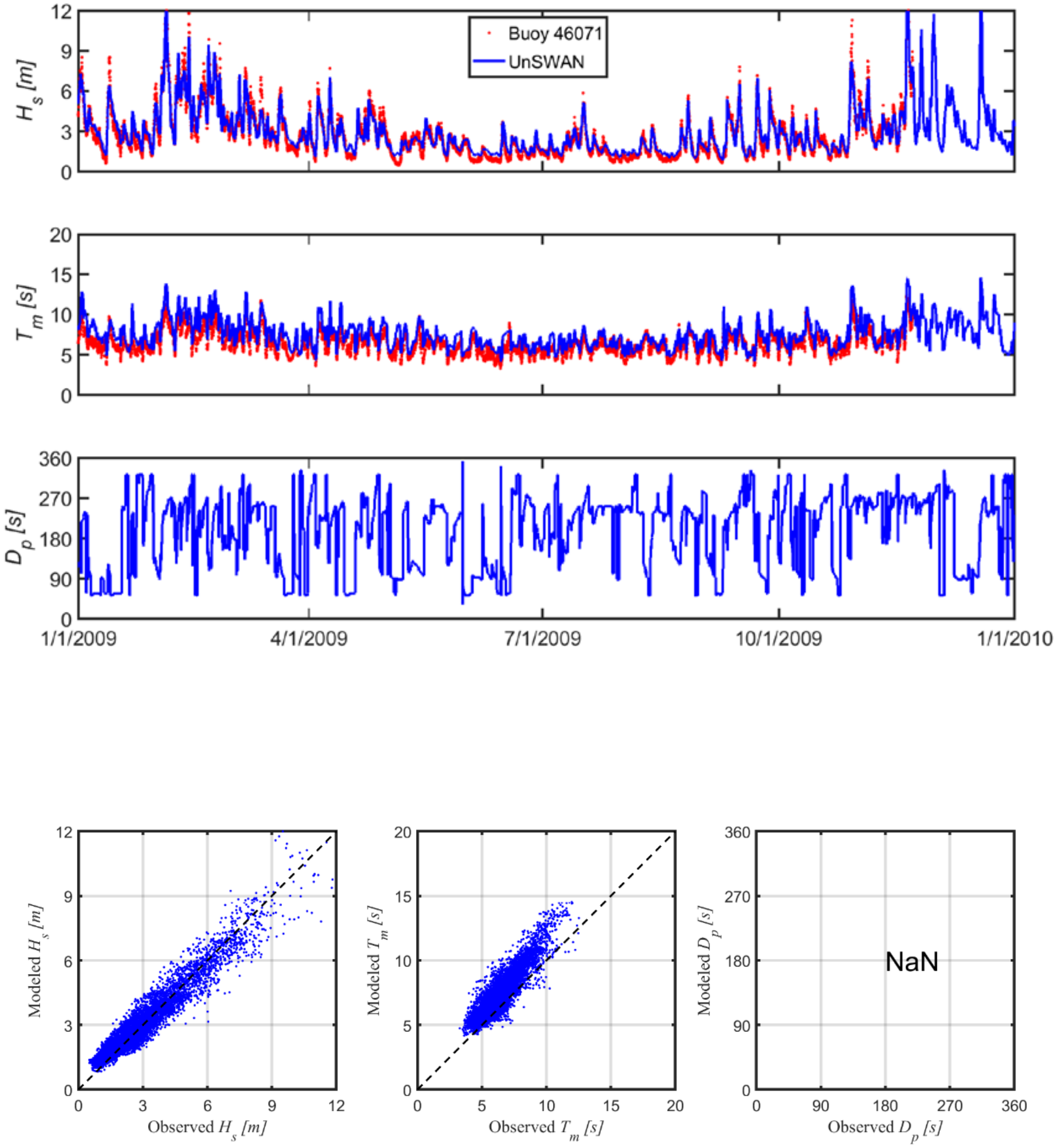

Figure B.80. Comparisons of time series (top) and scatter plots (bottom) of the three UnSWAN model-simulated bulk parameters with observed data at NDBC Buoy 46071 for 2009.

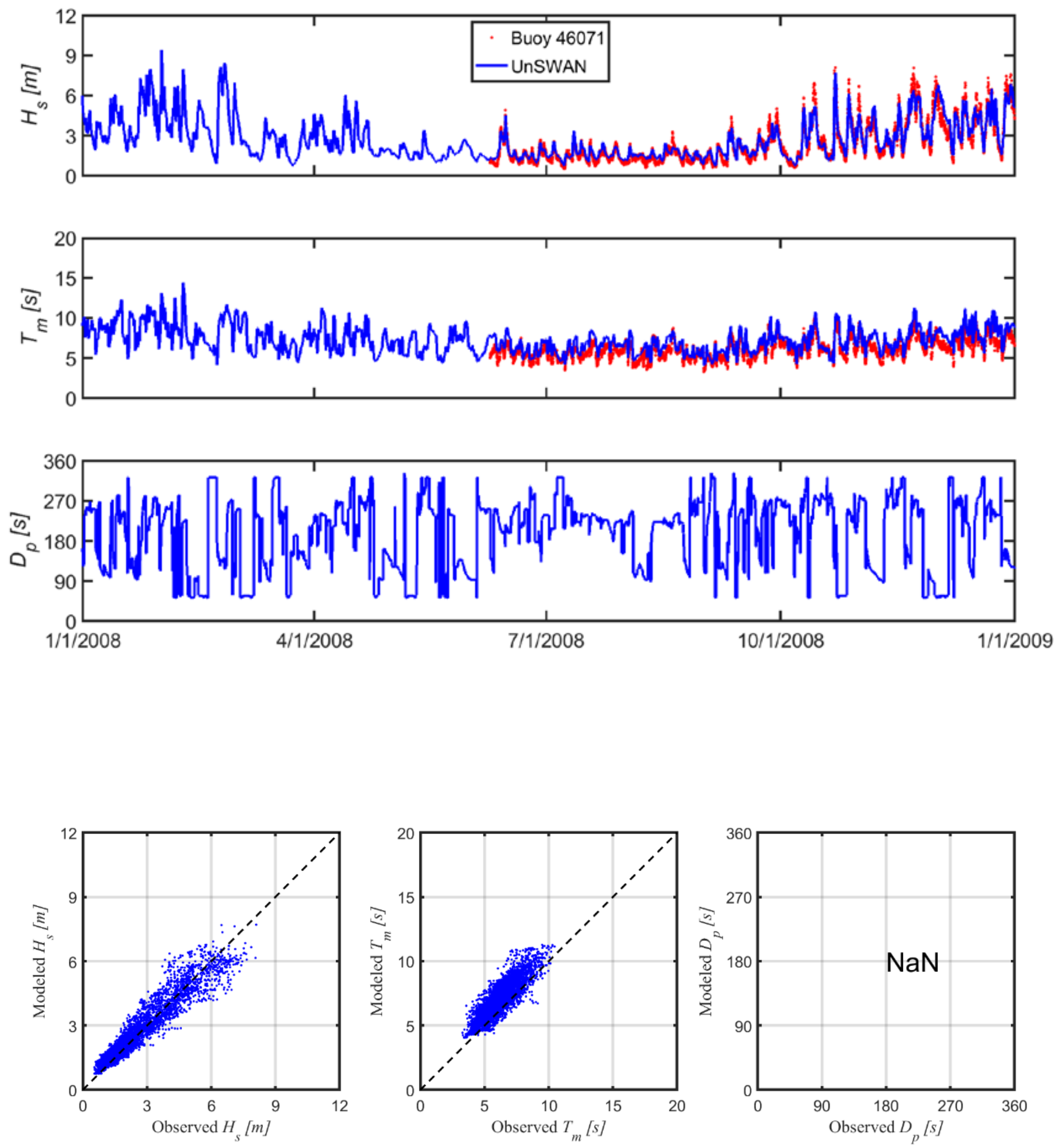

Figure B.81. Comparisons of time series (top) and scatter plots (bottom) of the three UnSWAN model-simulated bulk parameters with observed data at NDBC Buoy 46071 for 2008.

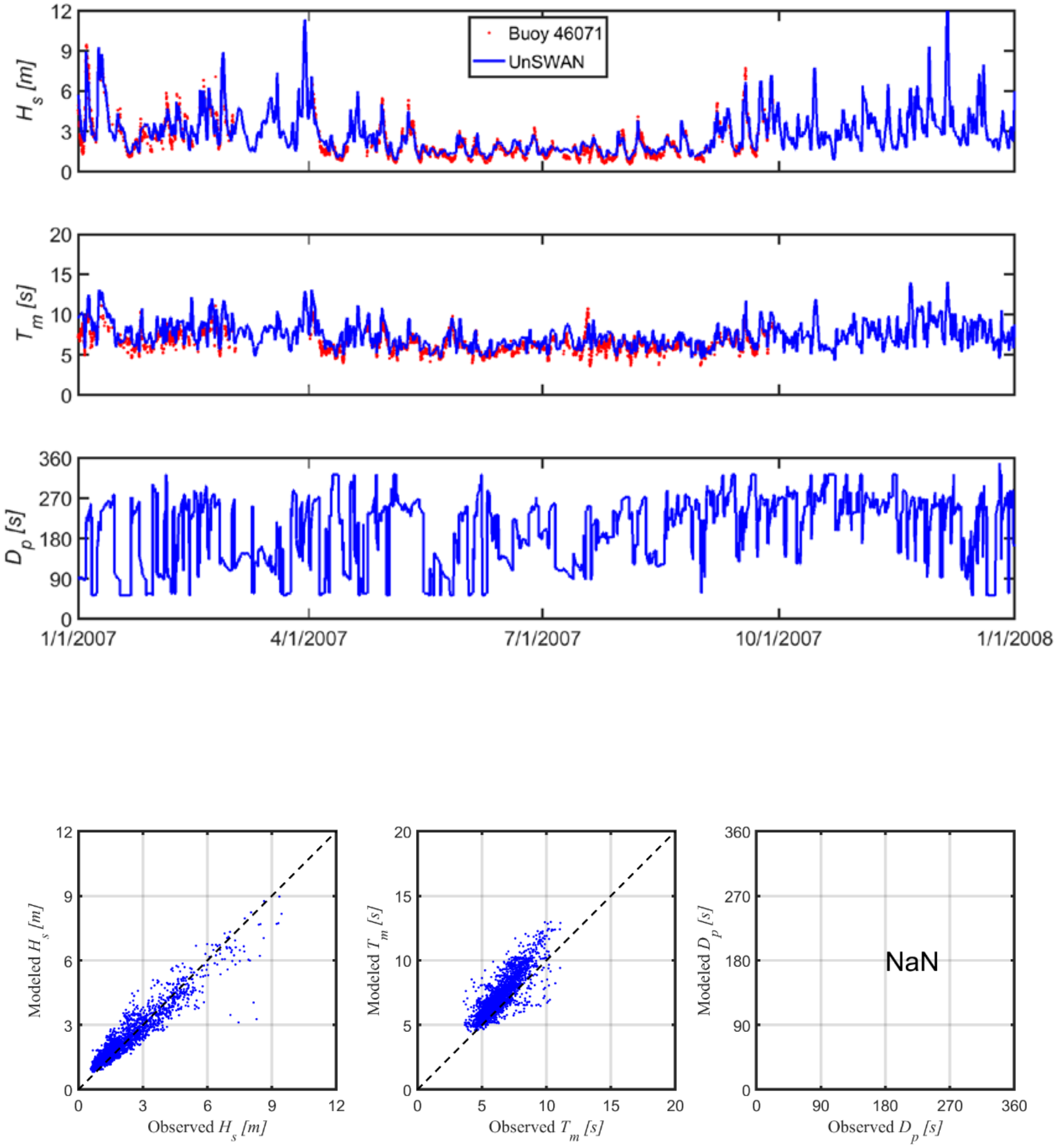

Figure B.82. Comparisons of time series (top) and scatter plots (bottom) of the three UnSWAN model-simulated bulk parameters with observed data at NDBC Buoy 46071 for 2007.

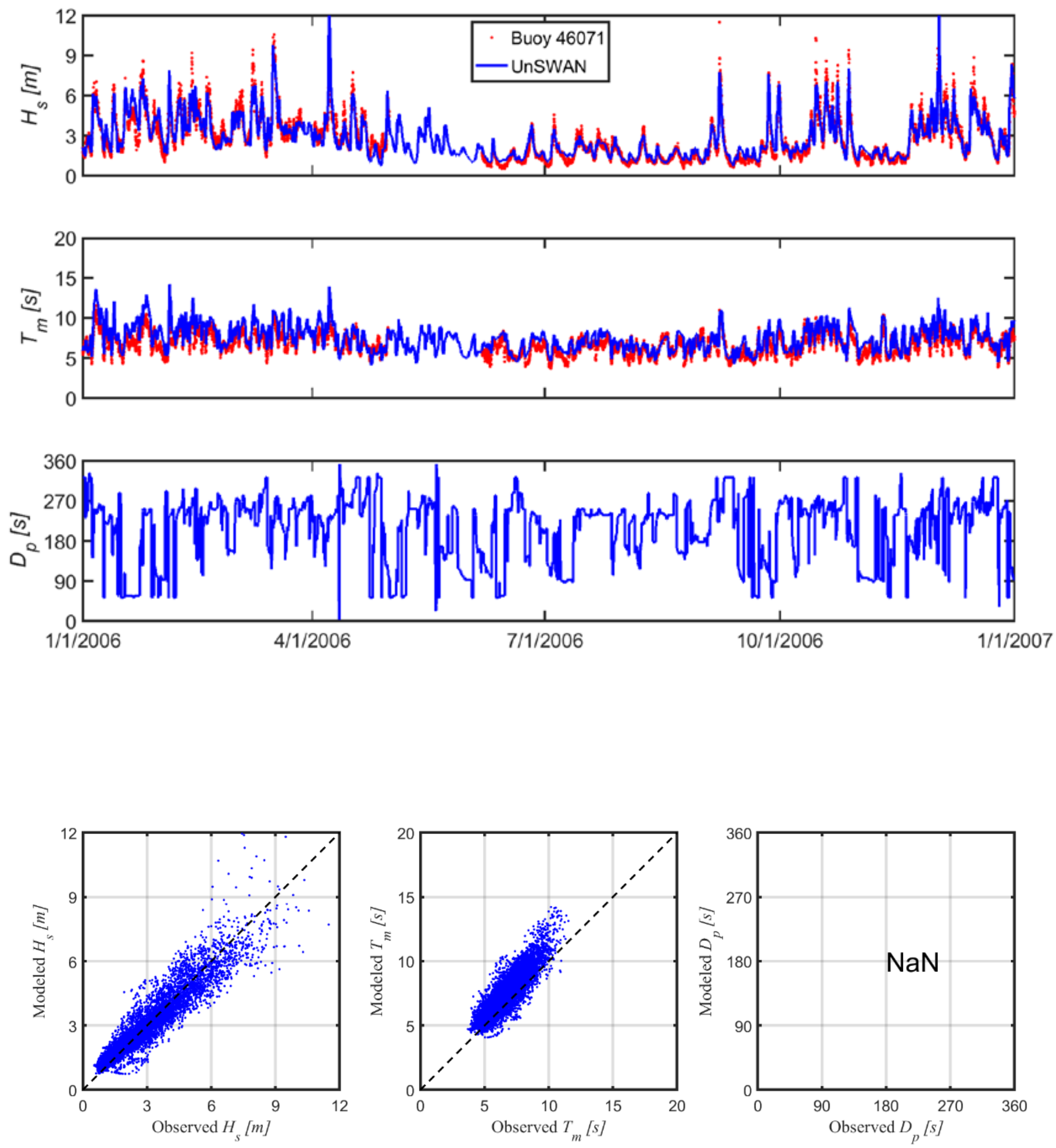

Figure B.83. Comparisons of time series (top) and scatter plots (bottom) of the three UnSWAN model-simulated bulk parameters with observed data at NDBC Buoy 46071 for 2006.

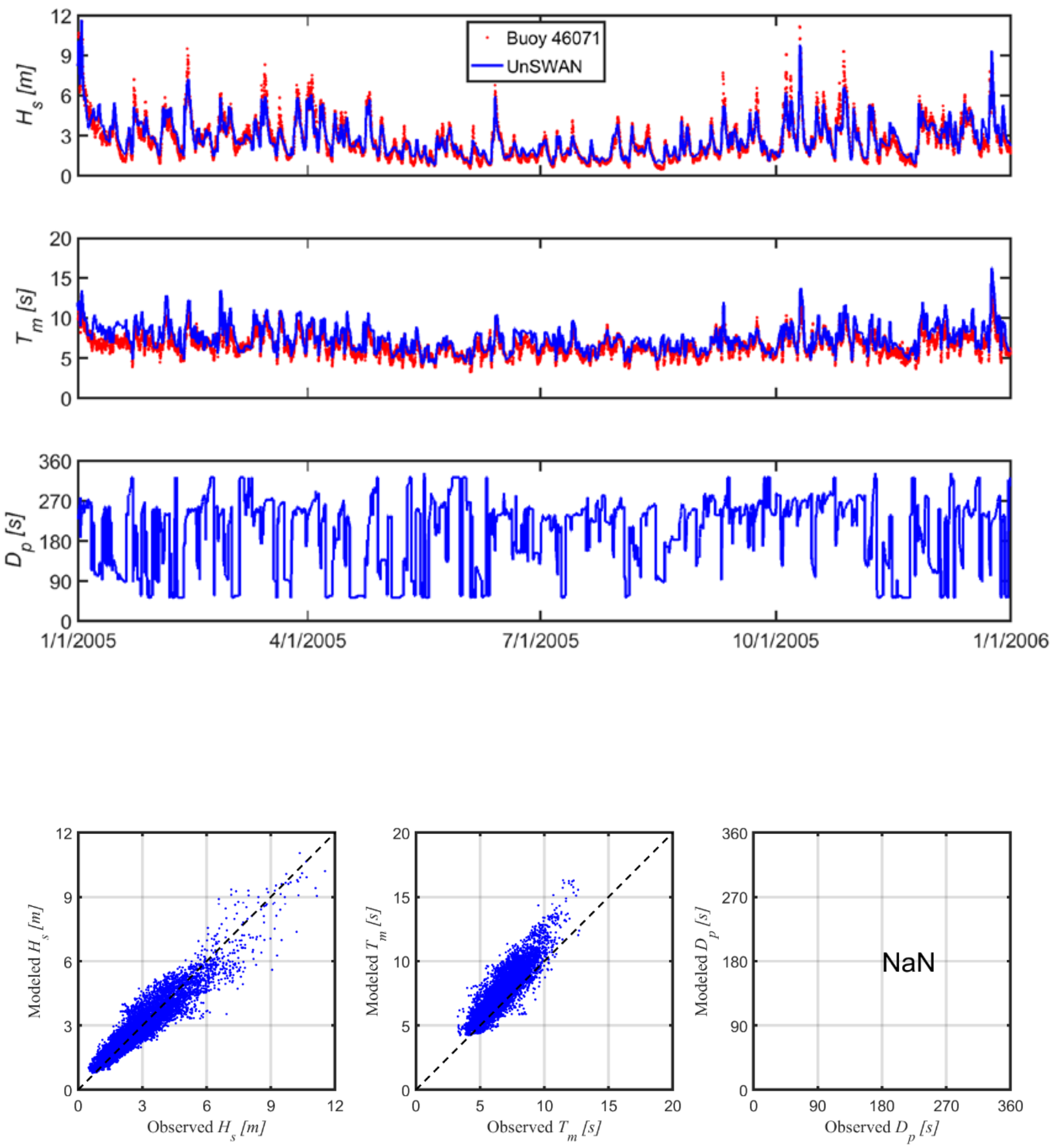

Figure B.84. Comparisons of time series (top) and scatter plots (bottom) of the three UnSWAN model-simulated bulk parameters with observed data at NDBC Buoy 46071 for 2005.

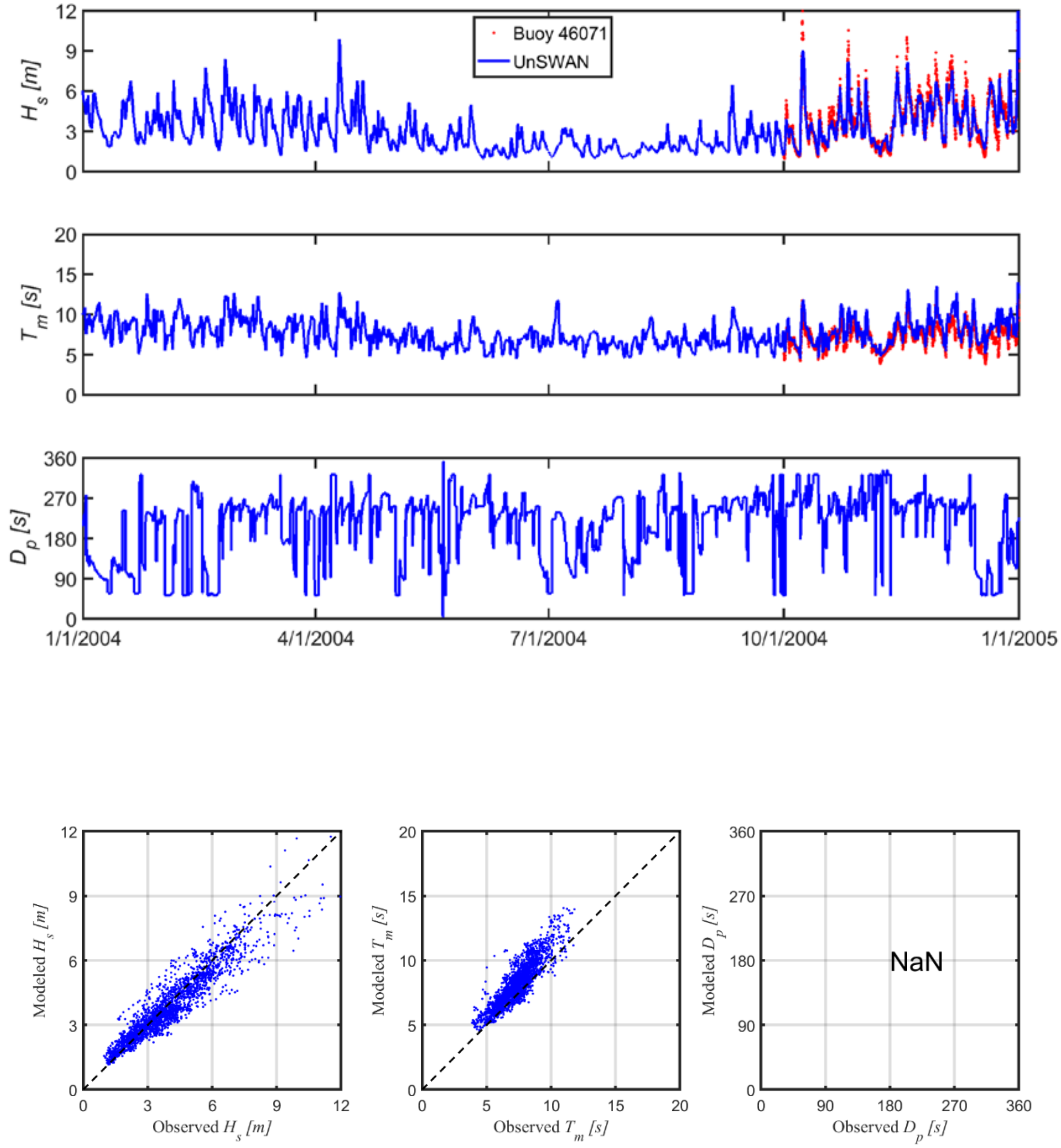

Figure B.85. Comparisons of time series (top) and scatter plots (bottom) of the three UnSWAN model-simulated bulk parameters with observed data at NDBC Buoy 46071 for 2004.

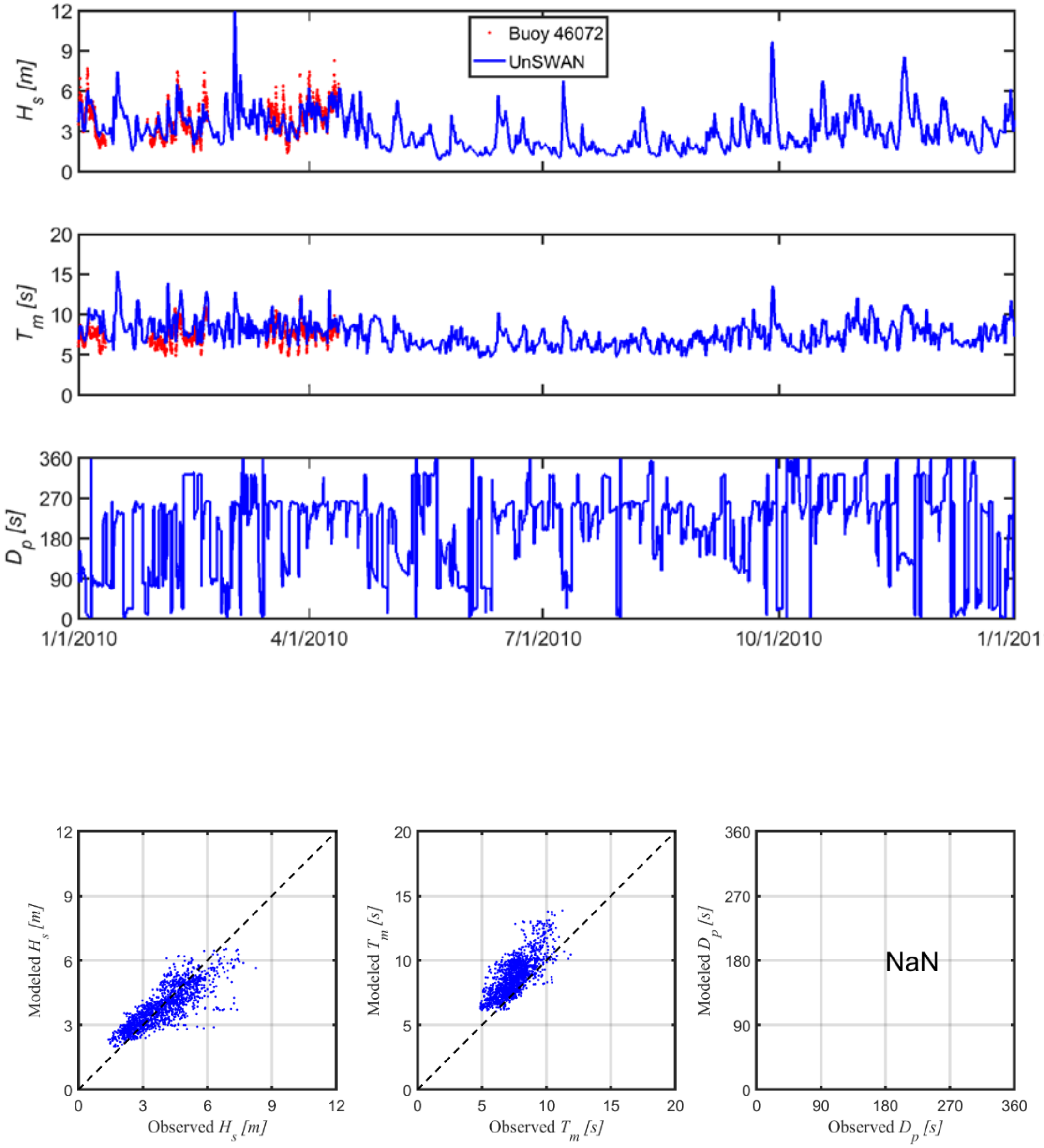

Figure B.86. Comparisons of time series (top) and scatter plots (bottom) of the three UnSWAN model-simulated bulk parameters with observed data at NDBC Buoy 46072 for 2010.

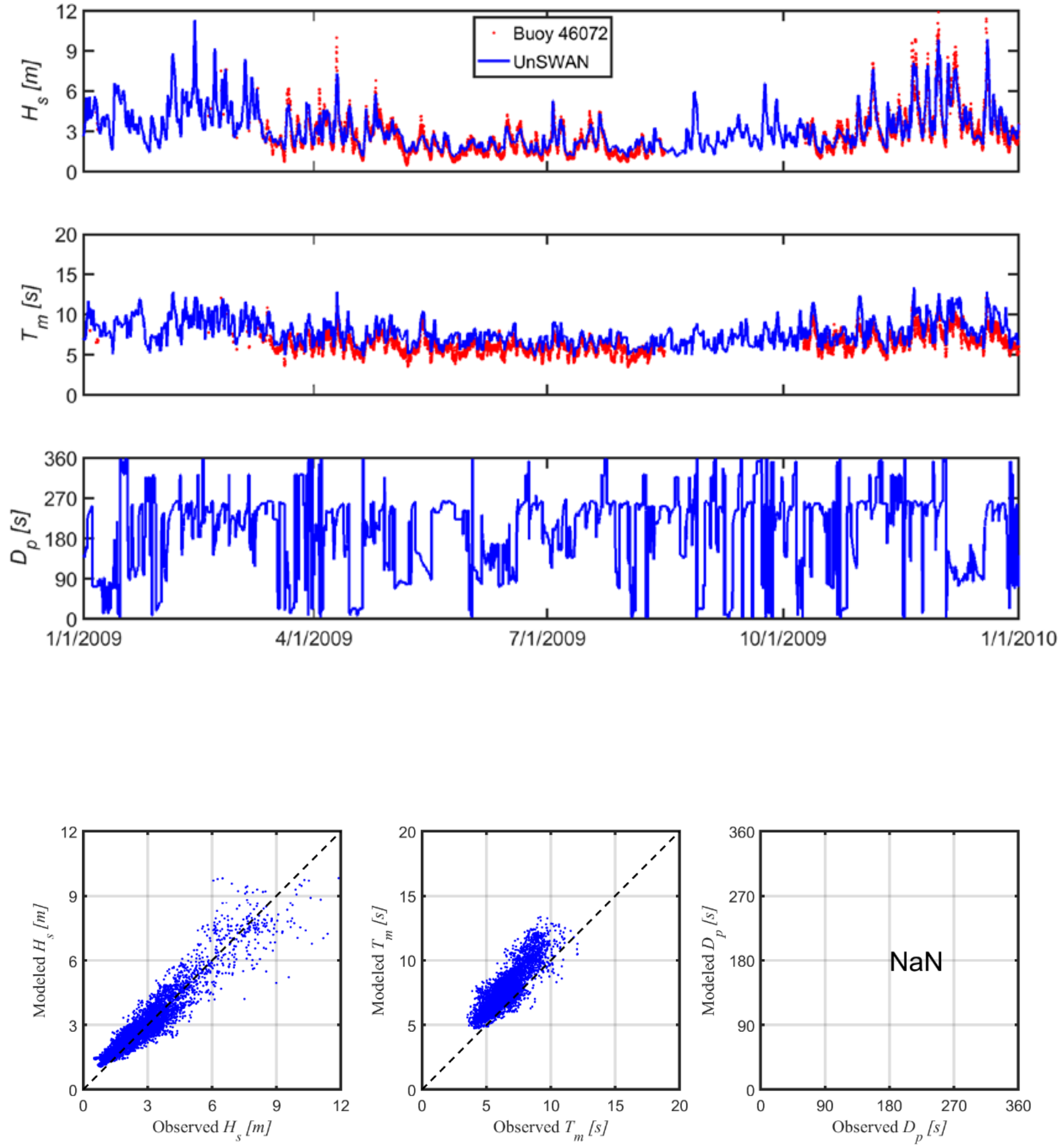

Figure B.87. Comparisons of time series (top) and scatter plots (bottom) of the three UnSWAN model-simulated bulk parameters with observed data at NDBC Buoy 46072 for 2009.

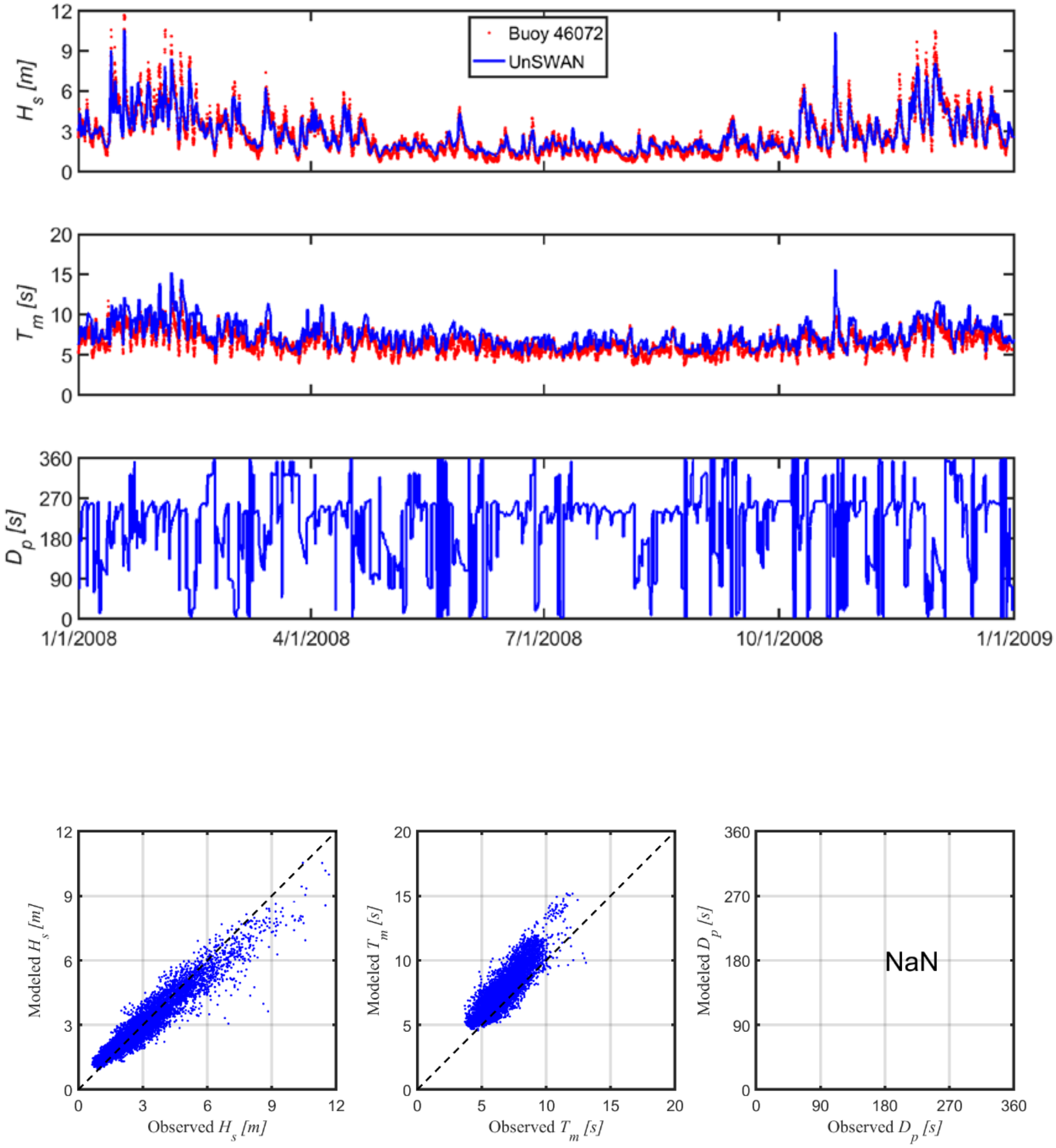

Figure B.88. Comparisons of time series (top) and scatter plots (bottom) of the three UnSWAN model-simulated bulk parameters with observed data at NDBC Buoy 46072 for 2008.

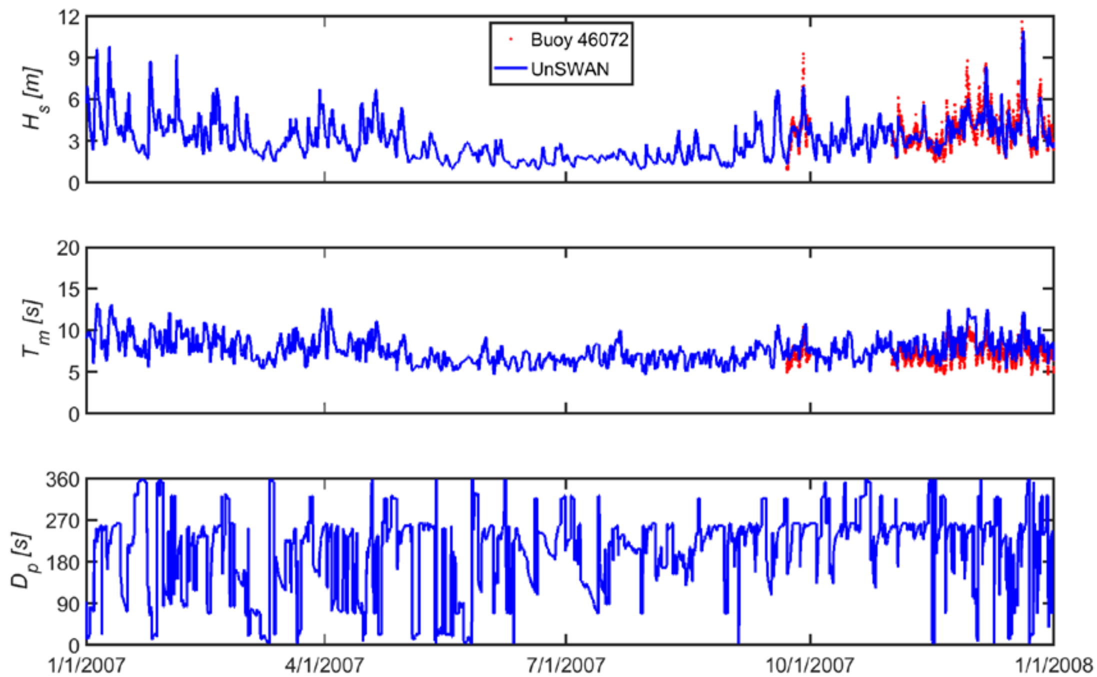

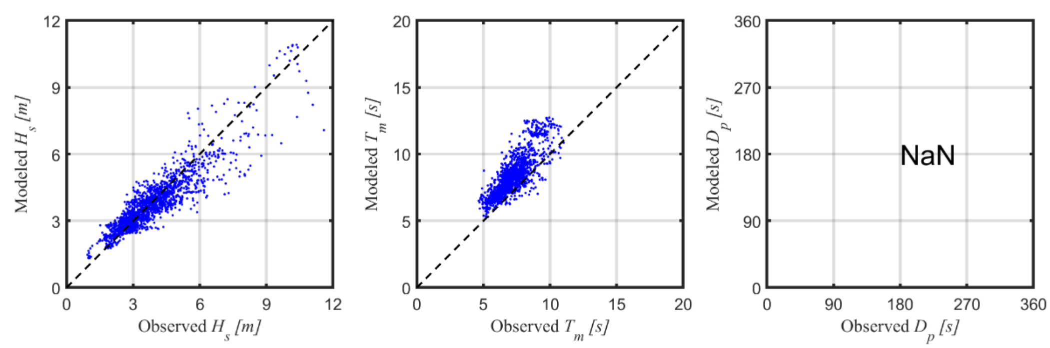

Figure B.89. Comparisons of time series (top) and scatter plots (bottom) of the three UnSWAN model-simulated bulk parameters with observed data at NDBC Buoy 46072 for 2007.

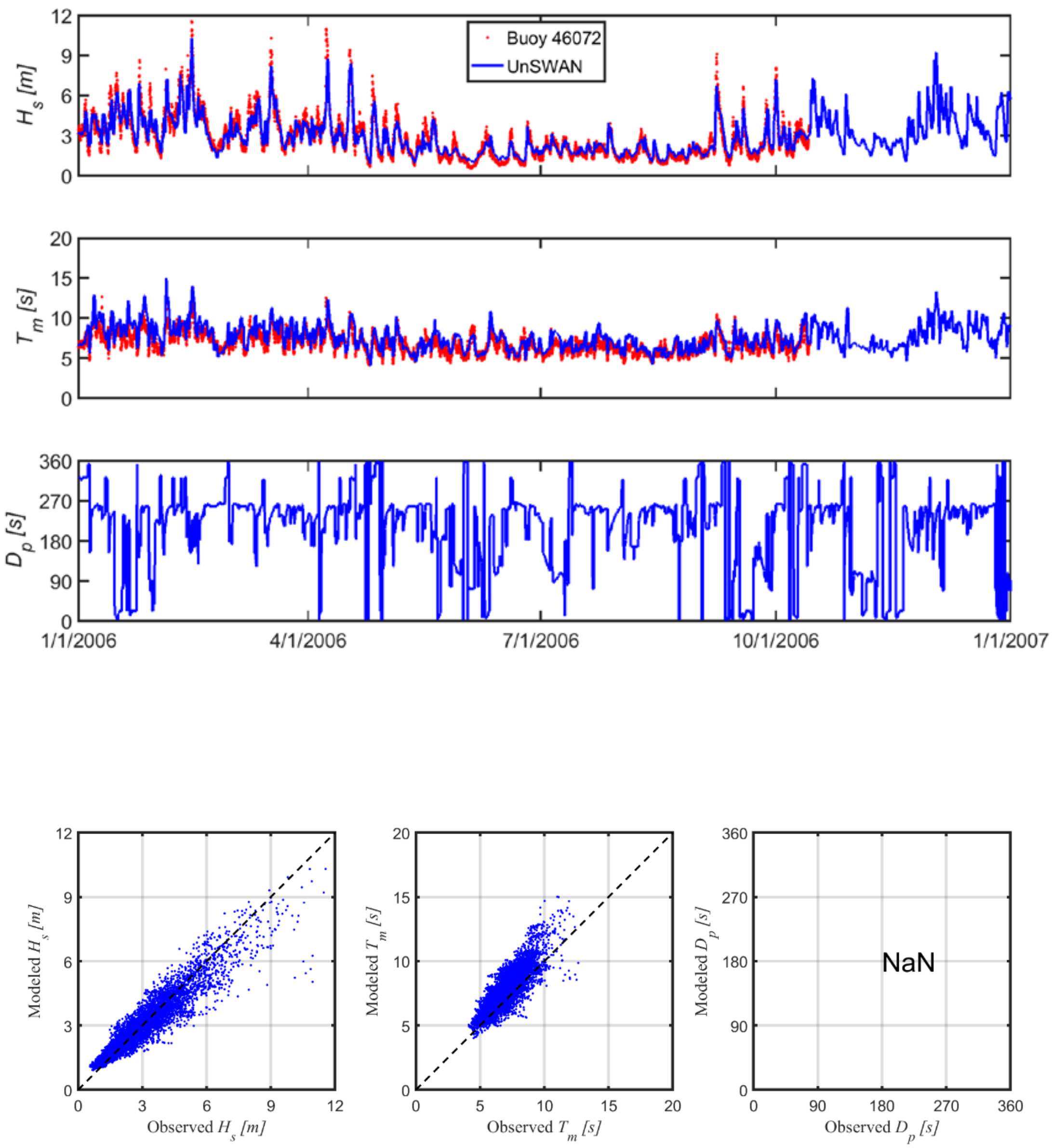

Figure B.90. Comparisons of time series (top) and scatter plots (bottom) of the three UnSWAN model-simulated bulk parameters with observed data at NDBC Buoy 46072 for 2006.

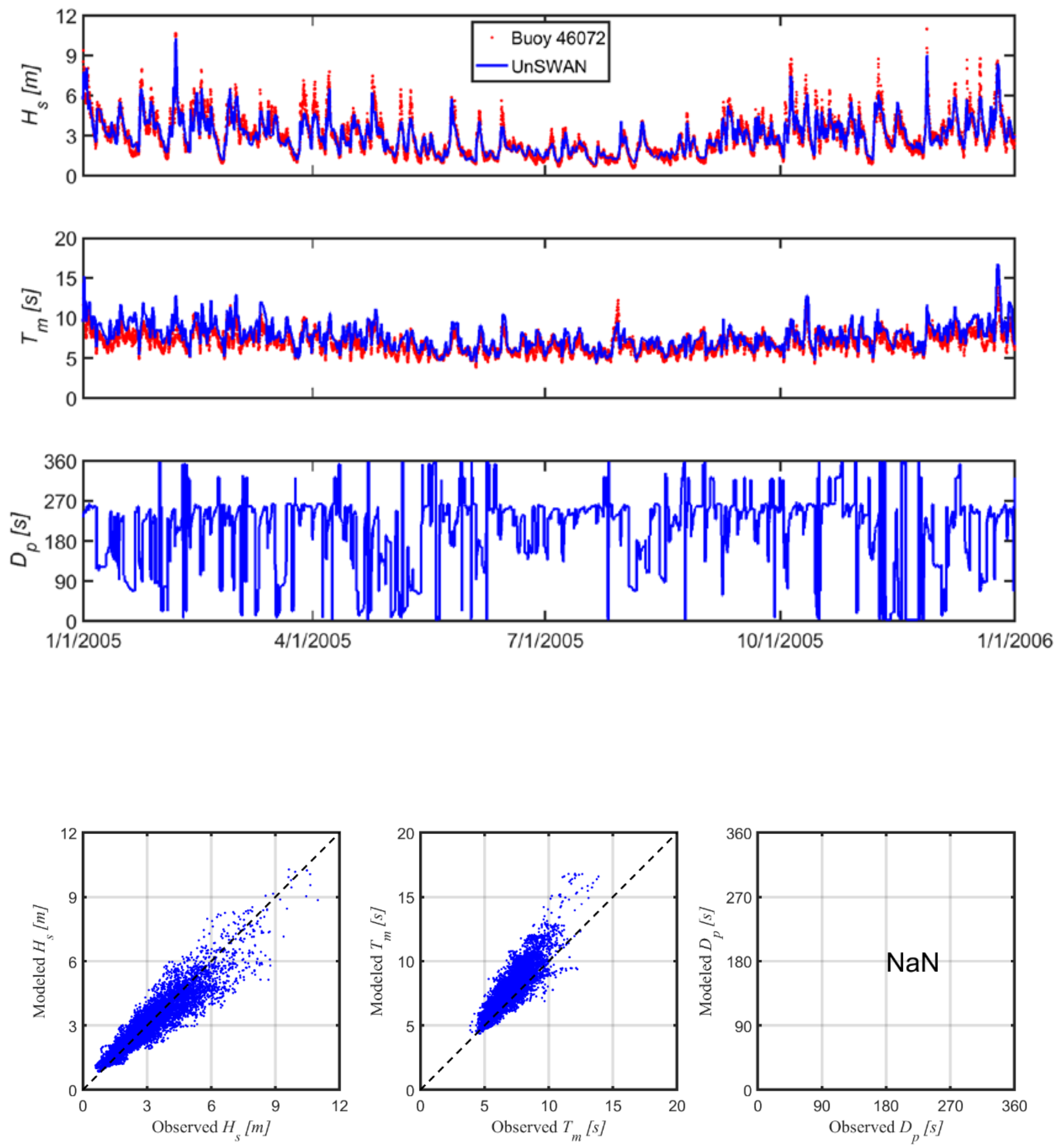

Figure B.91. Comparisons of time series (top) and scatter plots (bottom) of the three UnSWAN model-simulated bulk parameters with observed data at NDBC Buoy 46072 for 2005.

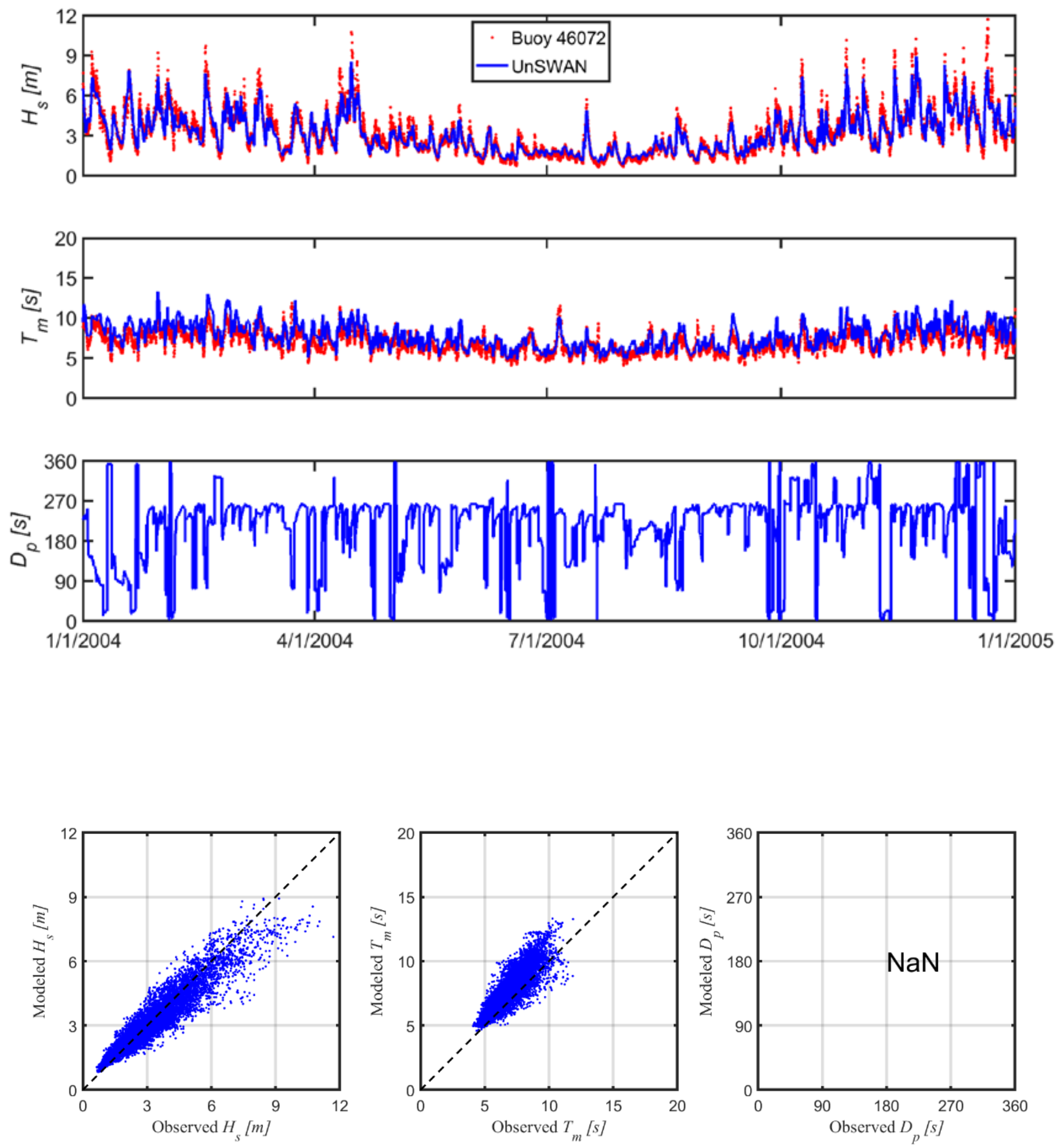

Figure B.92. Comparisons of time series (top) and scatter plots (bottom) of the three UnSWAN model-simulated bulk parameters with observed data at NDBC Buoy 46072 for 2004.

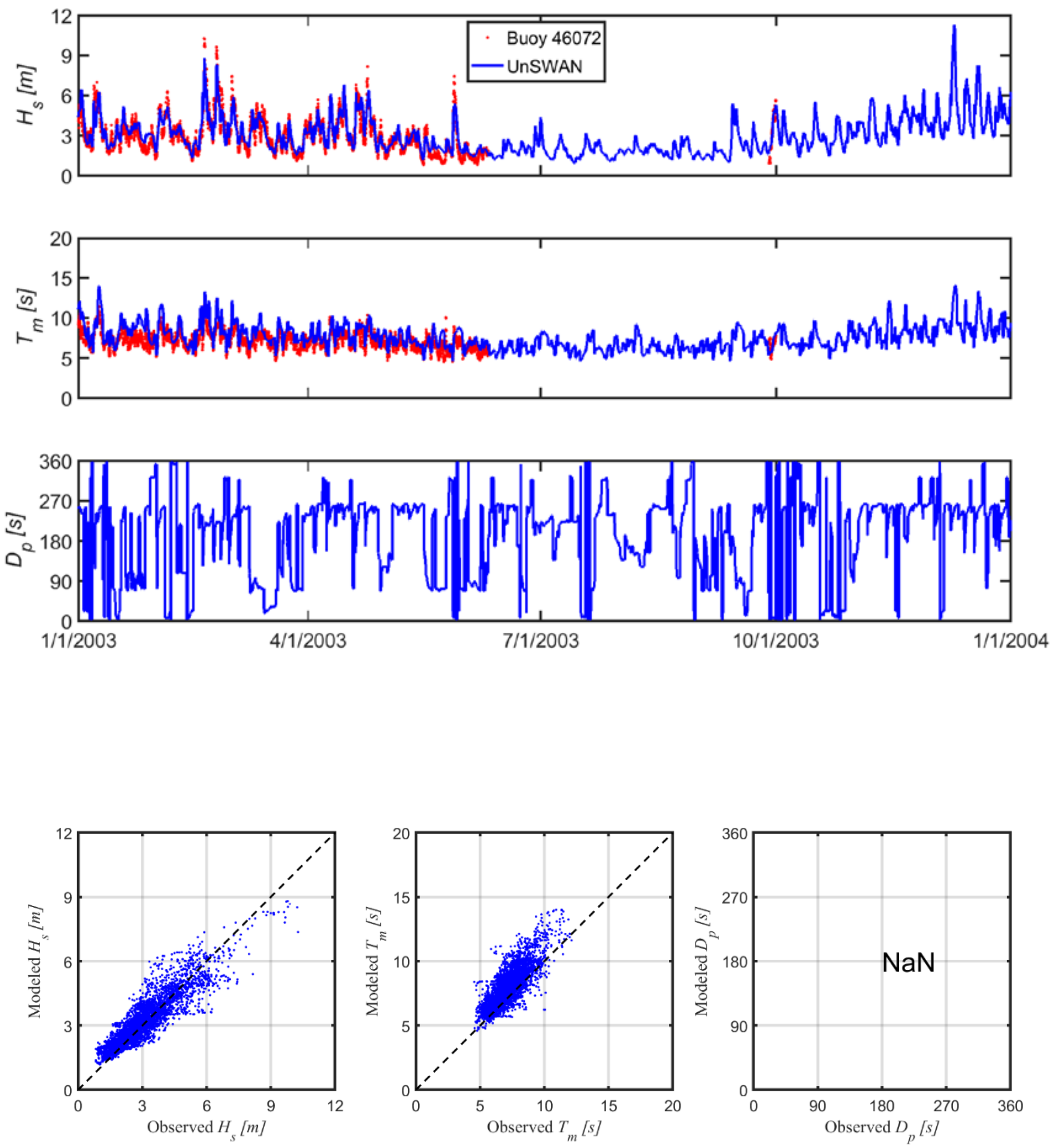

Figure B.93. Comparisons of time series (top) and scatter plots (bottom) of the three UnSWAN model-simulated bulk parameters with observed data at NDBC Buoy 46072 for 2003.

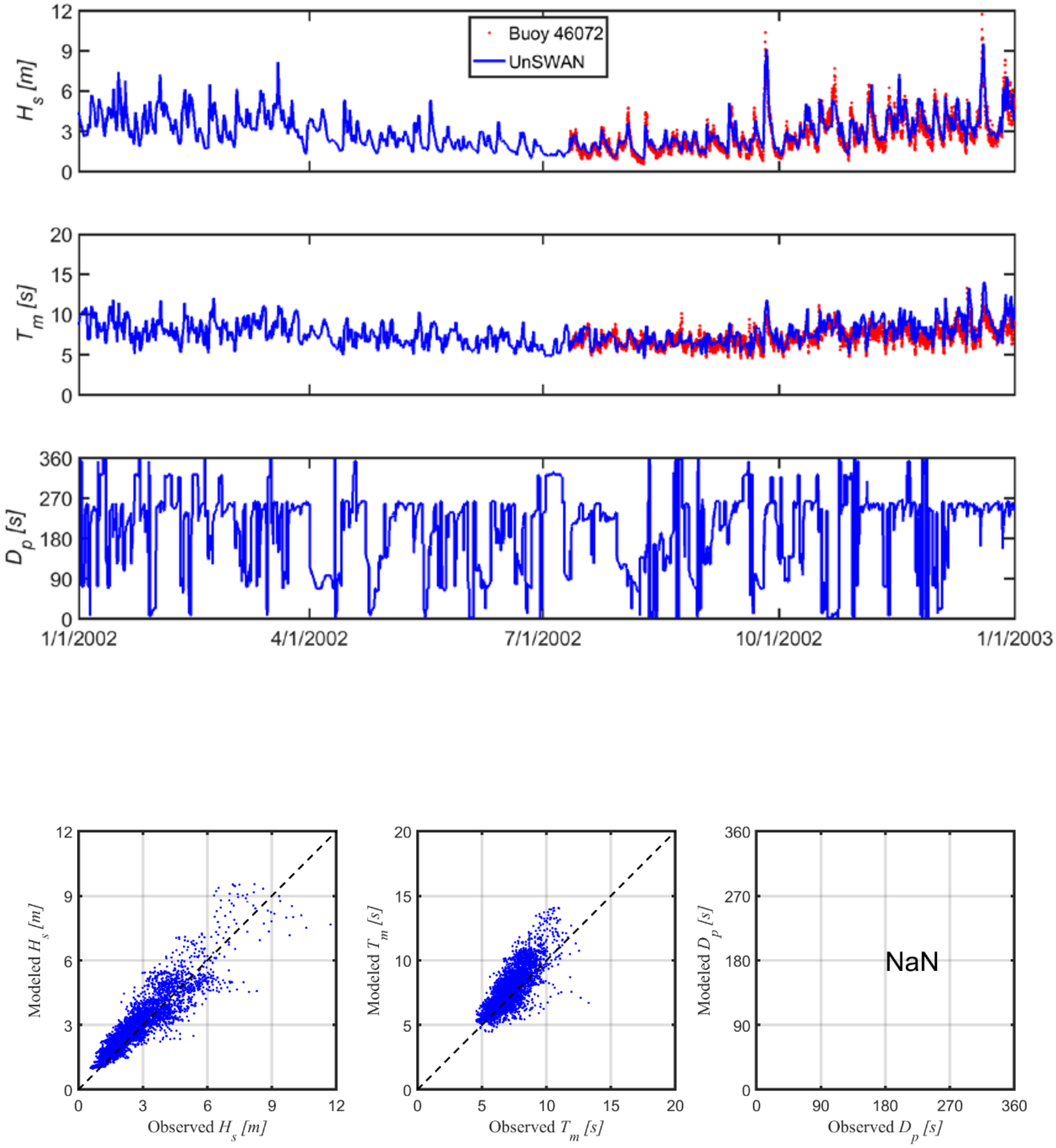

Figure B.94. Comparisons of time series (top) and scatter plots (bottom) of the three UnSWAN model-simulated bulk parameters with observed data at NDBC Buoy 46072 for 2002.

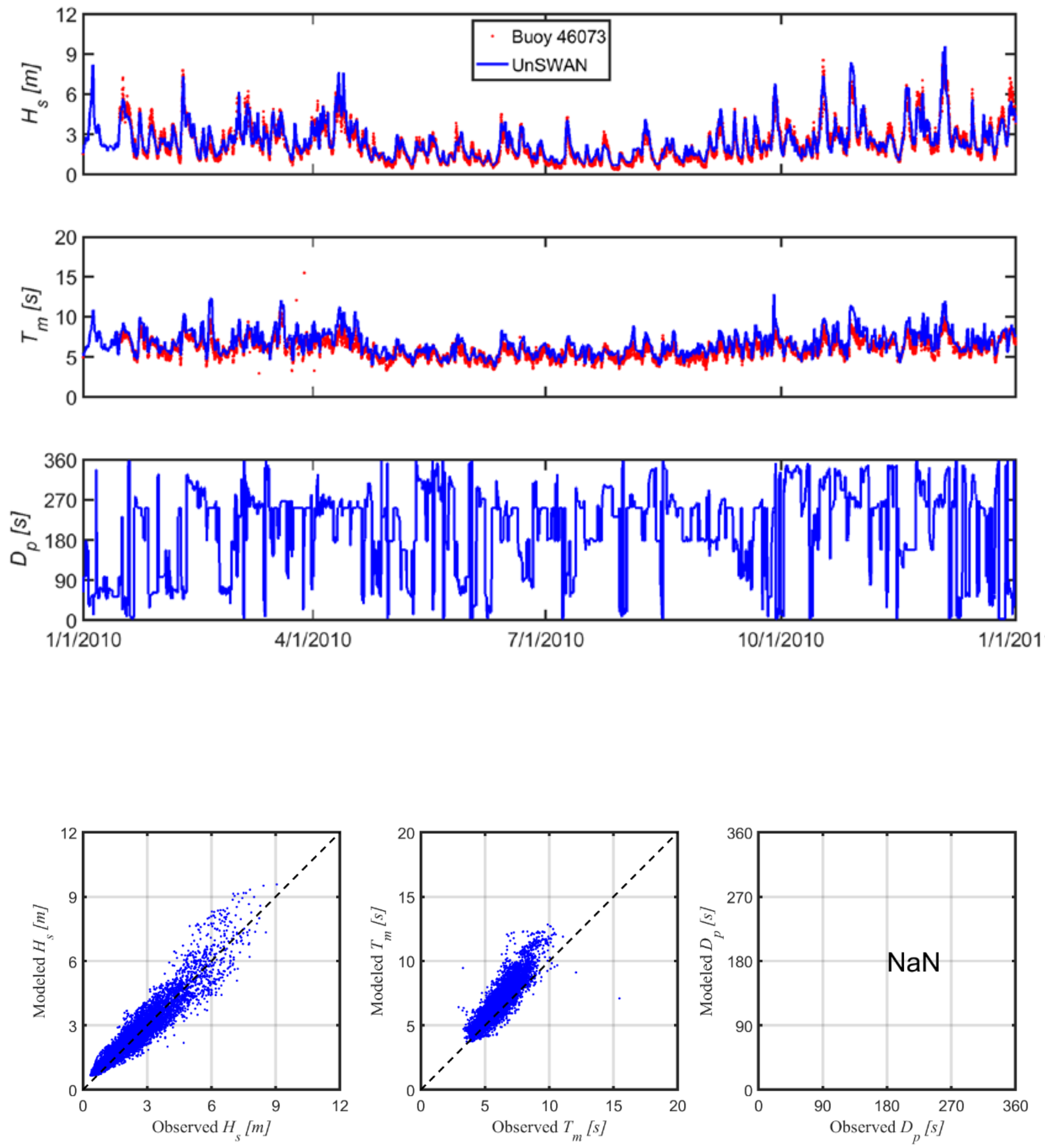

Figure B.95. Comparisons of time series (top) and scatter plots (bottom) of the three UnSWAN model-simulated bulk parameters with observed data at NDBC Buoy 46073 for 2010.

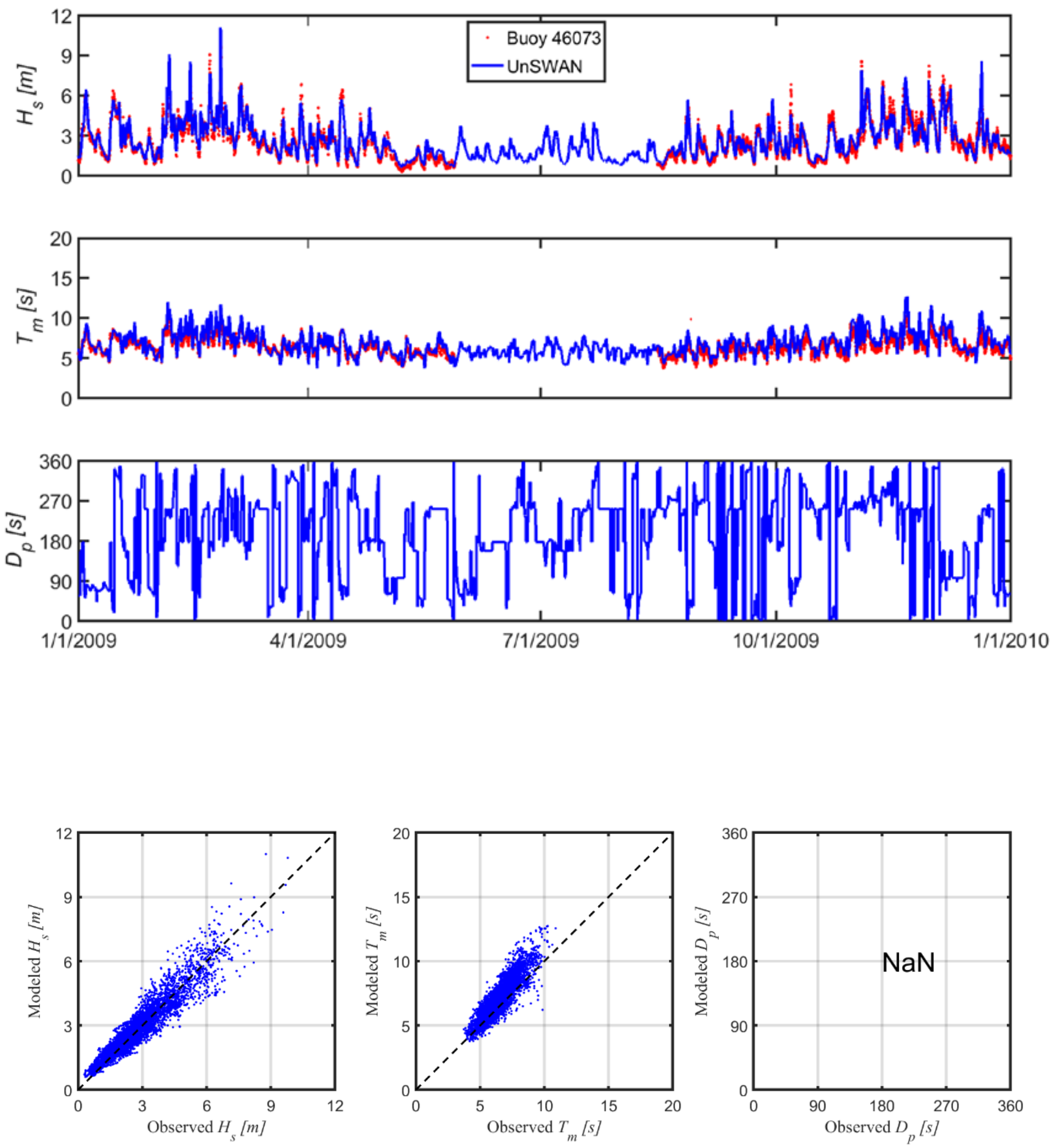

Figure B.96. Comparisons of time series (top) and scatter plots (bottom) of the three UnSWAN model-simulated bulk parameters with observed data at NDBC Buoy 46073 for 2009.

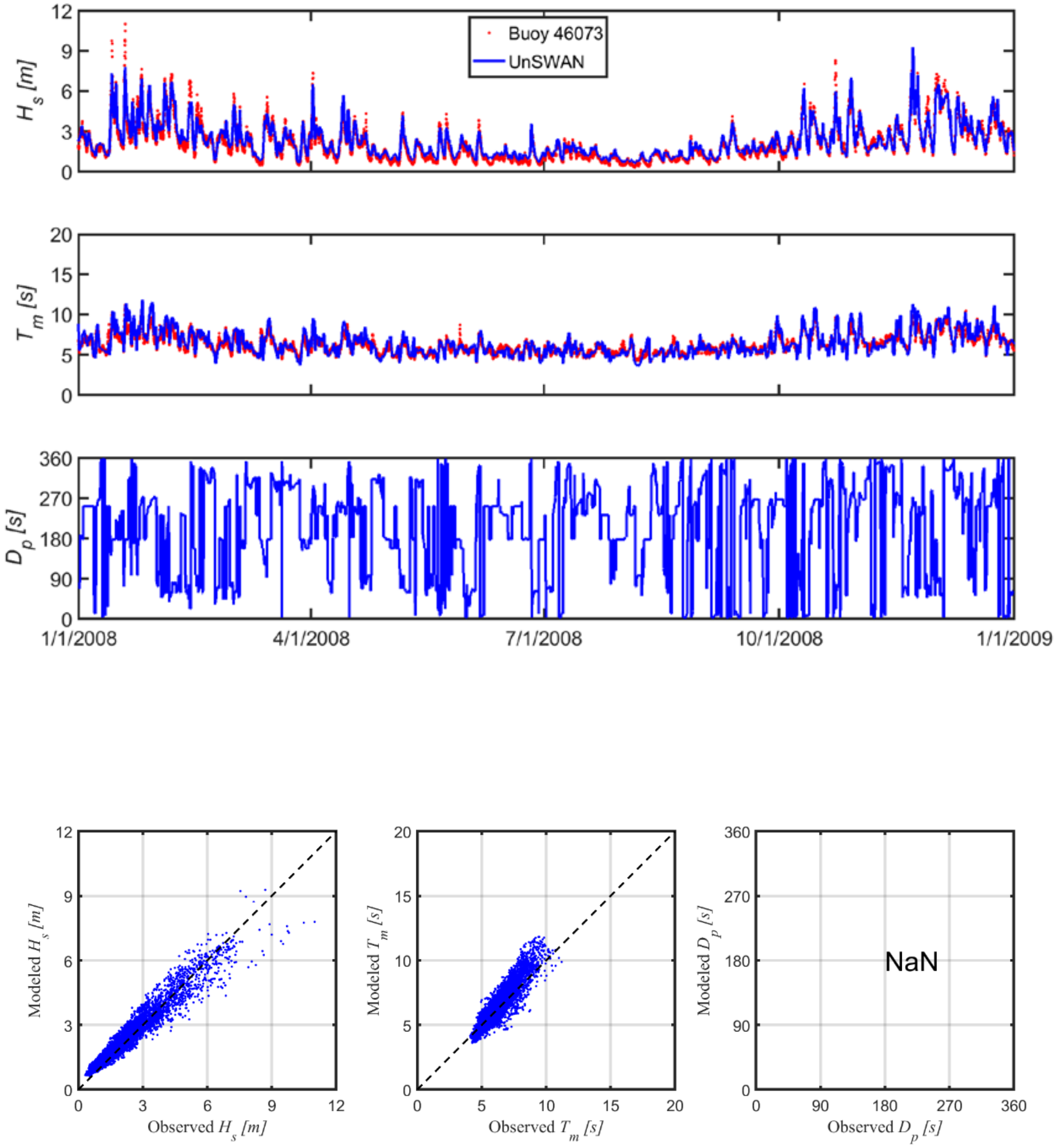

Figure B.97. Comparisons of time series (top) and scatter plots (bottom) of the three UnSWAN model-simulated bulk parameters with observed data at NDBC Buoy 46073 for 2008.

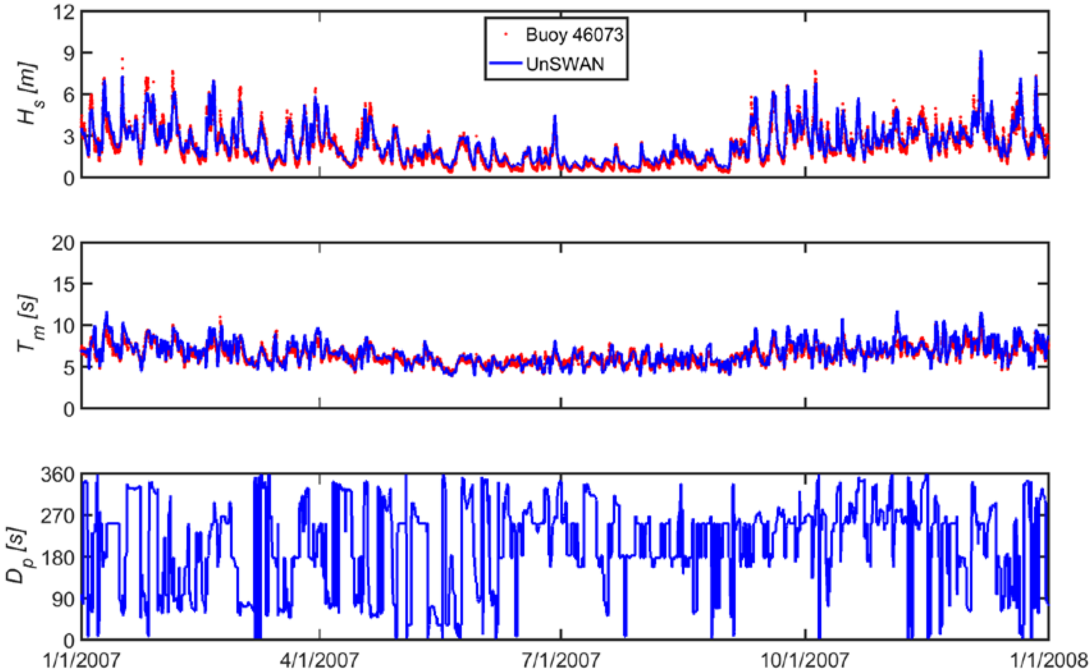

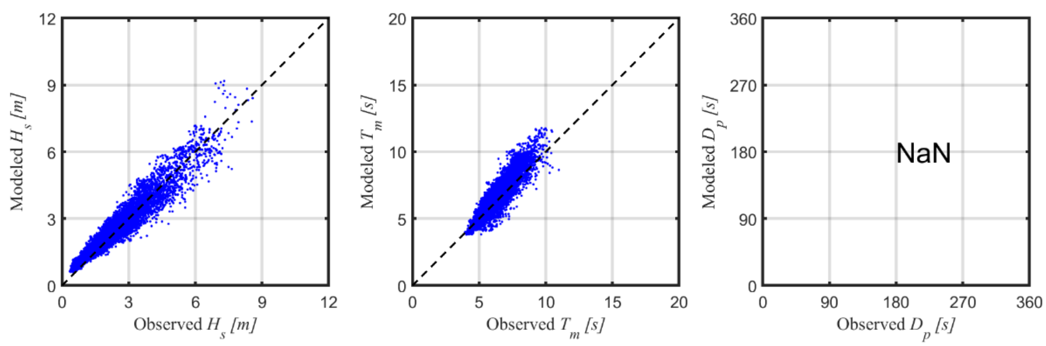

Figure B.98. Comparisons of time series (top) and scatter plots (bottom) of the three UnSWAN model-simulated bulk parameters with observed data at NDBC Buoy 46073 for 2007.

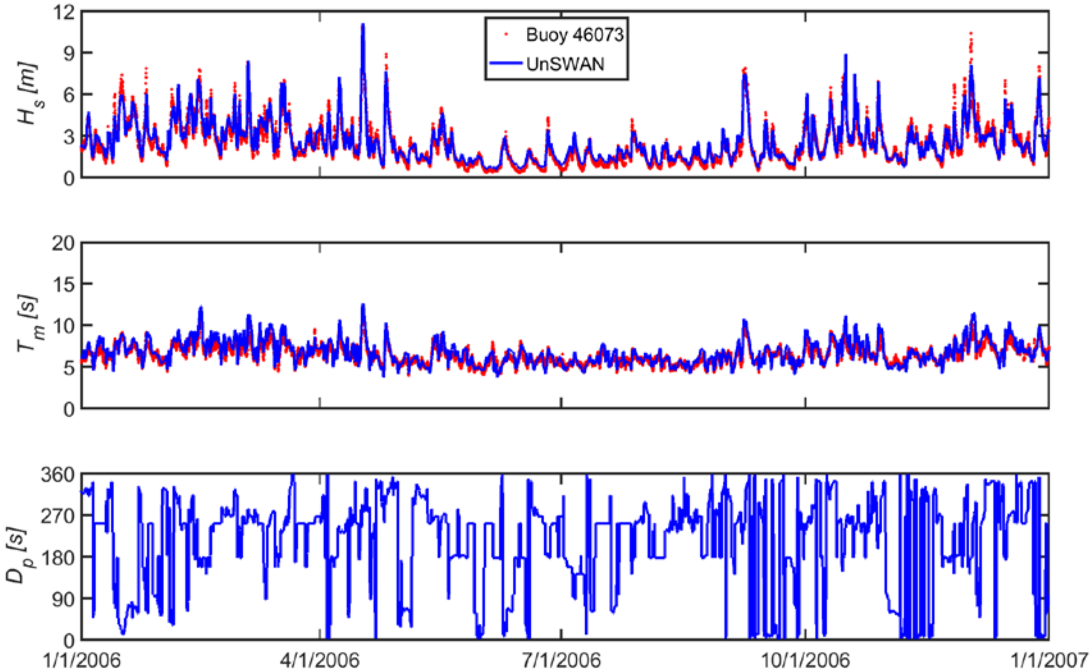

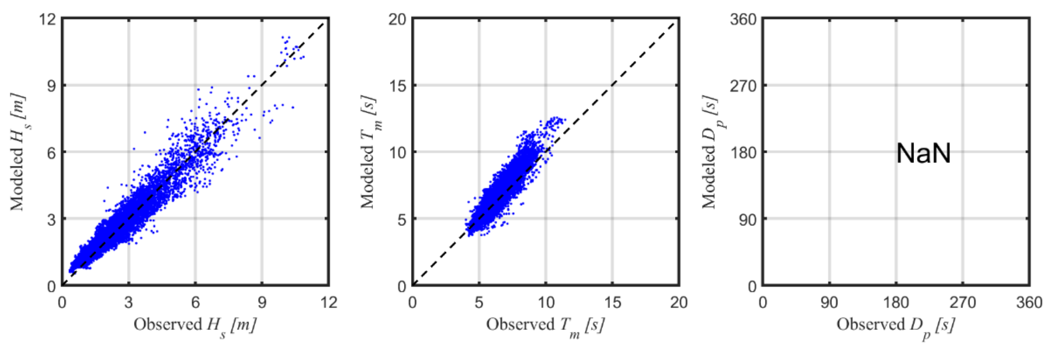

Figure B.99. Comparisons of time series (top) and scatter plots (bottom) of the three UnSWAN model-simulated bulk parameters with observed data at NDBC Buoy 46073 for 2006.

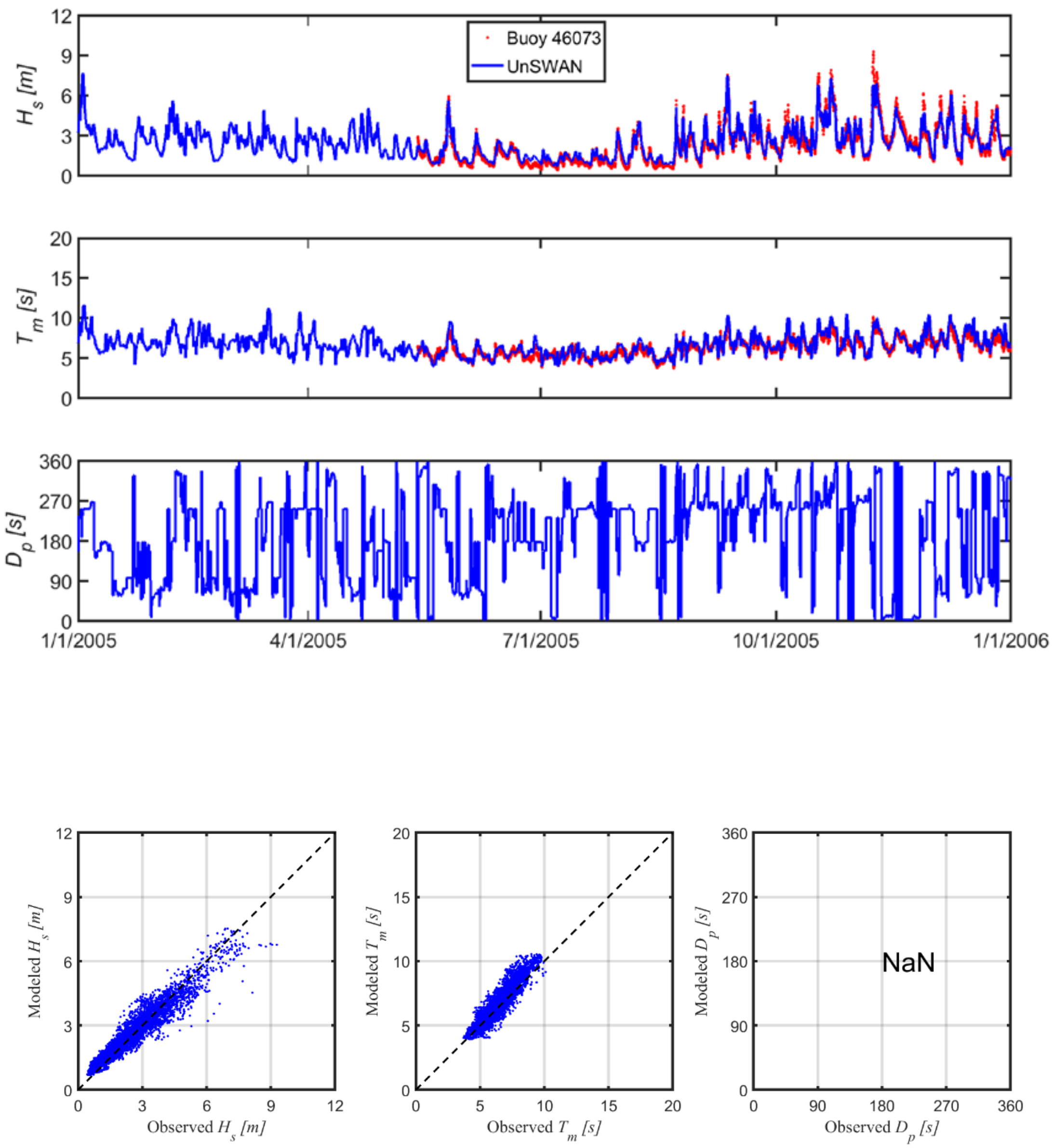

Figure B.100. Comparisons of time series (top) and scatter plots (bottom) of the three UnSWAN model-simulated bulk parameters with observed data at NDBC Buoy 46073 for 2005.

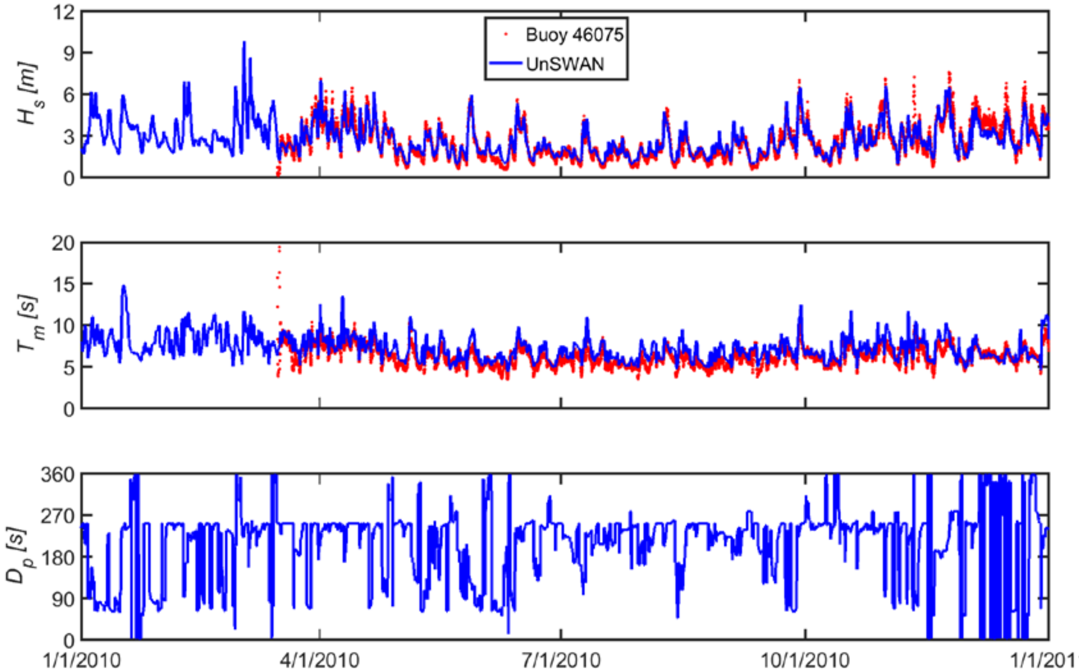

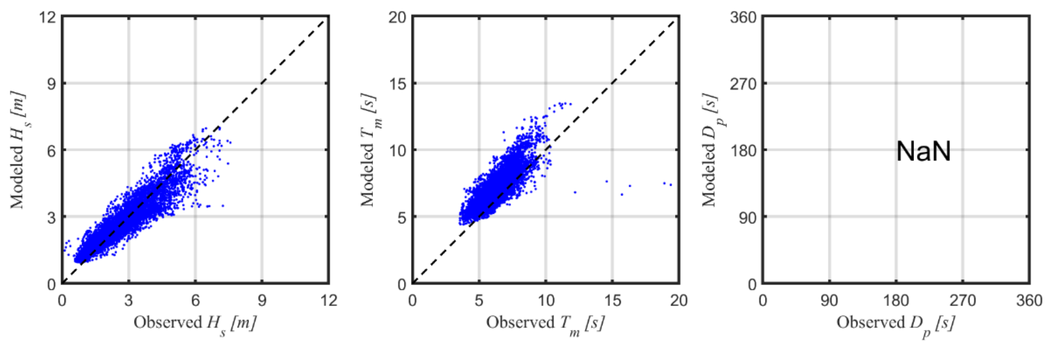

Figure B.101. Comparisons of time series (top) and scatter plots (bottom) of the three UnSWAN model-simulated bulk parameters with observed data at NDBC Buoy 46075 for 2010.

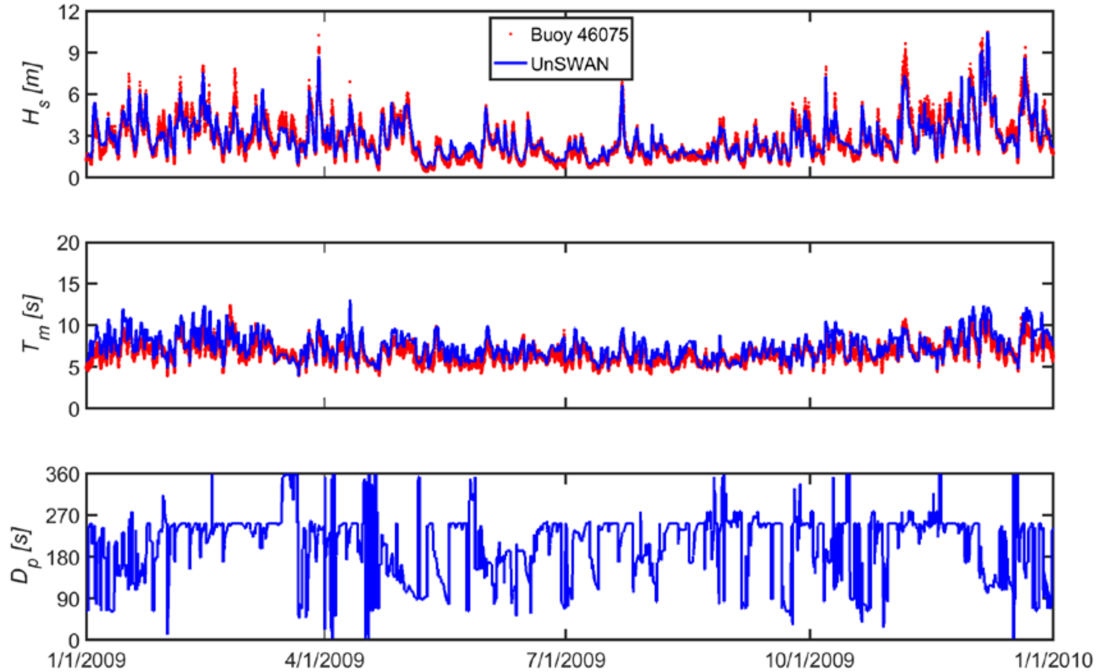

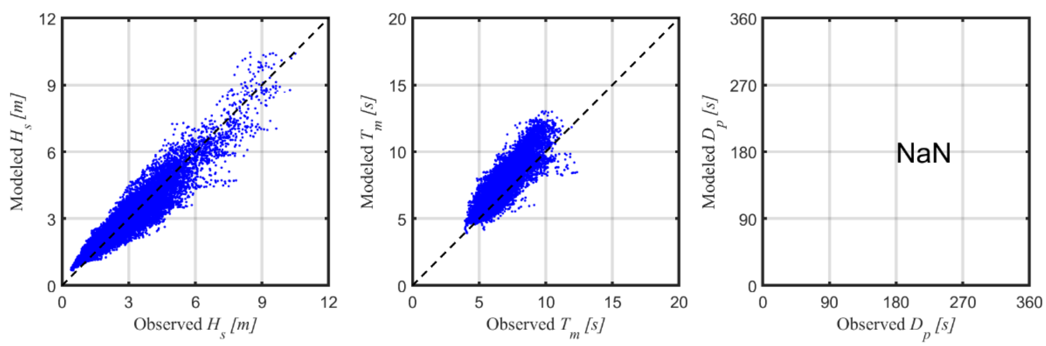

Figure B.102. Comparisons of time series (top) and scatter plots (bottom) of the three UnSWAN model-simulated bulk parameters with observed data at NDBC Buoy 46075 for 2009.

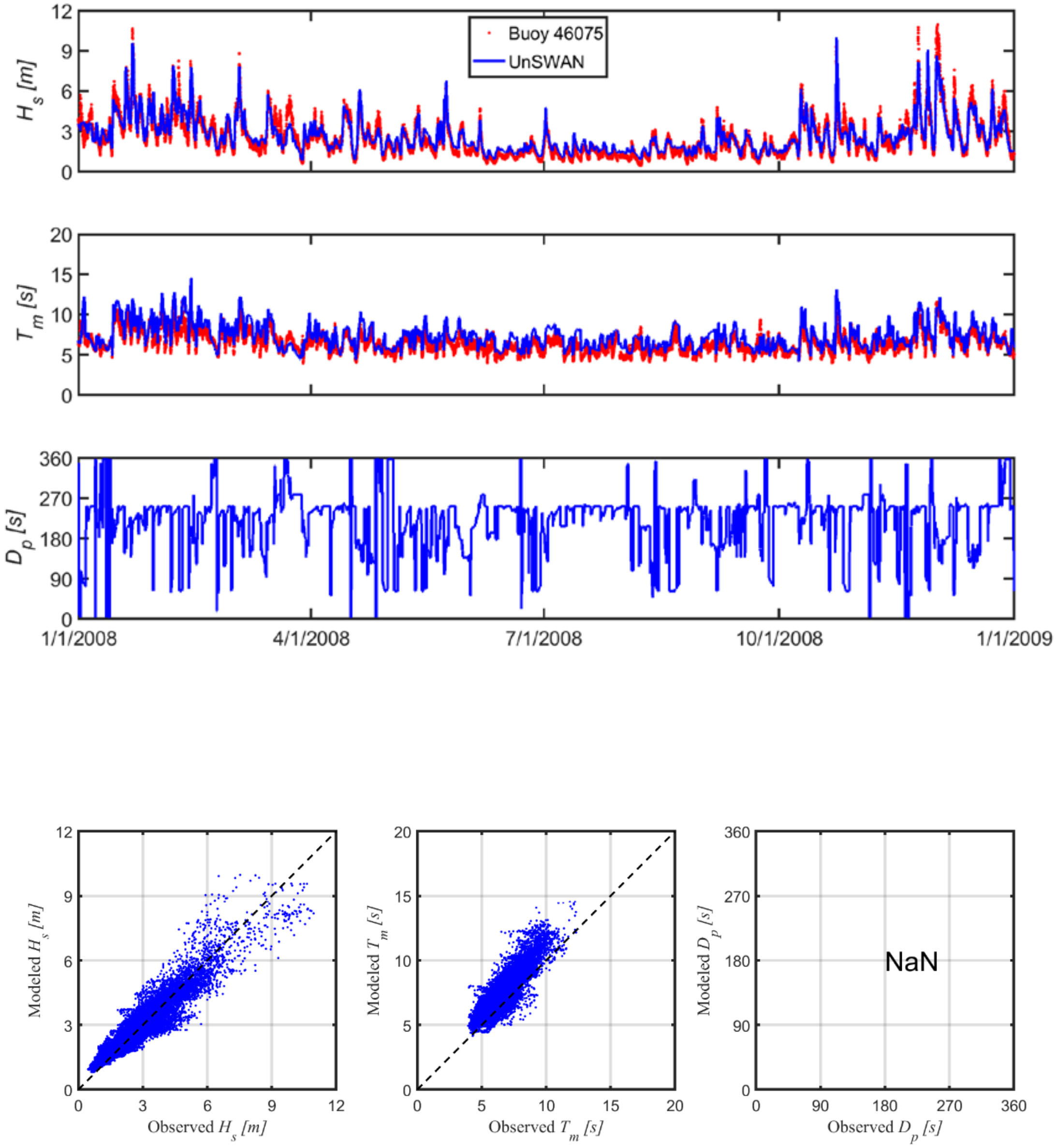

Figure B.103. Comparisons of time series (top) and scatter plots (bottom) of the three UnSWAN model-simulated bulk parameters with observed data at NDBC Buoy 46075 for 2008.

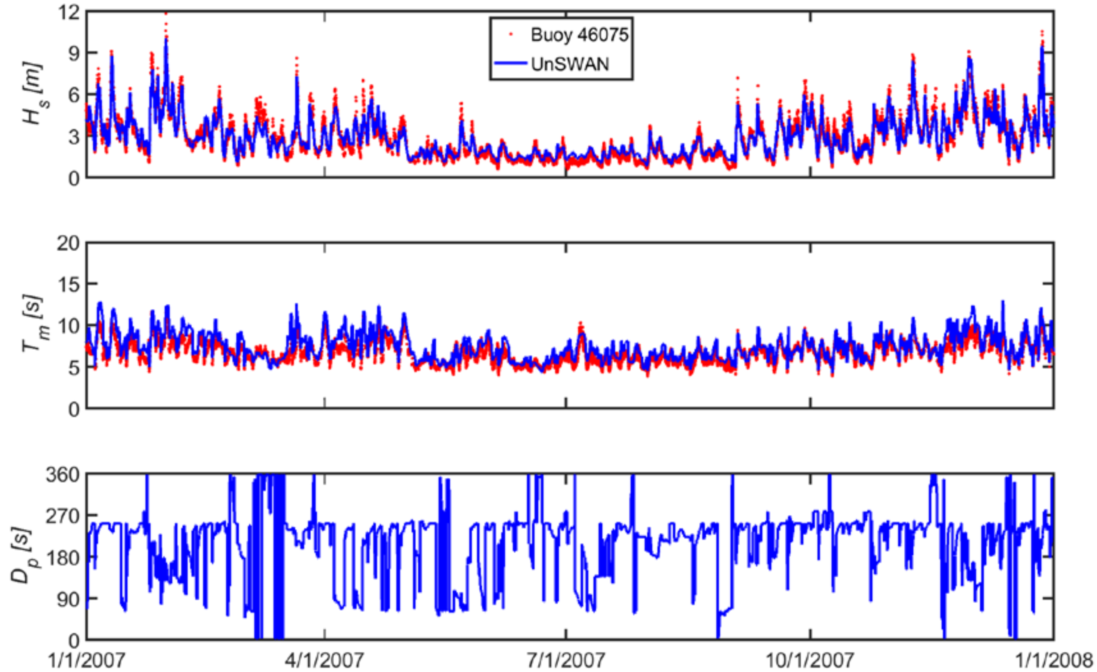

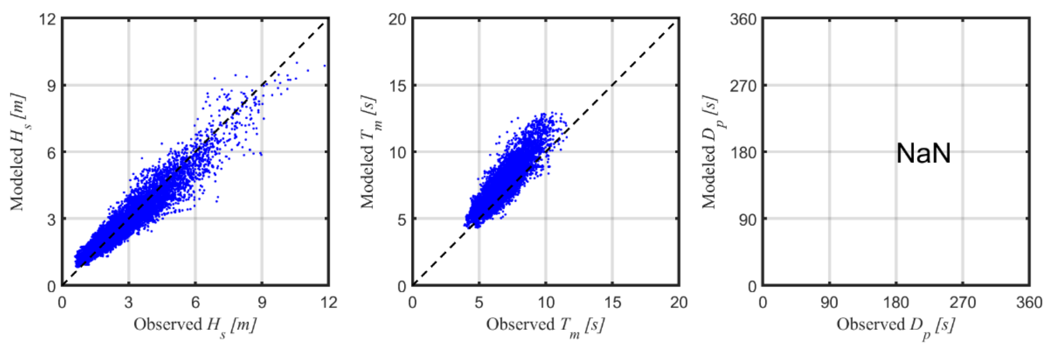

Figure B.104. Comparisons of time series (top) and scatter plots (bottom) of the three UnSWAN model-simulated bulk parameters with observed data at NDBC Buoy 46075 for 2007.

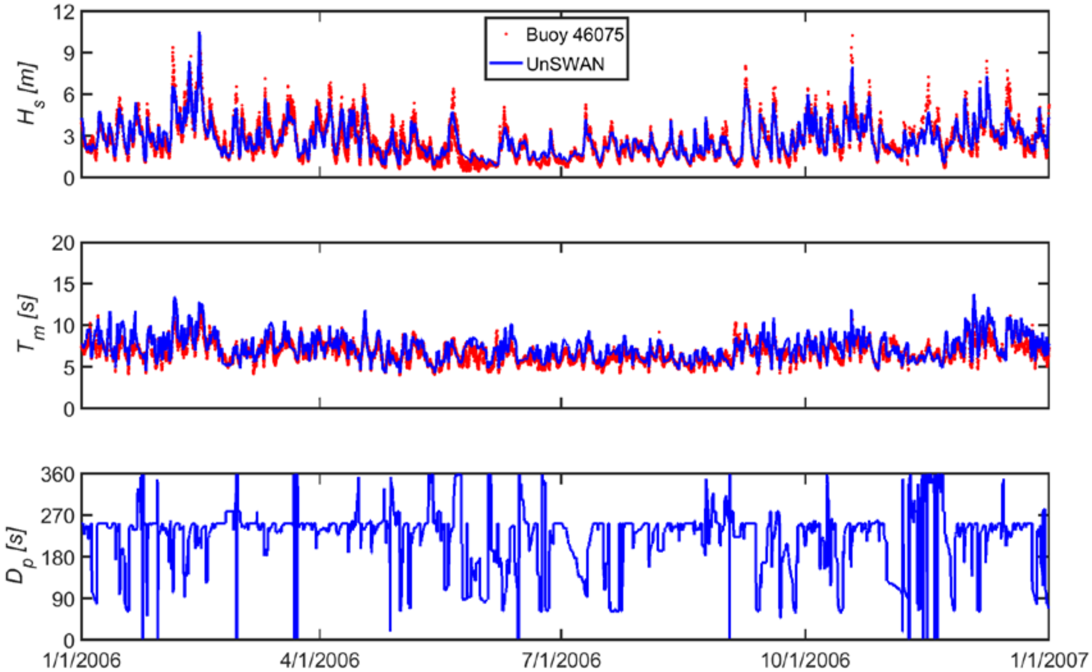

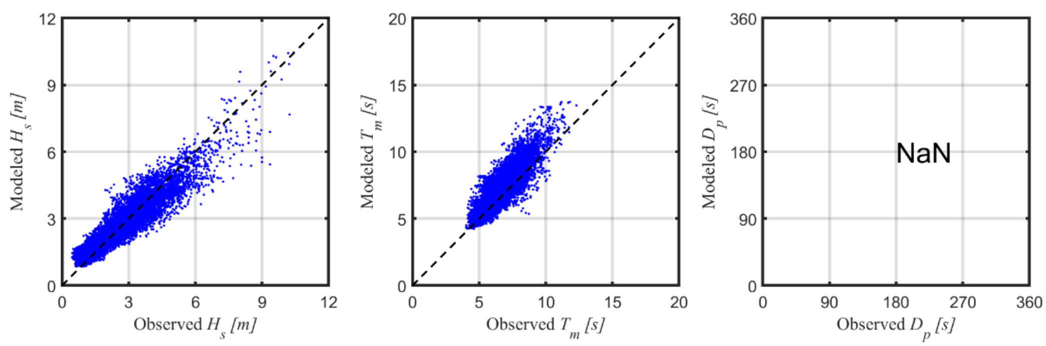

Figure B.105. Comparisons of time series (top) and scatter plots (bottom) of the three UnSWAN model-simulated bulk parameters with observed data at NDBC Buoy 46075 for 2006.

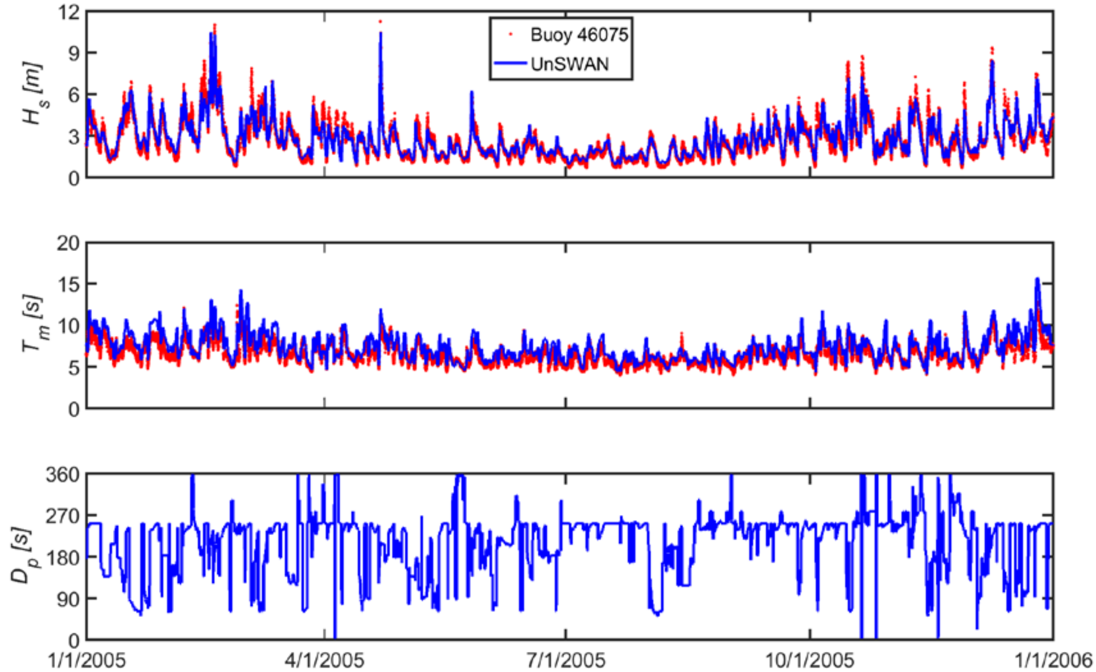

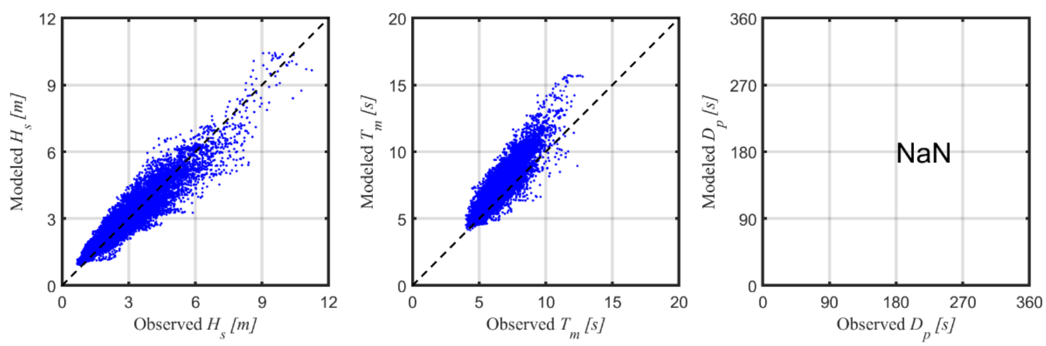

Figure B.106. Comparisons of time series (top) and scatter plots (bottom) of the three UnSWAN model-simulated bulk parameters with observed data at NDBC Buoy 46075 for 2005.

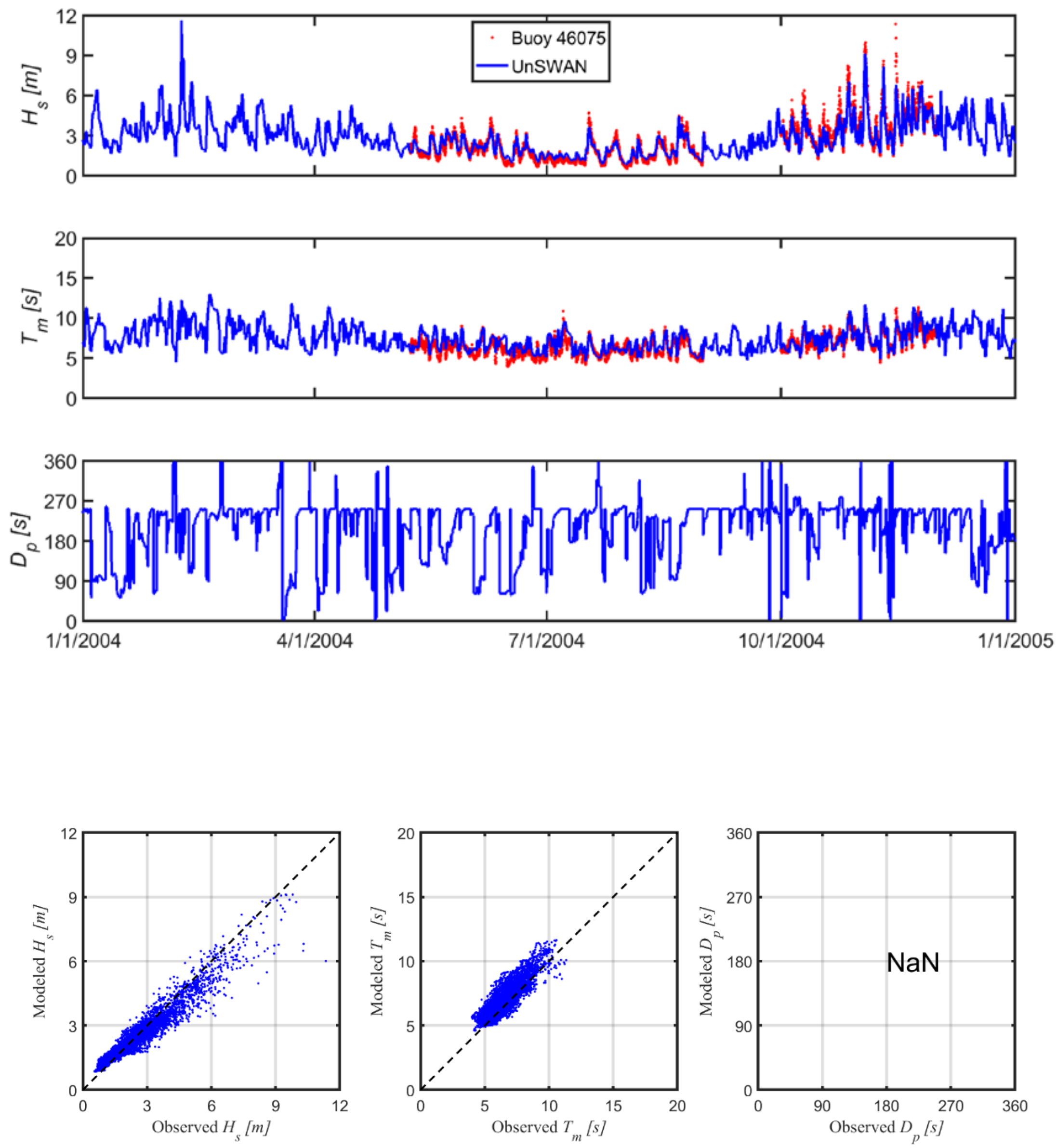

Figure B.107. Comparisons of time series (top) and scatter plots (bottom) of the three UnSWAN model-simulated bulk parameters with observed data at NDBC Buoy 46075 for 2004.

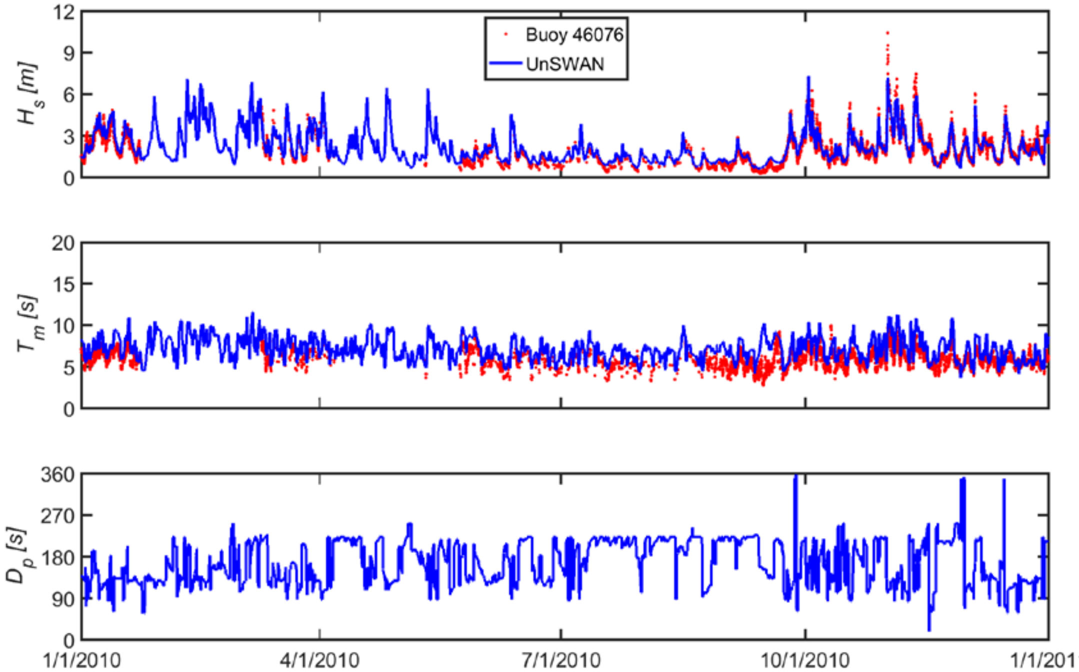

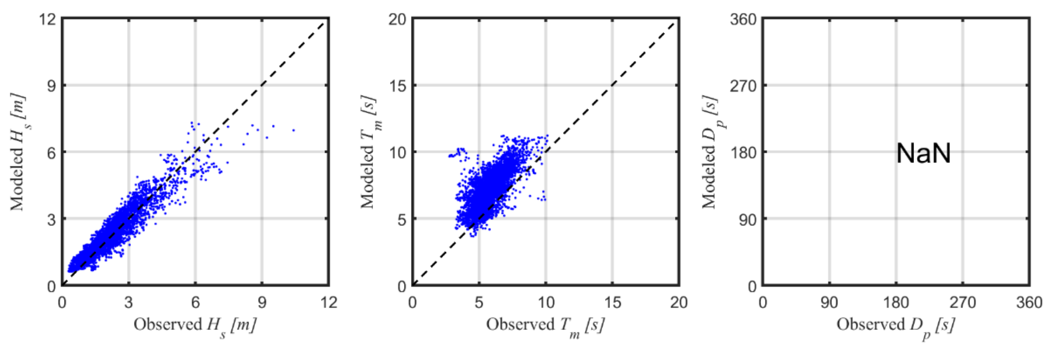

Figure B.108. Comparisons of time series (top) and scatter plots (bottom) of the three UnSWAN model-simulated bulk parameters with observed data at NDBC Buoy 46076 for 2010.

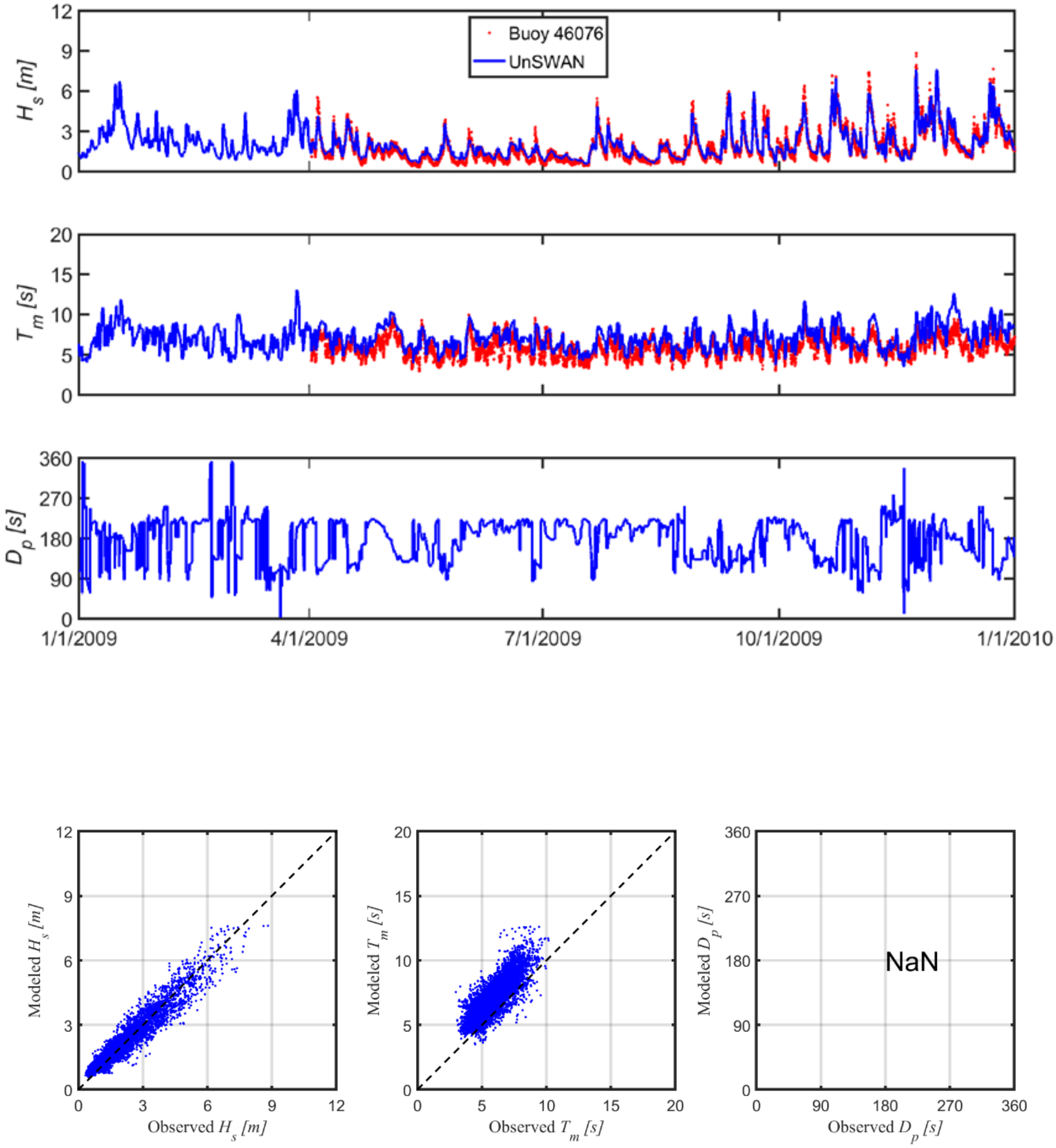

Figure B.109. Comparisons of time series (top) and scatter plots (bottom) of the three UnSWAN model-simulated bulk parameters with observed data at NDBC Buoy 46076 for 2009.

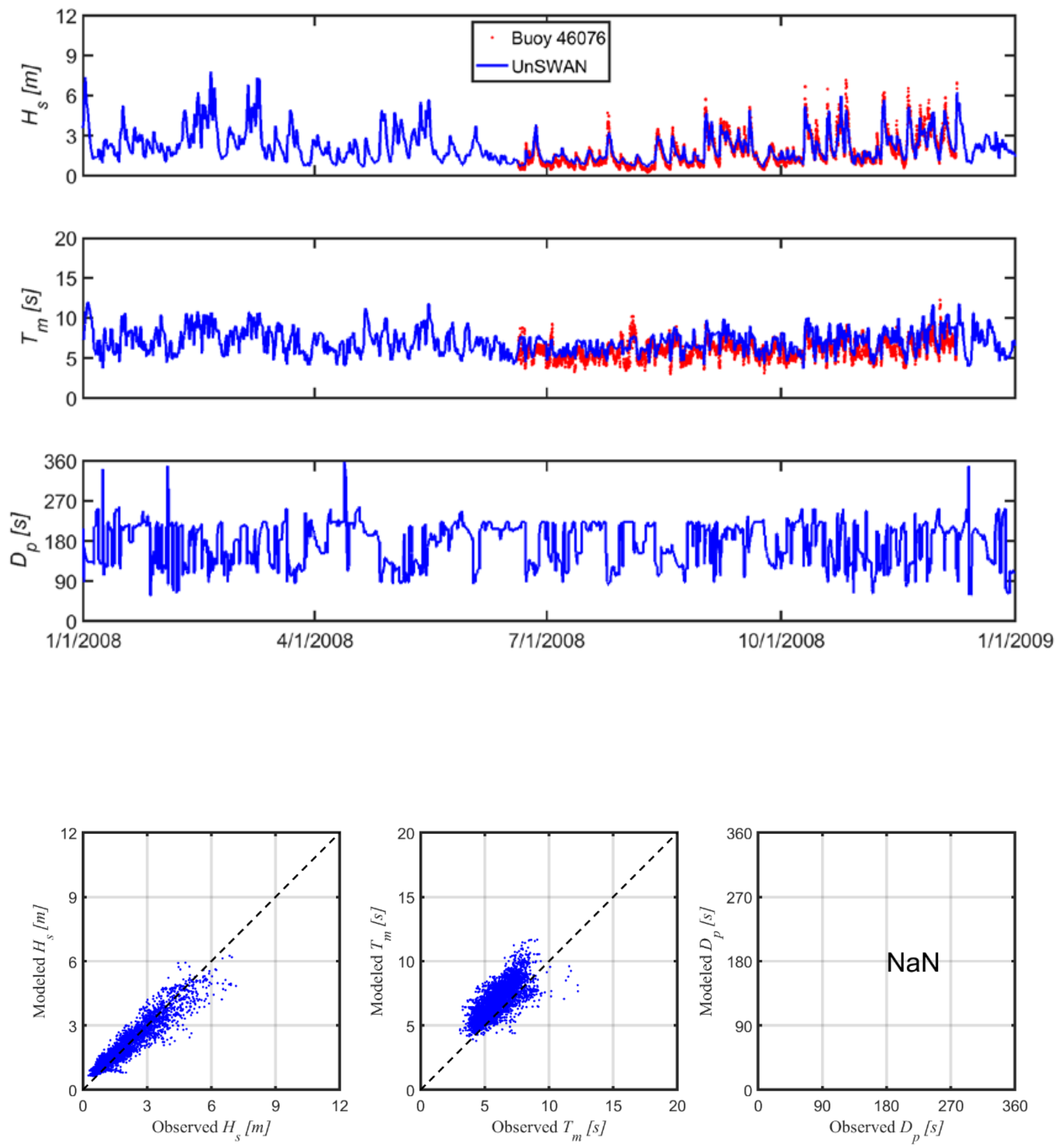

Figure B.110. Comparisons of time series (top) and scatter plots (bottom) of the three UnSWAN model-simulated bulk parameters with observed data at NDBC Buoy 46076 for 2008.

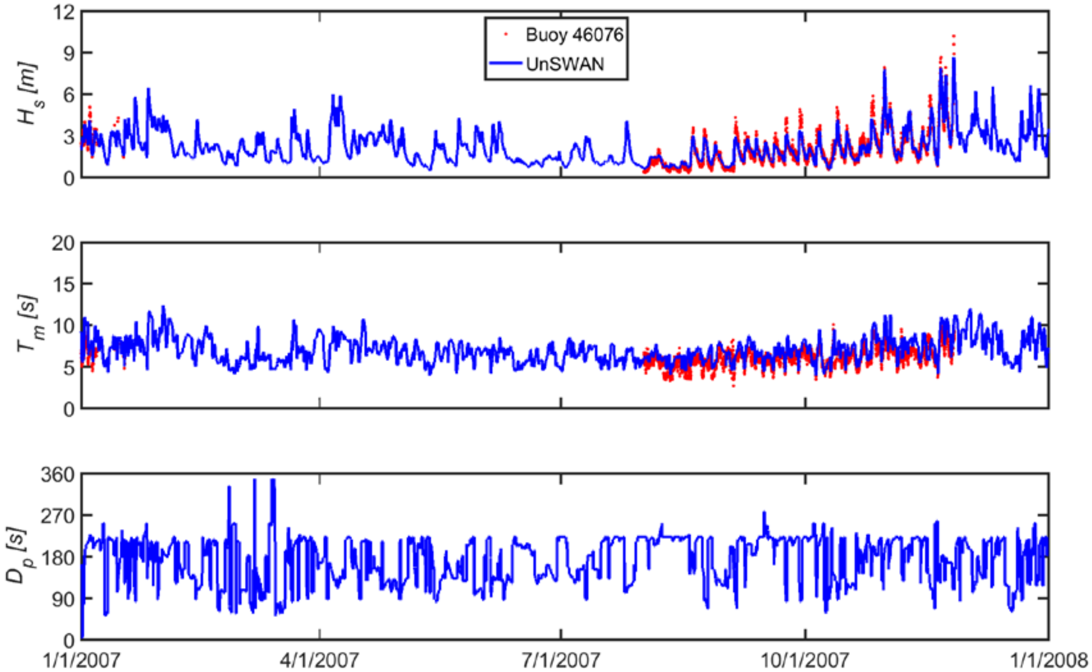

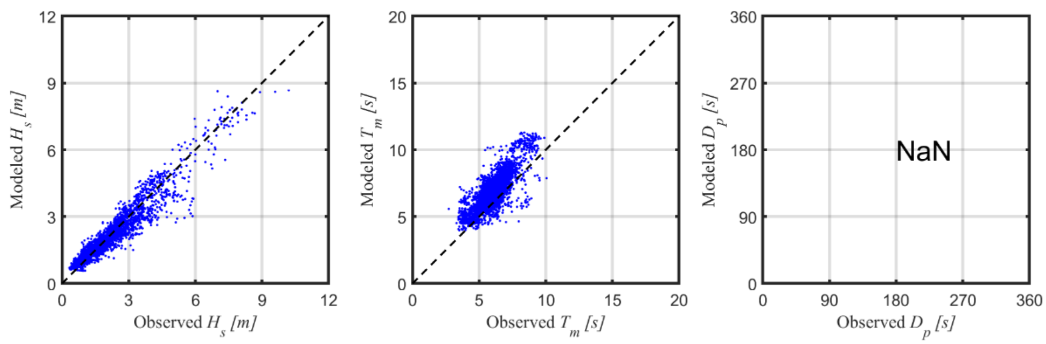

Figure B.111. Comparisons of time series (top) and scatter plots (bottom) of the three UnSWAN model-simulated bulk parameters with observed data at NDBC Buoy 46076 for 2007.

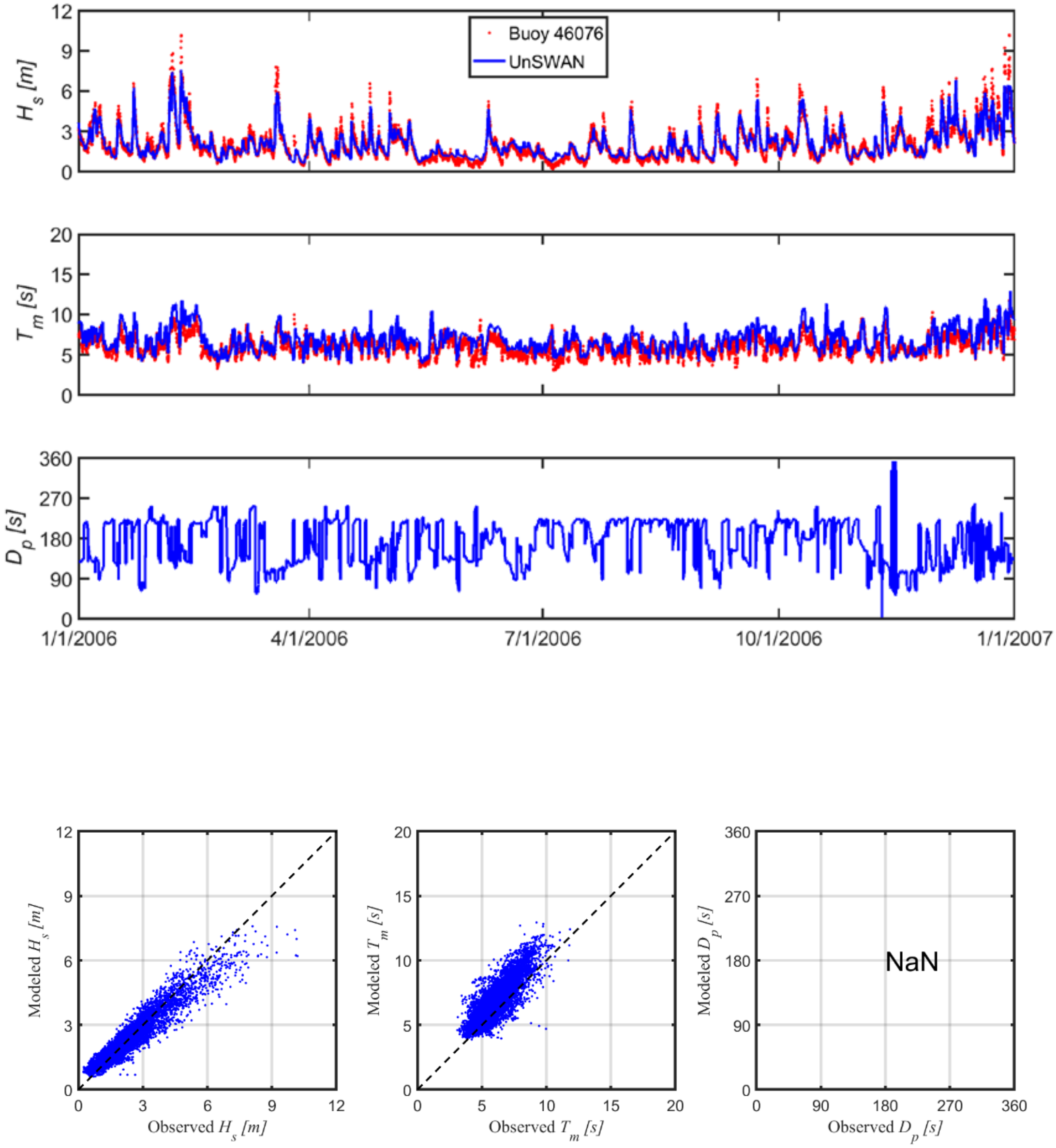

Figure B.112. Comparisons of time series (top) and scatter plots (bottom) of the three UnSWAN model-simulated bulk parameters with observed data at NDBC Buoy 46076 for 2006.

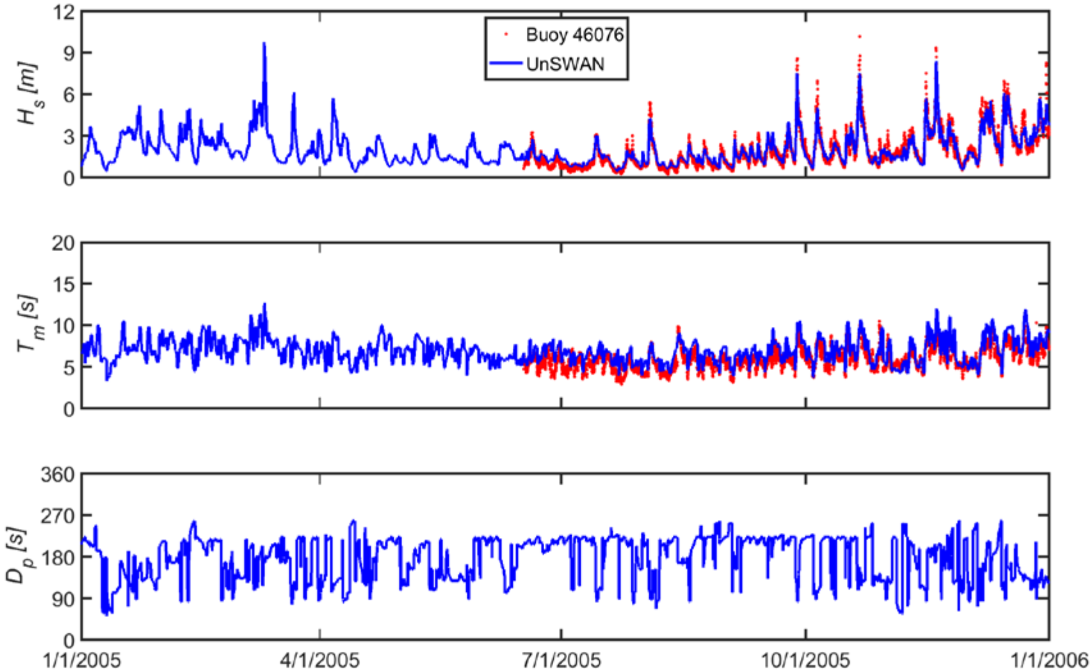

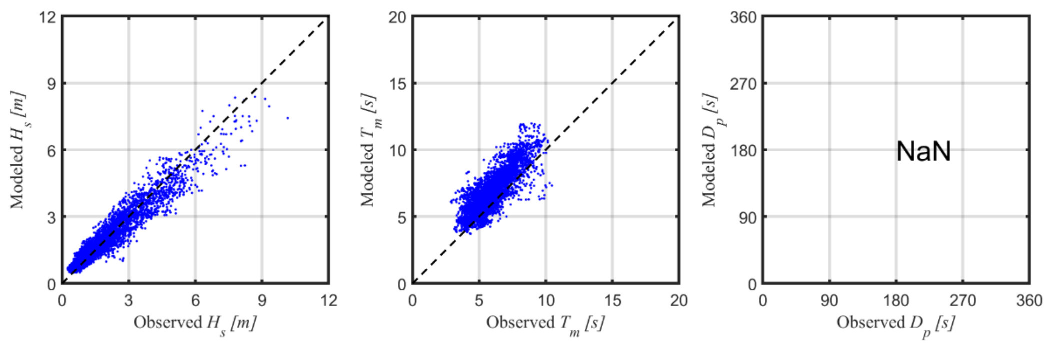

Figure B.113. Comparisons of time series (top) and scatter plots (bottom) of the three UnSWAN model-simulated bulk parameters with observed data at NDBC Buoy 46076 for 2005.

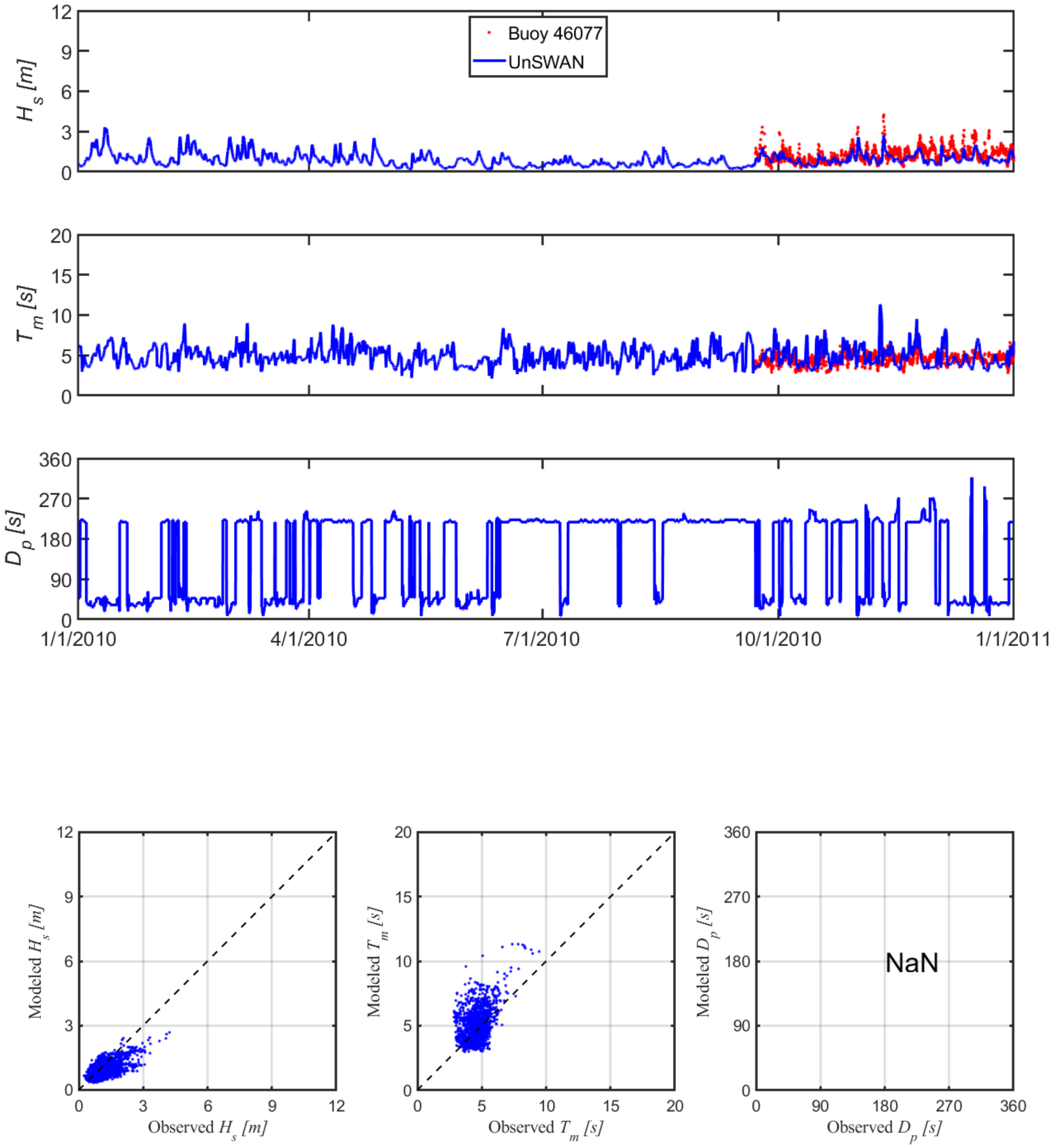

Figure B.114. Comparisons of time series (top) and scatter plots (bottom) of the three UnSWAN model-simulated bulk parameters with observed data at NDBC Buoy 46077 for 2010.

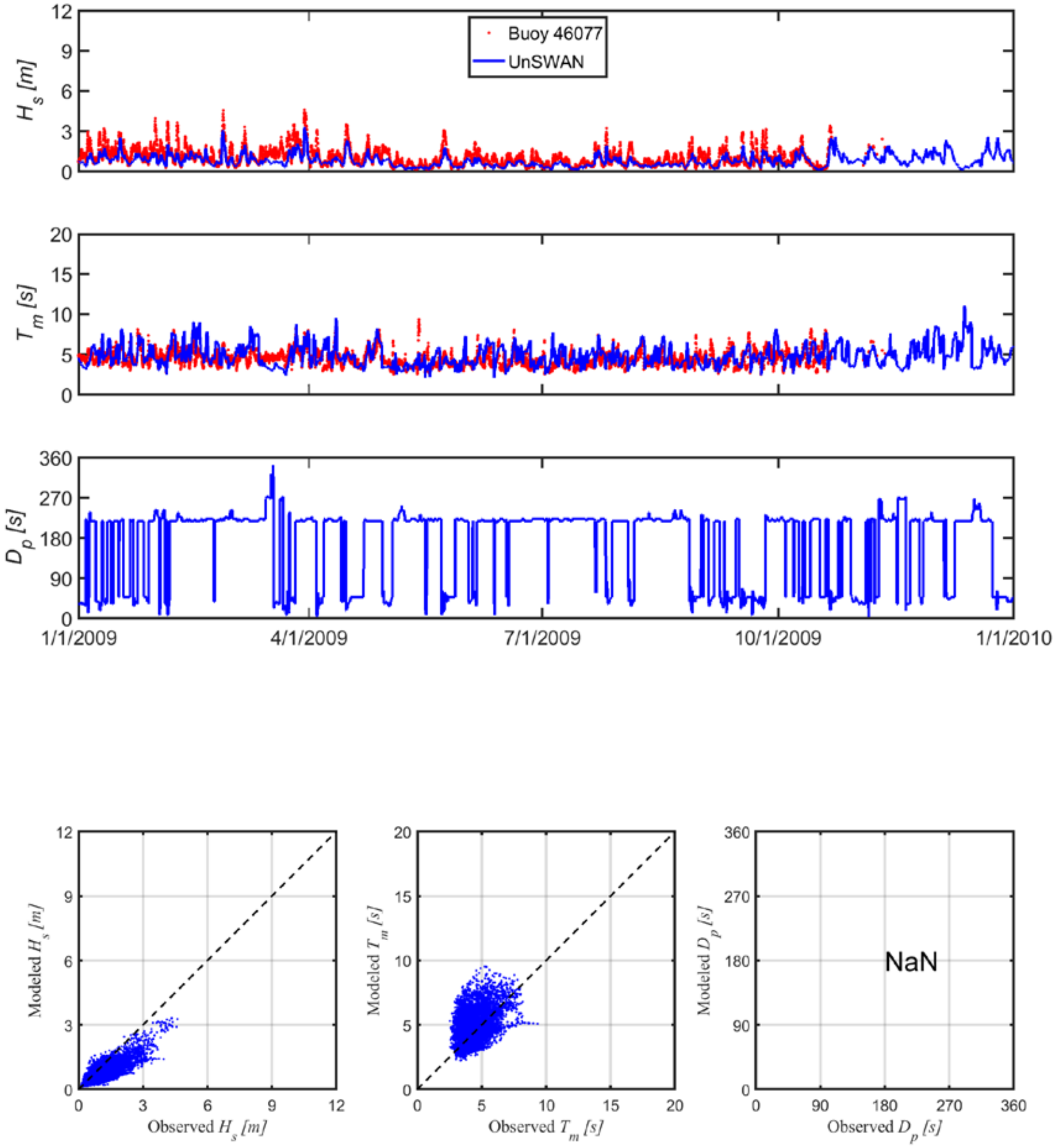

Figure B.115. Comparisons of time series (top) and scatter plots (bottom) of the three UnSWAN model-simulated bulk parameters with observed data at NDBC Buoy 46077 for 2009.

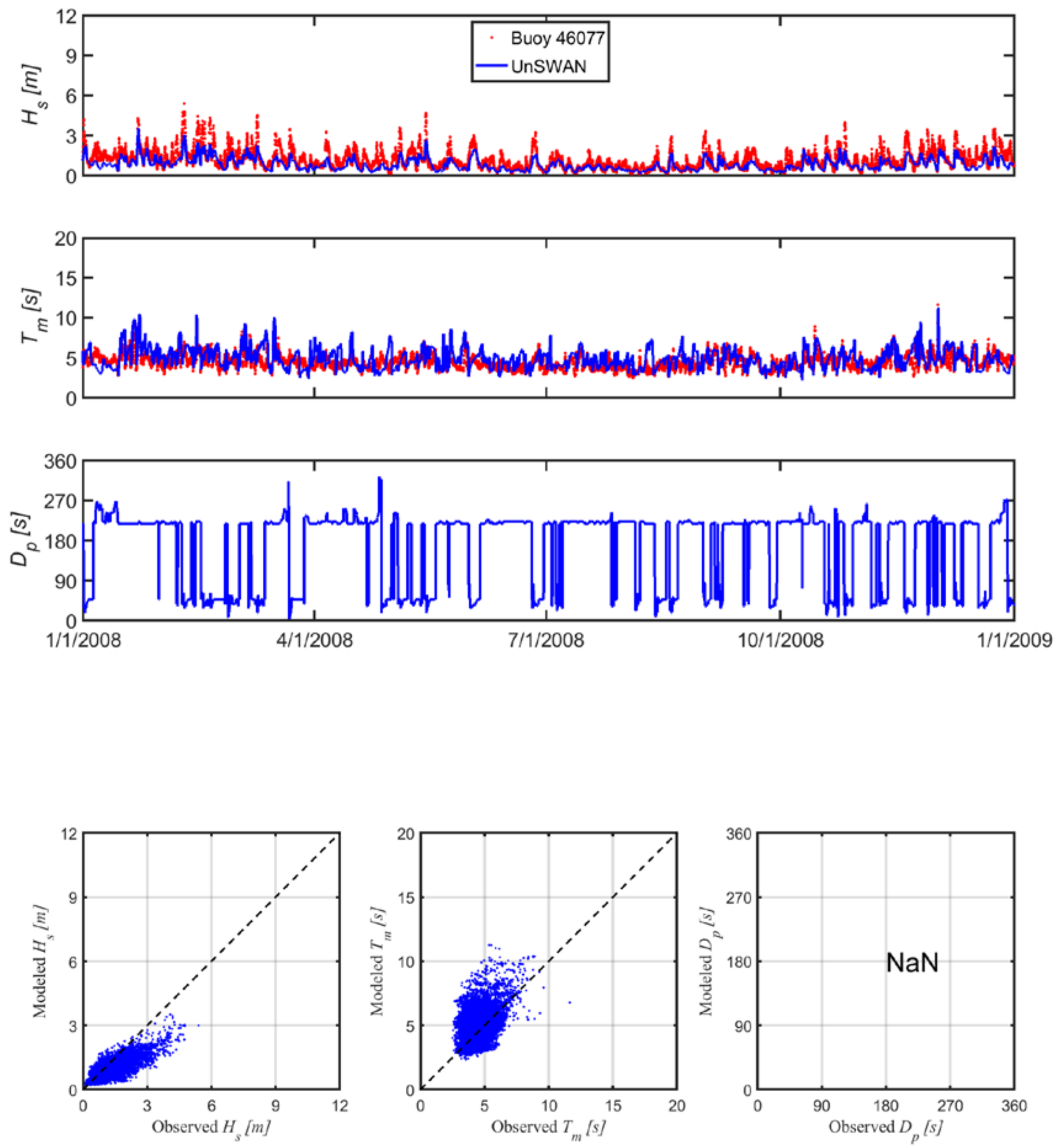

Figure B.116. Comparisons of time series (top) and scatter plots (bottom) of the three UnSWAN model-simulated bulk parameters with observed data at NDBC Buoy 46077 for 2008.

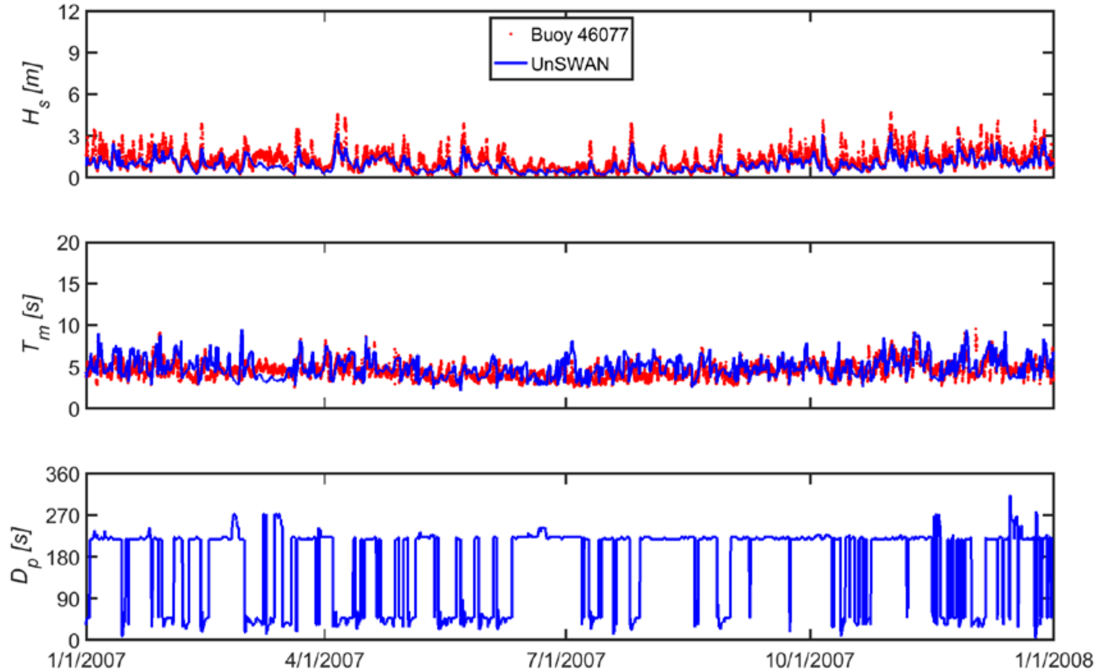

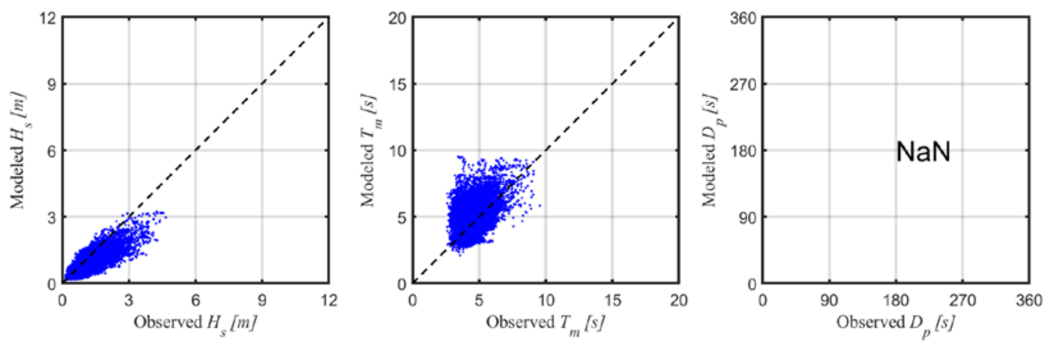

Figure B.117. Comparisons of time series (top) and scatter plots (bottom) of the three UnSWAN model-simulated bulk parameters with observed data at NDBC Buoy 46077 for 2007.

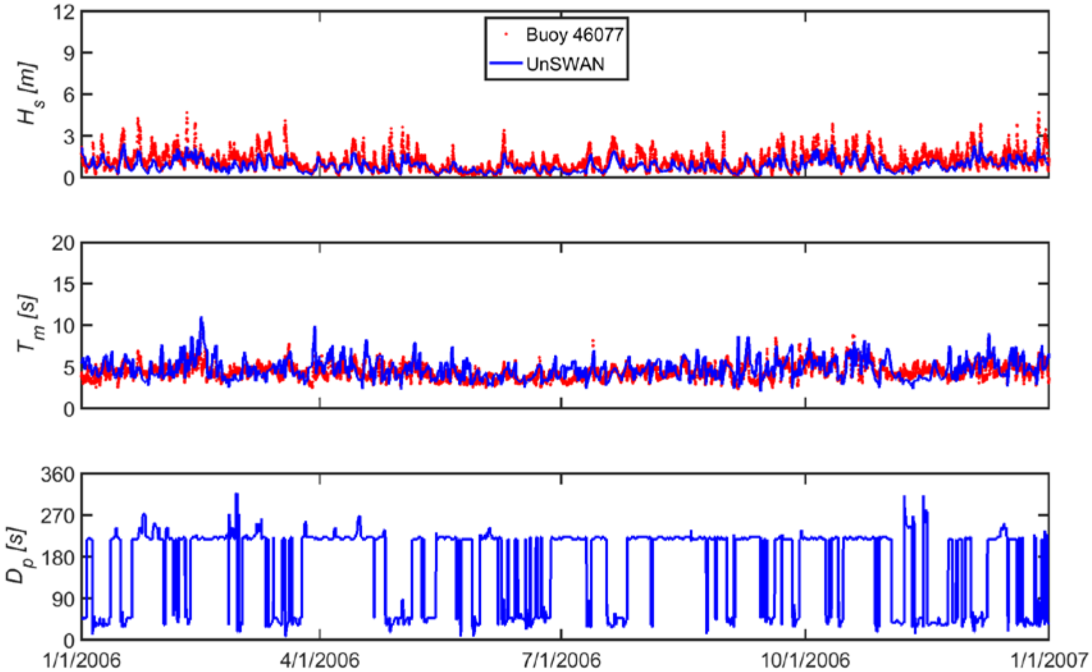

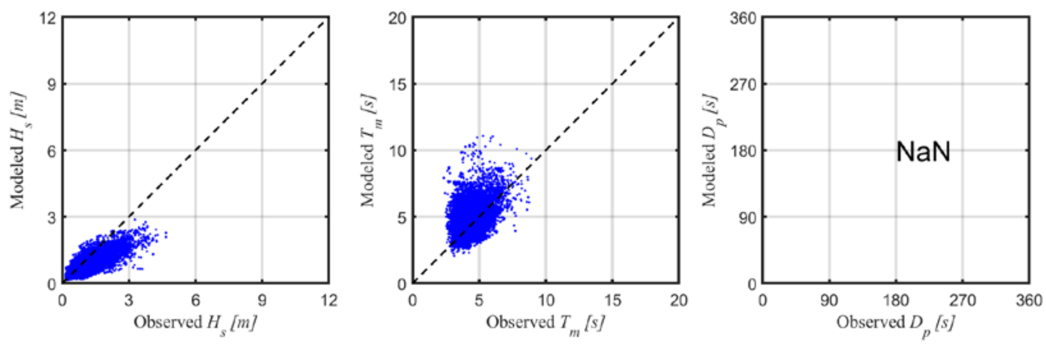

Figure B.118. Comparisons of time series (top) and scatter plots (bottom) of the three UnSWAN model-simulated bulk parameters with observed data at NDBC Buoy 46077 for 2006.

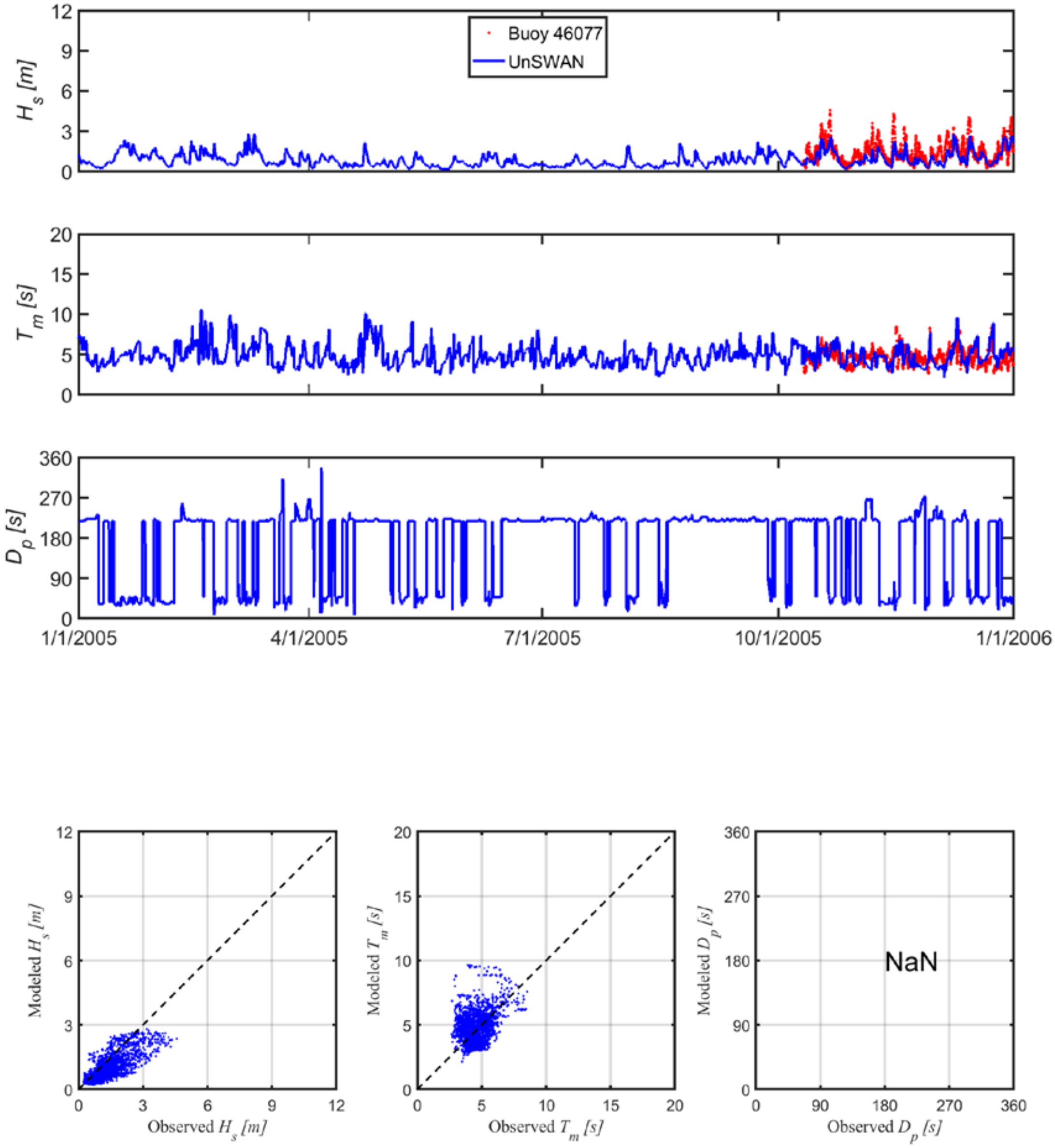

Figure B.119. Comparisons of time series (top) and scatter plots (bottom) of the three UnSWAN model-simulated bulk parameters with observed data at NDBC Buoy 46077 for 2005.

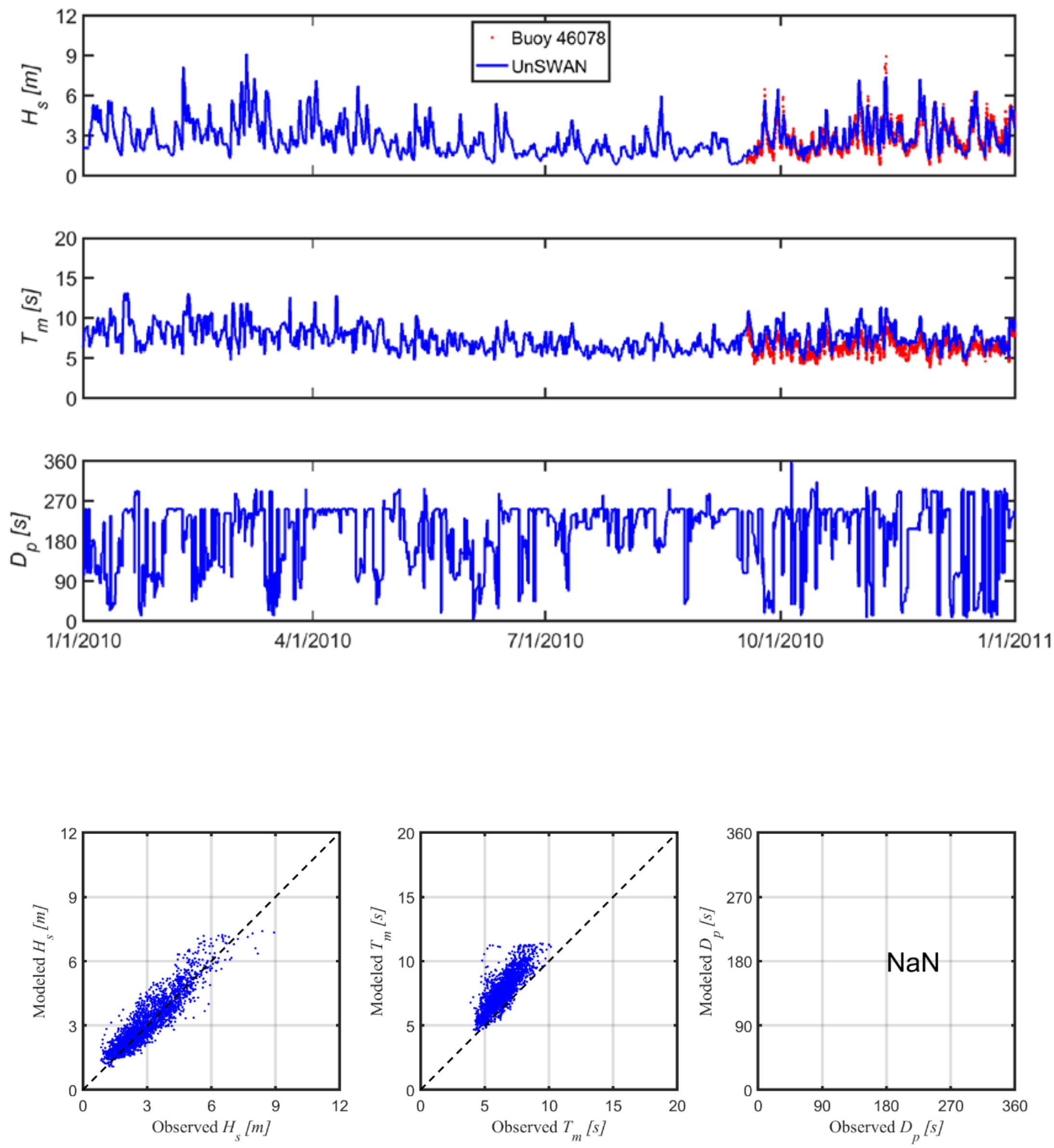

Figure B.120. Comparisons of time series (top) and scatter plots (bottom) of the three UnSWAN model-simulated bulk parameters with observed data at NDBC Buoy 46078 for 2010.

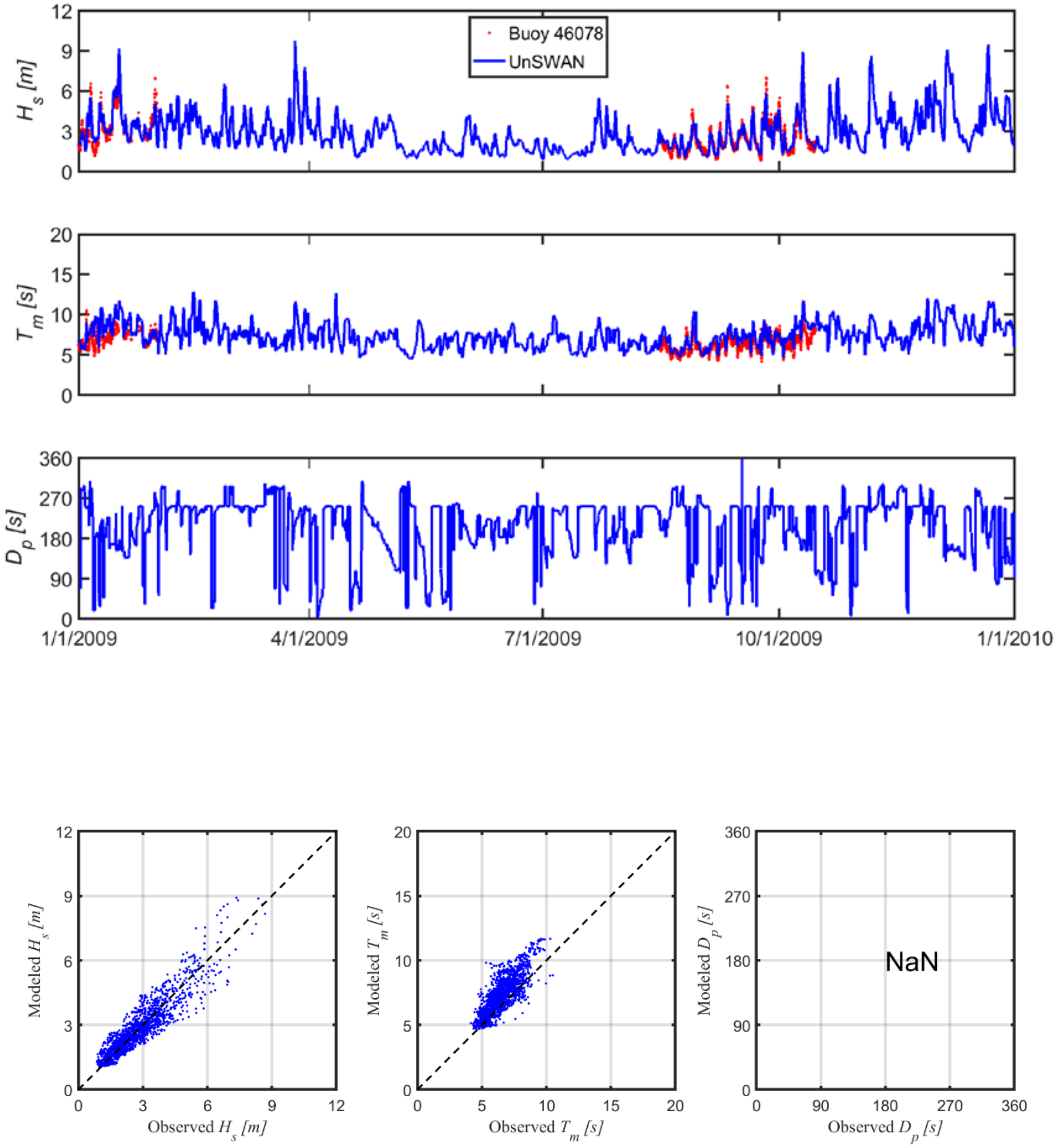

Figure B.121. Comparisons of time series (top) and scatter plots (bottom) of the three UnSWAN model-simulated bulk parameters with observed data at NDBC Buoy 46078 for 2009.

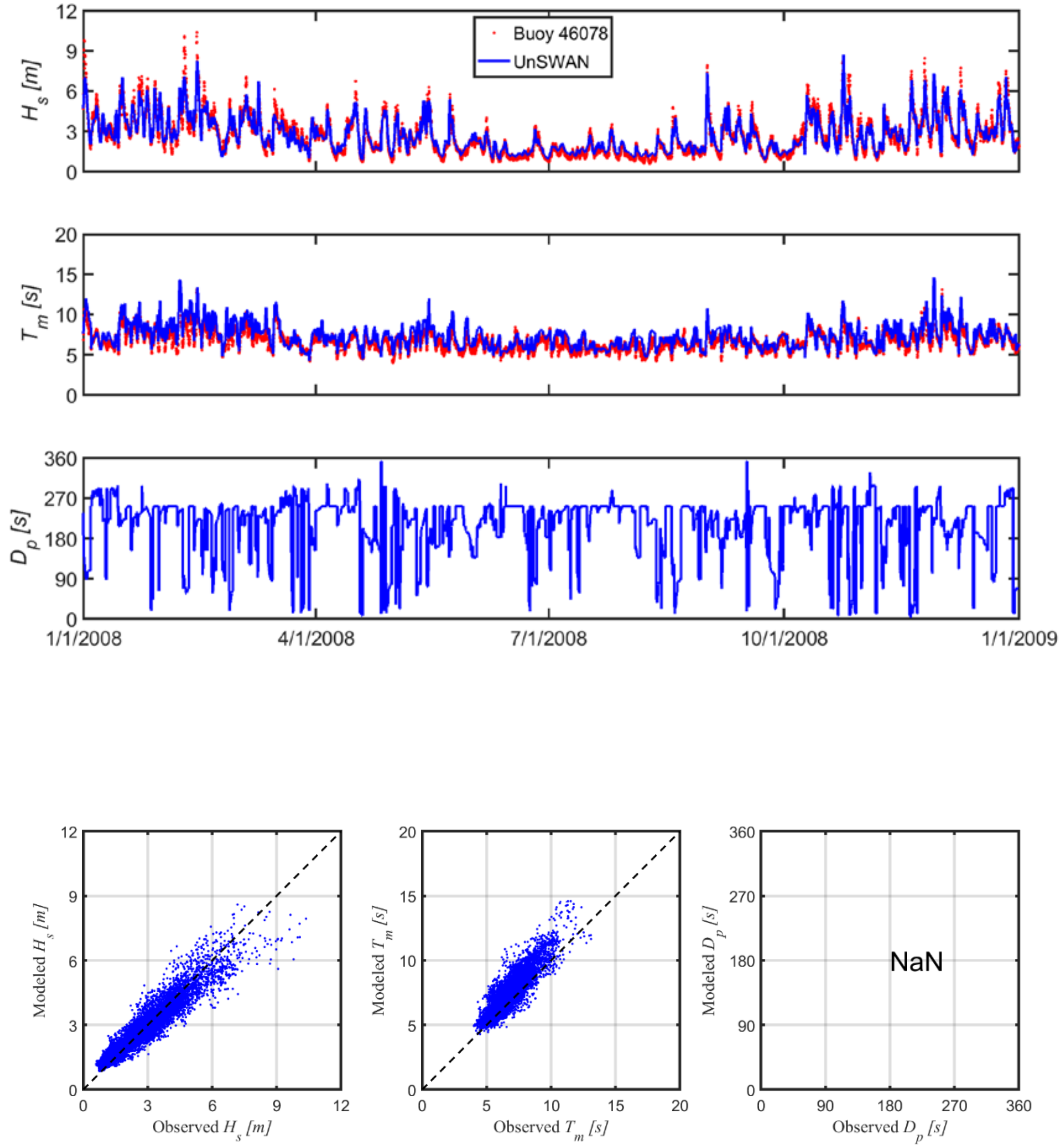

Figure B.122. Comparisons of time series (top) and scatter plots (bottom) of the three UnSWAN model-simulated bulk parameters with observed data at NDBC Buoy 46078 for 2008.

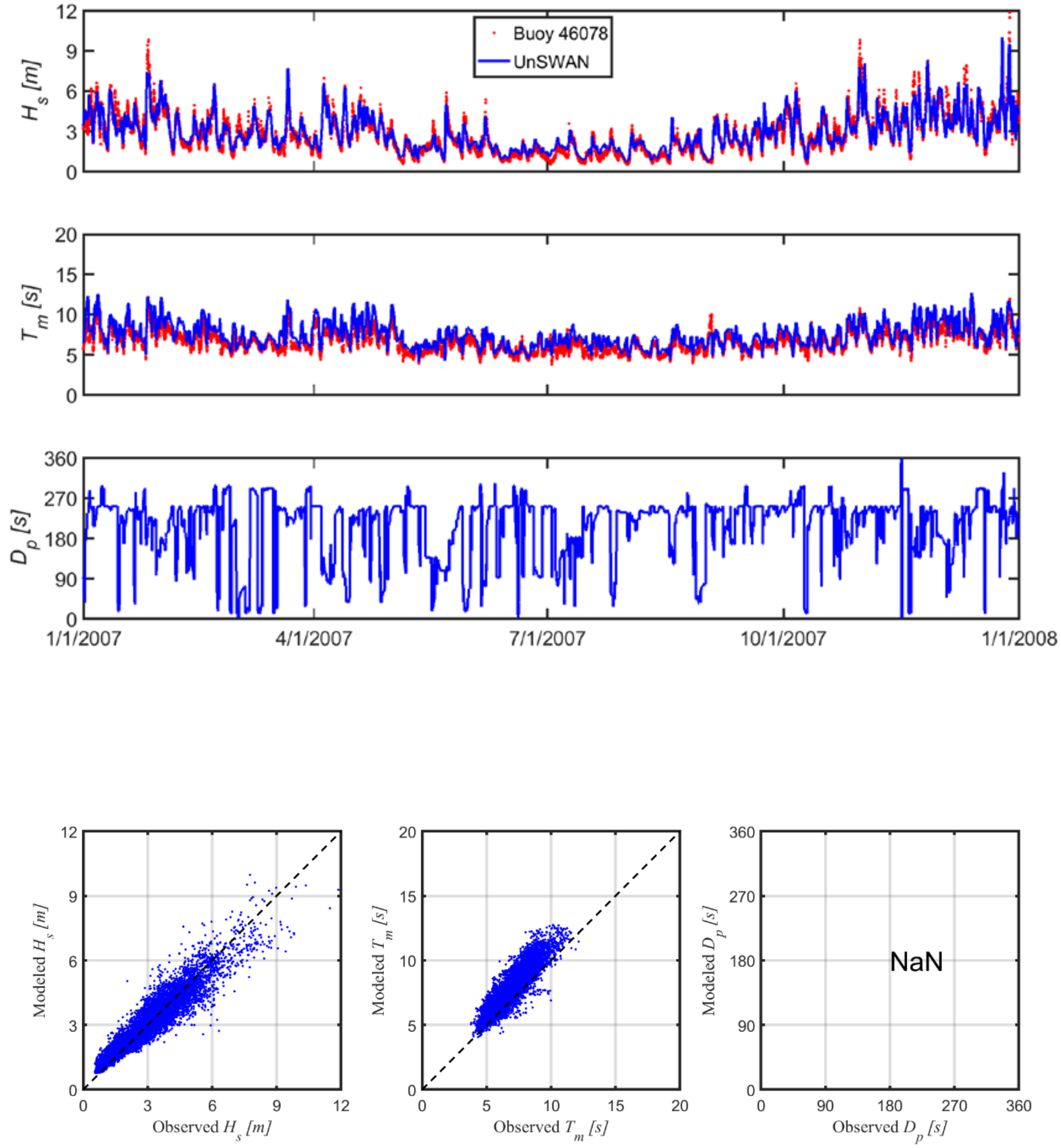

Figure B.123. Comparisons of time series (top) and scatter plots (bottom) of the three UnSWAN model-simulated bulk parameters with observed data at NDBC Buoy 46078 for 2007.

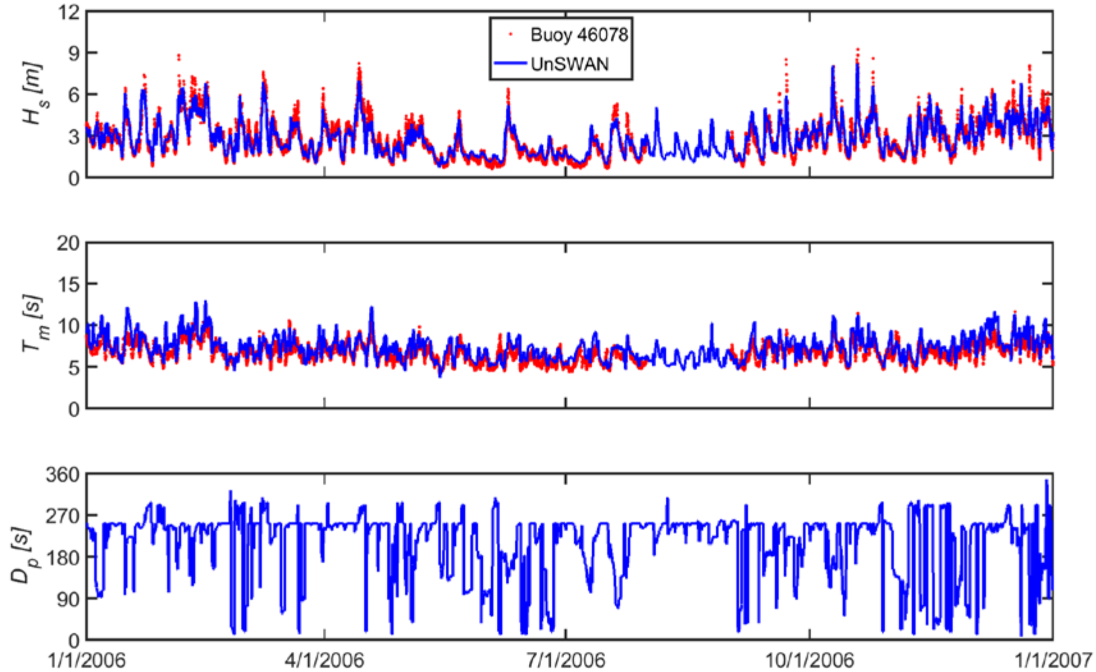

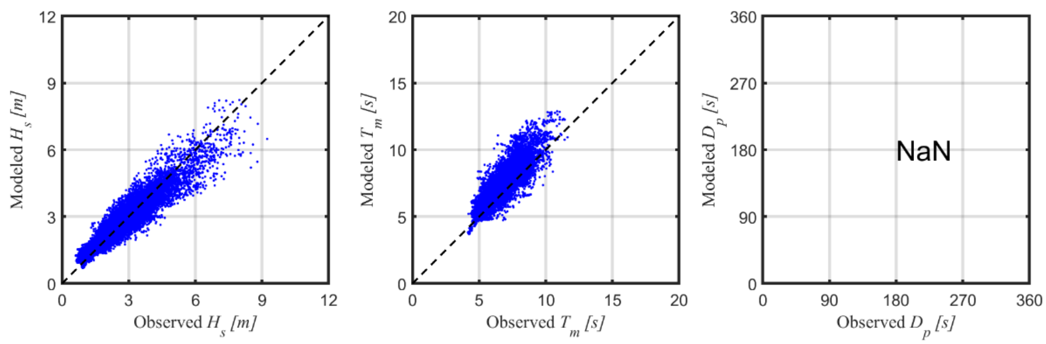

Figure B.124. Comparisons of time series (top) and scatter plots (bottom) of the three UnSWAN model-simulated bulk parameters with observed data at NDBC Buoy 46078 for 2006.

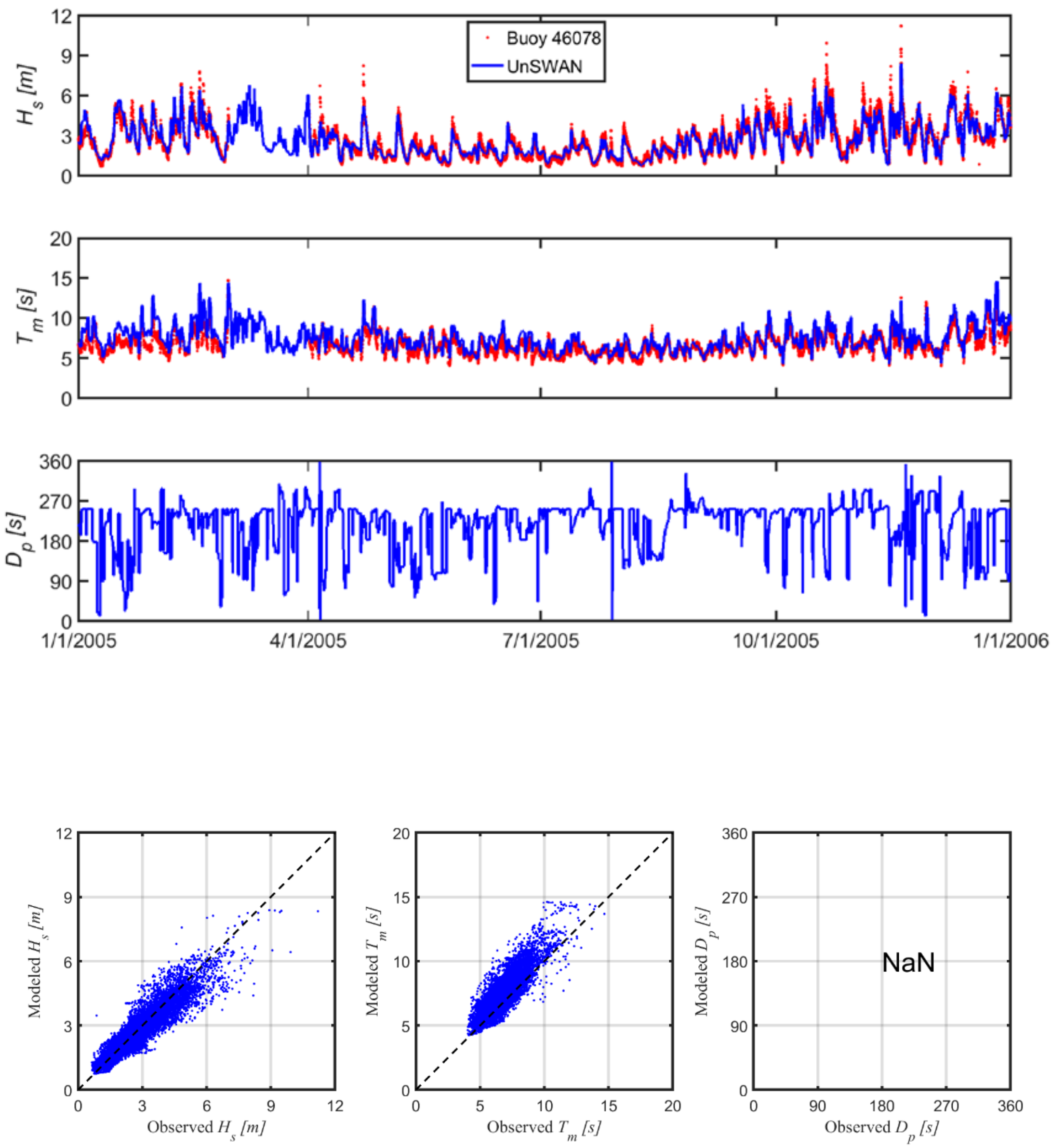

Figure B.125. Comparisons of time series (top) and scatter plots (bottom) of the three UnSWAN model-simulated bulk parameters with observed data at NDBC Buoy 46078 for 2005.

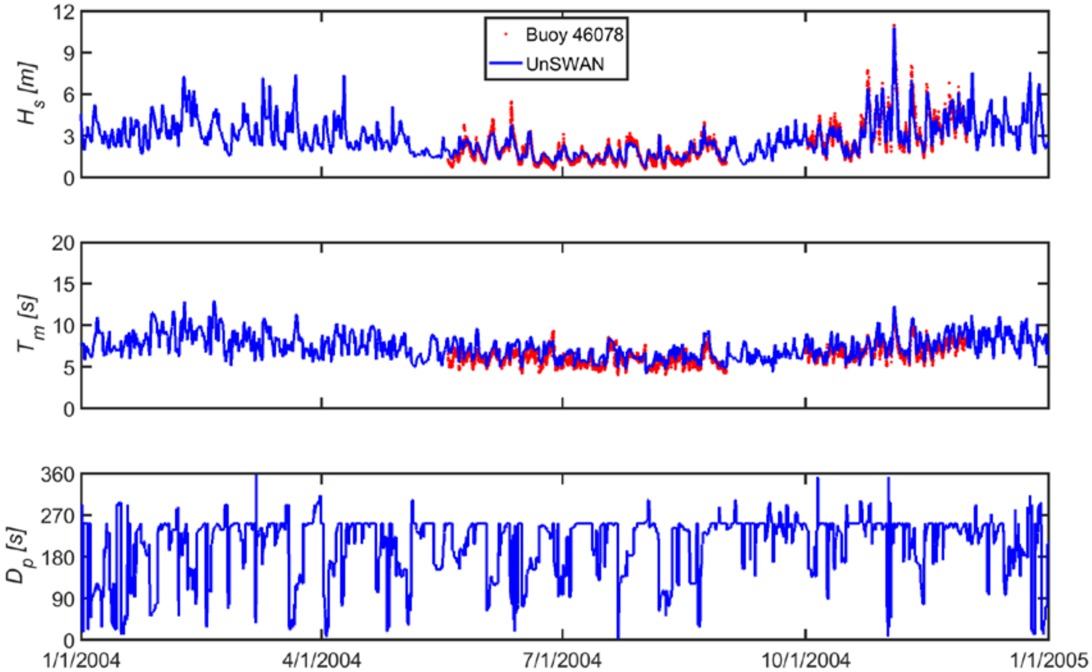

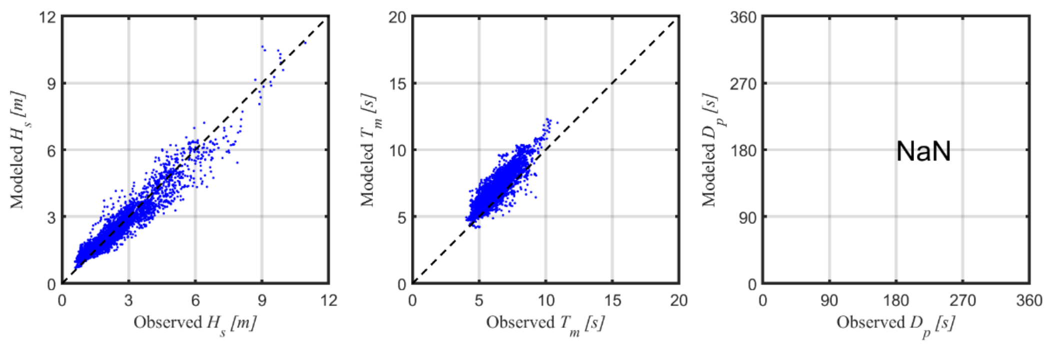

Figure B.126. Comparisons of time series (top) and scatter plots (bottom) of the three UnSWAN model-simulated bulk parameters with observed data at NDBC Buoy 46078 for 2004.

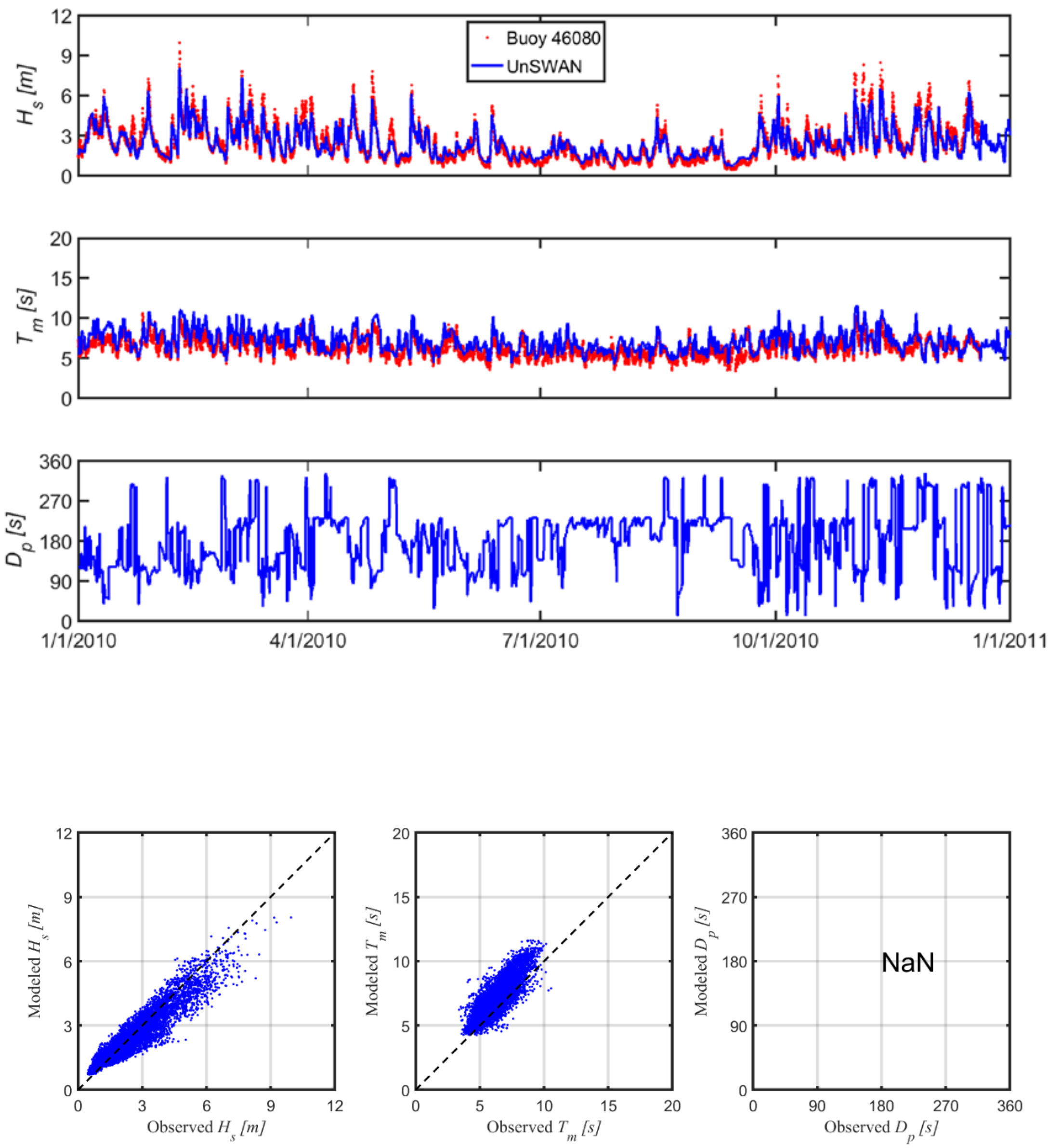

Figure B.127. Comparisons of time series (top) and scatter plots (bottom) of the three UnSWAN model-simulated bulk parameters with observed data at NDBC Buoy 46080 for 2010.

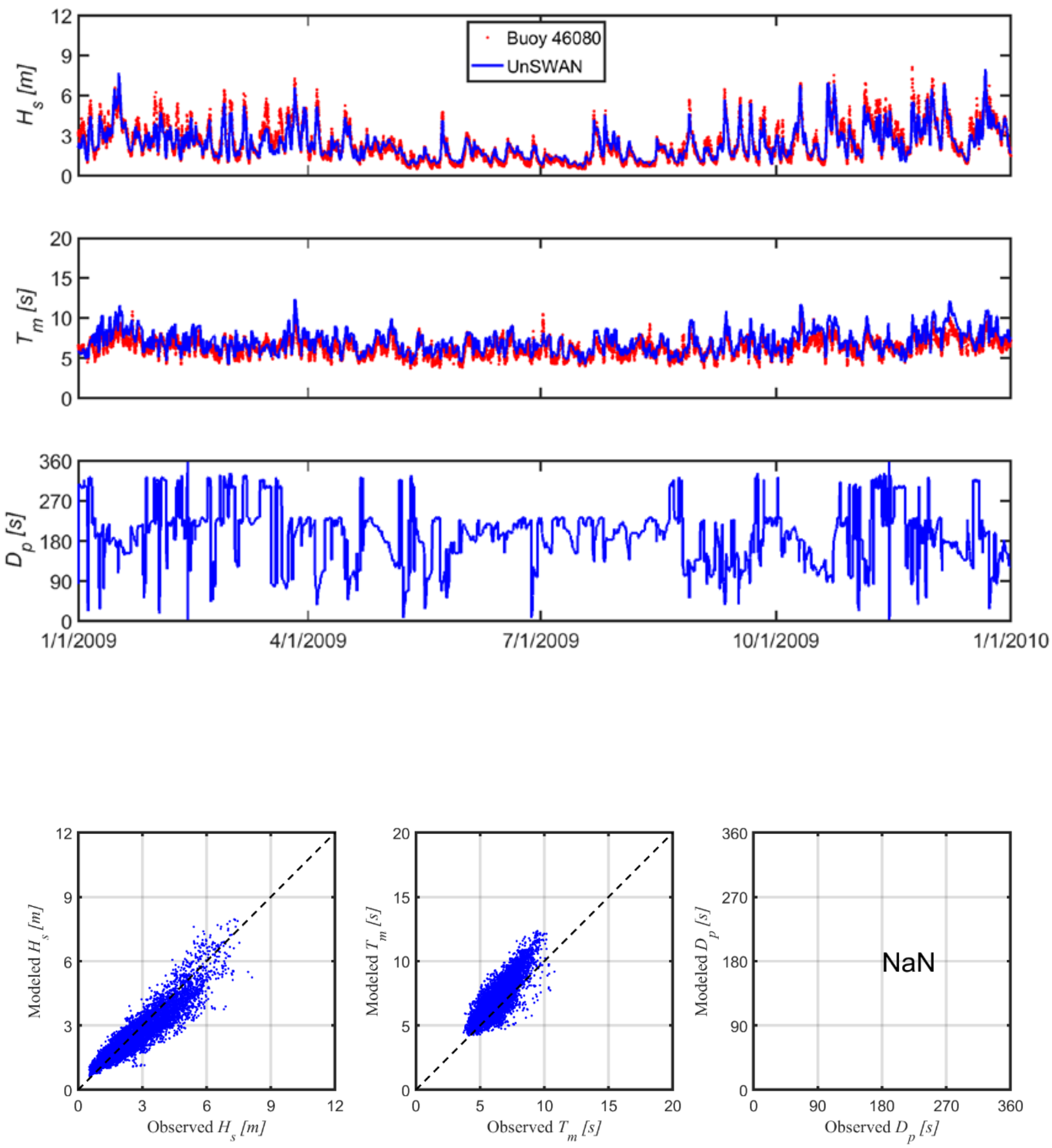

Figure B.128. Comparisons of time series (top) and scatter plots (bottom) of the three UnSWAN model-simulated bulk parameters with observed data at NDBC Buoy 46080 for 2009.

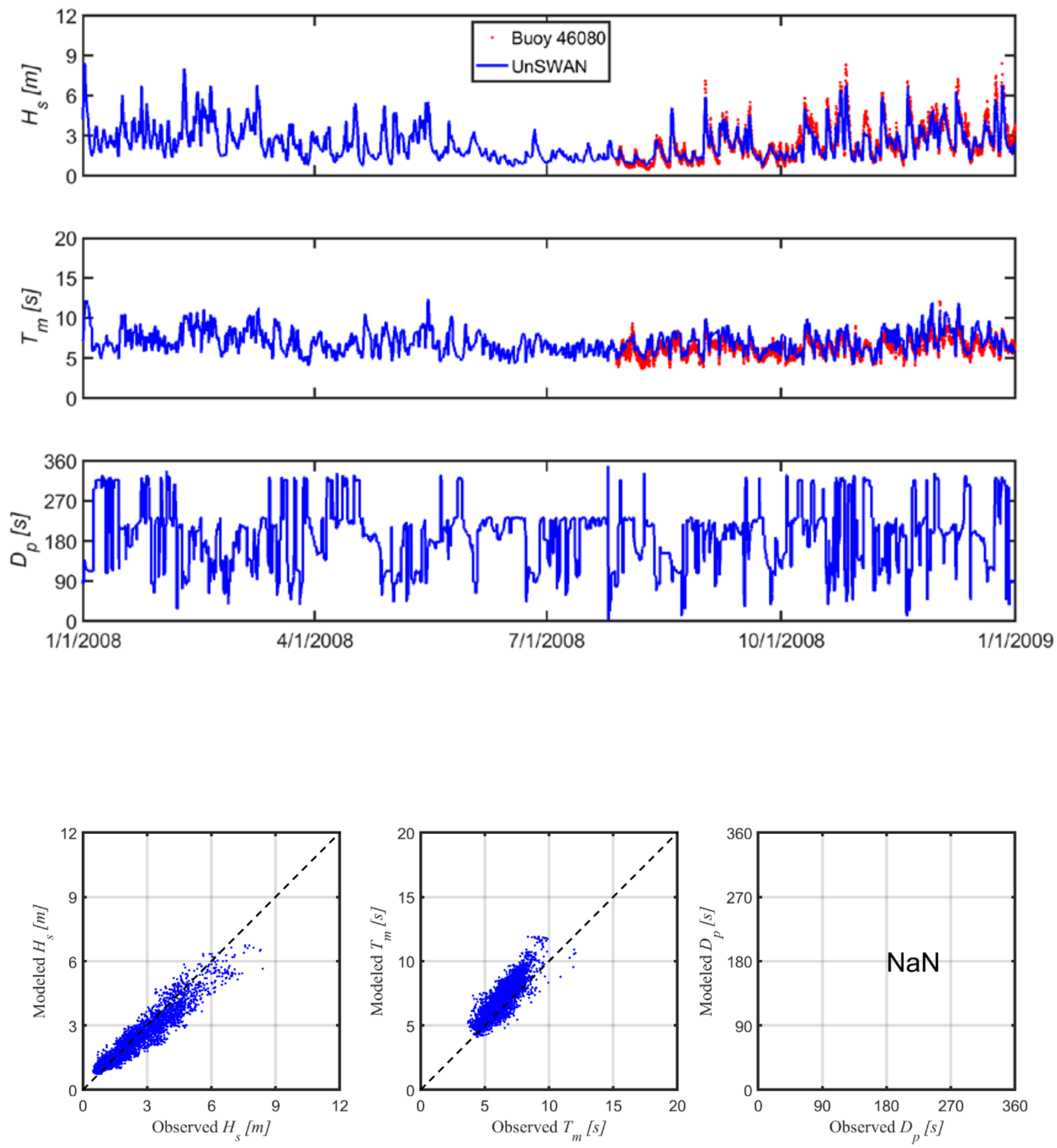

Figure B.129. Comparisons of time series (top) and scatter plots (bottom) of the three UnSWAN model-simulated bulk parameters with observed data at NDBC Buoy 46080 for 2008.

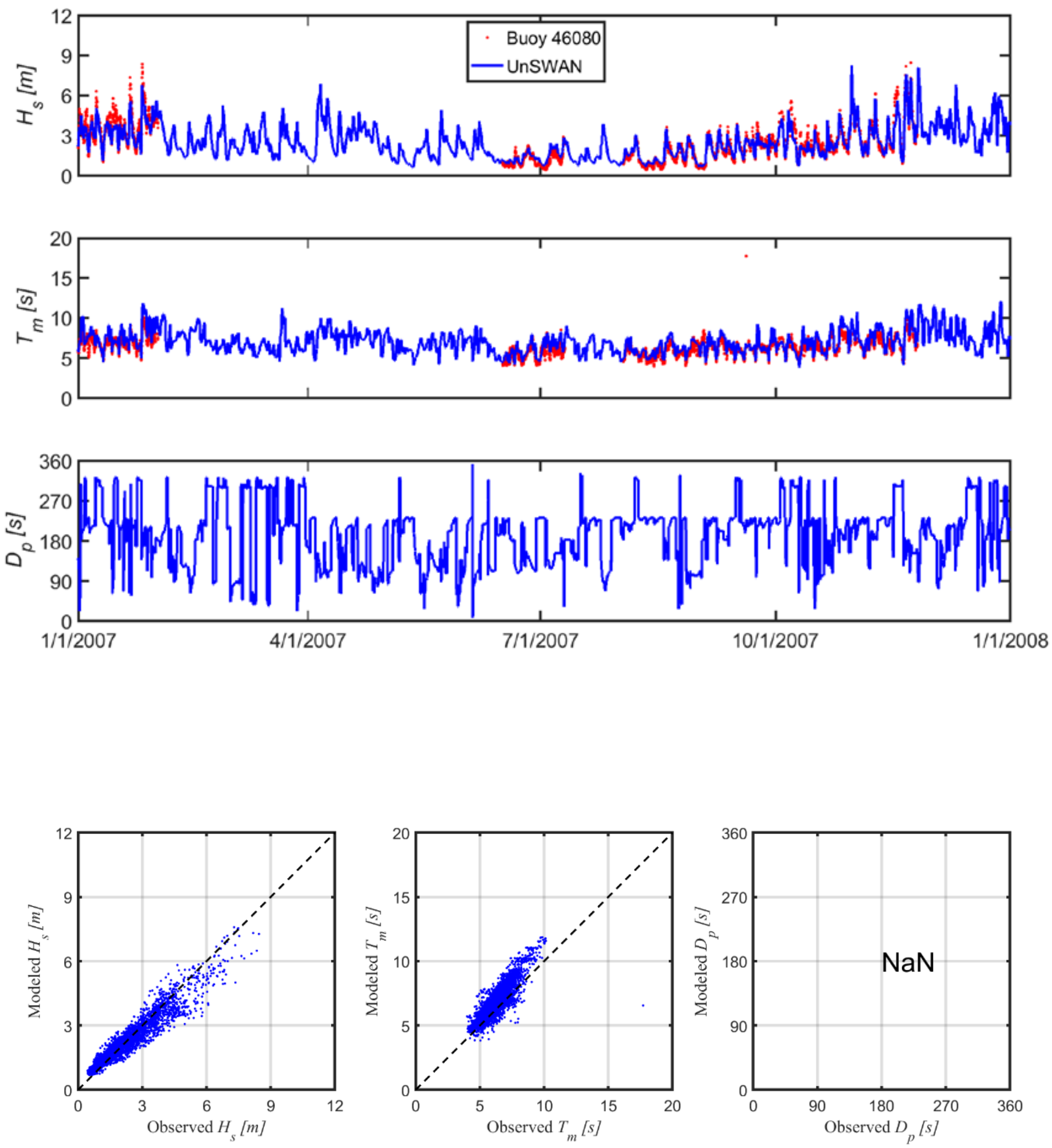

Figure B.130. Comparisons of time series (top) and scatter plots (bottom) of the three UnSWAN model-simulated bulk parameters with observed data at NDBC Buoy 46080 for 2007.

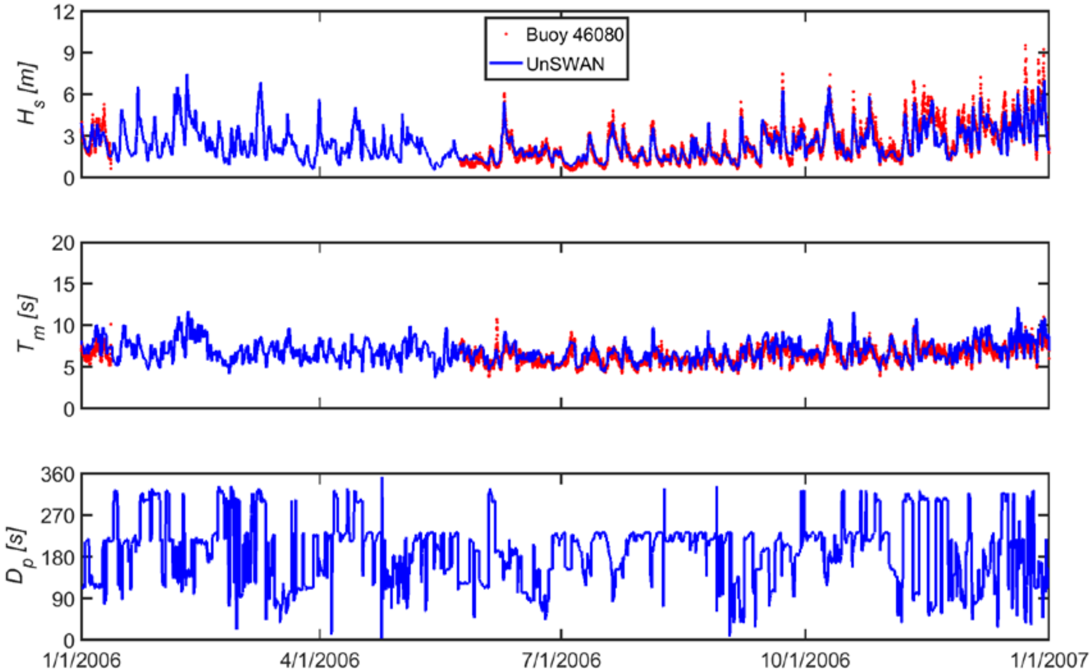

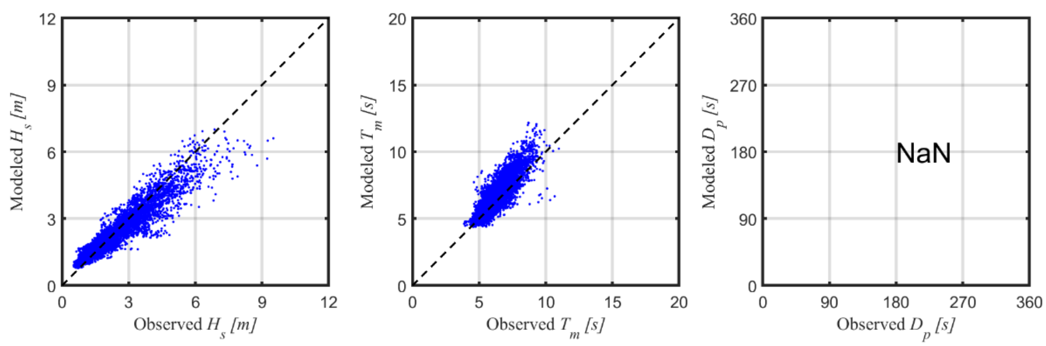

Figure B.131. Comparisons of time series (top) and scatter plots (bottom) of the three UnSWAN model-simulated bulk parameters with observed data at NDBC Buoy 46080 for 2006.

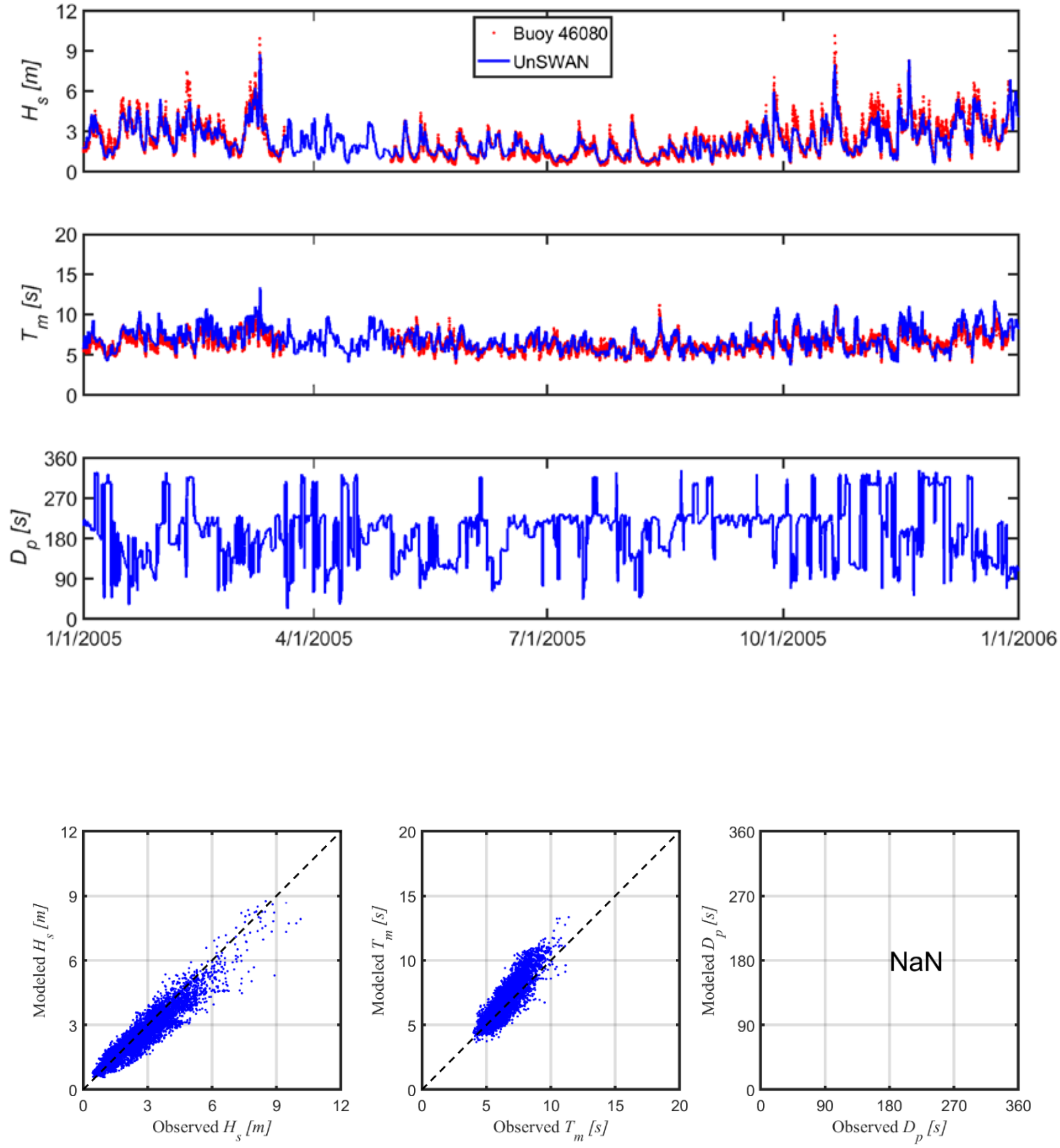

Figure B.132. Comparisons of time series (top) and scatter plots (bottom) of the three UnSWAN model-simulated bulk parameters with observed data at NDBC Buoy 46080 for 2005.

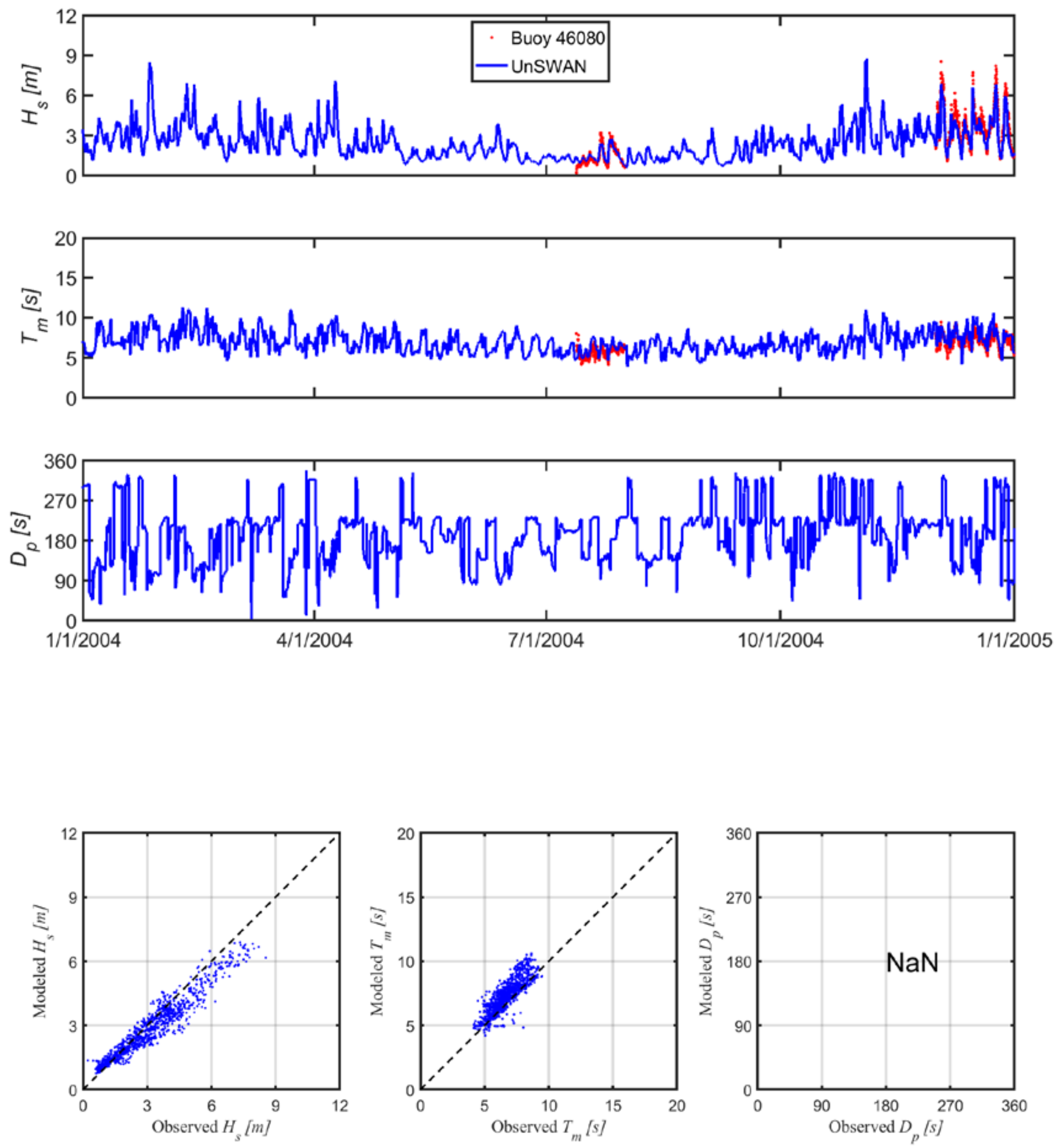

Figure B.133. Comparisons of time series (top) and scatter plots (bottom) of the three UnSWAN model-simulated bulk parameters with observed data at NDBC Buoy 46080 for 2004.

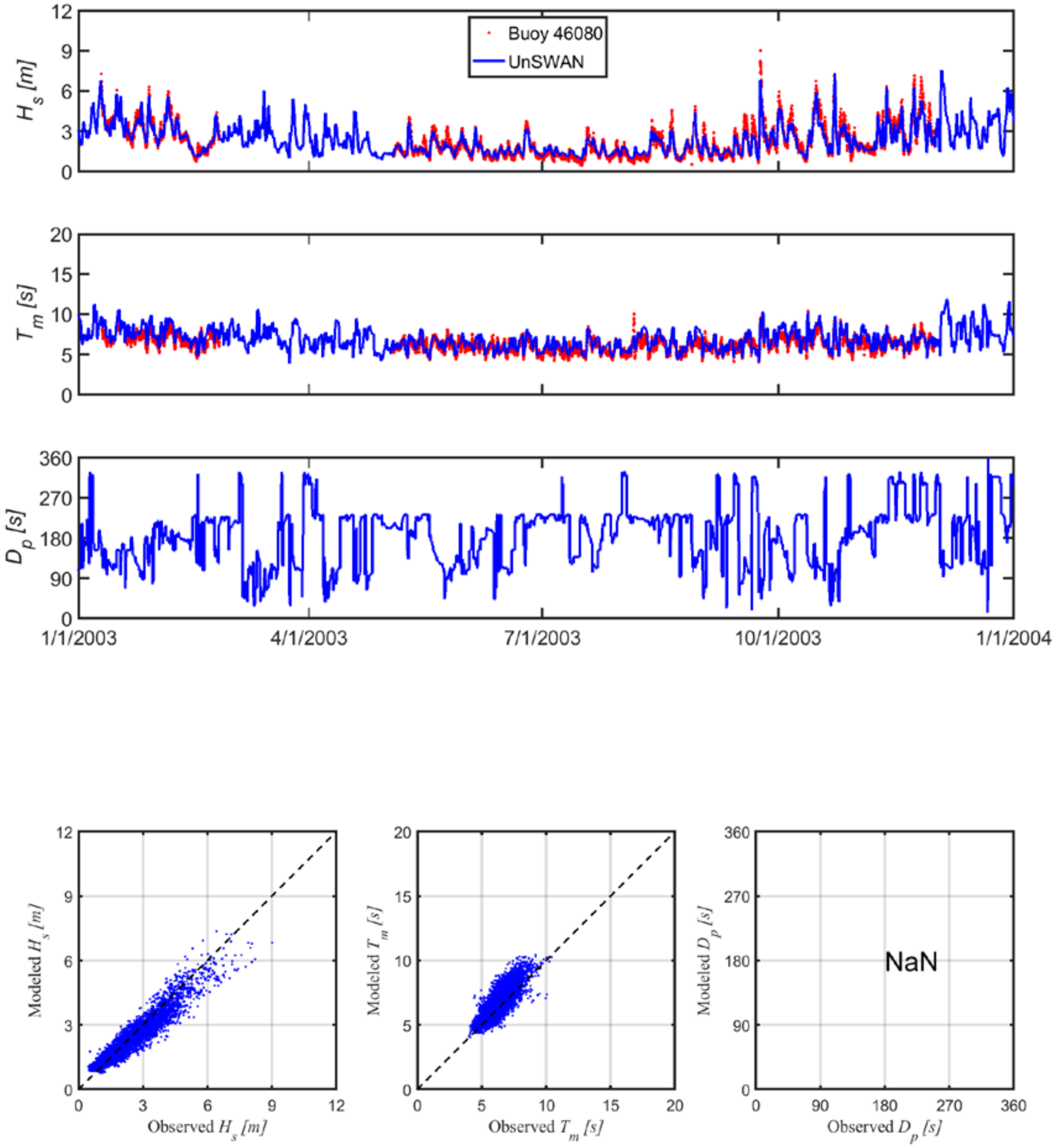

Figure B.134. Comparisons of time series (top) and scatter plots (bottom) of the three UnSWAN model-simulated bulk parameters with observed data at NDBC Buoy 46080 for 2003.

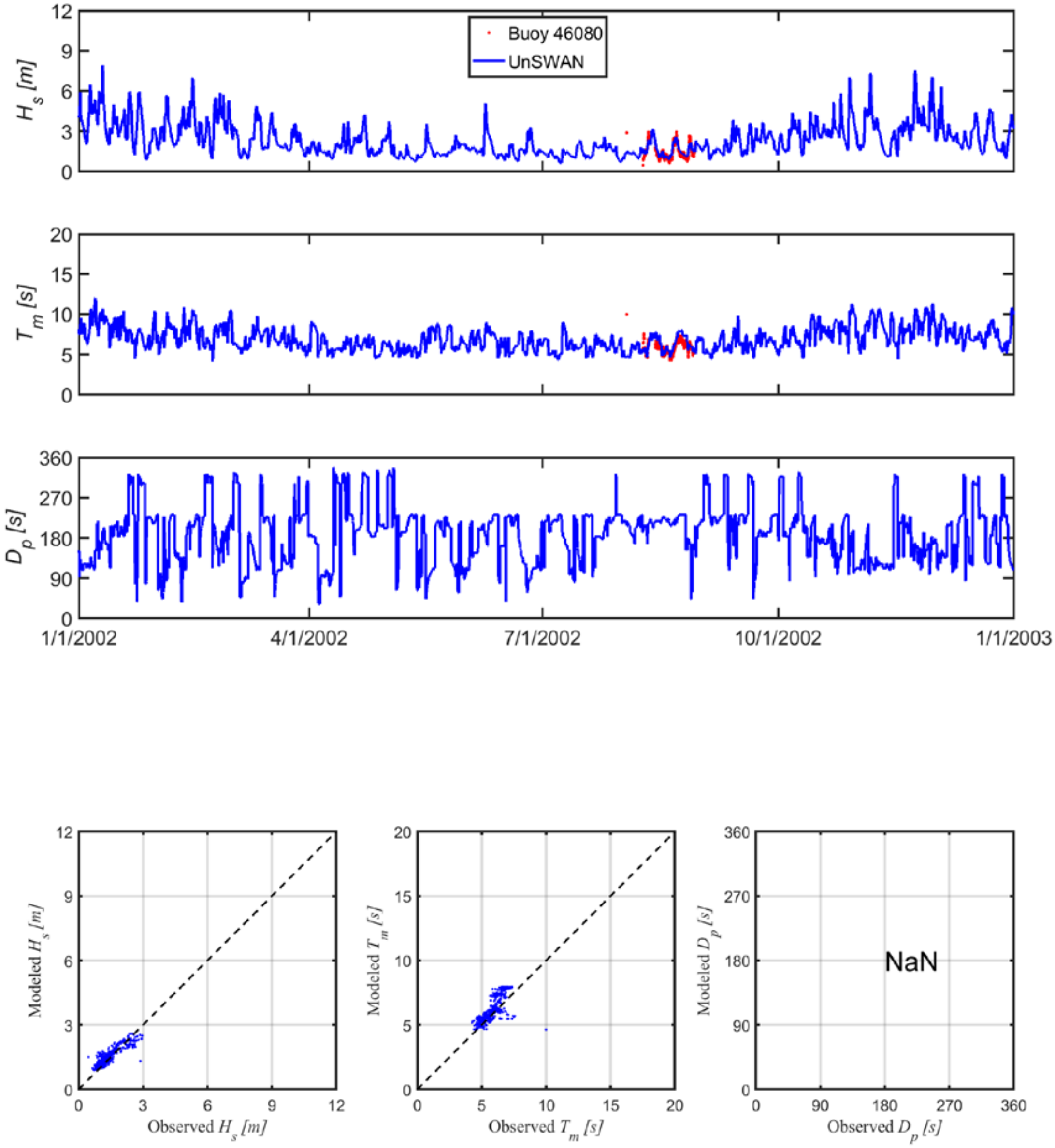

Figure B.135. Comparisons of time series (top) and scatter plots (bottom) of the three UnSWAN model-simulated bulk parameters with observed data at NDBC Buoy 46080 for 2002.

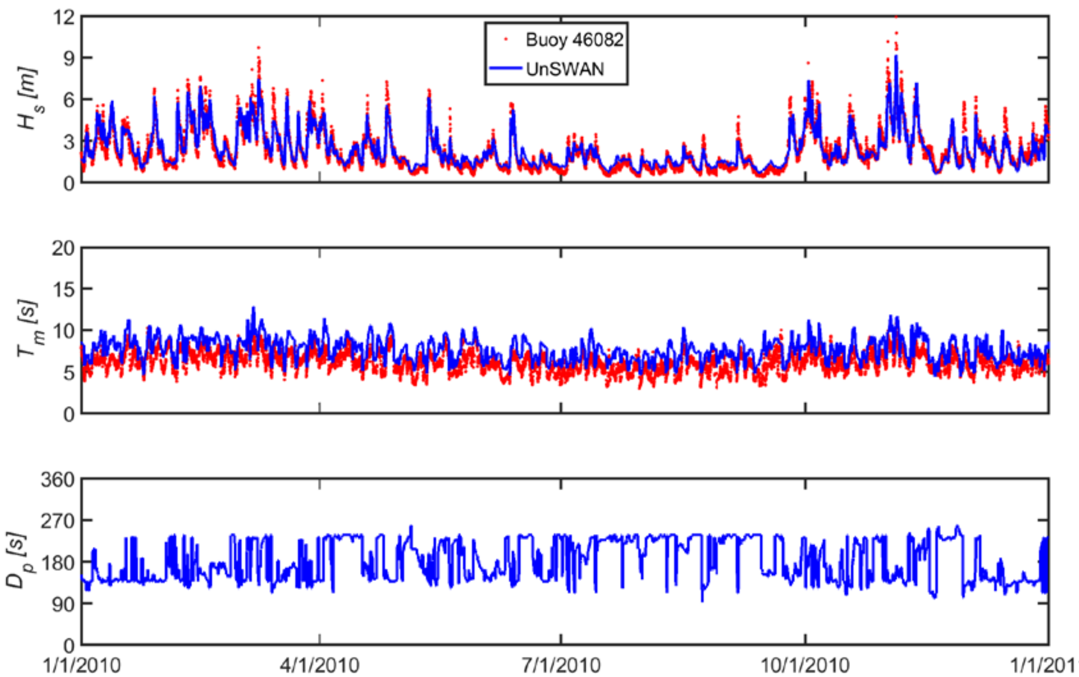

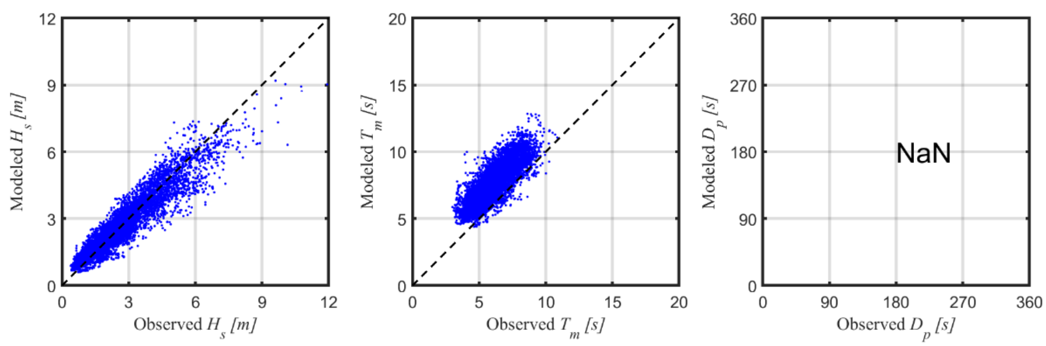

Figure B.136. Comparisons of time series (top) and scatter plots (bottom) of the three UnSWAN model-simulated bulk parameters with observed data at NDBC Buoy 46082 for 2010.

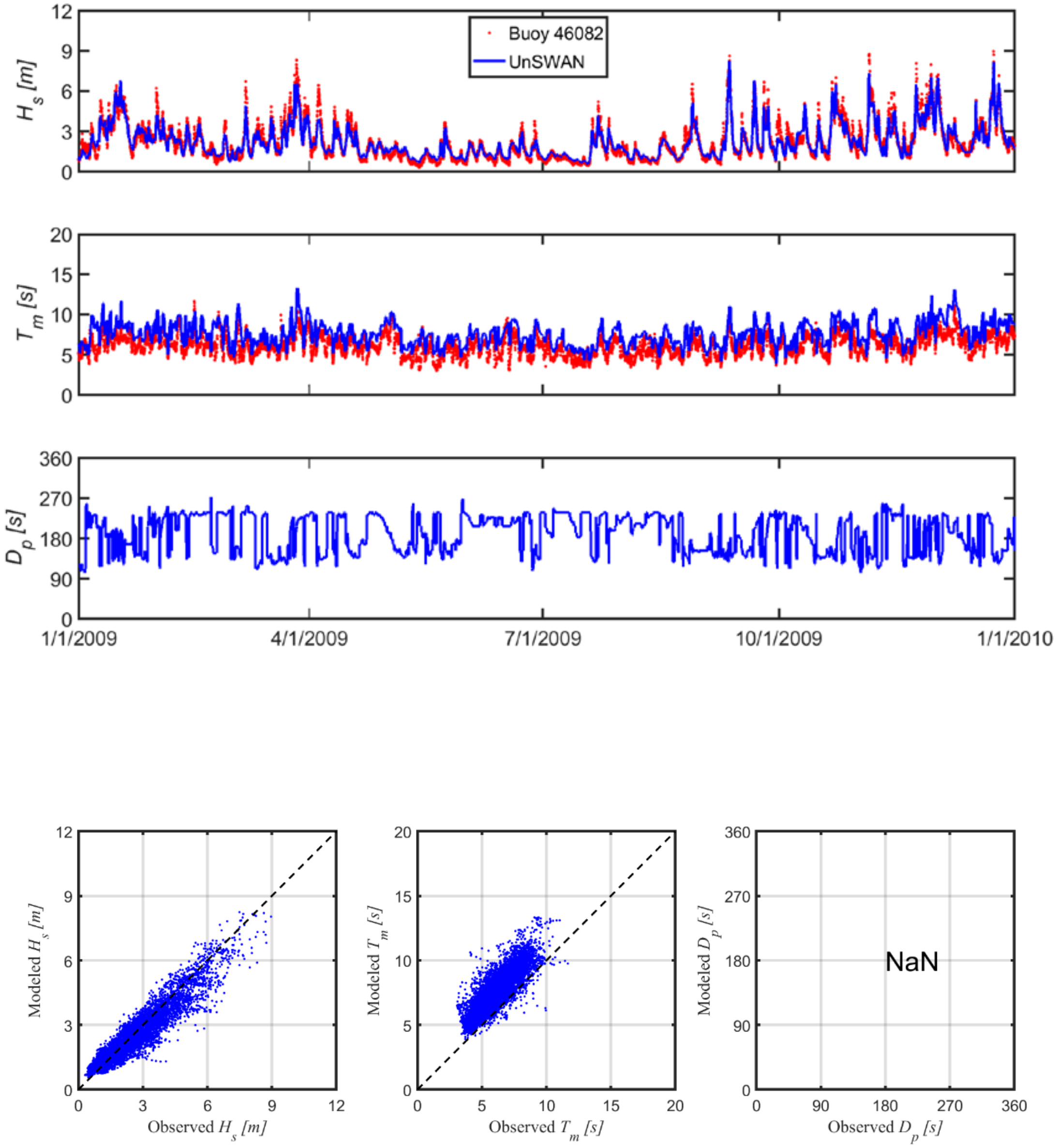

Figure B.137. Comparisons of time series (top) and scatter plots (bottom) of the three UnSWAN model-simulated bulk parameters with observed data at NDBC Buoy 46082 for 2009.

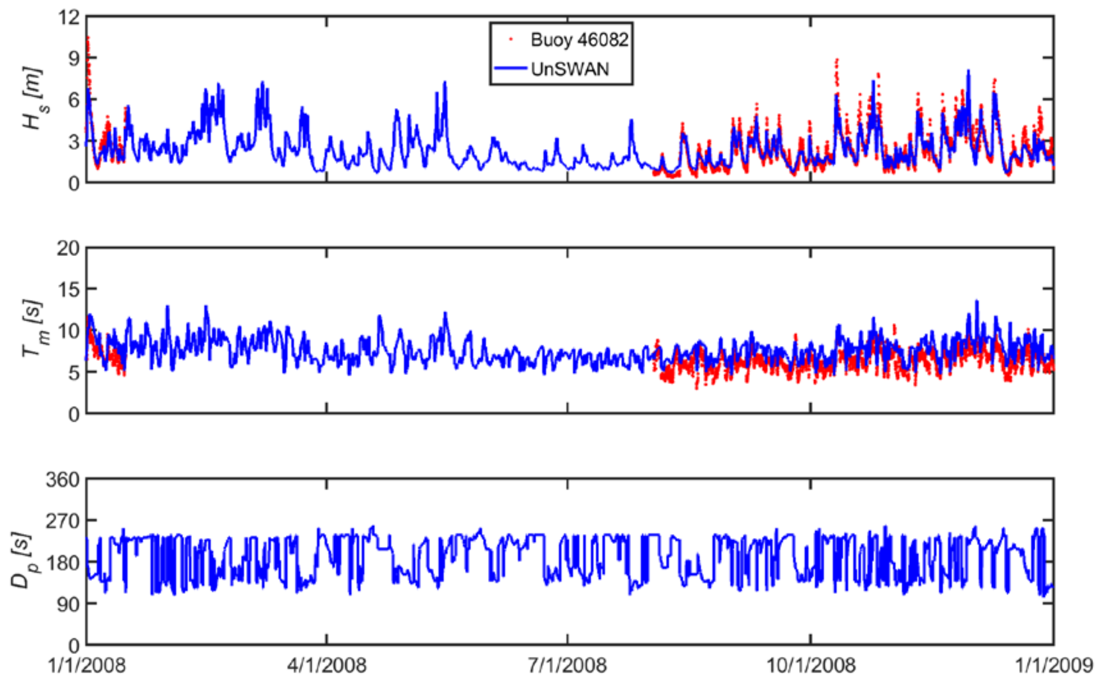

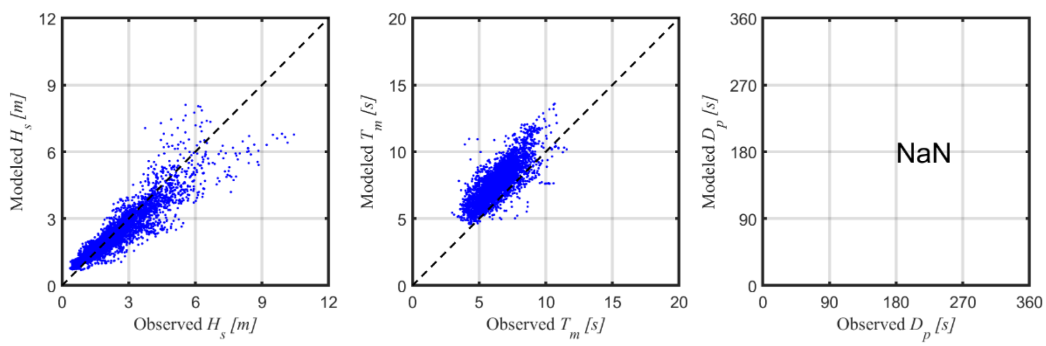

Figure B.138. Comparisons of time series (top) and scatter plots (bottom) of the three UnSWAN model-simulated bulk parameters with observed data at NDBC Buoy 46082 for 2008.

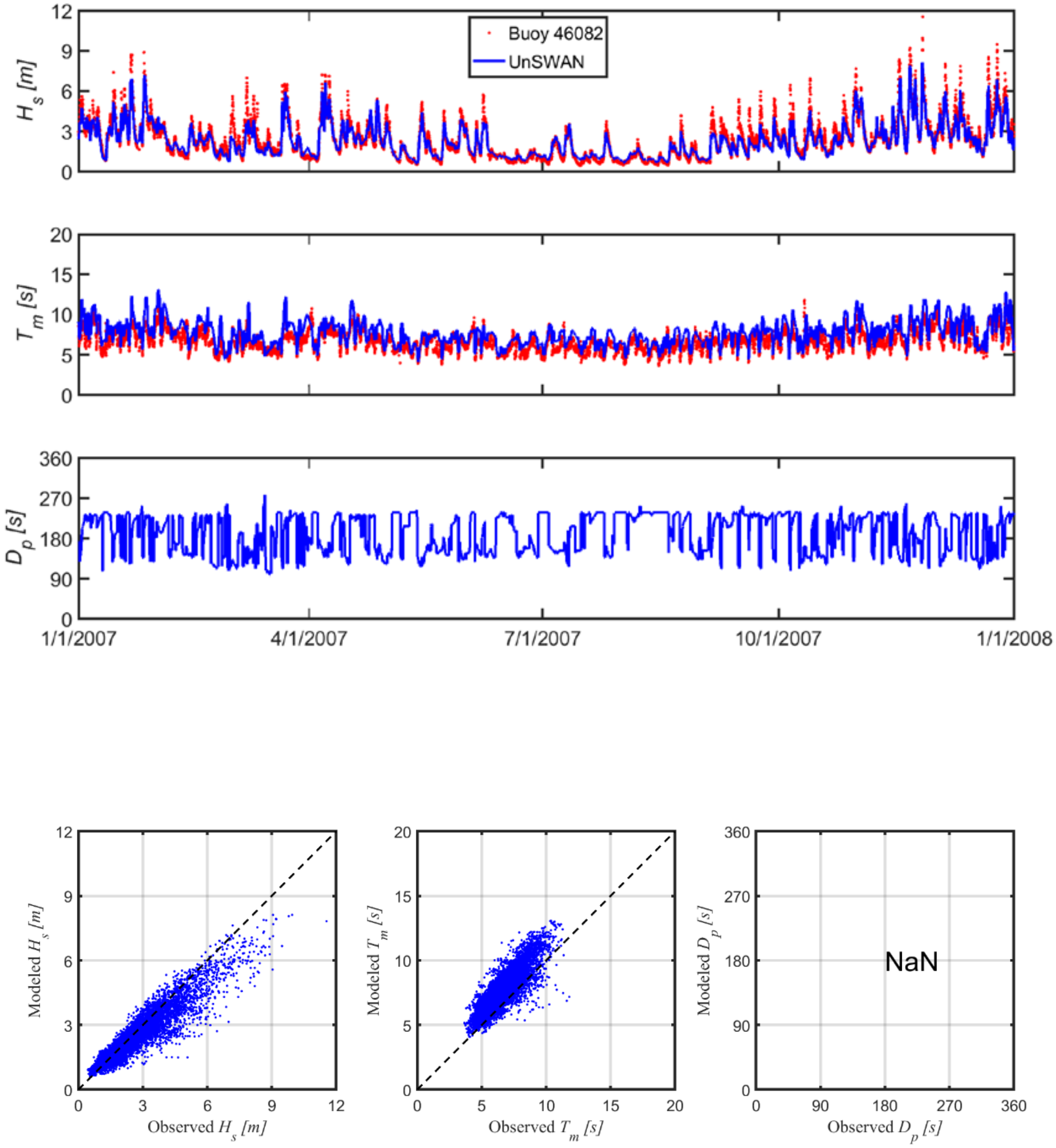

Figure B.139. Comparisons of time series (top) and scatter plots (bottom) of the three UnSWAN model-simulated bulk parameters with observed data at NDBC Buoy 46082 for 2007.

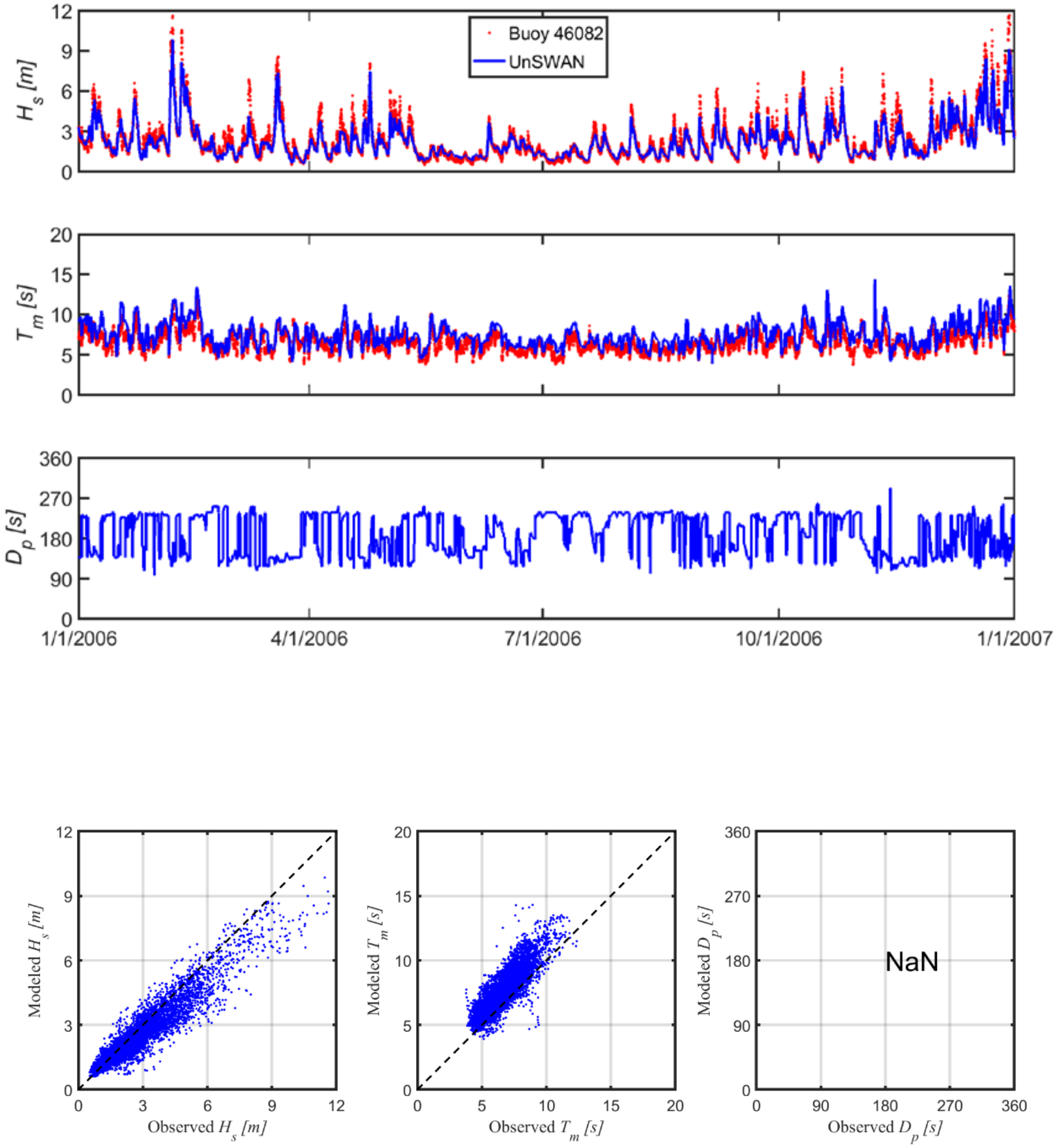

Figure B.140. Comparisons of time series (top) and scatter plots (bottom) of the three UnSWAN model-simulated bulk parameters with observed data at NDBC Buoy 46082 for 2006.

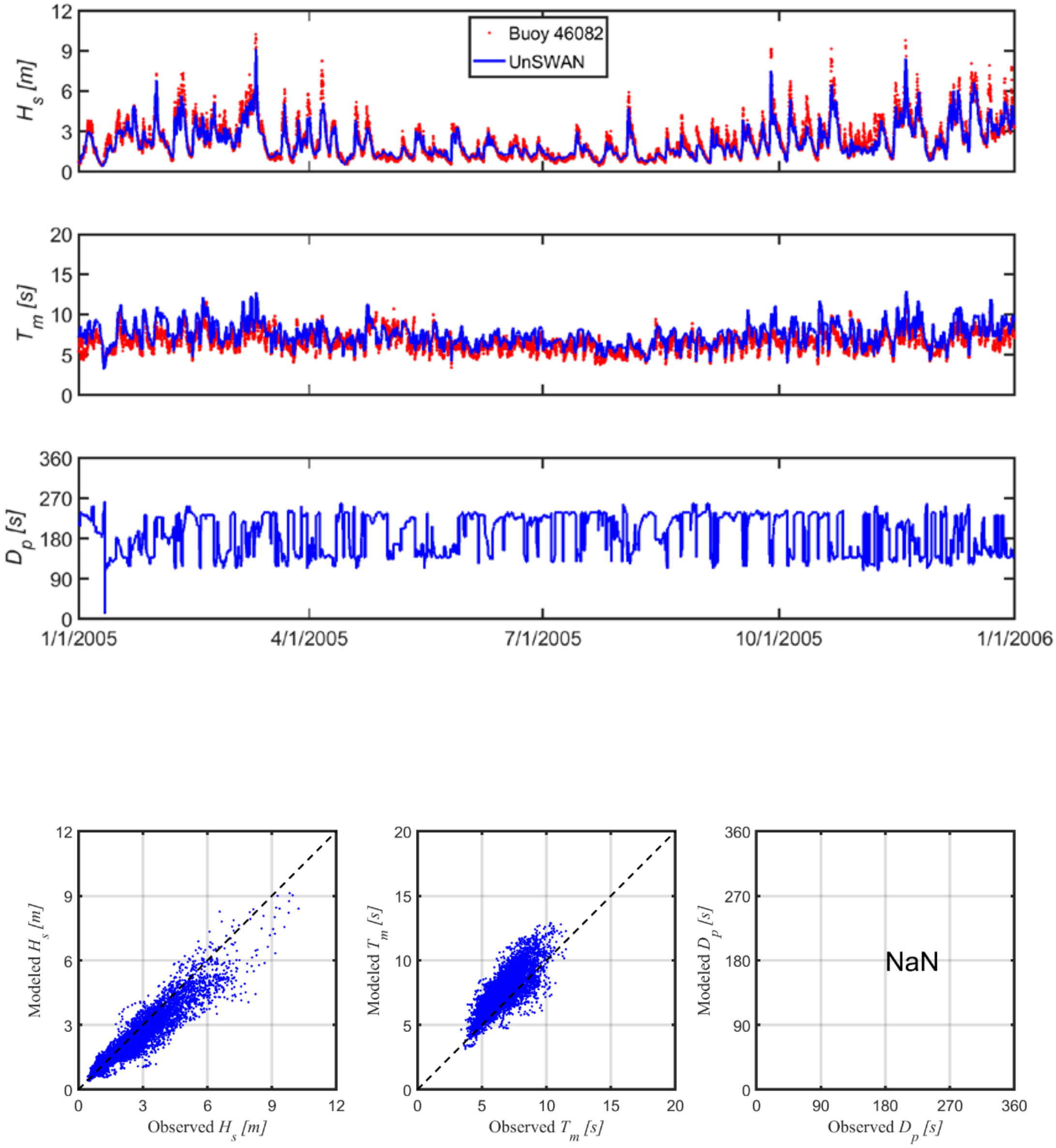

Figure B.141. Comparisons of time series (top) and scatter plots (bottom) of the three UnSWAN model-simulated bulk parameters with observed data at NDBC Buoy 46082 for 2005.

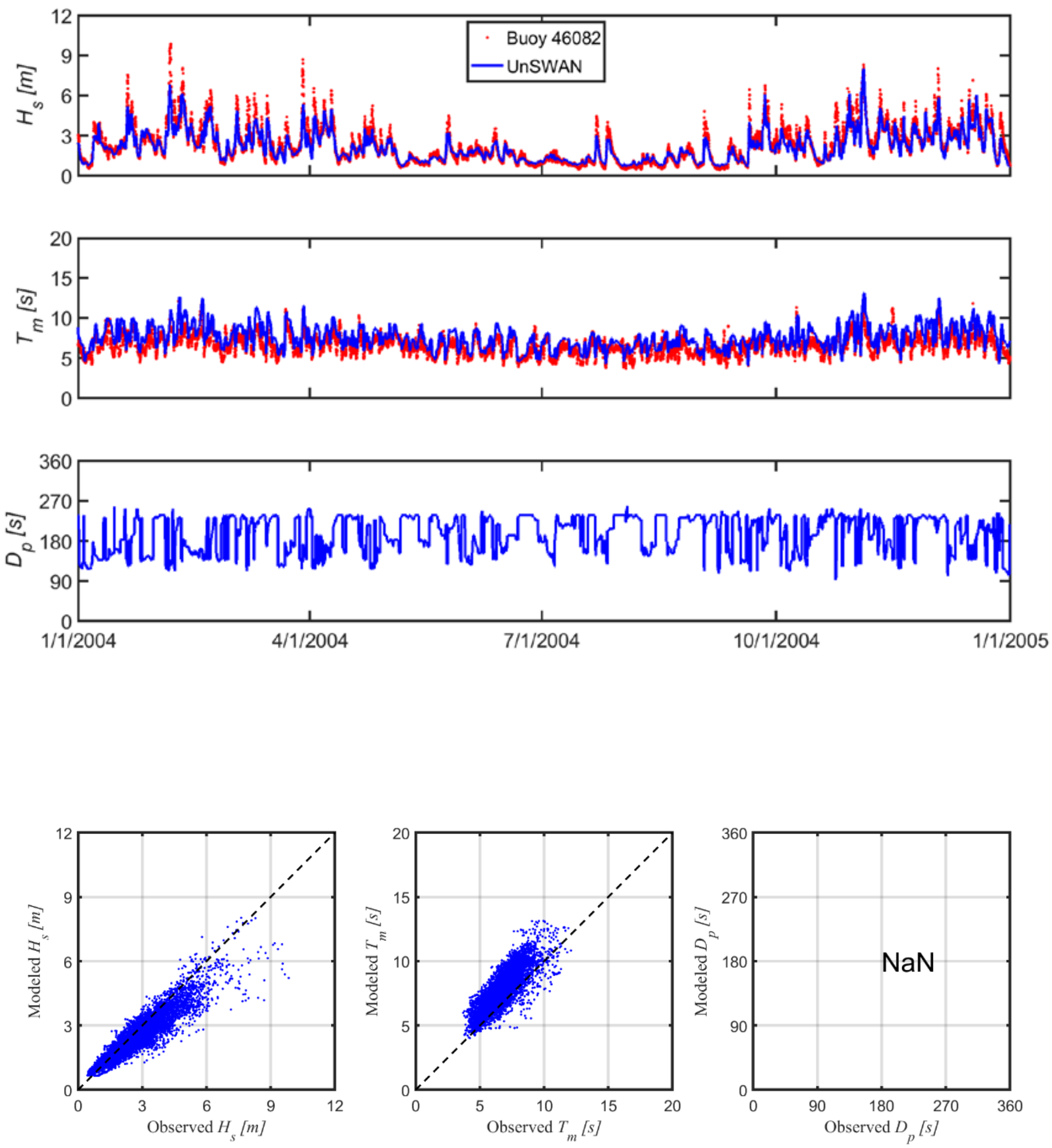

Figure B.142. Comparisons of time series (top) and scatter plots (bottom) of the three UnSWAN model-simulated bulk parameters with observed data at NDBC Buoy 46082 for 2004.

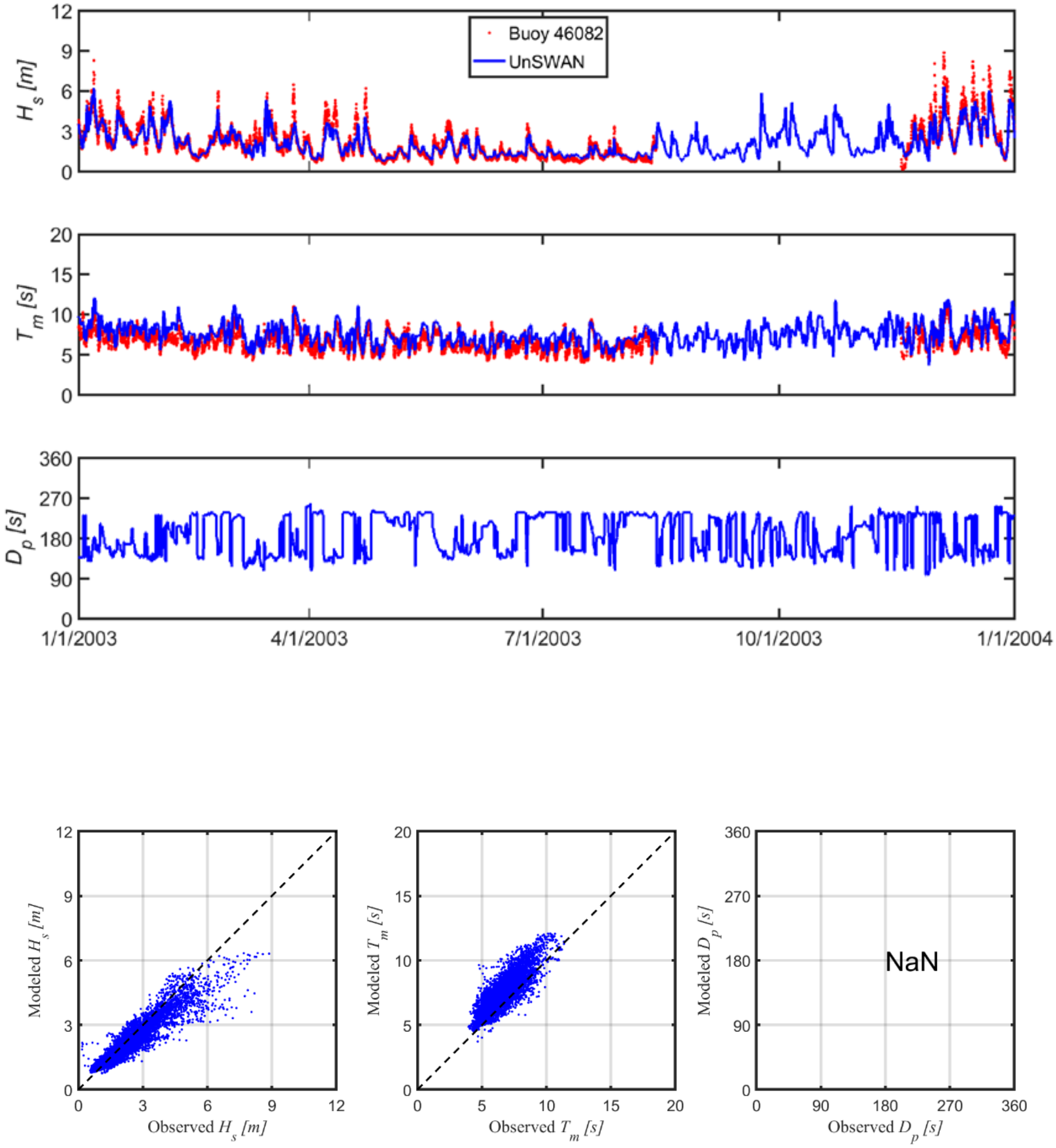

Figure B.143. Comparisons of time series (top) and scatter plots (bottom) of the three UnSWAN model-simulated bulk parameters with observed data at NDBC Buoy 46082 for 2003.

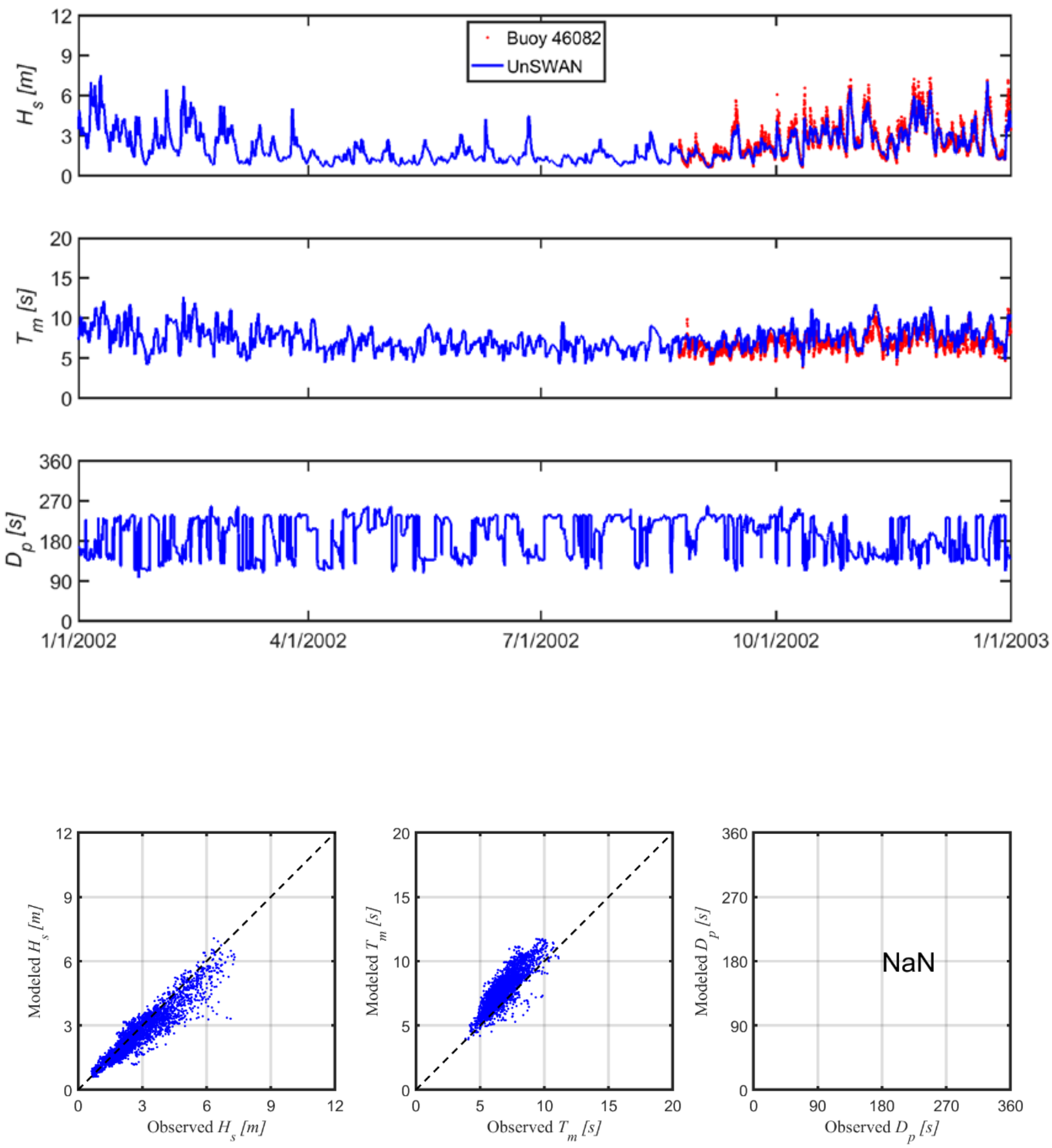

Figure B.144. Comparisons of time series (top) and scatter plots (bottom) of the three UnSWAN model-simulated bulk parameters with observed data at NDBC Buoy 46082 for 2002.

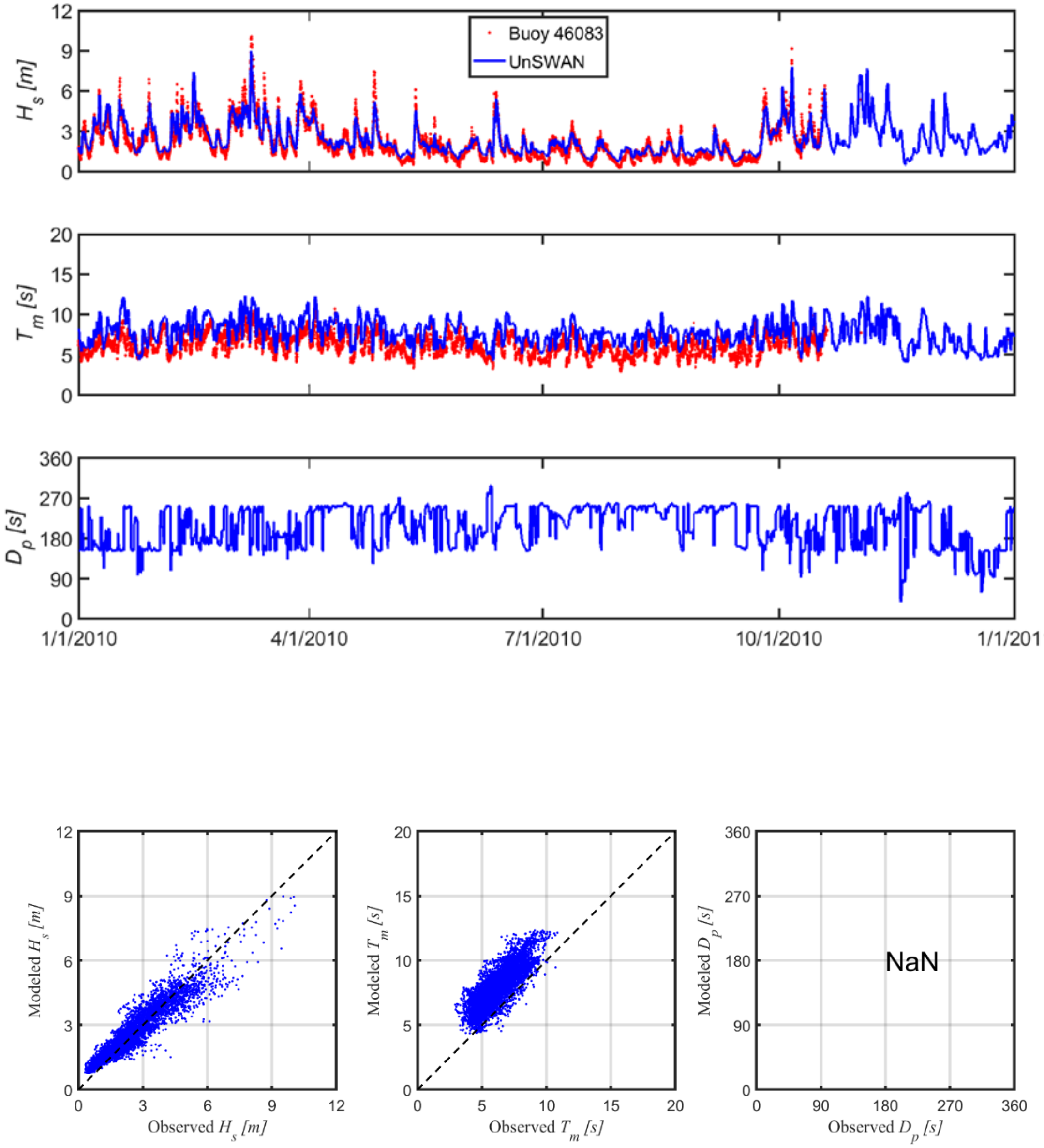

Figure B.145. Comparisons of time series (top) and scatter plots (bottom) of the three UnSWAN model-simulated bulk parameters with observed data at NDBC Buoy 46083 for 2010.

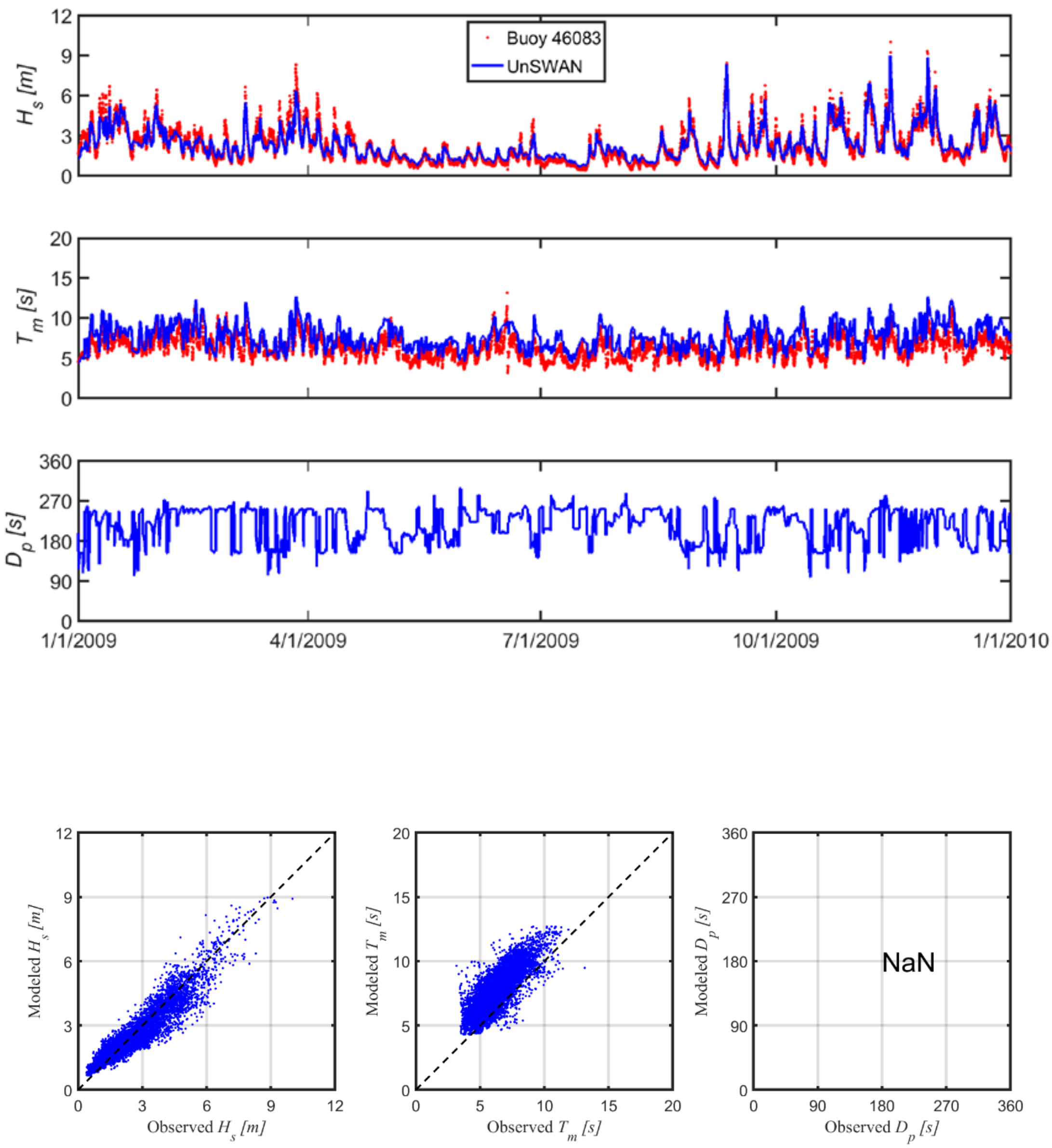

Figure B.146. Comparisons of time series (top) and scatter plots (bottom) of the three UnSWAN model-simulated bulk parameters with observed data at NDBC Buoy 46083 for 2009.

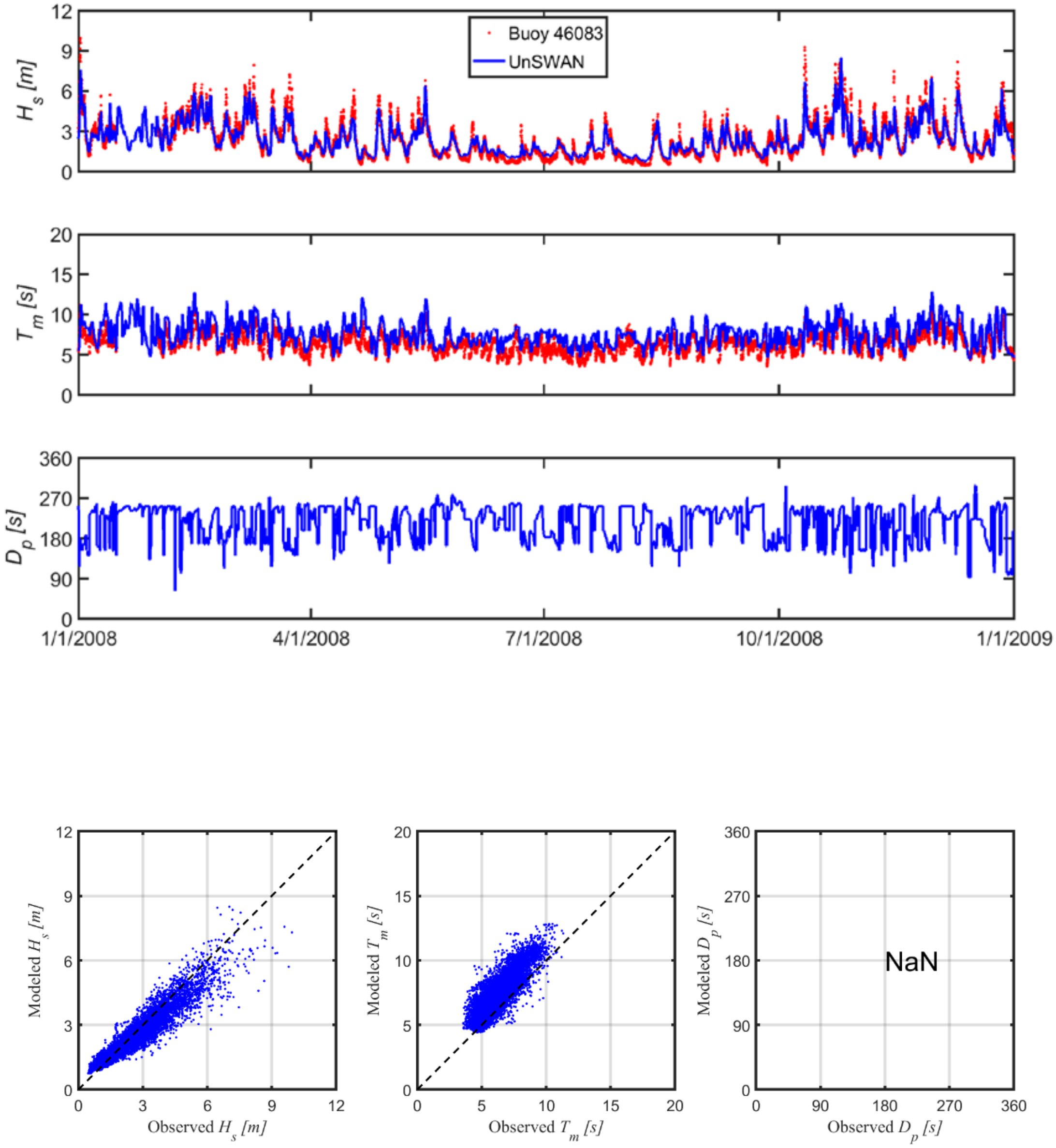

Figure B.147. Comparisons of time series (top) and scatter plots (bottom) of the three UnSWAN model-simulated bulk parameters with observed data at NDBC Buoy 46083 for 2008.

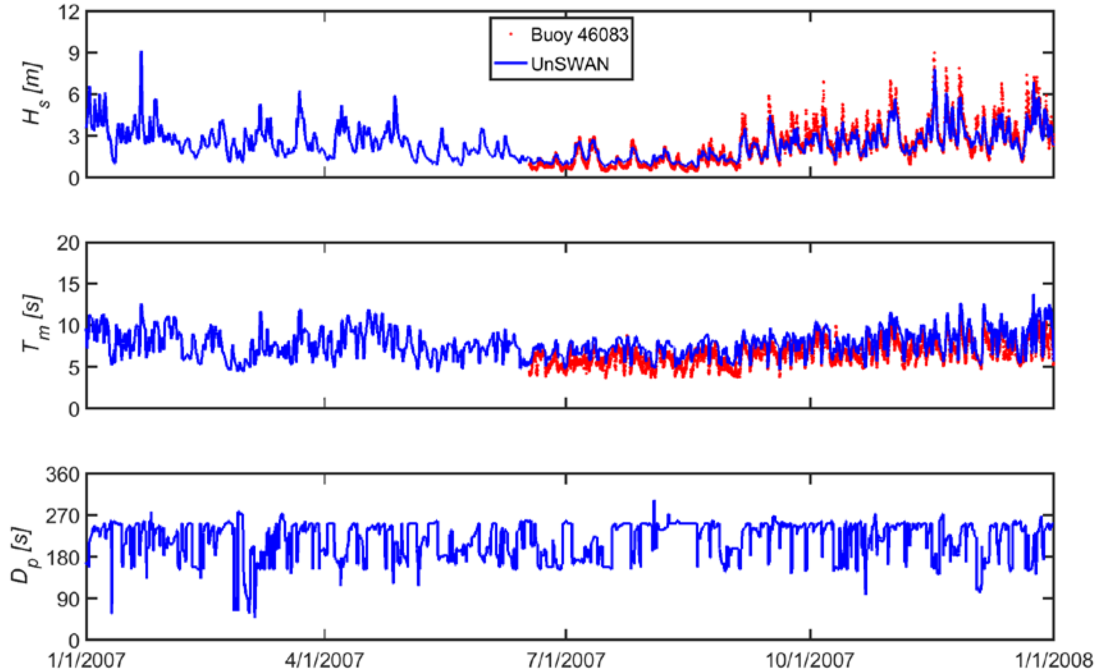

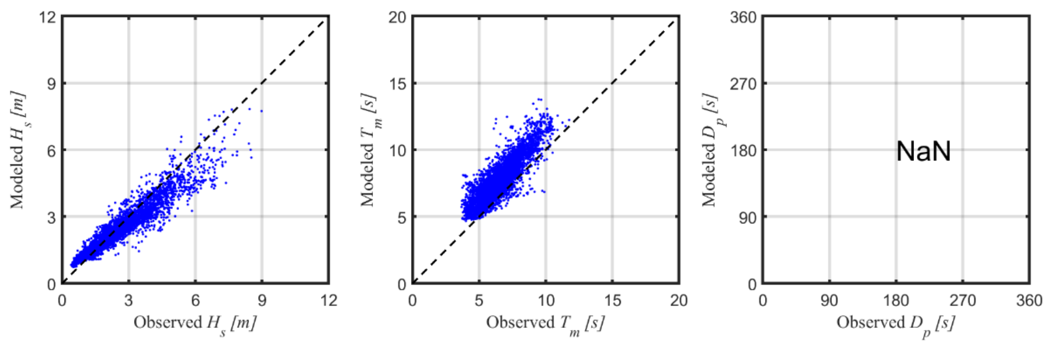

Figure B.148. Comparisons of time series (top) and scatter plots (bottom) of the three UnSWAN model-simulated bulk parameters with observed data at NDBC Buoy 46083 for 2007.

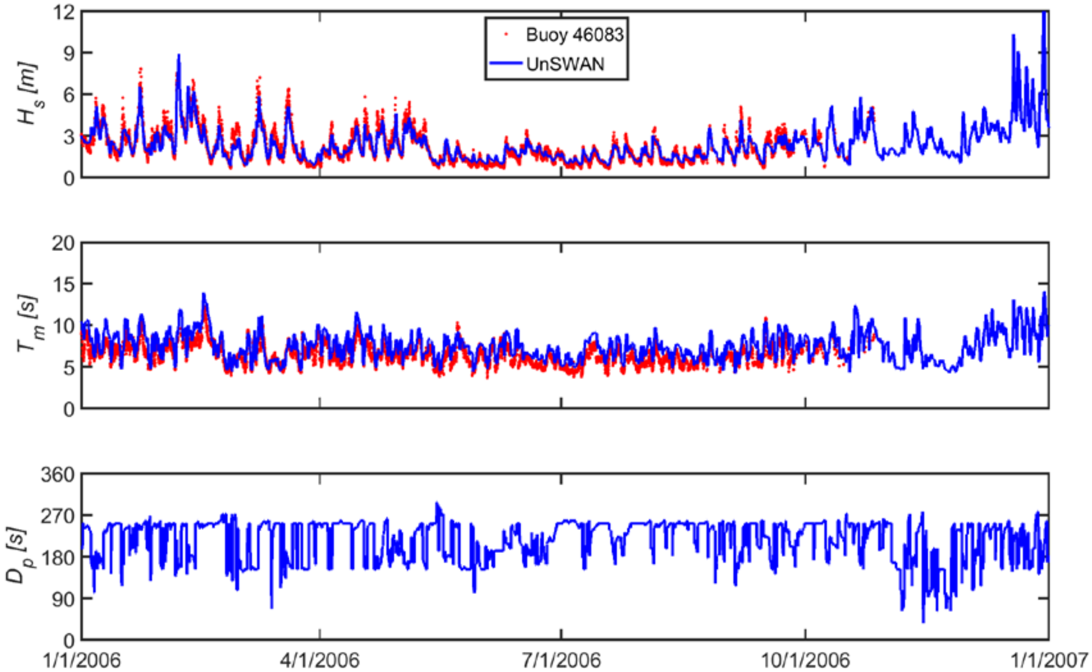

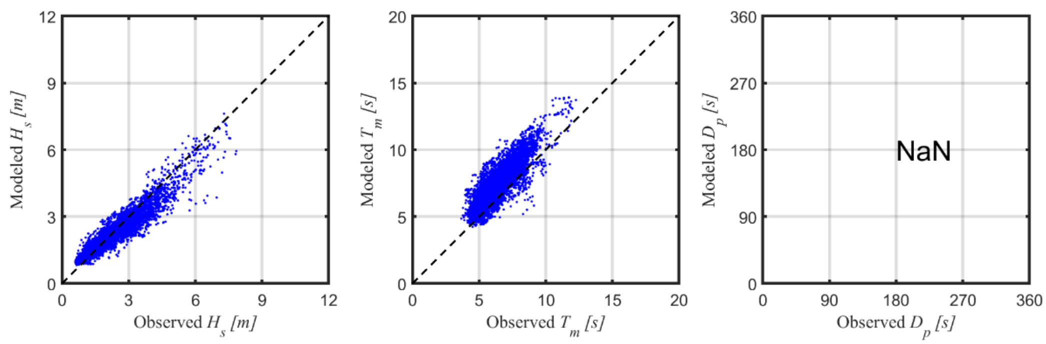

Figure B.149. Comparisons of time series (top) and scatter plots (bottom) of the three UnSWAN model-simulated bulk parameters with observed data at NDBC Buoy 46083 for 2006.

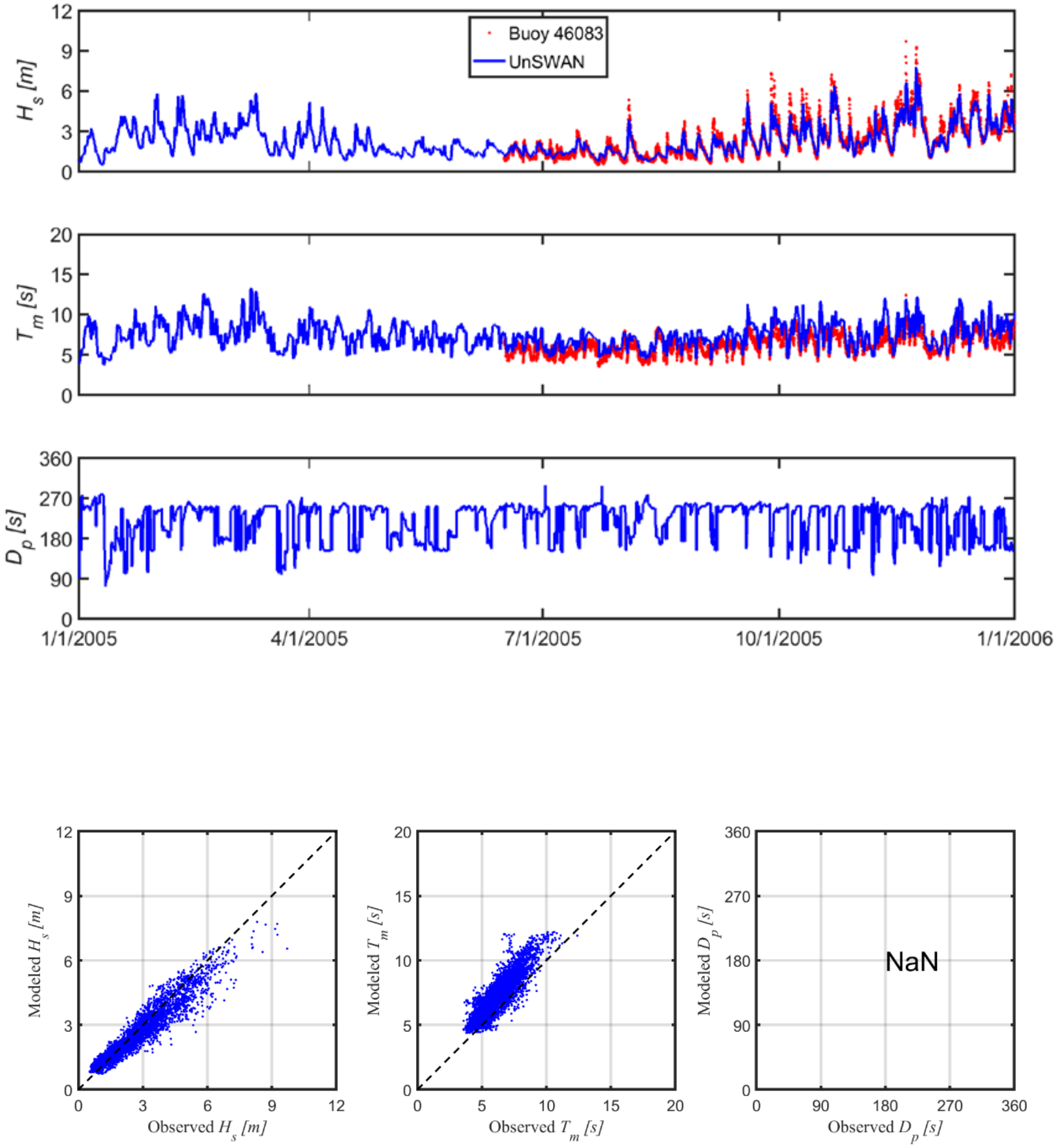

Figure B.150. Comparisons of time series (top) and scatter plots (bottom) of the three UnSWAN model-simulated bulk parameters with observed data at NDBC Buoy 46083 for 2005.

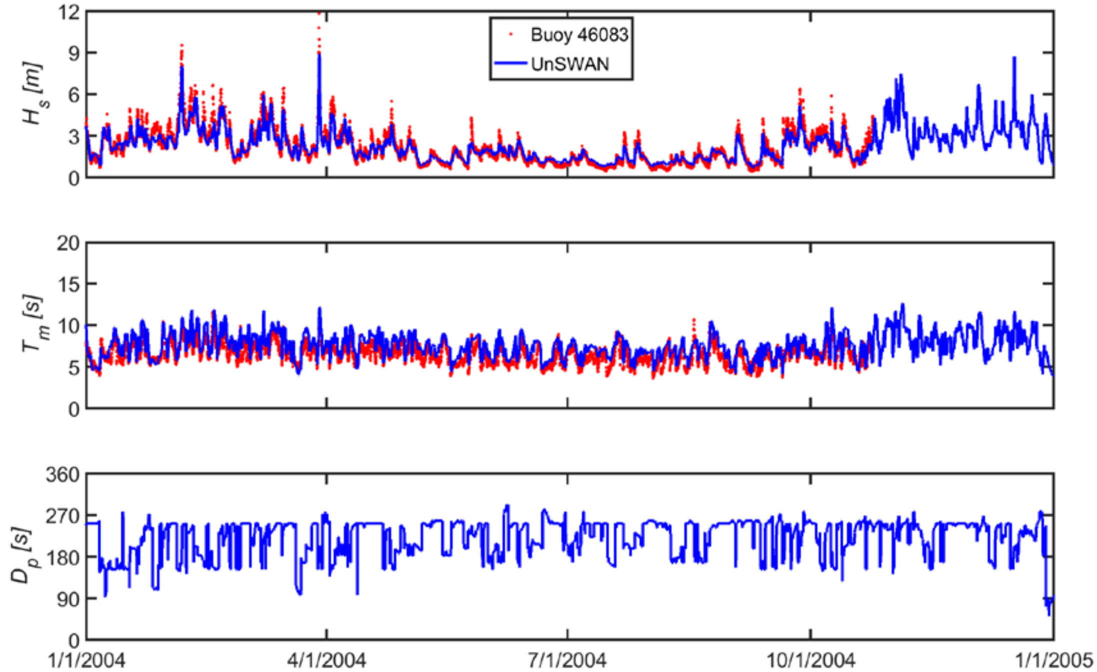

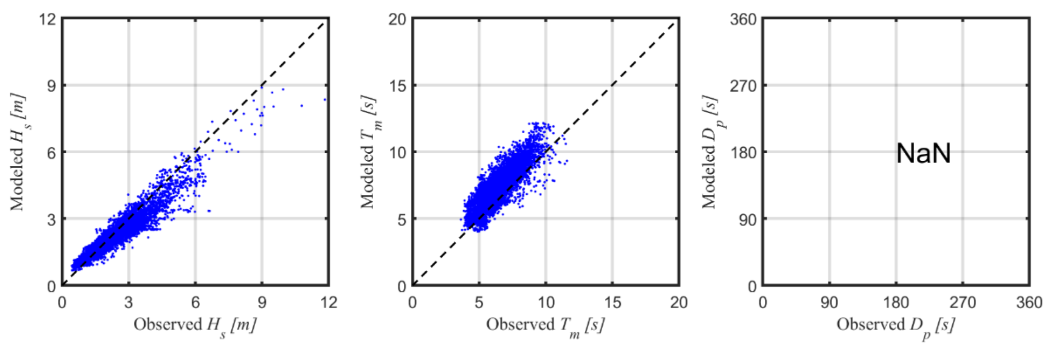

Figure B.151. Comparisons of time series (top) and scatter plots (bottom) of the three UnSWAN model-simulated bulk parameters with observed data at NDBC Buoy 46083 for 2004.

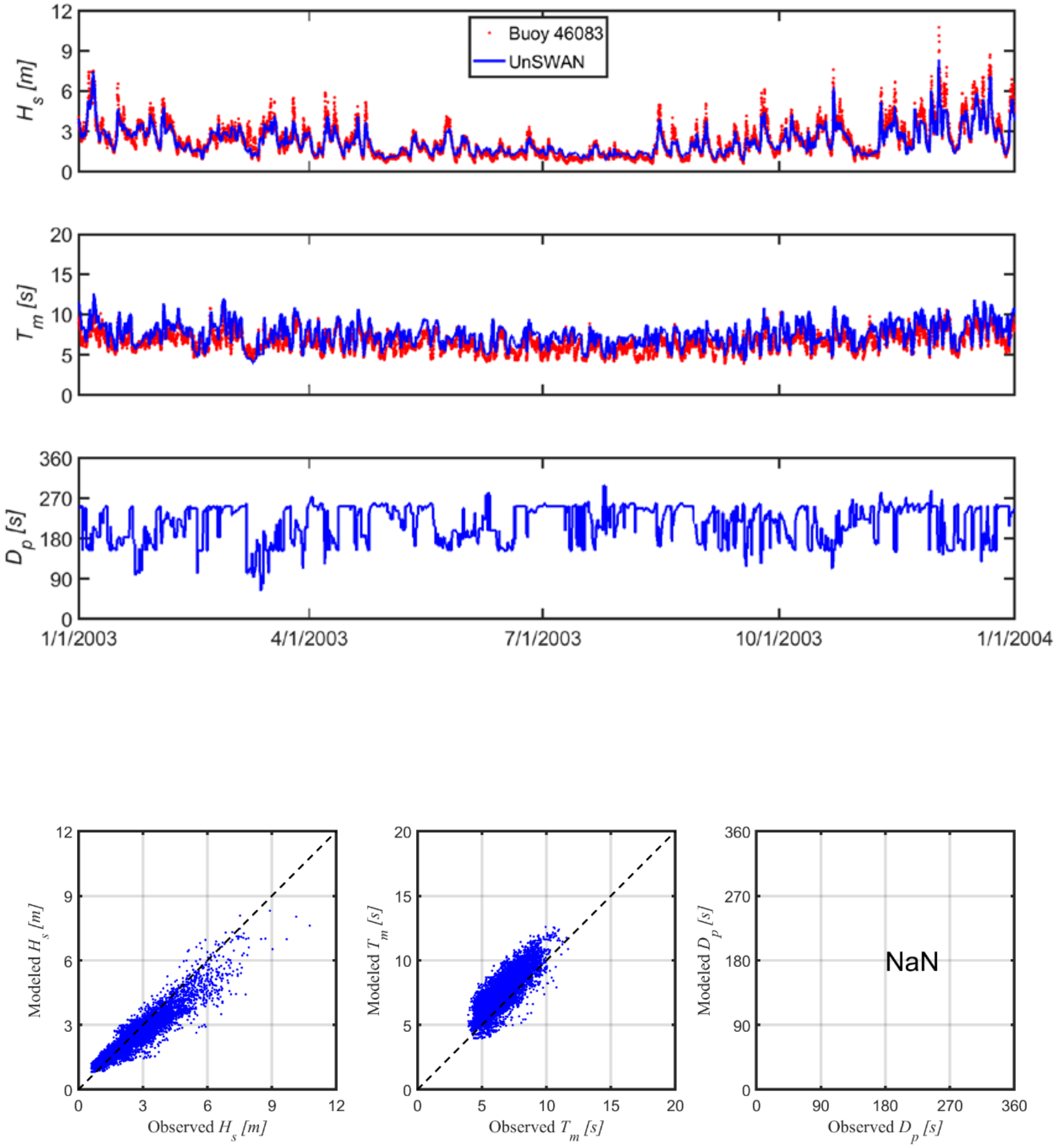

Figure B.152. Comparisons of time series (top) and scatter plots (bottom) of the three UnSWAN model-simulated bulk parameters with observed data at NDBC Buoy 46083 for 2003.

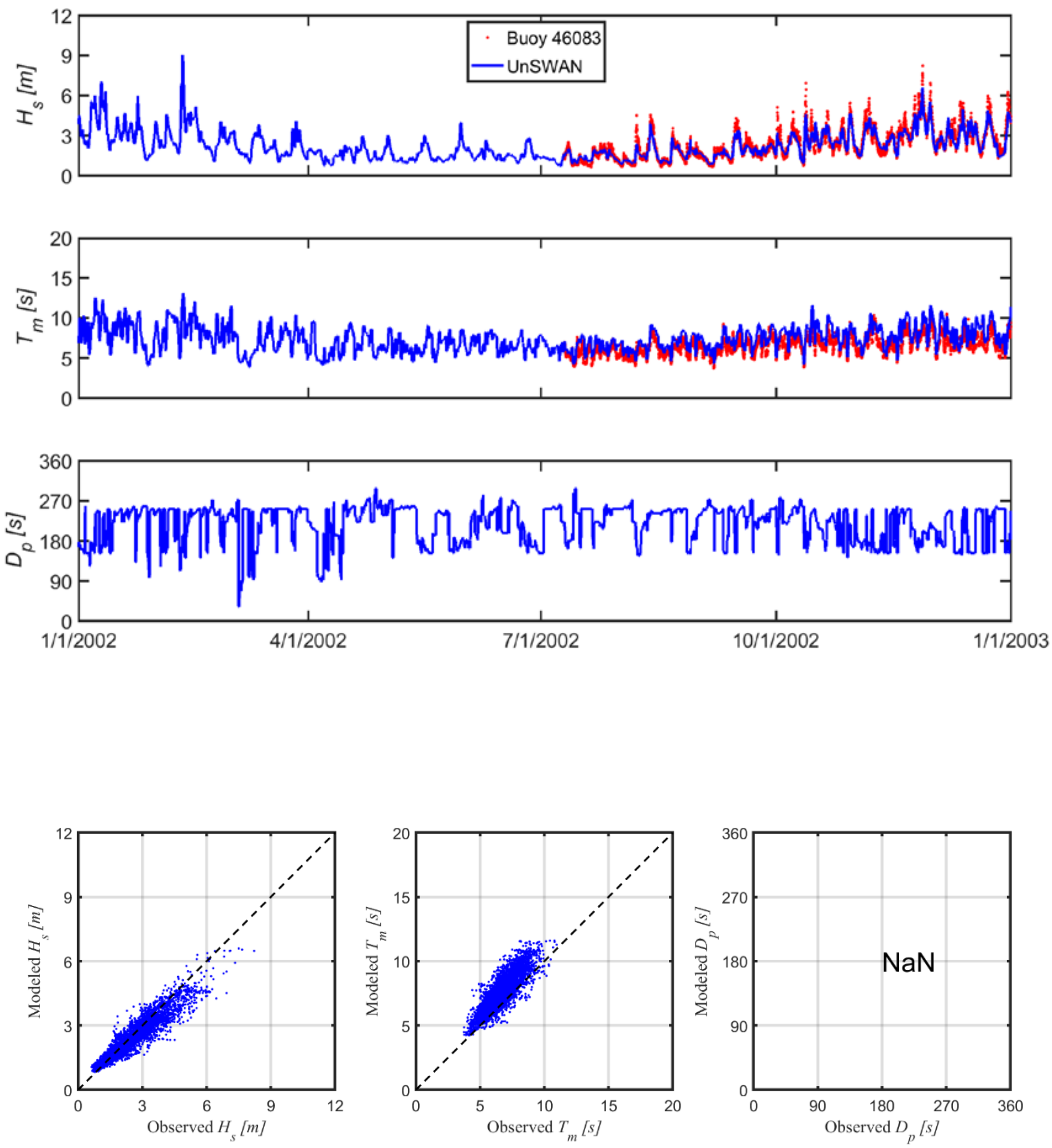

Figure B.153. Comparisons of time series (top) and scatter plots (bottom) of the three UnSWAN model-simulated bulk parameters with observed data at NDBC Buoy 46083 for 2002.

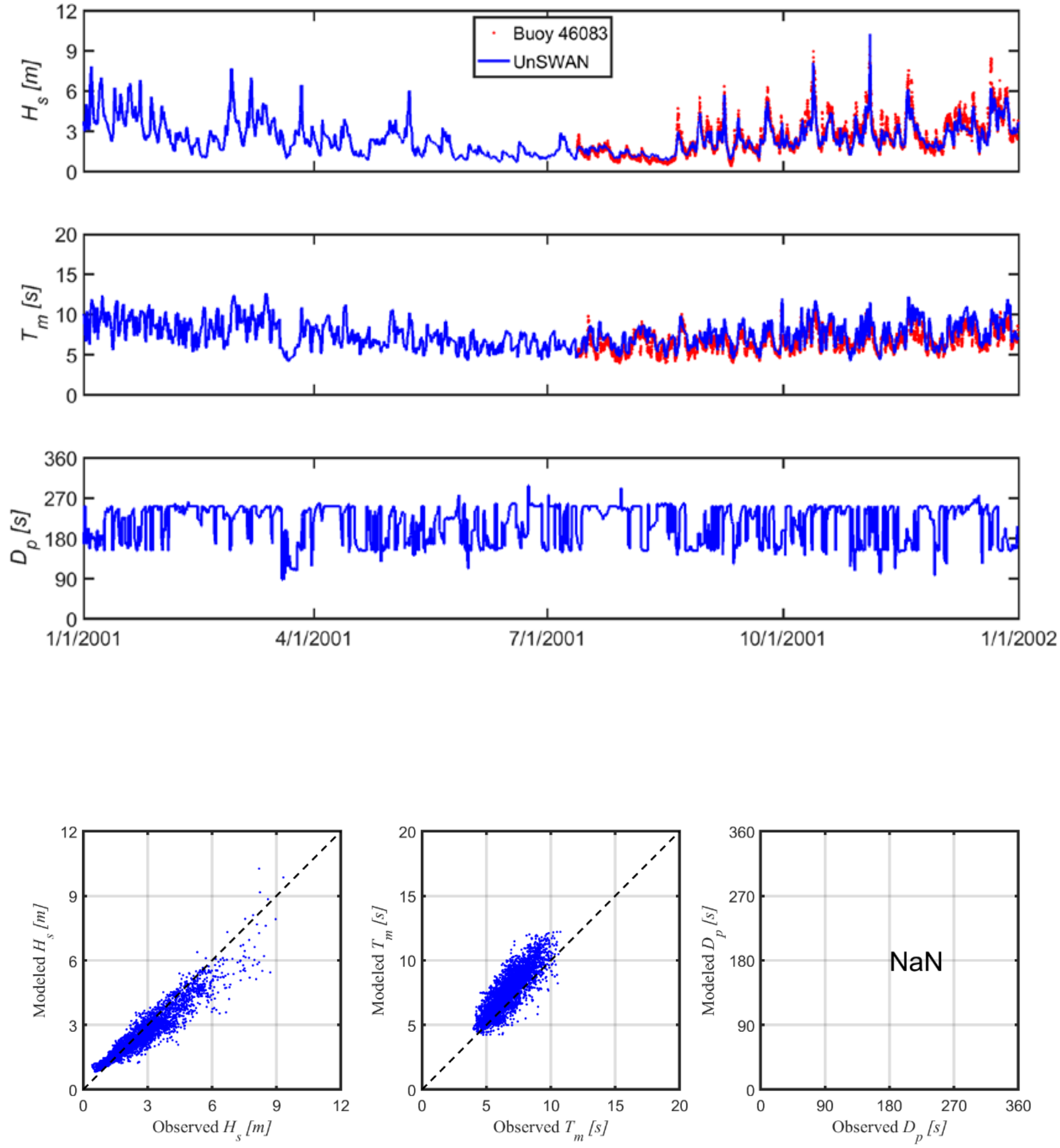

Figure B.154. Comparisons of time series (top) and scatter plots (bottom) of the three UnSWAN model-simulated bulk parameters with observed data at NDBC Buoy 46083 for 2001.

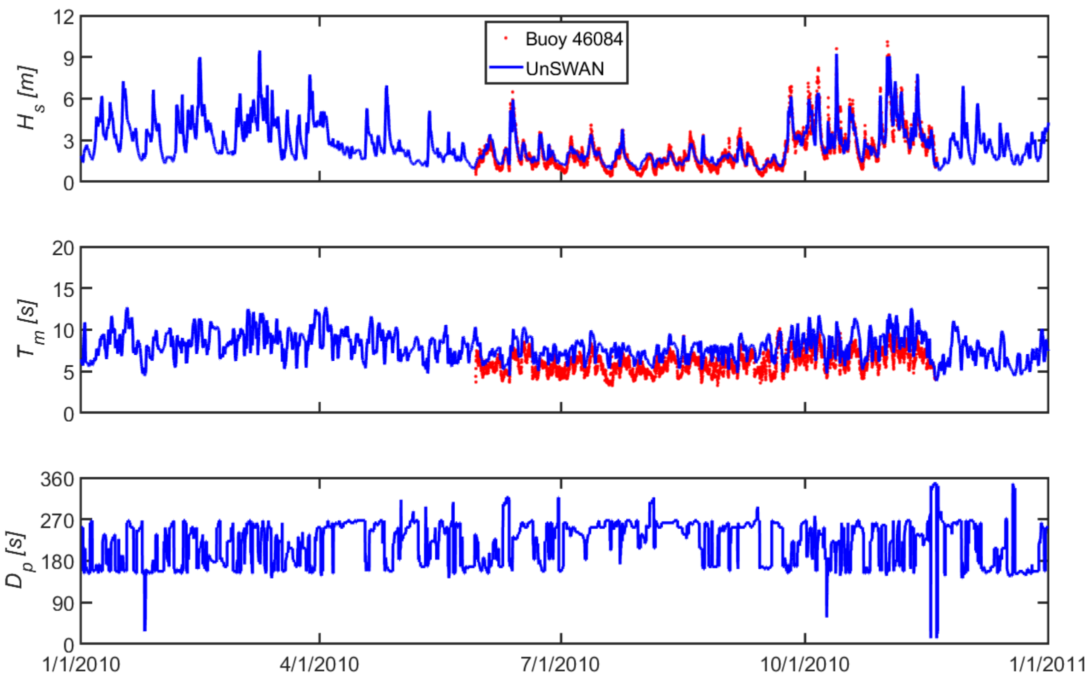

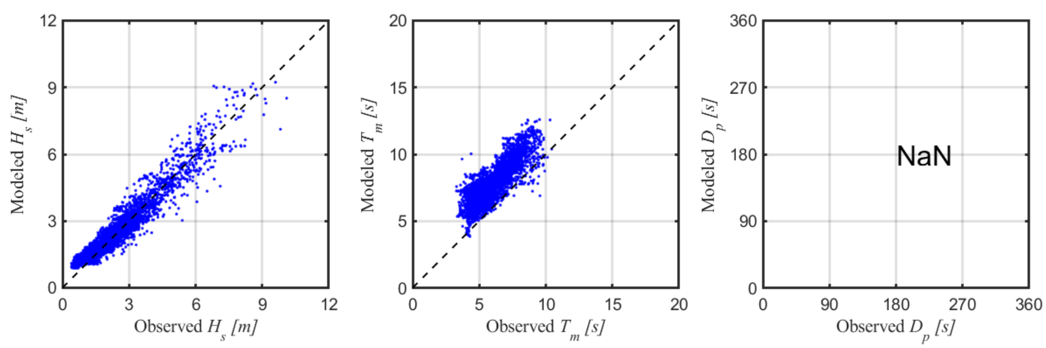

Figure B.155. Comparisons of time series (top) and scatter plots (bottom) of the three UnSWAN model-simulated bulk parameters with observed data at NDBC Buoy 46084 for 2010.

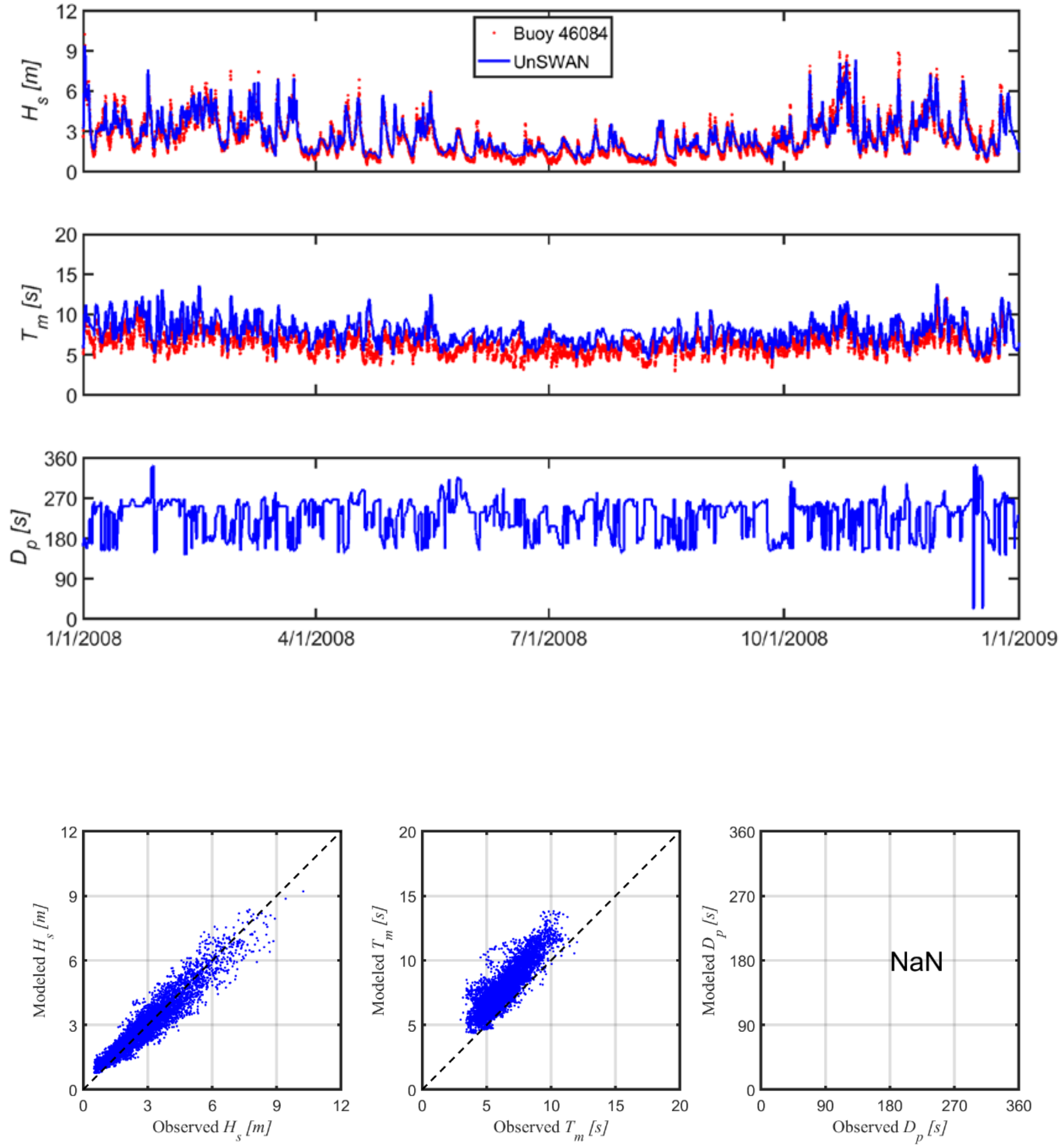

Figure B.156. Comparisons of time series (top) and scatter plots (bottom) of the three UnSWAN model-simulated bulk parameters with observed data at NDBC Buoy 46084 for 2008.

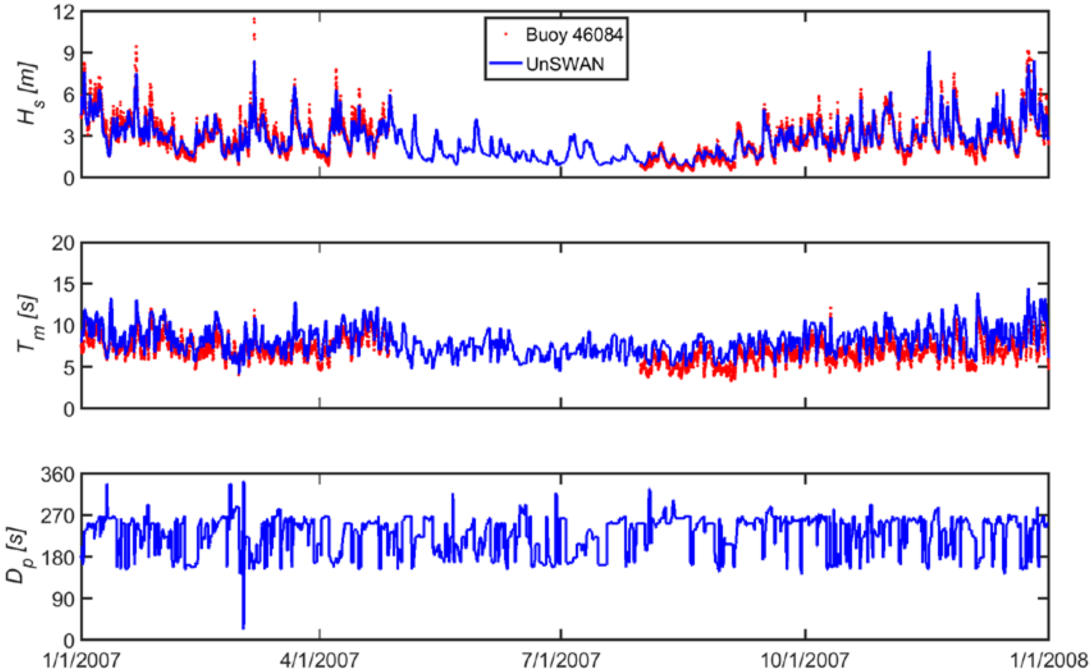

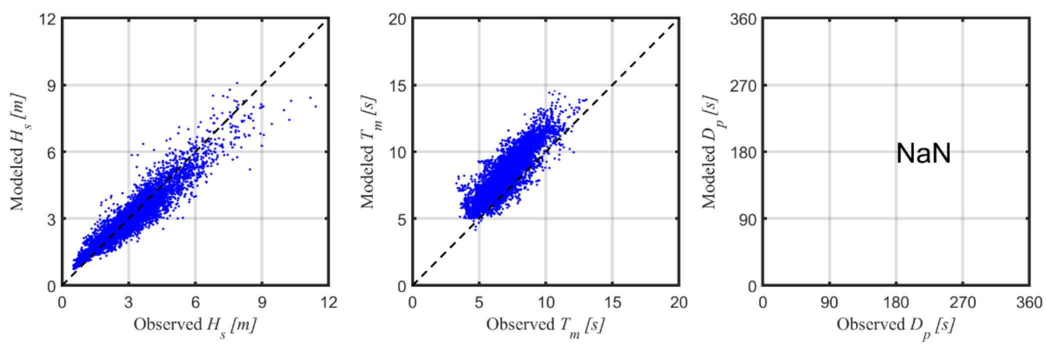

Figure B.157. Comparisons of time series (top) and scatter plots (bottom) of the three UnSWAN model-simulated bulk parameters with observed data at NDBC Buoy 46084 for 2007.

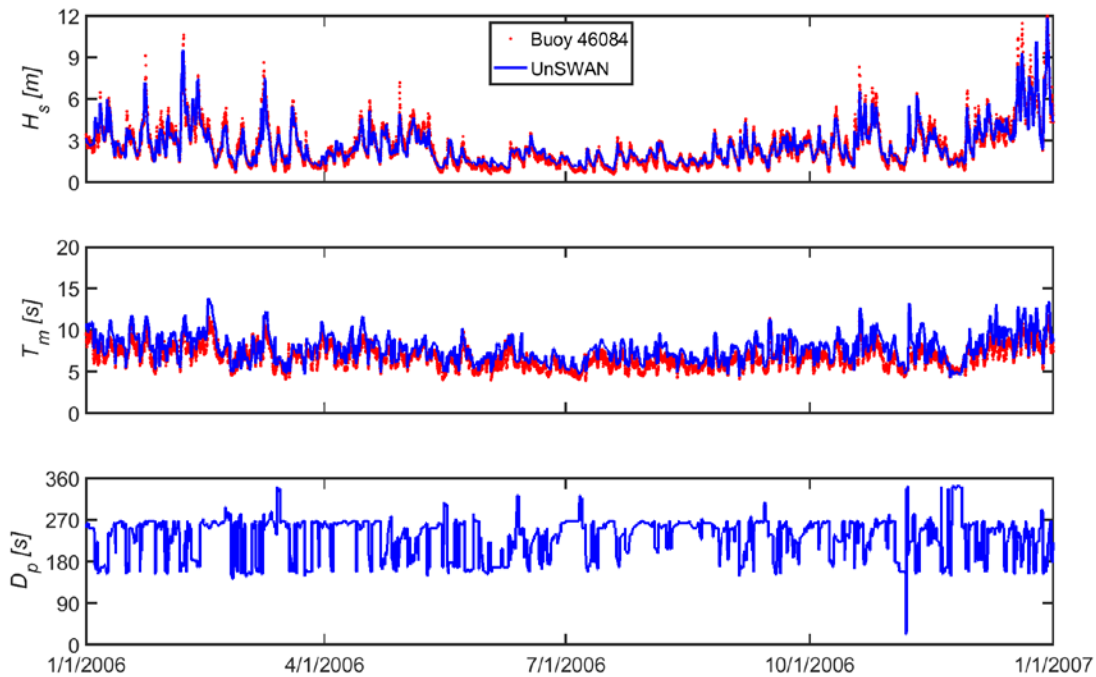

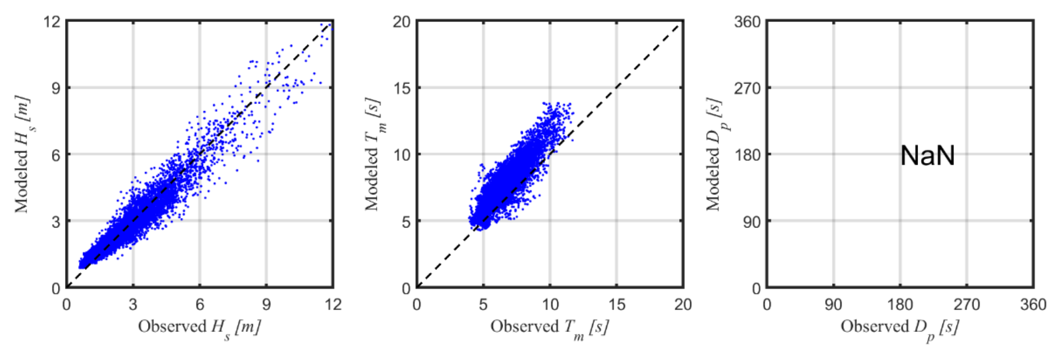

Figure B.158. Comparisons of time series (top) and scatter plots (bottom) of the three UnSWAN model-simulated bulk parameters with observed data at NDBC Buoy 46084 for 2006.

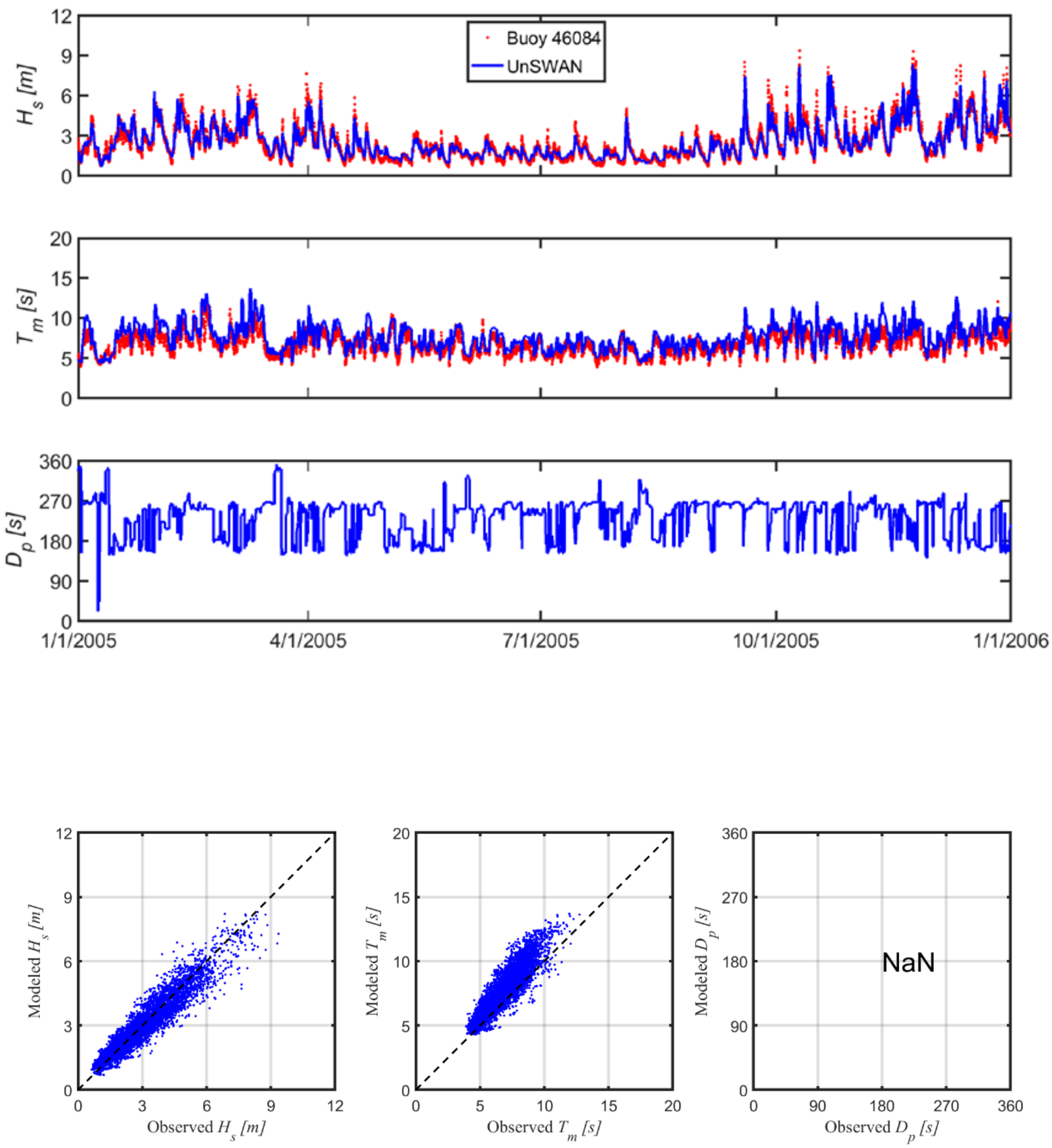

Figure B.159. Comparisons of time series (top) and scatter plots (bottom) of the three UnSWAN model-simulated bulk parameters with observed data at NDBC Buoy 46084 for 2005.

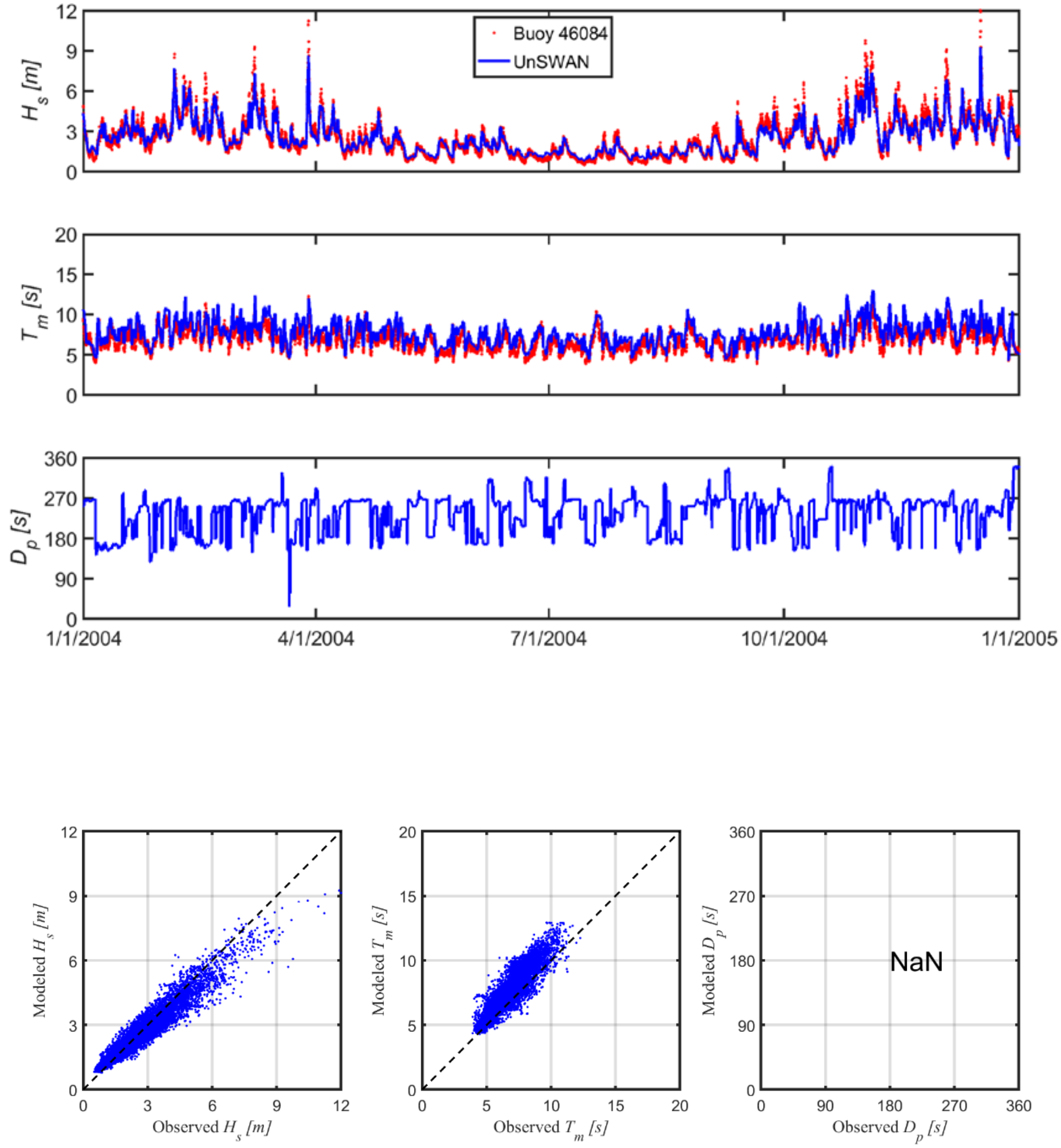

Figure B.160. Comparisons of time series (top) and scatter plots (bottom) of the three UnSWAN model-simulated bulk parameters with observed data at NDBC Buoy 46084 for 2004.

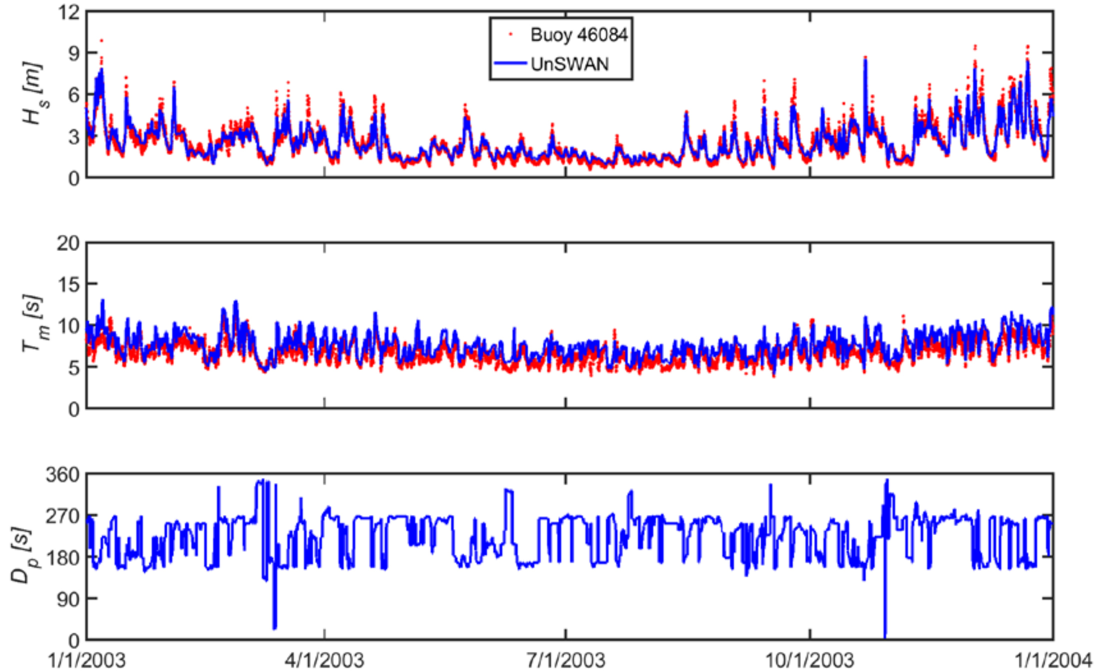

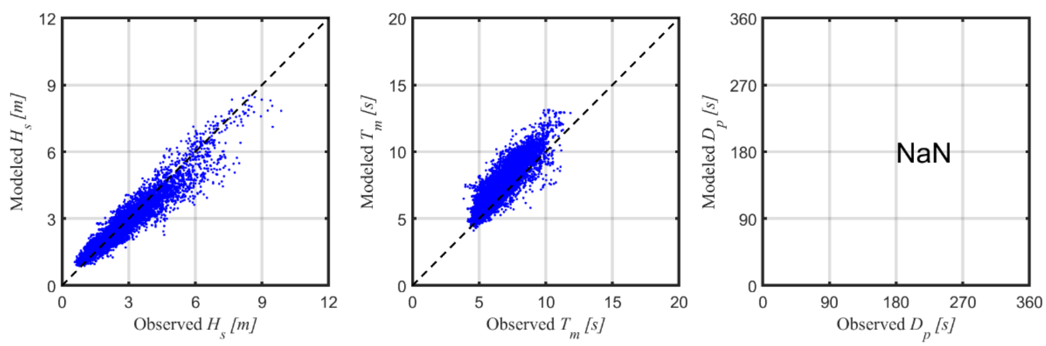

Figure B.161. Comparisons of time series (top) and scatter plots (bottom) of the three UnSWAN model-simulated bulk parameters with observed data at NDBC Buoy 46084 for 2003.

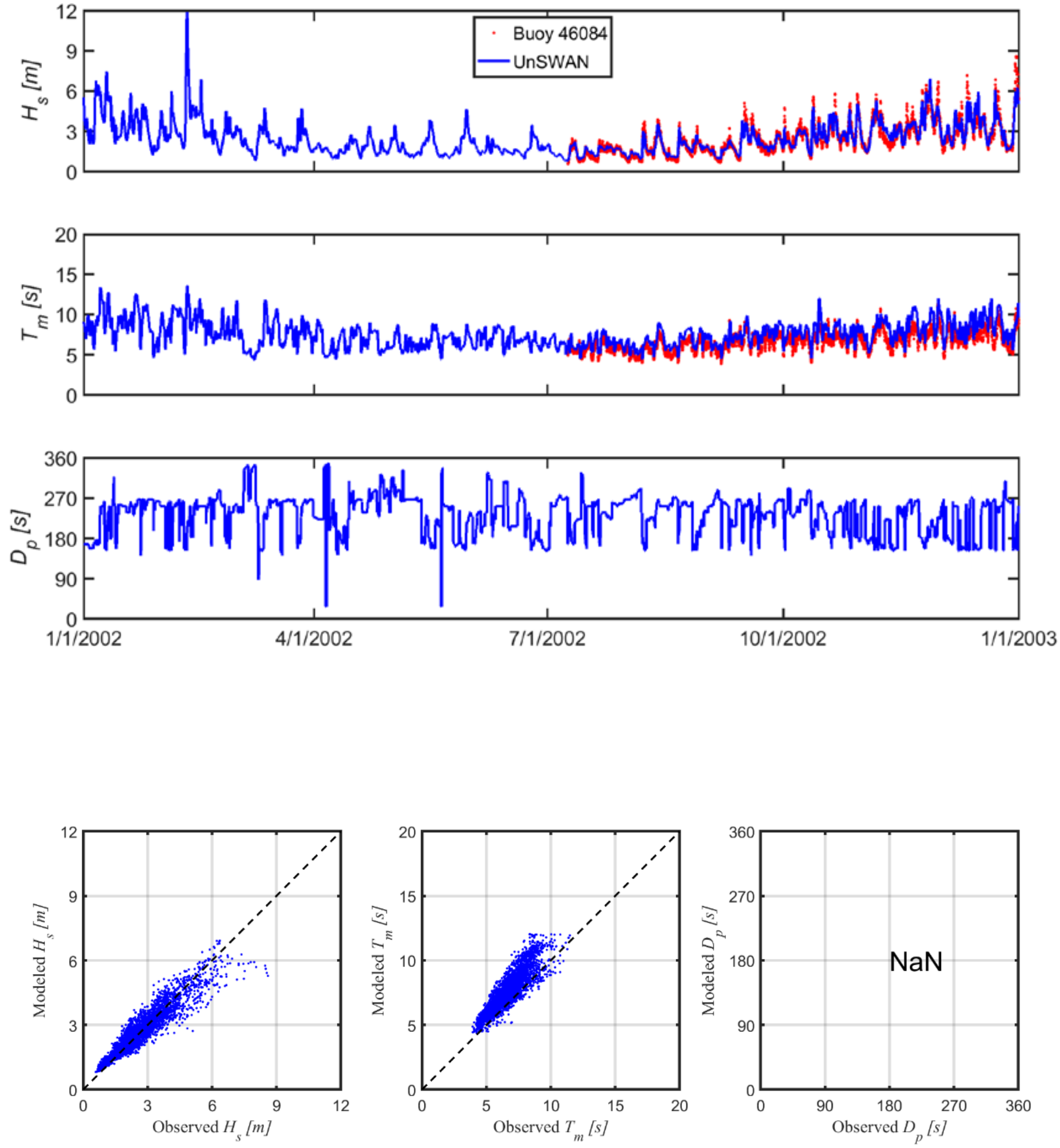

Figure B.162. Comparisons of time series (top) and scatter plots (bottom) of the three UnSWAN model-simulated bulk parameters with observed data at NDBC Buoy 46084 for 2002.

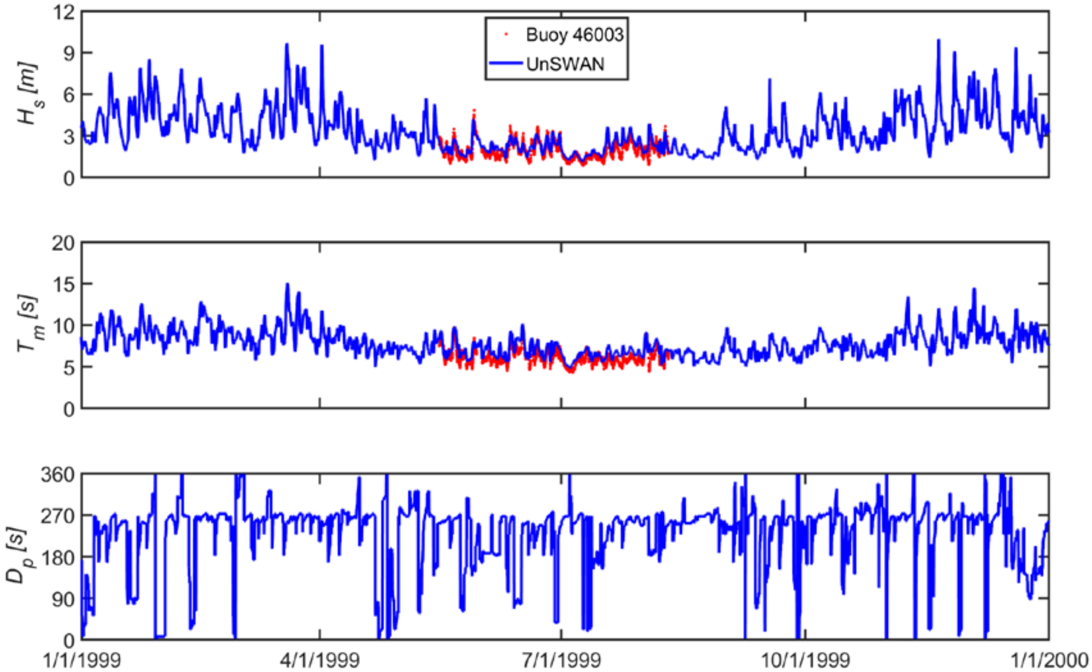

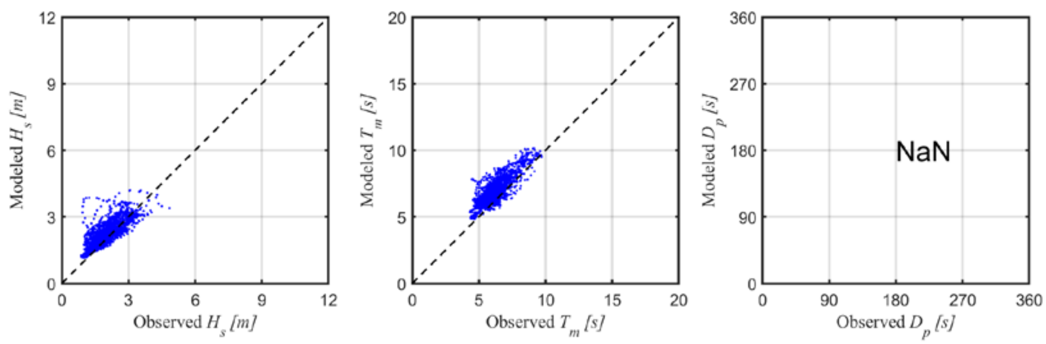

Figure B.163. Comparisons of time series (top) and scatter plots (bottom) of the three UnSWAN model-simulated bulk parameters with observed data at NDBC Buoy 46003 for 1999.

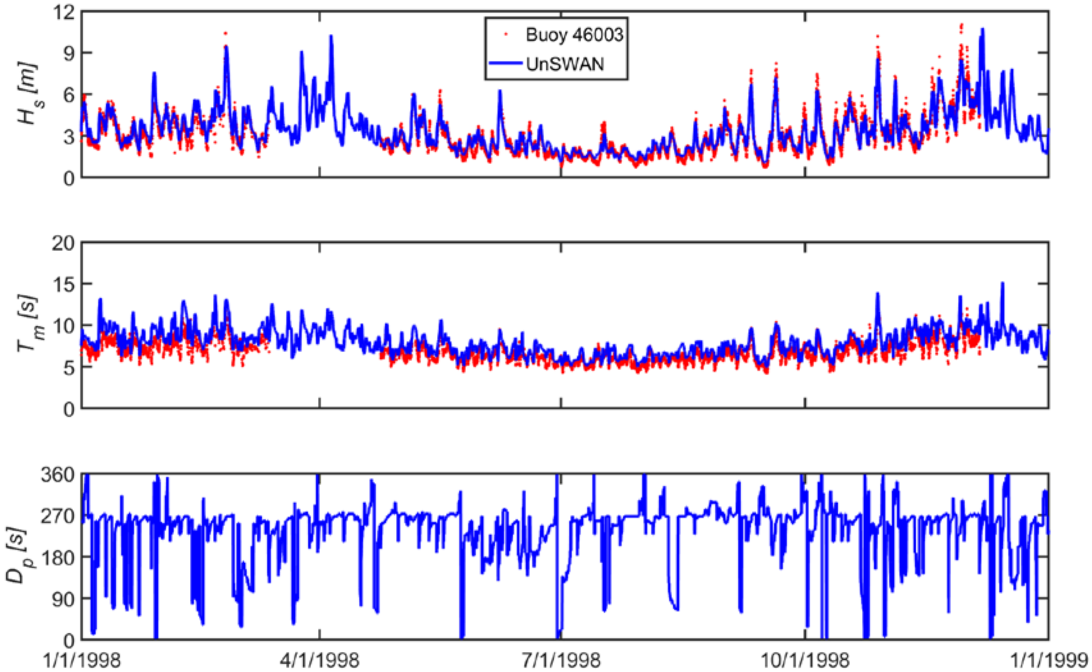

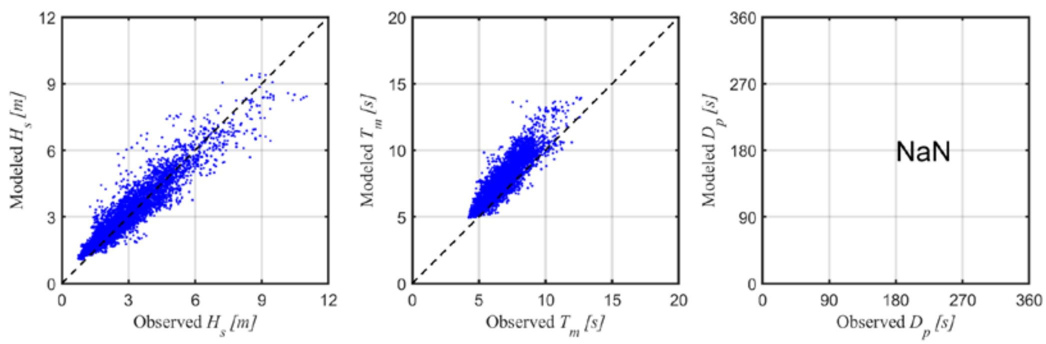

Figure B.164. Comparisons of time series (top) and scatter plots (bottom) of the three UnSWAN model-simulated bulk parameters with observed data at NDBC Buoy 46003 for 1998.

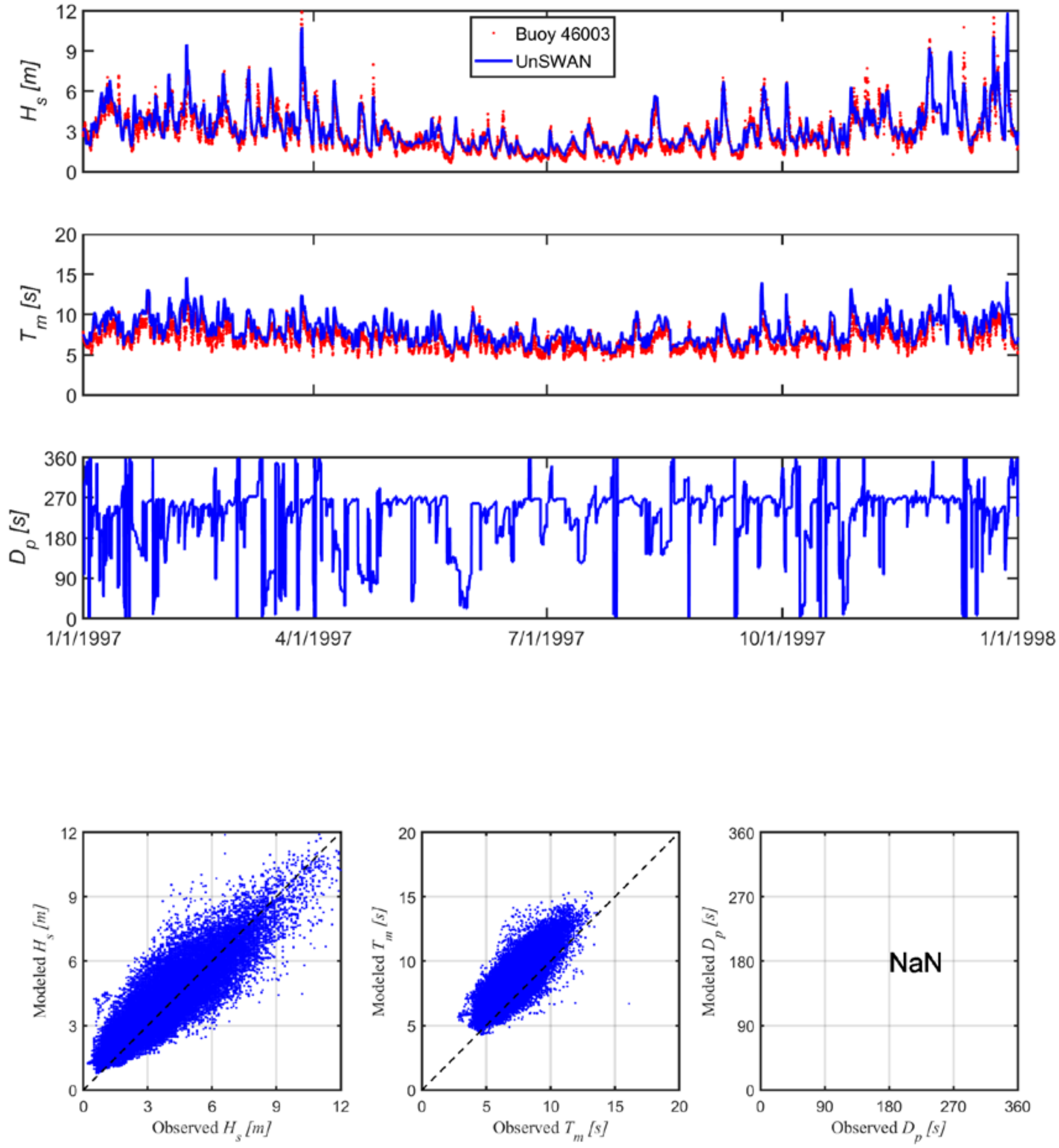

Figure B.165. Comparisons of time series (top) and scatter plots (bottom) of the three UnSWAN model-simulated bulk parameters with observed data at NDBC Buoy 46003 for 1997.

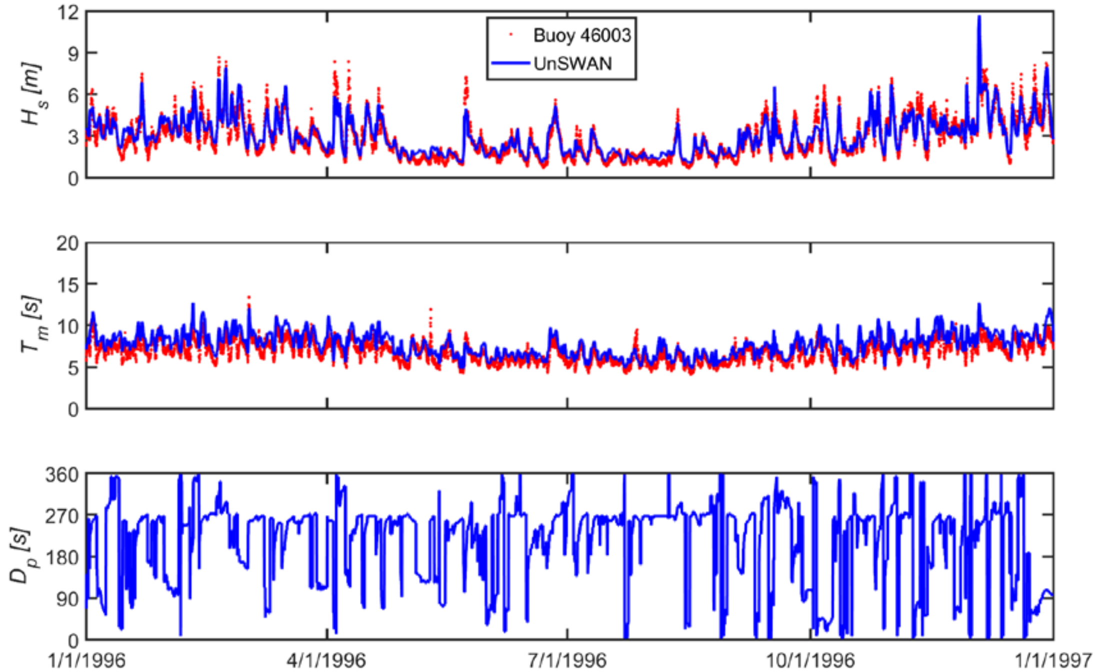

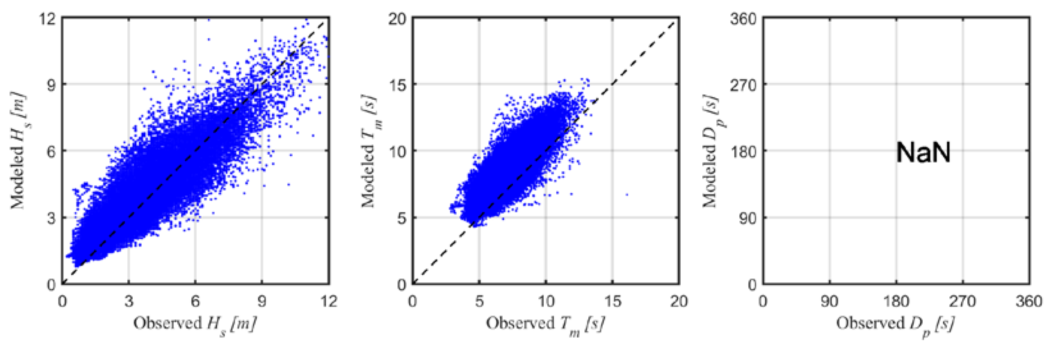

Figure B.166. Comparisons of time series (top) and scatter plots (bottom) of the three UnSWAN model-simulated bulk parameters with observed data at NDBC Buoy 46003 for 1996.

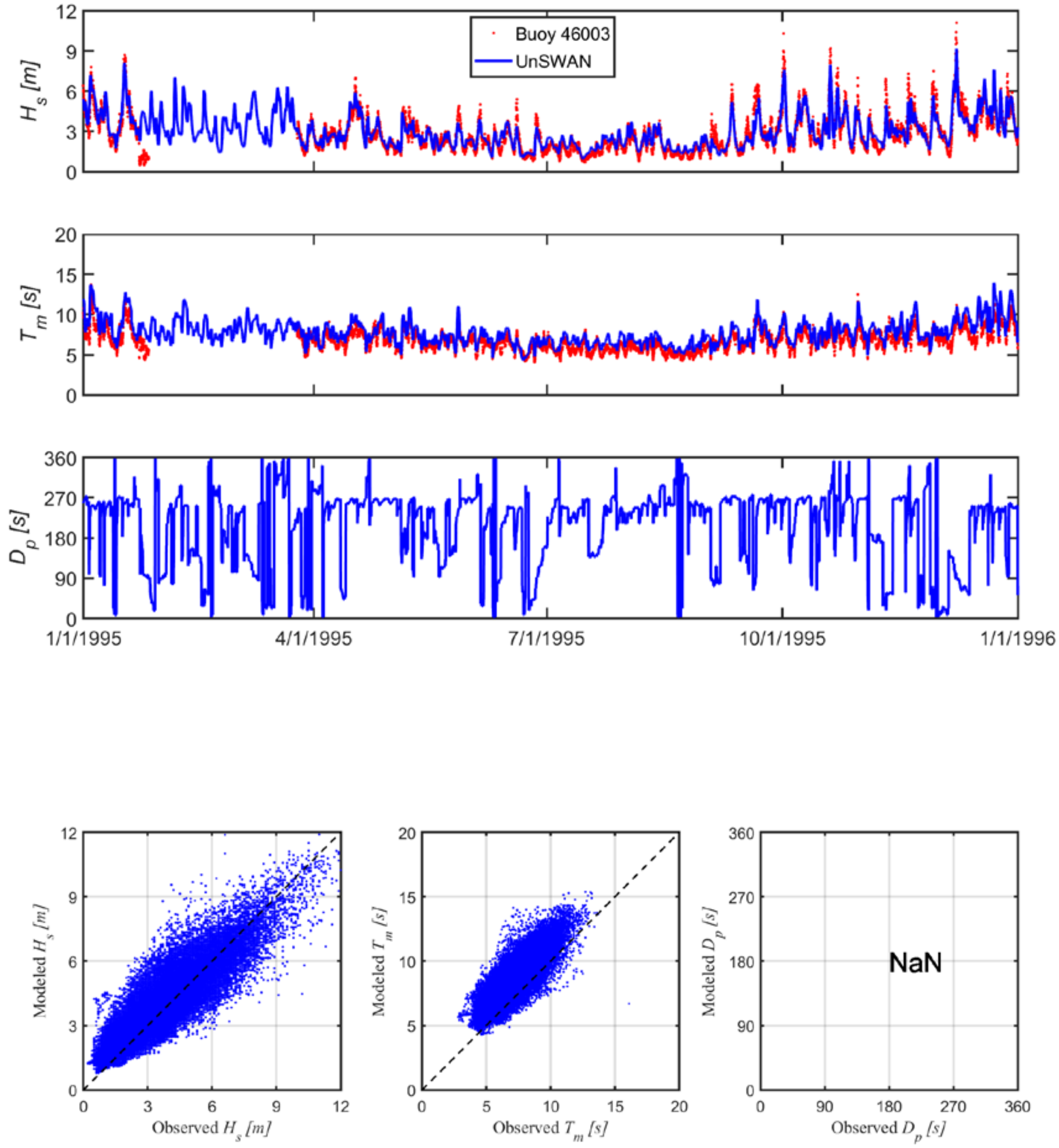

Figure B.167. Comparisons of time series (top) and scatter plots (bottom) of the three UnSWAN model-simulated bulk parameters with observed data at NDBC Buoy 46003 for 1995.

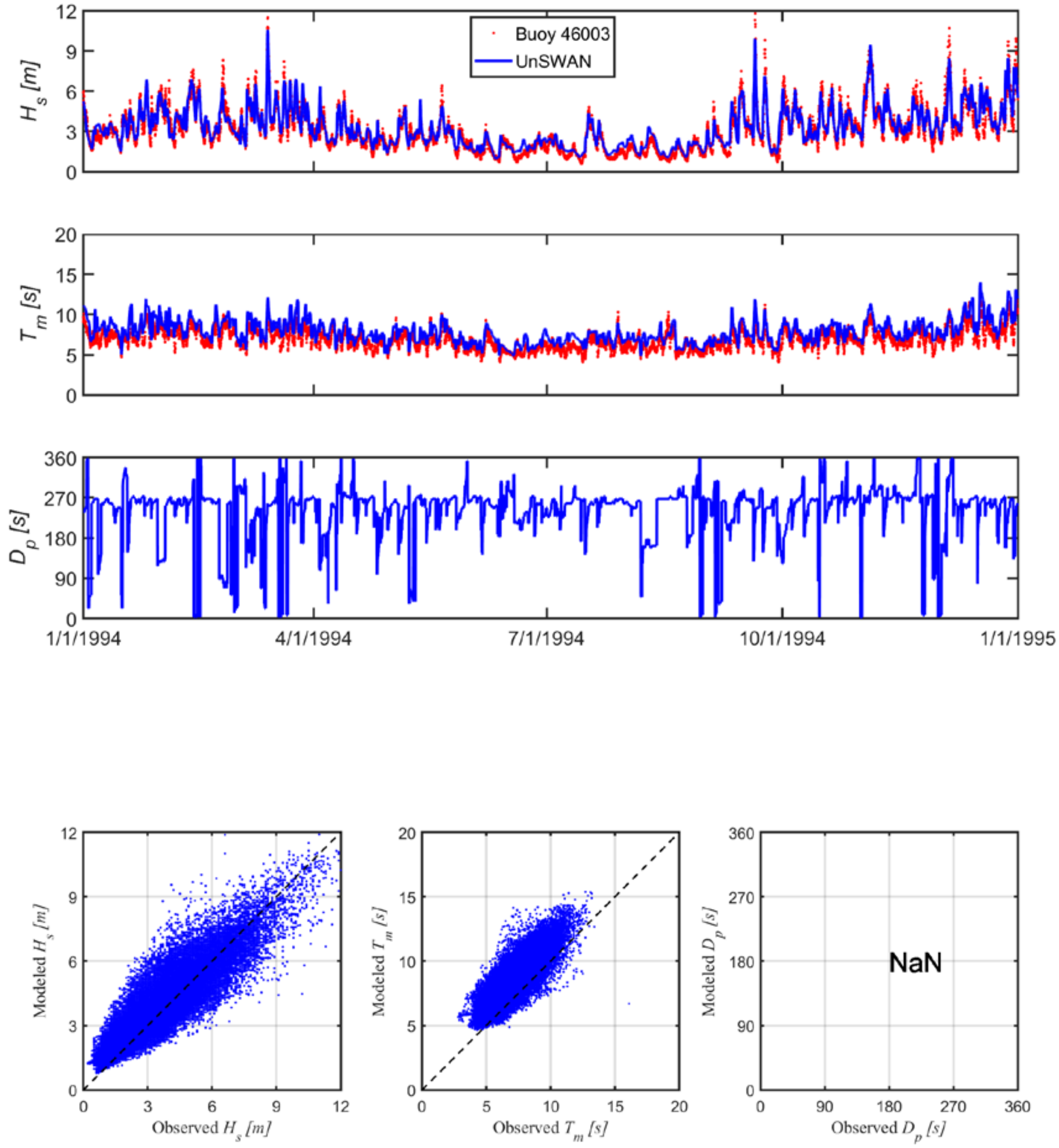

Figure B.168. Comparisons of time series (top) and scatter plots (bottom) of the three UnSWAN model-simulated bulk parameters with observed data at NDBC Buoy 46003 for 1994.

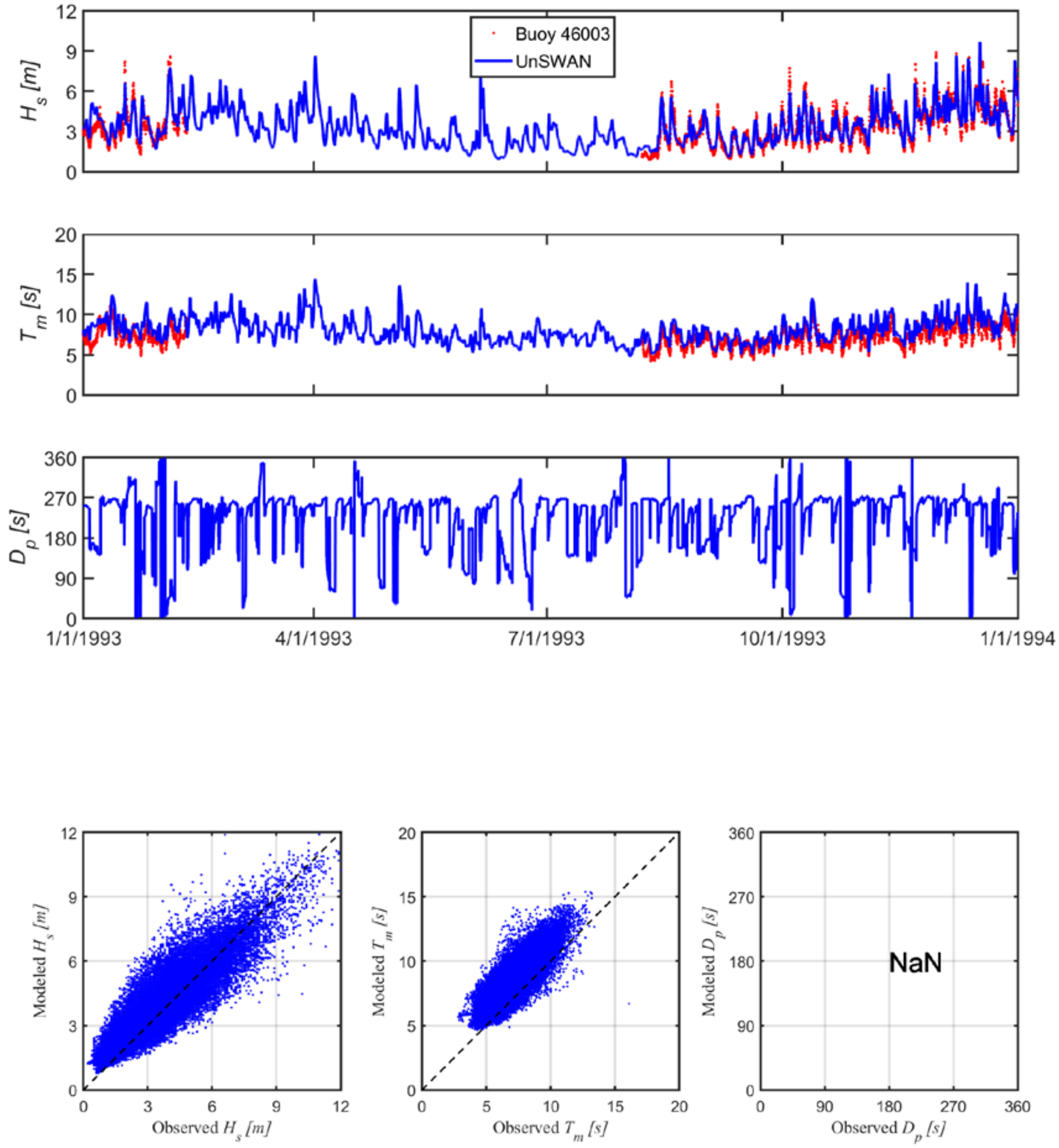

Figure B.169. Comparisons of time series (top) and scatter plots (bottom) of the three UnSWAN model-simulated bulk parameters with observed data at NDBC Buoy 46003 for 1993.

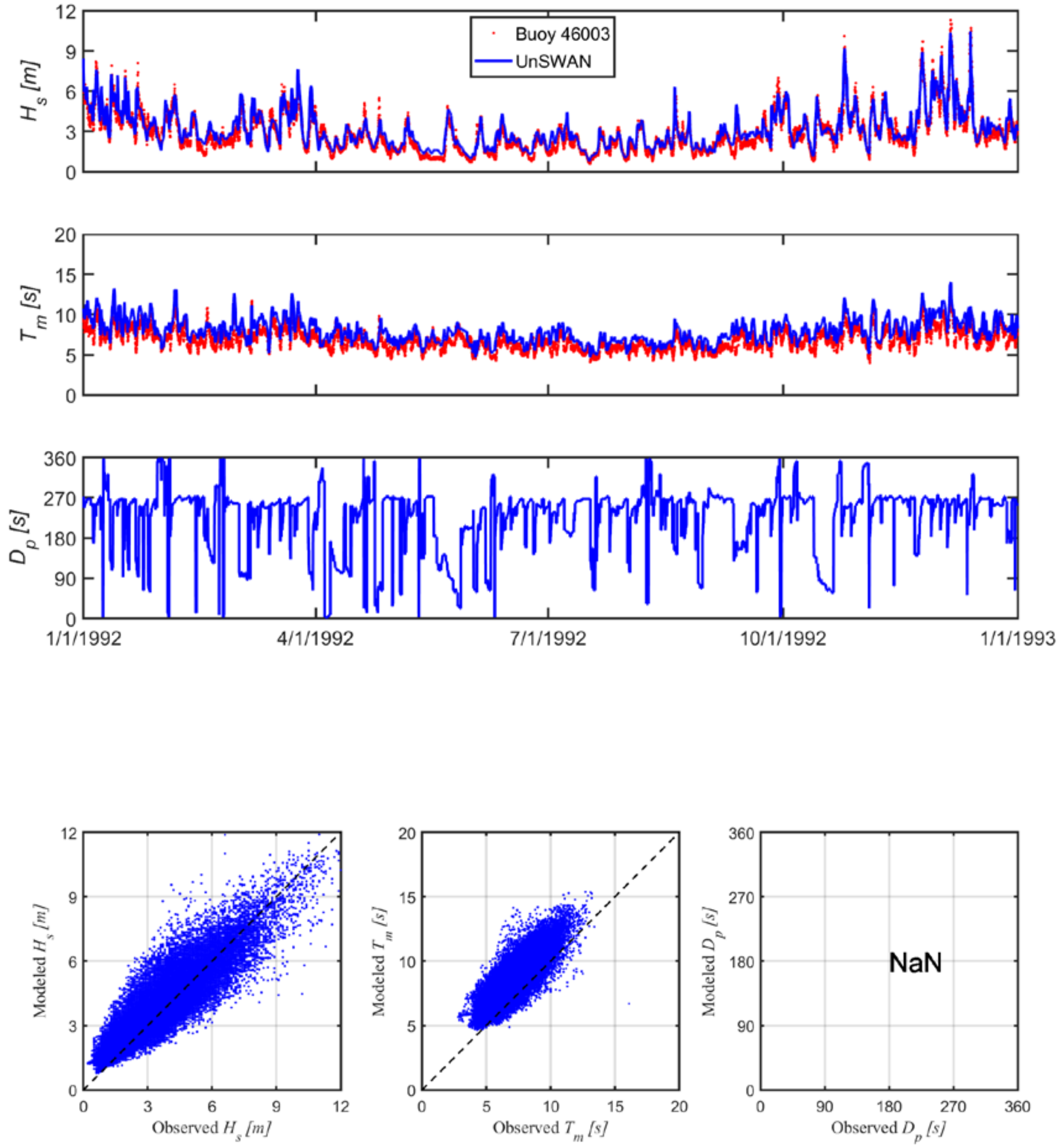

Figure B.170. Comparisons of time series (top) and scatter plots (bottom) of the three UnSWAN model-simulated bulk parameters with observed data at NDBC Buoy 46003 for 1992.

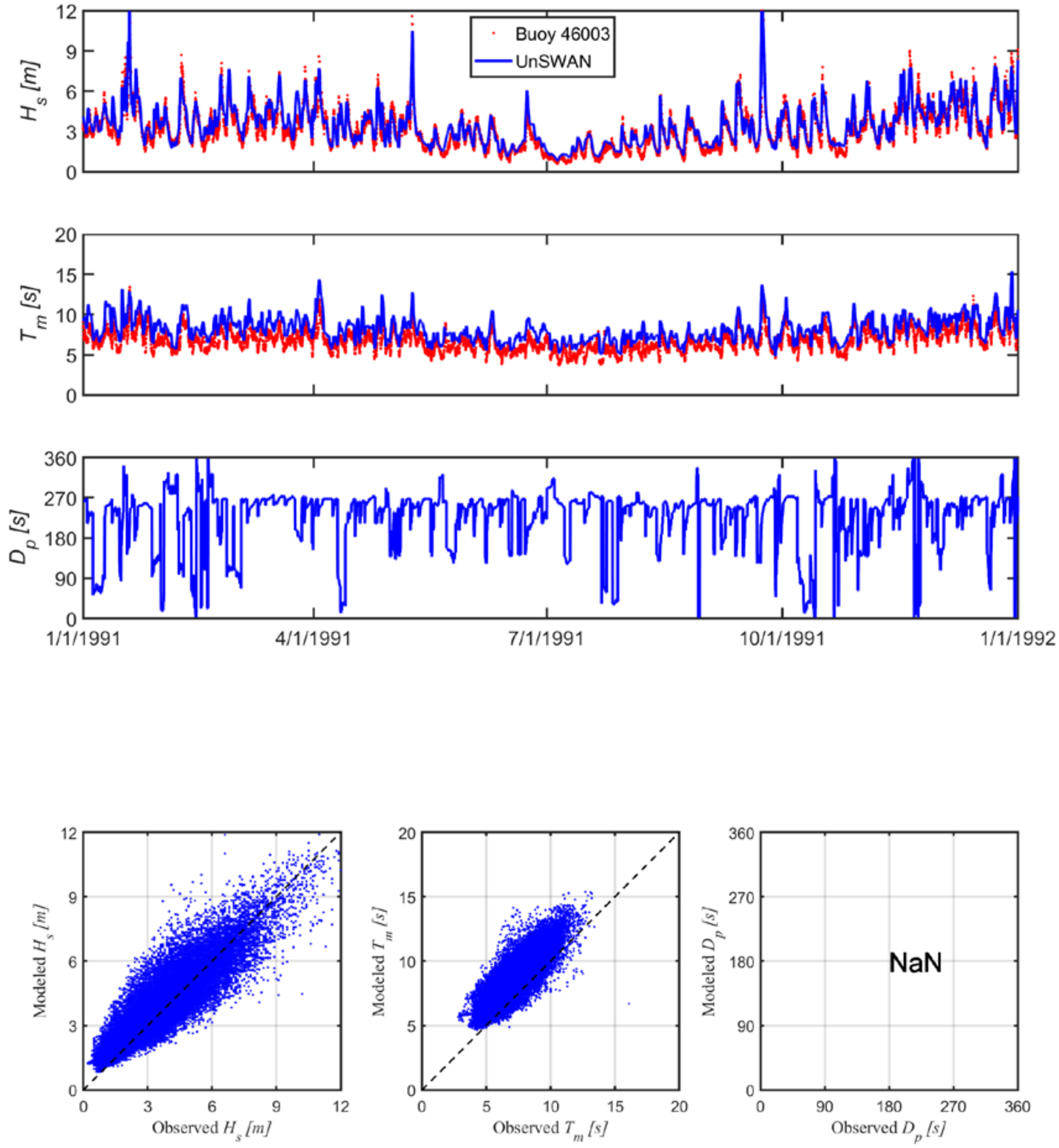

Figure B.171. Comparisons of time series (top) and scatter plots (bottom) of the three UnSWAN model-simulated bulk parameters with observed data at NDBC Buoy 46003 for 1991.

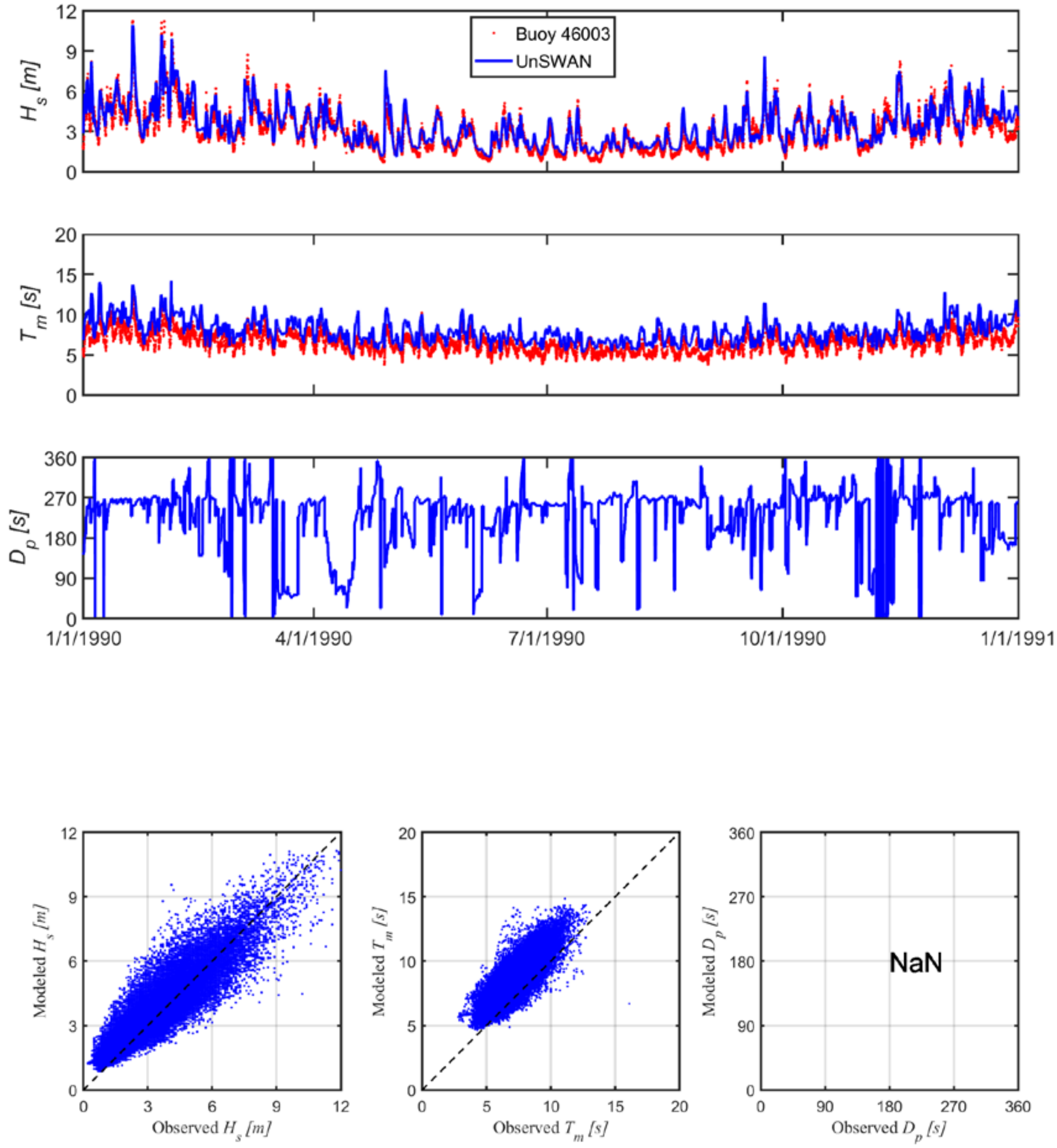

Figure B.172. Comparisons of time series (top) and scatter plots (bottom) of the three UnSWAN model-simulated bulk parameters with observed data at NDBC Buoy 46003 for 1990.

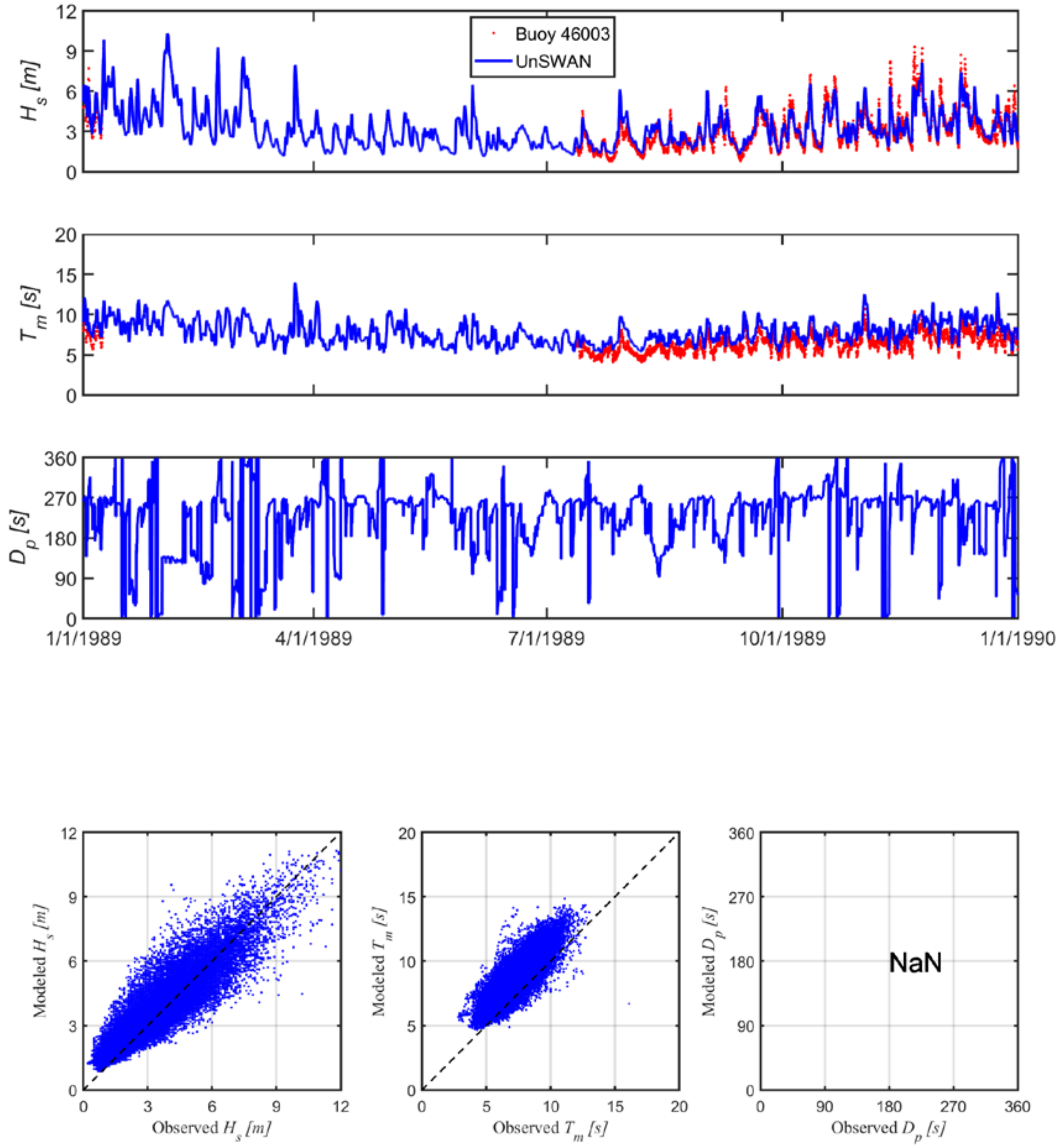

Figure B.173. Comparisons of time series (top) and scatter plots (bottom) of the three UnSWAN model-simulated bulk parameters with observed data at NDBC Buoy 46003 for 1989.

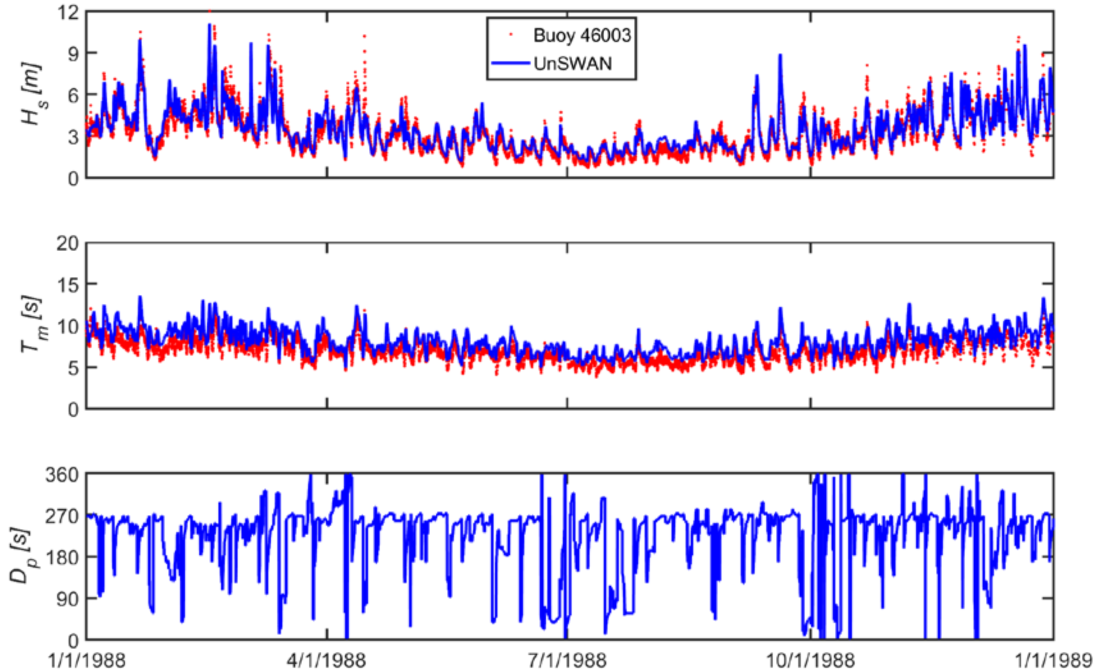

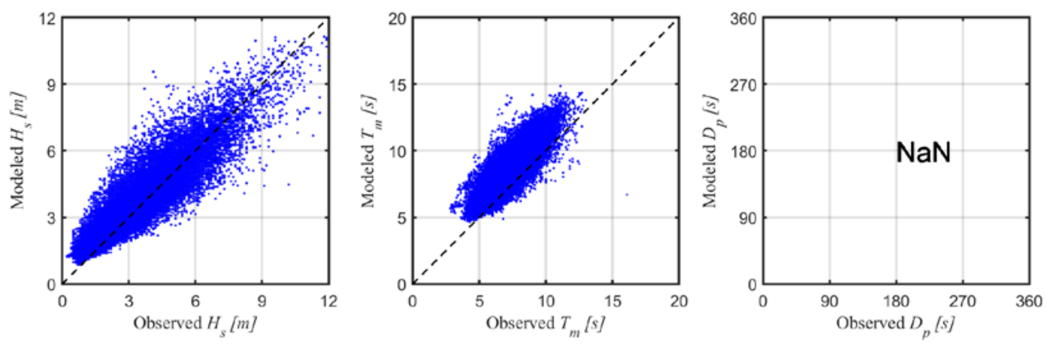

Figure B.174. Comparisons of time series (top) and scatter plots (bottom) of the three UnSWAN model-simulated bulk parameters with observed data at NDBC Buoy 46003 for 1988.

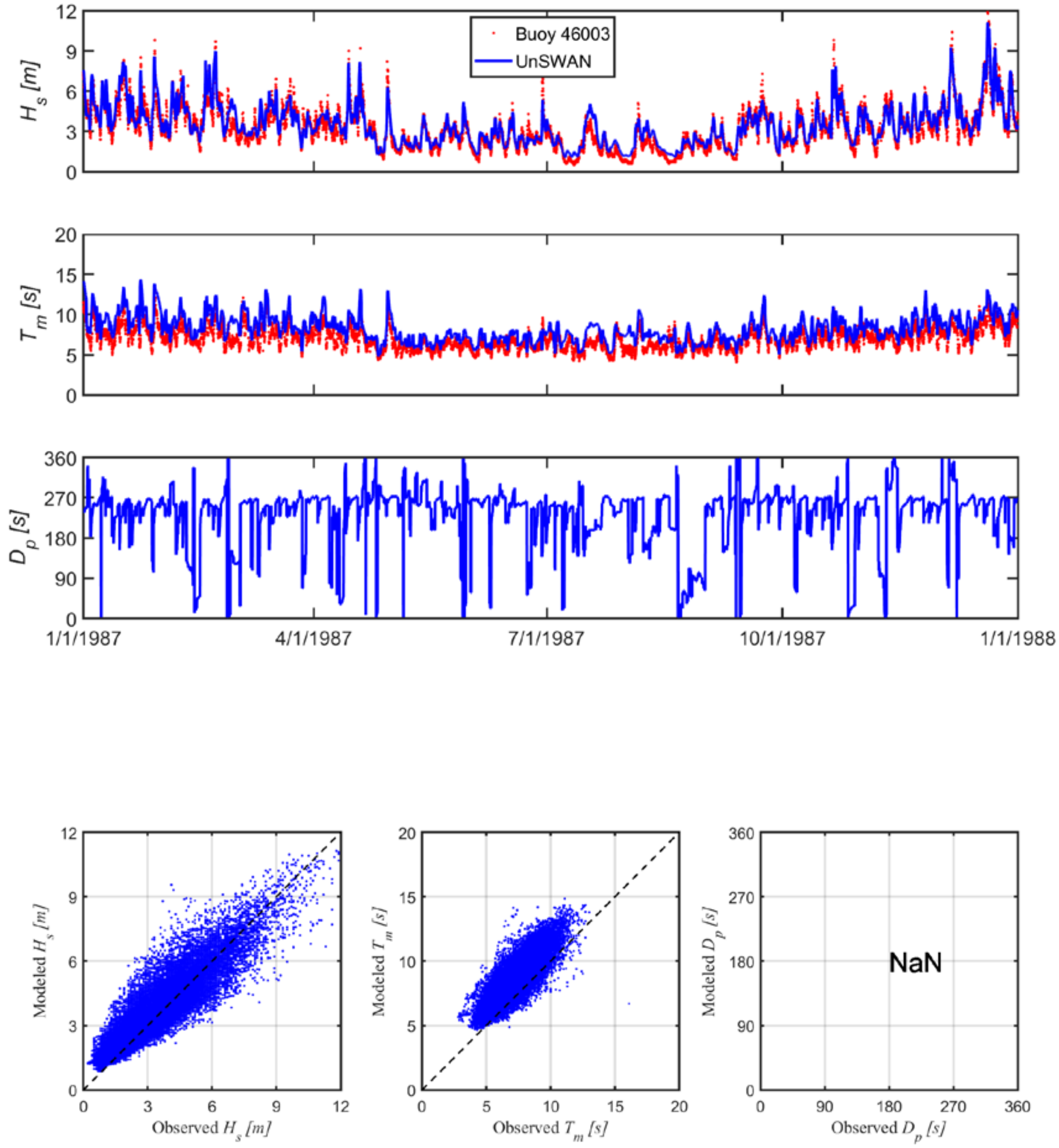

Figure B.175. Comparisons of time series (top) and scatter plots (bottom) of the three UnSWAN model-simulated bulk parameters with observed data at NDBC Buoy 46003 for 1987.

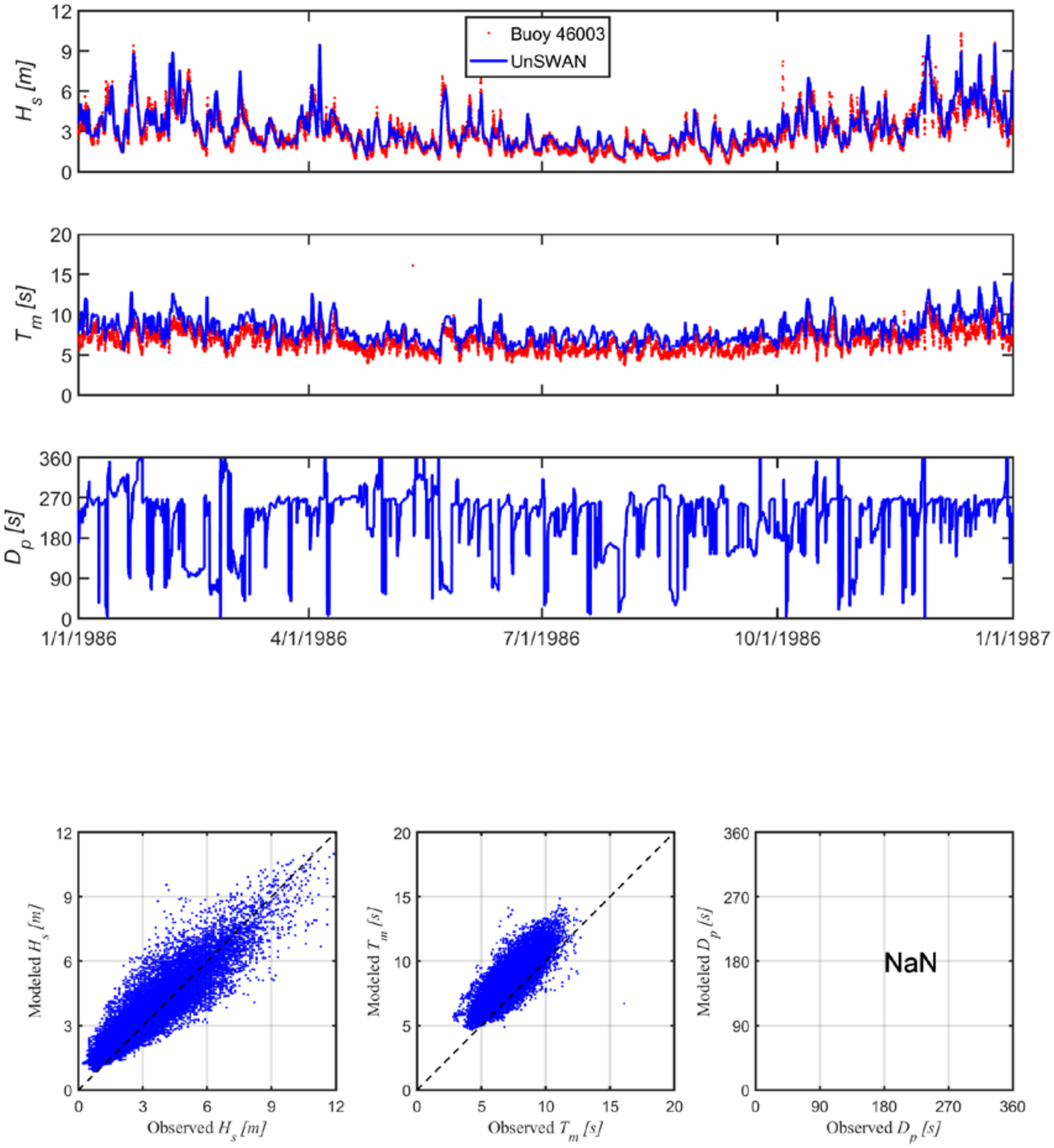

Figure B.176. Comparisons of time series (top) and scatter plots (bottom) of the three UnSWAN model-simulated bulk parameters with observed data at NDBC Buoy 46003 for 1986.

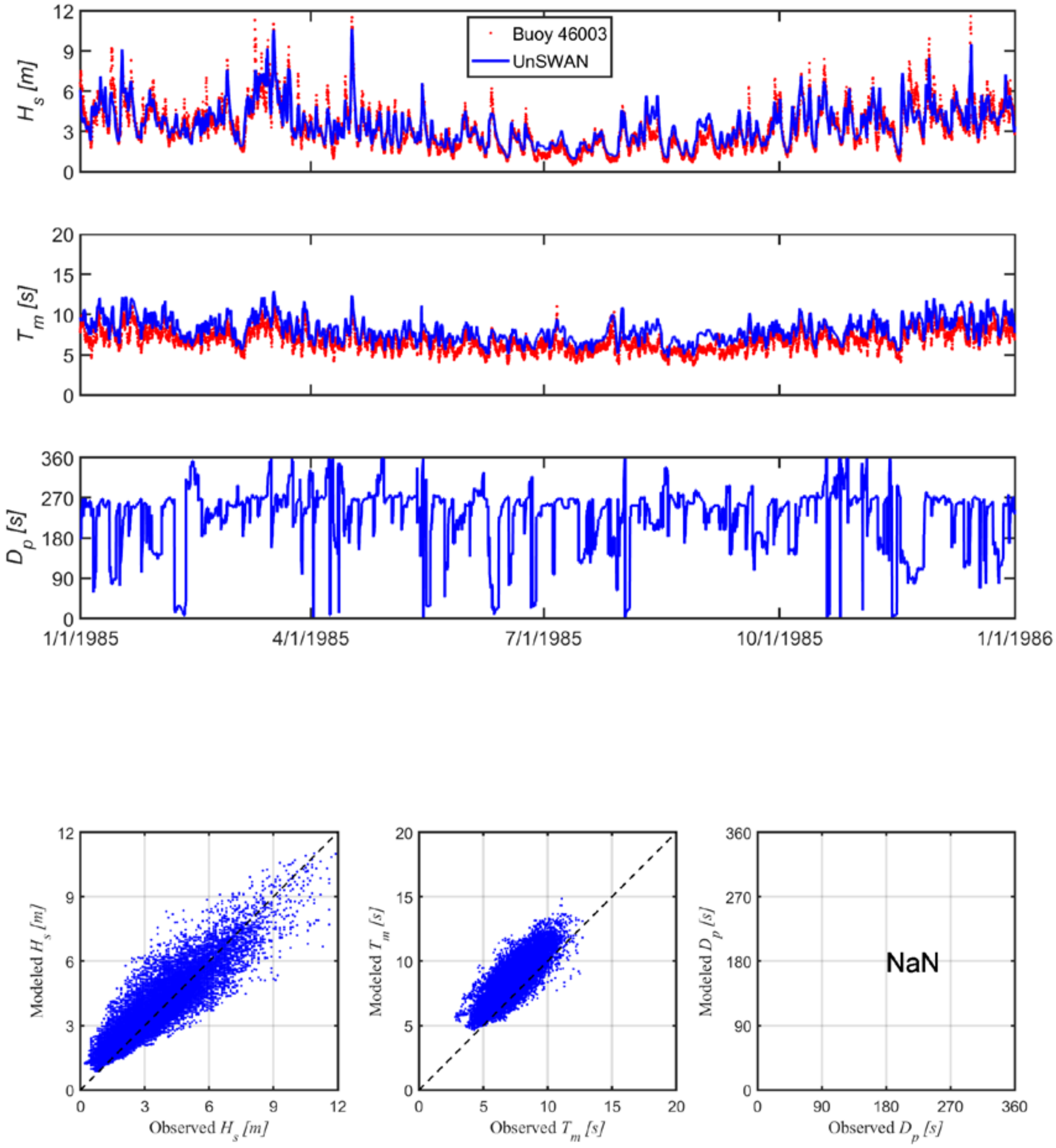

Figure B.177. Comparisons of time series (top) and scatter plots (bottom) of the three UnSWAN model-simulated bulk parameters with observed data at NDBC Buoy 46003 for 1985.

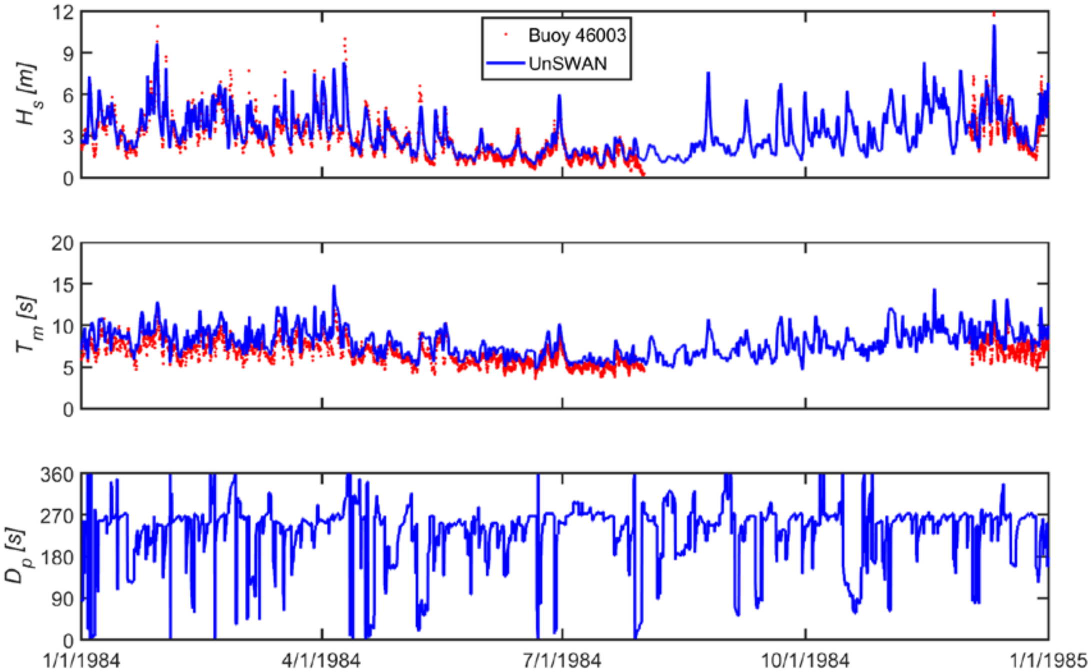

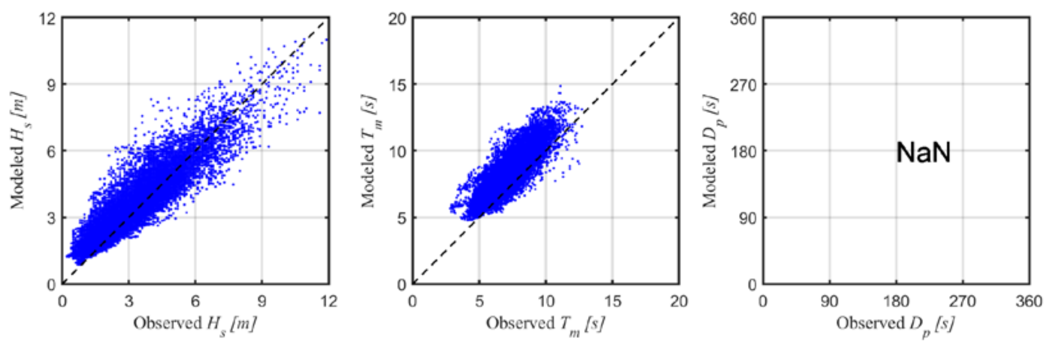

Figure B.178. Comparisons of time series (top) and scatter plots (bottom) of the three UnSWAN model-simulated bulk parameters with observed data at NDBC Buoy 46003 for 1984.

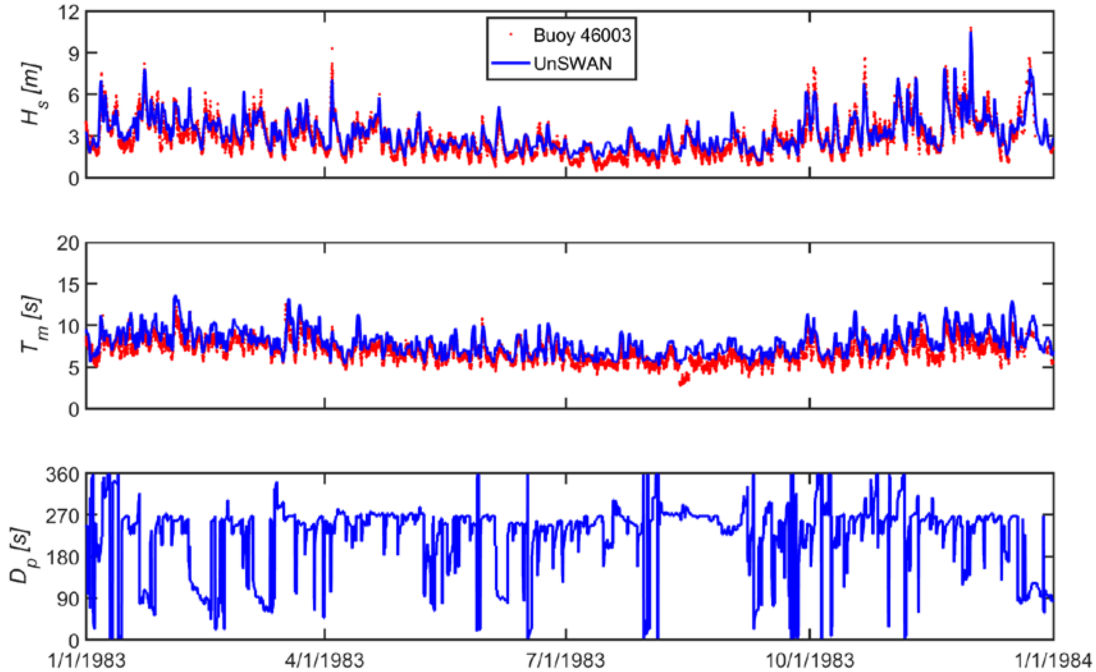

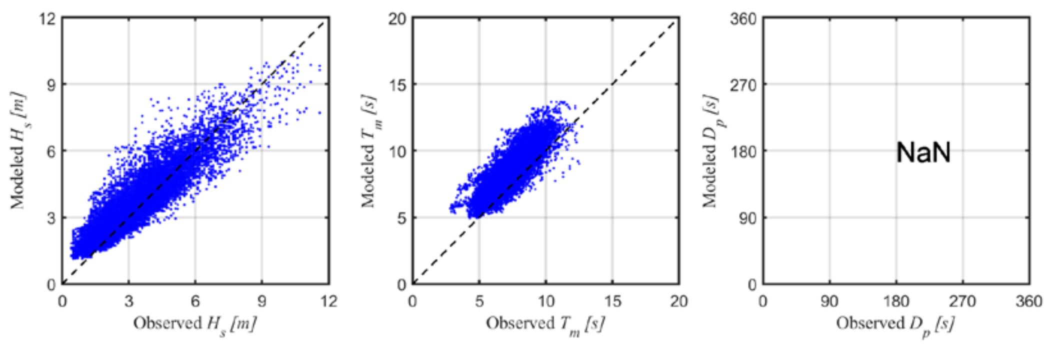

Figure B.179. Comparisons of time series (top) and scatter plots (bottom) of the three UnSWAN model-simulated bulk parameters with observed data at NDBC Buoy 46003 for 1983.

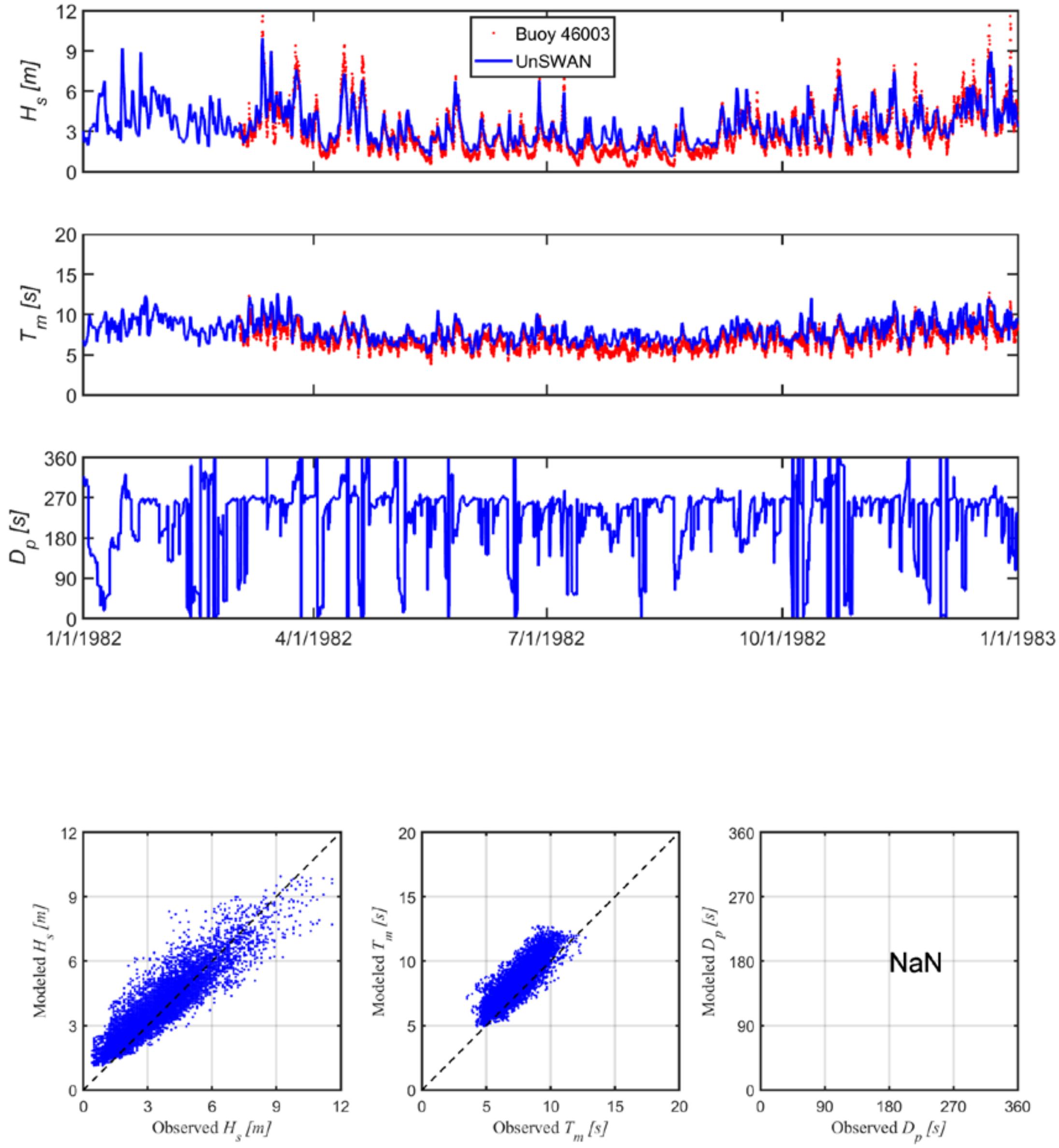

Figure B.180. Comparisons of time series (top) and scatter plots (bottom) of the three UnSWAN model-simulated bulk parameters with observed data at NDBC Buoy 46003 for 1982.

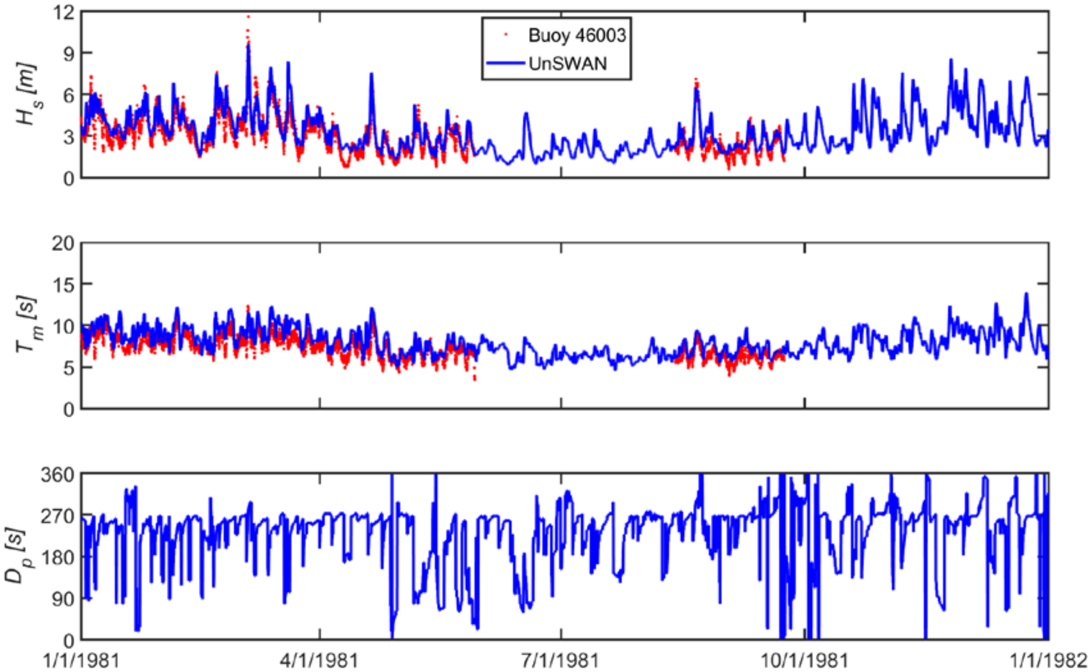

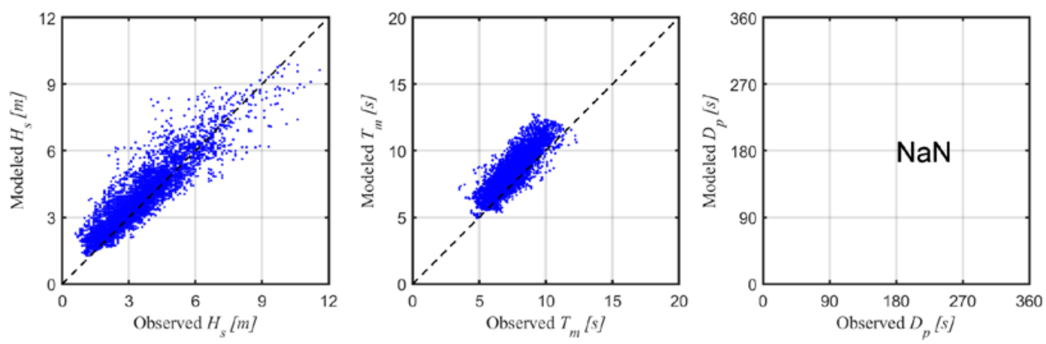

Figure B.181. Comparisons of time series (top) and scatter plots (bottom) of the three UnSWAN model-simulated bulk parameters with observed data at NDBC Buoy 46003 for 1981.

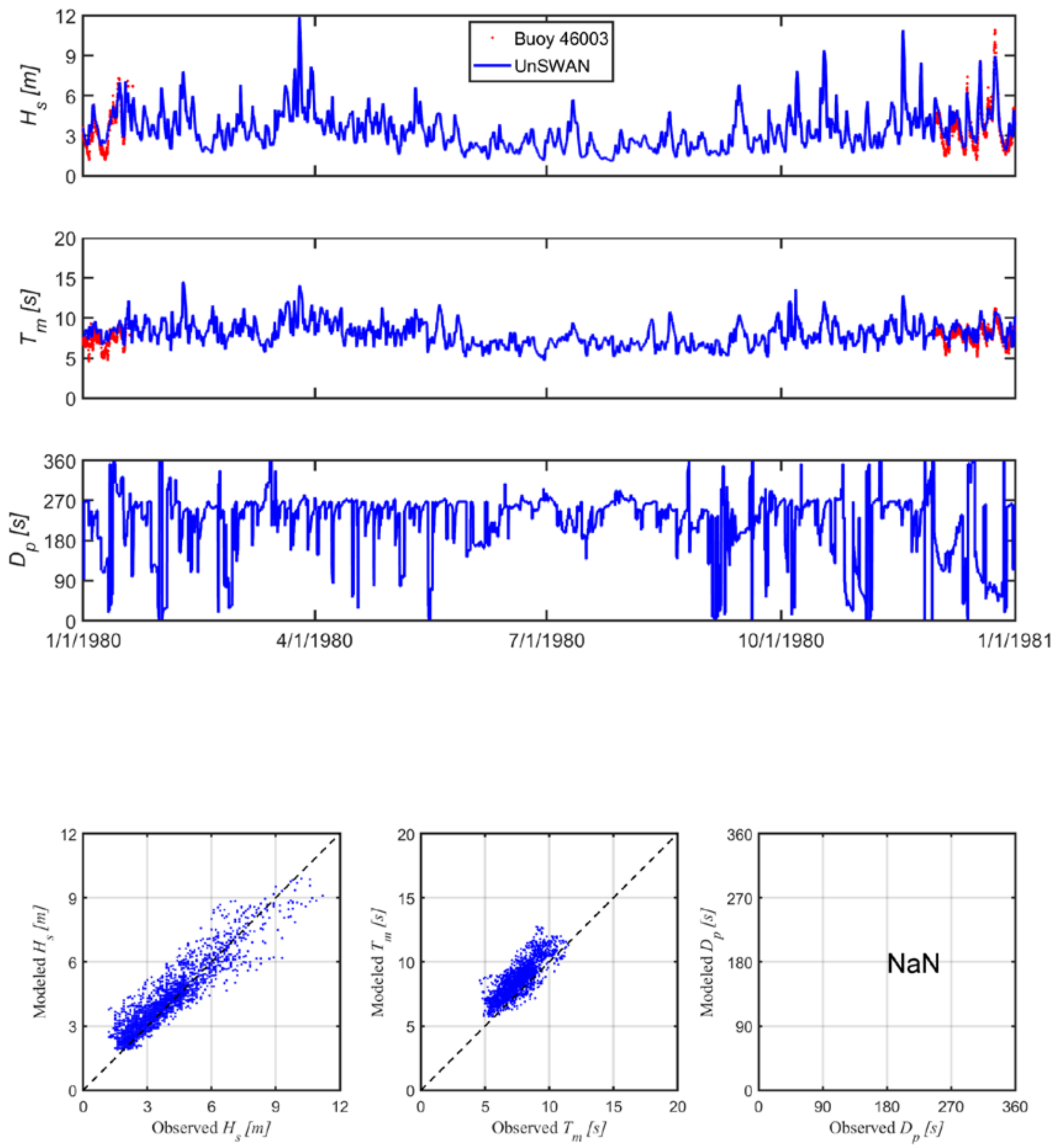

Figure B.182. Comparisons of time series (top) and scatter plots (bottom) of the three UnSWAN model-simulated bulk parameters with observed data at NDBC Buoy 46003 for 1980.

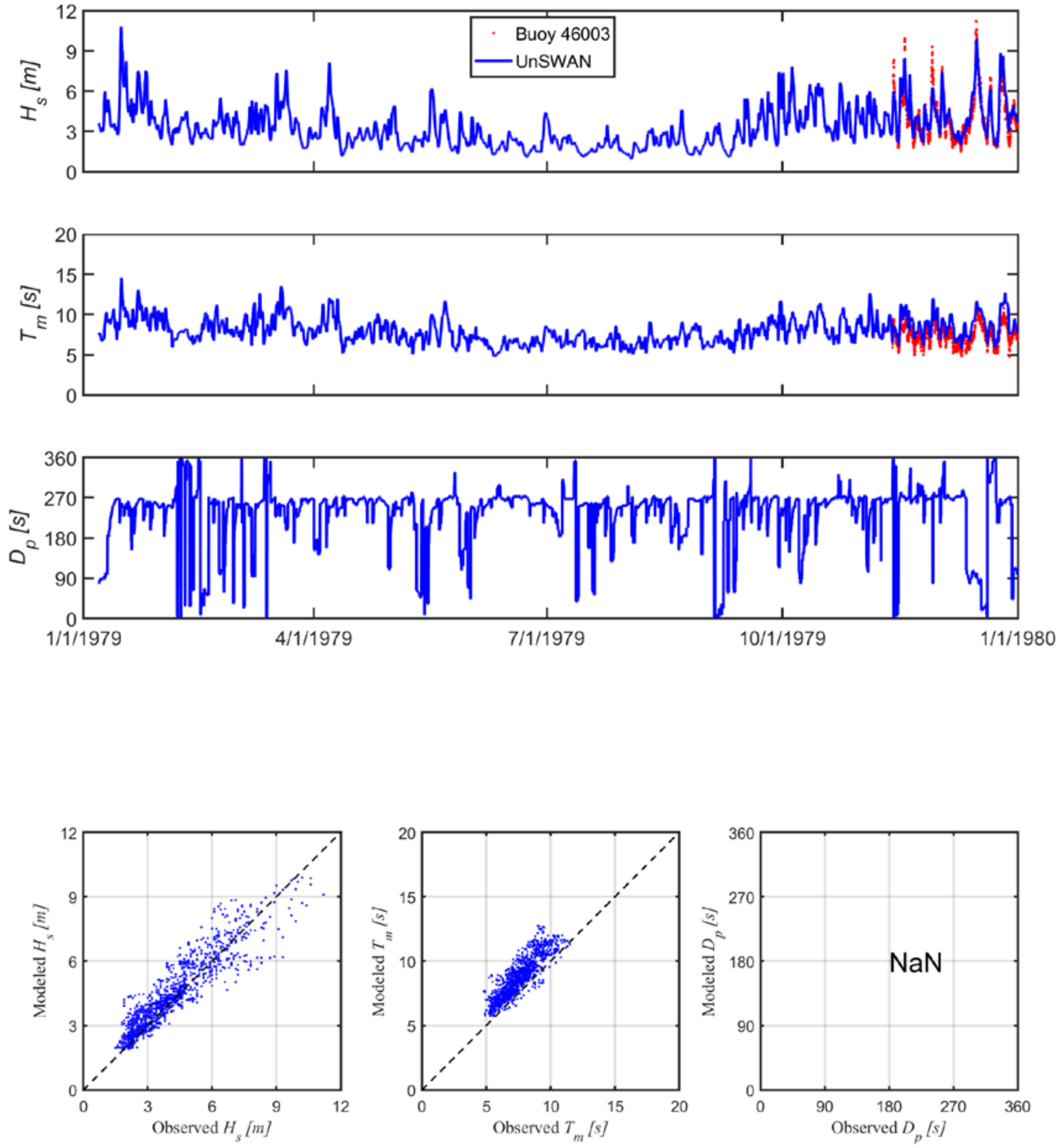

Figure B.183. Comparisons of time series (top) and scatter plots (bottom) of the three UnSWAN model-simulated bulk parameters with observed data at NDBC Buoy 46003 for 1979.

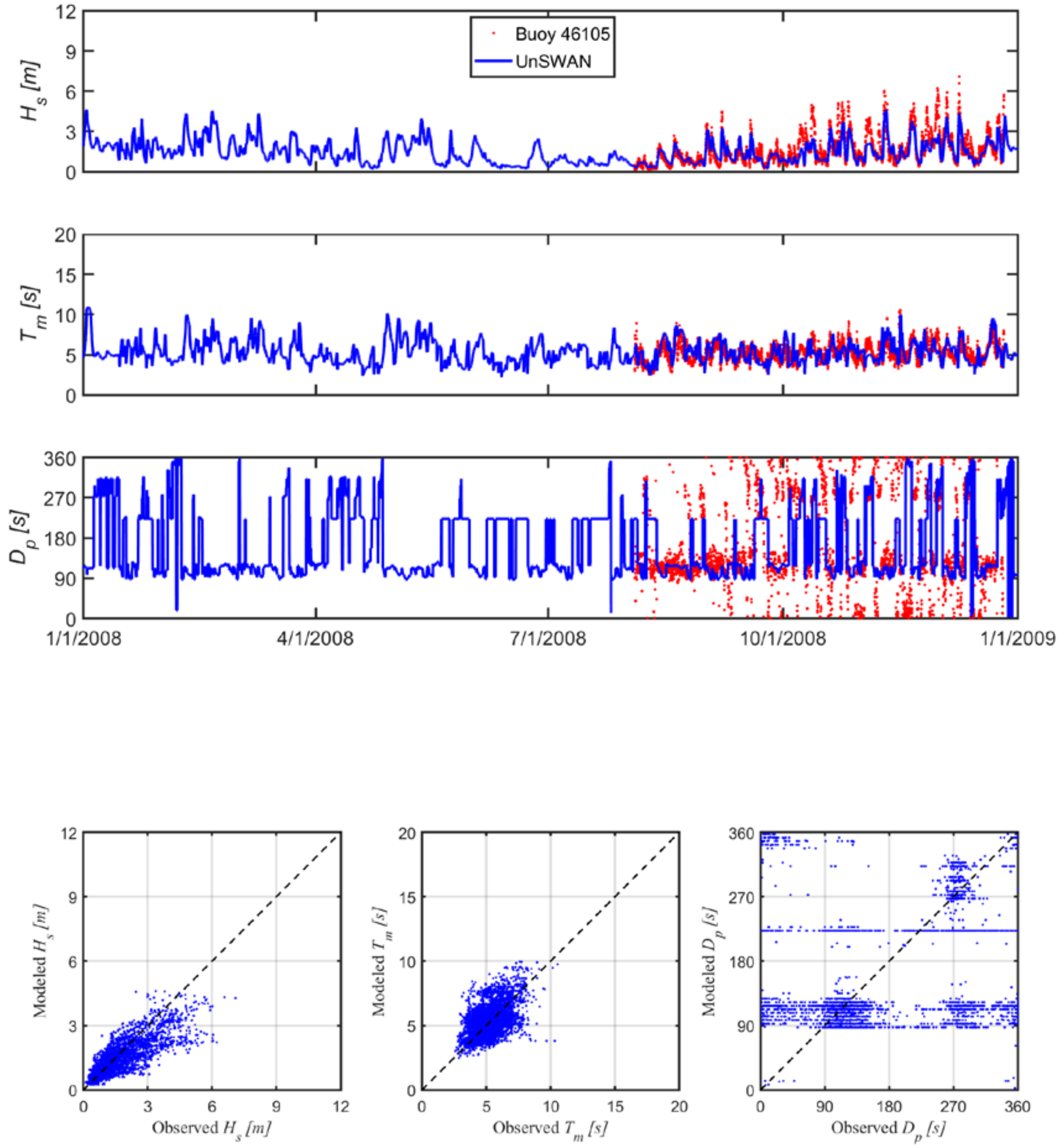

Figure B.184. Comparisons of time series (top) and scatter plots (bottom) of the three UnSWAN model-simulated bulk parameters with observed data at NDBC Buoy 46105 for 2008.

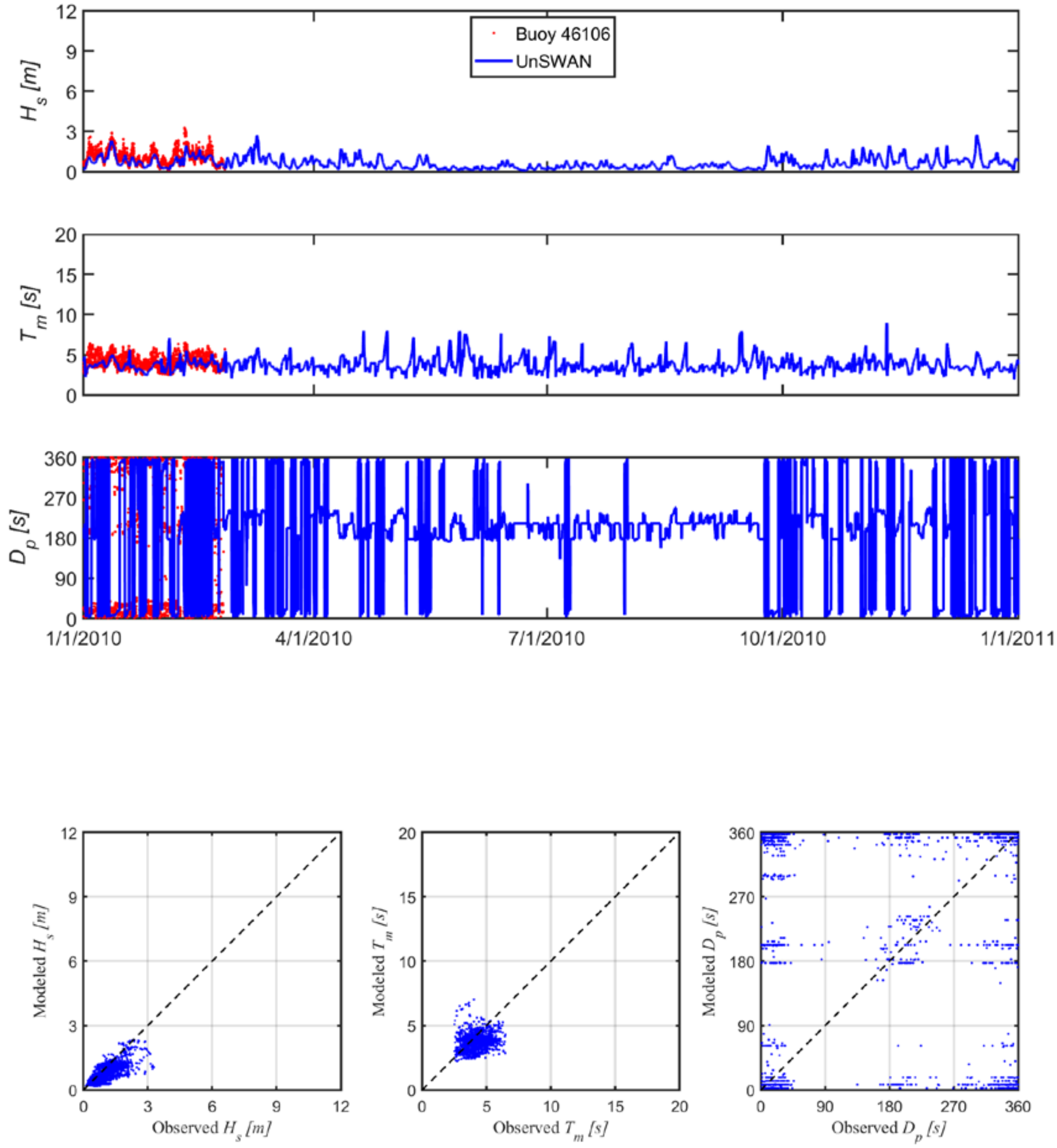

Figure B.185. Comparisons of time series (top) and scatter plots (bottom) of the three UnSWAN model-simulated bulk parameters with observed data at NDBC Buoy 46106 for 2010.

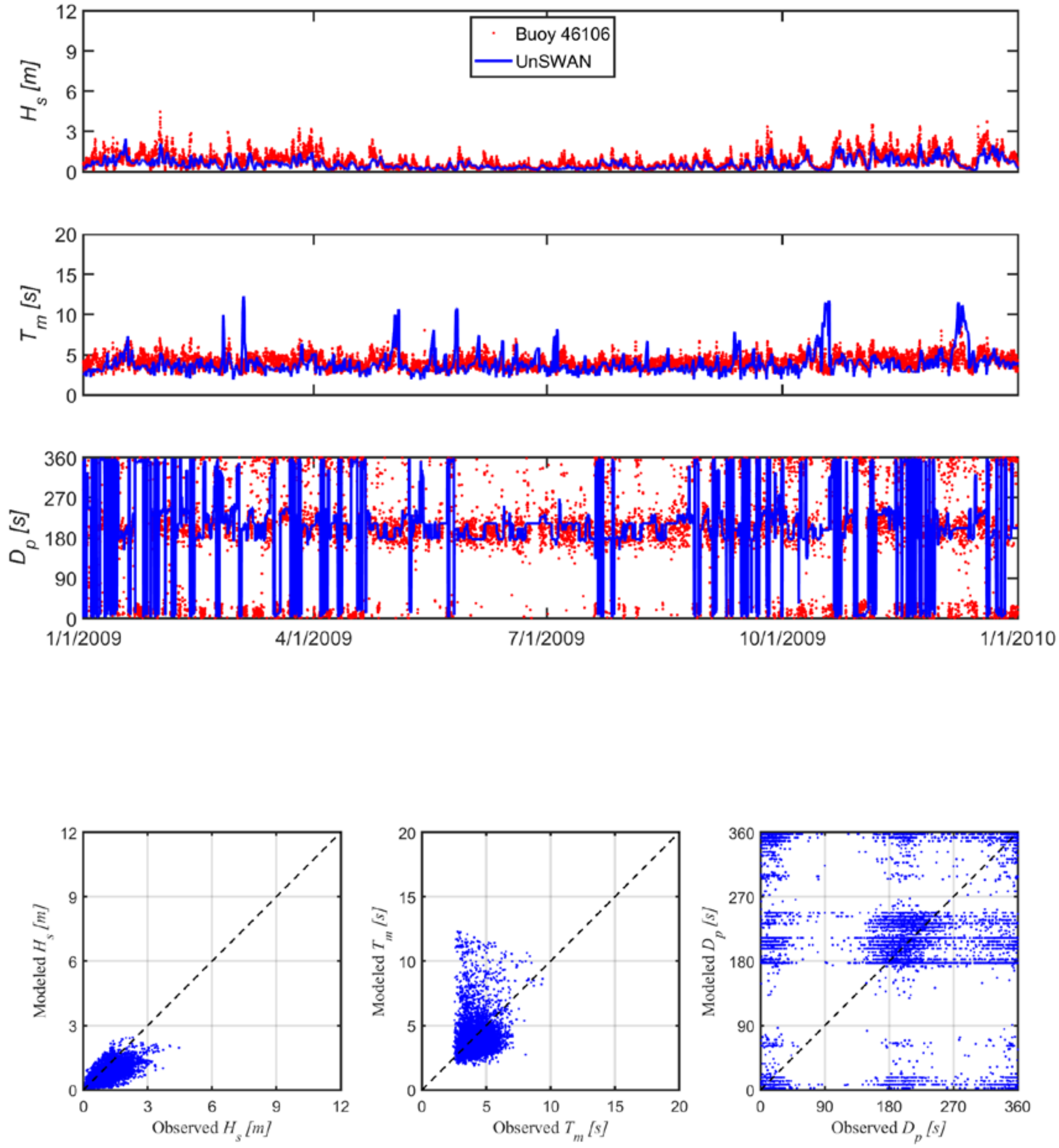

Figure B.186. Comparisons of time series (top) and scatter plots (bottom) of the three UnSWAN model-simulated bulk parameters with observed data at NDBC Buoy 46106 for 2009.

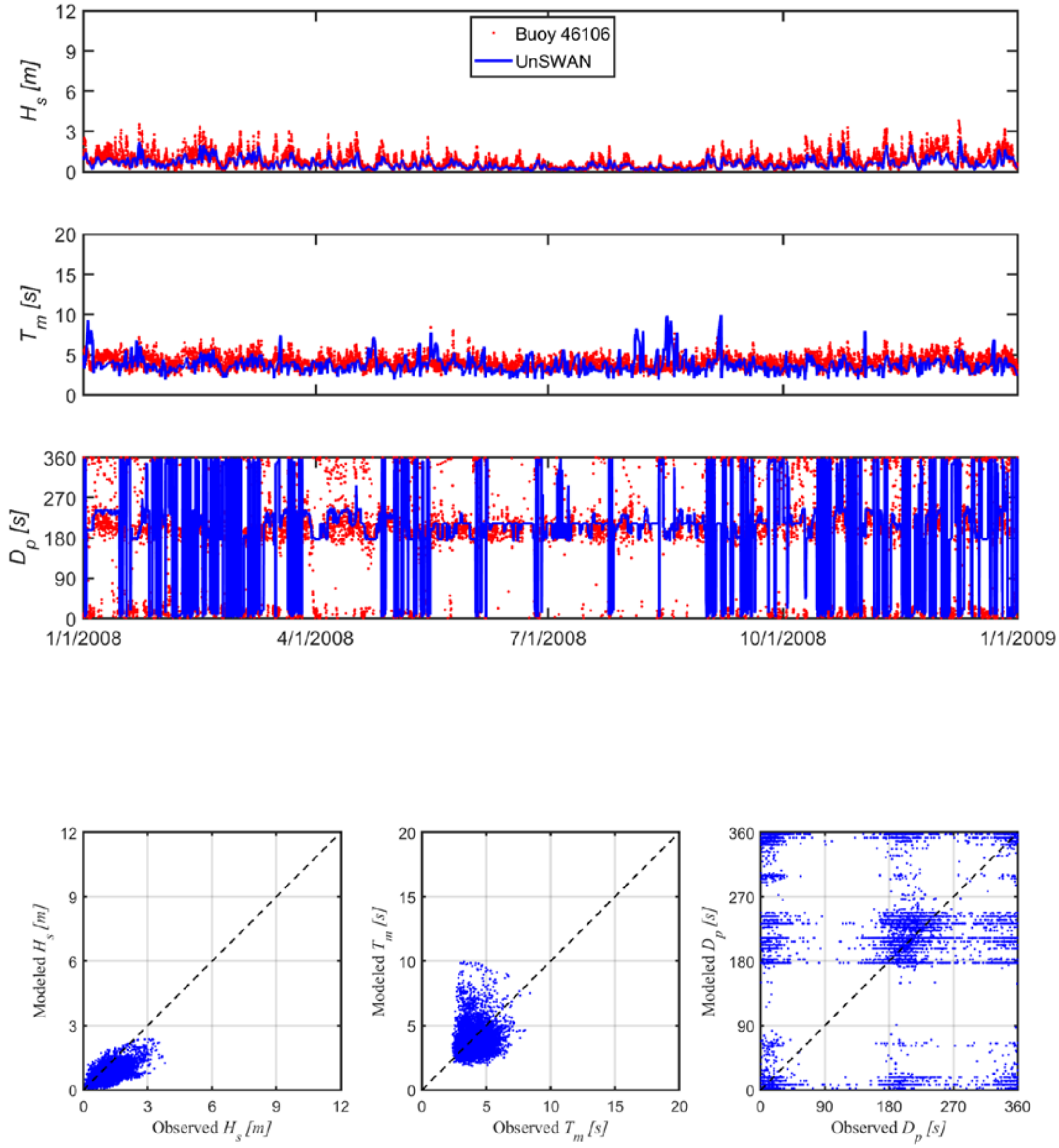

Figure B.187. Comparisons of time series (top) and scatter plots (bottom) of the three UnSWAN model-simulated bulk parameters with observed data at NDBC Buoy 46106 for 2008.

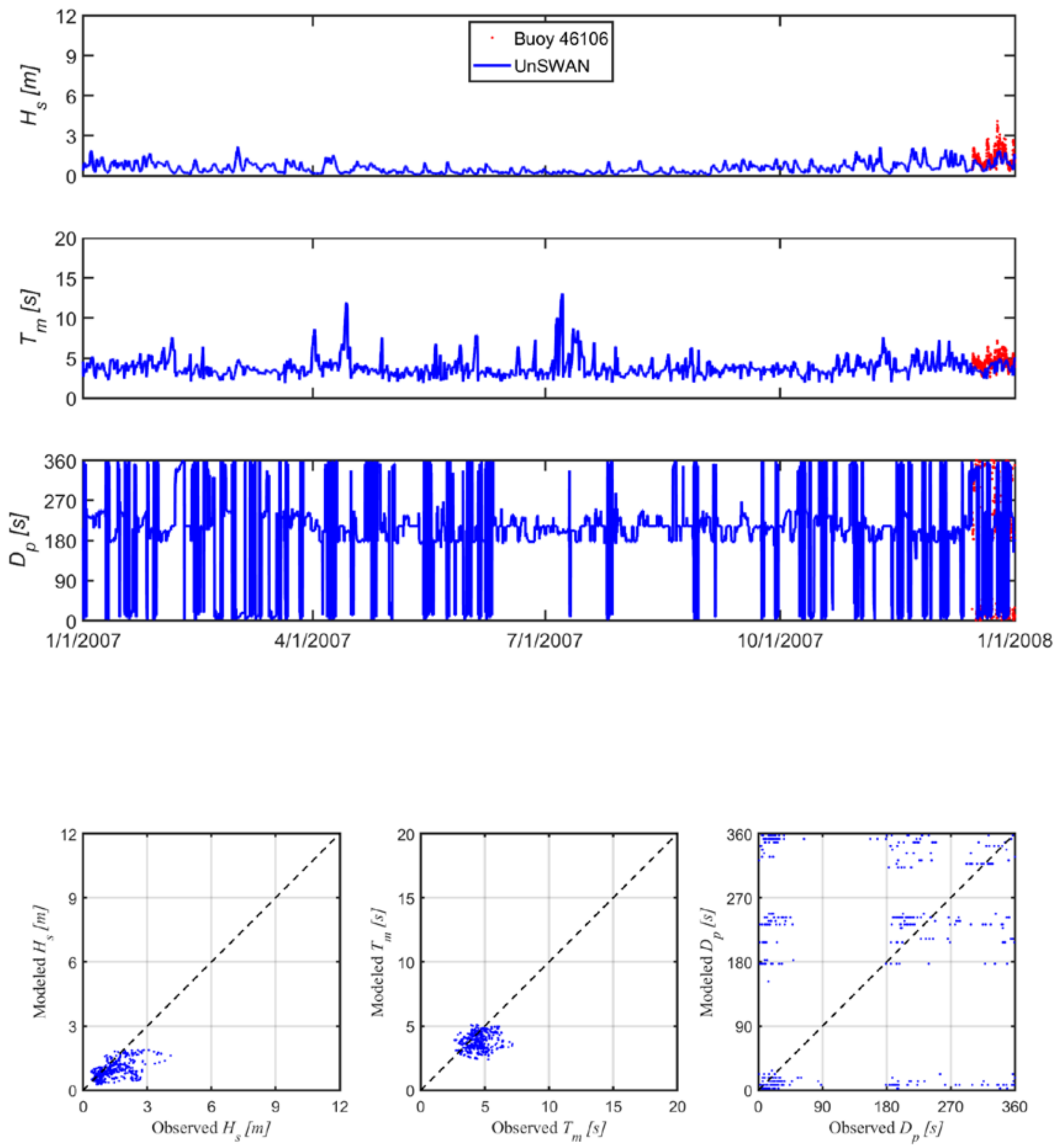

Figure B.188. Comparisons of time series (top) and scatter plots (bottom) of the three UnSWAN model-simulated bulk parameters with observed data at NDBC Buoy 46106 for 2007.

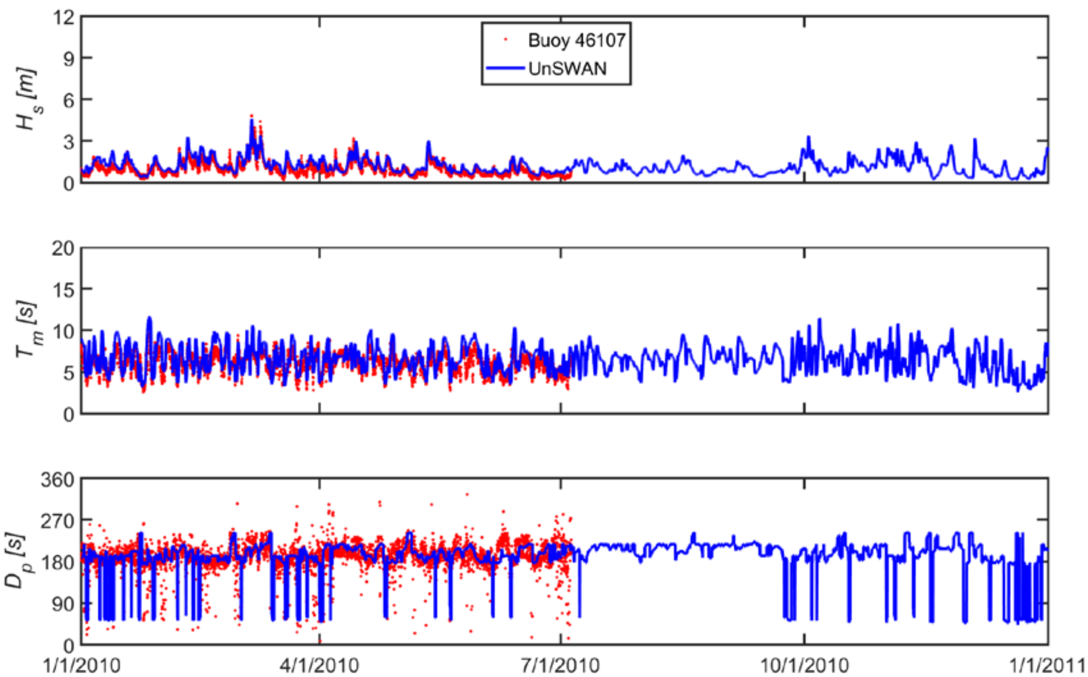

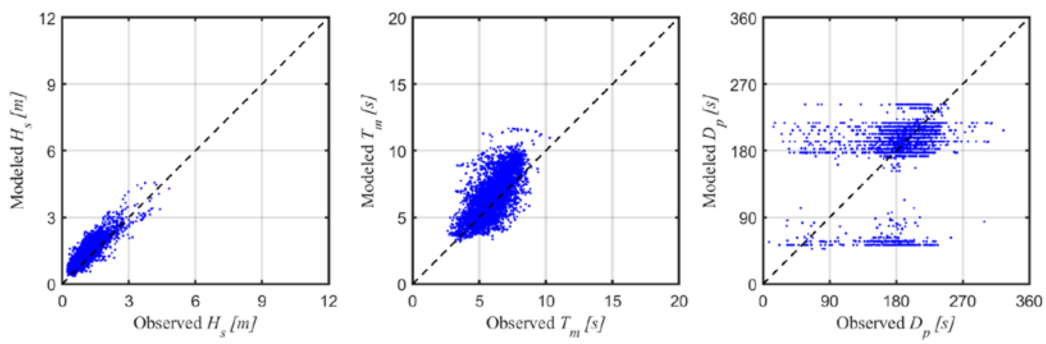

Figure B.189. Comparisons of time series (top) and scatter plots (bottom) of the three UnSWAN model-simulated bulk parameters with observed data at NDBC Buoy 46107 for 2010.

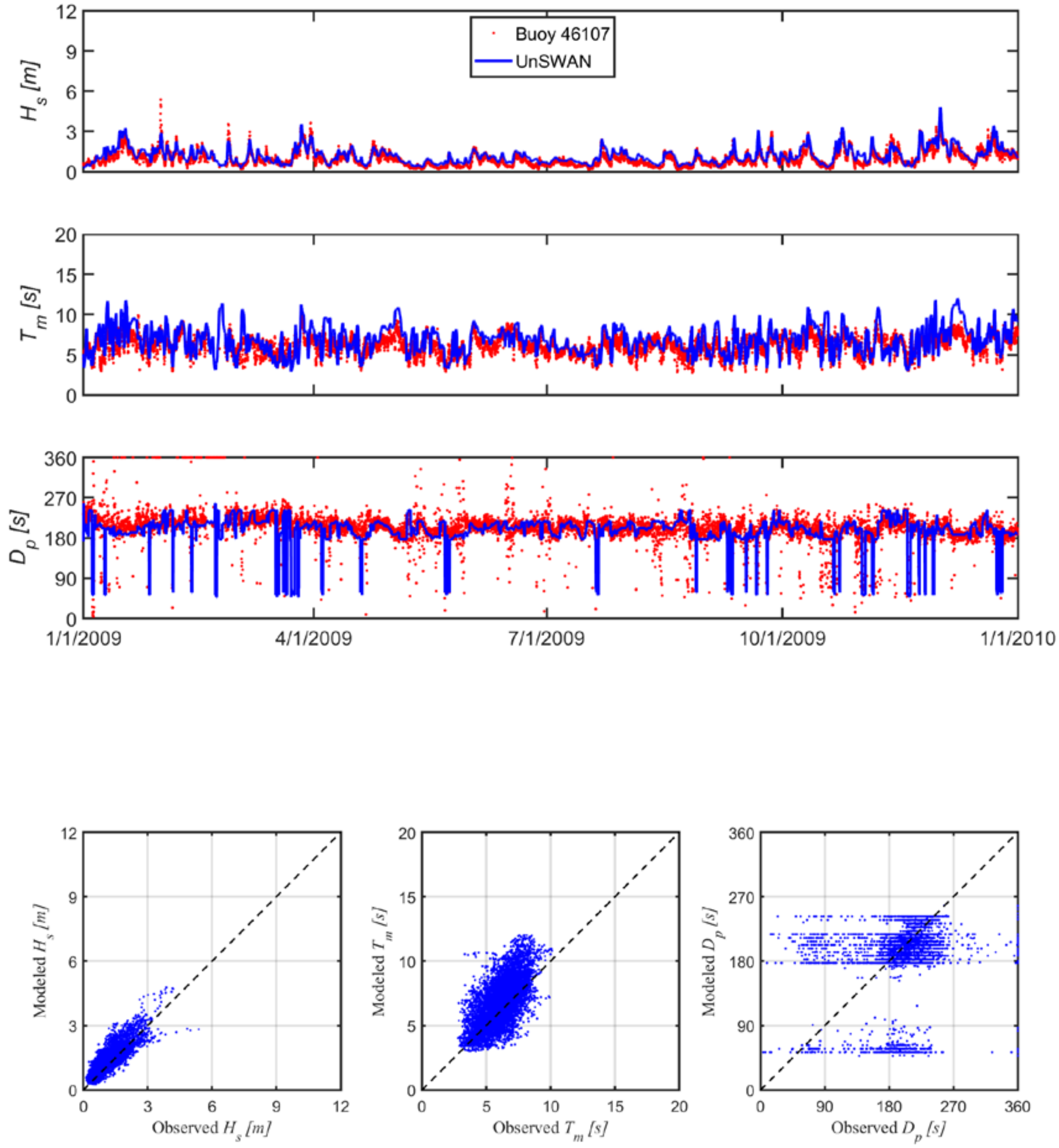

Figure B.190. Comparisons of time series (top) and scatter plots (bottom) of the three UnSWAN model-simulated bulk parameters with observed data at NDBC Buoy 46107 for 2009.

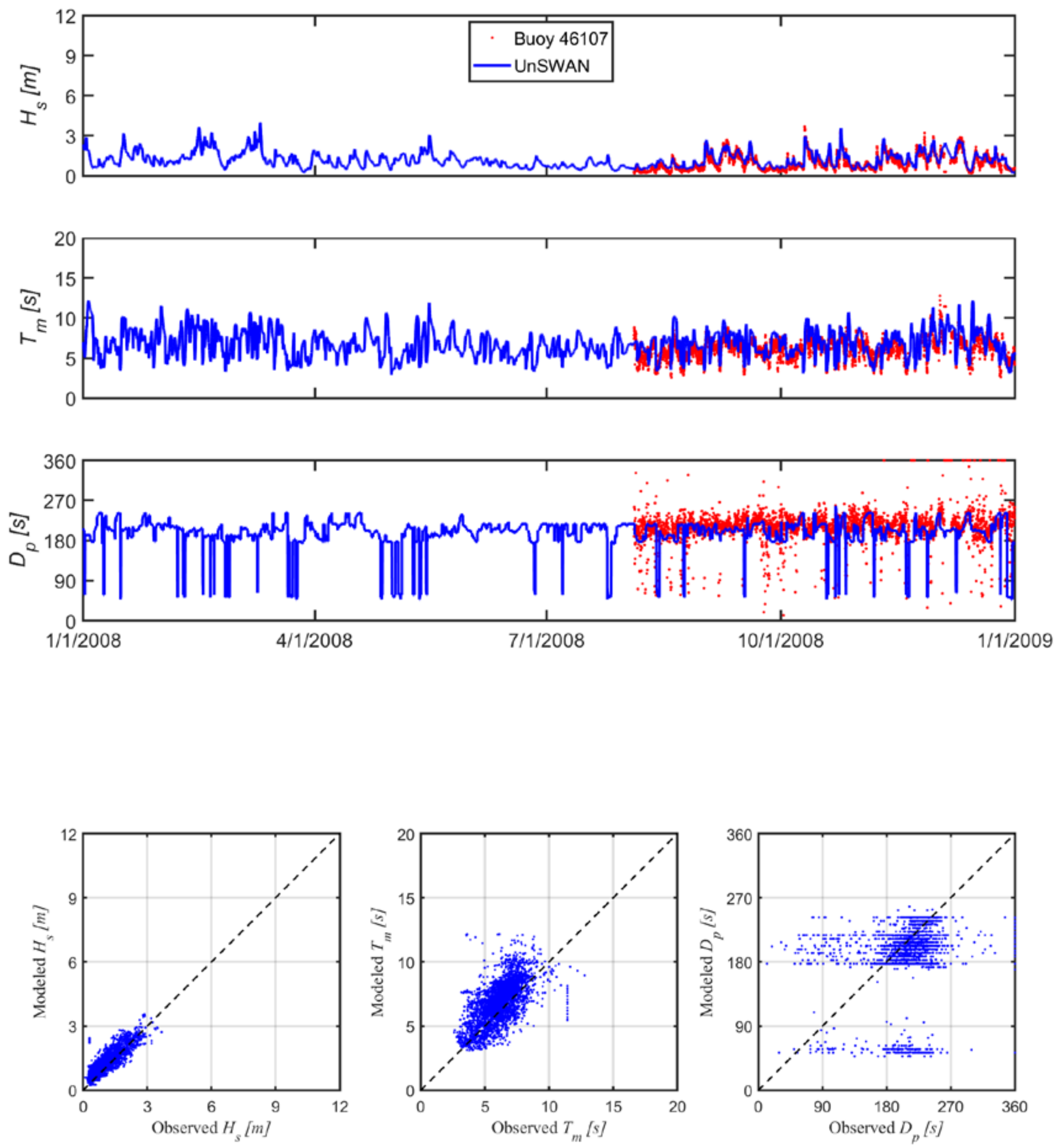

Figure B.191. Comparisons of time series (top) and scatter plots (bottom) of the three UnSWAN model-simulated bulk parameters with observed data at NDBC Buoy 46107 for 2008.

Appendix C – Performance Metrics for Simulated Wave Bulk Parameters

Table C.1. UnSWAN performance metrics for NDBC Station 46001 for 2010.

Parameter	RMSE	PE (%)	SI	Bias	Bias (%)	R
H_s (m)	0.47	11.0	0.17	0.16	6.1	0.94
T_m (s)	1.6	22.1	0.20	1.4	21.8	0.87

Table C.2. UnSWAN performance metrics for NDBC Station 46001 for 2009.

Parameter	RMSE	PE (%)	SI	Bias	Bias (%)	R
H_s (m)	0.44	9.2	0.16	0.11	4.4	0.95
T_m (s)	1.4	19.9	0.19	1.2	19.7	0.89

Table C.3. UnSWAN performance metrics for NDBC Station 46001 for 2008.

Parameter	RMSE	PE (%)	SI	Bias	Bias (%)	R
H_s (m)	0.47	9.3	0.17	0.11	4.0	0.95
T_m (s)	1.4	20.5	0.19	1.3	20.1	0.88

Table C.4. UnSWAN performance metrics for NDBC Station 46001 for 2007.

Parameter	RMSE	PE (%)	SI	Bias	Bias (%)	R
H_s (m)	0.45	4.6	0.14	0.03	0.9	0.96
T_m (s)	1.4	18.8	0.18	1.2	18.5	0.89

Table C.5. UnSWAN performance metrics for NDBC Station 46001 for 2006.

Parameter	RMSE	PE (%)	SI	Bias	Bias (%)	R
H_s (m)	0.41	4.9	0.16	0.02	0.8	0.95
T_m (s)	1.1	13.7	0.15	0.9	13.5	0.89

Table C.6. UnSWAN performance metrics for NDBC Station 46001 for 2005.

Parameter	RMSE	PE (%)	SI	Bias	Bias (%)	R
H_s (m)	0.44	5.9	0.17	0.05	1.7	0.95
T_m (s)	1.1	11.7	0.15	0.8	11.8	0.88

Table C.7. UnSWAN performance metrics for NDBC Station 46001 for 2004.

Parameter	RMSE	PE (%)	SI	Bias	Bias (%)	R
H_s (m)	0.44	3.1	0.16	-0.06	-2.2	0.96
T_m (s)	0.9	9.3	0.12	0.6	9.2	0.90

Table C.8. UnSWAN performance metrics for NDBC Station 46001 for 2003.

Parameter	RMSE	PE (%)	SI	Bias	Bias (%)	R
H_s (m)	0.42	4.3	0.16	0.01	0.3	0.95
T_m (s)	1.0	10.8	0.13	0.7	10.8	0.88

Table C.9. UnSWAN performance metrics for NDBC Station 46001 for 2002.

Parameter	RMSE	PE (%)	SI	Bias	Bias (%)	R
H_s (m)	0.42	4.4	0.15	0.00	0.0	0.96
T_m (s)	1.0	10.8	0.14	0.7	11.0	0.90

Table C.10. UnSWAN performance metrics for NDBC Station 46001 for 2001.

Parameter	RMSE	PE (%)	SI	Bias	Bias (%)	R
H_s (m)	0.47	3.3	0.17	-0.04	-1.4	0.96
T_m (s)	1.1	11.7	0.14	0.8	11.8	0.90

Table C.11. UnSWAN performance metrics for NDBC Station 46001 for 2000

Parameter	RMSE	PE (%)	SI	Bias	Bias (%)	R
H_s (m)	0.50	3.1	0.18	-0.03	-1.0	0.94
T_m (s)	1.2	12.0	0.15	0.8	12.3	0.90

Table C.12. UnSWAN performance metrics for NDBC Station 46001 for 1999.

Parameter	RMSE	PE (%)	SI	Bias	Bias (%)	R
H_s (m)	0.52	4.8	0.18	0.03	1.1	0.93
T_m (s)	1.2	13.0	0.16	0.9	13.0	0.87

Table C.13. UnSWAN performance metrics for NDBC Station 46001 for 1998.

Parameter	RMSE	PE (%)	SI	Bias	Bias (%)	R
H_s (m)	0.47	5.3	0.16	0.04	1.6	0.94
T_m (s)	1.2	13.6	0.16	0.9	13.7	0.88

Table C.14. UnSWAN performance metrics for NDBC Station 46001 for 1997.

Parameter	RMSE	PE (%)	SI	Bias	Bias (%)	R
H_s (m)	0.46	7.8	0.17	0.12	4.4	0.94
T_m (s)	1.3	14.9	0.17	1.0	15.0	0.87

Table C.15. UnSWAN performance metrics for NDBC Station 46001 for 1996.

Parameter	RMSE	PE (%)	SI	Bias	Bias (%)	R
H_s (m)	0.41	4.5	0.16	0.00	0.0	0.95
T_m (s)	1.0	11.1	0.14	0.7	11.0	0.88

Table C.16. UnSWAN performance metrics for NDBC Station 46001 for 1995

Parameter	RMSE	PE (%)	SI	Bias	Bias (%)	R
H_s (m)	0.44	5.7	0.16	0.05	1.9	0.94
T_m (s)	1.1	12.5	0.15	0.8	12.7	0.88

Table C.17. UnSWAN performance metrics for NDBC Station 46001 for 1994.

Parameter	RMSE	PE (%)	SI	Bias	Bias (%)	R
H_s (m)	0.47	8.7	0.17	0.04	1.6	0.96
T_m (s)	1.0	12.0	0.14	0.8	11.7	0.88

Table C.18. UnSWAN performance metrics for NDBC Station 46001 for 1993.

Parameter	RMSE	PE (%)	SI	Bias	Bias (%)	R
H_s (m)	0.46	9.8	0.16	0.13	5.1	0.94
T_m (s)	1.3	15.6	0.17	1.1	15.5	0.87

Table C.19. UnSWAN performance metrics for NDBC Station 46001 for 1992.

Parameter	RMSE	PE (%)	SI	Bias	Bias (%)	R
H_s (m)	0.47	8.4	0.17	0.12	4.3	0.94
T_m (s)	1.3	15.0	0.17	1.0	15.1	0.87

Table C.20. UnSWAN performance metrics for NDBC Station 46001 for 1991.

Parameter	RMSE	PE (%)	SI	Bias	Bias (%)	R
H_s (m)	0.52	11.6	0.18	0.17	6.2	0.94
T_m (s)	1.4	16.2	0.17	1.1	16.1	0.87

Table C.21. UnSWAN performance metrics for NDBC Station 46001 for 1990

Parameter	RMSE	PE (%)	SI	Bias	Bias (%)	R
H_s (m)	0.56	6.3	0.17	0.06	1.8	0.93
T_m (s)	1.3	15.0	0.17	1.0	14.8	0.85

Table C.22. UnSWAN performance metrics for NDBC Station 46001 for 1989.

Parameter	RMSE	PE (%)	SI	Bias	Bias (%)	R
H_s (m)	0.47	10.7	0.17	0.13	4.8	0.94
T_m (s)	1.3	16.2	0.17	1.0	15.8	0.85

Table C.23. UnSWAN performance metrics for NDBC Station 46001 for 1988.

Parameter	RMSE	PE (%)	SI	Bias	Bias (%)	R
H_s (m)	0.48	7.0	0.16	0.08	2.8	0.95
T_m (s)	1.4	17.0	0.17	1.2	16.9	0.90

Table C.24. UnSWAN performance metrics for NDBC Station 46001 for 1987.

Parameter	RMSE	PE (%)	SI	Bias	Bias (%)	R
H_s (m)	0.51	9.3	0.17	0.13	4.4	0.94
T_m (s)	1.5	19.5	0.19	1.3	19.2	0.86

Table C.25. UnSWAN performance metrics for NDBC Station 46001 for 1986.

Parameter	RMSE	PE (%)	SI	Bias	Bias (%)	R
H_s (m)	0.44	10.2	0.15	0.16	6.0	0.95
T_m (s)	1.3	16.7	0.17	1.1	16.6	0.89

Table C.26. UnSWAN performance metrics for NDBC Station 46001 for 1985

Parameter	RMSE	PE (%)	SI	Bias	Bias (%)	R
H_s (m)	0.50	7.4	0.17	0.06	1.9	0.94
T_m (s)	1.4	16.2	0.17	1.1	16.1	0.88

Table C.27. UnSWAN performance metrics for NDBC Station 46001 for 1984.

Parameter	RMSE	PE (%)	SI	Bias	Bias (%)	R
H_s (m)	0.47	9.3	0.17	0.09	3.2	0.94
T_m (s)	1.8	26.5	0.23	1.6	25.3	0.80

Table C.28. UnSWAN performance metrics for NDBC Station 46001 for 1983.

Parameter	RMSE	PE (%)	SI	Bias	Bias (%)	R
H_s (m)	0.47	9.3	0.17	0.09	3.2	0.94
T_m (s)	1.8	26.5	0.23	1.6	25.3	0.80

Table C.29. UnSWAN performance metrics for NDBC Station 46001 for 1982.

Parameter	RMSE	PE (%)	SI	Bias	Bias (%)	R
H_s (m)	0.51	10.6	0.18	0.06	2.1	0.94
T_m (s)	1.6	23.3	0.21	1.4	21.4	0.78

Table C.30. UnSWAN performance metrics for NDBC Station 46001 for 1981.

Parameter	RMSE	PE (%)	SI	Bias	Bias (%)	R
H_s (m)	0.52	13.5	0.18	0.16	6.1	0.94
T_m (s)	1.4	17.6	0.18	1.1	16.9	0.85

Table C.31. UnSWAN performance metrics for NDBC Station 46001 for 1980.

Parameter	RMSE	PE (%)	SI	Bias	Bias (%)	R
H_s (m)	0.56	16.0	0.19	0.23	8.5	0.92
T_m (s)	1.3	16.1	0.17	1.1	15.4	0.83

Table C.32. UnSWAN performance metrics for NDBC Station 46001 for 1979.

Parameter	RMSE	PE (%)	SI	Bias	Bias (%)	R
H_s (m)	0.61	17.6	0.20	0.31	11.4	0.93
T_m (s)	1.2	10.4	0.15	0.7	10.4	0.83

Table C.33. UnSWAN performance metrics for NDBC Station 46060 for 2010.

Parameter	RMSE	PE (%)	SI	Bias	Bias (%)	R
H_s (m)	0.28	16.3	0.34	0.06	8.5	0.82
T_m (s)	2.1	25.7	0.34	1.1	21.8	0.44
D_p (deg)	73.4	-	-	2	-	0.26

Table C.34. UnSWAN performance metrics for NDBC Station 46060 for 2009.

Parameter	RMSE	PE (%)	SI	Bias	Bias (%)	R
H_s (m)	0.29	16.0	0.40	0.04	5.3	0.80
T_m (s)	2.3	37.4	0.37	1.5	32.4	0.50
D_p (deg)	65.5	-	-	-2	-	0.42

Table C.35. UnSWAN performance metrics for NDBC Station 46060 for 2008.

Parameter	RMSE	PE (%)	SI	Bias	Bias (%)	R
H_s (m)	0.27	16.3	0.37	0.03	4.1	0.83
T_m (s)	2.4	39.2	0.39	1.6	35.2	0.44
D_p (deg)	63.4	-	-	5	-	0.41

Table C.36. UnSWAN performance metrics for NDBC Station 46060 for 2007.

Parameter	RMSE	PE (%)	SI	Bias	Bias (%)	R
H_s (m)	0.26	8.6	0.36	0.00	0.0	0.85
T_m (s)	2.5	41.2	0.39	1.7	36.2	0.47
D_p (deg)	66.9	-	-	17	-	0.27

Table C.37. UnSWAN performance metrics for NDBC Station 46060 for 2006.

Parameter	RMSE	PE (%)	SI	Bias	Bias (%)	R
H_s (m)	0.29	5.7	0.41	-0.03	-4.4	0.82
T_m (s)	2.3	36.2	0.39	1.4	31.2	0.42

Table C.38. UnSWAN performance metrics for NDBC Station 46060 for 2005.

Parameter	RMSE	PE (%)	SI	Bias	Bias (%)	R
H_s (m)	0.29	9.6	0.42	0.00	-0.4	0.80
T_m (s)	2.4	40.5	0.39	1.6	35.1	0.38

Table C.39. UnSWAN performance metrics for NDBC Station 46060 for 2004.

Parameter	RMSE	PE (%)	SI	Bias	Bias (%)	R
H_s (m)	0.26	20.8	0.41	0.04	6.7	0.81
T_m (s)	2.0	30.1	0.32	1.3	26.1	0.51

Table C.40. UnSWAN performance metrics for NDBC Station 46060 for 2003.

Parameter	RMSE	PE (%)	SI	Bias	Bias (%)	R
H_s (m)	0.25	15.0	0.36	0.03	4.9	0.82
T_m (s)	1.9	17.6	0.31	0.8	14.5	0.50

Table C.41. UnSWAN performance metrics for NDBC Station 46060 for 2002.

Parameter	RMSE	PE (%)	SI	Bias	Bias (%)	R
H_s (m)	0.25	14.6	0.35	0.03	4.7	0.87
T_m (s)	2.0	25.2	0.33	1.1	22.1	0.47

Table C.42. UnSWAN performance metrics for NDBC Station 46060 for 2001.

Parameter	RMSE	PE (%)	SI	Bias	Bias (%)	R
H_s (m)	0.26	8.7	0.36	0.00	-0.7	0.88
T_m (s)	1.9	20.8	0.32	0.9	17.7	0.50

Table C.43. UnSWAN performance metrics for NDBC Station 46060 for 2000

Parameter	RMSE	PE (%)	SI	Bias	Bias (%)	R
H_s (m)	0.24	11.4	0.34	0.02	3.0	0.85
T_m (s)	2.0	25.8	0.32	1.1	21.6	0.53

Table C.44. UnSWAN performance metrics for NDBC Station 46060 for 1999.

Parameter	RMSE	PE (%)	SI	Bias	Bias (%)	R
H_s (m)	0.25	1.3	0.36	-0.04	-5.9	0.82
T_m (s)	2.0	24.8	0.34	1.1	21.0	0.46

Table C.45. UnSWAN performance metrics for NDBC Station 46060 for 1998.

Parameter	RMSE	PE (%)	SI	Bias	Bias (%)	R
H_s (m)	0.25	12.7	0.34	0.02	3.1	0.81
T_m (s)	1.8	20.8	0.30	0.9	17.6	0.51

Table C.46. UnSWAN performance metrics for NDBC Station 46060 for 1997.

Parameter	RMSE	PE (%)	SI	Bias	Bias (%)	R
H_s (m)	0.25	12.6	0.34	0.03	4.1	0.87
T_m (s)	2.1	28.7	0.34	1.3	25.8	0.53

Table C.47. UnSWAN performance metrics for NDBC Station 46060 for 1996.

Parameter	RMSE	PE (%)	SI	Bias	Bias (%)	R
H_s (m)	0.24	9.0	0.38	0.00	0.7	0.80
T_m (s)	1.9	22.5	0.33	1.0	19.1	0.55

Table C.48. UnSWAN performance metrics for NDBC Station 46060 for 1995

Parameter	RMSE	PE (%)	SI	Bias	Bias (%)	R
H_s (m)	0.25	14.6	0.37	0.02	2.7	0.80
T_m (s)	1.9	24.1	0.31	1.0	20.4	0.51

Table C.49. UnSWAN performance metrics for NDBC Station 46061 for 2010.

Parameter	RMSE	PE (%)	SI	Bias	Bias (%)	R
H_s (m)	0.52	23.6	0.28	0.28	17.6	0.91
T_m (s)	1.7	23.5	0.23	1.3	22.3	0.72

Table C.50. UnSWAN performance metrics for NDBC Station 46061 for 2009.

Parameter	RMSE	PE (%)	SI	Bias	Bias (%)	R
H_s (m)	0.46	22.6	0.27	0.22	14.9	0.92
T_m (s)	1.6	22.0	0.22	1.3	21.1	0.75

Table C.51. UnSWAN performance metrics for NDBC Station 46061 for 2008.

Parameter	RMSE	PE (%)	SI	Bias	Bias (%)	R
H_s (m)	0.46	22.4	0.25	0.22	13.4	0.92
T_m (s)	1.6	22.6	0.22	1.3	21.4	0.72

Table C.52. UnSWAN performance metrics for NDBC Station 46061 for 2007.

Parameter	RMSE	PE (%)	SI	Bias	Bias (%)	R
H_s (m)	0.45	20.2	0.25	0.19	11.9	0.92
T_m (s)	1.6	22.5	0.22	1.3	21.4	0.77

Table C.53. UnSWAN performance metrics for NDBC Station 46061 for 2006.

Parameter	RMSE	PE (%)	SI	Bias	Bias (%)	R
H_s (m)	0.42	13.9	0.25	0.11	6.9	0.92
T_m (s)	1.3	12.6	0.18	0.7	12.1	0.74

Table C.54. UnSWAN performance metrics for NDBC Station 46061 for 2005.

Parameter	RMSE	PE (%)	SI	Bias	Bias (%)	R
H_s (m)	0.41	13.8	0.24	0.12	7.4	0.93
T_m (s)	1.3	14.0	0.18	0.8	13.1	0.72

Table C.55. UnSWAN performance metrics for NDBC Station 46061 for 2004.

Parameter	RMSE	PE (%)	SI	Bias	Bias (%)	R
H_s (m)	0.39	14.8	0.23	0.11	7.4	0.92
T_m (s)	1.3	15.4	0.18	0.9	14.7	0.74

Table C.56. UnSWAN performance metrics for NDBC Station 46061 for 2003.

Parameter	RMSE	PE (%)	SI	Bias	Bias (%)	R
H_s (m)	0.41	12.1	0.25	0.10	6.5	0.91
T_m (s)	1.2	13.7	0.17	0.8	12.9	0.75

Table C.57. UnSWAN performance metrics for NDBC Station 46061 for 2002.

Parameter	RMSE	PE (%)	SI	Bias	Bias (%)	R
H_s (m)	0.44	13.6	0.25	0.14	8.6	0.93
T_m (s)	1.3	16.2	0.19	0.9	15.3	0.76

Table C.58. UnSWAN performance metrics for NDBC Station 46061 for 2001.

Parameter	RMSE	PE (%)	SI	Bias	Bias (%)	R
H_s (m)	0.44	14.7	0.25	0.13	7.8	0.93
T_m (s)	1.2	12.9	0.18	0.8	12.4	0.78

Table C.59. UnSWAN performance metrics for NDBC Station 46061 for 2000

Parameter	RMSE	PE (%)	SI	Bias	Bias (%)	R
H_s (m)	0.41	14.3	0.24	0.13	8.3	0.93
T_m (s)	1.3	14.0	0.18	0.8	13.0	0.76

Table C.60. UnSWAN performance metrics for NDBC Station 46061 for 1999.

Parameter	RMSE	PE (%)	SI	Bias	Bias (%)	R
H_s (m)	0.43	11.6	0.26	0.08	5.2	0.90
T_m (s)	1.4	14.5	0.19	0.8	13.7	0.72

Table C.61. UnSWAN performance metrics for NDBC Station 46061 for 1998.

Parameter	RMSE	PE (%)	SI	Bias	Bias (%)	R
H_s (m)	0.45	16.9	0.25	0.16	9.6	0.90
T_m (s)	1.2	12.1	0.17	0.7	11.5	0.75

Table C.62. UnSWAN performance metrics for NDBC Station 46061 for 1997.

Parameter	RMSE	PE (%)	SI	Bias	Bias (%)	R
H_s (m)	0.43	19.7	0.24	0.20	12.3	0.94
T_m (s)	1.4	14.9	0.19	0.9	14.1	0.73

Table C.63. UnSWAN performance metrics for NDBC Station 46061 for 1996.

Parameter	RMSE	PE (%)	SI	Bias	Bias (%)	R
H_s (m)	0.38	16.4	0.25	0.12	8.7	0.91
T_m (s)	1.3	14.5	0.19	0.8	13.4	0.74

Table C.64. UnSWAN performance metrics for NDBC Station 46061 for 1995

Parameter	RMSE	PE (%)	SI	Bias	Bias (%)	R
H_s (m)	0.34	18.8	0.23	0.15	11.5	0.94
T_m (s)	1.3	17.3	0.19	1.0	16.3	0.72

Table C.65. UnSWAN performance metrics for NDBC Station 46066 for 2010.

Parameter	RMSE	PE (%)	SI	Bias	Bias (%)	R
H_s (m)	0.52	14.3	0.17	0.25	9.1	0.95
T_m (s)	1.7	24.5	0.22	1.5	24.0	0.88

Table C.66. UnSWAN performance metrics for NDBC Station 46066 for 2009.

Parameter	RMSE	PE (%)	SI	Bias	Bias (%)	R
H_s (m)	0.48	7.7	0.15	0.11	3.7	0.96
T_m (s)	1.5	21.2	0.19	1.4	21.0	0.90

Table C.67. UnSWAN performance metrics for NDBC Station 46066 for 2008.

Parameter	RMSE	PE (%)	SI	Bias	Bias (%)	R
H_s (m)	0.46	11.9	0.16	0.16	5.9	0.96
T_m (s)	1.5	20.9	0.19	1.3	20.5	0.90

Table C.68. UnSWAN performance metrics for NDBC Station 46066 for 2007.

Parameter	RMSE	PE (%)	SI	Bias	Bias (%)	R
H_s (m)	0.46	7.6	0.15	0.08	2.7	0.96
T_m (s)	1.4	19.6	0.18	1.3	19.2	0.91

Table C.69. UnSWAN performance metrics for NDBC Station 46066 for 2006.

Parameter	RMSE	PE (%)	SI	Bias	Bias (%)	R
H_s (m)	0.50	4.7	0.16	0.03	0.9	0.94
T_m (s)	1.4	17.9	0.18	1.2	17.7	0.88

Table C.70. UnSWAN performance metrics for NDBC Station 46066 for 2005.

Parameter	RMSE	PE (%)	SI	Bias	Bias (%)	R
H_s (m)	0.39	7.8	0.16	0.06	2.6	0.95
T_m (s)	1.2	16.1	0.17	1.0	15.9	0.87

Table C.71. UnSWAN performance metrics for NDBC Station 46066 for 2004.

Parameter	RMSE	PE (%)	SI	Bias	Bias (%)	R
H_s (m)	0.52	3.2	0.16	-0.04	-1.3	0.95
T_m (s)	1.2	14.0	0.15	1.0	13.6	0.89

Table C.72. UnSWAN performance metrics for NDBC Station 46066 for 2003.

Parameter	RMSE	PE (%)	SI	Bias	Bias (%)	R
H_s (m)	0.46	4.2	0.15	0.02	0.5	0.95
T_m (s)	1.0	12.0	0.14	0.8	11.9	0.89

Table C.73. UnSWAN performance metrics for NDBC Station 46066 for 2002.

Parameter	RMSE	PE (%)	SI	Bias	Bias (%)	R
H_s (m)	0.44	5.4	0.15	0.03	1.1	0.96
T_m (s)	1.1	12.5	0.14	0.9	12.5	0.90

Table C.74. UnSWAN performance metrics for NDBC Station 46066 for 2001.

Parameter	RMSE	PE (%)	SI	Bias	Bias (%)	R
H_s (m)	0.51	3.9	0.16	-0.02	-0.6	0.96
T_m (s)	1.1	12.8	0.14	0.9	12.6	0.92

Table C.75. UnSWAN performance metrics for NDBC Station 46066 for 2000

Parameter	RMSE	PE (%)	SI	Bias	Bias (%)	R
H_s (m)	0.39	12.7	0.17	0.14	6.3	0.95
T_m (s)	0.9	11.7	0.13	0.7	11.4	0.86

Table C.76. UnSWAN performance metrics for NDBC Station 46070 for 2009.

Parameter	RMSE	PE (%)	SI	Bias	Bias (%)	R
H_s (m)	0.43	3.1	0.17	-0.07	-2.8	0.97
T_m (s)	1.1	15.9	0.16	0.9	15.9	0.92

Table C.77. UnSWAN performance metrics for NDBC Station 46070 for 2008.

Parameter	RMSE	PE (%)	SI	Bias	Bias (%)	R
H_s (m)	0.43	3.1	0.17	-0.07	-2.8	0.97
T_m (s)	1.1	15.9	0.16	0.9	15.9	0.92

Table C.78. UnSWAN performance metrics for NDBC Station 46070 for 2007.

Parameter	RMSE	PE (%)	SI	Bias	Bias (%)	R
H_s (m)	0.45	0.2	0.18	-0.13	-4.7	0.96
T_m (s)	1.2	16.6	0.17	1.0	16.5	0.89

Table C.79. UnSWAN performance metrics for NDBC Station 46070 for 2006.

Parameter	RMSE	PE (%)	SI	Bias	Bias (%)	R
H_s (m)	0.47	-3.4	0.18	-0.16	-5.8	0.94
T_m (s)	1.1	14.7	0.16	0.9	14.9	0.87

Table C.80. UnSWAN performance metrics for NDBC Station 46071 for 2009.

Parameter	RMSE	PE (%)	SI	Bias	Bias (%)	R
H_s (m)	0.50	12.2	0.17	0.12	4.4	0.97
T_m (s)	1.3	16.2	0.17	1.0	15.9	0.89

Table C.81. UnSWAN performance metrics for NDBC Station 46071 for 2008.

Parameter	RMSE	PE (%)	SI	Bias	Bias (%)	R
H_s (m)	0.46	10.8	0.18	0.11	4.7	0.96
T_m (s)	1.1	14.0	0.16	0.8	13.5	0.86

Table C.82. UnSWAN performance metrics for NDBC Station 46071 for 2007.

Parameter	RMSE	PE (%)	SI	Bias	Bias (%)	R
H_s (m)	0.49	14.6	0.21	0.14	6.4	0.94
T_m (s)	1.2	13.4	0.16	0.8	12.9	0.83

Table C.83. UnSWAN performance metrics for NDBC Station 46071 for 2006.

Parameter	RMSE	PE (%)	SI	Bias	Bias (%)	R
H_s (m)	0.60	7.4	0.21	0.05	1.8	0.94
T_m (s)	1.1	11.7	0.15	0.8	11.5	0.87

Table C.84. UnSWAN performance metrics for NDBC Station 46071 for 2005.

Parameter	RMSE	PE (%)	SI	Bias	Bias (%)	R
H_s (m)	0.51	8.0	0.19	0.06	2.4	0.94
T_m (s)	1.2	12.9	0.16	0.8	12.7	0.88

Table C.85. UnSWAN performance metrics for NDBC Station 46071 for 2004.

Parameter	RMSE	PE (%)	SI	Bias	Bias (%)	R
H_s (m)	0.65	0.5	0.17	-0.11	-2.8	0.94
T_m (s)	1.2	11.7	0.14	0.8	11.7	0.89

Table C.86. UnSWAN performance metrics for NDBC Station 46072 for 2010.

Parameter	RMSE	PE (%)	SI	Bias	Bias (%)	R
H_s (m)	0.71	3.0	0.18	-0.04	-1.1	0.83
T_m (s)	1.6	17.0	0.18	1.2	16.2	0.75

Table C.87. UnSWAN performance metrics for NDBC Station 46072 for 2009.

Parameter	RMSE	PE (%)	SI	Bias	Bias (%)	R
H_s (m)	0.53	10.4	0.17	0.12	4.5	0.94
T_m (s)	1.4	18.9	0.18	1.2	18.3	0.86

Table C.88. UnSWAN performance metrics for NDBC Station 46072 for 2008.

Parameter	RMSE	PE (%)	SI	Bias	Bias (%)	R
H_s (m)	0.49	7.4	0.18	0.02	0.8	0.96
T_m (s)	1.2	14.9	0.17	0.9	14.5	0.86

Table C.89. UnSWAN performance metrics for NDBC Station 46072 for 2007.

Parameter	RMSE	PE (%)	SI	Bias	Bias (%)	R
H_s (m)	0.66	1.6	0.17	-0.07	-1.7	0.90
T_m (s)	1.4	16.3	0.17	1.2	16.0	0.82

Table C.90. UnSWAN performance metrics for NDBC Station 46072 for 2006.

Parameter	RMSE	PE (%)	SI	Bias	Bias (%)	R
H_s (m)	0.55	5.7	0.19	0.00	-0.2	0.94
T_m (s)	1.0	9.4	0.14	0.6	9.4	0.85

Table C.91. UnSWAN performance metrics for NDBC Station 46072 for 2005.

Parameter	RMSE	PE (%)	SI	Bias	Bias (%)	R
H_s (m)	0.54	3.1	0.18	-0.03	-1.1	0.93
T_m (s)	1.1	11.0	0.14	0.8	11.0	0.87

Table C.92. UnSWAN performance metrics for NDBC Station 46072 for 2004.

Parameter	RMSE	PE (%)	SI	Bias	Bias (%)	R
H_s (m)	0.59	1.6	0.18	-0.08	-2.6	0.94
T_m (s)	1.1	11.6	0.14	0.8	11.4	0.85

Table C.93. UnSWAN performance metrics for NDBC Station 46072 for 2003.

Parameter	RMSE	PE (%)	SI	Bias	Bias (%)	R
H_s (m)	0.61	10.2	0.19	0.15	5.1	0.90
T_m (s)	1.2	11.6	0.15	0.8	11.3	0.78

Table C.94. UnSWAN performance metrics for NDBC Station 46072 for 2002.

Parameter	RMSE	PE (%)	SI	Bias	Bias (%)	R
H_s (m)	0.64	13.4	0.22	0.22	8.2	0.90
T_m (s)	1.1	8.0	0.14	0.6	7.8	0.77

Table C.95. UnSWAN performance metrics for NDBC Station 46073 for 2010.

Parameter	RMSE	PE (%)	SI	Bias	Bias (%)	R
H_s (m)	0.47	11.7	0.19	0.14	5.8	0.95
T_m (s)	1.0	10.9	0.15	0.7	10.9	0.87

Table C.96. UnSWAN performance metrics for NDBC Station 46073 for 2009.

Parameter	RMSE	PE (%)	SI	Bias	Bias (%)	R
H_s (m)	0.46	7.6	0.17	0.09	3.4	0.95
T_m (s)	0.9	8.3	0.13	0.5	8.5	0.89

Table C.97. UnSWAN performance metrics for NDBC Station 46073 for 2008.

Parameter	RMSE	PE (%)	SI	Bias	Bias (%)	R
H_s (m)	0.39	14.0	0.17	0.14	6.5	0.97
T_m (s)	0.7	2.9	0.10	0.2	3.3	0.91

Table C.98. UnSWAN performance metrics for NDBC Station 46073 for 2007.

Parameter	RMSE	PE (%)	SI	Bias	Bias (%)	R
H_s (m)	0.40	13.5	0.16	0.13	5.9	0.96
T_m (s)	0.7	3.6	0.10	0.3	4.0	0.91

Table C.99. UnSWAN performance metrics for NDBC Station 46073 for 2006.

Parameter	RMSE	PE (%)	SI	Bias	Bias (%)	R
H_s (m)	0.42	10.5	0.17	0.10	4.0	0.96
T_m (s)	0.7	4.2	0.10	0.3	4.6	0.92

Table C.100. UnSWAN performance metrics for NDBC Station 46073 for 2005.

Parameter	RMSE	PE (%)	SI	Bias	Bias (%)	R
H_s (m)	0.41	11.2	0.17	0.09	3.8	0.96
T_m (s)	0.6	3.8	0.09	0.3	4.0	0.92

Table C.101. UnSWAN performance metrics for NDBC Station 46075 for 2010.

Parameter	RMSE	PE (%)	SI	Bias	Bias (%)	R
H_s (m)	0.49	7.6	0.19	0.03	1.1	0.92
T_m (s)	1.1	13.3	0.16	0.8	12.5	0.81

Table C.102. UnSWAN performance metrics for NDBC Station 46075 for 2009.

Parameter	RMSE	PE (%)	SI	Bias	Bias (%)	R
H_s (m)	0.49	7.4	0.17	0.06	2.3	0.95
T_m (s)	1.1	11.0	0.14	0.7	10.9	0.86

Table C.103. UnSWAN performance metrics for NDBC Station 46075 for 2008.

Parameter	RMSE	PE (%)	SI	Bias	Bias (%)	R
H_s (m)	0.50	11.5	0.19	0.12	4.6	0.94
T_m (s)	1.1	13.1	0.16	0.8	12.9	0.87

Table C.104. UnSWAN performance metrics for NDBC Station 46075 for 2007.

Parameter	RMSE	PE (%)	SI	Bias	Bias (%)	R
H_s (m)	0.46	8.6	0.17	0.05	2.0	0.96
T_m (s)	1.0	11.2	0.14	0.7	11.1	0.89

Table C.105. UnSWAN performance metrics for NDBC Station 46075 for 2006.

Parameter	RMSE	PE (%)	SI	Bias	Bias (%)	R
H_s (m)	0.53	7.8	0.20	0.03	1.0	0.93
T_m (s)	1.0	8.3	0.13	0.6	8.2	0.84

Table C.106. UnSWAN performance metrics for NDBC Station 46075 for 2005.

Parameter	RMSE	PE (%)	SI	Bias	Bias (%)	R
H_s (m)	0.45	6.9	0.16	0.08	2.9	0.95
T_m (s)	1.1	11.6	0.15	0.8	11.8	0.90

Table C.107. UnSWAN performance metrics for NDBC Station 46075 for 2004.

Parameter	RMSE	PE (%)	SI	Bias	Bias (%)	R
H_s (m)	0.48	4.9	0.19	-0.06	-2.4	0.96
T_m (s)	0.8	8.4	0.12	0.5	7.9	0.86

Table C.108. UnSWAN performance metrics for NDBC Station 46076 for 2010.

Parameter	RMSE	PE (%)	SI	Bias	Bias (%)	R
H_s (m)	0.41	12.8	0.19	0.11	5.1	0.94
T_m (s)	1.7	24.1	0.24	1.3	22.7	0.69

Table C.109. UnSWAN performance metrics for NDBC Station 46076 for 2009.

Parameter	RMSE	PE (%)	SI	Bias	Bias (%)	R
H_s (m)	0.38	13.8	0.19	0.11	5.6	0.96
T_m (s)	1.5	21.5	0.21	1.2	20.5	0.82

Table C.110. UnSWAN performance metrics for NDBC Station 46076 for 2008.

Parameter	RMSE	PE (%)	SI	Bias	Bias (%)	R
H_s (m)	0.41	15.3	0.21	0.09	4.9	0.95
T_m (s)	1.3	16.8	0.18	0.9	15.6	0.74

Table C.111. UnSWAN performance metrics for NDBC Station 46076 for 2007.

Parameter	RMSE	PE (%)	SI	Bias	Bias (%)	R
H_s (m)	0.40	6.8	0.19	-0.01	-0.3	0.96
T_m (s)	1.2	14.6	0.17	0.8	13.9	0.79

Table C.112. UnSWAN performance metrics for NDBC Station 46076 for 2006.

Parameter	RMSE	PE (%)	SI	Bias	Bias (%)	R
H_s (m)	0.41	8.9	0.20	0.03	1.3	0.95
T_m (s)	1.2	13.7	0.17	0.8	13.2	0.83

Table C.113. UnSWAN performance metrics for NDBC Station 46076 for 2005.

Parameter	RMSE	PE (%)	SI	Bias	Bias (%)	R
H_s (m)	0.42	10.3	0.21	0.03	1.3	0.95
T_m (s)	1.2	15.8	0.18	0.9	14.9	0.82

Table C.114. UnSWAN performance metrics for NDBC Station 46077 for 2010.

Parameter	RMSE	PE (%)	SI	Bias	Bias (%)	R
H_s (m)	0.54	-16.7	0.56	-0.32	-25.0	0.59
T_m (s)	1.3	8.2	0.26	0.3	6.7	0.39

Table C.115. UnSWAN performance metrics for NDBC Station 46077 for 2009.

Parameter	RMSE	PE (%)	SI	Bias	Bias (%)	R
H_s (m)	0.52	-22.1	0.69	-0.33	-30.7	0.83
T_m (s)	1.3	9.5	0.26	0.3	7.1	0.41

Table C.116. UnSWAN performance metrics for NDBC Station 46077 for 2008.

Parameter	RMSE	PE (%)	SI	Bias	Bias (%)	R
H_s (m)	0.57	-21.6	0.68	-0.36	-30.1	0.81
T_m (s)	1.3	12.1	0.27	0.4	9.8	0.40

Table C.117. UnSWAN performance metrics for NDBC Station 46077 for 2007.

Parameter	RMSE	PE (%)	SI	Bias	Bias (%)	R
H_s (m)	0.55	-20.3	0.60	-0.35	-27.7	0.82
T_m (s)	1.3	12.2	0.26	0.4	9.4	0.40

Table C.118. UnSWAN performance metrics for NDBC Station 46077 for 2006.

Parameter	RMSE	PE (%)	SI	Bias	Bias (%)	R
H_s (m)	0.54	-19.9	0.63	-0.33	-27.9	0.78
T_m (s)	1.3	10.9	0.26	0.4	8.3	0.38

Table C.119. UnSWAN performance metrics for NDBC Station 46077 for 2005.

Parameter	RMSE	PE (%)	SI	Bias	Bias (%)	R
H_s (m)	0.65	-22.5	0.61	-0.41	-27.8	0.77
T_m (s)	1.3	7.6	0.27	0.2	4.7	0.33

Table C.120. UnSWAN performance metrics for NDBC Station 46078 for 2010.

Parameter	RMSE	PE (%)	SI	Bias	Bias (%)	R
H_s (m)	0.51	8.2	0.17	0.15	5.3	0.92
T_m (s)	1.5	20.3	0.19	1.3	19.9	0.82

Table C.121. UnSWAN performance metrics for NDBC Station 46078 for 2009.

Parameter	RMSE	PE (%)	SI	Bias	Bias (%)	R
H_s (m)	0.49	4.3	0.18	0.04	1.5	0.92
T_m (s)	1.2	12.7	0.16	0.8	12.5	0.80

Table C.122. UnSWAN performance metrics for NDBC Station 46078 for 2008.

Parameter	RMSE	PE (%)	SI	Bias	Bias (%)	R
H_s (m)	0.47	6.6	0.17	0.03	1.2	0.95
T_m (s)	1.0	9.6	0.13	0.6	9.5	0.87

Table C.123. UnSWAN performance metrics for NDBC Station 46078 for 2007.

Parameter	RMSE	PE (%)	SI	Bias	Bias (%)	R
H_s (m)	0.49	8.9	0.17	0.08	2.9	0.94
T_m (s)	1.0	11.7	0.14	0.8	11.6	0.90

Table C.124. UnSWAN performance metrics for NDBC Station 46078 for 2006.

Parameter	RMSE	PE (%)	SI	Bias	Bias (%)	R
H_s (m)	0.46	4.9	0.17	0.01	0.3	0.94
T_m (s)	1.0	9.5	0.13	0.6	9.3	0.85

Table C.125. UnSWAN performance metrics for NDBC Station 46078 for 2005.

Parameter	RMSE	PE (%)	SI	Bias	Bias (%)	R
H_s (m)	0.45	2.7	0.18	-0.03	-1.0	0.94
T_m (s)	0.9	9.0	0.13	0.6	8.9	0.86

Table C.126. UnSWAN performance metrics for NDBC Station 46078 for 2004.

Parameter	RMSE	PE (%)	SI	Bias	Bias (%)	R
H_s (m)	0.40	6.0	0.17	0.02	0.7	0.96
T_m (s)	0.9	11.2	0.13	0.7	11.0	0.88

Table C.127. UnSWAN performance metrics for NDBC Station 46080 for 2010.

Parameter	RMSE	PE (%)	SI	Bias	Bias (%)	R
H_s (m)	0.49	4.8	0.20	-0.05	-2.0	0.94
T_m (s)	1.1	14.0	0.16	0.9	13.6	0.83

Table C.128. UnSWAN performance metrics for NDBC Station 46080 for 2009.

Parameter	RMSE	PE (%)	SI	Bias	Bias (%)	R
H_s (m)	0.50	2.9	0.21	-0.08	-3.4	0.94
T_m (s)	1.1	11.7	0.15	0.7	11.5	0.83

Table C.129. UnSWAN performance metrics for NDBC Station 46080 for 2008.

Parameter	RMSE	PE (%)	SI	Bias	Bias (%)	R
H_s (m)	0.49	1.8	0.20	-0.12	-4.7	0.94
T_m (s)	1.0	11.2	0.14	0.7	11.0	0.84

Table C.130. UnSWAN performance metrics for NDBC Station 46080 for 2007.

Parameter	RMSE	PE (%)	SI	Bias	Bias (%)	R
H_s (m)	0.45	6.2	0.19	-0.04	-1.7	0.95
T_m (s)	0.9	8.6	0.13	0.5	8.6	0.85

Table C.131. UnSWAN performance metrics for NDBC Station 46080 for 2006.

Parameter	RMSE	PE (%)	SI	Bias	Bias (%)	R
H_s (m)	0.49	2.1	0.20	-0.09	-3.8	0.94
T_m (s)	0.8	7.3	0.12	0.5	7.3	0.84

Table C.132. UnSWAN performance metrics for NDBC Station 46080 for 2005.

Parameter	RMSE	PE (%)	SI	Bias	Bias (%)	R
H_s (m)	0.45	1.1	0.20	-0.10	-4.2	0.95
T_m (s)	0.8	6.6	0.12	0.4	6.8	0.88

Table C.133. UnSWAN performance metrics for NDBC Station 46080 for 2004.

Parameter	RMSE	PE (%)	SI	Bias	Bias (%)	R
H_s (m)	0.57	-0.1	0.23	-0.24	-8.1	0.96
T_m (s)	0.9	9.6	0.13	0.6	9.3	0.85

Table C.134. UnSWAN performance metrics for NDBC Station 46080 for 2003.

Parameter	RMSE	PE (%)	SI	Bias	Bias (%)	R
H_s (m)	0.38	3.2	0.17	-0.04	-1.9	0.95
T_m (s)	0.8	6.7	0.11	0.4	6.6	0.83

Table C.135. UnSWAN performance metrics for NDBC Station 46080 for 2002.

Parameter	RMSE	PE (%)	SI	Bias	Bias (%)	R
H_s (m)	0.27	11.7	0.19	0.10	7.1	0.89
T_m (s)	0.8	6.8	0.13	0.4	6.7	0.73

Table C.136. UnSWAN performance metrics for NDBC Station 46082 for 2010.

Parameter	RMSE	PE (%)	SI	Bias	Bias (%)	R
H_s (m)	0.48	10.1	0.20	0.05	2.0	0.95
T_m (s)	1.8	26.7	0.23	1.6	25.3	0.82

Table C.137. UnSWAN performance metrics for NDBC Station 46082 for 2009.

Parameter	RMSE	PE (%)	SI	Bias	Bias (%)	R
H_s (m)	0.46	4.9	0.21	-0.05	-2.3	0.95
T_m (s)	1.6	24.2	0.22	1.4	23.0	0.83

Table C.138. UnSWAN performance metrics for NDBC Station 46082 for 2008.

Parameter	RMSE	PE (%)	SI	Bias	Bias (%)	R
H_s (m)	0.60	5.0	0.26	-0.09	-3.9	0.91
T_m (s)	1.6	22.1	0.21	1.3	20.7	0.79

Table C.139. UnSWAN performance metrics for NDBC Station 46082 for 2007.

Parameter	RMSE	PE (%)	SI	Bias	Bias (%)	R
H_s (m)	0.57	0.4	0.25	-0.16	-6.7	0.94
T_m (s)	1.3	15.7	0.17	1.0	15.3	0.85

Table C.140. UnSWAN performance metrics for NDBC Station 46082 for 2006.

Parameter	RMSE	PE (%)	SI	Bias	Bias (%)	R
H_s (m)	0.59	-2.9	0.26	-0.21	-8.5	0.95
T_m (s)	1.2	15.1	0.17	1.0	14.7	0.86

Table C.141. UnSWAN performance metrics for NDBC Station 46082 for 2005.

Parameter	RMSE	PE (%)	SI	Bias	Bias (%)	R
H_s (m)	0.54	-3.6	0.25	-0.21	-8.7	0.94
T_m (s)	1.2	13.8	0.16	0.9	13.3	0.81

Table C.142. UnSWAN performance metrics for NDBC Station 46082 for 2004.

Parameter	RMSE	PE (%)	SI	Bias	Bias (%)	R
H_s (m)	0.53	-1.2	0.25	-0.18	-7.8	0.94
T_m (s)	1.3	15.3	0.17	1.0	14.9	0.83

Table C.143. UnSWAN performance metrics for NDBC Station 46082 for 2003.

Parameter	RMSE	PE (%)	SI	Bias	Bias (%)	R
H_s (m)	0.52	1.2	0.25	-0.13	-6.0	0.94
T_m (s)	1.1	13.6	0.15	0.9	13.0	0.84

Table C.144. UnSWAN performance metrics for NDBC Station 46082 for 2002.

Parameter	RMSE	PE (%)	SI	Bias	Bias (%)	R
H_s (m)	0.52	-5.3	0.20	-0.22	-7.8	0.94
T_m (s)	1.2	13.7	0.15	0.9	13.5	0.85

Table C.145. UnSWAN performance metrics for NDBC Station 46083 for 2010.

Parameter	RMSE	PE (%)	SI	Bias	Bias (%)	R
H_s (m)	0.48	16.1	0.20	0.14	6.2	0.94
T_m (s)	1.9	28.5	0.24	1.7	27.0	0.81

Table C.146. UnSWAN performance metrics for NDBC Station 46083 for 2009.

Parameter	RMSE	PE (%)	SI	Bias	Bias (%)	R
H_s (m)	0.46	8.0	0.20	0.00	0.0	0.94
T_m (s)	1.7	23.1	0.22	1.4	21.8	0.80

Table C.147. UnSWAN performance metrics for NDBC Station 46083 for 2008.

Parameter	RMSE	PE (%)	SI	Bias	Bias (%)	R
H_s (m)	0.50	5.2	0.21	-0.08	-3.2	0.95
T_m (s)	1.4	18.8	0.19	1.2	18.0	0.82

Table C.148. UnSWAN performance metrics for NDBC Station 46083 for 2007.

Parameter	RMSE	PE (%)	SI	Bias	Bias (%)	R
H_s (m)	0.50	7.6	0.22	-0.08	-3.6	0.96
T_m (s)	1.5	19.8	0.19	1.2	18.9	0.86

Table C.149. UnSWAN performance metrics for NDBC Station 46083 for 2006.

Parameter	RMSE	PE (%)	SI	Bias	Bias (%)	R
H_s (m)	0.40	3.8	0.19	-0.05	-2.2	0.95
T_m (s)	1.3	16.3	0.17	1.0	15.8	0.85

Table C.150. UnSWAN performance metrics for NDBC Station 46083 for 2005.

Parameter	RMSE	PE (%)	SI	Bias	Bias (%)	R
H_s (m)	0.46	2.2	0.19	-0.09	-3.6	0.95
T_m (s)	1.3	17.4	0.18	1.1	17.0	0.87

Table C.151. UnSWAN performance metrics for NDBC Station 46083 for 2004.

Parameter	RMSE	PE (%)	SI	Bias	Bias (%)	R
H_s (m)	0.42	3.0	0.20	-0.09	-4.1	0.96
T_m (s)	1.1	13.6	0.15	0.9	13.1	0.85

Table C.152. UnSWAN performance metrics for NDBC Station 46083 for 2003.

Parameter	RMSE	PE (%)	SI	Bias	Bias (%)	R
H_s (m)	0.47	1.5	0.21	-0.11	-4.5	0.95
T_m (s)	1.2	14.5	0.16	0.9	14.0	0.83

Table C.153. UnSWAN performance metrics for NDBC Station 46083 for 2002.

Parameter	RMSE	PE (%)	SI	Bias	Bias (%)	R
H_s (m)	0.41	0.2	0.18	-0.09	-3.8	0.94
T_m (s)	1.2	15.0	0.16	1.0	14.7	0.85

Table C.154. UnSWAN performance metrics for NDBC Station 46083 for 2001.

Parameter	RMSE	PE (%)	SI	Bias	Bias (%)	R
H_s (m)	0.50	1.1	0.20	-0.14	-5.6	0.95
T_m (s)	1.2	12.6	0.16	0.8	12.4	0.85

Table C.155. UnSWAN performance metrics for NDBC Station 46084 for 2010.

Parameter	RMSE	PE (%)	SI	Bias	Bias (%)	R
H_s (m)	0.42	13.2	0.17	0.12	5.2	0.96
T_m (s)	1.9	29.5	0.24	1.7	28.0	0.84

Table C.156. UnSWAN performance metrics for NDBC Station 46084 for 2008.

Parameter	RMSE	PE (%)	SI	Bias	Bias (%)	R
H_s (m)	0.42	10.0	0.16	0.08	3.3	0.96
T_m (s)	1.7	24.7	0.22	1.5	23.7	0.86

Table C.157. UnSWAN performance metrics for NDBC Station 46084 for 2007.

Parameter	RMSE	PE (%)	SI	Bias	Bias (%)	R
H_s (m)	0.49	3.6	0.17	-0.05	-1.6	0.94
T_m (s)	1.6	20.1	0.19	1.3	19.1	0.85

Table C.158. UnSWAN performance metrics for NDBC Station 46084 for 2006.

Parameter	RMSE	PE (%)	SI	Bias	Bias (%)	R
H_s (m)	0.42	5.9	0.16	0.02	0.8	0.96
T_m (s)	1.3	15.4	0.17	1.0	15.3	0.89

Table C.159. UnSWAN performance metrics for NDBC Station 46084 for 2005.

Parameter	RMSE	PE (%)	SI	Bias	Bias (%)	R
H_s (m)	0.41	3.0	0.16	-0.01	-0.5	0.96
T_m (s)	1.1	13.0	0.15	0.9	13.1	0.90

Table C.160. UnSWAN performance metrics for NDBC Station 46084 for 2004.

Parameter	RMSE	PE (%)	SI	Bias	Bias (%)	R
H_s (m)	0.45	3.4	0.18	-0.07	-2.6	0.96
T_m (s)	1.1	12.6	0.14	0.9	12.4	0.89

Table C.161. UnSWAN performance metrics for NDBC Station 46084 for 2003.

Parameter	RMSE	PE (%)	SI	Bias	Bias (%)	R
H_s (m)	0.41	4.1	0.16	-0.02	-0.6	0.96
T_m (s)	1.1	13.7	0.15	0.9	13.3	0.87

Table C.162. UnSWAN performance metrics for NDBC Station 46084 for 2002.

Parameter	RMSE	PE (%)	SI	Bias	Bias (%)	R
H_s (m)	0.40	4.8	0.16	0.03	1.0	0.95
T_m (s)	1.2	14.2	0.15	0.9	14.1	0.88

Table C.163. UnSWAN performance metrics for NDBC Station 46003 for 1999.

Parameter	RMSE	PE (%)	SI	Bias	Bias (%)	R
H_s (m)	0.47	16.9	0.21	0.25	12.9	0.77
T_m (s)	0.9	12.3	0.13	0.7	11.8	0.84

Table C.164. UnSWAN performance metrics for NDBC Station 46003 for 1998.

Parameter	RMSE	PE (%)	SI	Bias	Bias (%)	R
H_s (m)	0.53	9.2	0.17	0.14	4.6	0.94
T_m (s)	1.1	13.9	0.15	0.9	13.6	0.89

Table C.165. UnSWAN performance metrics for NDBC Station 46003 for 1997.

Parameter	RMSE	PE (%)	SI	Bias	Bias (%)	R
H_s (m)	0.61	11.0	0.19	0.19	6.5	0.92
T_m (s)	1.3	15.0	0.16	1.0	14.7	0.89

Table C.166. UnSWAN performance metrics for NDBC Station 46003 for 1996.

Parameter	RMSE	PE (%)	SI	Bias	Bias (%)	R
H_s (m)	0.57	9.3	0.19	0.09	3.0	0.93
T_m (s)	1.1	12.8	0.14	0.9	12.4	0.86

Table C.167. UnSWAN performance metrics for NDBC Station 46003 for 1995.

Parameter	RMSE	PE (%)	SI	Bias	Bias (%)	R
H_s (m)	0.64	10.7	0.21	0.09	3.2	0.89
T_m (s)	1.1	13.2	0.15	0.9	12.9	0.88

Table C.168. UnSWAN performance metrics for NDBC Station 46003 for 1994.

Parameter	RMSE	PE (%)	SI	Bias	Bias (%)	R
H_s (m)	0.61	10.0	0.19	0.14	4.5	0.93
T_m (s)	1.2	14.3	0.15	1.0	13.9	0.87

Table C.169. UnSWAN performance metrics for NDBC Station 46003 for 1993.

Parameter	RMSE	PE (%)	SI	Bias	Bias (%)	R
H_s (m)	0.67	7.7	0.19	0.12	3.5	0.89
T_m (s)	1.3	14.4	0.15	1.0	13.9	0.85

Table C.170. UnSWAN performance metrics for NDBC Station 46003 for 1992.

Parameter	RMSE	PE (%)	SI	Bias	Bias (%)	R
H_s (m)	0.61	13.9	0.20	0.25	8.6	0.93
T_m (s)	1.3	16.3	0.16	1.1	15.9	0.88

Table C.171. UnSWAN performance metrics for NDBC Station 46003 for 1991.

Parameter	RMSE	PE (%)	SI	Bias	Bias (%)	R
H_s (m)	0.70	13.1	0.20	0.26	8.1	0.91
T_m (s)	1.5	20.5	0.19	1.3	19.8	0.87

Table C.172. UnSWAN performance metrics for NDBC Station 46003 for 1990.

Parameter	RMSE	PE (%)	SI	Bias	Bias (%)	R
H_s (m)	0.66	12.4	0.19	0.25	8.1	0.92
T_m (s)	1.6	21.7	0.20	1.4	21.2	0.87

Table C.173. UnSWAN performance metrics for NDBC Station 46003 for 1989.

Parameter	RMSE	PE (%)	SI	Bias	Bias (%)	R
H_s (m)	0.64	9.8	0.19	0.15	4.8	0.90
T_m (s)	1.5	20.9	0.19	1.3	20.2	0.85

Table C.174. UnSWAN performance metrics for NDBC Station 46003 for 1988.

Parameter	RMSE	PE (%)	SI	Bias	Bias (%)	R
H_s (m)	0.66	9.9	0.20	0.15	4.8	0.91
T_m (s)	1.3	16.6	0.17	1.1	16.1	0.88

Table C.175. UnSWAN performance metrics for NDBC Station 46003 for 1987.

Parameter	RMSE	PE (%)	SI	Bias	Bias (%)	R
H_s (m)	0.65	12.2	0.19	0.21	6.4	0.92
T_m (s)	1.5	18.2	0.18	1.2	17.8	0.87

Table C.176. UnSWAN performance metrics for NDBC Station 46003 for 1986.

Parameter	RMSE	PE (%)	SI	Bias	Bias (%)	R
H_s (m)	0.63	10.7	0.20	0.18	6.2	0.91
T_m (s)	1.6	20.9	0.20	1.4	20.3	0.85

Table C.177. UnSWAN performance metrics for NDBC Station 46003 for 1985.

Parameter	RMSE	PE (%)	SI	Bias	Bias (%)	R
H_s (m)	0.72	11.1	0.21	0.15	4.5	0.90
T_m (s)	1.5	20.2	0.19	1.3	19.3	0.87

Table C.178. UnSWAN performance metrics for NDBC Station 46003 for 1984.

Parameter	RMSE	PE (%)	SI	Bias	Bias (%)	R
H_s (m)	0.68	20.0	0.24	0.28	10.3	0.93
T_m (s)	1.5	19.7	0.20	1.3	19.3	0.89

Table C.179. UnSWAN performance metrics for NDBC Station 46003 for 1983.

Parameter	RMSE	PE (%)	SI	Bias	Bias (%)	R
H_s (m)	0.65	16.4	0.21	0.27	9.4	0.89
T_m (s)	1.3	15.8	0.17	1.0	14.9	0.85

Table C.180. UnSWAN performance metrics for NDBC Station 46003 for 1982.

Parameter	RMSE	PE (%)	SI	Bias	Bias (%)	R
H_s (m)	0.73	24.0	0.22	0.32	10.8	0.92
T_m (s)	1.1	13.7	0.14	0.9	12.9	0.85

Table C.181. UnSWAN performance metrics for NDBC Station 46003 for 1981.

Parameter	RMSE	PE (%)	SI	Bias	Bias (%)	R
H_s (m)	0.76	18.7	0.21	0.38	12.4	0.88
T_m (s)	1.2	13.3	0.15	1.0	12.8	0.87

Table C.182. UnSWAN performance metrics for NDBC Station 46003 for 1980.

Parameter	RMSE	PE (%)	SI	Bias	Bias (%)	R
H_s (m)	0.74	17.0	0.22	0.34	9.5	0.92
T_m (s)	1.1	11.8	0.14	0.8	10.9	0.76

Table C.183. UnSWAN performance metrics for NDBC Station 46003 for 1979.

Parameter	RMSE	PE (%)	SI	Bias	Bias (%)	R
H_s (m)	0.75	10.2	0.23	0.28	6.9	0.92
T_m (s)	1.4	16.5	0.18	1.2	16.0	0.87

Table C.184. UnSWAN performance metrics for NDBC Station 46105 for 2008.

Parameter	RMSE	PE (%)	SI	Bias	Bias (%)	R
H_s (m)	0.71	0.42	0.50	-0.22	-13.54	0.81
T_m (s)	1.24	4.11	0.23	0.10	1.92	0.51
D_p (deg)	105.30	-	-	-14.07	-	0.29

Table C.185. UnSWAN performance metrics for NDBC Station 46106 for 2010.

Parameter	RMSE	PE (%)	SI	Bias	Bias (%)	R
H_s (m)	0.50	-20.7	0.59	-0.31	-26.8	0.71
T_m (s)	1.1	-7.6	0.28	-0.4	-10.6	0.22
D_p (deg)	219.4	-	-	33	-	-0.06

Table C.186. UnSWAN performance metrics for NDBC Station 46106 for 2009.

Parameter	RMSE	PE (%)	SI	Bias	Bias (%)	R
H_s (m)	0.46	-17.4	0.80	-0.24	-29.5	0.74
T_m (s)	1.5	-1.8	0.38	-0.2	-4.7	0.19
D_p (deg)	142.5	-	-	27	-	-0.02

Table C.187. UnSWAN performance metrics for NDBC Station 46106 for 2008.

Parameter	RMSE	PE (%)	SI	Bias	Bias (%)	R
H_s (m)	0.47	-19.0	0.82	-0.26	-30.8	0.76
T_m (s)	1.2	-5.0	0.32	-0.3	-7.8	0.16
D_p (deg)	151.0	-	-	35	-	0.05

Table C.188. UnSWAN performance metrics for NDBC Station 46106 for 2007.

Parameter	RMSE	PE (%)	SI	Bias	Bias (%)	R
H_s (m)	0.73	-23.9	0.77	-0.46	-32.6	0.56
T_m (s)	1.2	-13.2	0.31	-0.7	-15.6	0.20
D_p (deg)	175.9	-	-	51	-	0.19

Table C.189. UnSWAN performance metrics for NDBC Station 46107 for 2010.

Parameter	RMSE	PE (%)	SI	Bias	Bias (%)	R
H_s (m)	0.37	33.5	0.30	0.25	24.9	0.87
T_m (s)	1.4	11.8	0.20	0.7	11.0	0.69
D_p (deg)	41.3	-	-	-1	-	0.30

Table C.190. UnSWAN performance metrics for NDBC Station 46107 for 2009.

Parameter	RMSE	PE (%)	SI	Bias	Bias (%)	R
H_s (m)	0.36	32.2	0.30	0.21	21.9	0.88
T_m (s)	1.5	13.0	0.21	0.7	12.1	0.66
D_p (deg)	49.8	-	-	-10	-	0.20

Table C.191. UnSWAN performance metrics for NDBC Station 46107 for 2008.

Parameter	RMSE	PE (%)	SI	Bias	Bias (%)	R
H_s (m)	0.35	35.4	0.29	0.20	19.7	0.88
T_m (s)	1.4	12.7	0.21	0.7	11.1	0.65
D_p (deg)	56.2	-	-	-19	-	0.16

Appendix D – Monthly Averaged Distributions of Simulated IEC Parameter in Alaska Coast

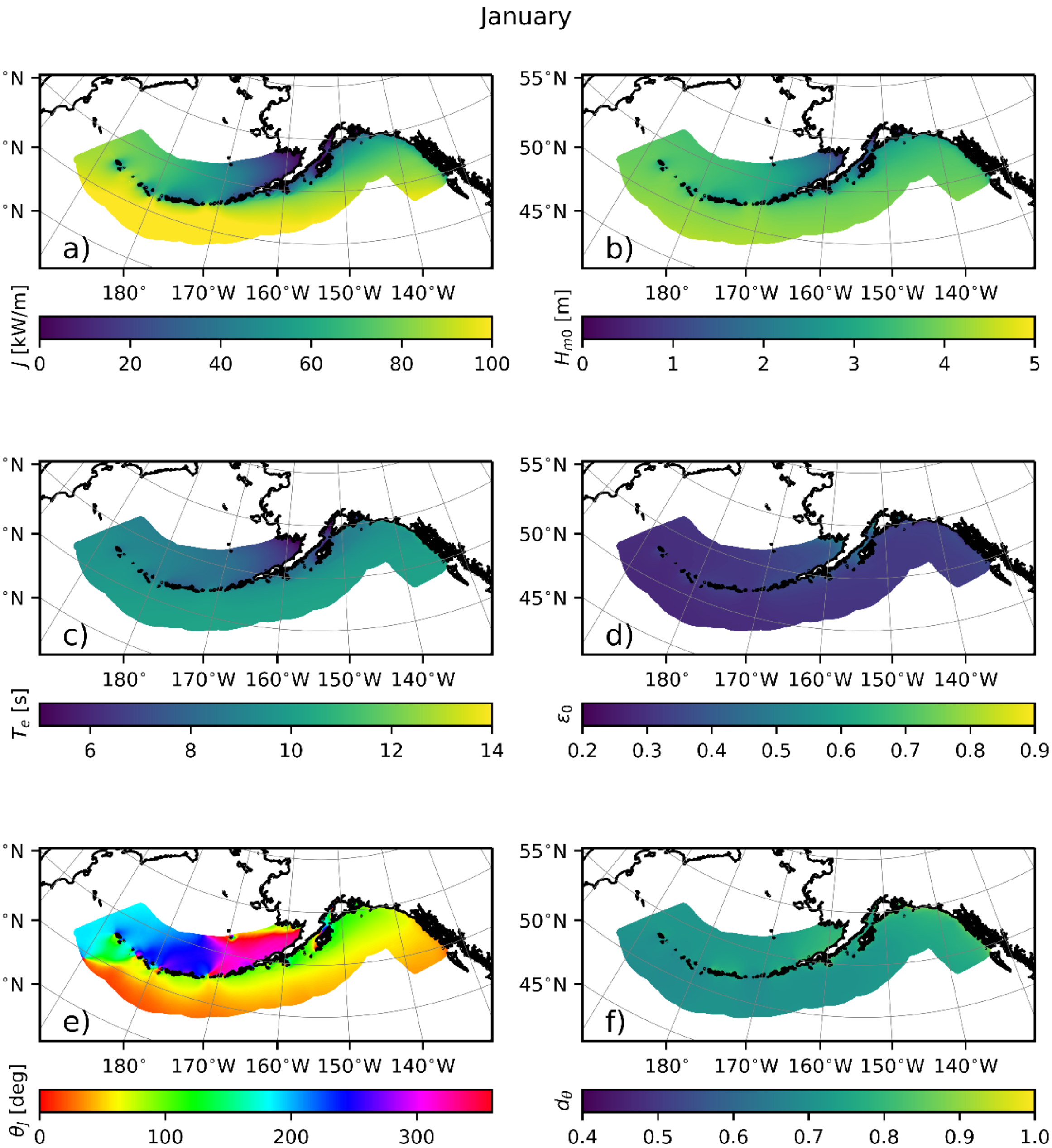

Figure D.1. Monthly distributions of six IEC parameters in January: (a) omnidirectional wave power, (b) significant wave height, (c) energy period, (d) spectral width, (e) direction of maximum directionally resolved wave power, and (f) directionality coefficient around Alaska.

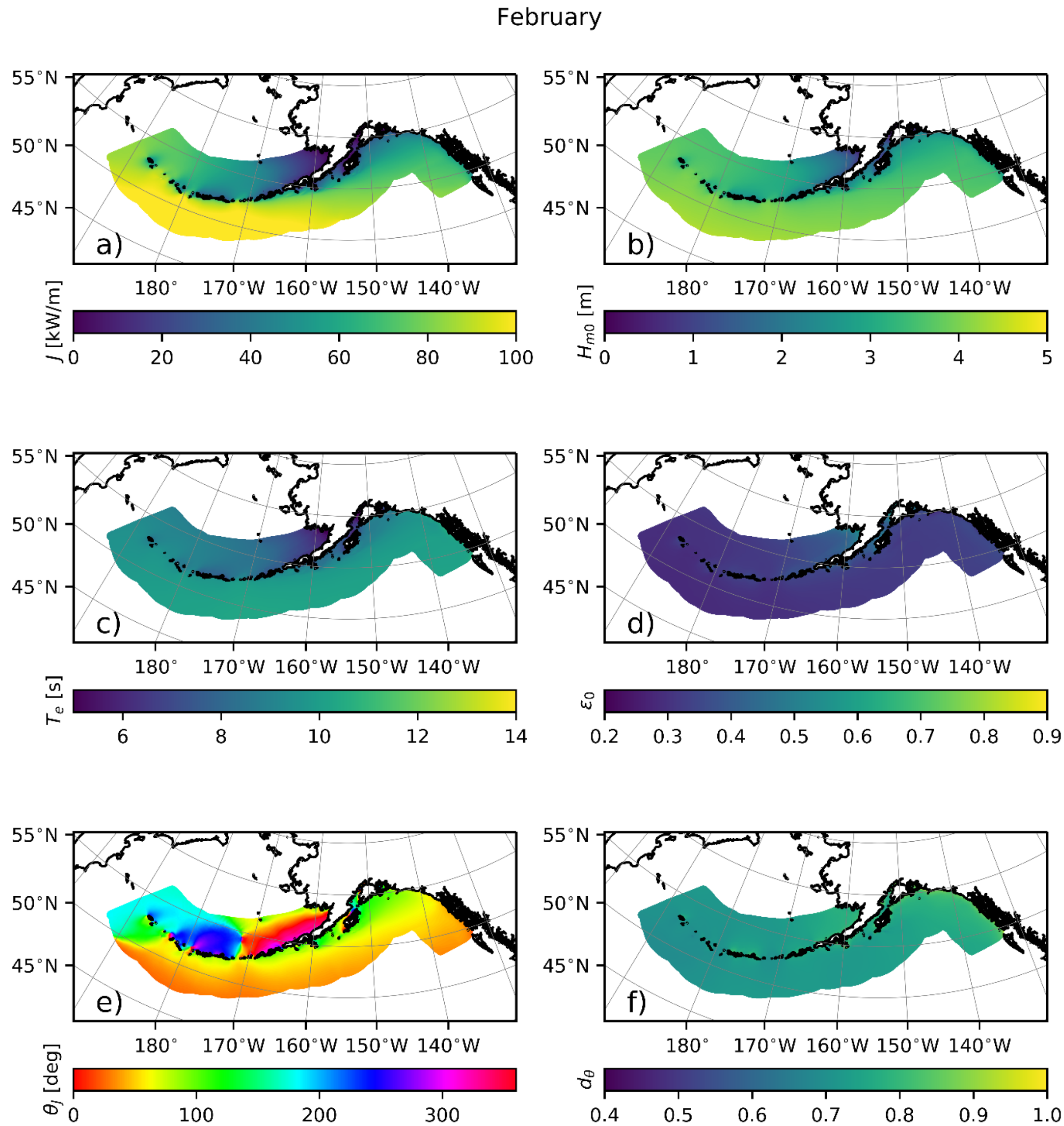

Figure D.2. Monthly distributions of six IEC parameters in February: (a) omnidirectional wave power, (b) significant wave height, (c) energy period, (d) spectral width, (e) direction of maximum directionally resolved wave power, and (f) directionality coefficient around Alaska.

March

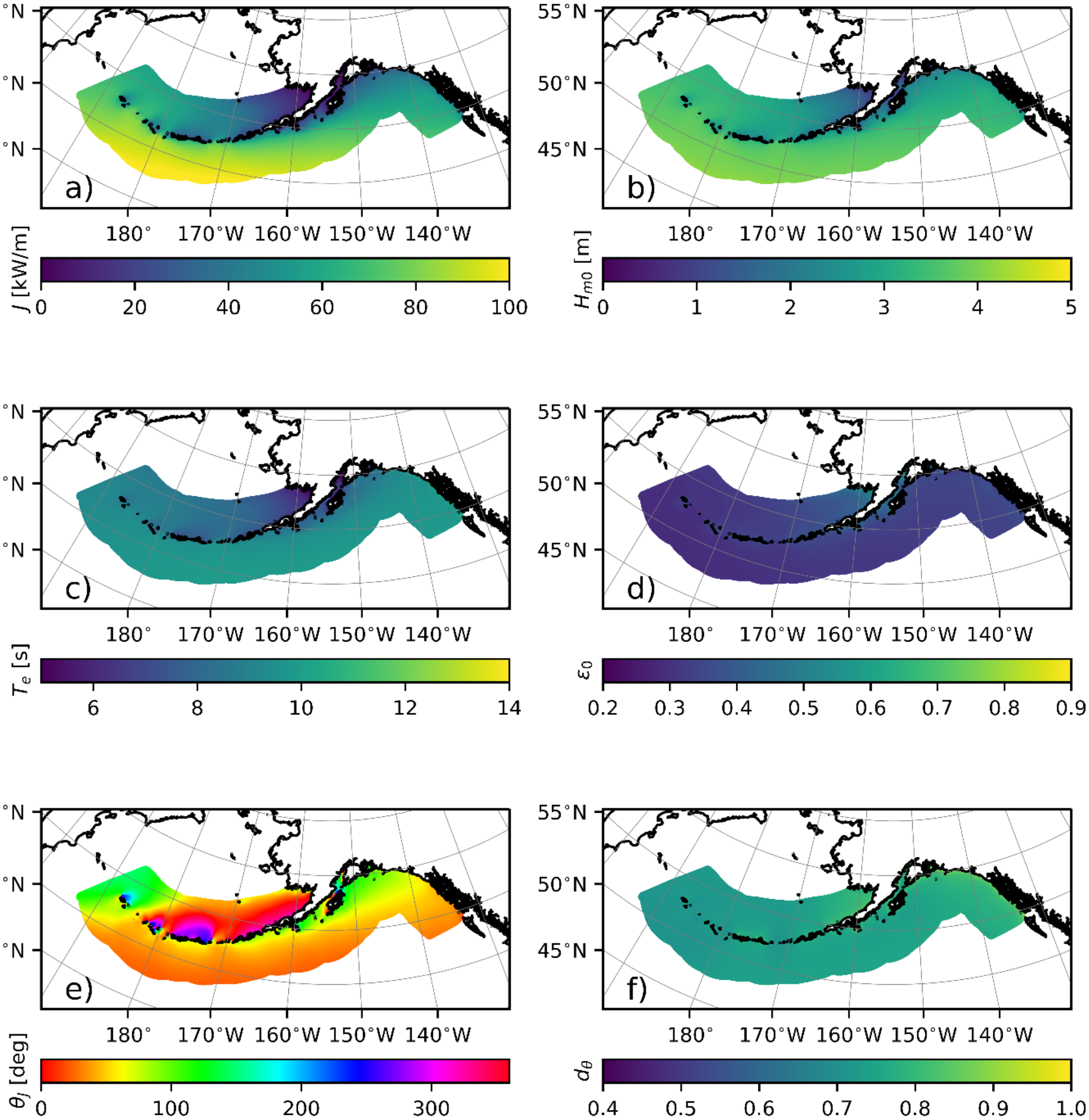

Figure D.3. Monthly distributions of six IEC parameters in March: (a) omnidirectional wave power, (b) significant wave height, (c) energy period, (d) spectral width, (e) direction of maximum directionally resolved wave power, and (f) directionality coefficient around Alaska.

April

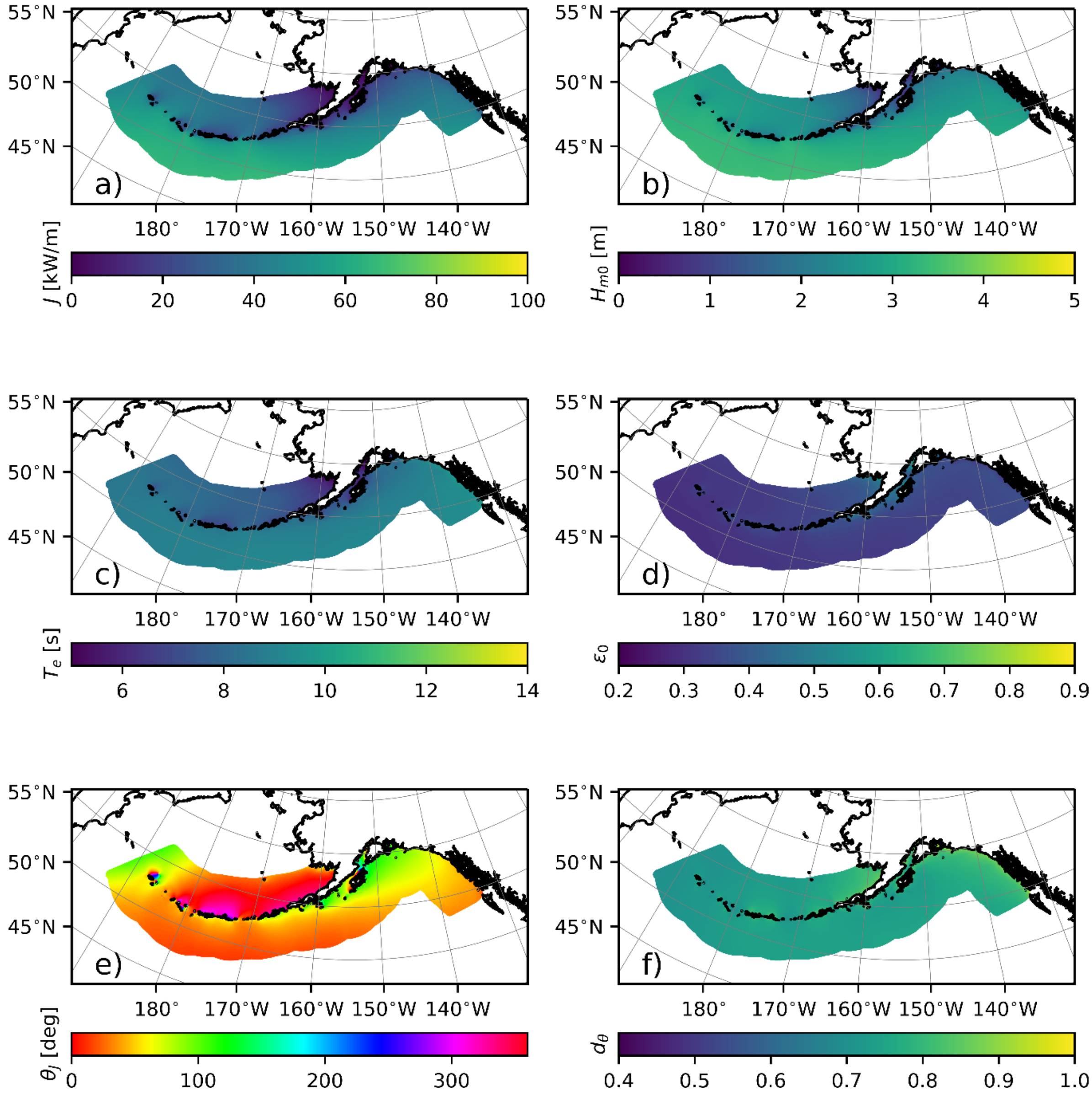

Figure D.4. Monthly distributions of six IEC parameters in April: (a) omnidirectional wave power, (b) significant wave height, (c) energy period, (d) spectral width, (e) direction of maximum directionally resolved wave power, and (f) directionality coefficient around Alaska.

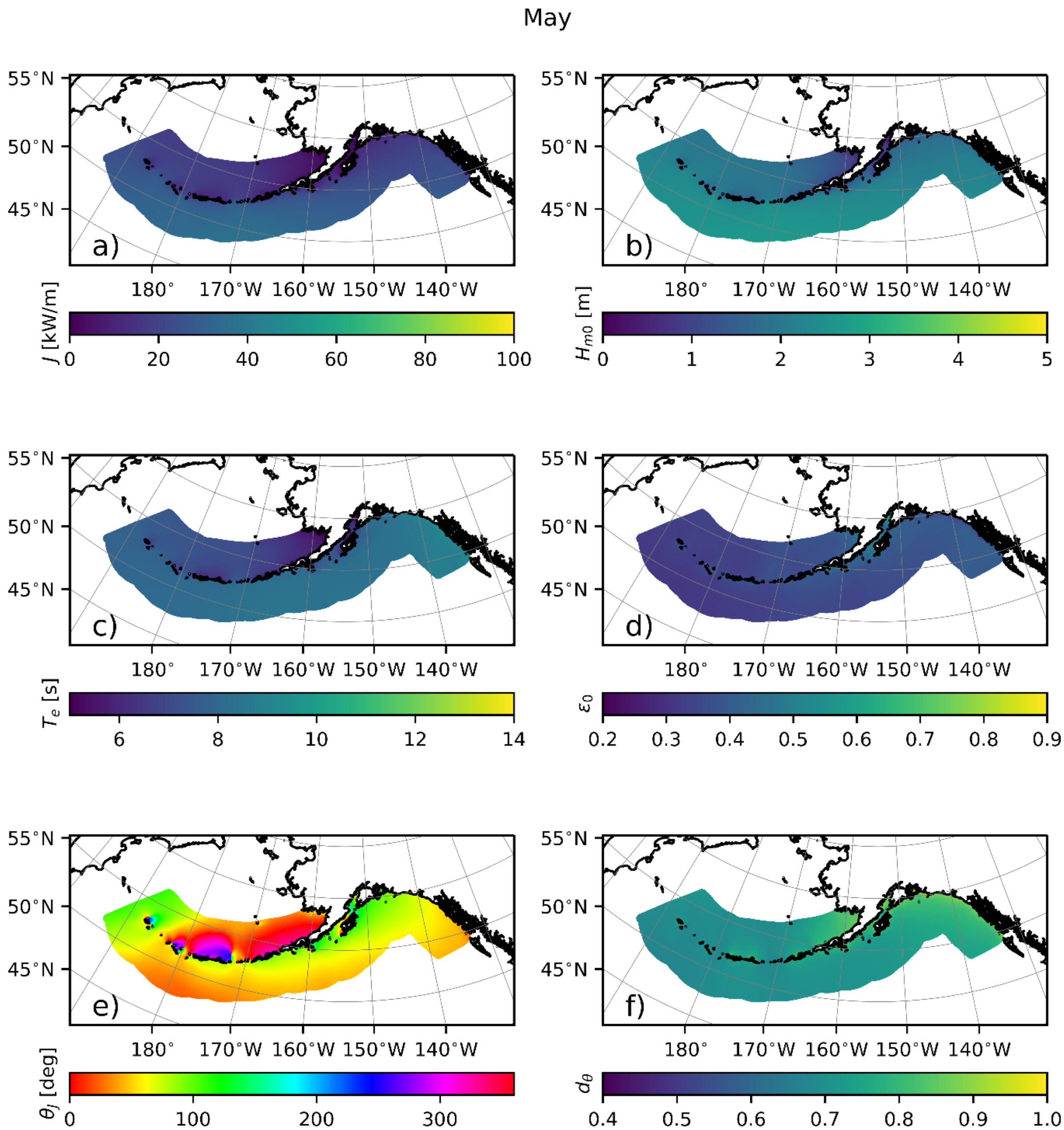

Figure D.5. Monthly distributions of six IEC parameters in May: (a) omnidirectional wave power, (b) significant wave height, (c) energy period, (d) spectral width, (e) direction of maximum directionally resolved wave power, and (f) directionality coefficient around Alaska.

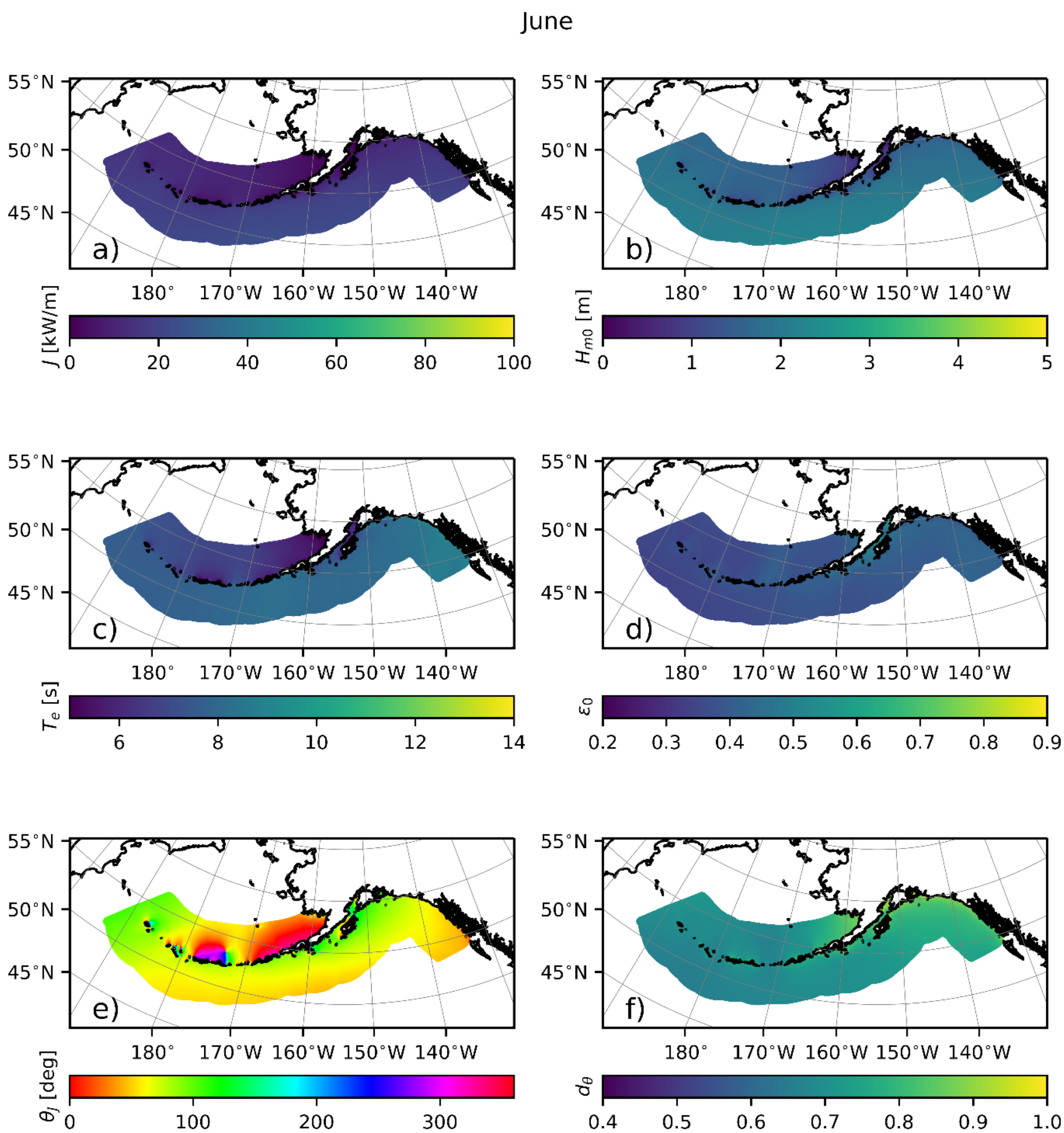

Figure D.6. Monthly distributions of six IEC parameters in June: (a) omnidirectional wave power, (b) significant wave height, (c) energy period, (d) spectral width, (e) direction of maximum directionally resolved wave power, and (f) directionality coefficient around Alaska.

July

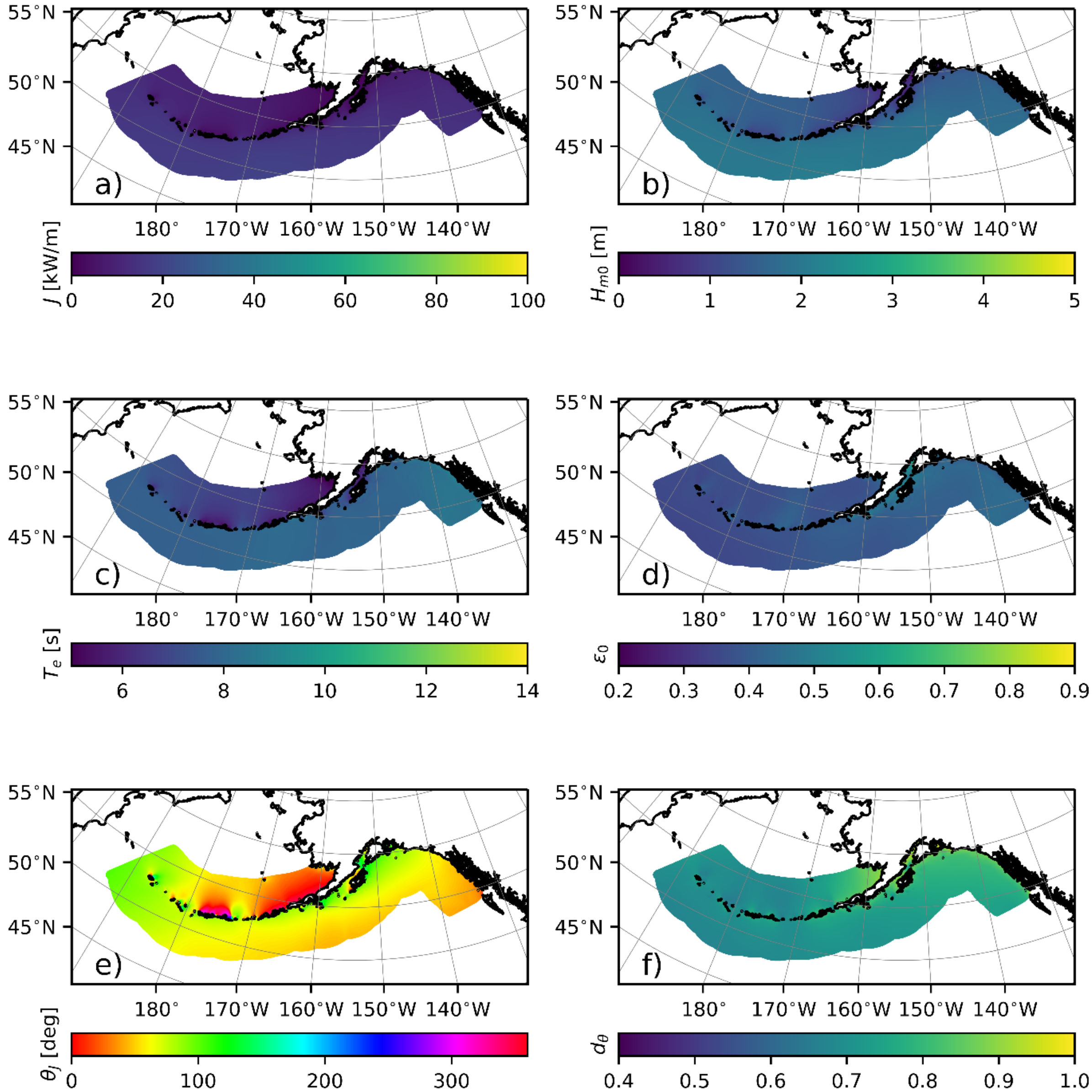

Figure D.7. Monthly distributions of six IEC parameters in July: (a) omnidirectional wave power, (b) significant wave height, (c) energy period, (d) spectral width, (e) direction of maximum directionally resolved wave power, and (f) directionality coefficient around Alaska.

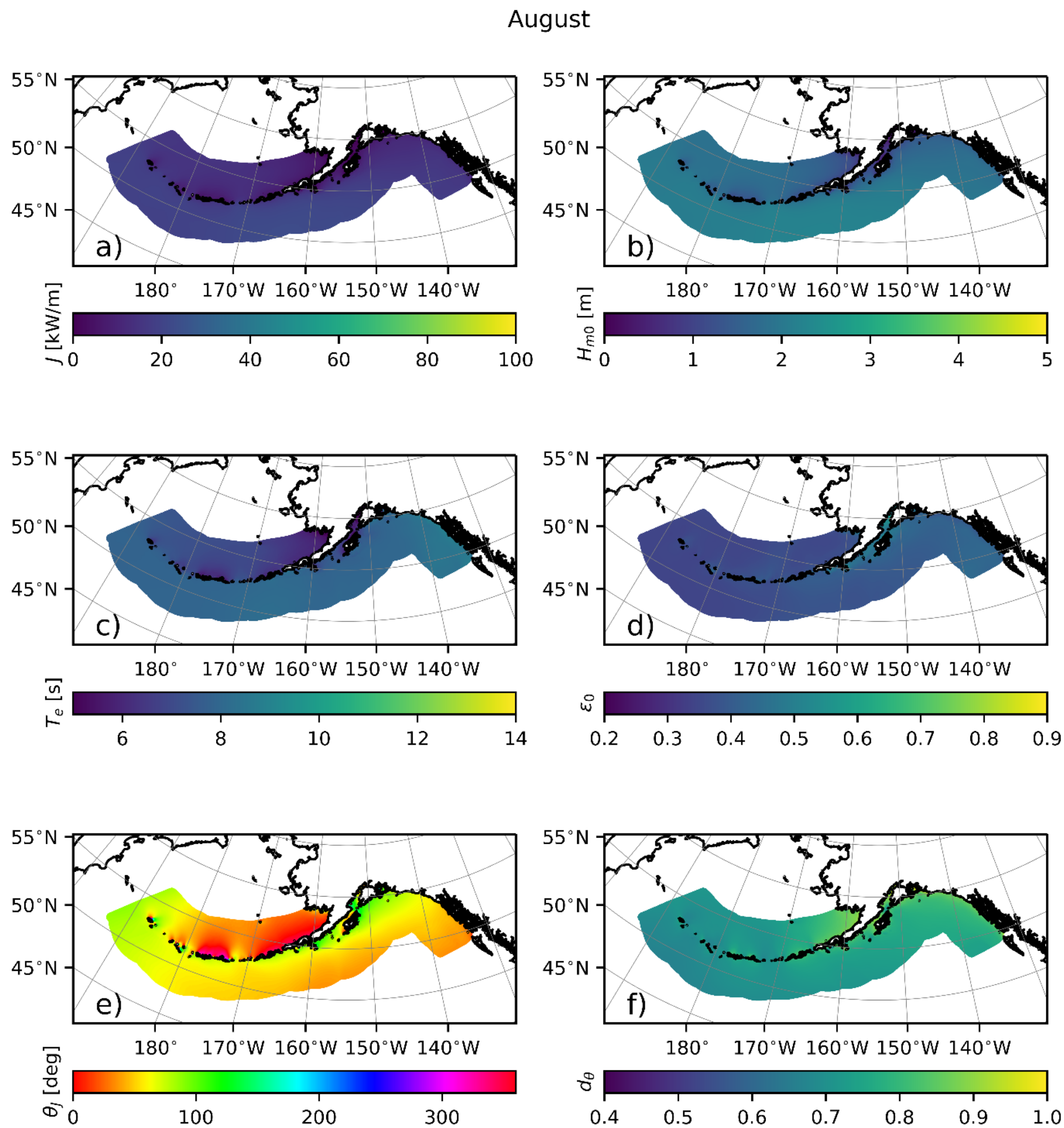

Figure D.8. Monthly distributions of six IEC parameters in August: (a) omnidirectional wave power, (b) significant wave height, (c) energy period, (d) spectral width, (e) direction of maximum directionally resolved wave power, and (f) directionality coefficient around Alaska.

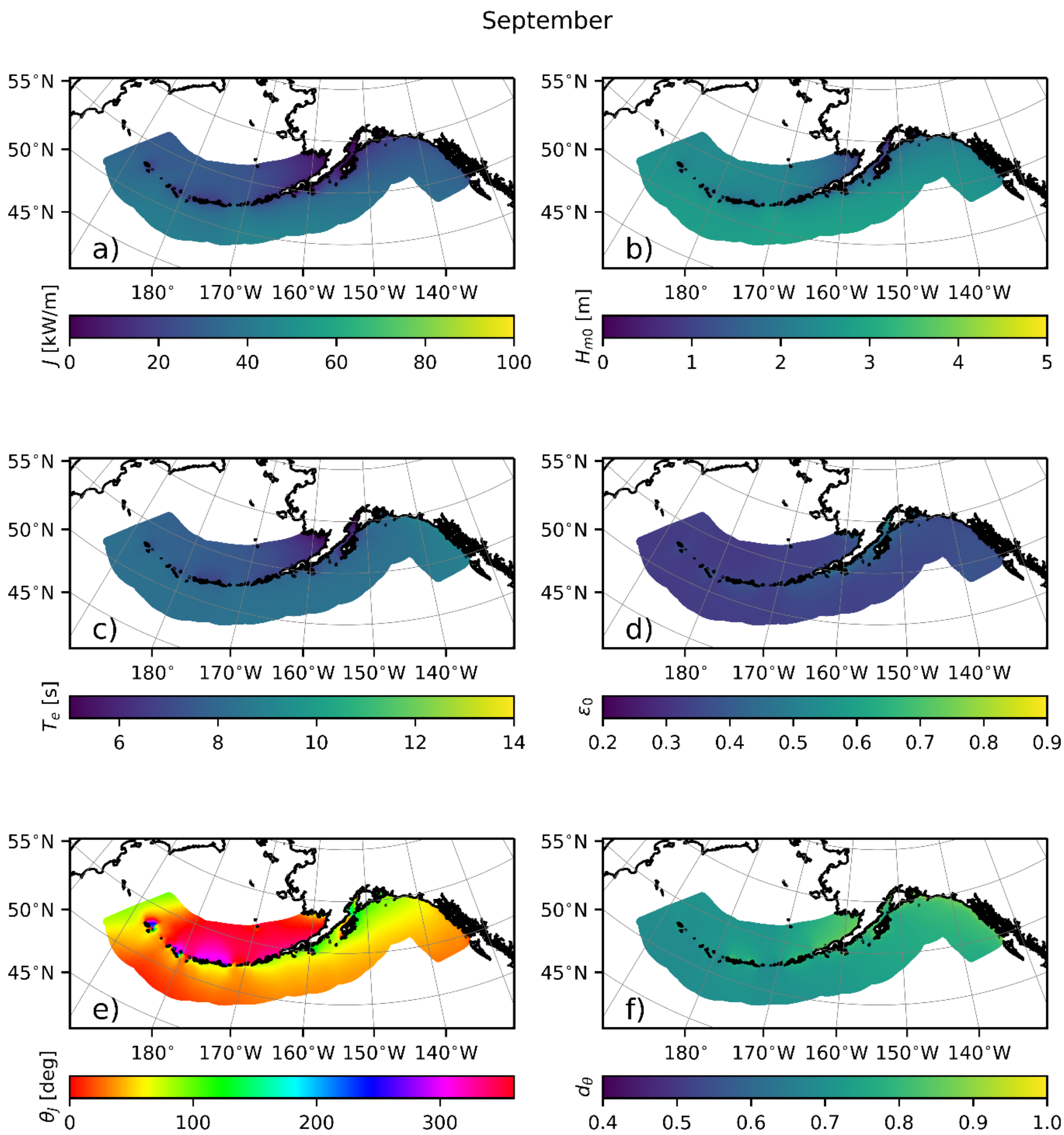

Figure D.9. Monthly distributions of six IEC parameters in September: (a) omnidirectional wave power, (b) significant wave height, (c) energy period, (d) spectral width, (e) direction of maximum directionally resolved wave power, and (f) directionality coefficient around Alaska.

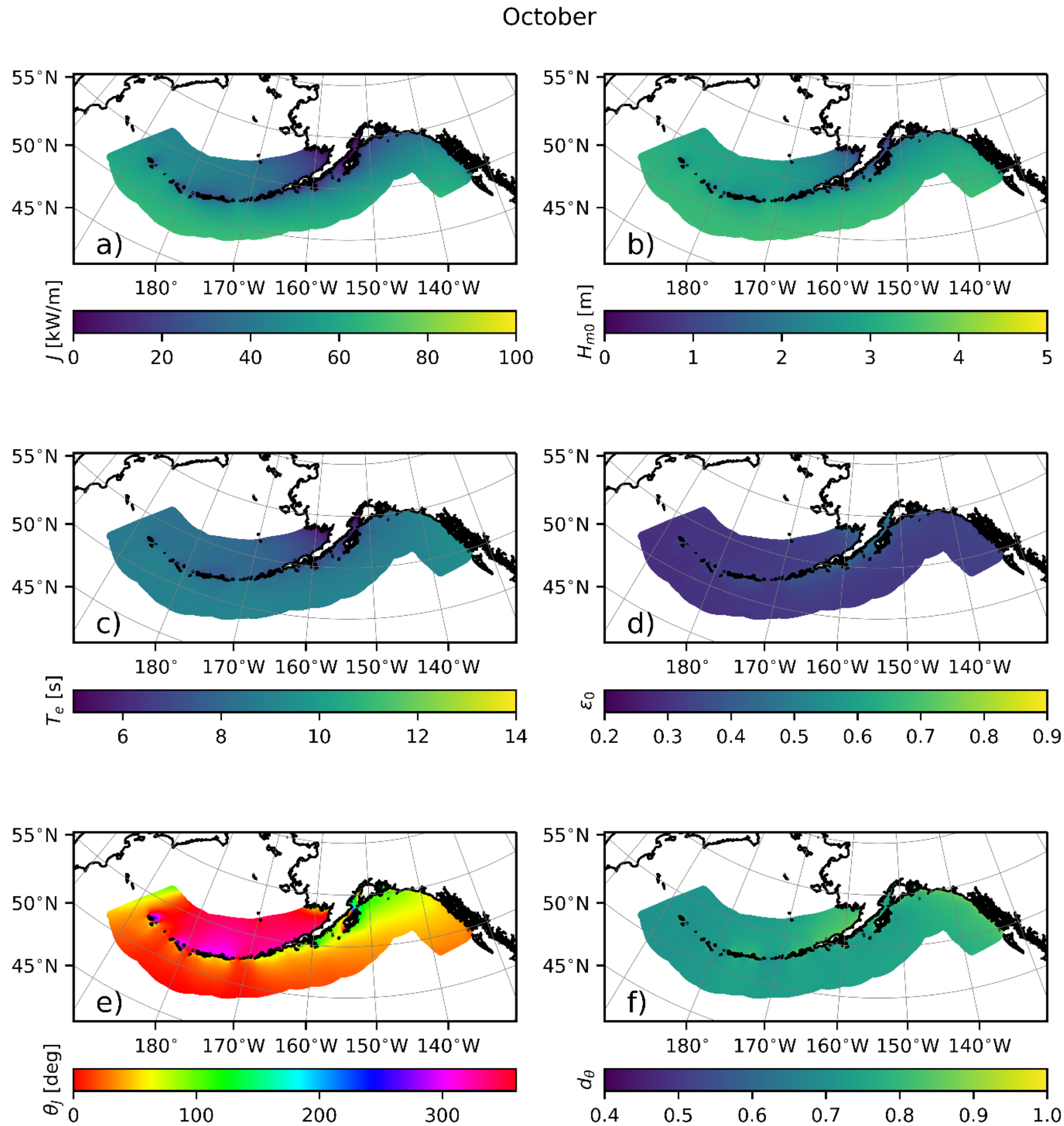

Figure D.10. Monthly distributions of six IEC parameters in October: (a) omnidirectional wave power, (b) significant wave height, and (c) energy period, (d) spectral width, (e) direction of maximum directionally resolved wave power, and (f) directionality coefficient around Alaska.

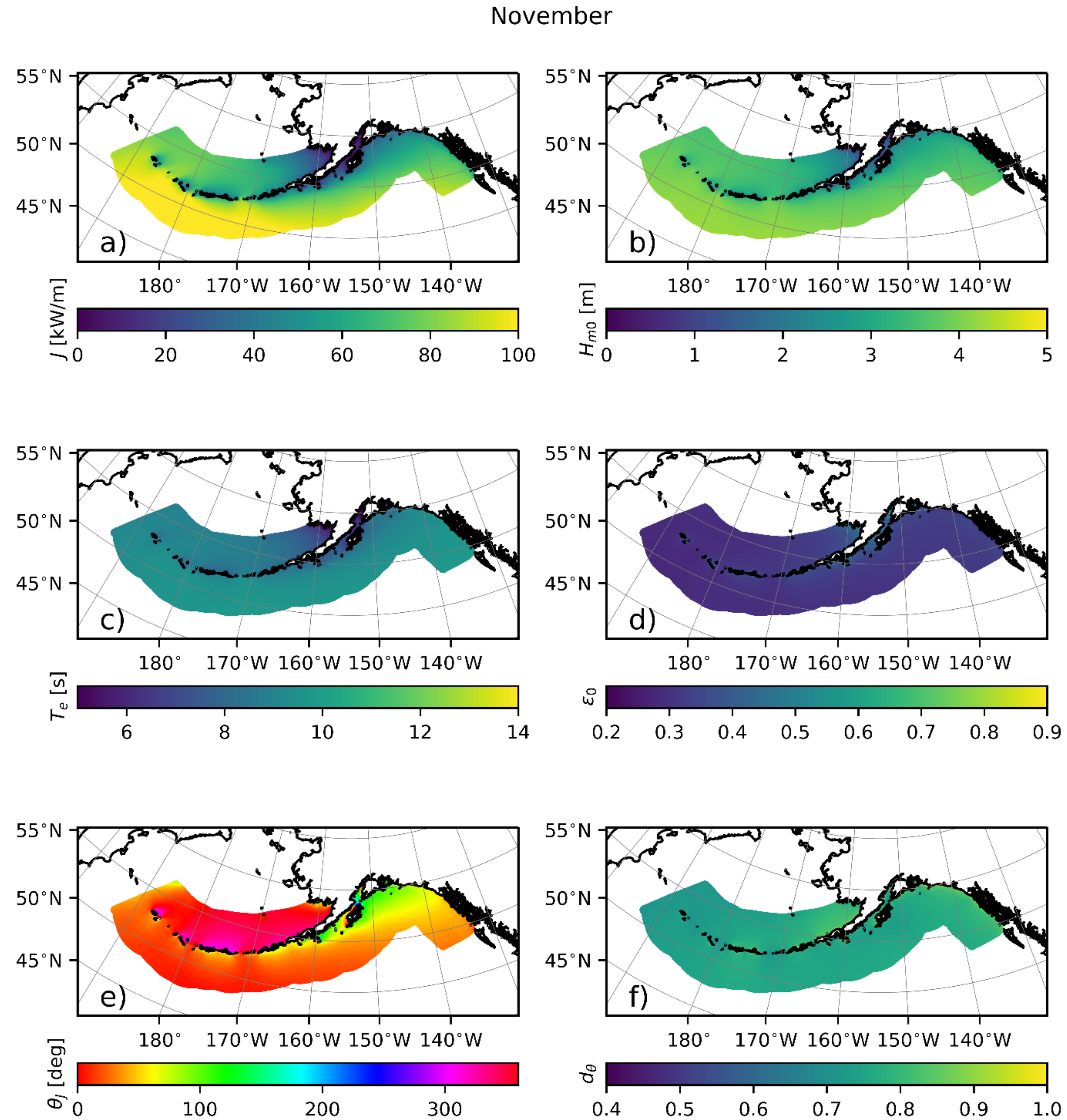

Figure D.11. Monthly distributions of six IEC parameters in November: (a) omnidirectional wave power, (b) significant wave height, (c) energy period, (d) spectral width, (e) direction of maximum directionally resolved wave power, and (f) directionality coefficient around Alaska.

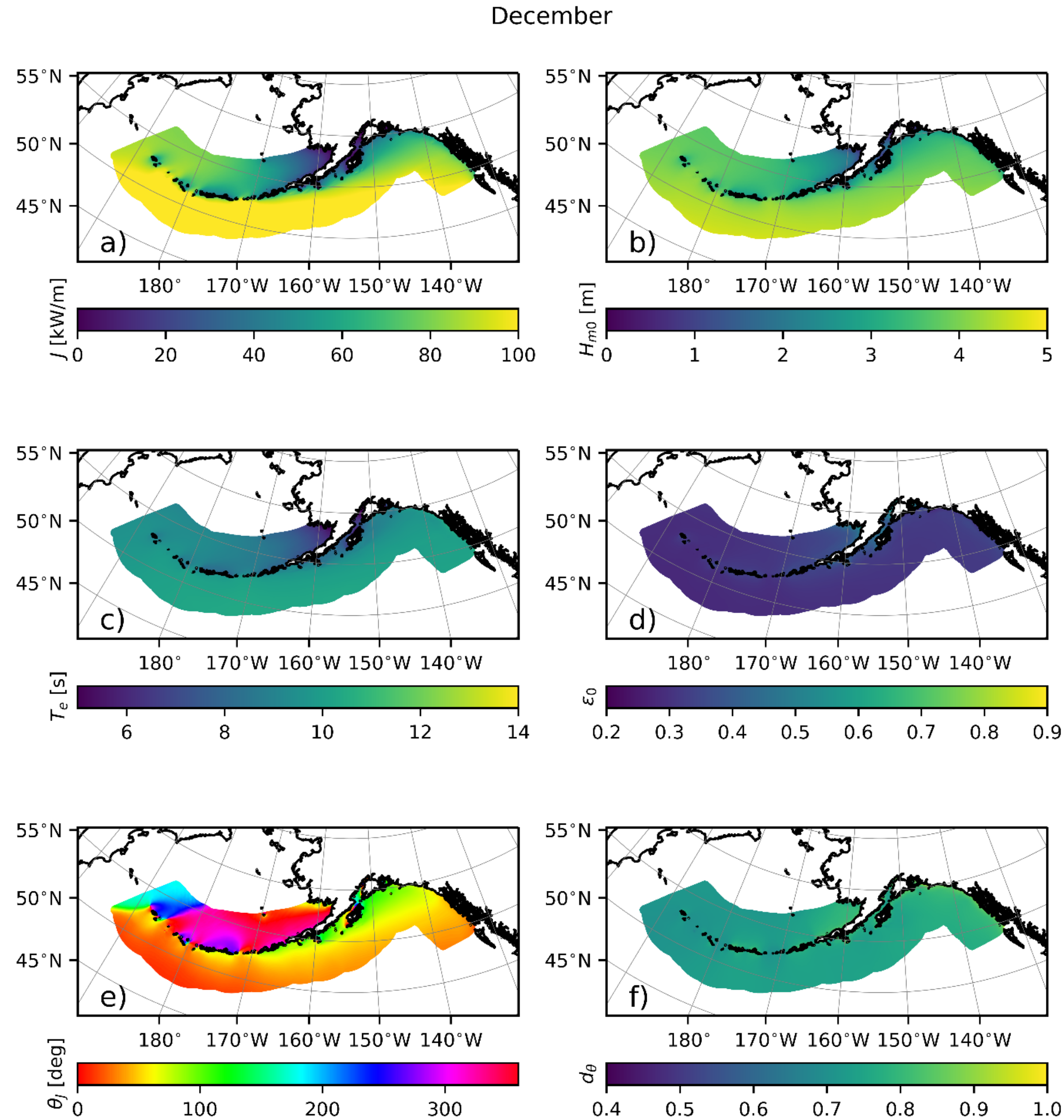

Figure D.12. Monthly distributions of six IEC parameters in December: (a) omnidirectional wave power, (b) significant wave height, (c) energy period, (d) spectral width, (e) direction of maximum directionally resolved wave power, and (f) directionality coefficient around Alaska.

Appendix E – Comparison of Model-Simulated IEC Parameters with Buoy Data

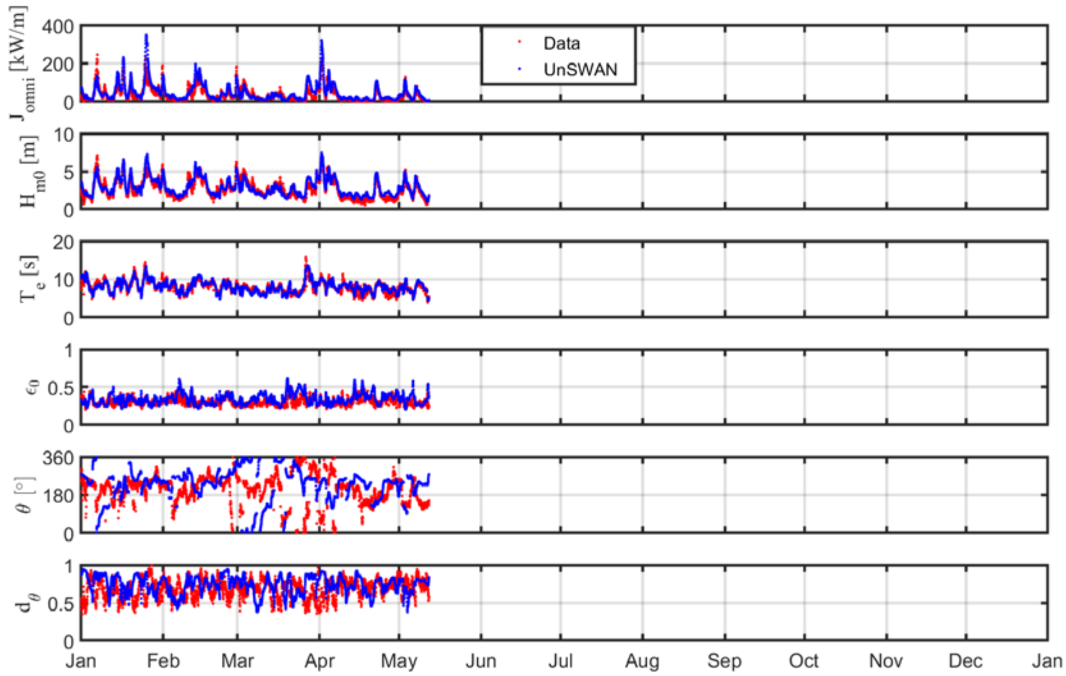

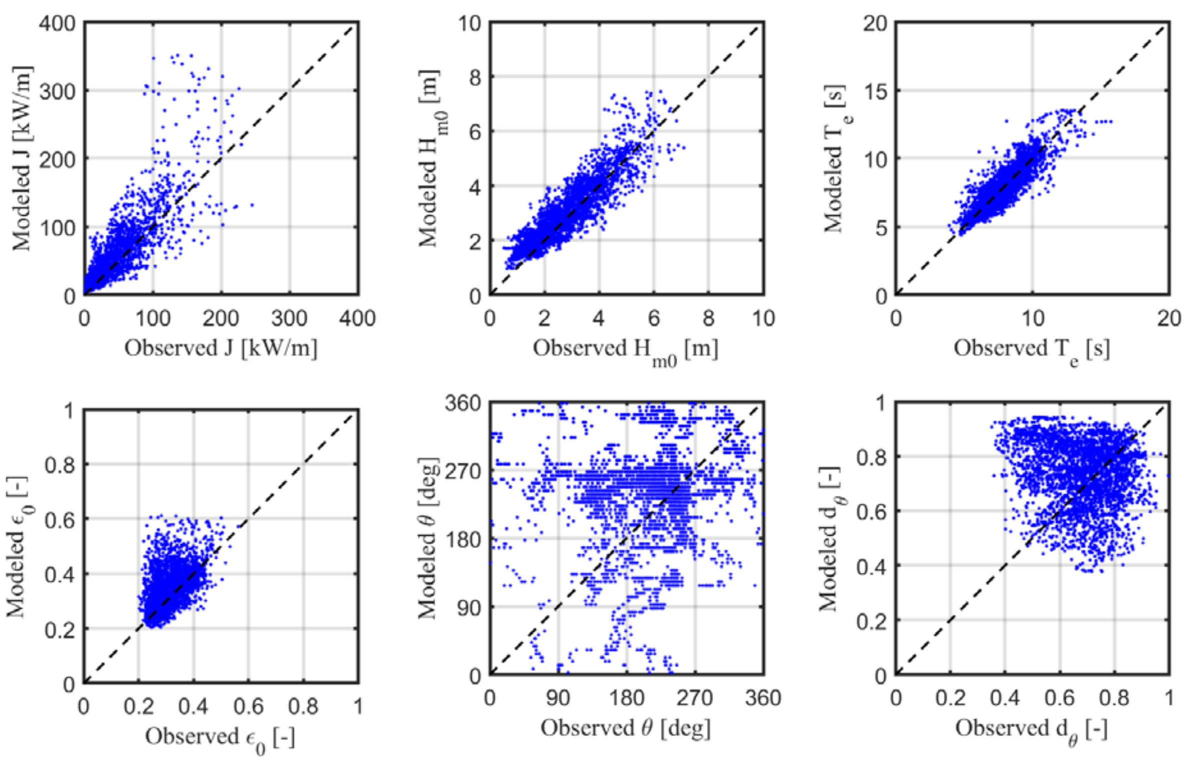

Figure E.1. Comparisons of time series (top) and scatter plots (bottom) of the six UnSWAN model-simulated IEC parameters with observed data at NDBC Buoy 46001 for 2017.

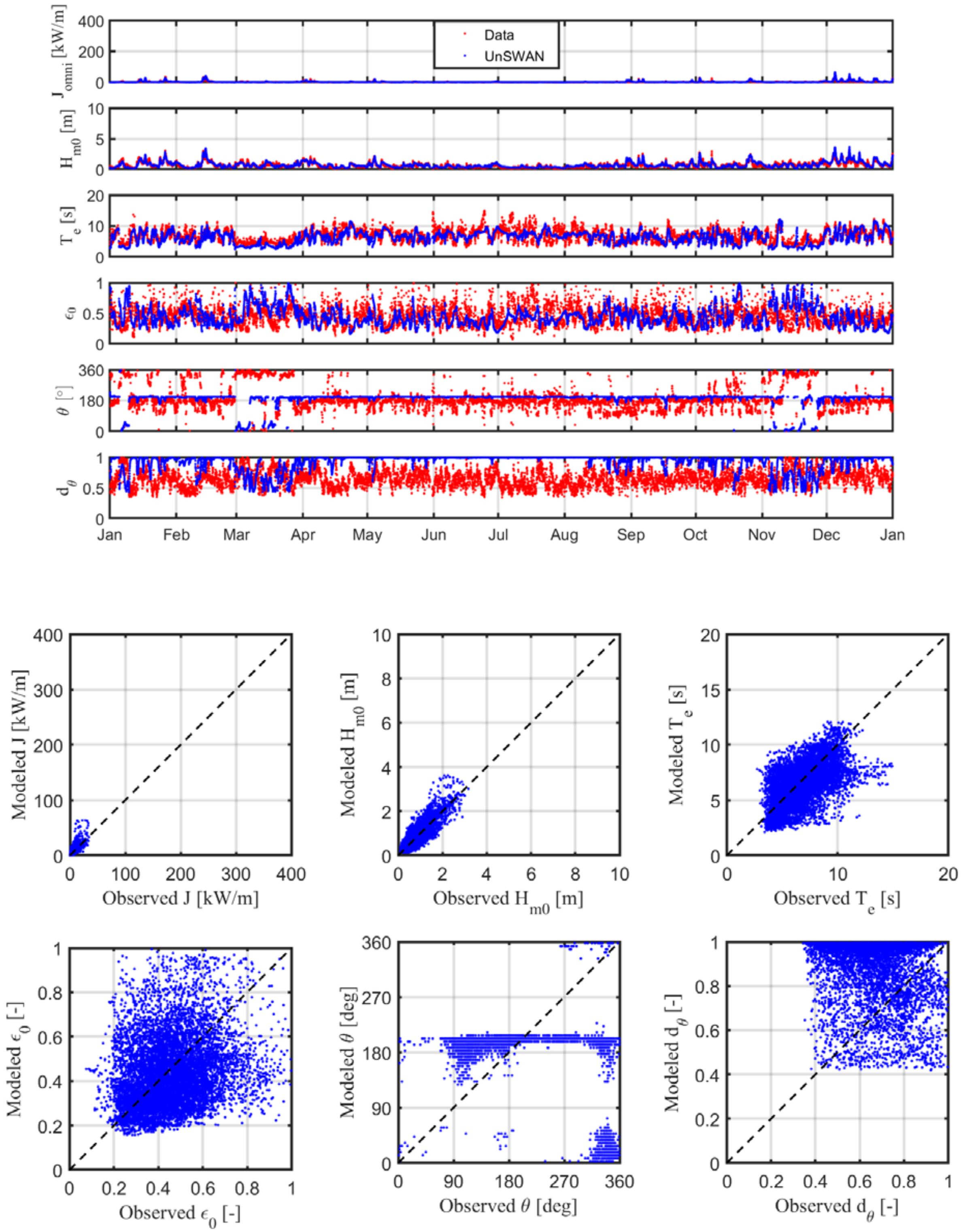

Figure E.2. Comparisons of time series (top) and scatter plots (bottom) of the six UnSWAN model-simulated IEC parameters with observed data at NDBC Buoy 46060 for 2017.

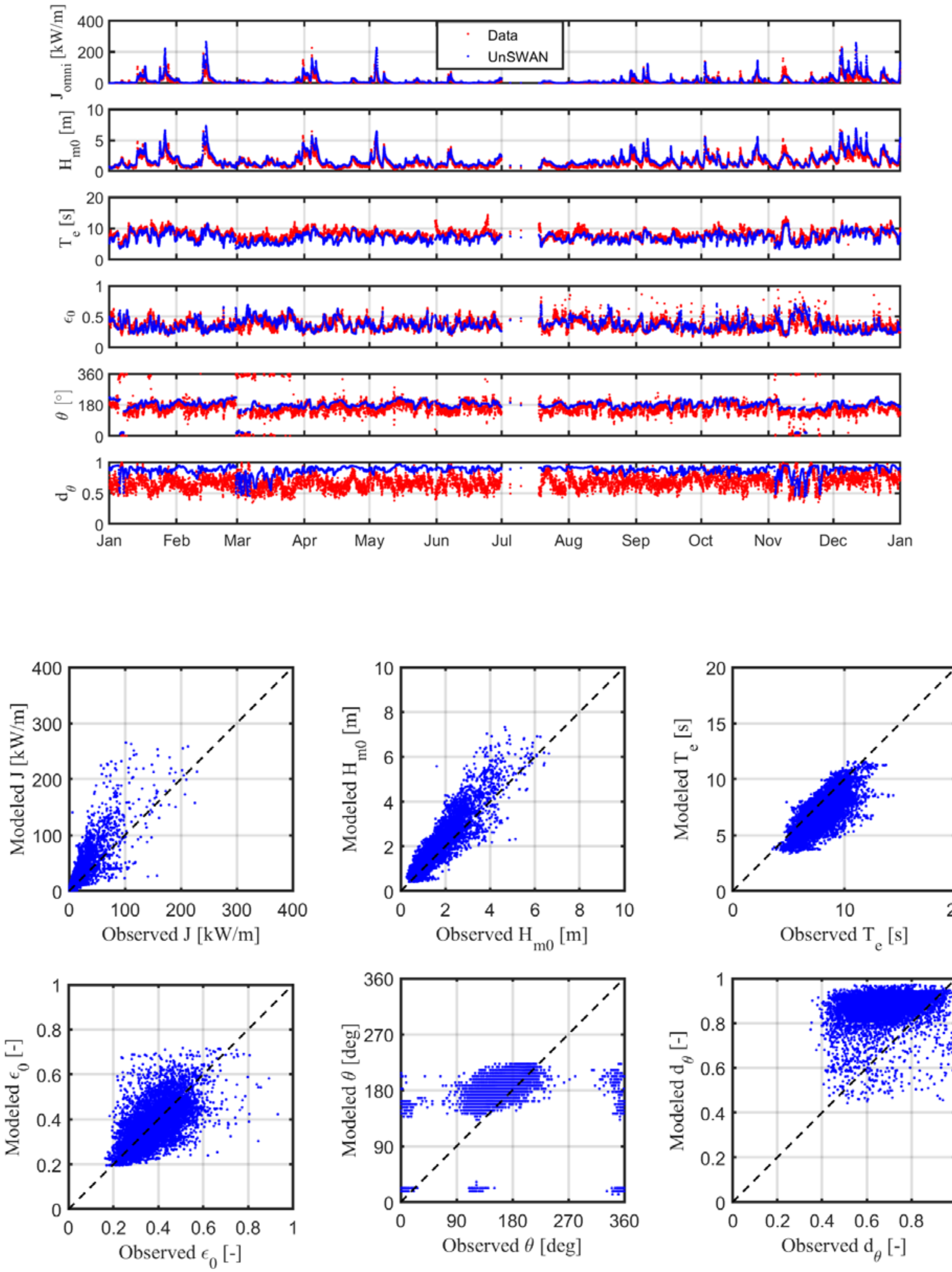

Figure E.3. Comparisons of time series (top) and scatter plots (bottom) of the six UnSWAN model-simulated IEC parameters with observed data at NDBC Buoy 46061 for 2017.

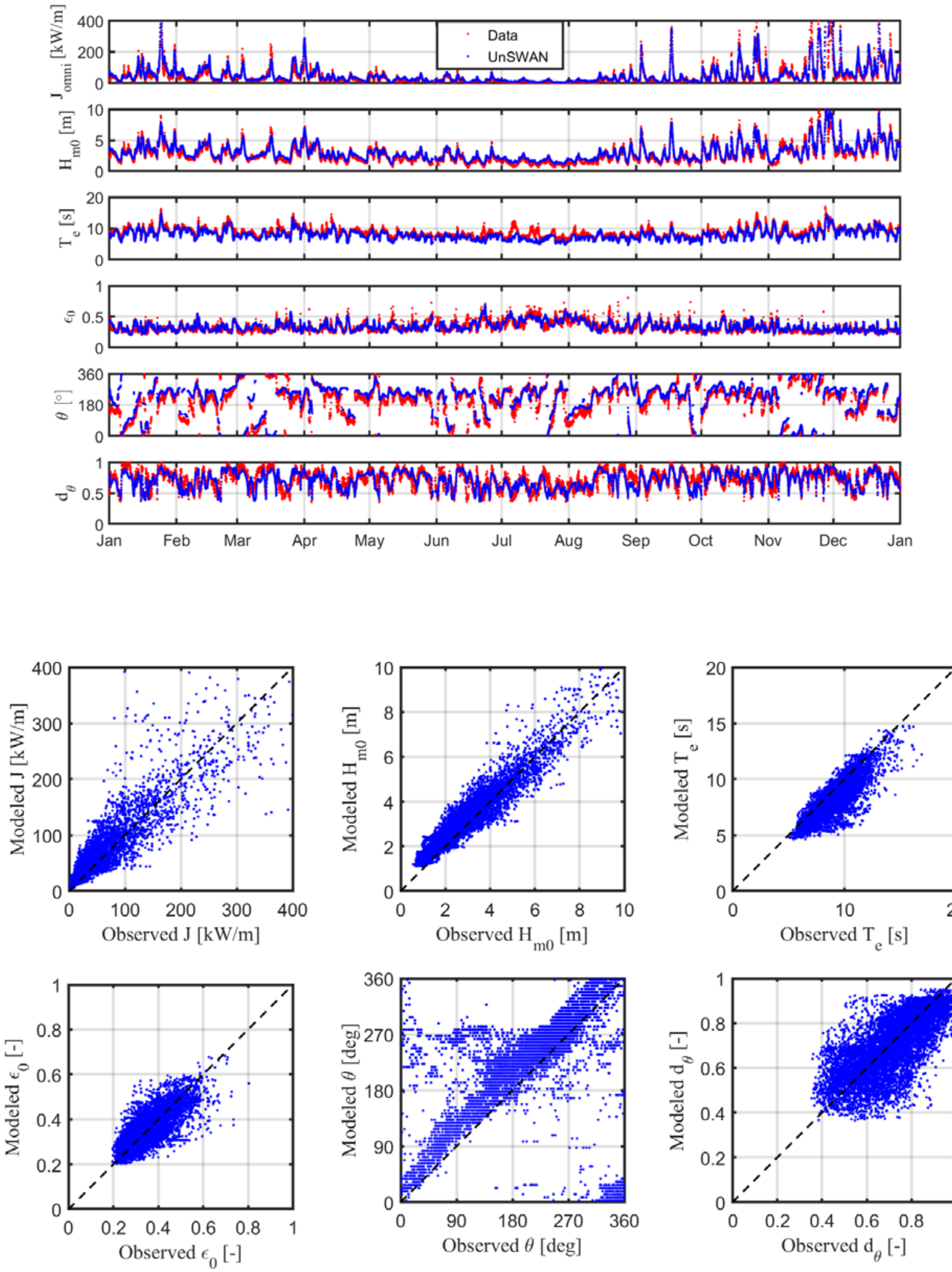

Figure E.4. Comparisons of time series (top) and scatter plots (bottom) of the six UnSWAN model-simulated IEC parameters with observed data at NDBC Buoy 46066 for 2017.

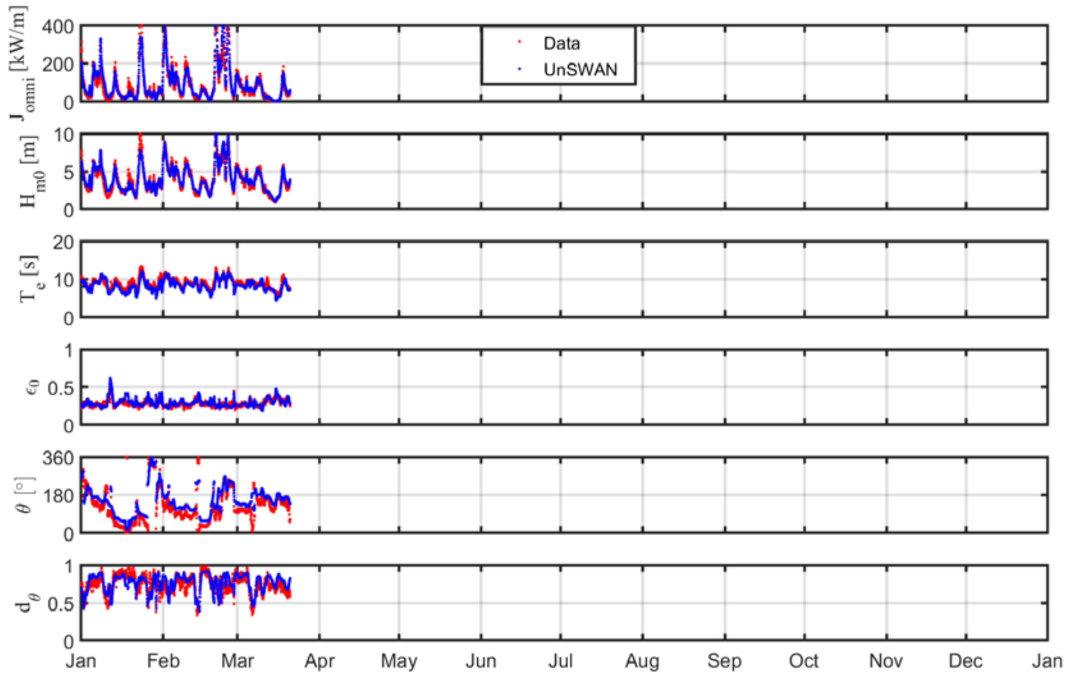

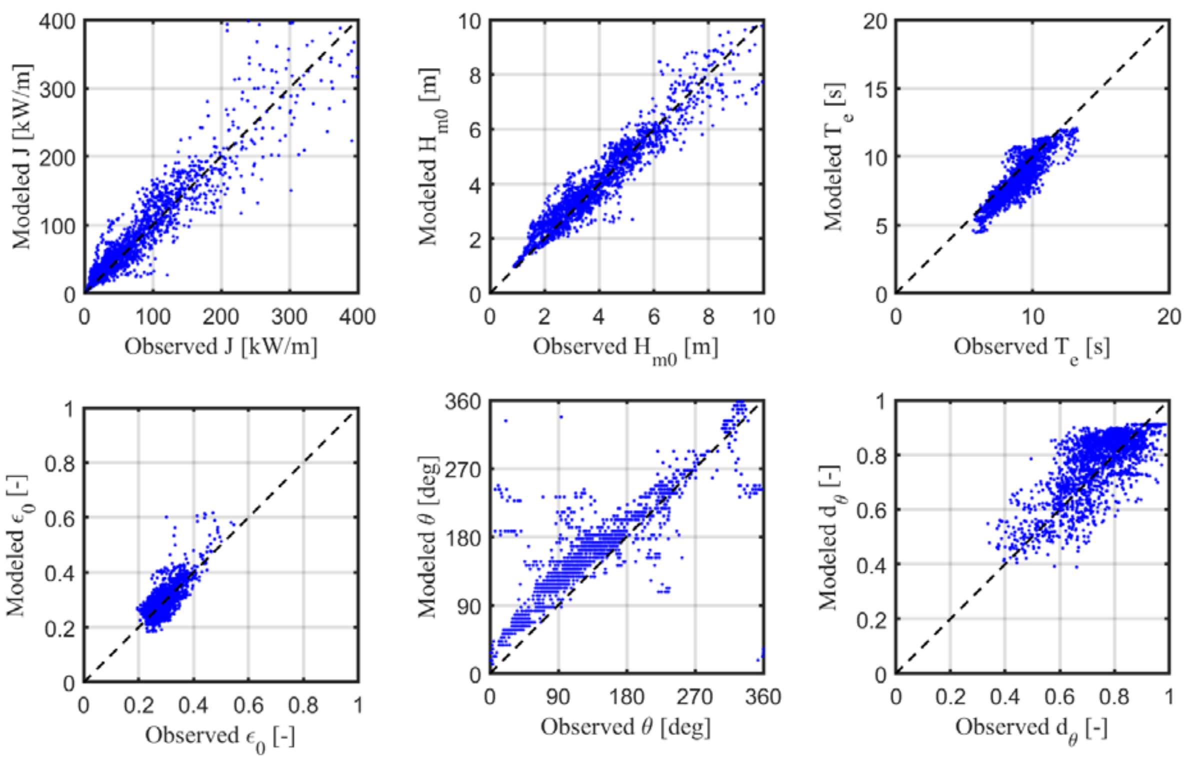

Figure E.5. Comparisons of time series (top) and scatter plots (bottom) of the six UnSWAN model-simulated IEC parameters with observed data at NDBC Buoy 46070 for 2017.

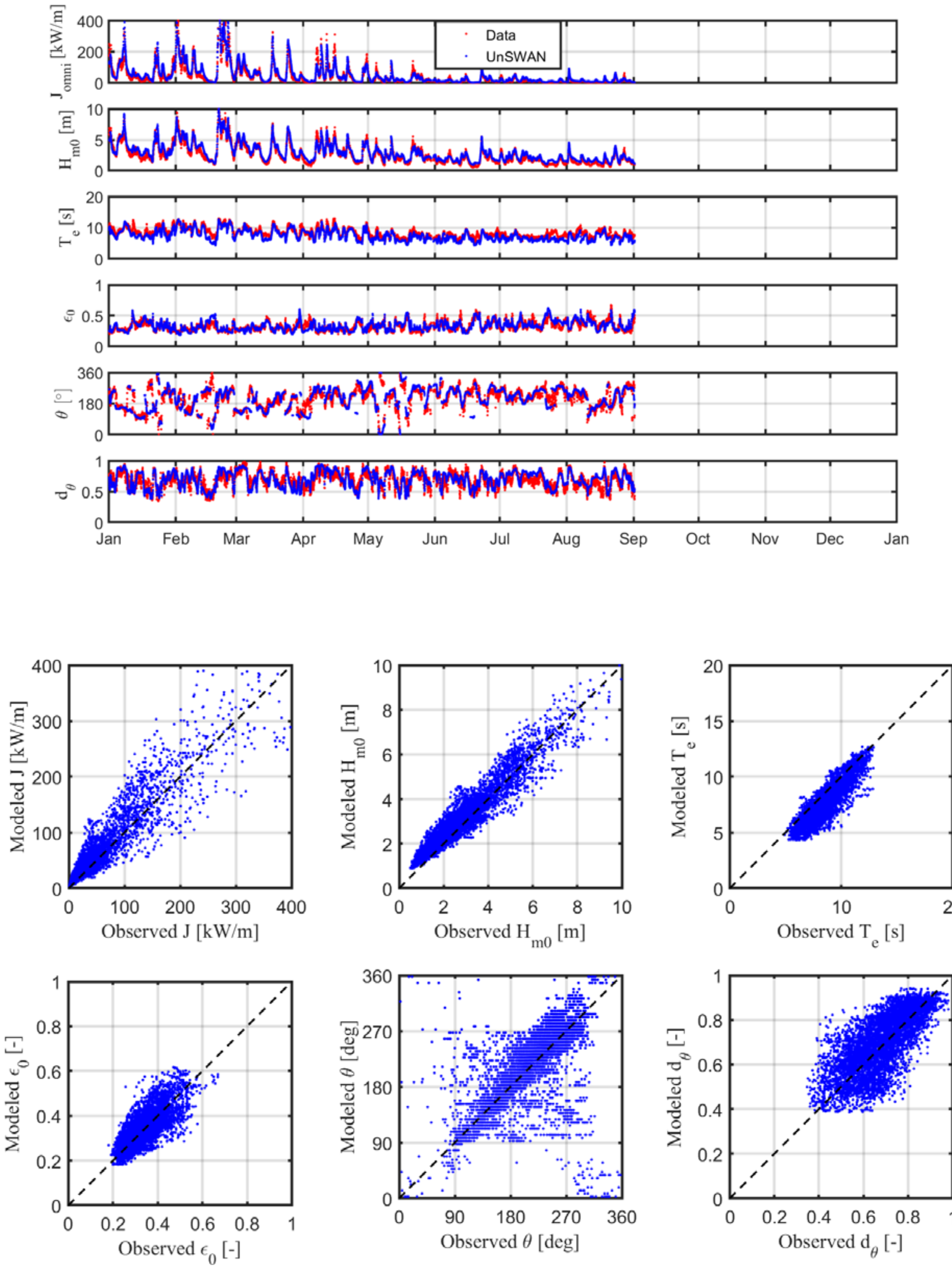

Figure E.6. Comparisons of time series (top) and scatter plots (bottom) of the six UnSWAN model-simulated IEC parameters with observed data at NDBC Buoy 46071 for 2017.

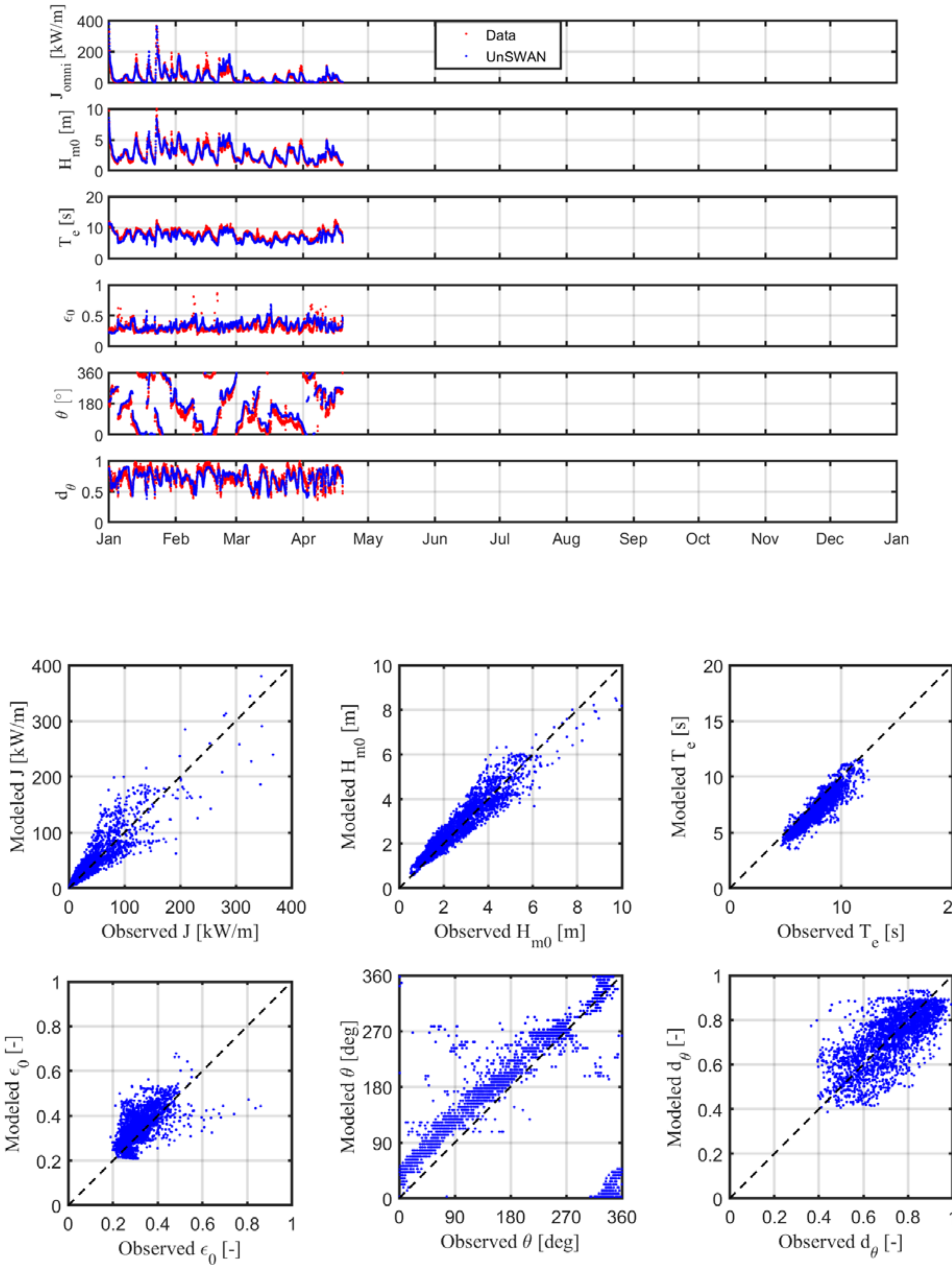

Figure E.7. Comparisons of time series (top) and scatter plots (bottom) of the six UnSWAN model-simulated IEC parameters with observed data at NDBC Buoy 46073 for 2017.

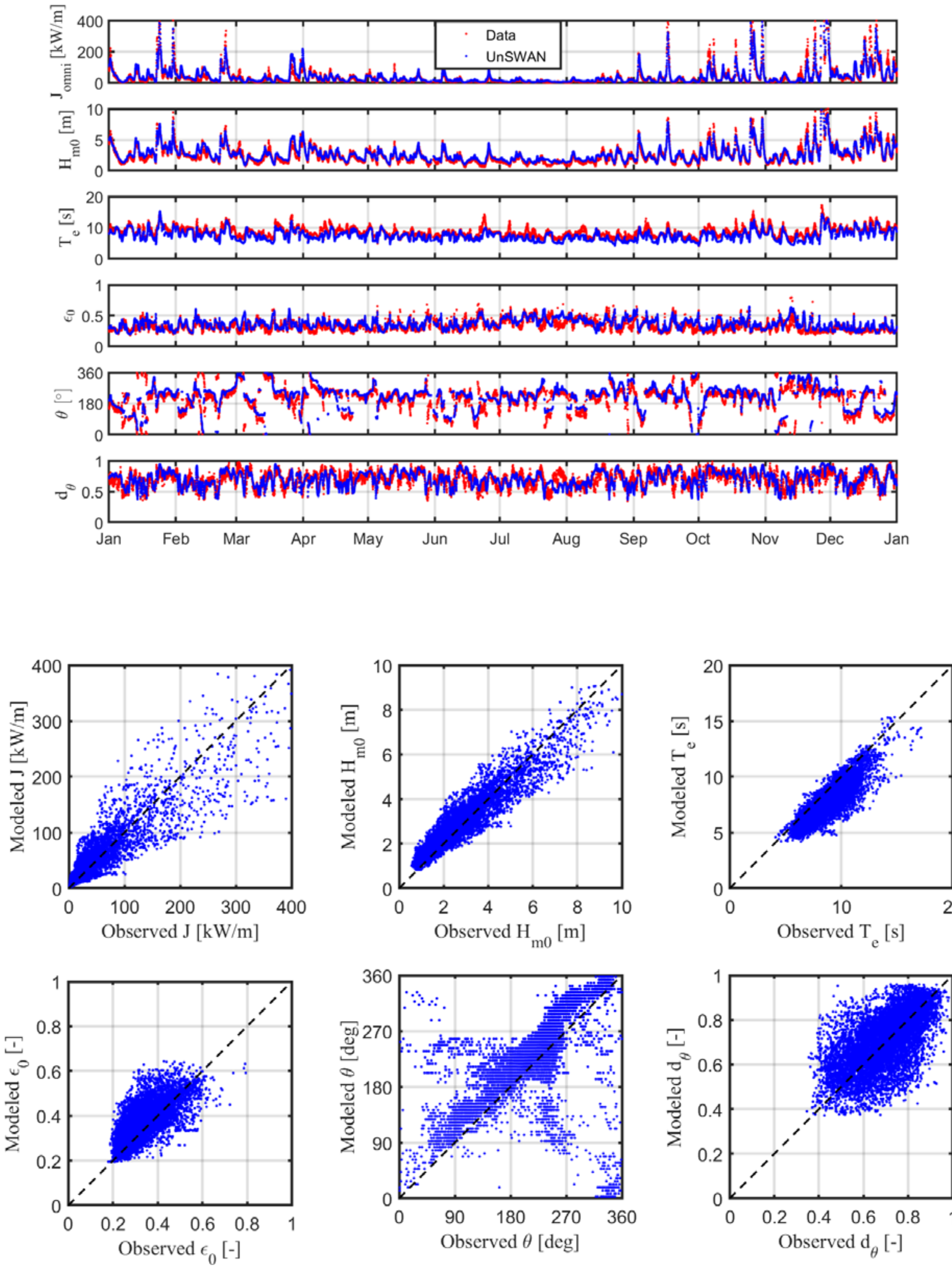

Figure E.8. Comparisons of time series (top) and scatter plots (bottom) of the six UnSWAN model-simulated IEC parameters with observed data at NDBC Buoy 46075 for 2017.

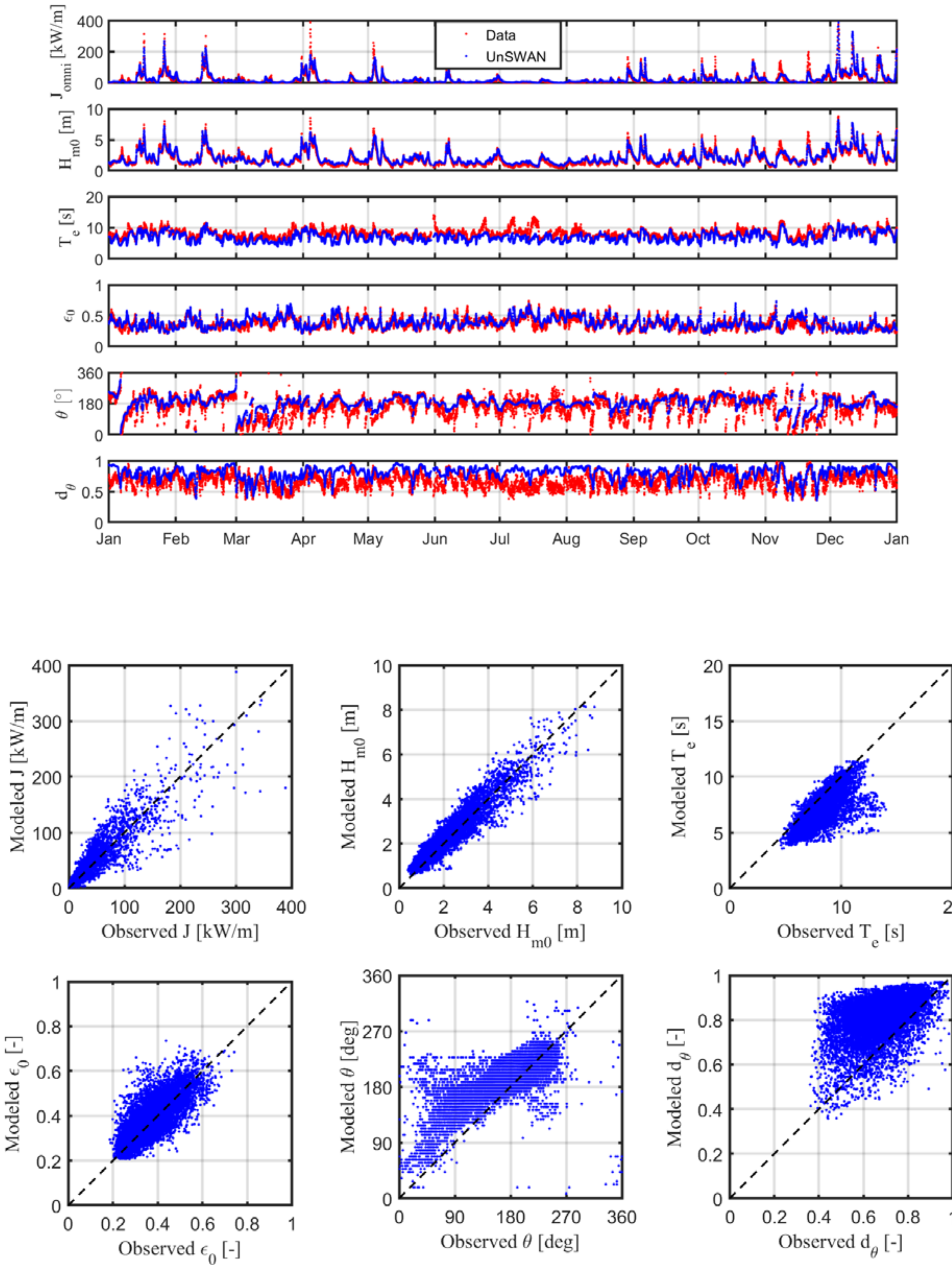

Figure E.9. Comparisons of time series (top) and scatter plots (bottom) of the six UnSWAN model-simulated IEC parameters with observed data at NDBC Buoy 46076 for 2017.

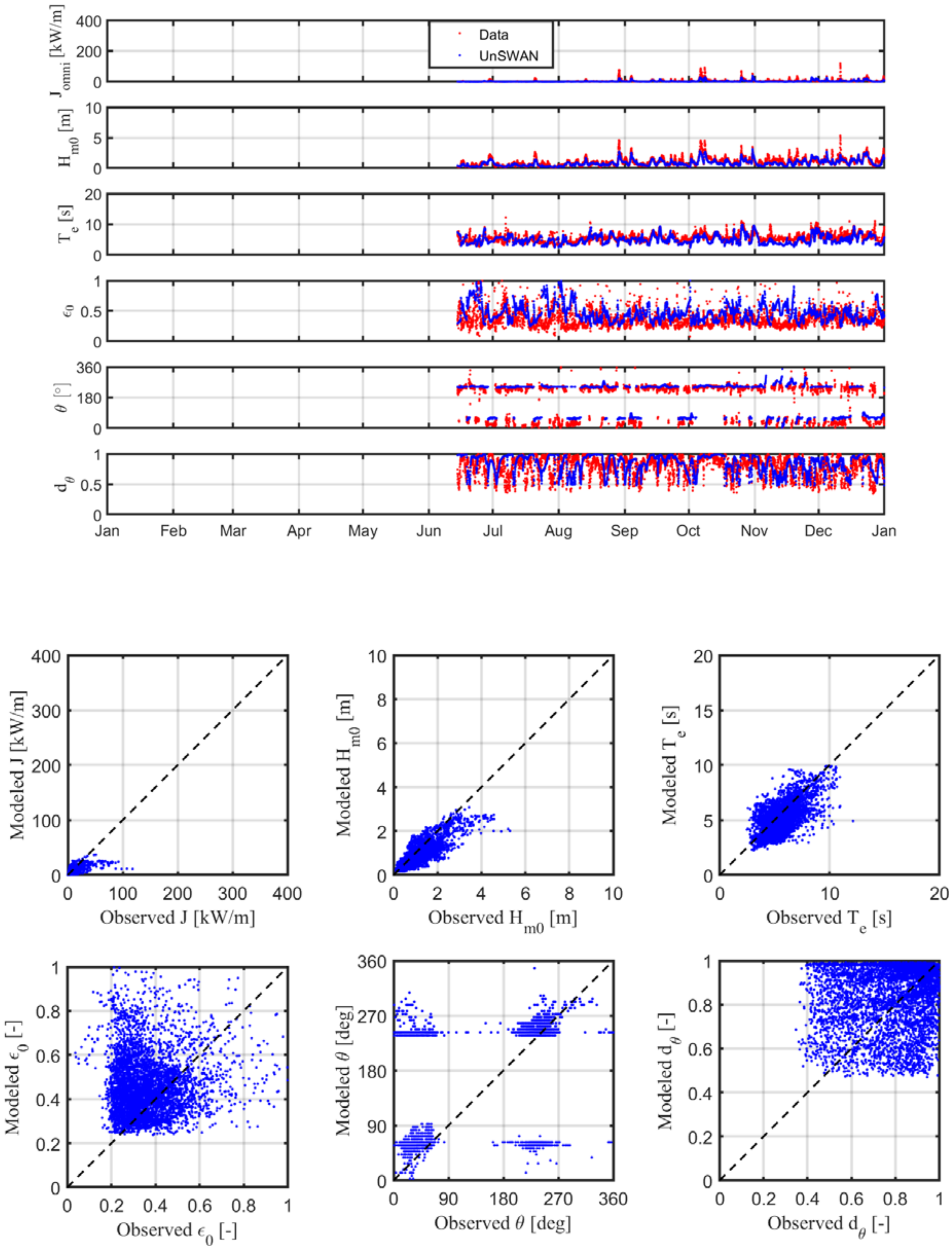

Figure E.10. Comparisons of time series (top) and scatter plots (bottom) of the six UnSWAN model-simulated IEC parameters with observed data at NDBC Buoy 46077 for 2017.

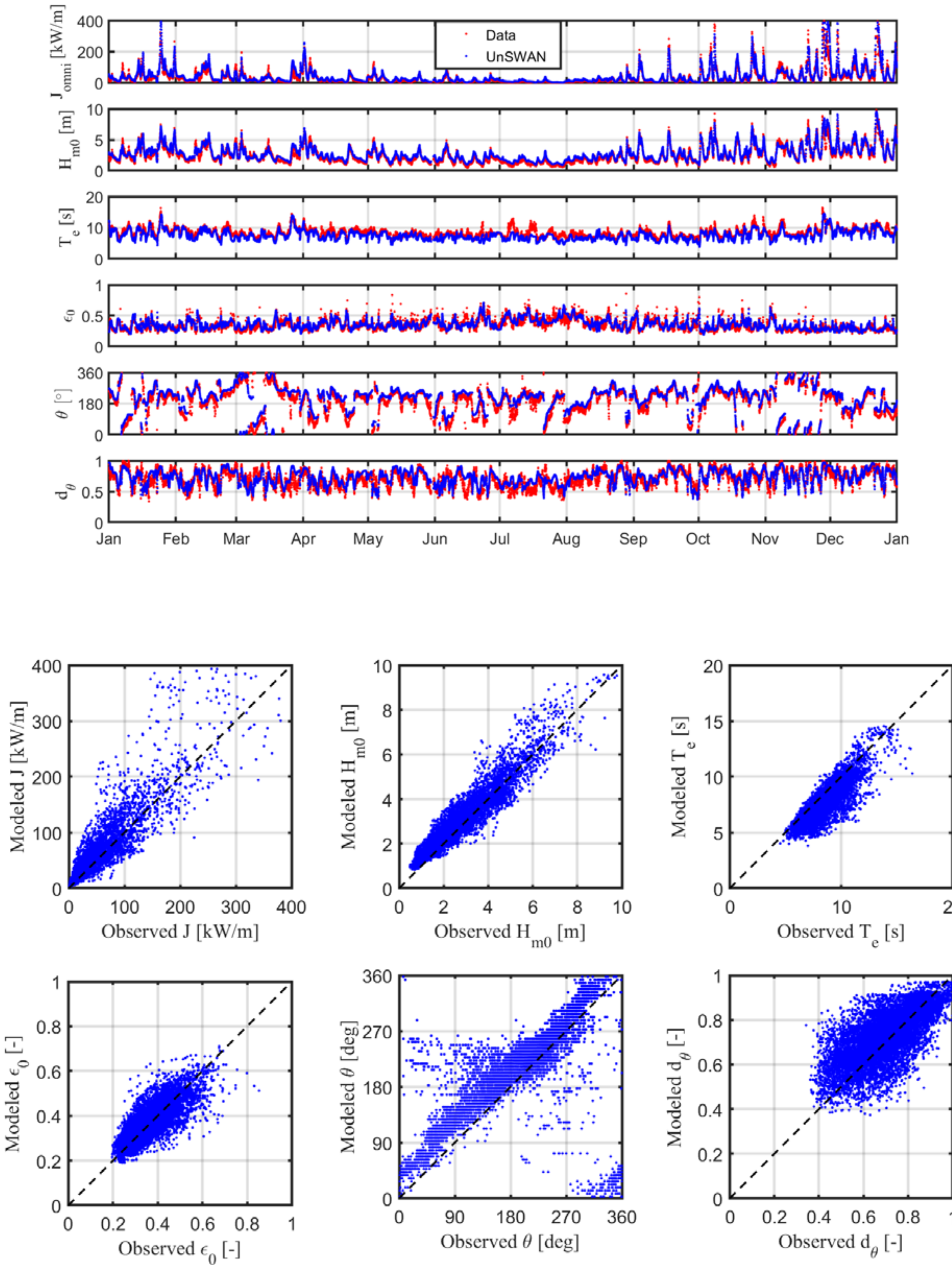

Figure E.11. Comparisons of time series (top) and scatter plots (bottom) of the six UnSWAN model-simulated IEC parameters with observed data at NDBC Buoy 46078 for 2017.

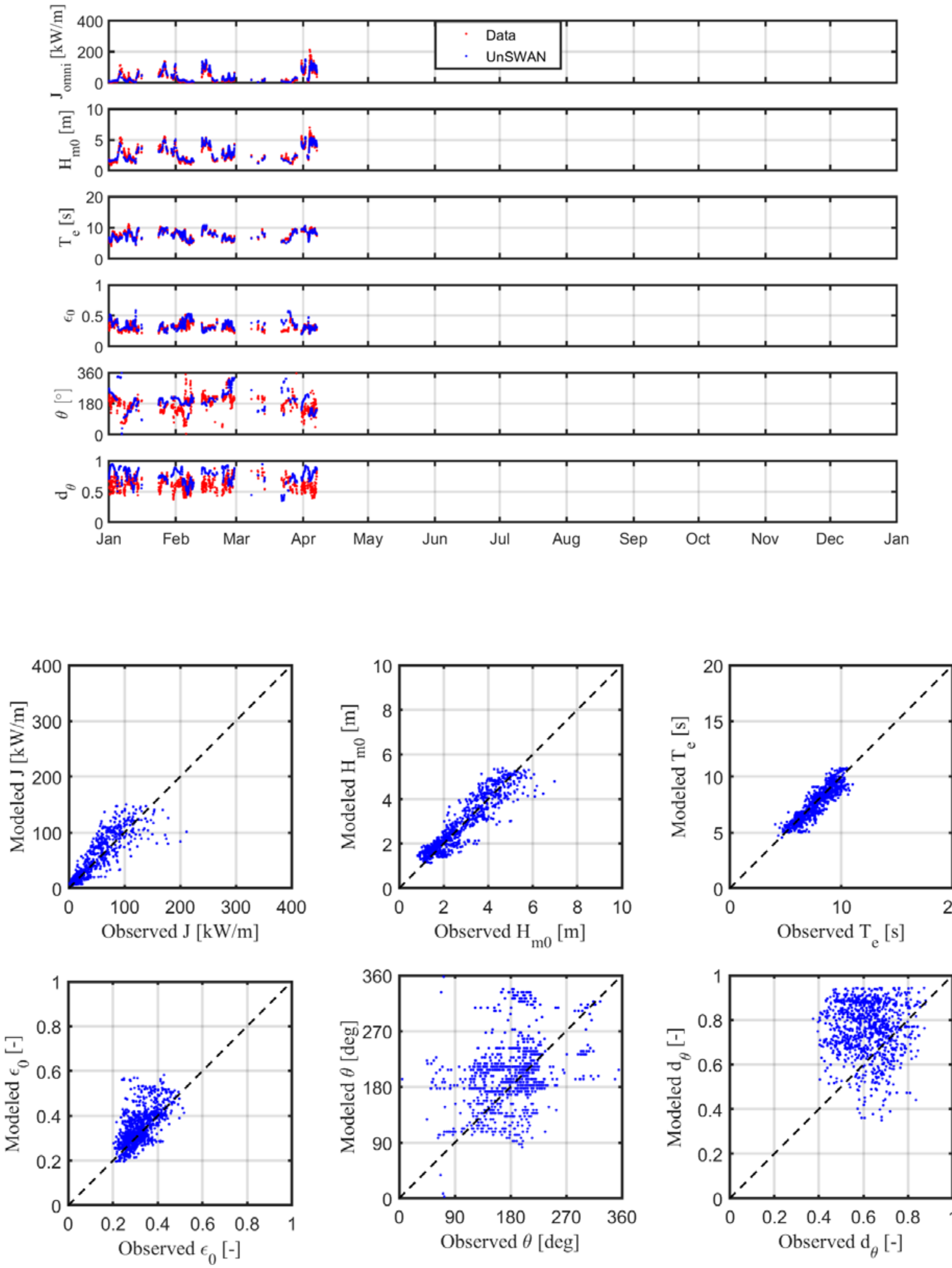

Figure E.12. Comparisons of time series (top) and scatter plots (bottom) of the six UnSWAN model-simulated IEC parameters with observed data at NDBC Buoy 46080 for 2017.

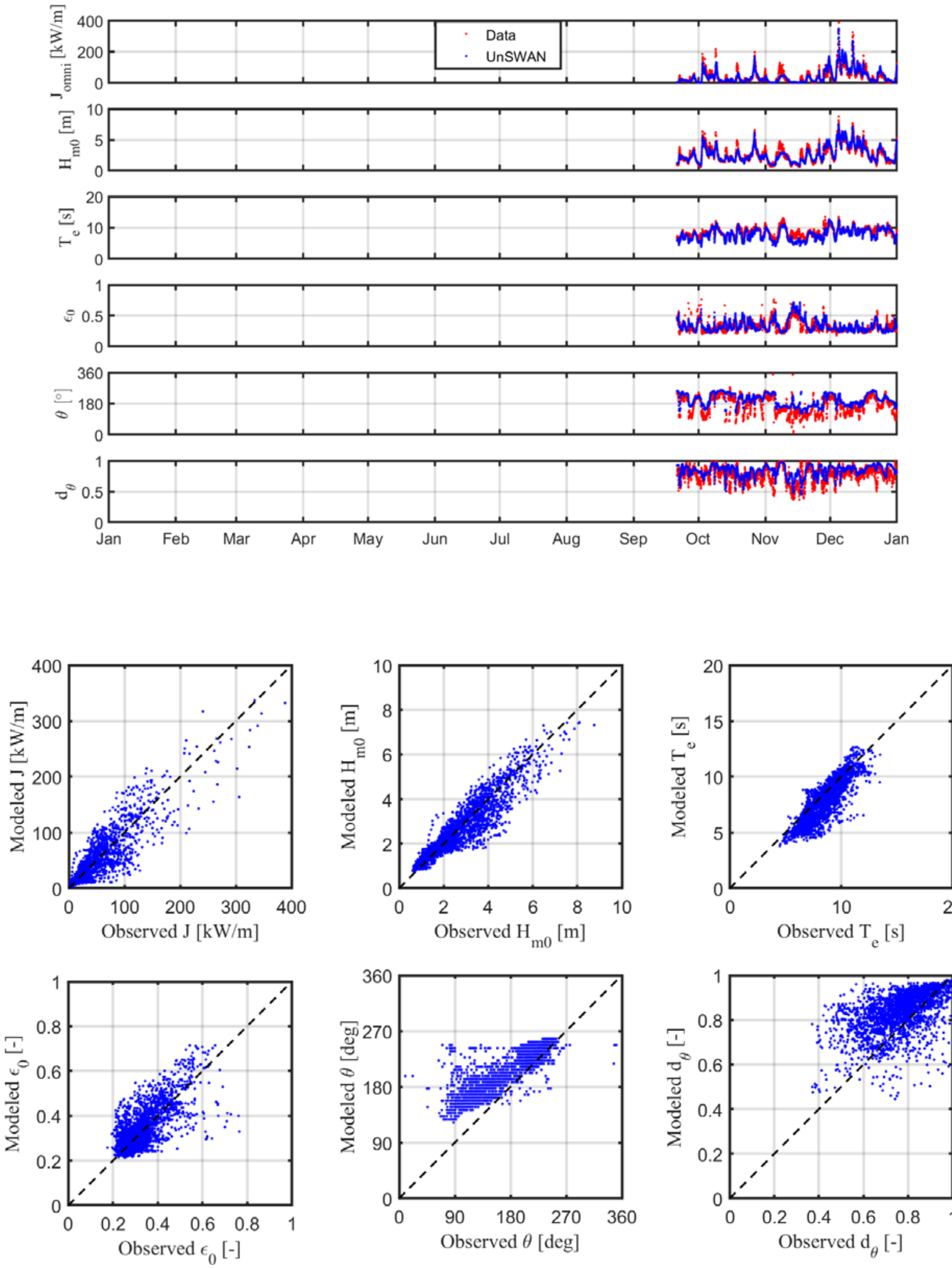

Figure E.13. Comparisons of time series (top) and scatter plots (bottom) of the six UnSWAN model-simulated IEC parameters with observed data at NDBC Buoy 46082 for 2017.

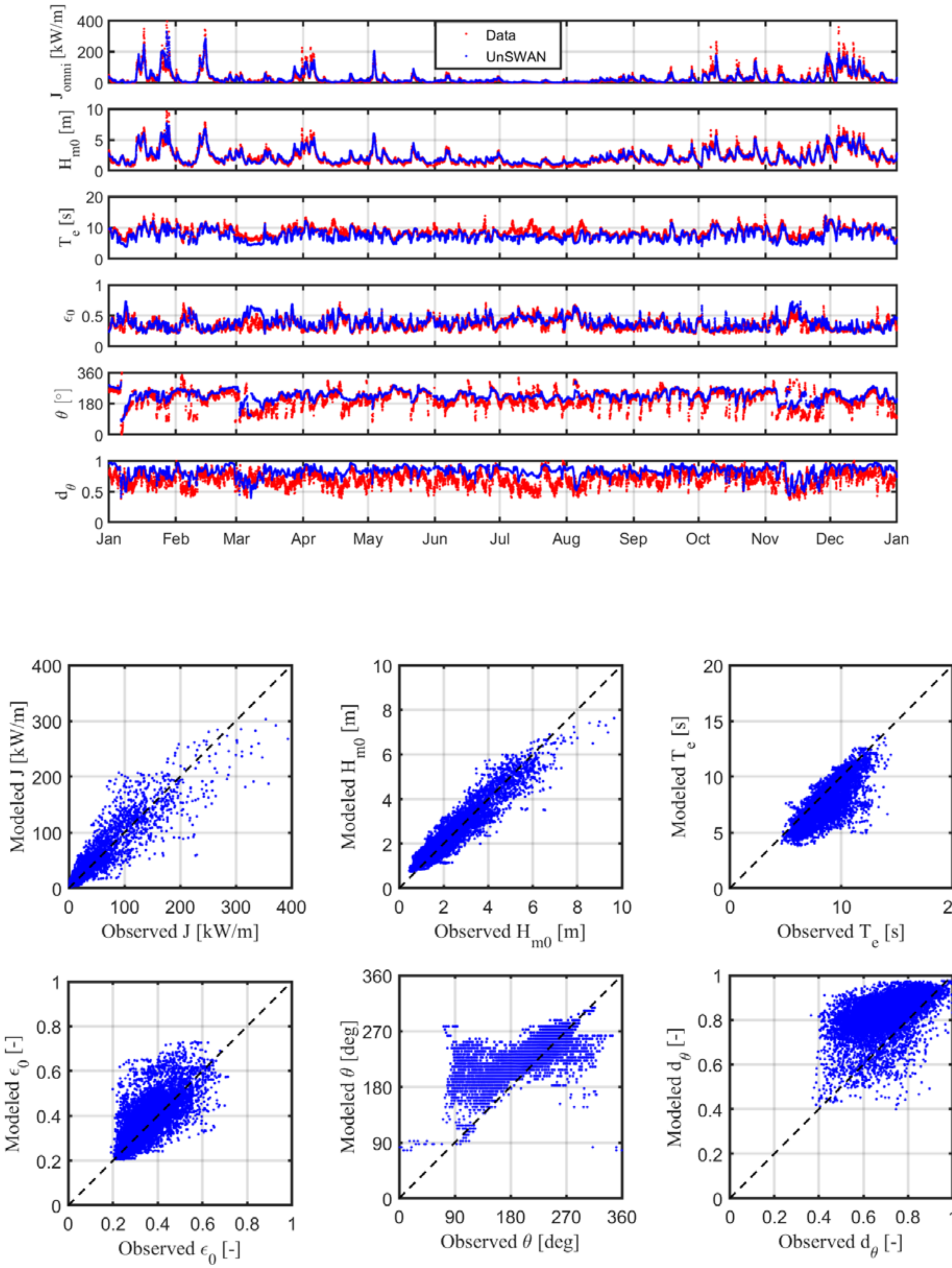

Figure E.14. Comparisons of time series (top) and scatter plots (bottom) of the six UnSWAN model-simulated IEC parameters with observed data at NDBC Buoy 46083 for 2017.

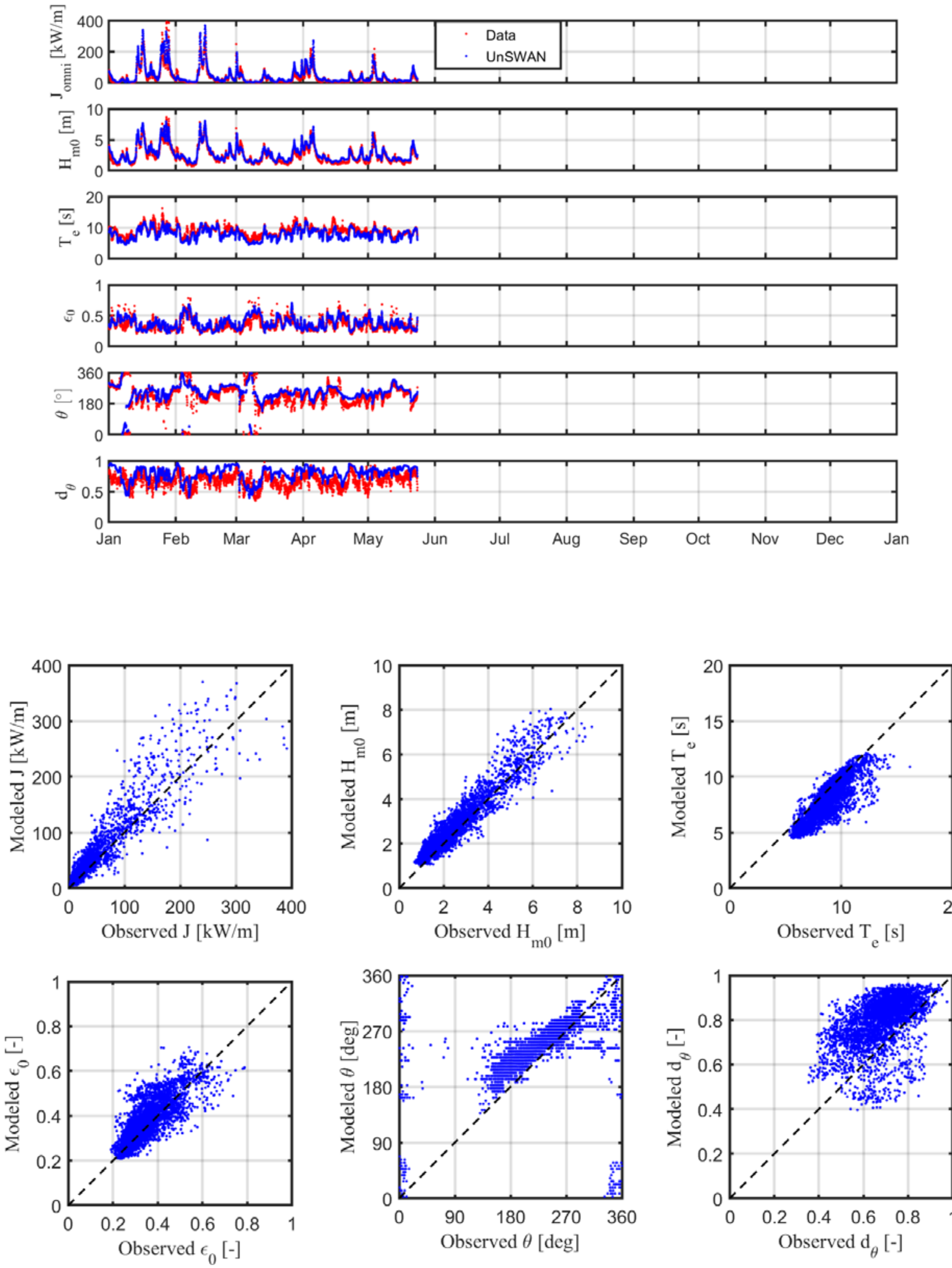

Figure E.15. Comparisons of time series (top) and scatter plots (bottom) of the six UnSWAN model-simulated IEC parameters with observed data at NDBC Buoy 46084 for 2017.

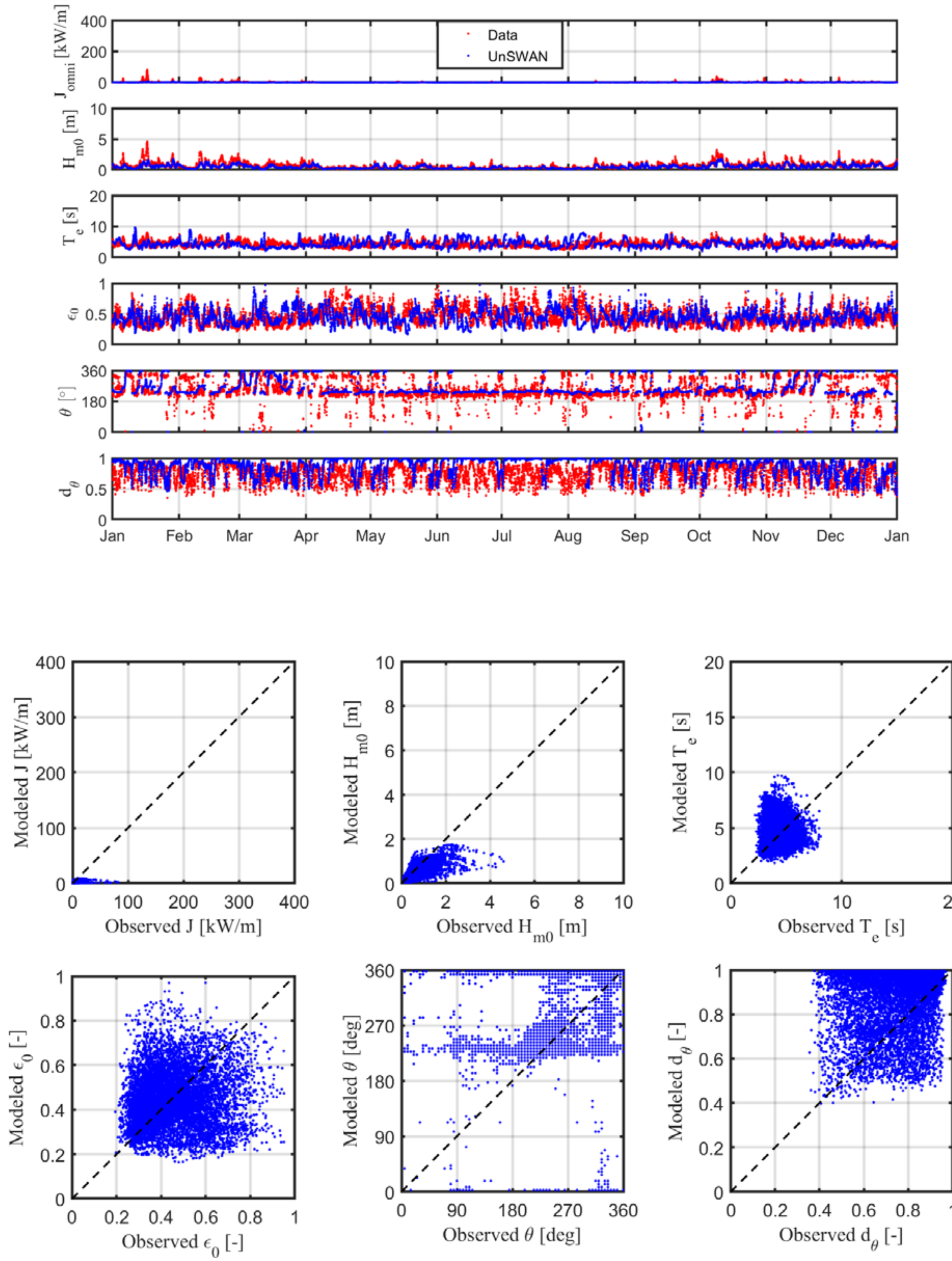

Figure E.16. Comparisons of time series (top) and scatter plots (bottom) of the six UnSWAN model-simulated IEC parameters with observed data at NDBC Buoy 46108 for 2017.

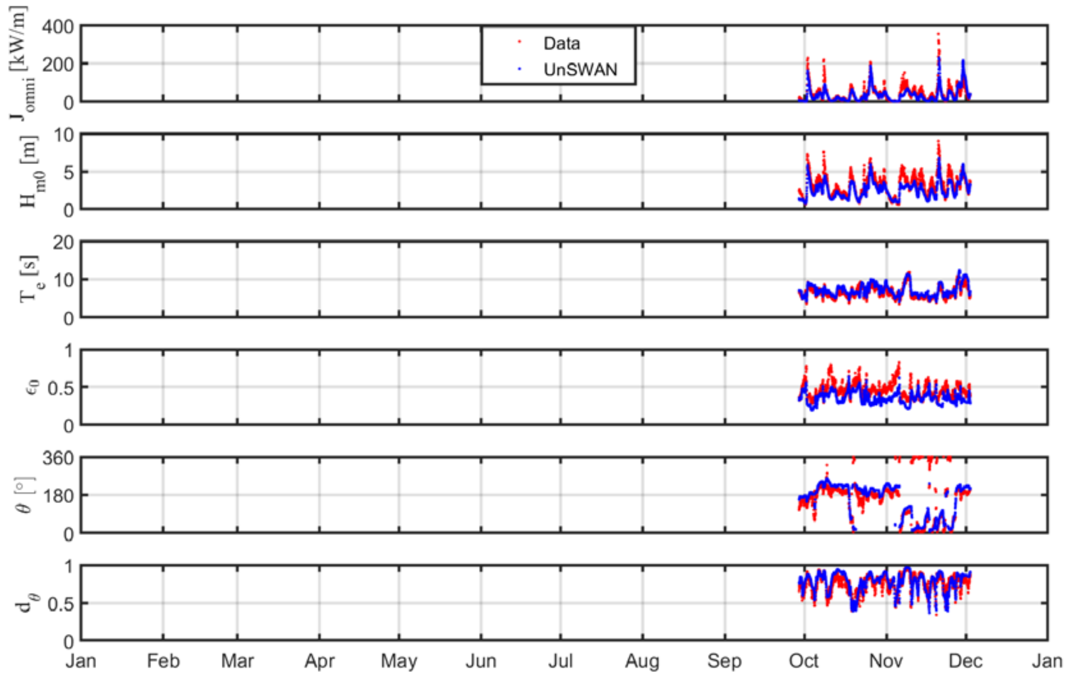

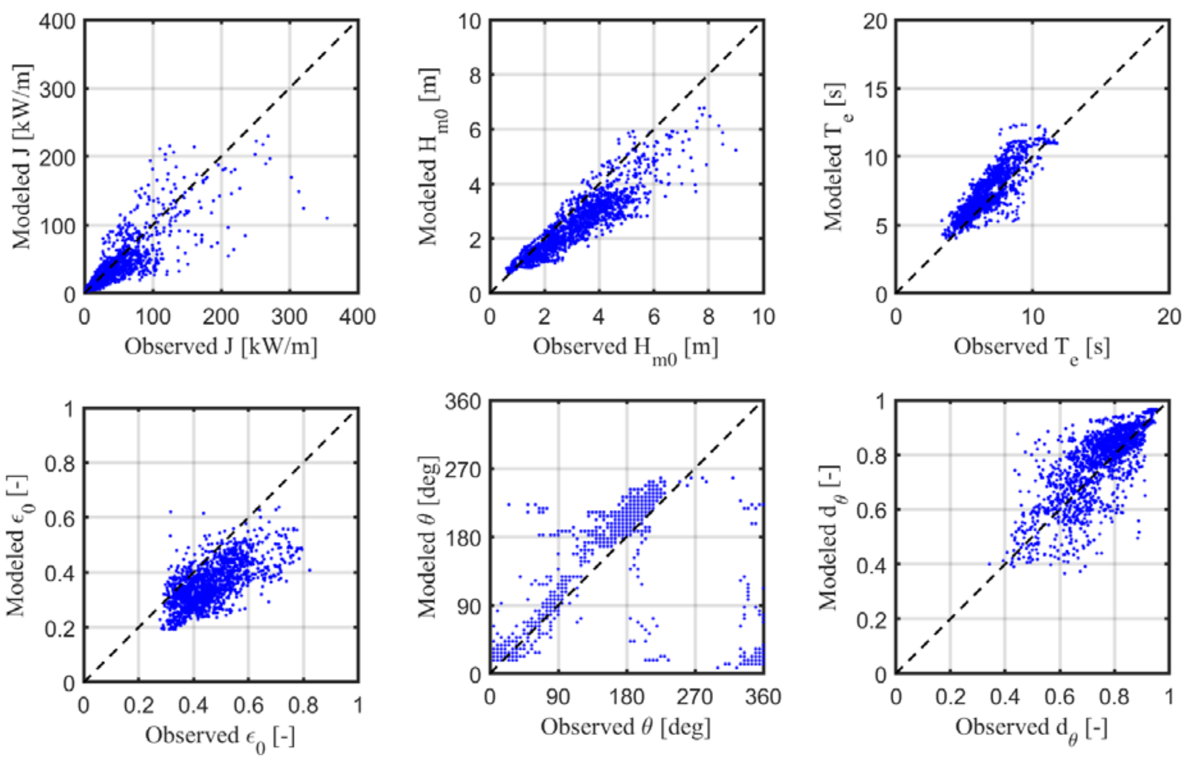

Figure E.17. Comparisons of time series (top) and scatter plots (bottom) of the six UnSWAN model-simulated IEC parameters with observed data at NDBC Buoy 46264 for 2017.

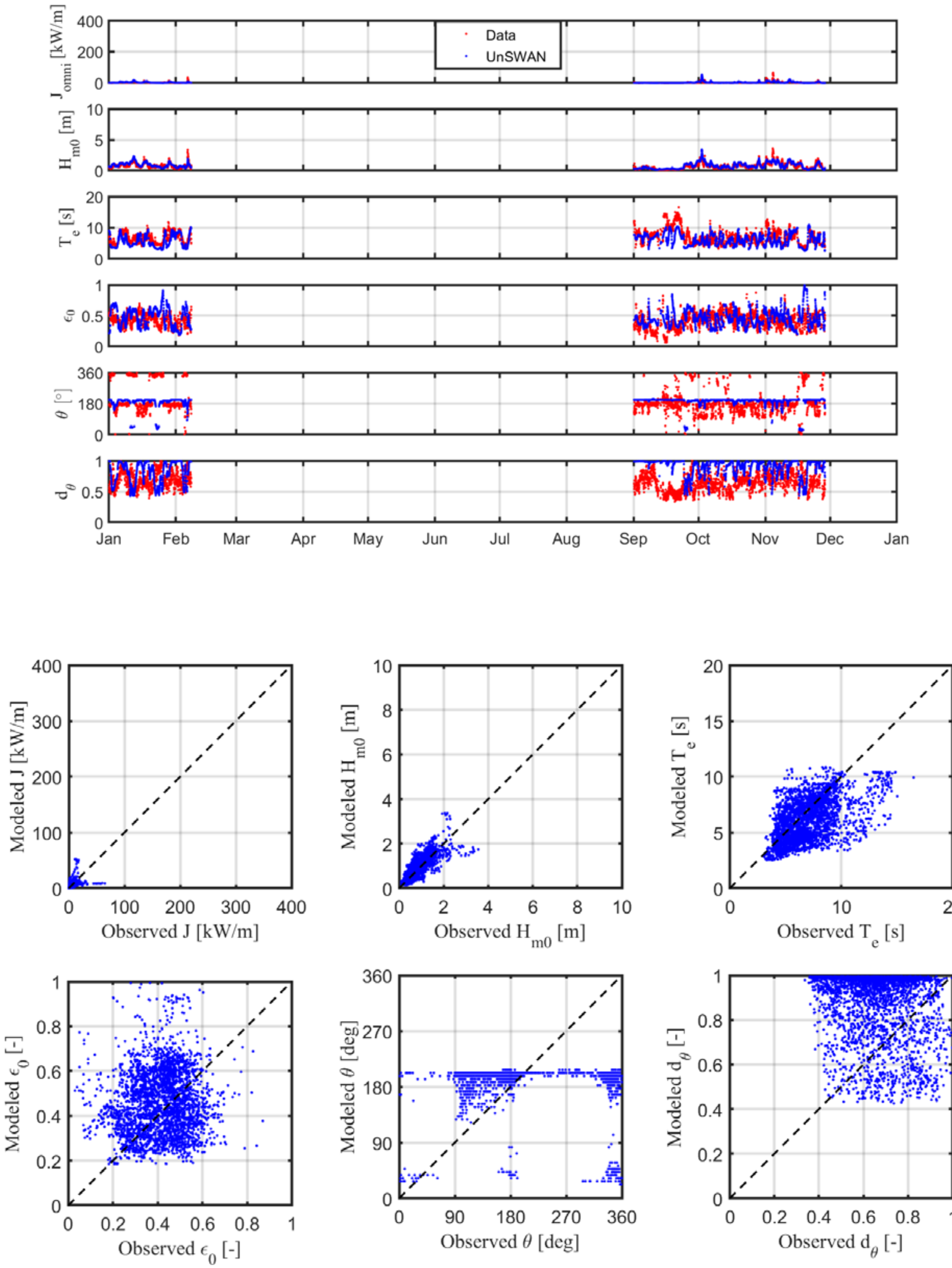

Figure E.18. Comparisons of time series (top) and scatter plots (bottom) of the six UnSWAN model-simulated IEC parameters with observed data at NDBC Buoy 46060 for 2010.

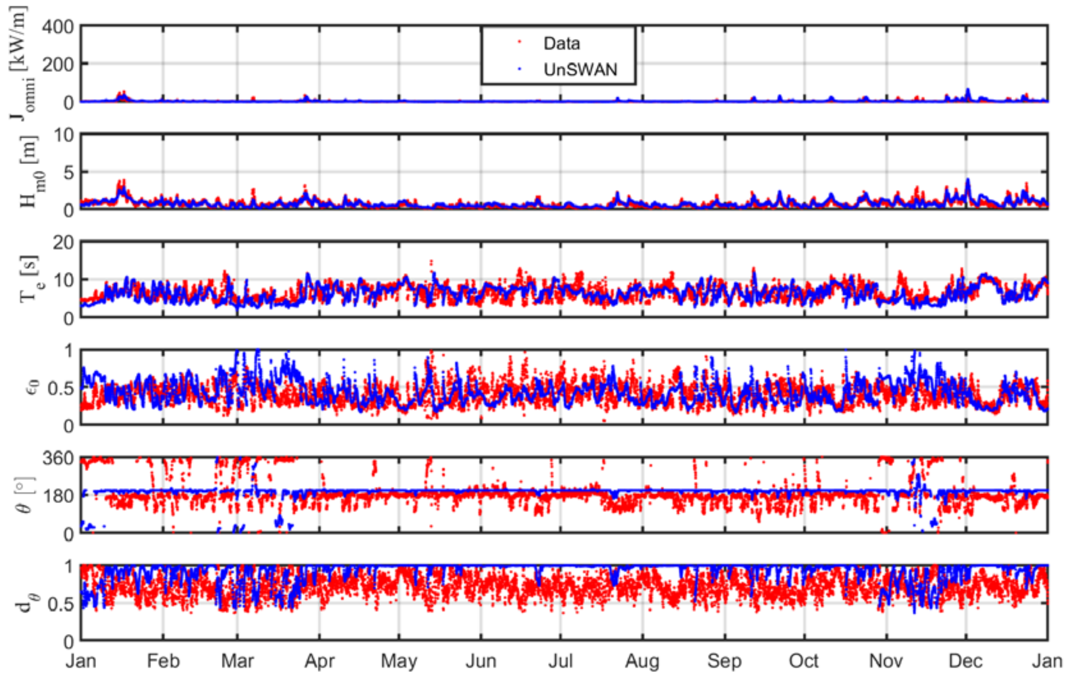

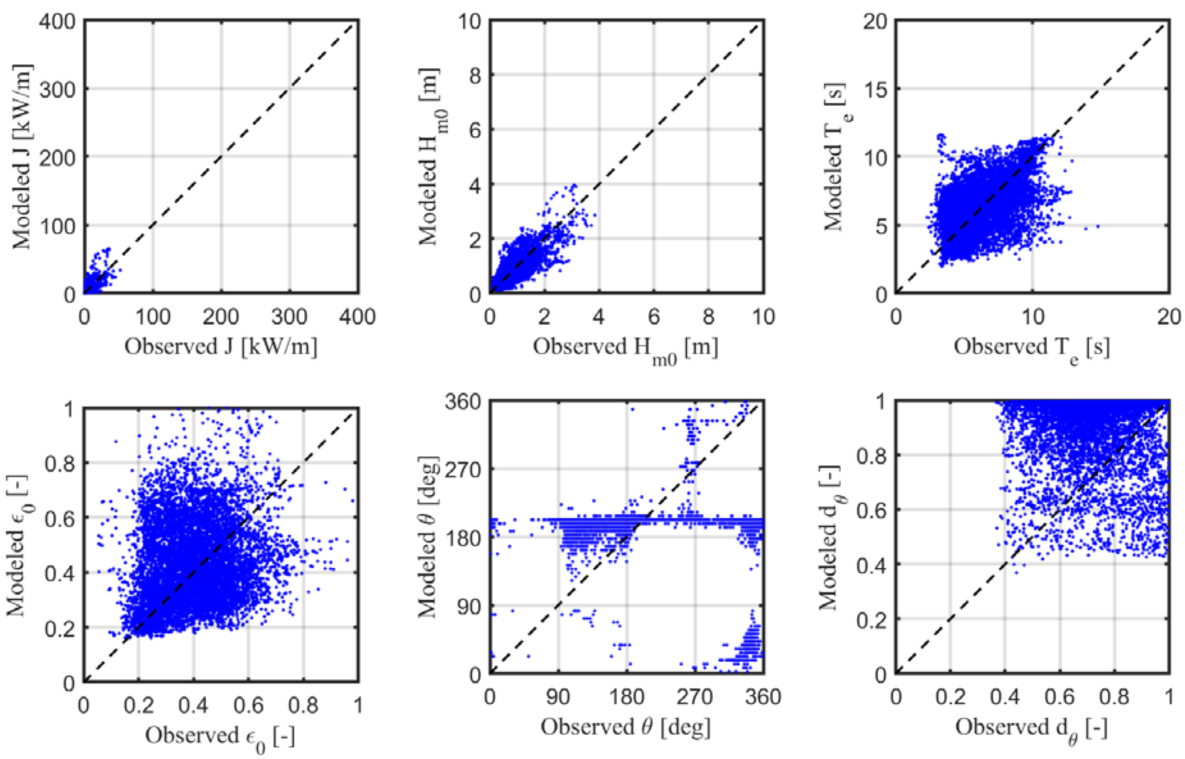

Figure E.19. Comparisons of time series (top) and scatter plots (bottom) of the six UnSWAN model-simulated IEC parameters with observed data at NDBC Buoy 46060 for 2009.

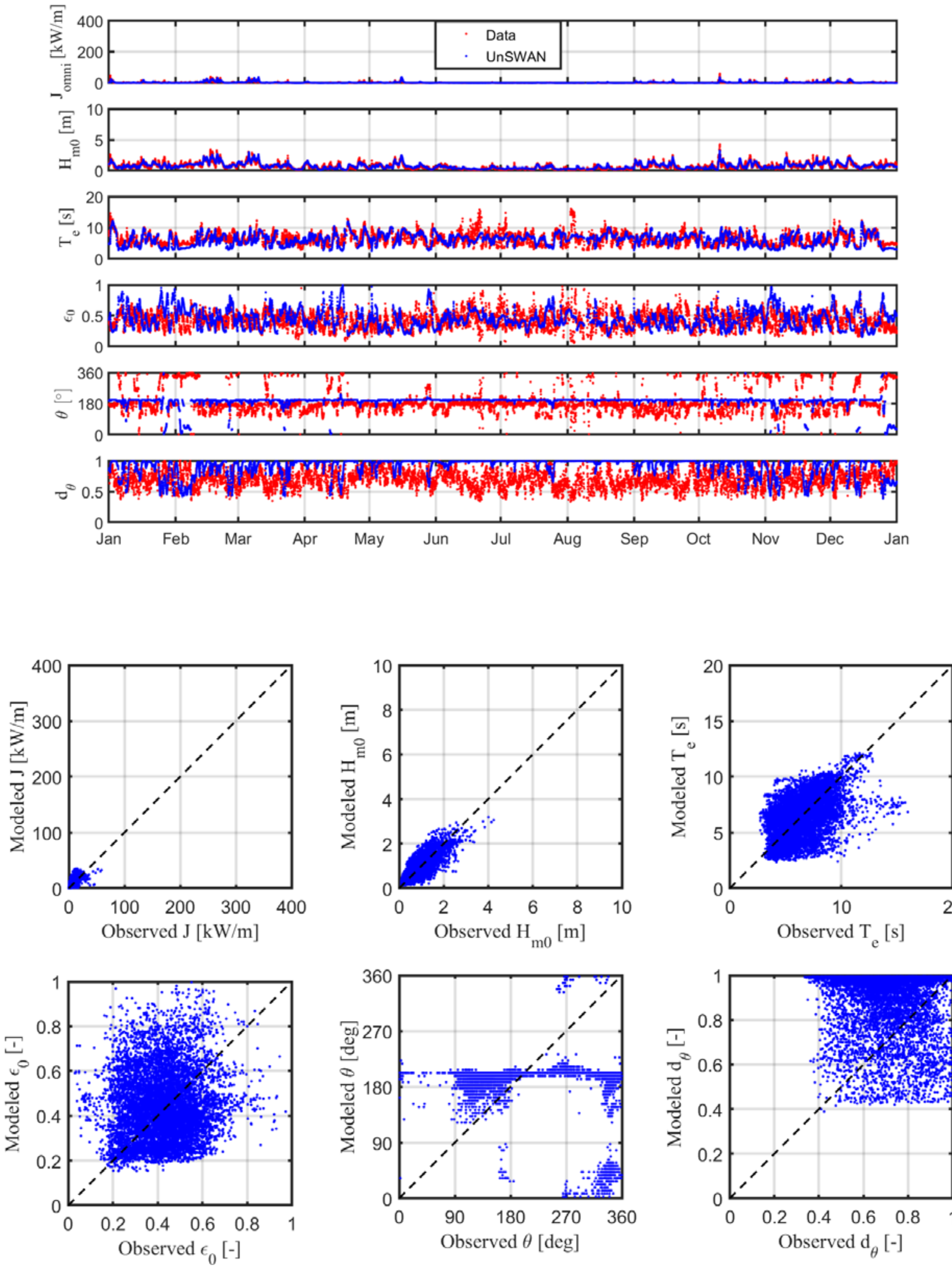

Figure E.20. Comparisons of time series (top) and scatter plots (bottom) of the six UnSWAN model-simulated IEC parameters with observed data at NDBC Buoy 46060 for 2008.

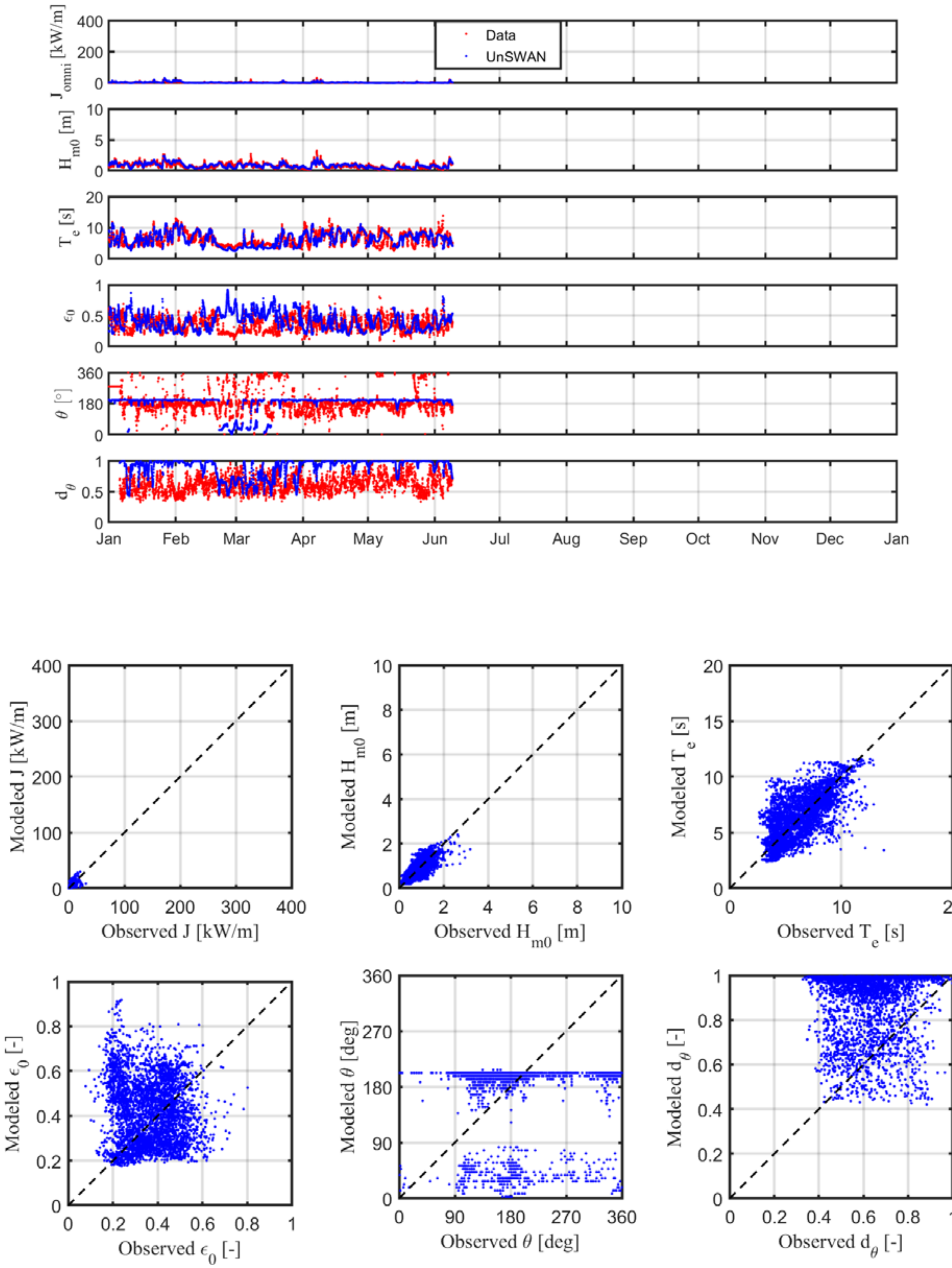

Figure E.21. Comparisons of time series (top) and scatter plots (bottom) of the six UnSWAN model-simulated IEC parameters with observed data at NDBC Buoy 46060 for 2007.

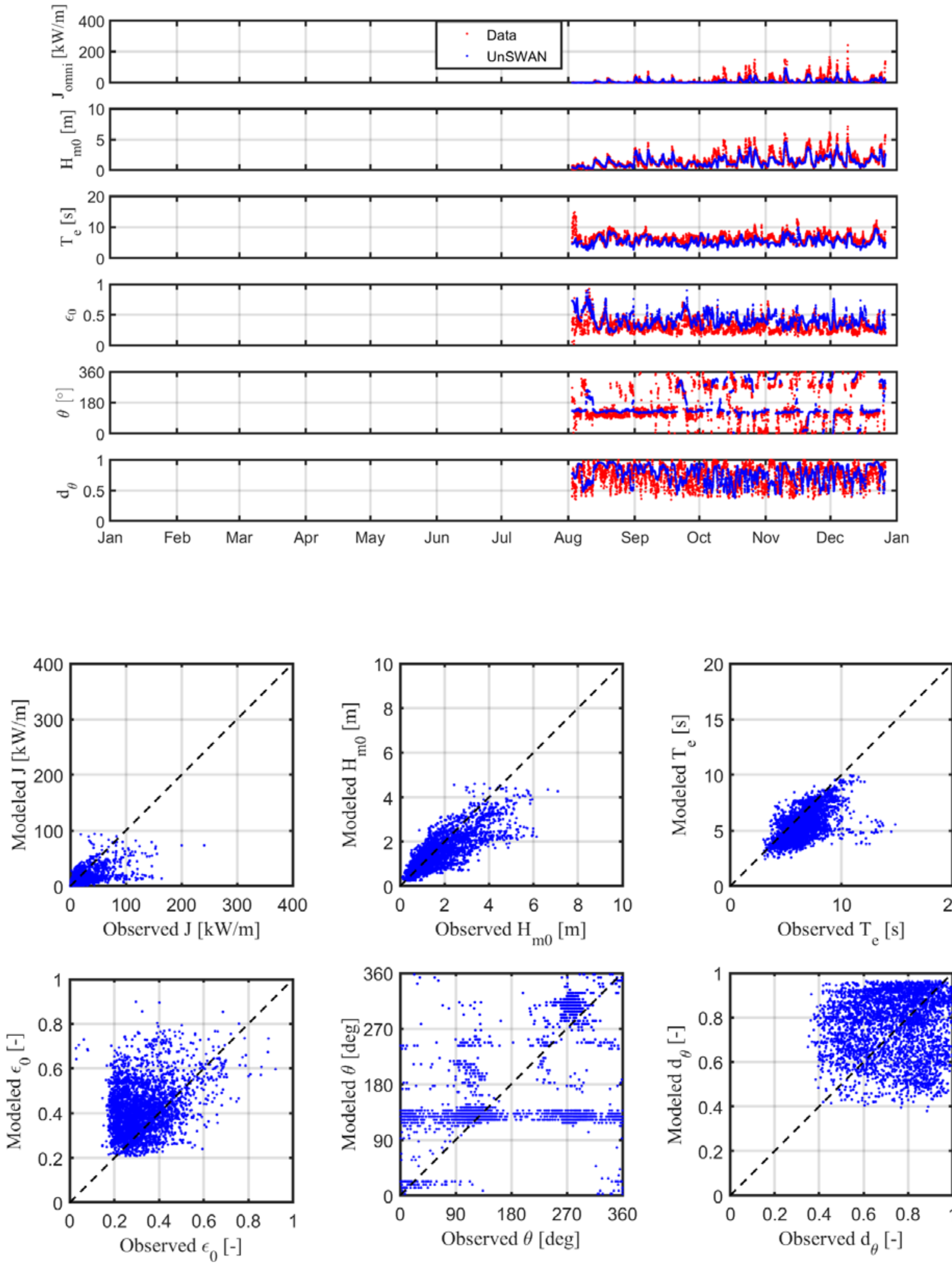

Figure E.22. Comparisons of time series (top) and scatter plots (bottom) of the six UnSWAN model-simulated IEC parameters with observed data at NDBC Buoy 46105 for 2008.

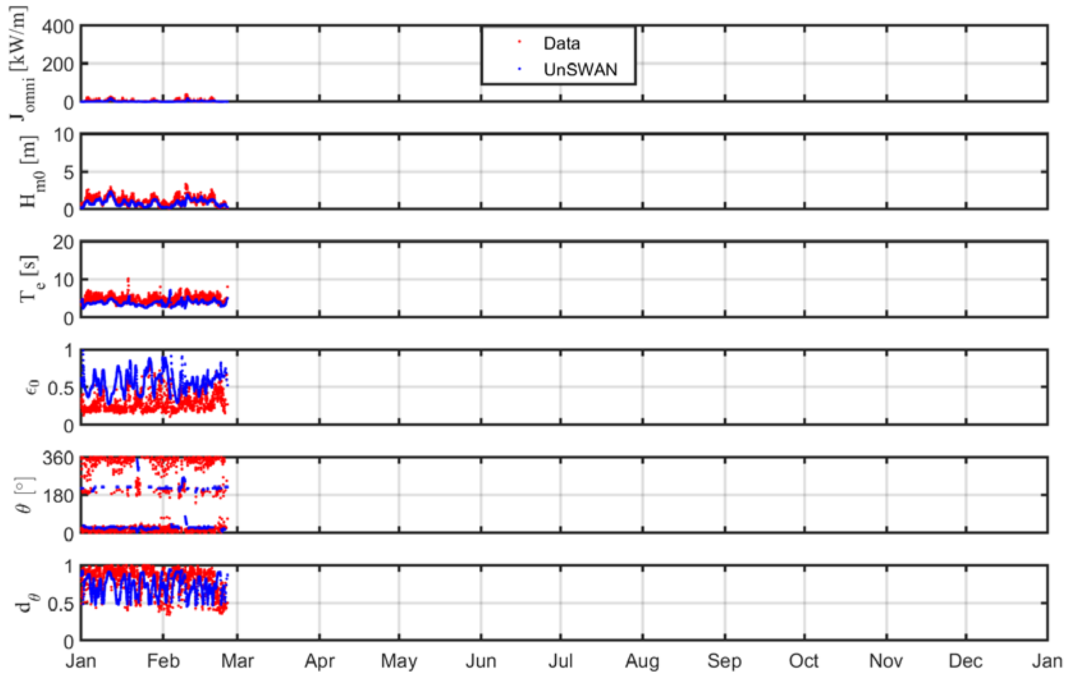

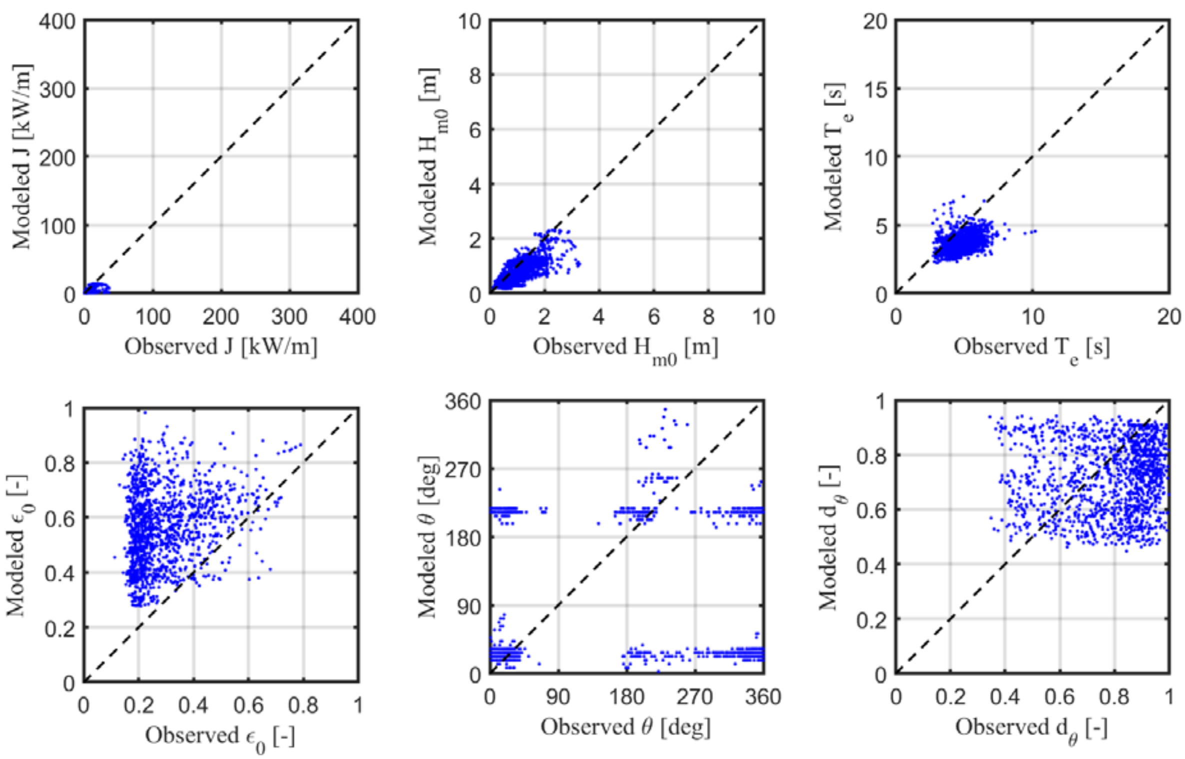

Figure E.23. Comparisons of time series (top) and scatter plots (bottom) of the six UnSWAN model-simulated IEC parameters with observed data at NDBC Buoy 46106 for 2010.

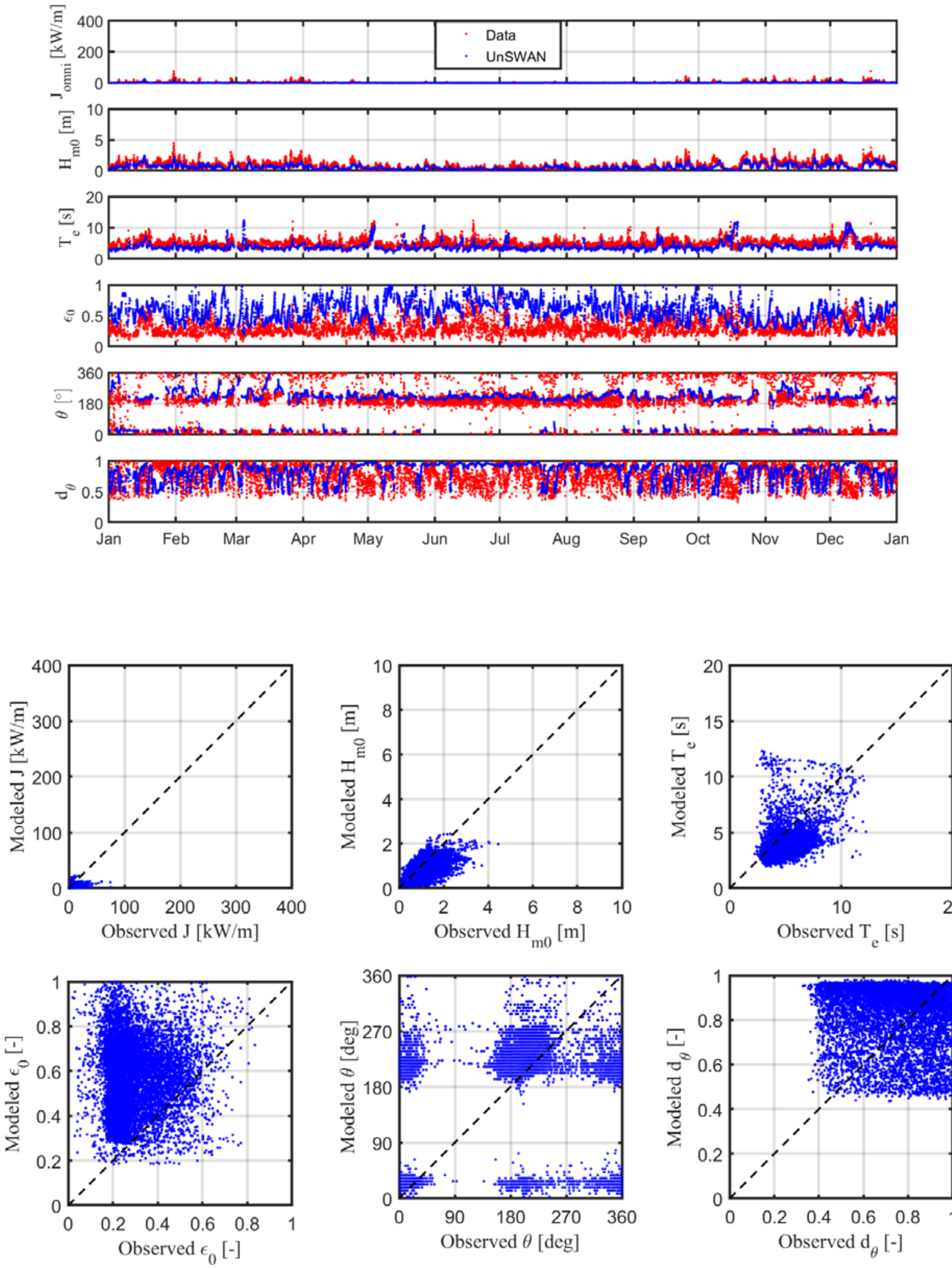

Figure E.24. Comparisons of time series (top) and scatter plots (bottom) of the six UnSWAN model-simulated IEC parameters with observed data at NDBC Buoy 46106 for 2009.

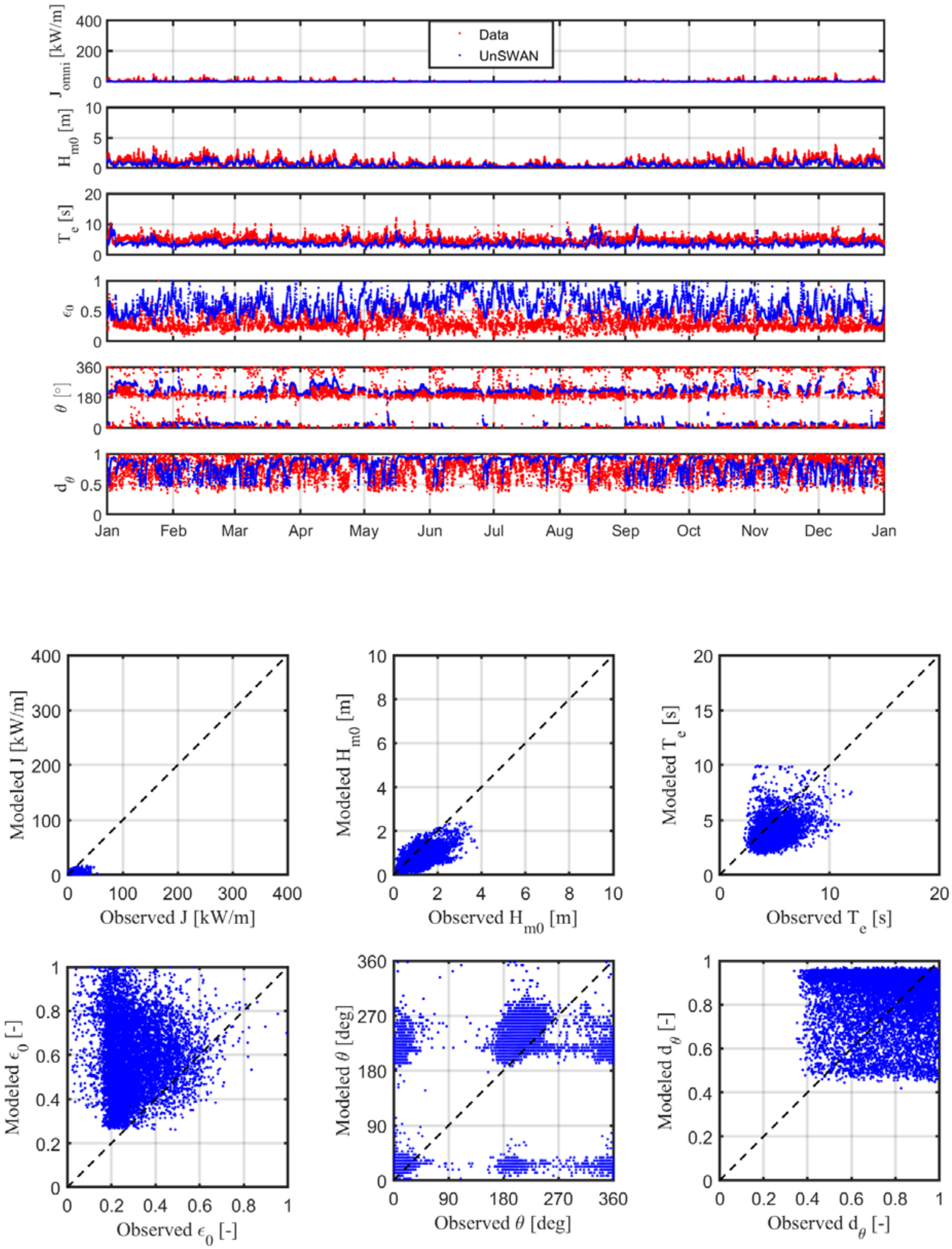

Figure E.25. Comparisons of time series (top) and scatter plots (bottom) of the six UnSWAN model-simulated IEC parameters with observed data at NDBC Buoy 46106 for 2008.

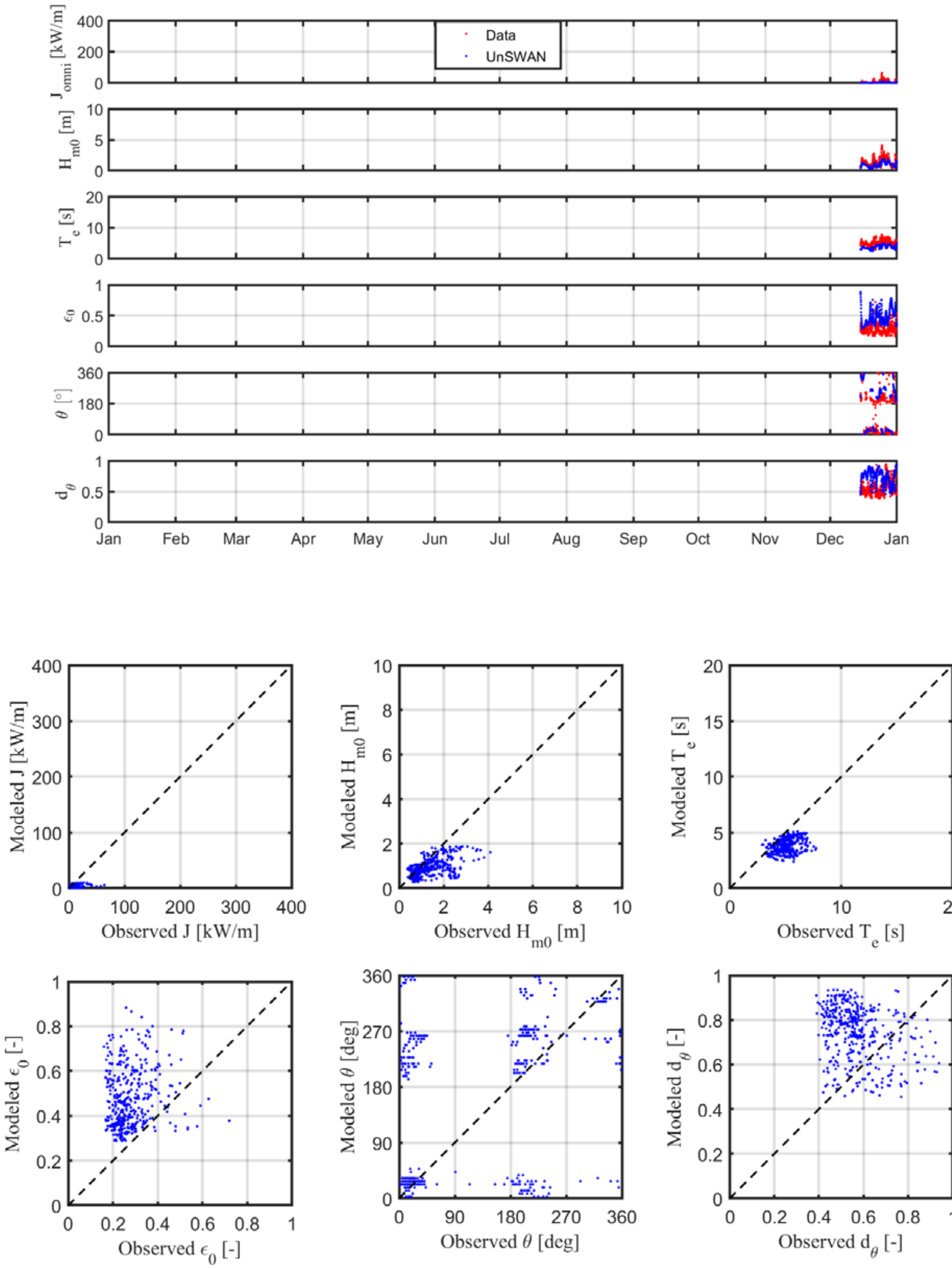

Figure E.26. Comparisons of time series (top) and scatter plots (bottom) of the six UnSWAN model-simulated IEC parameters with observed data at NDBC Buoy 46106 for 2007.

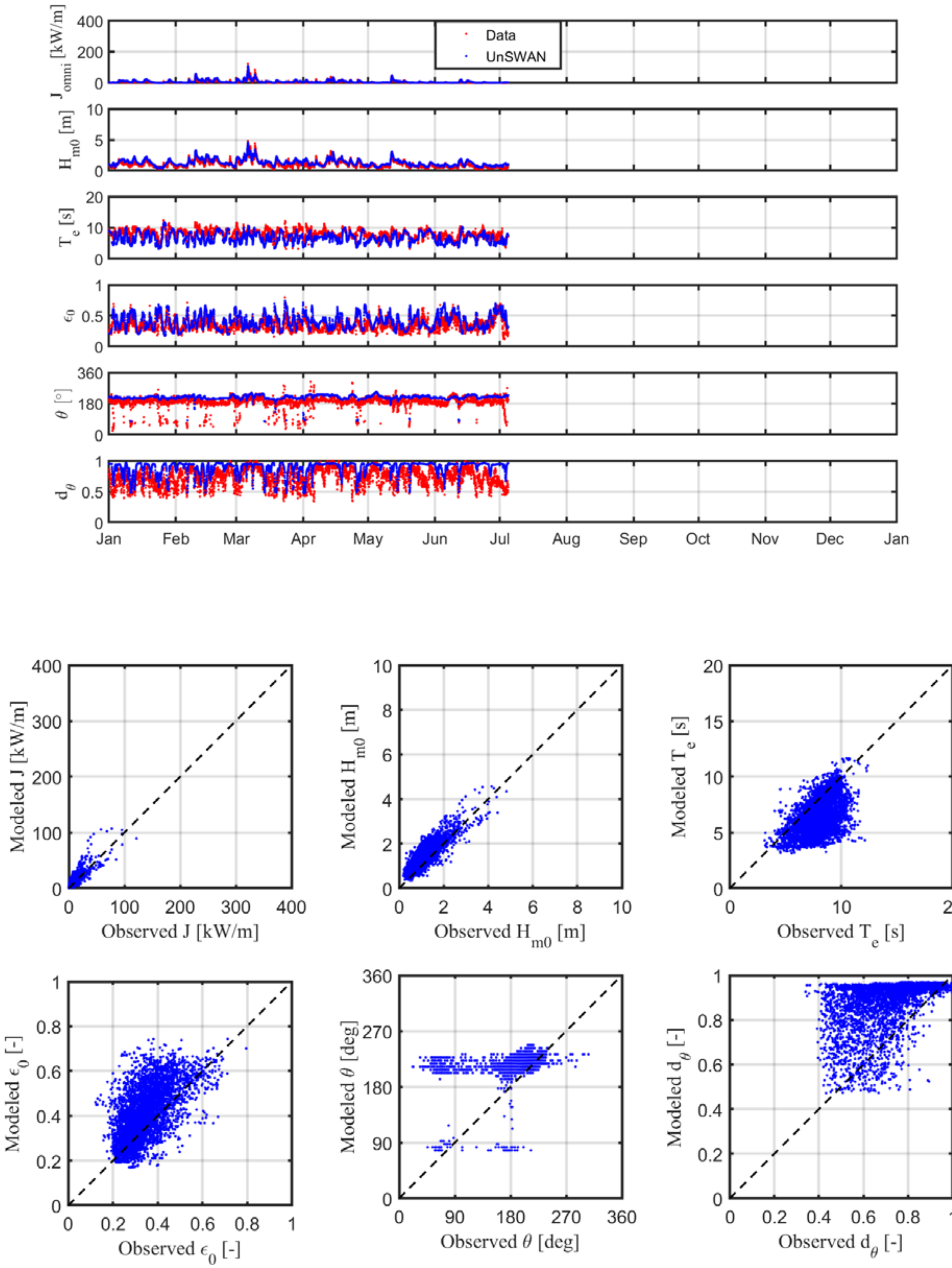

Figure E.27. Comparisons of time series (top) and scatter plots (bottom) of the six UnSWAN model-simulated IEC parameters with observed data at NDBC Buoy 46107 for 2010.

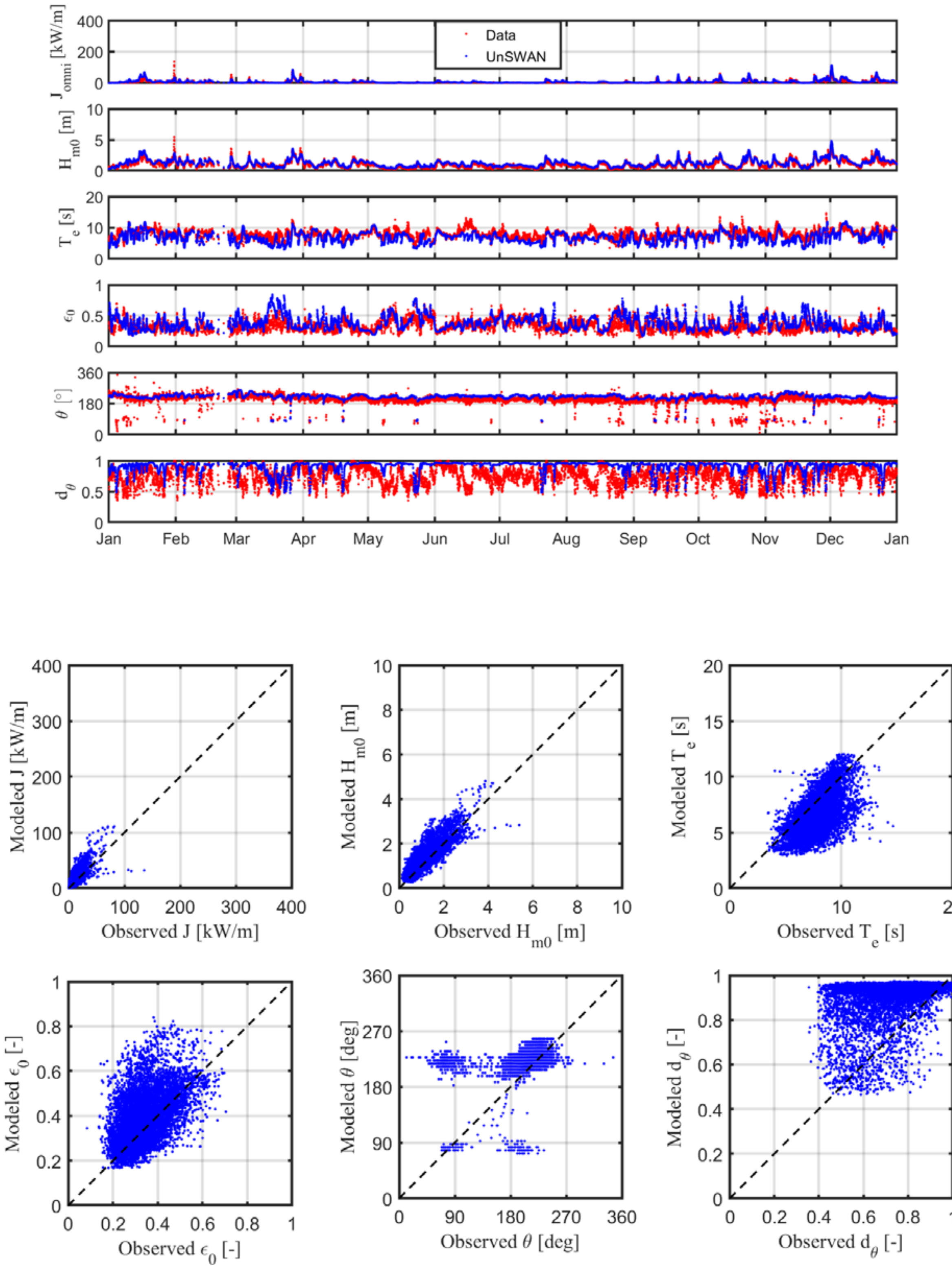

Figure E.28. Comparisons of time series (top) and scatter plots (bottom) of the six UnSWAN model-simulated IEC parameters with observed data at NDBC Buoy 46107 for 2009.

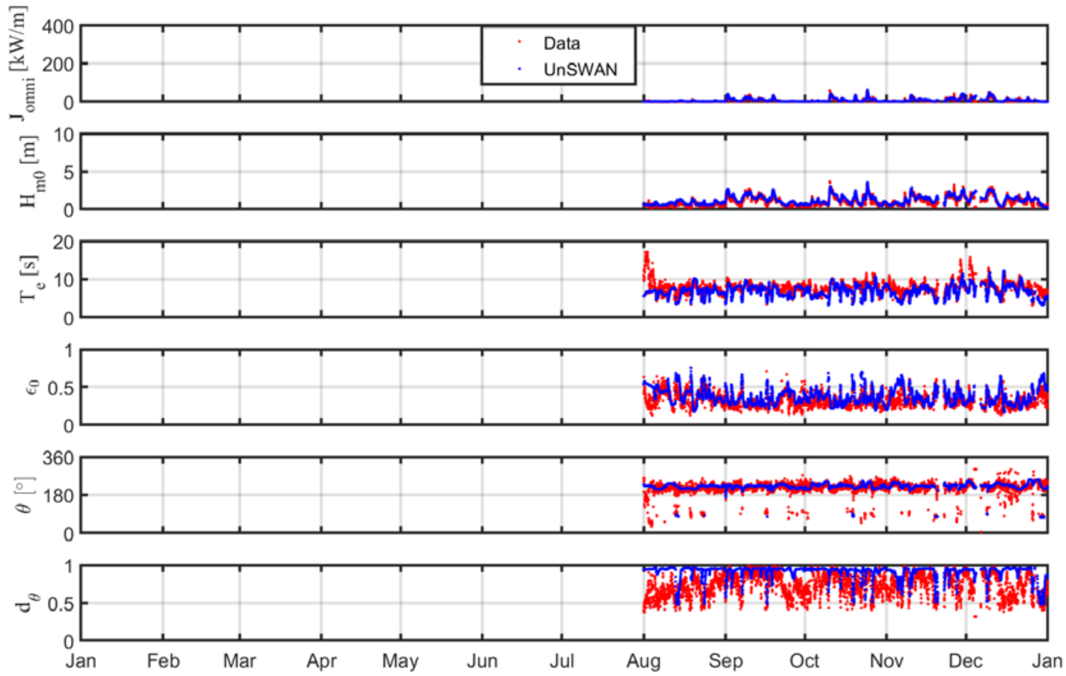

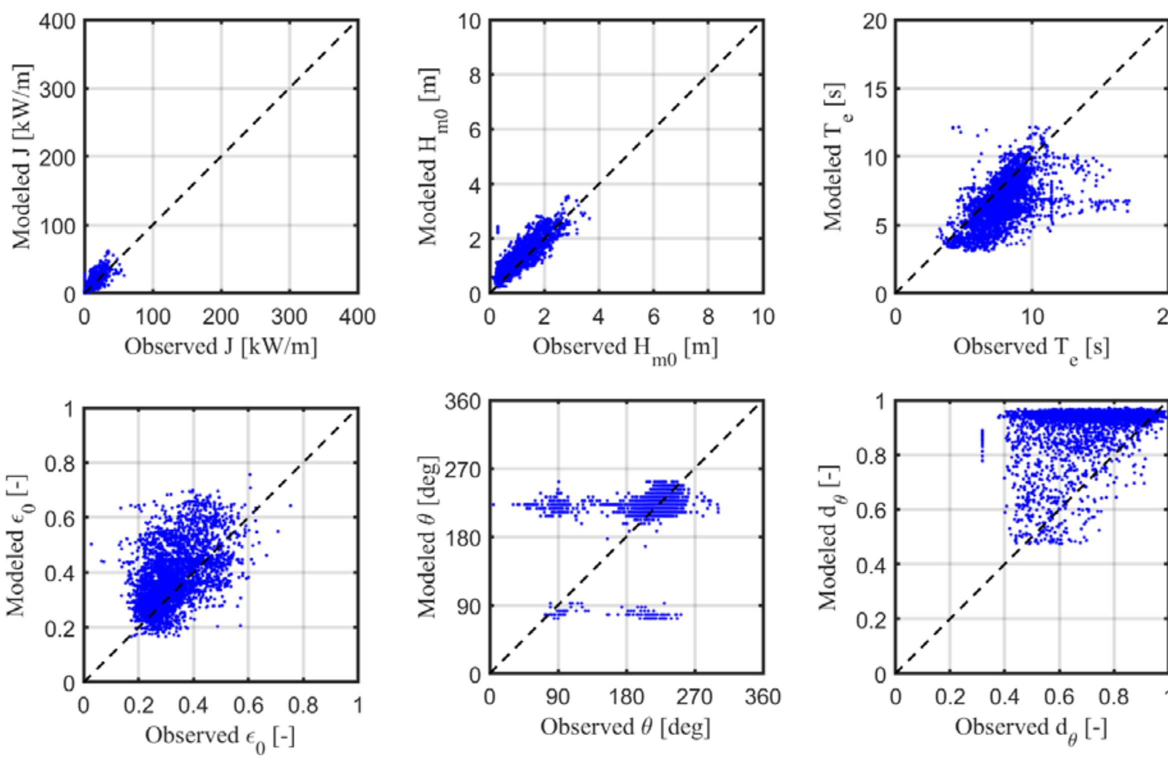

Figure E.29. Comparisons of time series (top) and scatter plots (bottom) of the six UnSWAN model-simulated IEC parameters with observed data at NDBC Buoy 46107 for 2008.

Appendix F – Comparison of Model-Simulated IEC Parameters with Buoy Data

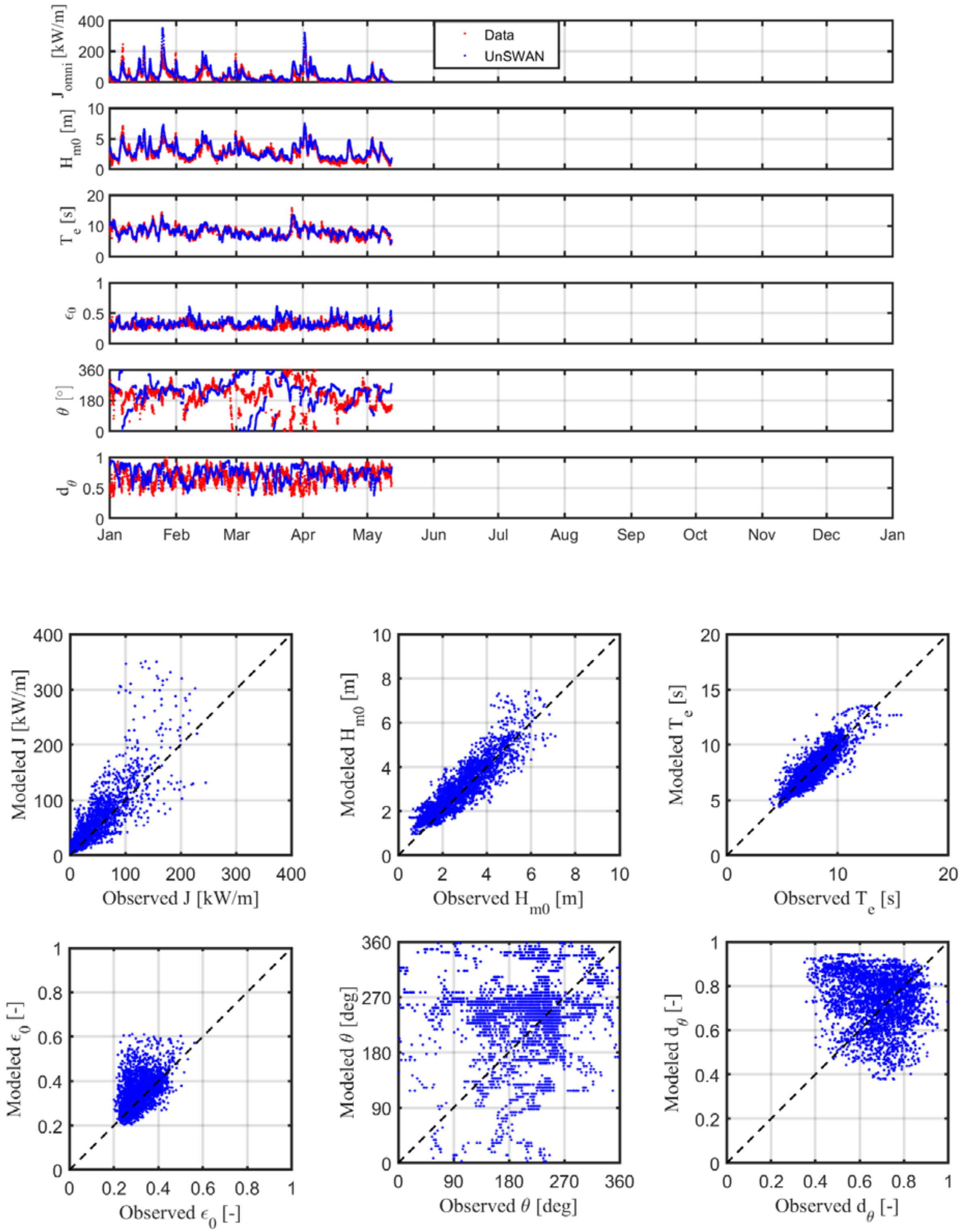

Figure F.1. Comparisons of time series (top) and scatter plots (bottom) of the six UnSWAN model-simulated IEC parameters with observed data at NDBC Buoy 46001 for 2017.

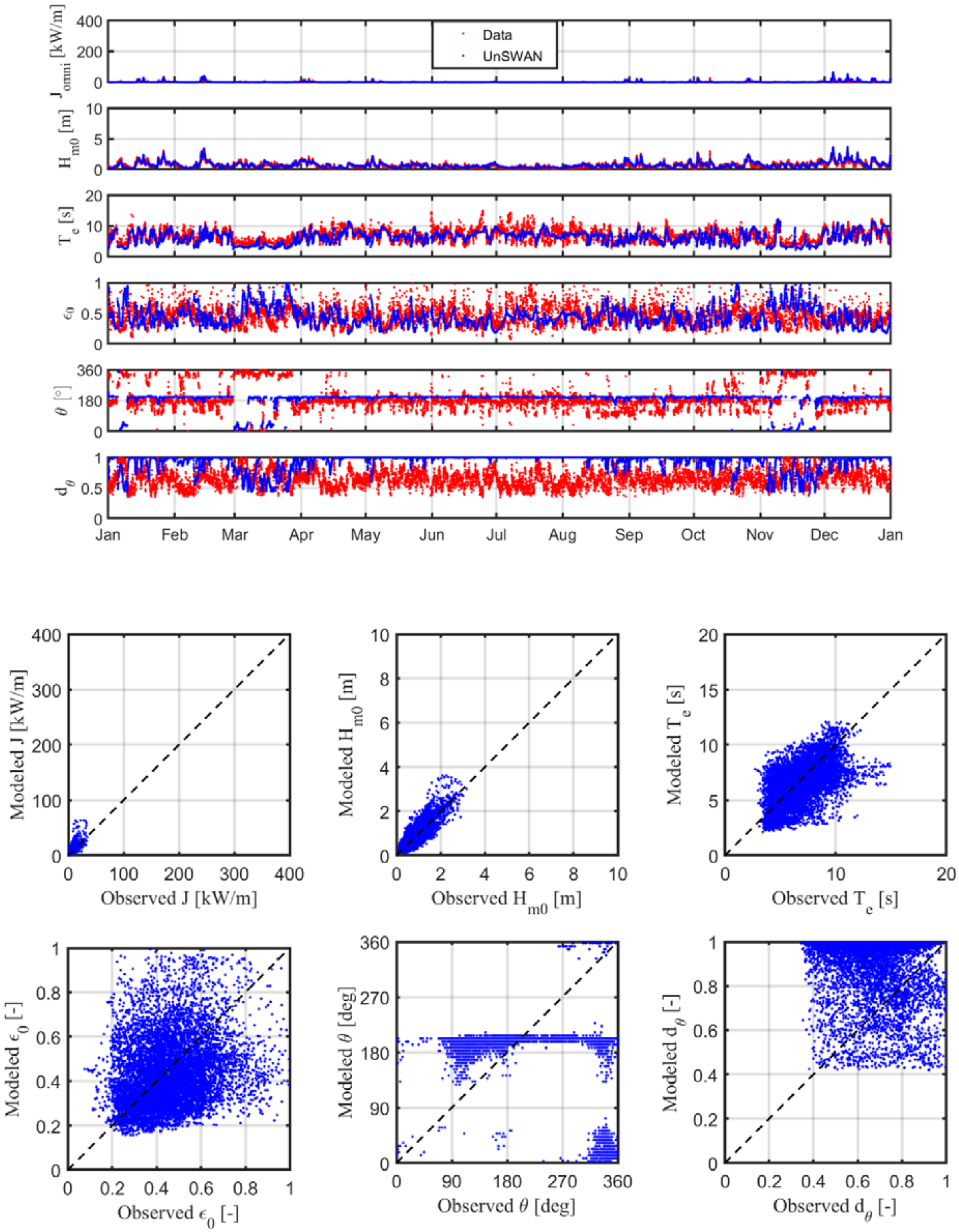

Figure F.2. Comparisons of time series (top) and scatter plots (bottom) of the six UnSWAN model-simulated IEC parameters with observed data at NDBC Buoy 46060 for 2017.

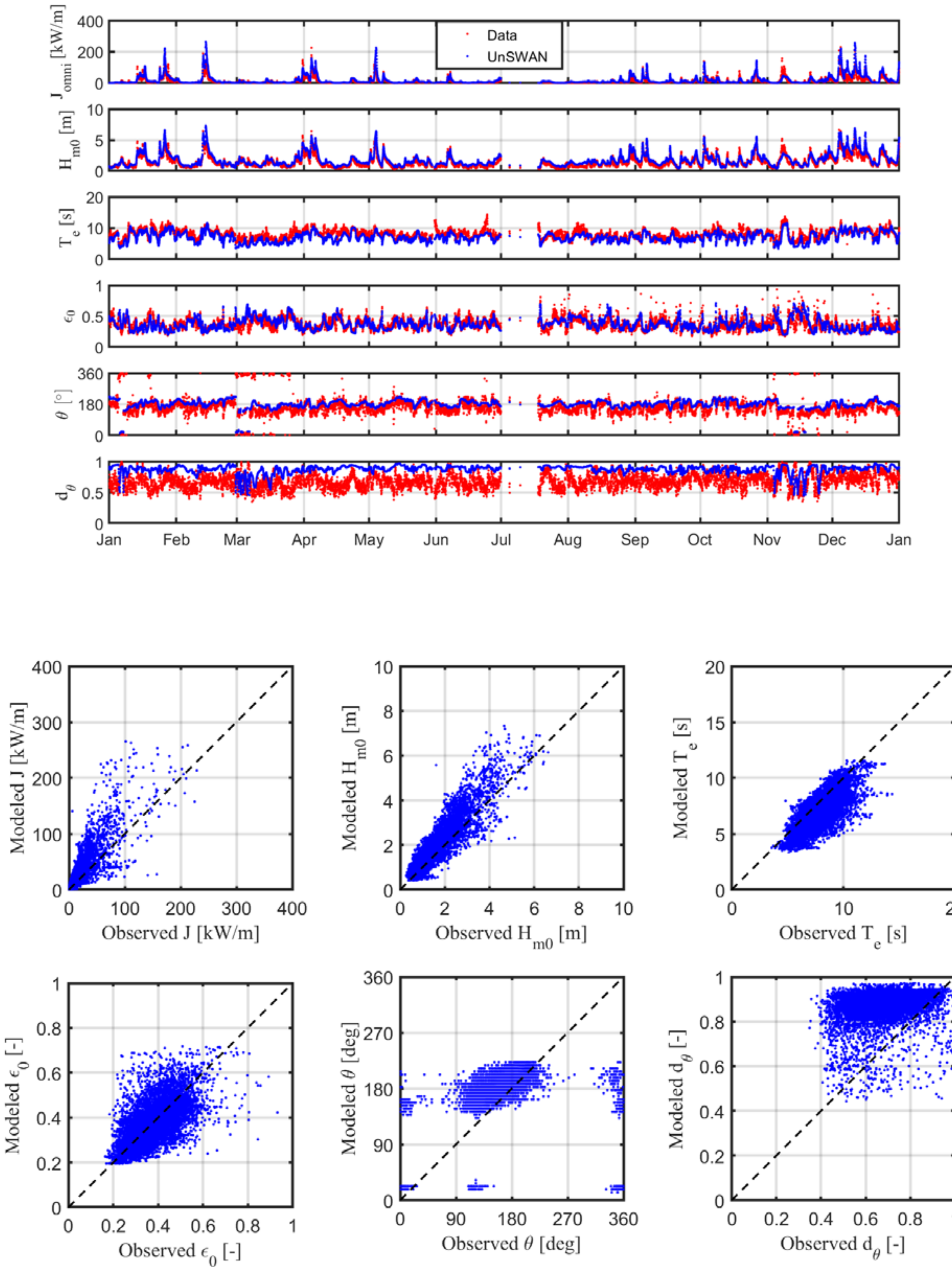

Figure F.3. Comparisons of time series (top) and scatter plots (bottom) of the six UnSWAN model-simulated IEC parameters with observed data at NDBC Buoy 46061 for 2017.

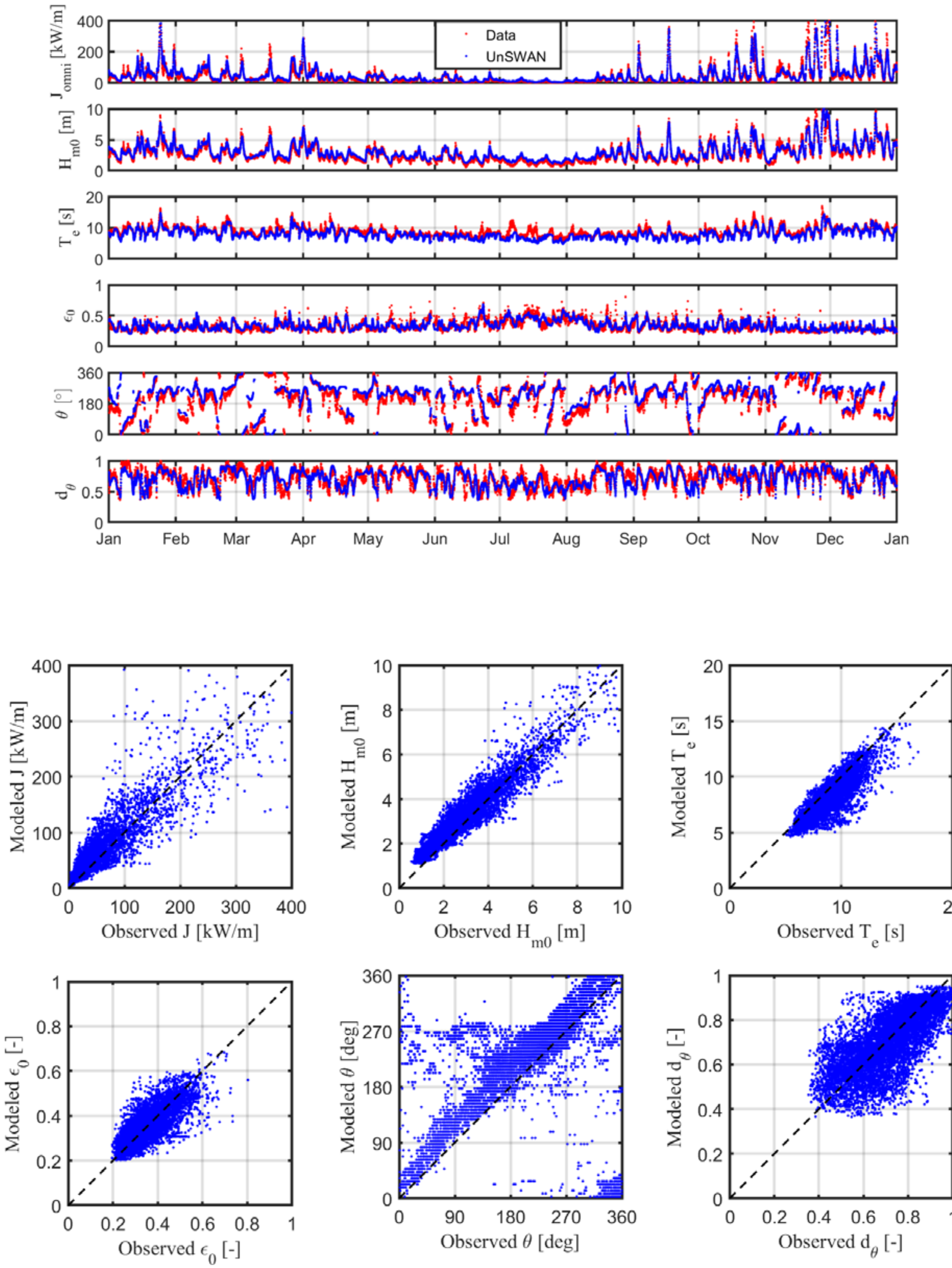

Figure F.4. Comparisons of time series (top) and scatter plots (bottom) of the six UnSWAN model-simulated IEC parameters with observed data at NDBC Buoy 46066 for 2017.

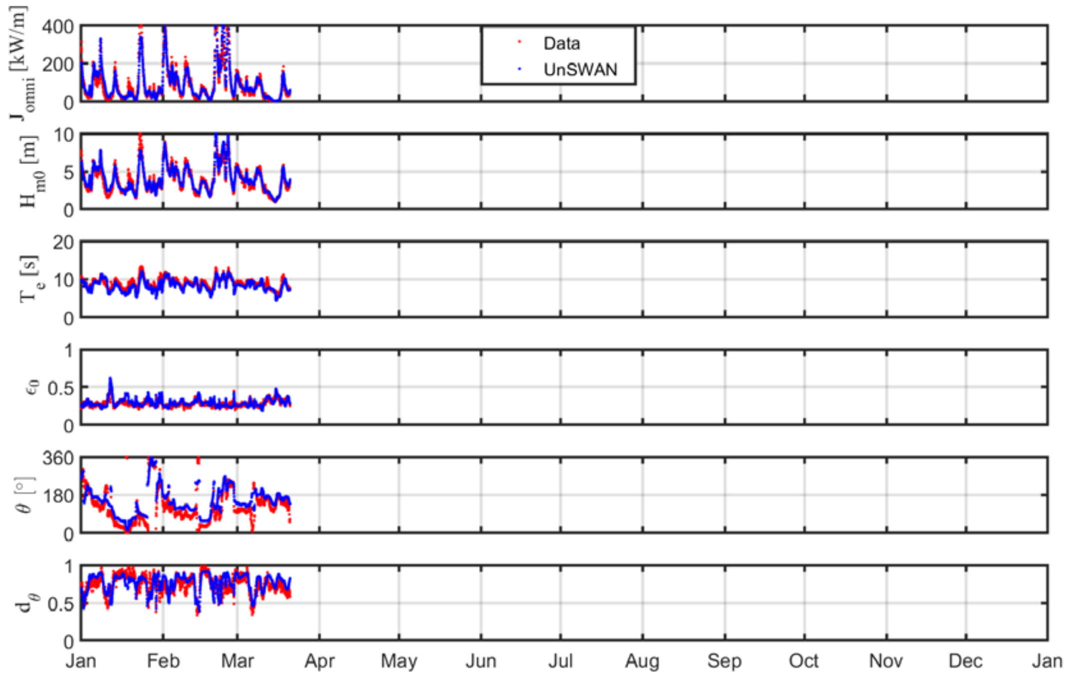

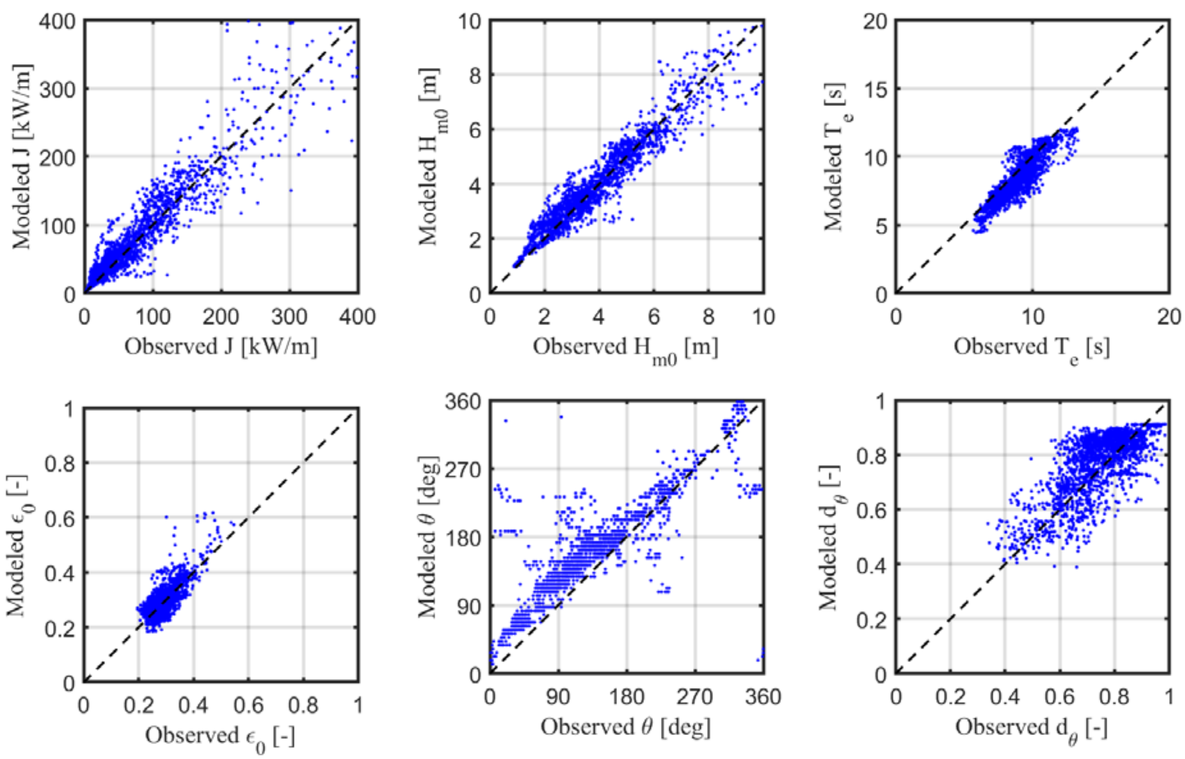

Figure F.5. Comparisons of time series (top) and scatter plots (bottom) of the six UnSWAN model-simulated IEC parameters with observed data at NDBC Buoy 46070 for 2017.

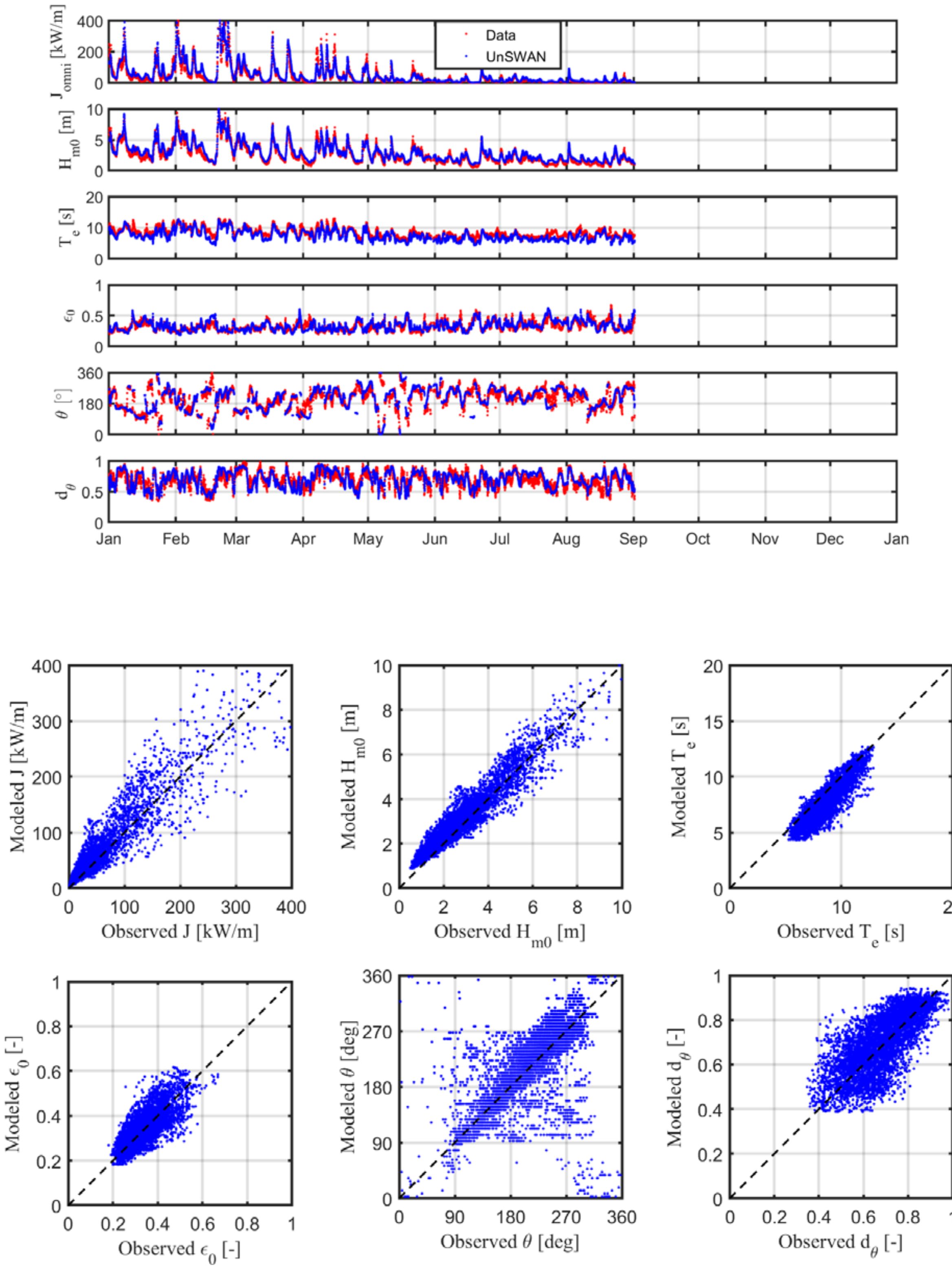

Figure F.6. Comparisons of time series (top) and scatter plots (bottom) of the six UnSWAN model-simulated IEC parameters with observed data at NDBC Buoy 46071 for 2017.

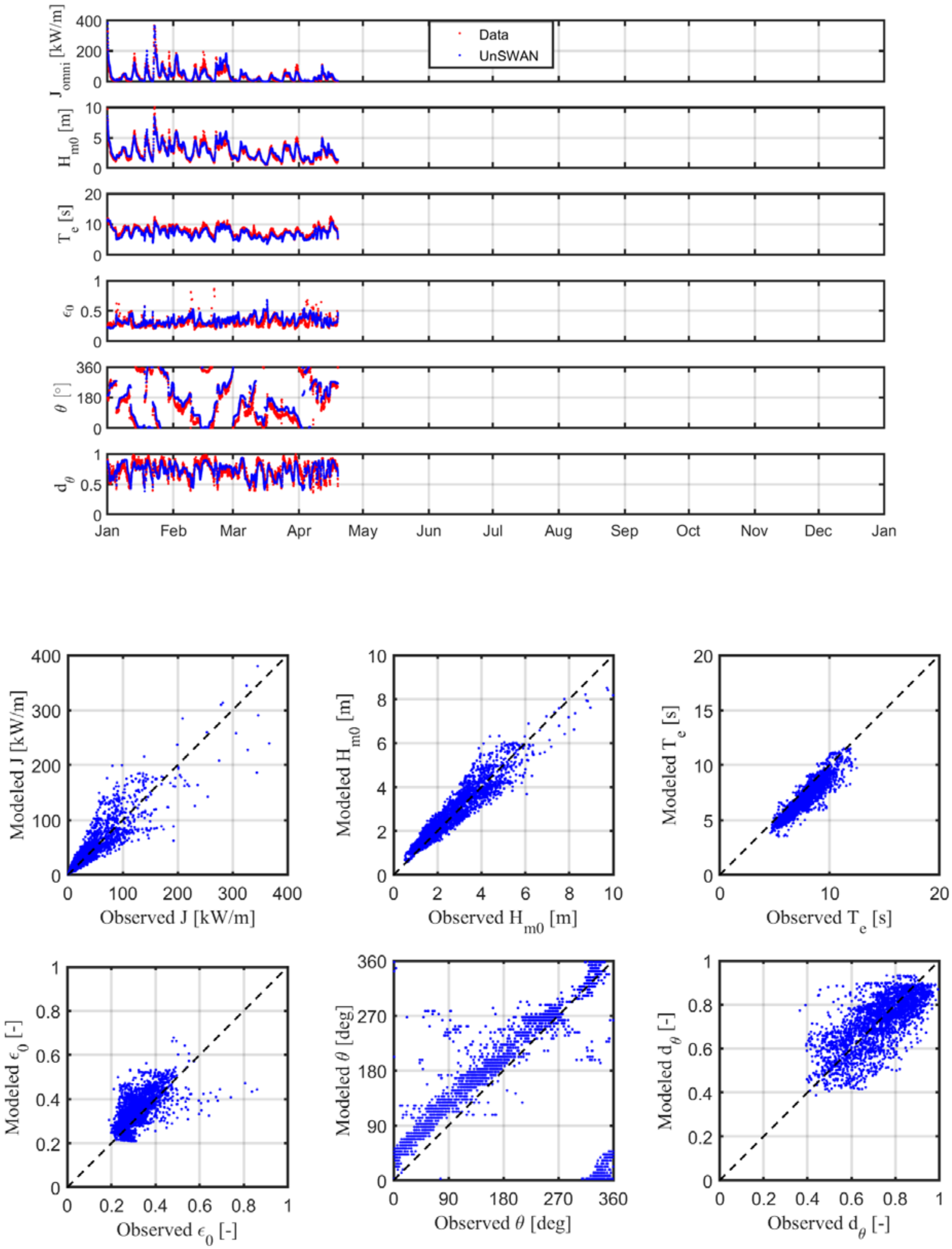

Figure F.7. Comparisons of time series (top) and scatter plots (bottom) of the six UnSWAN model-simulated IEC parameters with observed data at NDBC Buoy 46073 for 2017.

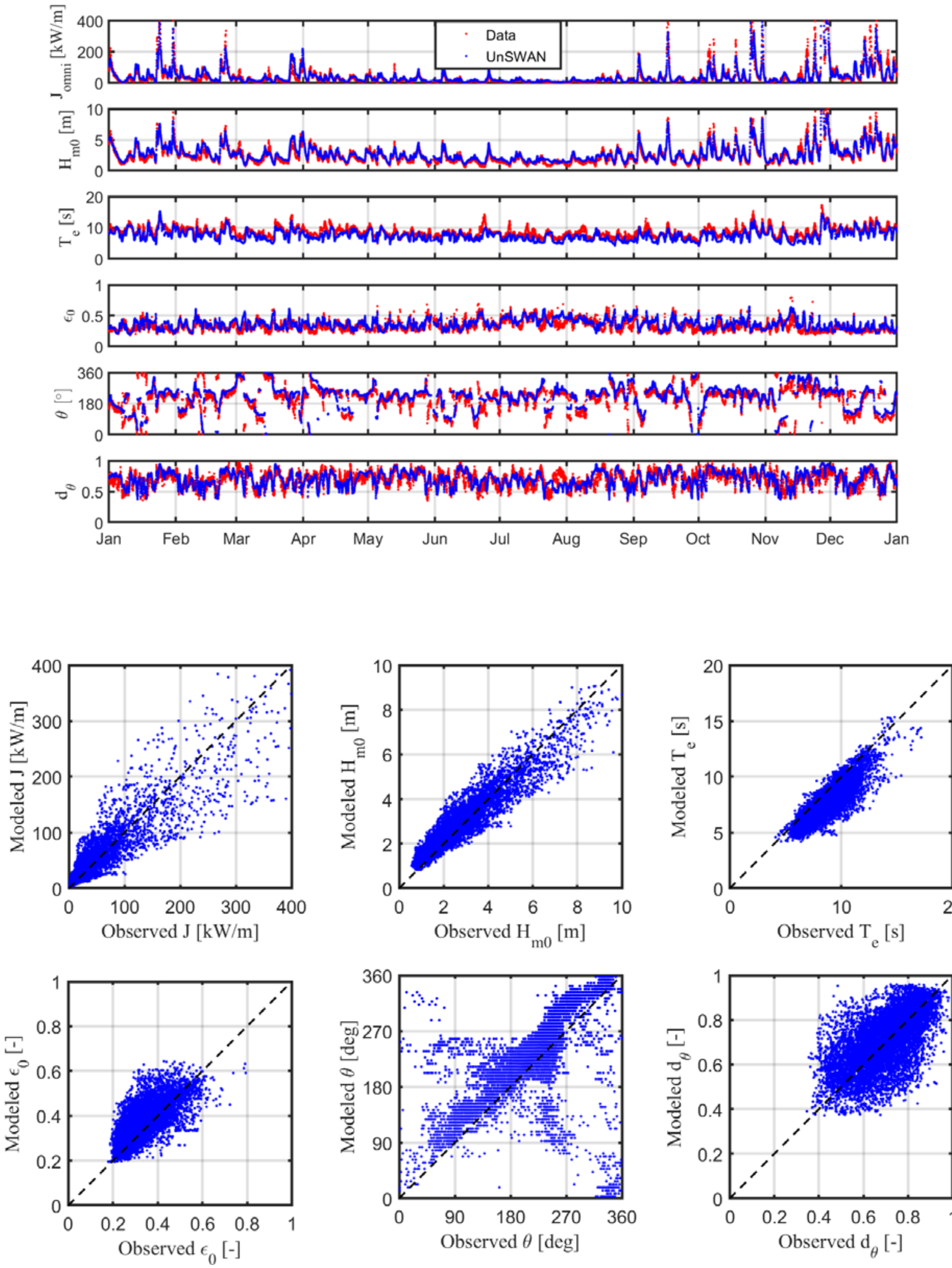

Figure F.8. Comparisons of time series (top) and scatter plots (bottom) of the six UnSWAN model-simulated IEC parameters with observed data at NDBC Buoy 46075 for 2017.

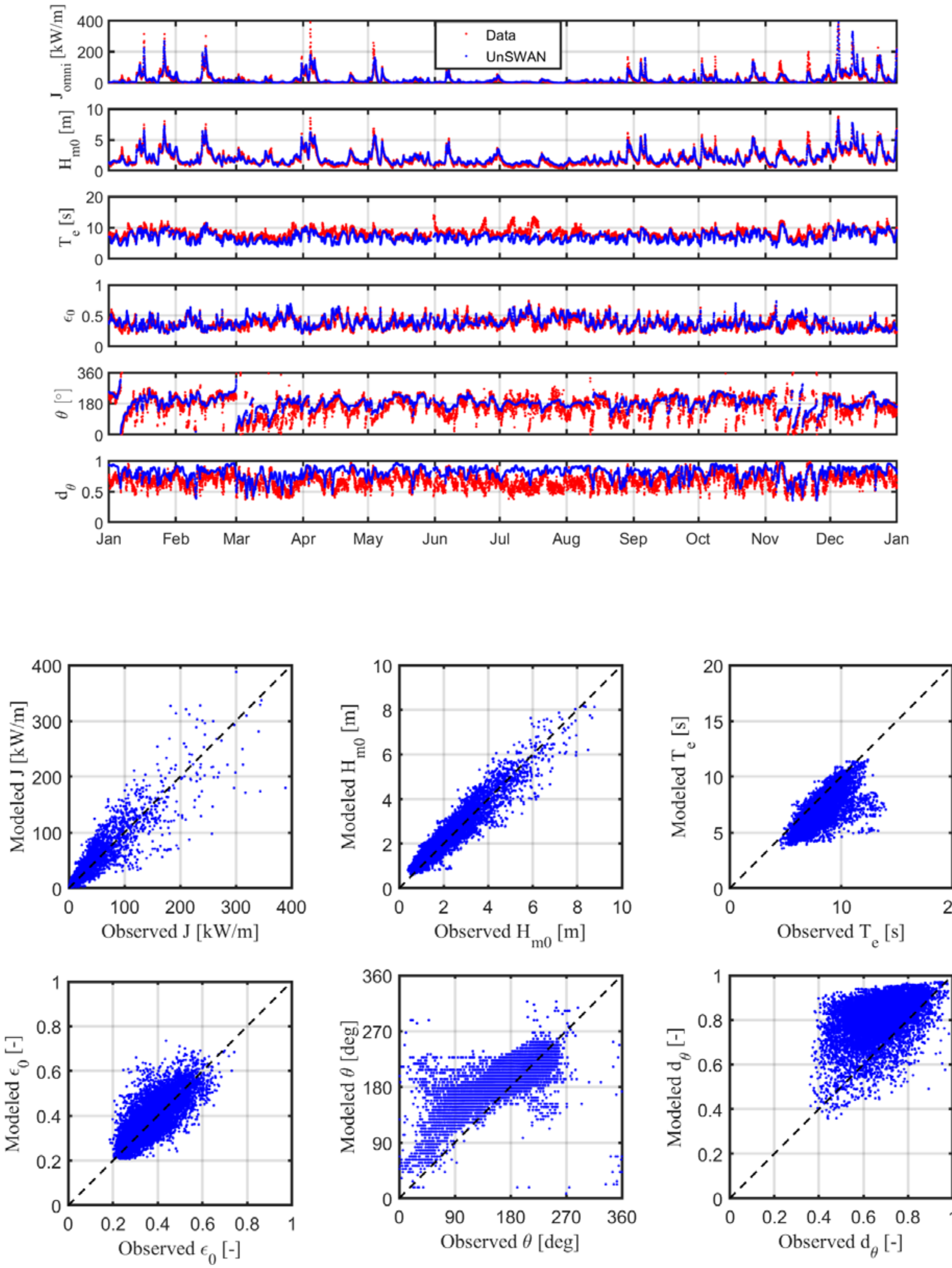

Figure F.9. Comparisons of time series (top) and scatter plots (bottom) of the six UnSWAN model-simulated IEC parameters with observed data at NDBC Buoy 46076 for 2017.

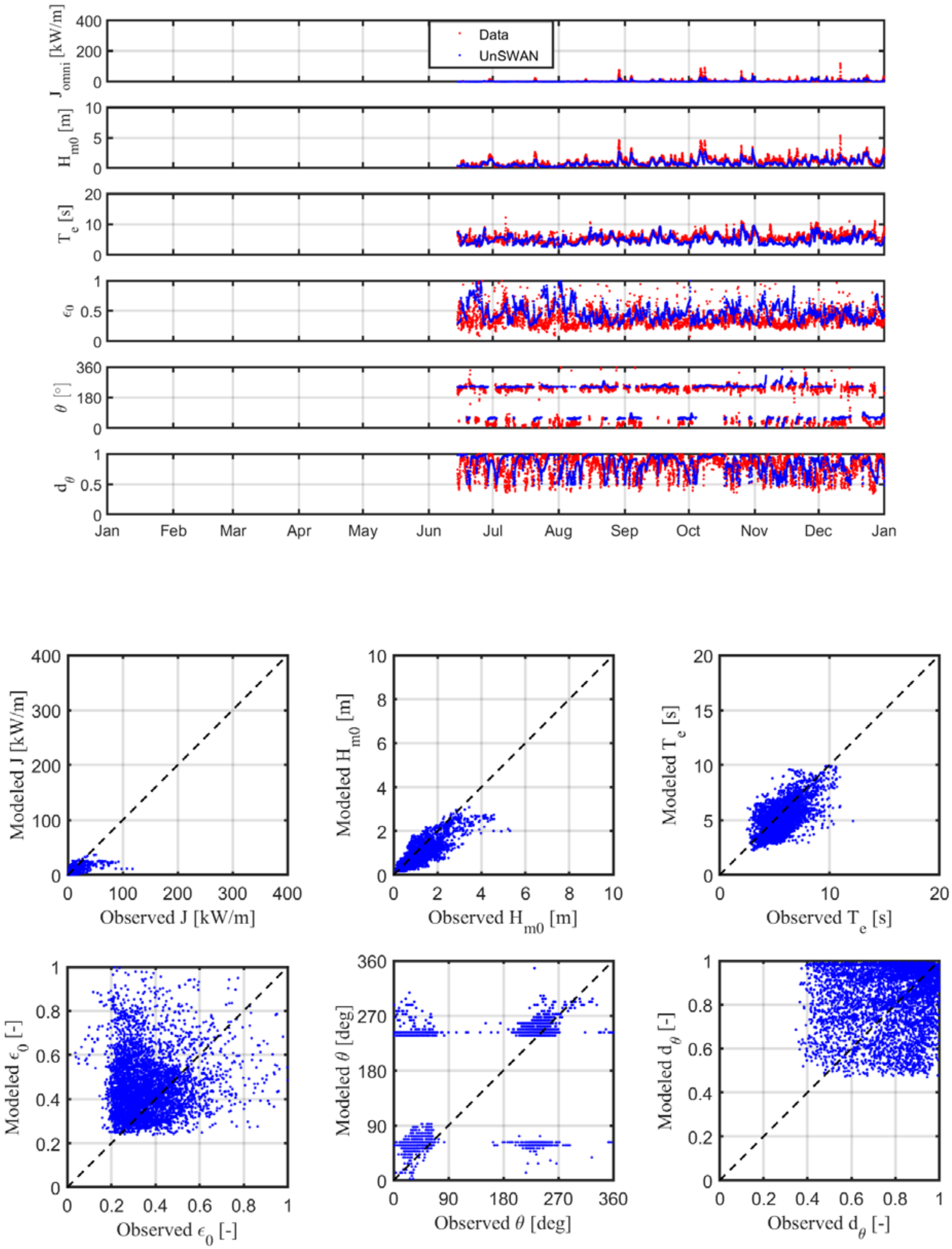

Figure F.10. Comparisons of time series (top) and scatter plots (bottom) of the six UnSWAN model-simulated IEC parameters with observed data at NDBC Buoy 46077 for 2017.

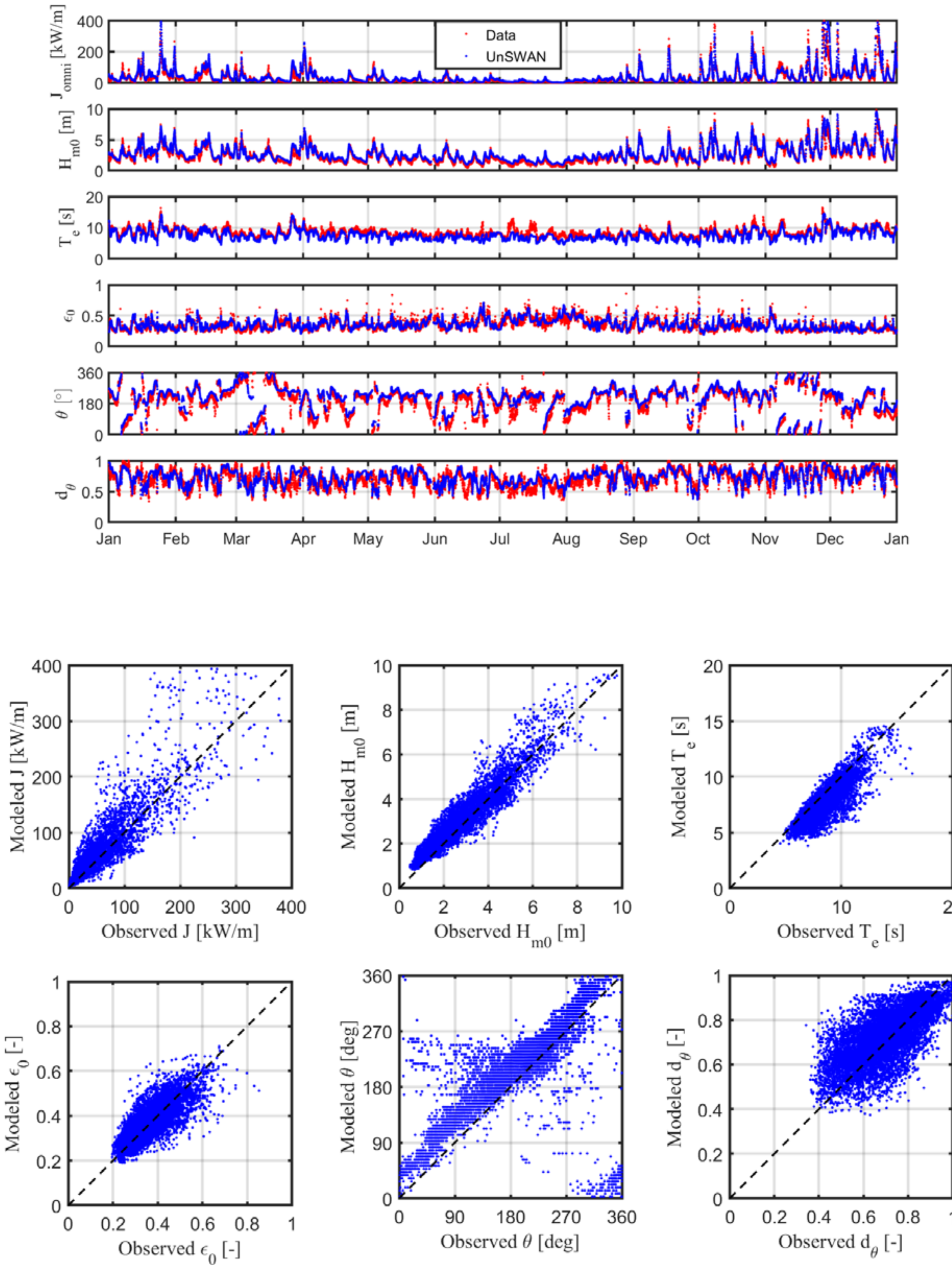

Figure F.11. Comparisons of time series (top) and scatter plots (bottom) of the six UnSWAN model-simulated IEC parameters with observed data at NDBC Buoy 46078 for 2017.

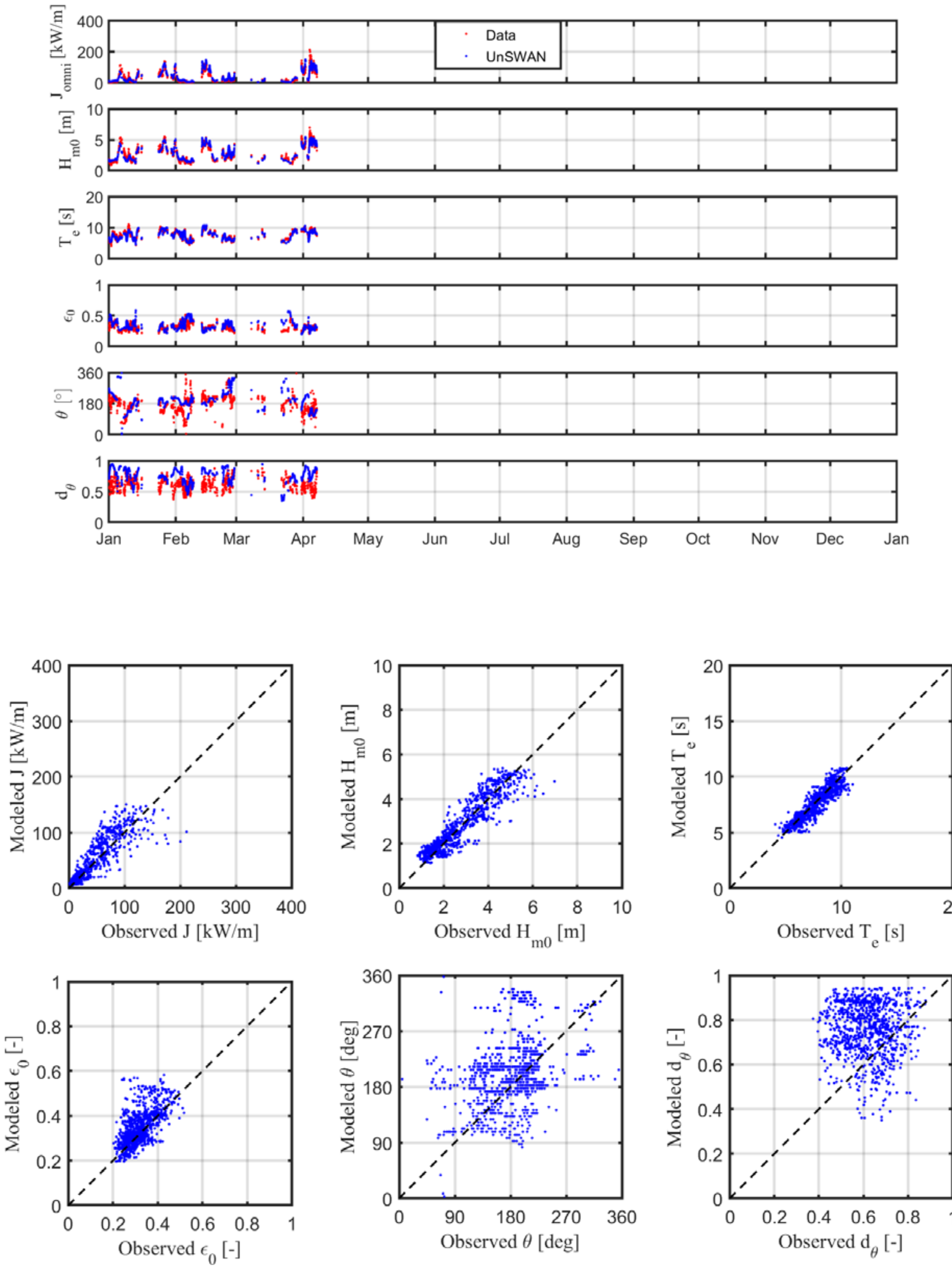

Figure F.12. Comparisons of time series (top) and scatter plots (bottom) of the six UnSWAN model-simulated IEC parameters with observed data at NDBC Buoy 46080 for 2017.

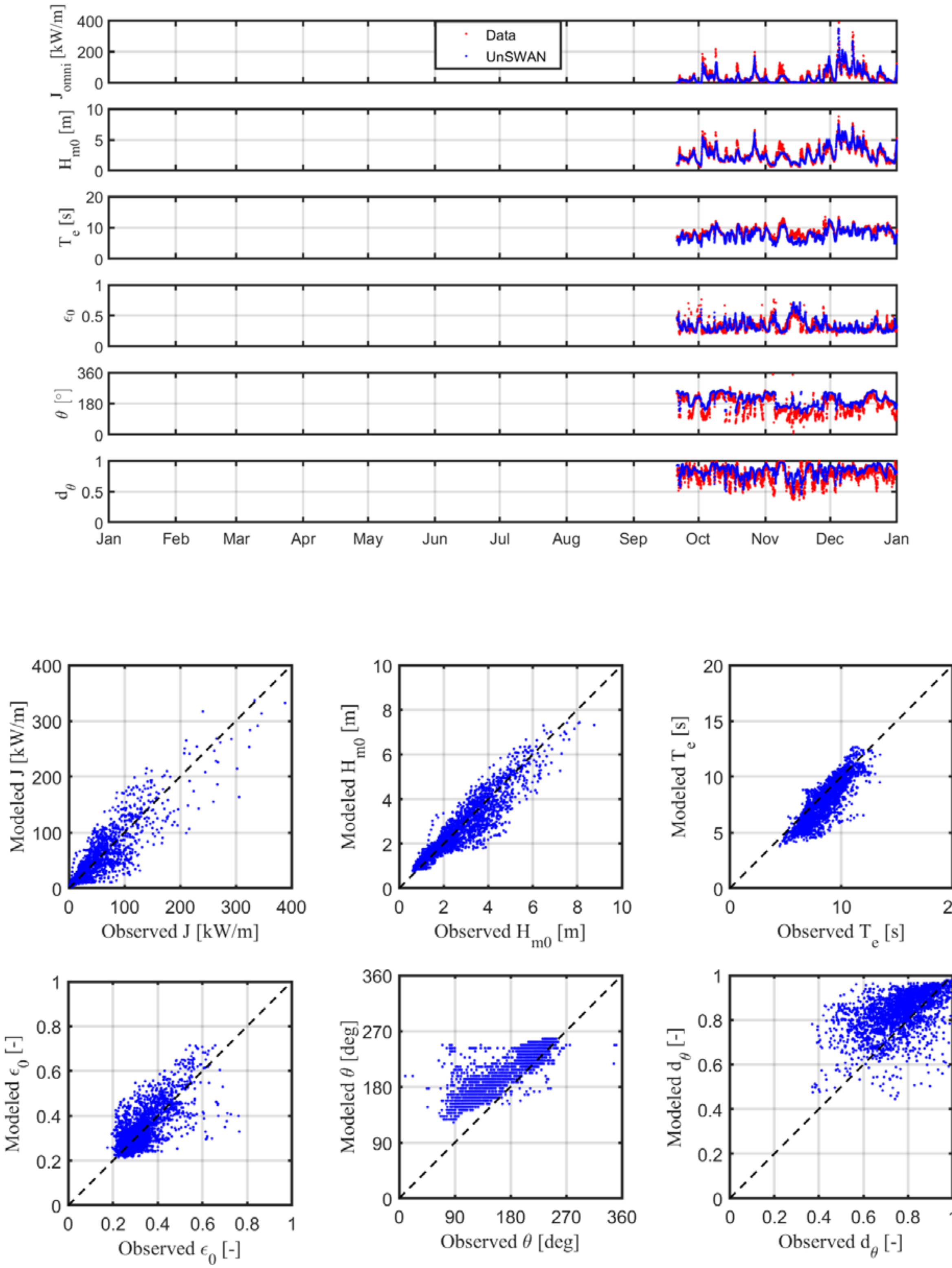

Figure F.13. Comparisons of time series (top) and scatter plots (bottom) of the six UnSWAN model-simulated IEC parameters with observed data at NDBC Buoy 46082 for 2017.

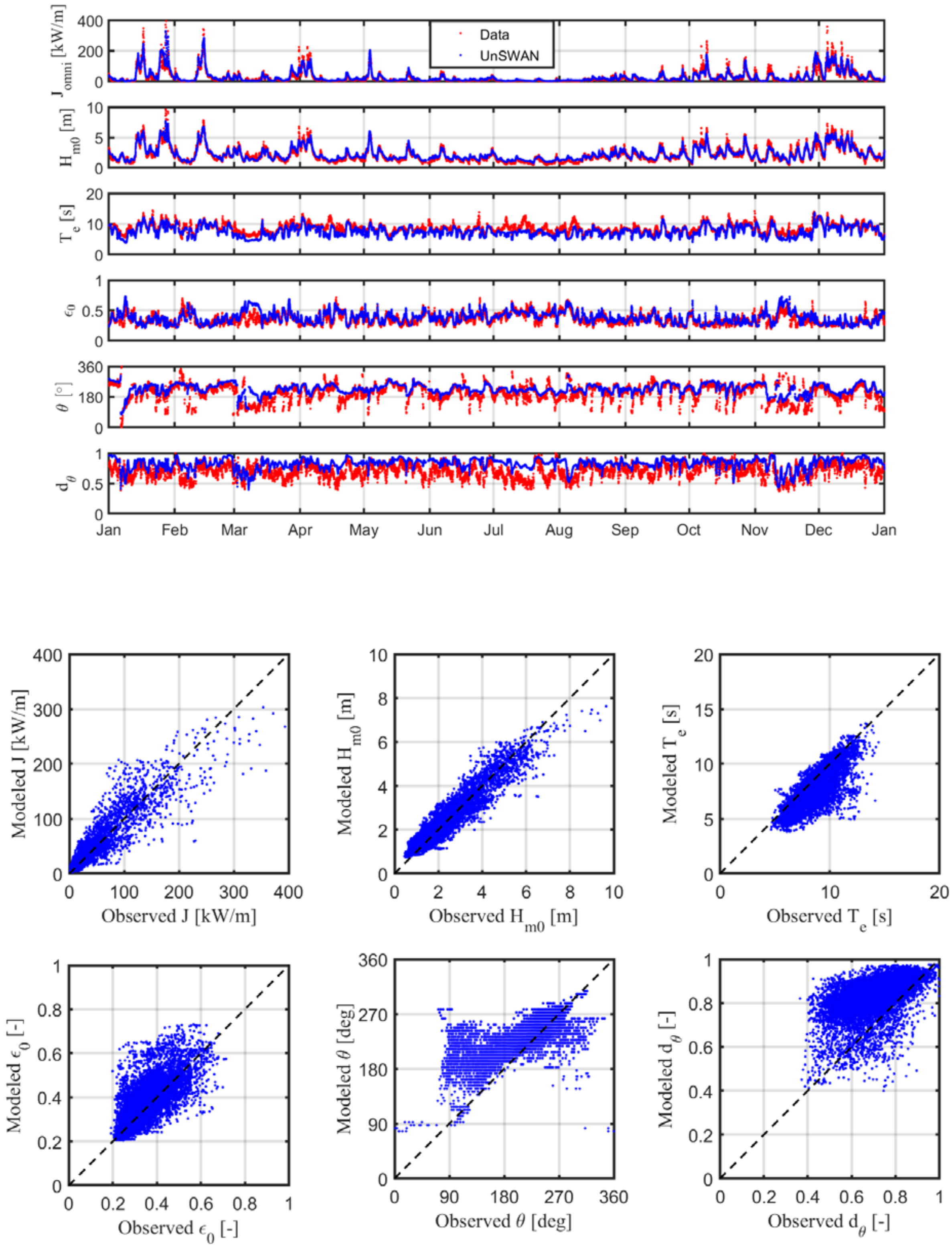

Figure F.14. Comparisons of time series (top) and scatter plots (bottom) of the six UnSWAN model-simulated IEC parameters with observed data at NDBC Buoy 46083 for 2017.

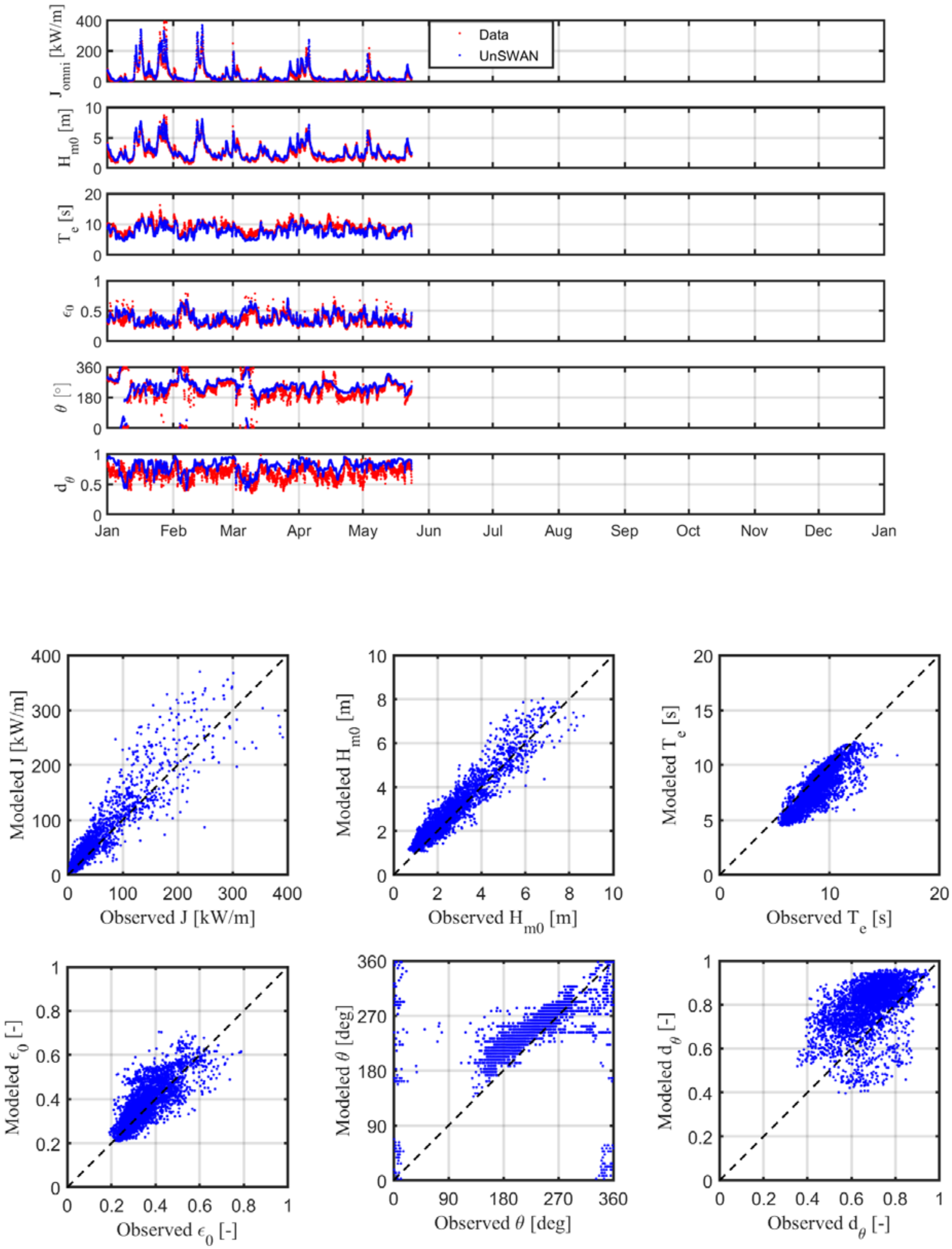

Figure F.15. Comparisons of time series (top) and scatter plots (bottom) of the six UnSWAN model-simulated IEC parameters with observed data at NDBC Buoy 46084 for 2017.

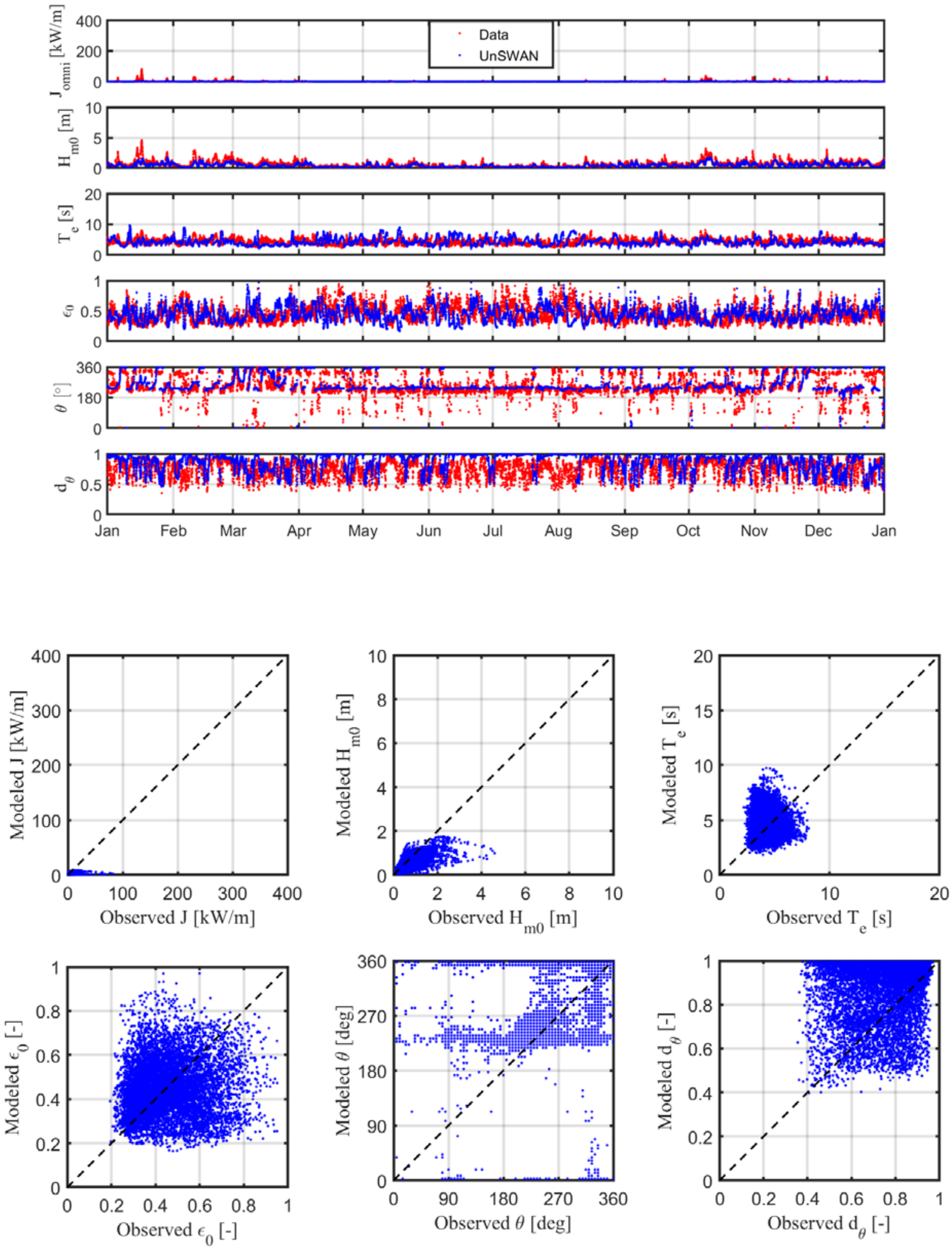

Figure F.16. Comparisons of time series (top) and scatter plots (bottom) of the six UnSWAN model-simulated IEC parameters with observed data at NDBC Buoy 46108 for 2017.

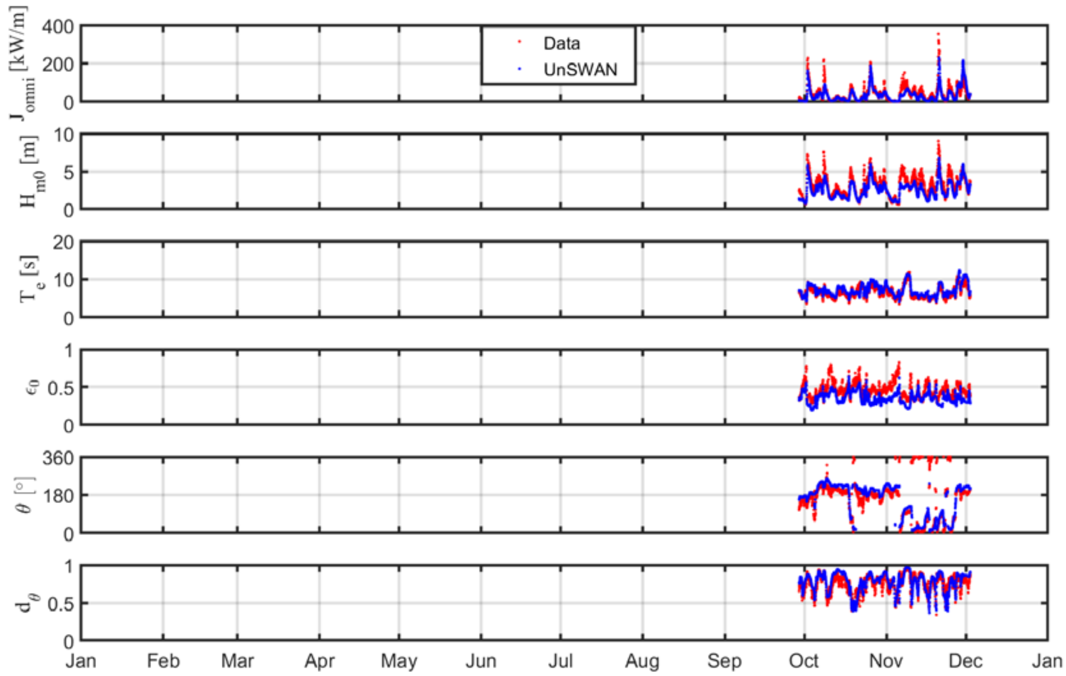

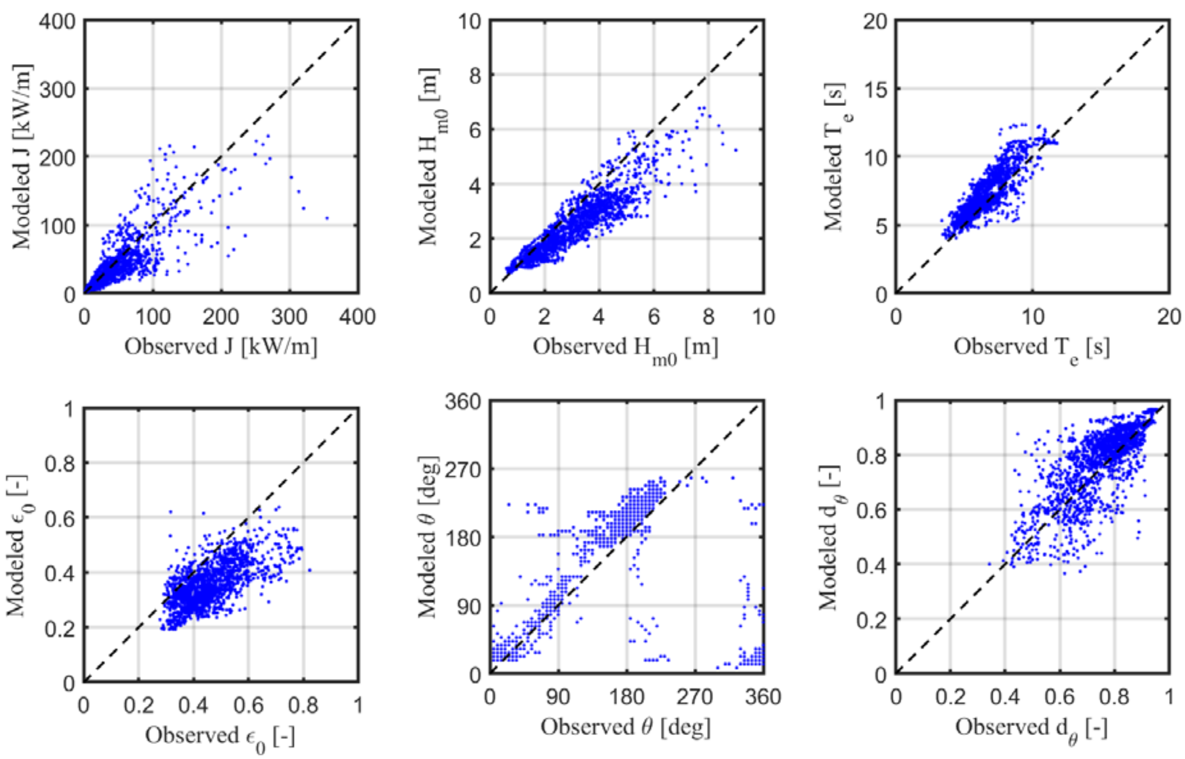

Figure F.17. Comparisons of time series (top) and scatter plots (bottom) of the six UnSWAN model-simulated IEC parameters with observed data at NDBC Buoy 46264 for 2017.

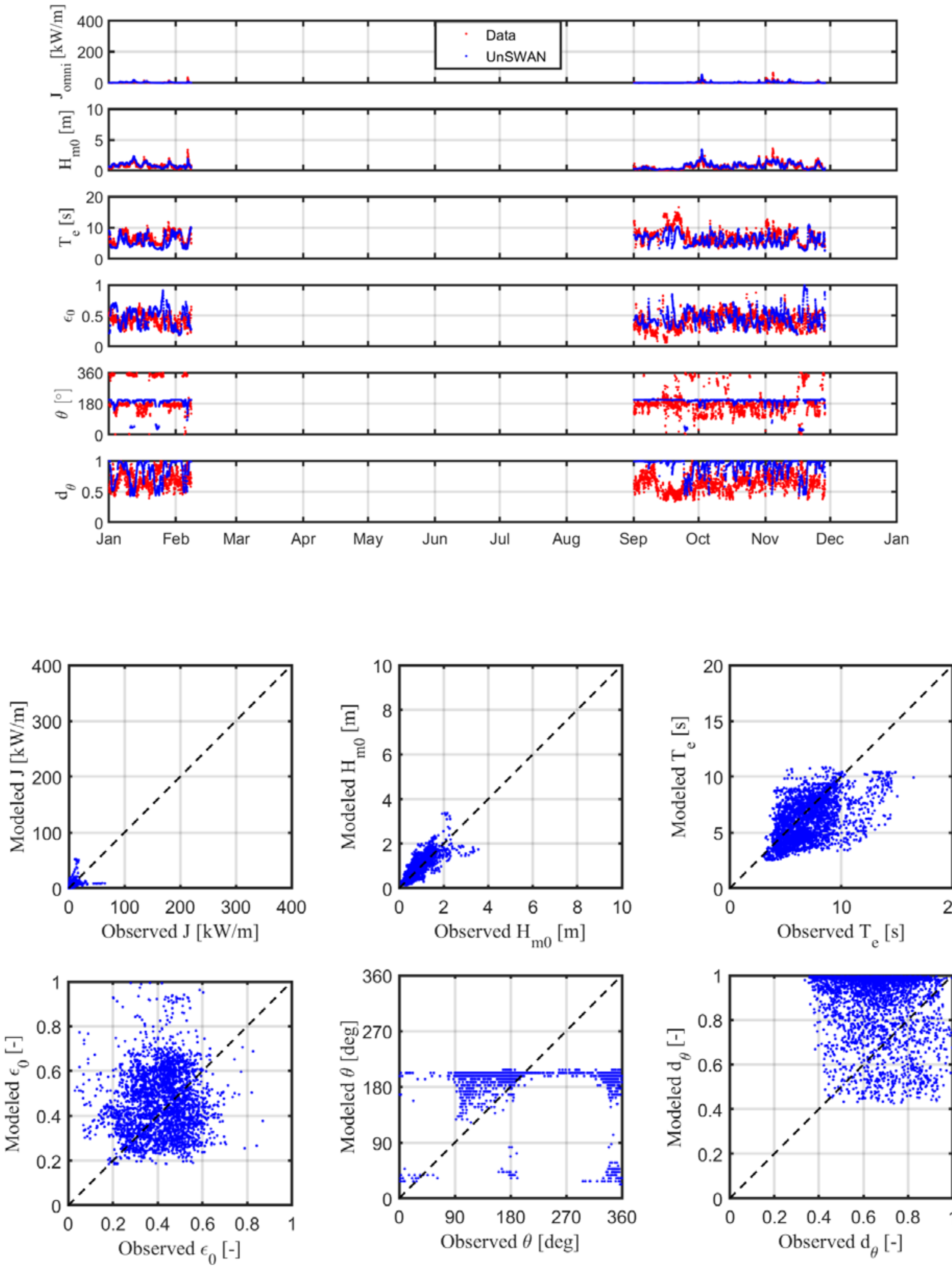

Figure F.18. Comparisons of time series (top) and scatter plots (bottom) of the six UnSWAN model-simulated IEC parameters with observed data at NDBC Buoy 46060 for 2010.

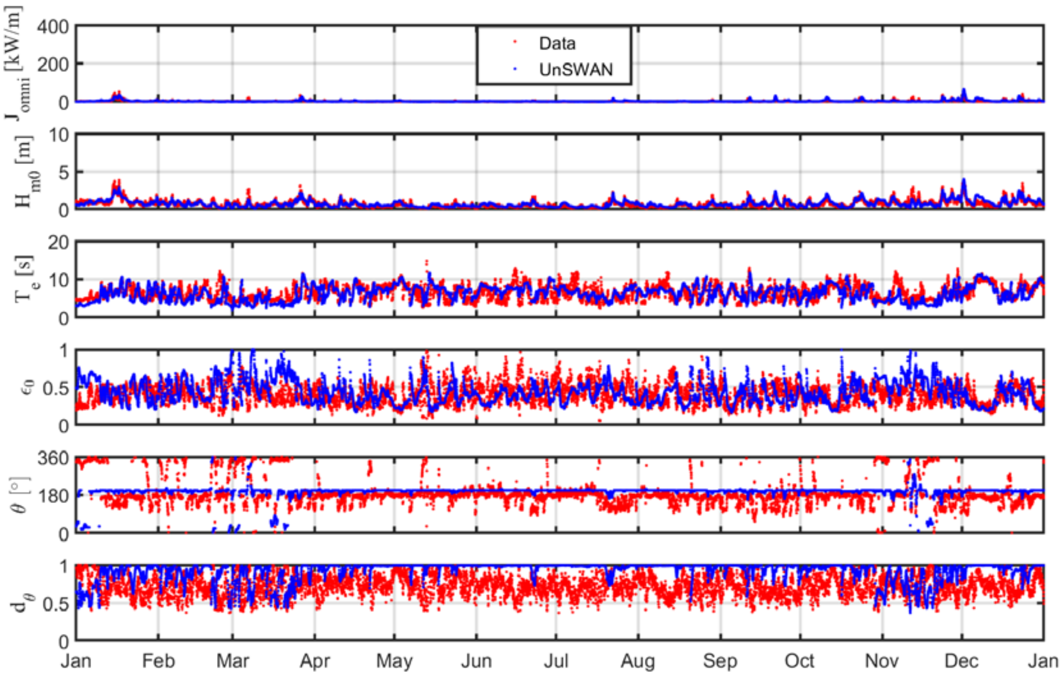

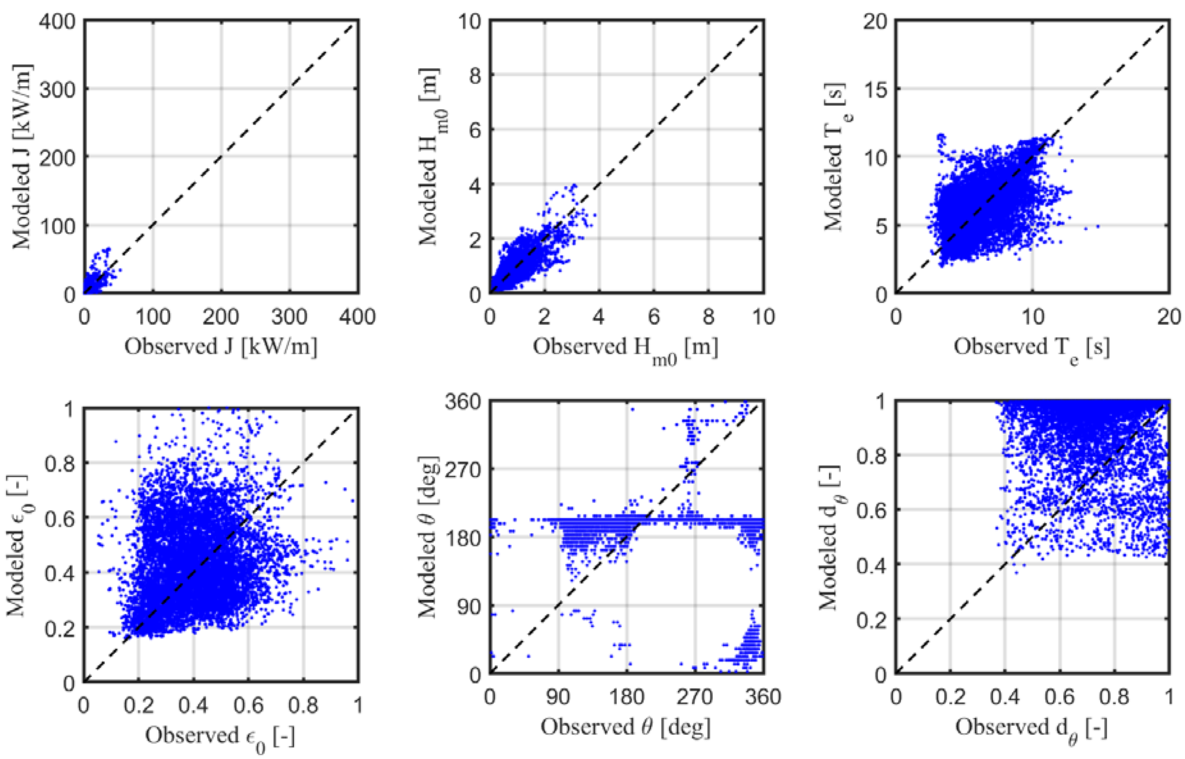

Figure F.19. Comparisons of time series (top) and scatter plots (bottom) of the six UnSWAN model-simulated IEC parameters with observed data at NDBC Buoy 46060 for 2009.

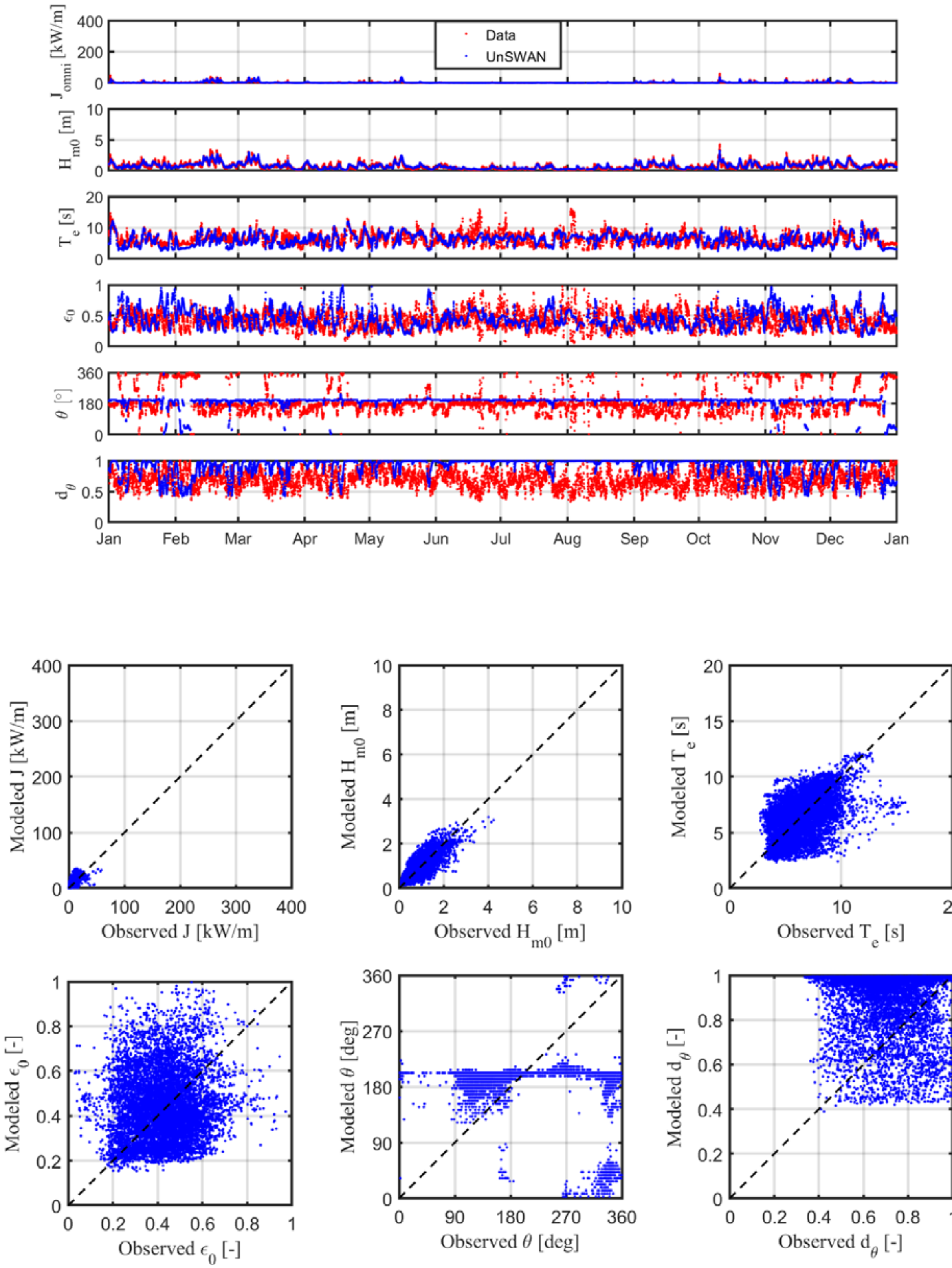

Figure F.20. Comparisons of time series (top) and scatter plots (bottom) of the six UnSWAN model-simulated IEC parameters with observed data at NDBC Buoy 46060 for 2008.

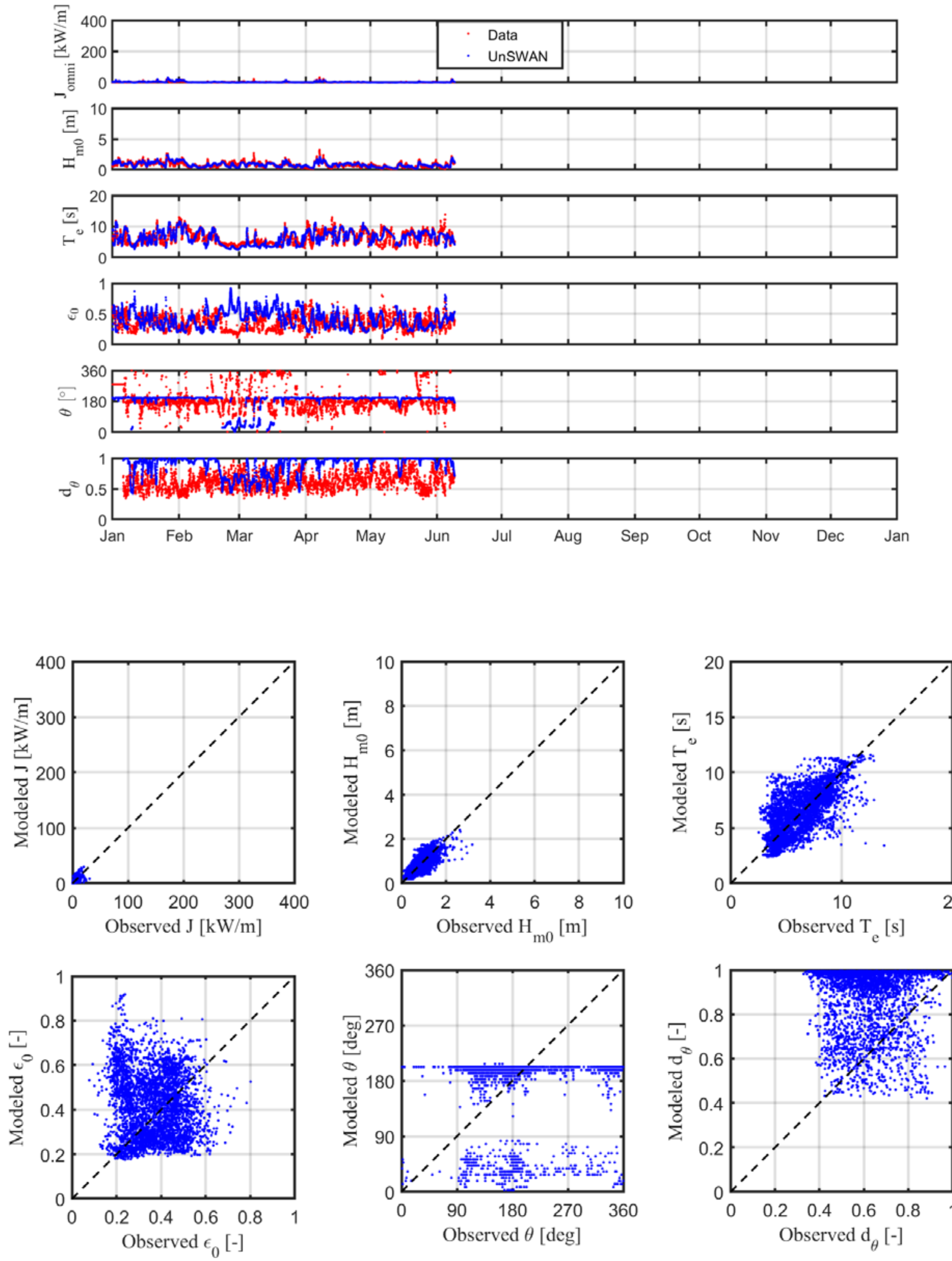

Figure F.21. Comparisons of time series (top) and scatter plots (bottom) of the six UnSWAN model-simulated IEC parameters with observed data at NDBC Buoy 46060 for 2007.

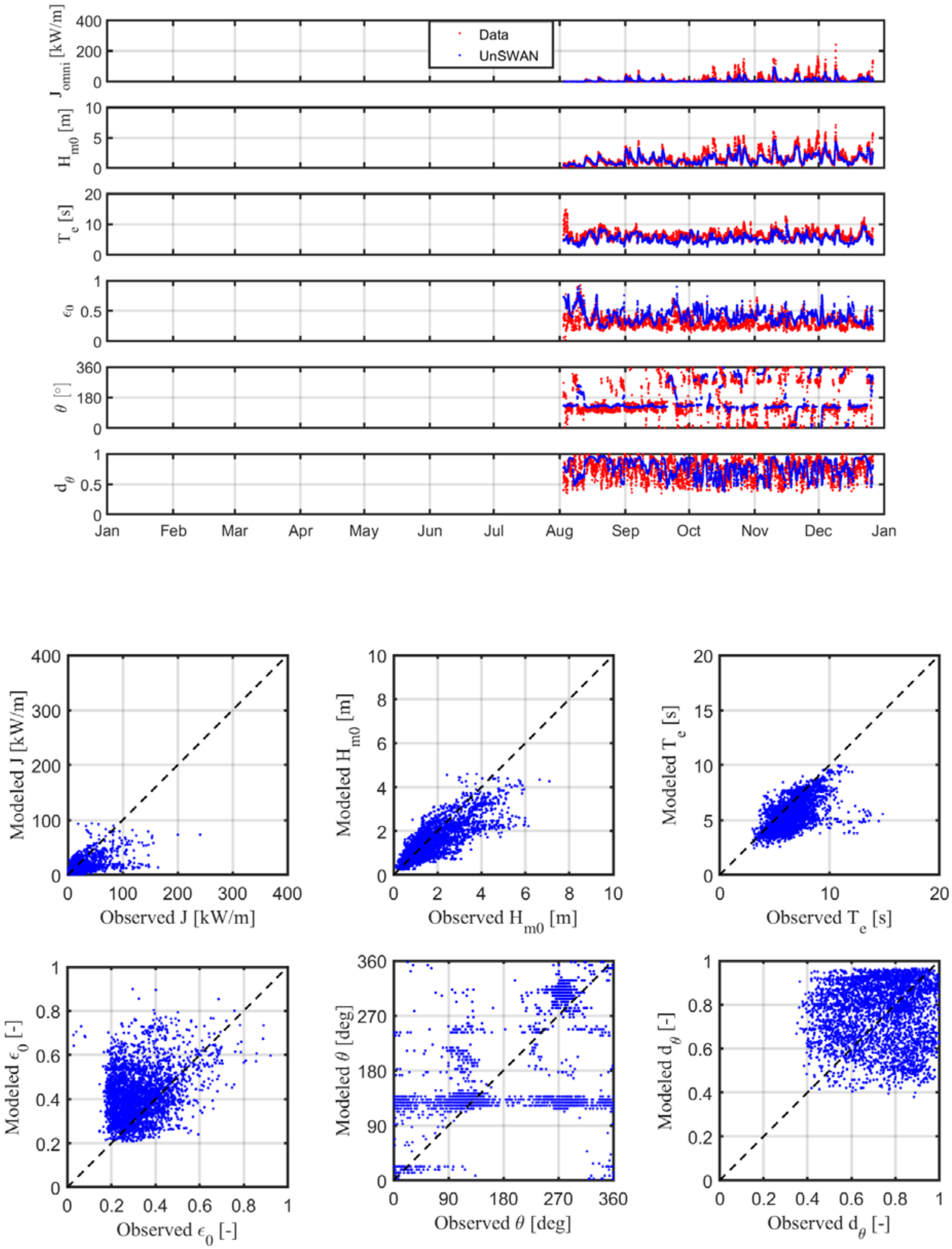

Figure F.22. Comparisons of time series (top) and scatter plots (bottom) of the six UnSWAN model-simulated IEC parameters with observed data at NDBC Buoy 46105 for 2008.

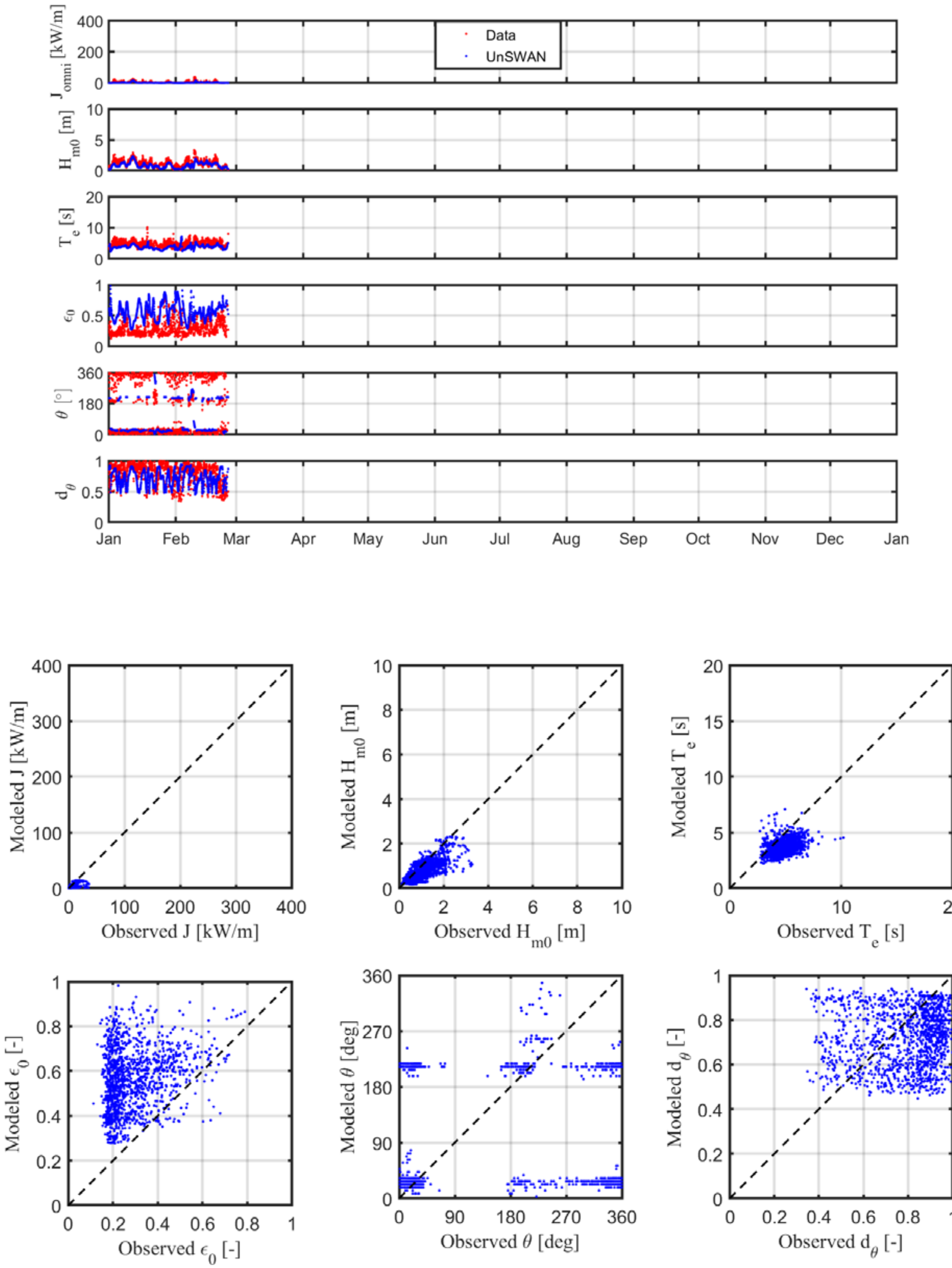

Figure F.23. Comparisons of time series (top) and scatter plots (bottom) of the six UnSWAN model-simulated IEC parameters with observed data at NDBC Buoy 46106 for 2010.

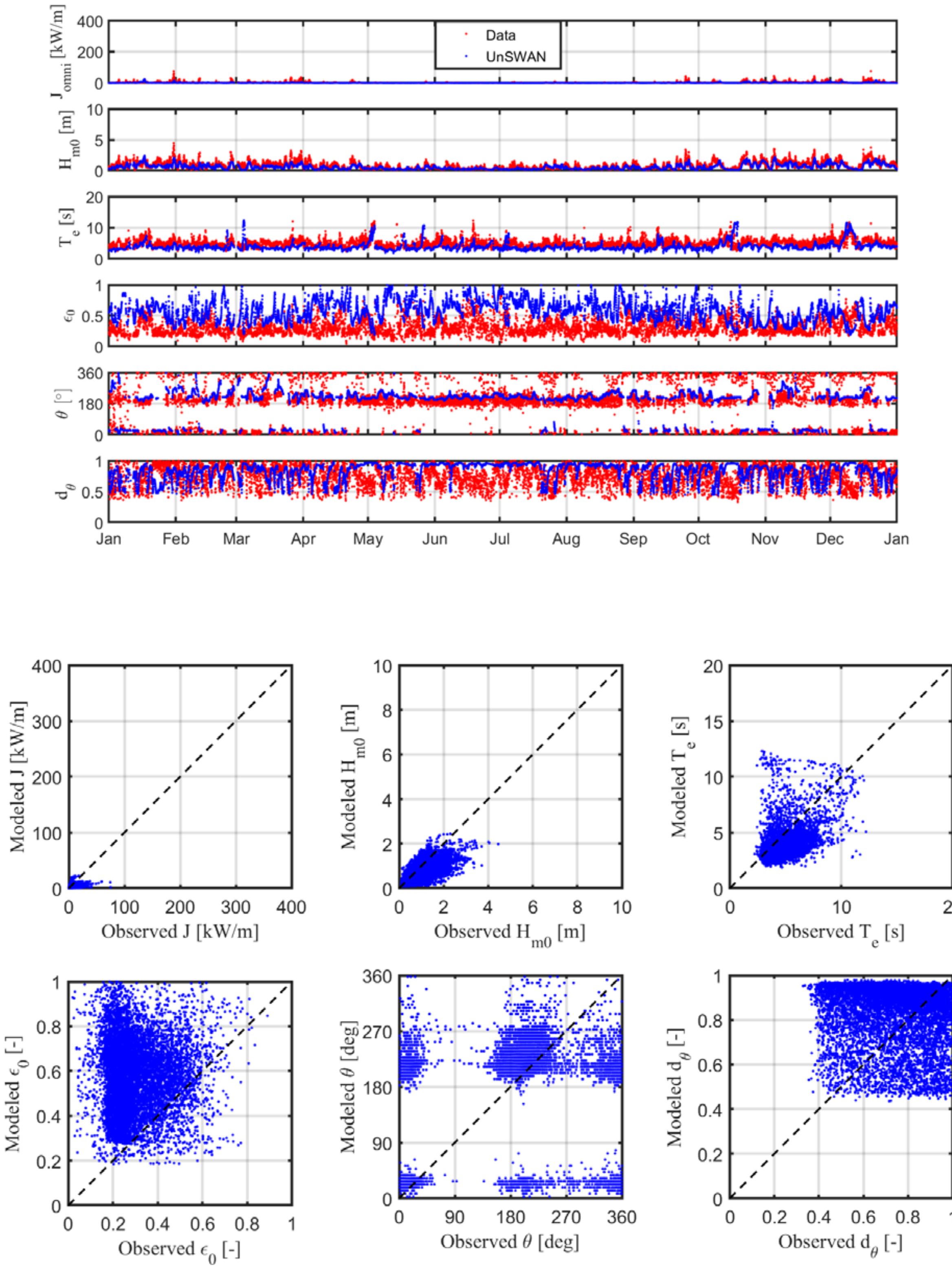

Figure F.24. Comparisons of time series (top) and scatter plots (bottom) of the six UnSWAN model-simulated IEC parameters with observed data at NDBC Buoy 46106 for 2009.

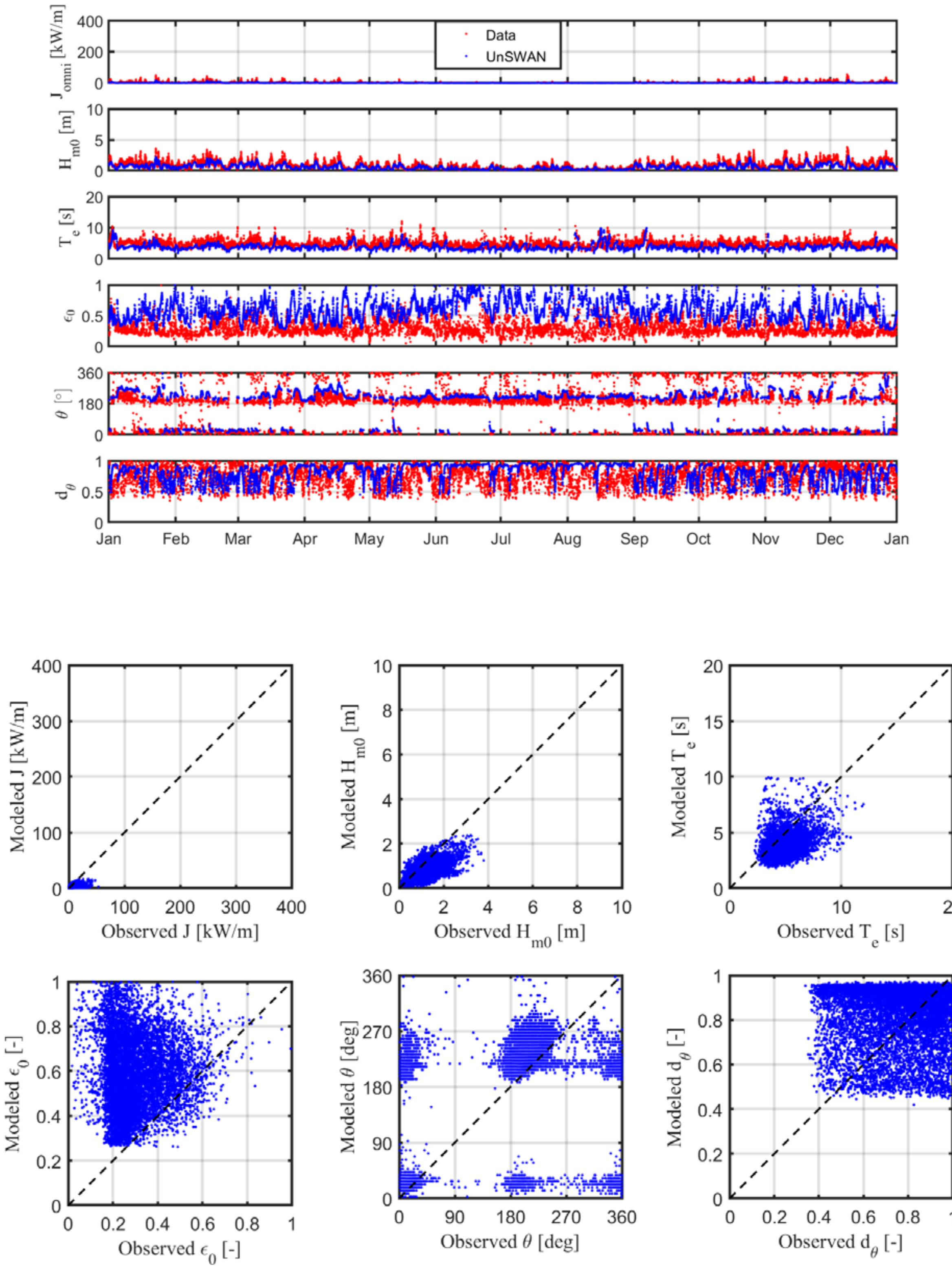

Figure F.25. Comparisons of time series (top) and scatter plots (bottom) of the six UnSWAN model-simulated IEC parameters with observed data at NDBC Buoy 46106 for 2008.

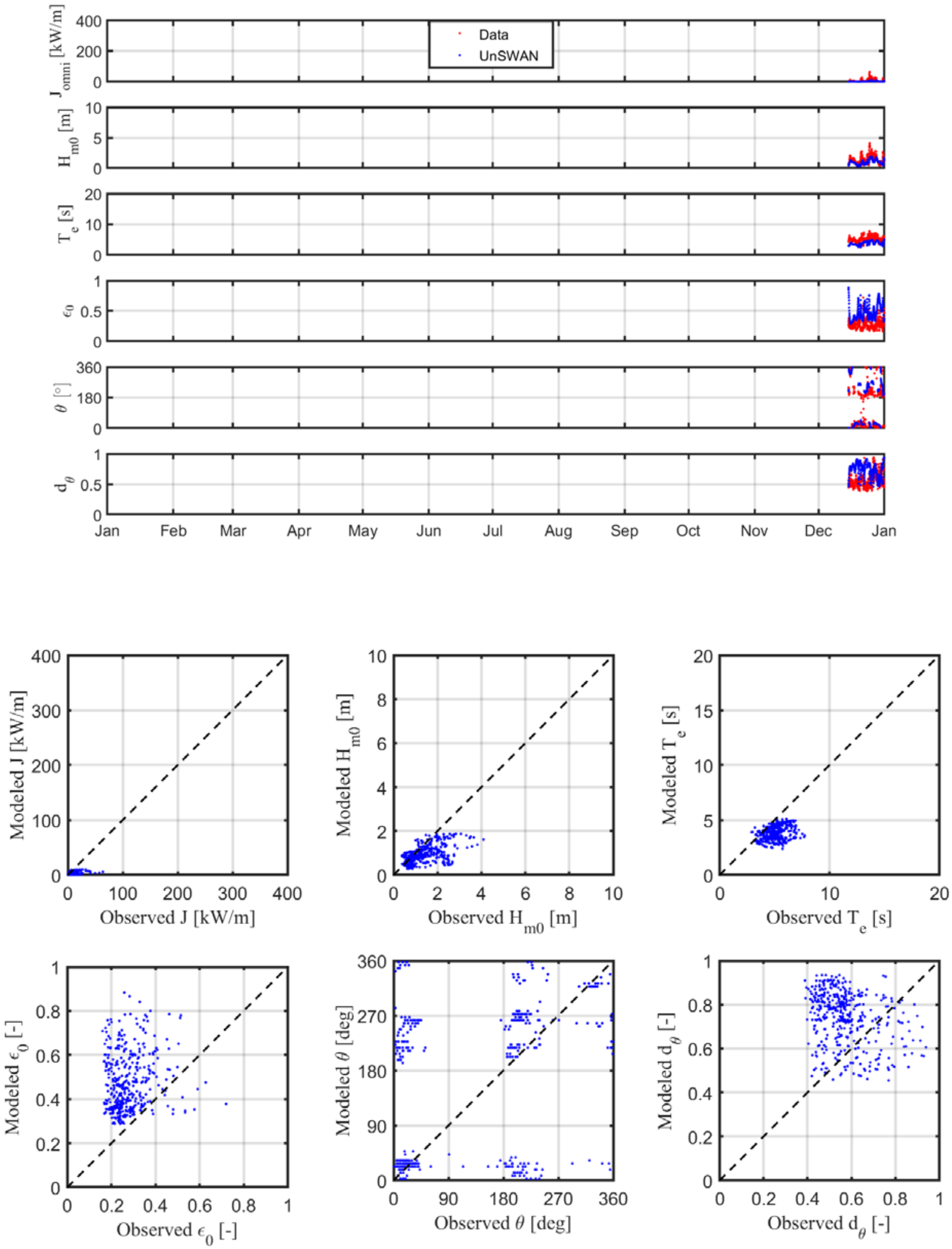

Figure F.26. Comparisons of time series (top) and scatter plots (bottom) of the six UnSWAN model-simulated IEC parameters with observed data at NDBC Buoy 46106 for 2007.

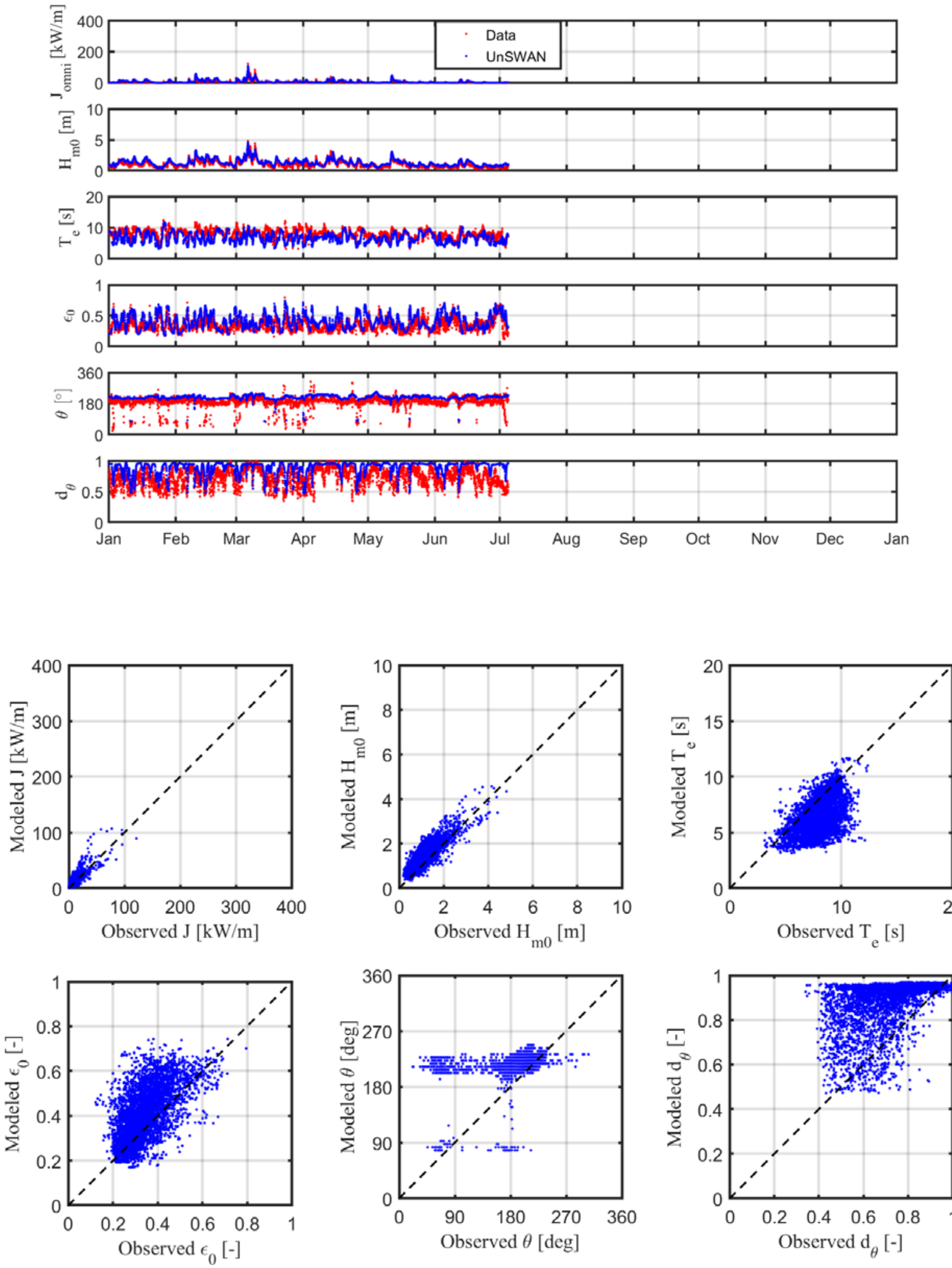

Figure F.27. Comparisons of time series (top) and scatter plots (bottom) of the six UnSWAN model-simulated IEC parameters with observed data at NDBC Buoy 46107 for 2010.

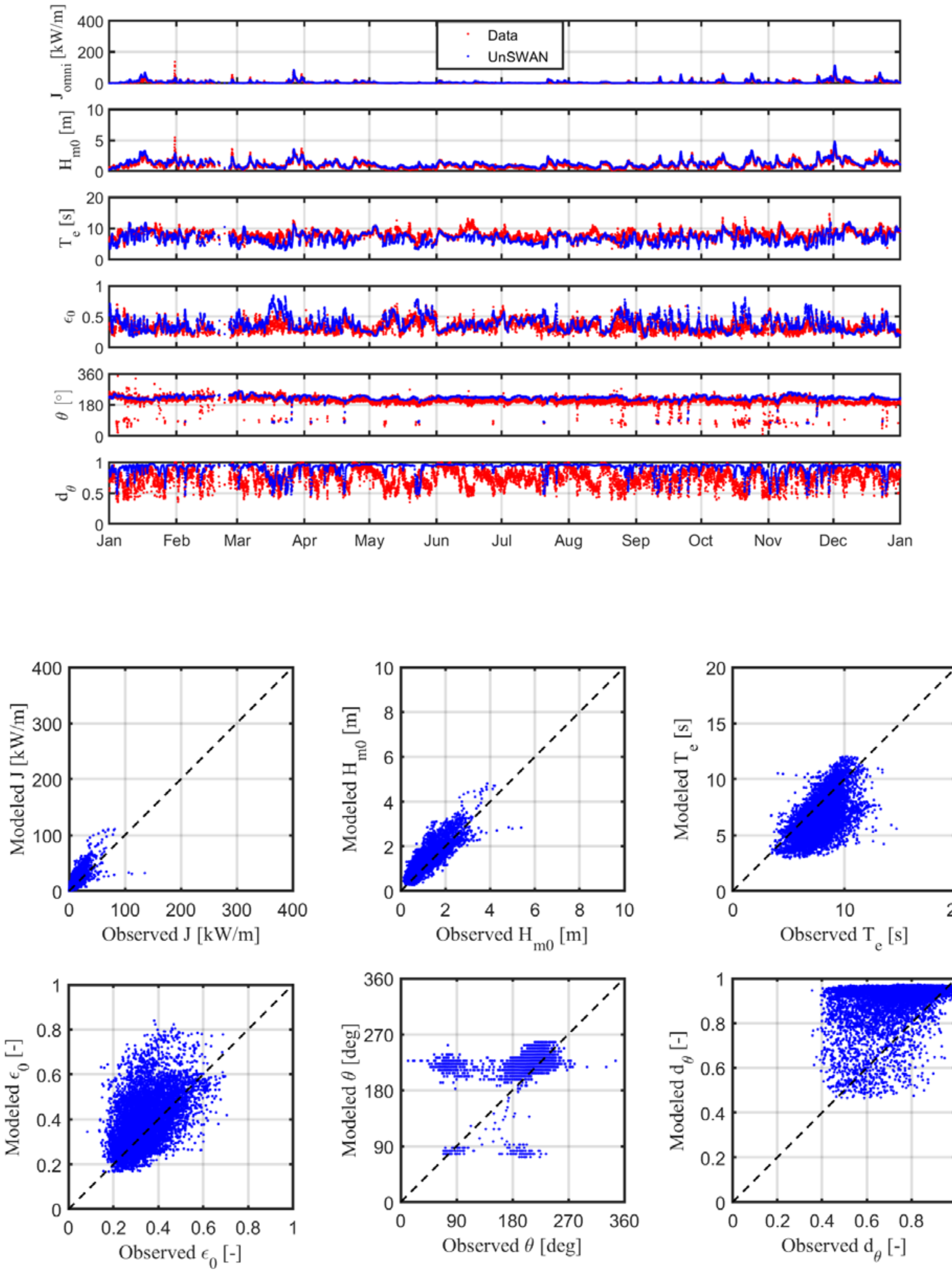

Figure F.28. Comparisons of time series (top) and scatter plots (bottom) of the six UnSWAN model-simulated IEC parameters with observed data at NDBC Buoy 46107 for 2009.

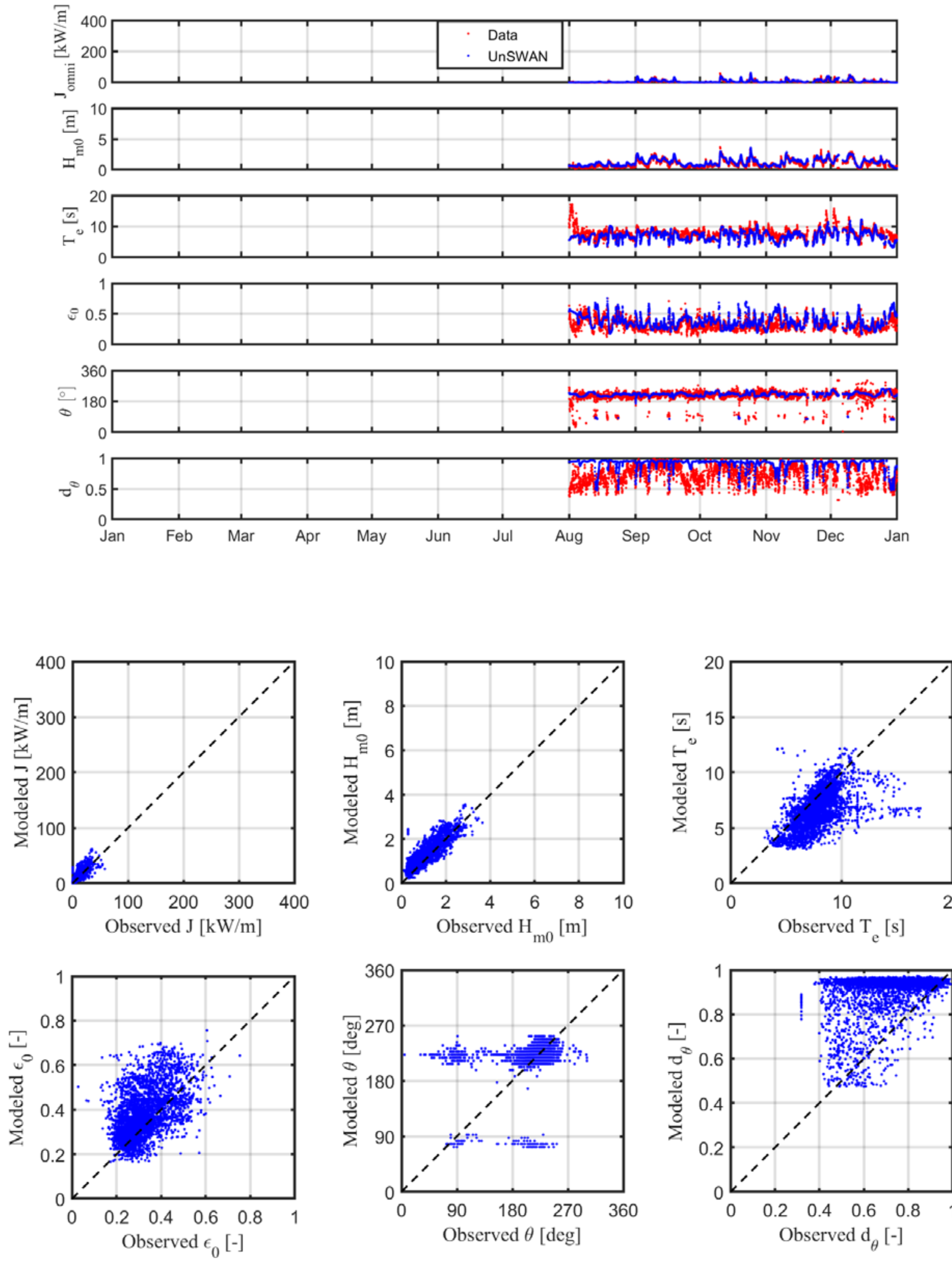

Figure F.29. Comparisons of time series (top) and scatter plots (bottom) of the six UnSWAN model-simulated IEC parameters with observed data at NDBC Buoy 46107 for 2008.

Pacific Northwest National Laboratory

902 Battelle Boulevard
P.O. Box 999
Richland, WA 99354
1-888-375-PNNL (7665)

www.pnnl.gov